CONFORMATIONAL AND STRUCTURAL DETERMINATIONS OF SUBSTITUTED FOUR AND FIVE MEMBERED RINGS BY INFRARED, RAMAN, AND MICROWAVE SPECTRAL STUDIES

A DISSERTATION IN
Chemistry
and
Geosciences

Presented to the Faculty of the University
of Missouri-Kansas City in partial fulfillment of
the requirements for the degree

DOCTOR OF PHILOSOPHY

by

Joshua John Klaassen

B.S., Nebraska Wesleyan University, 2007

Kansas City, Missouri

2014

© 2014
JOSHUA JOHN KLAASSEN
ALL RIGHTS RESERVED

AN ABSTRACT IN A UNIVERSITY OF MISSOURI-

KANSAS CITY DISSERTATION: CONFORMATIONAL AND STRUCTURAL DETERMINATIONS OF SUBSTITUTED FOUR AND FIVE MEMBERED RINGS BY INFRARED, RAMAN, AND MICROWAVE

SPECTRAL STUDIES

Joshua John Klaassen, Candidate for the Doctor of Philosophy

University of Missouri-Kansas City, 2014

ABSTRACT

Studies of the structure and conformational stabilities of molecules have become increasingly important due in part to advances in the fields of biochemistry and nano-chemistry. Specifically the conformation of organoamines is currently at work in every human alive with this arising from the amino acids in proteins and the substituted bases in DNA and RNA. The importance of conformational stability is further demonstrated in biological systems by enzyme binding where the conformational changes of the protein can change the binding site either enhancing or deactivating the enzyme. These systems however tend to have relatively large molecules with many conformers. Thus in this work we explore the use of multiple spectroscopies to stuy four and five membered rings and amines. Infrared, far-infrared, and Raman spectroscopy to of vapor, liquid, solid, and rare gas solutions to determine vibrational assignments, conformational stabilities, and even some structural parameters. We combine this vibrational approach with ab initio

calculations and microwave spectroscopy for greatly improved conformational and structural studies. Also explored are new methodologies of variable temperature Raman spectra of rare gas solutions to improve conformational stuies of polar compounds or compounds with four or more conformers. Additionally chirped-pulse FT microwave spectroscopy has been applied to structural problems to greatly improve the structural parameters.

The faculty listed below, appointed by the Dean of the College of Arts and Sciences have examined a thesis titled “Conformational and Structural Determinations of Substituted Foure and Five Membered Rings by Infrared, Raman, and Microwave Spectral Studies.” presented by Joshua J Klaassen, candidate for the Doctor of Philosophy, and certify that in their opinion it is worthy of acceptance.

Supervisory Committee

James R. Durig, Ph.D., Committee Chair
Department of Chemistry

Andrew J. Holder, Ph.D.
Department of Chemistry

Zhonghua Peng, Ph.D.
Department of Chemistry

James B. Murowchick, Ph.D.
Department of Geosciences

Jejung Lee, Ph.D.
Department of Geosciences

CONTENTS

ABSTRACT iii

LIST OF TABLES ix

LIST OF ILLUSTRATIONS xix

ACKNOWLEDGMENTS xxviii

CHAPTER

1. INTRODUCTION 1

2. EXPERIMENTAL AND THEORETICAL METHODS 8

3. THE r_0 STRUCTURAL PARAMETERS, CONFORMATIONAL STABILITY, AND VIBRATIONAL ASSIGNMENT OF EQUATORIAL AND AXIAL CYANOCYCLOBUTANE 15

4. THE r_0 STRUCTURAL PARAMETERS, CONFORMATIONAL STABILITY, AND VIBRATIONAL ASSIGNMENT OF EQUATORIAL AND AXIAL BROMOCYCLOBUTANE 47

5. CONFORMATIONAL STABILITY, r_0 STRUCTURAL PARAMETERS, AND VIBRATIONAL ASSIGNMENTS OF MONO-SUBSTITUTED CYCLOBUTANES: FLUOROCYCLOBUTANE 86

6. CONFORMATIONAL AND STRUCTURAL STUDIES OF CYCLOBUTYLSILANE FROM TEMPERATURE DEPENDENT INFRARED SPECTRA OF XENON SOLUTIONS AND AB INITIO CALCULATIONS 116

7. STRUCTURAL AND CONFORMATIONAL STUDIES FROM TEMPERATURE DEPENDENT INFRARED SPECTRA OF XENON SOLUTIONS AND AB INITIO CALCULATATIONS OF CYCLOBUTYLGERMANE 149

8. MICROWAVE AND INFRARED SPECTRA, ADJUSTED r_0 STRUCTURAL PARAMETERS, CONFORMATIONAL STABILITIES, VIBRATIONAL ASSIGNMENTS AND THEORETICAL CALCULATIONS OF CYCLOBUTYLCARBOXYLIC ACID CHLORIDE 188

9. INFRARED AND RAMAN SPECTRA, AB INITIO CALCULATIONS, CONFORMATIONAL STABILITY AND VIBRATIONAL ASSIGNMENT OF 1-BROMO-1-SILACYCLOPENTANE 239

10. CONFORMATIONAL AND STRUCTURAL STUDIES OF ETHYNYLCYCLOPENTANE FROM TEMPERATURE DEPENDENT RAMAN SPECTRA OF XENON SOLUTIONS AND AB INITIO CALCULATIONS 268

11. MICROWAVE, INFRARED, AND RAMAN SPECTRA, STRUCTURAL PARAMETERS, VIBRATIONAL ASSIGNMENTS AND THEORETICAL CALCULATIONS OF 1,3-DISILACYCLOPENTANE 301

12. MICROWAVE, INFRARED, RAMAN SPECTRA, STRUCTURAL PARAMETERS, VIBRATIONAL ASSIGNMENTS AND THEORETICAL CALCULATIONS OF 1,1,3,3-TETRAFLUORO-1,3-DISILACYCLOPENTANE 331

13. CONFORMATIONAL AND STRUCTURAL STUDIES OF 2,2-DIFLUOROETHYLAMINE FROM TEMPERATURE DEPENDENT INFRARED SPECTRA OF XENON SOLUTION AND AB INITIO CALCULATIONS 366

14. CONFORMATIONAL AND STRUCTURAL STUDIES OF N-PROPYLAMINE FROM TEMPERATURE DEPENDENT RAMAN AND FAR INFRARED SPECTRA OF XENON SOLUTIONS AND AB INITIO CALCULATIONS 404

15. CONFORMATIONAL AND STRUCTURAL STUDIES OF 2,2,2-TRIFLUOROETHYLAMINE FROM TEMPERATURE DEPENDENT RAMAN SPECTRA OF XENON SOLUTIONS AND AB INITIO CALCULATIONS 428

16. CONFORMATIONAL, VIBRATIONAL, AND STRUCTURAL STUDIES OF 2,2,3,3,3- PENTAFLUOROPROPYLAMINE FROM RAMAN AND INFRARED SPECTRA OF GAS, LIQUID, XENON SOLUTIONS, AND SOLID SUPPORTED BY AB INITIO CALCULATIONS 463

17. CONFORMATIONAL AND STRUCTURAL STUDIES OF ISOPROPYLAMINE FROM TEMPERATURE DEPENDENT RAMAN SPECTRA OF XENON SOLUTIONS AND AB INITIO CALCULATIONS 493

18. INFRARED AND RAMAN SPECTRA, r_0 STRUCTURAL PARAMETERS, CONFORMATIONAL STABILITY, AND VIBRATIONAL ASSIGNMENT OF 2-CYANOETHYLAMINE 532

19. THE R0 STRUCTURAL PARAMETERS, CONFORMATIONAL STABILITY, BARRIERS TO INTERNAL ROTAION, AND

VIBRATIONAL ASSIGNMENTS FOR TRANS AND GAUCHE ETHANOL 561

20. MICROWAVE, INFRARED, AND RAMAN SPECTRA, r_0 STRUCTURAL PARAMETERS, CONFORMATIONAL, STABILTIY, AND VIBRATIONAL ASSIGNMENT OF ALLYL THIOL.....593

REFERENCE LIST 636

Appendix

A. SUPPLEMENTAL INFORMATION.....653

VITA xxxii

TABLES

Table Page

1. Observed and calculated frequencies for the equatorial conformer of cyanocyclobutane. 18

2. Observed and calculated frequencies for the axial conformer of cyanocyclobutane. 20

3. Calculated energies (H) and energy differences (cm^{-1}) for the two conformers, transition state of cyanocyclobutane, and barrier to linearity of the $\angle C_{\alpha}CN$ angle. 27

4. Structural parameters (Å and degrees), rotational constants (MHz) and dipole moments (Debye) for equatorial and axial cyanocyclobutane. 28

5. Comparison of rotational constants (MHz) obtained from modified ab initio, MP2(full)/6-311+G(d,p) structural parameters and the experimental values from the microwave spectra of cyanocyclobutane. 35

6. Temperature and intensity ratios of the equatorial and axial bands of cyanocyclobutane. 39

7. Quadratic centrifugal distortion constants (kHz) for equatorial and axial conformers of cyanocyclobutane. 45

8. Structural parameters (Å and degree) for cyclobutane, cyanocyclobutane, chlorocyclobutane, cyclobutanol, cyanocyclopropane, cyclopropane, methyl cyanide, and ethyl cyanide. 46

9. Observed and calculated frequencies for the equatorial conformer of bromocyclobutane. 54

10. Observed and calculated frequencies for the equatorial conformer of bromocyclobutane-d1. 56

11. Observed and calculated frequencies for the equatorial conformer of bromocyclobutane-d4. 57

12. Observed and calculated frequencies for the axial conformer of bromocyclobutane. 59

13. Calculated energies in (H) and energy differences (cm^{-1}) for the two conformers, and transition states of bromocyclobutane. 61

14. Structural parameters (Å and degrees), rotational constants (MHz) and dipole moments (Debye) for equatorial and axial ^{79}bromocyclobutane. 63

15. Comparison of rotational constants (MHz) obtained from modified ab initio, MP2(full)/6-311+G(d,p) structural parameters and the experimental values from the microwave spectra of two isotopes of bromocyclobutane. 67

16. Temperature and intensity ratios of the equatorial and axial bands of bromocyclobutane. 74

17. Structural parameters (Å and degrees) of cyclobutane and some bromoalkanes and bromoalkenes. 78

18. Rotational transition frequencies and residuals (MHz) of bromocyclobutane-^{79}Br and ^{81}Br. 80

19. Rotational, centrifugal distortion and quadrupole coupling constants of bromocyclobutane. 82

20. Observed and calculated frequencies (cm^{-1}) for the ring-puckering vibrations of bromocyclobutane. 84

21. Observed and calculated frequencies for the equatorial conformer of fluorocyclobutane. 89

22. Observed and calculated frequencies for the axial conformer of fluorocyclobutane. 91

23. Calculated energies in (H) and energy differences (cm^{-1}) for the two conformers, and transition state of fluorocyclobutane. 95

24. Structural parameters (Å and degrees), rotational constants (MHz) and dipole moments (Debye) for equatorial and axial fluorocyclobutane. 97

25. Temperature and intensity ratios of the equatorial and axial bands of fluorocyclobutane. 102

26. Comparison of rotational constants (MHz) obtained from modified ab initio, MP2(full)/6-311+G(d,p) structural parameters and the experimental values from the microwave spectra of equatorial and axial fluorocyclobutane. 105

27. Observed and calculated frequencies (cm^{-1}) for the ring-puckering vibrations of fluorocyclobutane. 106

28. Structural parameters (Å and degrees) of cyclobutane and some fluoroalkanes and fluoroalkenes. 111

29. Structural parameters of the ring for a few four-membered ring molecules (Å and degree).....113

30. Quadratic centrifugal distortion constants (kHz) for equatorial and axial conformers of fluorocyclobutane. 115

31. Observed and calculated frequencies (cm^{-1}) for Eq cyclobutylsilane. 120

32. Observed and calculated frequencies (cm^{-1}) for Ax cyclobutylsilane. 122

33. Calculated energies in Hartrees (H) and energy differences (cm^{-1}) for the two conformers and transition state of cyclobutylsilane.....124

34. Structural parameters (Å and degrees), rotational constants (MHz) and dipole moments (Debye) for Eq and Ax cyclobutylsilane. 128

35. Temperature and intensity ratios of the Eq and Ax bands of cyclobutylsilane. 141

36. Comparison of rotational constants (MHz) obtained from modified ab initio, MP2(full)/6-311+G(d,p) structural parameters and the experimental values from the microwave spectra of Eq and Ax cyclobutylsilane. 144

37. Quadratic centrifugal distortion constants (kHz) for Eq and Ax conformers of cyclobutylsilane. 148

38. Observed and calculated frequencies (cm^{-1}) for Eq cyclobutylgermane. 153

39. Observed and calculated frequencies (cm^{-1}) for Ax cyclobutylgermane. 155

40. Structural parameters (Å and degrees), rotational constants (MHz) and dipole moments (Debye) for Eq cyclobutylgermane. 160

41. Structural parameters (Å and degrees), rotational constants (MHz) and dipole moments (Debye) for Ax cyclobutylgermane.....162

42. Temperature and intensity ratios of the Eq and Ax bands of cyclobutylgermane. 174

43. Comparison of rotational constants (MHz) obtained from modified ab initio, MP2(full)/6-311+G(d,p) structural parameters and the experimental values from the microwave spectra of Eq and Ax cyclobutylgermane. 178

44. Microwave spectrum for the g-Eq form of c-$C_4H_7C(O)^{35}Cl$. Observed frequencies of hyperfine components of rotational transitions (MHz) and deviations of calculated values (kHz). 194

45. Microwave spectrum for the g-Eq form of c-$C_4H_7C(O)^{37}Cl$. Observed frequencies of hyperfine components of rotational transitions (MHz) and deviations of calculated values (kHz) 196

46. Observed and predicted fundamental frequencies for the g-Eq conformer of cyclobutylcarboxylic acid chloride. 199

47. Observed and predicted fundamental frequencies for the g-Ax conformer of cyclobutylcarboxylic acid chloride. 201

48. Observed and predicted fundamental frequencies for the t-Eq conformer of cyclobutylcarboxylic acid chloride. 203

49. Calculated energies in (H) and energy differences (cm^{-1}) for the four possible conformers of cyclobutylcarboxylic acid chloride 206

50. Structural parameters (Å and degrees), rotational constants (MHz) and dipole moments (Debye) for g-Eq form of cyclobutylcarboxylic acid chloride. 208

51. Rotational Constants (MHz), Quadratic centrifugal distortion constants (kHz) and quadrupole coupling constants (MHz) for the ^{35}Cl and ^{37}Cl isotopomers of the g-Eq conformer of cyclobutylcarboxylic acid chloride. 214

52A. Temperature and intensity ratios of the g-Eq and g-Ax bands of cyclobutylcarboxylic acid chloride. 223

52B. Temperature and intensity ratios of the g-Eq and t-Eq bands of cyclobutanecarbonyl chloride. 217

52C. Temperature and intensity ratios of the g-Ax and t-Eq bands of cyclobutanecarbonyl chloride. 225

53. Comparison of rotational constants (MHz) obtained from modified ab initio MP2(full)/6-311+G(d,p) structural parameters and the experimental values from the microwave spectra of g-Eq conformer of cyclobutylcarboxylic acid chloride. 228

54. Structural parameters of a few acetyl chloride molecules of the form R-C(O)Cl (Å and degree)....232

55. Structural parameters of a few four-membered ring molecules of the form c-C_4H_7X (Å and degree). 235

56. Calculated and observed frequencies (cm-1) for 1-bromo-1-silacyclopentane twisted (C1) form. 246

57. Calculated electronic energies (hartree) and energy differences (cm^{-1}) for the twisted (C1), envelope-axial (Cs), envelope-equatorial (Cs), and planar (Cs) forms of 1-bromo-1-silacyclopentane. 248

58. Structural parameters (Å and degree), rotational constants (MHz) and dipole moment (debye) for 1-^{79}bromo-1-silacyclopentane twisted (C1) form. 250

59. Calculated and Observed Frequencies (cm^{-1}) for Ethynylcyclopentane Eq (Cs) Form. 276

60. Calculated and Observed Frequencies (cm^{-1}) for Ethynylcyclopentane Ax (Cs) Form. 278

61. Calculated Electronic Energies (Hartree) for the Eq (Cs) and Energy Differences (cm^{-1}) for Ax (Cs), Twisted (C1), and Planar (Cs) Forms of Ethynylcyclopentane. 281

62. Structural Parameters (Å and Degree), Rotational Constants (MHz) and Dipole Moment (Debye) for Ethynylcyclopentane Eq and Ax (Cs) Forms. 285

63. Temperature and Activity Ratios of the Eq and Ax Bands of Ethynylcyclopentane. 292

64. Comparison of Rotational Constants (MHz) Obtained from Ab Initio MP2(full)/6-311+G(d,p) Predictions, Experimental Values from Microwave Spectra, and Adjusted r_0 Structural Parameters for Ethynylcyclopentane. 295

65. Rotational transition frequencies (MHz) of the ground vibrational state of c-$C_3H_6Si_2H_4$. 306

66. Rotational transition frequencies (MHz) of the ground vibrational state of c-$C_3H_6Si_2H_4$. 307

67. Rotational transition frequencies (MHz) of the ground vibrational state of c-$C_3H_6Si_2H_4$. 308

68. Experimental rotational and centrifugal distortion constants of the ground vibrational state of c-$C_3H_6Si_2H_4$ isotopologues. 309

69. Observed and calculated frequencies (cm^{-1}) and potential energy distributions (P.E.D.s) for the twist (C2) conformer of c-$C_3H_6Si_2H_4$. 310

70. Calculated energies in Hartrees (H) and energy differences (cm^{-1}) for the three conformers of c-$C_3H_6Si_2H_4$. 317

71. Structural parameters (Å and degrees), rotational constants (MHz) and dipole moments (Debye) for twist conformer c-$C_3H_6Si_2H_4$. 320

72. Comparison of rotational constants (MHz) obtained from experimental values from microwave spectra, and from the adjusted r_0 structural parameters for c-$C_3H_6Si_2H_4$. 322

73. Rotational transition frequencies (MHz) of the ground vibrational state of c-$C_3H_6Si_2F_4$. 338

74. Rotational transition frequencies (MHz) of the ground vibrational state of c-$C_3H_6Si_2F_4$. 341

75. Rotational transition frequencies (MHz) of the ground vibrational state of c-$C_3H_6Si_2F_4$. 344

76. Experimental rotational and centrifugal distortion constants of c-$C_3H_6Si_2F_4$ isotopologues 345

77. Calculated and observed frequencies (cm^{-1}) for the twist form of c-$C_3H_6Si_2F_4$ (C2). 348

78. Calculated energies in Hartrees (H) and energy differences (cm^{-1}) for the two conformers and transition state of c-$C_3H_6Si_2F_4$ 351

79. Structural parameters (Å and degrees), rotational constants (MHz) and dipole moments (Debye) for twist conformer c-$C_3H_6Si_2F_4$. 357

80. Comparison of rotational constants (MHz) obtained from experimental values from microwave spectra, and from the adjusted r_0 structural parameters for c-$C_3H_6Si_2F_4$. 360

81. Observed and calculated frequencies for the Trans-trans conformer of 2,2-difluoroethylamine. 375

82. Observed and calculated frequencies for the Gauche-gauche conformer of 2,2-difluoroethylamine 377

83. Observed and calculated frequencies for the Gauche-trans conformer of 2,2-difluoroethylamine.....379

84. Calculated energies in (H) and energy differences (cm^{-1}) for the five conformers of 2,2-difluoroethylamine. 381

85. Structural parameters (Å and degree), rotational constants (MHz), and dipole moment (Debye) for Trans-trans, Gauche-gauche and Gauche-trans forms of 2,2-difluoroethylamine. 384

86. Temperature and intensity ratios of the Trans-trans, Gauche-gauche, and Gauche-trans bands of 2,2-difluoroethylamine.....394

87. Comparison of rotational constants obtained from ab initio MP2(full)/6-311+G(d,p) predictions, experimental values from microwave spectra, and adjusted r_0 structural parameters for 2,2-difluoroethylamine. 397

88. Quadratic centrifugal distortion constants (kHz) for conformers of 2,2-difluoroethylamine. 401

89. Observed and predicted wavenumbers (cm^{-1}) for conformers of n-propylamine. 411

90. Calculated energies in (H) and energy differences (cm^{-1}) for the five conformers of n-propylamine. 416

91. Temperature and intensity ratios of the Tt, Tg, Gg, Gg′, and Gt bands of n-propylamine. 424

92. Observed and calculated wavenumbers (cm^{-1}) for trans 2,2,2 trifluoroethylamine. 436

93. Observed and calculated wavenumbers (cm^{-1}) for gauche 2,2,2 trifluoroethylamine. 438

94. Calculated energies (hartree) and energy differences (cm^{-1}) for the two conformers of 2,2,2 trifluoroethylamine. 440

95. Structural parameters, rotational constants, and dipole moments for trans and gauche 2,2,2 trifluoroethylamine. 443

96. Temperature and intensity ratios of the trans and gauche bands of 2,2,2 trifluoroethylamine. 452

97. Comparison of rotational constants obtained from experimental values from microwave spectra and adjusted r_0 structural parameters for trans 2,2,2 trifluoroethylamine. 455

98. Quadratic centrifugal distortion constants (kHz) and quadrupole coupling constants (MHz) for conformers of 2,2,2 trifluoroethylamine. 459

99. Observed and calculated wavenumbers (cm^{-1}) for trans-trans 2,2,3,3,3-pentafluoropropylamine. 474

100. Observed and calculated wavenumbers (cm^{-1}) for trans-gauche 2,2,3,3,3-pentafluoropropylamine. 476

101. Calculated energies in (H) and energy differences (cm^{-1}) for the five conformers of 2,2,3,3,3-pentafluoropropylamine. 478

102. Structural parameters (Å and degree), rotational constants (MHz) and dipole moment (debye) for 2,2,3,3,3-pentafluoropropylamine trans-trans (Cs) and trans-gauche (C1) forms. 480

103. Temperature and intensity ratios of the trans-trans and trans-gauche bands of 2,2,3,3,3-pentafluoropropylamine. 489

104. Observed and calculated frequencies (cm^{-1}) for trans isopropylamine. 503

105. Observed and calculated frequencies (cm^{-1}) for gauche isopropylamine. 505

106. Calculated energies (hartree) and energy differences (cm^{-1}) for the two conformers and transition states of isopropylamine. 507

107. Structural parameters, rotational constants, and dipole moments for trans and gauche isopropylamine. 509

108. Temperature and intensity ratios of the trans and gauche bands of isopropylamine. 521

109. Comparison of rotational constants obtained from ab initio MP2(full)/6-311+G(d,p) predictions, experimental values from microwave spectra, and adjusted r_0 structural parameters for trans isopropylamine. 525

110. Quadratic centrifugal distortion constants (kHz) and quadrupole coupling constants (MHz) for conformers of isopropylamine. 532

111. Observed and calculated frequencies (cm^{-1}) and potential energy distributions (P.E.D.s) for the Gg conformer of 2-cyanoethylamine. 540

112. Observed and calculated frequencies (cm^{-1}) and potential energy distributions (P.E.D.s) for the Gt conformer of 2-cyanoethylamine.....542

113. Calculated energies in (H) and energy differences (cm^{-1}) for the five conformers of 2-cyanoethylamine. 544

114. Structural parameters (Å and °) and rotational constants (MHz) for the Gg and Gt conformers of 2-cyanoethylamine.....546

115. Comparison of experimental rotational constants obtained from microwave spectra and adjusted r_0 structural parameters of 2-cyanoethylamine. 555

116. Quadratic centrifugal distortion constants (kHz) and quadrupole coupling constants (MHz) for Gg and Gt conformers of 2-cyanoethylamine. 559

117. Observed and calculated frequencies (cm^{-1}) for trans ethanol.....566

118. Observed and calculated frequencies (cm^{-1}) for gauche ethanol. 568

119. Calculated energies (hartree) and energy differences (cm^{-1}) for the two conformers and transition states of ethanol. 571

120. Structural parameters, rotational constants, and dipole moments for trans and gauche ethanol.....575

121. Temperature and intensity ratios of the trans and gauche bands of ethanol. 584

122. Comparison of rotational constants obtained from modified ab initio, MP2/6-311+G(d,p) structural parameters and those from microwave spectra for ethanol.....587

123. Quadratic centrifugal distortion constants (MHz) for trans and gauche-ethanol.....593

124. Rotational transitional frequencies (MHz) for Gg form of allyl thiol in the ground state.....599

125. Rotational constants (MHz) and quadratic centrifugal distortion constants (kHz) for Gg conformer of allyl thiol. 600

126. Observed and calculated wavenumbers (cm^{-1}) for Gg form of allyl thiol. 605

127. Observed and calculated wavenumbers (cm^{-1}) for Cg form of allyl thiol. 608

128. Observed and calculated wavenumbers (cm^{-1}) for Gg' form of allyl thiol. 610

129. Observed and calculated wavenumbers (cm^{-1}) for Gt form of allyl thiol. 612

130A. Calculated energies in (Hatrees) and energy differences (cm^{-1}) for the five possible conformers of allyl thiol. 615

130B. Temperature and intensity ratios of the Gg, Cg, Gg′, and Gt bands of allyl thiol. 616

131. Structural parameters (Å and degrees), rotational constants (MHz) and dipole moments (Debye) for Gg and Cg conformers of allyl thiol. 617

132. Structural parameters (Å and degrees) for carbon skeleton gauche and cis forms of allyl alcohol, allyl amine, and allyl fluoride.....635

ILLUSTRATIONS

Figure Page

1. Comparison of experimental and predicted infrared spectra of cyanocyclobutane: (A) gas; (B) Xe solution at -70ºC; (C) simulated spectrum of mixture of equatorial and axial conformers at -70°C with ΔH = 254 cm^{-1}; (D) simulated spectrum of axial conformer; (E) simulated spectrum of equatorial conformer; (F) annealed solid. 23

2. Comparison of experimental and predicted Raman spectra of cyanocyclobutane: (A) liquid; (B) simulated spectrum of the mixture of equatorial and axial conformers at 25ºC with ΔH = 254 cm^{-1}; (C) simulated spectrum of axial conformer; (D) simulated spectrum of equatorial conformer. 24

3. Cyanocyclobutane showing atomic numbering. 29

4. Mid-infrared spectra of cyanocyclobutane (A) gas; (B) Xe solution at -70°C. 33

5. Infrared spectra of cyanocyclobutane, in Xe solution at different temperatures. 38

6. Far-infrared spectrum of gaseous cyanocyclobutane. 42

7. Comparison of experimental and predicted infrared spectra of bromocyclobutane: (A) Xe solution at -70ºC; (B) simulated spectrum of mixture of equatorial and axial conformers at -70°C with ΔH = 291 cm^{-1}; (C) simulated spectrum of axial conformer; (D) simulated spectrum of equatorial conformer. 52

8. Comparison of experimental and predicted Raman spectra of bromocyclobutane: (A) liquid; (B) simulated spectrum of the mixture of equatorial and axial conformers at 25ºC with ΔH = 291 cm^{-1}; (C) simulated spectrum of axial conformer; (D) simulated spectrum of equatorial conformer. 53

9. Bromocyclobutane showing atomic numbering. 64

10. Mid-infrared spectra of bromocyclobutane (A) gas; (B) Xe solution at -70°C; asterisk denotes axial fundamentals. 70

11. Infrared spectra of bromocyclobutane, in Xe solution at different temperatures. 72

12. Potential function governing the ring-puckering vibration of bromocyclobutane. V (cm^{-1}) = (7.02 ± 0.97) x 10^5X^4 + (3.87 ± 0.52) x 10^4X^3 – (3.42 ± 0.28) x 10^4X^2 with a reduced mass of 214 amu. 85

13. Comparison of experimental and predicted mid-infrared spectra of fluorocyclobutane: (A) simulated spectrum of equatorial conformer; (B) observed infrared spectrum of the gas, asterisk denotes an impurity; (C) Xe solution at -70ºC.....94

14. Fluorocyclobutane showing atomic numbering.....97

15. Low frequency spectra of gaseous fluorocyclobutane: (A) background; (B) far infrared; (C) Raman.....108

16. Potential function governing the ring-puckering vibration of fluorocyclobutane. V (cm^{-1}) = (8.46 ± 0.12) x 10^5X^4 – (4.05 ± 0.18) x 10^4X^2 + (6.01 ± 0.11) x 10^4X^3 with a reduced mass of 214 amu. 109

17. Experimental and predicted infrared spectra of cyclobutylsilane: (A) simulated spectrum of mixture of Eq and Ax (ΔH = 67 cm^{-1}) conformers at 25°C; (B) gas; (C) polycrystalline; (D) annealed solid; (E) simulated Ax conformer; (F) simulated Eq conformer. 126

18. Experimental and predicted infrared spectra of cyclobutylsilane: (A) simulated spectrum of mixture of Eq and Ax (ΔH = 67 cm^{-1}) conformers at -70°C; (B) xenon solutions at various temperatures; (C) simulated Ax conformer; (D) simulated Eq conformer.....127

19. Experimental and predicted Raman spectra of cyclobutylsilane: (A) gas; (B) simulated spectrum of mixture of Eq and Ax (ΔH = 67 cm^{-1}) conformers at 25°C; (C) simulated Ax conformer; (D) simulated Eq conformer. 134

20. Experimental and predicted Raman spectra of cyclobutylsilane: (A) simulated spectrum of mixture of Eq and Ax (ΔH = 67 cm^{-1}) conformers at 25°C; (B) liquid; (C) solid; (D) simulated Ax conformer; (E) simulated Eq conformer.....135

21. Experimental and predicted infrared spectra of cyclobutylgermane: (A) xenon solution at -70°C; (B) gas; (C) simulated spectrum of mixture of Eq and Ax (ΔH = 112 cm^{-1}) conformers at 25°C; (D) simulated Eq conformer; (F) simulated Ax conformer.....158

22. Labeled cyclobutylgermane molecule (A) Axial conformer; (B) Equitorial conformer.....164

23. Experimental and predicted Raman spectra of cyclobutylgermane: (A) Gas; (B) liquid; (C) simulated spectrum of mixture of Eq and Ax (ΔH = 112 cm^{-1}) conformers at 25°C; (D) simulated Eq conformer; (F) simulated Ax conformer. 167

24. Temperature (-70 to -100°C) dependent mid-infrared spectrum of cyclobutylgermane dissolved in liquid xenon....173

25. Labeled conformers of cyclobutylcarboxylic acid chloride with atomic numbering. 190

26. Mid-infrared spectra of cyclobutylcarboxylic acid chloride (A) spectrum of gas; (B) spectrum of xenon solution at -80°C with bands used in the enthalpy determination assigned on spectra. 205

27. Experimental and predicted mid-infrared spectra of cyclobutylcarboxylic acid chloride: (A) observed spectra of xenon solutions at -80, -90, and -100°C; (B) simulated spectrum of mixture of g-Eq, g-Ax (ΔH = 91 cm^{-1}), and t-Eq (ΔH = 173 cm^{-1}) conformers at -80°C; (C) simulated g-Eq conformer; (D) simulated g-Ax conformer; (E) simulated t-Eq conformer. 210

28. Temperature (-70 to -100°C) dependent mid-infrared spectrum of cyclobutylcarboxylic acid chloride dissolved in liquid xenon....220

29. Comparison of experimental and calculated infrared spectra of 1-bromo-1-silacyclopentane: (A) observed infrared spectrum of gas; (B) observed infrared spectrum of solid; (C) simulated infrared spectrum of twist (C1) conformer. 244

30. Comparison of experimental and calculated Raman spectra of 1-bromo-1-silacyclopentane: (A) observed Raman spectrum of the liquid; (B) simulated Raman spectrum of twist conformer (C1). 245

31. Planar (Cs) conformer of 1-bromo-1-silacyclopentane showing atom numbering and internal coordinates. 252

32. Comparison of experimental and calculated infrared spectra of 1-bromo-1-silacyclopentane: (A) observed infrared spectrum of solid; (B) simulated infrared spectrum of twist conformer; (C) simulated infrared spectrum of envelope-axial conformer; (D) simulated infrared spectrum of envelope-equatorial conformer. 256

33. Comparison of experimental and calculated infrared spectra (990-1200 cm^{-1}) of 1-bromo-1-silacyclopentane: (A) simulated spectra of twist (C1) conformer at 0.5 cm^{-1} and 4.0 cm^{-1} resolutions; (B) observed infrared

spectrum of the gas showing typical B-, A- and A/C-type band contours at 1157, 1080 and 1033 cm^{-1}, respectively, measured at 0.5 cm^{-1} resolution. 258

34. Raman spectra (0-1550 cm^{-1}) showing the polarized and the depolarized bands for 1-bromo-1-silacyclopentane. 262

35. Comparison of experimental and calculated infrared spectra of ethynylcyclopentane: (A) observed spectrum of gas; (B) simulated spectrum of a mixture of Eq and Ax conformers (ΔH = 94 cm^{-1}) at 25°C; (C) simulated spectrum of Ax conformer; (D) simulated spectrum of Eq conformer; (E) observed spectrum of solid. 273

36. Comparison of experimental and calculated Raman spectra of ethynylcyclopentane: (A) observed spectrum of liquid; (B) observed spectrum of Xe solution at -60°C; (C) simulated spectrum of a mixture of Eq and Ax conformers (ΔH = 94 cm^{-1}) at -60°C; (D) simulated spectrum of Ax conformer; (E) simulated spectrum of Eq conformer. 275

37. Conformers of ethynylcyclopentane (A) Eq; (B) Ax.....284

38. Infrared and Raman spectra of ethynylcyclopentane (A) observed mid-infrared spectrum of gas; (B) Raman spectrum of Xe solution at -60°C.....288

39. Temperature (-50 to -100°C) dependent Raman spectrum of ethynylcyclopentane dissolved in liquid xenon. 291

40. Comparison of experimental and calculated infrared spectra of c-$C_3H_6Si_2H_4$: (A) observed spectrum of gas; (B) simulated spectrum of twist conformer.....314

41. Comparison of experimental and calculated Raman spectra of c-$C_3H_6Si_2H_4$: (A) observed spectrum of liquid; (B) simulated spectrum of twist conformer.....315

42. Model of c-$C_3H_6Si_2H_4$ showing atomic numbering.....324

43. Comparison of experimental (path length = 9.5 cm & gas pressure = 400 mTorr) and calculated infrared spectra of c-$C_3H_6Si_2F_4$: (A) observed spectrum of gas; (B) simulated spectrum of twist conformer.....346

44. Comparison of experimental and calculated Raman spectra of c-$C_3H_6Si_2F_4$: (A) observed spectrum of liquid; (B) simulated spectrum of twist conformer.....347

45. Model of c-$C_3H_6Si_2F_4$ showing atomic numbering. 354

46. Mid-infrared spectra of 2,2-difluoroethylamine (A) gas; (B) Xe solution at -65°C. 371

47. Comparison of experimental and predicted infrared spectra of 2,2-difluoroethylamine: (A) infrared spectra of the solid; (B) simulated spectrum of Tt conformer. 372

48. Comparison of experimental and predicted Raman spectra of 2,2-difluoroethylamine: (A) observed spectrum of the liquid; (B) simulated spectrum of a mixture of Tt, Gg ($\Delta H = 83$ cm^{-1}), Gt ($\Delta H = 235$ cm^{-1}) conformers at 25°C; (C) simulated spectrum of Gt conformer; (D) simulated spectrum of Gg conformer; (E) simulated spectrum of Tt conformer. 374

49. Possible stable conformers of 2,2-difluoroethylamine. 383

50. Comparison of experimental and predicted infrared spectra of 2,2-difluoroethylamine: (A) observed spectrum of Xe solution at -65°C; (B) simulated spectrum of mixture of Tt, Gg ($\Delta H = 83$ cm^{-1}), Gt ($\Delta H = 235$ cm^{-1}) conformers at -65°C; (C) simulated spectrum of Gt conformer; (D) simulated spectrum of Gg conformer; (E) simulated spectrum of Tt conformer. 387

51. Temperature (-60 to -100°C) dependent mid-infrared spectrum in the 725-835 cm^{-1} region of 2,2-difluoroethylamine dissolved in liquid xenon.....392

52. Raman spectra (650-1700 cm^{-1}) showing the polarized and the depolarized bands for 2,2-difluoroethylamine.....399

53. Five conformers of n-propylamine showing atomic numbering.....407

54. Experimental and predicted infrared spectra of n-propylamine: (A) gas; (B) simulated spectrum of mixture of Tt, Tg ($\Delta H = 79$ cm^{-1}), Gg ($\Delta H = 91$ cm^{-1}), Gg′ ($\Delta H = 135$ cm^{-1}), and Gt ($\Delta H = 143$ cm^{-1}) conformers at 25°C.; (C) simulated Tt conformer; (D) simulated Tg conformer; (E) simulated Gg conformer; (F) simulated Gg′ conformer; (G) simulated Gt conformer; (H) solid. 410

55. Raman spectra of the xenon solution (Top) and infrared spectra of the gaseous vapor (Bottom) of n-propylamine (A) 920 - 800 cm^{-1}; (B) 500 – 425 cm^{-1}. 413

56. Experimental and predicted Raman spectra of n-propylamine: (A) xenon solution at -100°C; (B) simulated spectrum of mixture of Tt, Tg ($\Delta H = 79$ cm^{-1}), Gg ($\Delta H = 91$ cm^{-1}), Gg′ ($\Delta H = 135$ cm^{-1}), and Gt ($\Delta H = 143$ cm^{-1}) conformers at -100°C.; (C) simulated Tt conformer; (D) simulated Tg conformer; (E) simulated Gg conformer; (F) simulated Gg′ conformer; (G) simulated Gt conformer. 415

57. Experimental and predicted Raman spectra of 2,2,2 trifluoroethylamine: (A) xenon solution at -100°C; (B) simulated spectrum of Trans and gauche; enthalpy difference of 267 cm^{-1} at -100°C; (C) simulated spectrum of gauche conformer; (D) simulated spectrum of Trans conformer.....435

58. 2,2,2 trifluoroethylamine molecule showing atomic numbering. 442

59. Raman spectra of 2,2,2 trifluoroethylamine in xenon solution at different temperatures. 451

60. Mid-infrared spectra of normal 2,2,3,3,3-pentafluoropropylamine (A) gas; (B) Xe solution at -70°C; (C) simulated spectrum of Tt conformer; (D) infrared spectra of the solid.....468

61. Comparison of experimental and predicted Raman spectra of 2,2,3,3,3-pentafluoropropylamine: (A) gas; (B) simulated spectrum of Tt and Tg; enthalpy difference of 280 cm^{-1} at 25°C; (C) simulated spectrum of Tg conformer; (D) simulated spectrum of A′ modes of Tt conformer. 471

62. Comparison of experimental and predicted Raman spectra of 2,2,3,3,3-pentafluoropropylamine-ND_2: (A) gas; (B) simulated spectrum of Tt and Tg; enthalpy difference of 280 cm^{-1} at 25°C; (C) simulated spectrum of Tg conformer; (D) simulated spectrum of A′ modes of Tt conformer. 472

63. Comparison of experimental and predicted Raman spectra of 2,2,3,3,3-pentafluoropropylamine: (A) liquid; (B) simulated spectrum of Tt and Tg; enthalpy difference of 280 cm^{-1} at 25°C; (C) simulated spectrum of Tg conformer; (D) simulated spectrum of Tt conformer. 473

64. Five conformers of 2,2,3,3,3-pentafluoropropylamine showing atomic numbering. 480

65. Infrared spectra of 2,2,3,3,3-pentafluoropropylamine in xenon solution at different temperatures. 487

66. Experimental and predicted infrared spectra of isopropylamine: (A) gas; (B) simulated spectrum of T and G; enthalpy difference of 113 cm^{-1} at 25°C; (C) simulated spectrum of G conformer; (D) simulated spectrum of T conformer (D) solid. 501

67. Experimental and predicted Raman spectra of isopropylamine: (A) xenon solution at -100°C; (B) simulated spectrum of T and G; enthalpy difference of 113 cm^{-1} at -100°C; (C) simulated spectrum of G conformer; (D) simulated spectrum of T conformer. 502

68. Experimental and predicted Raman spectra of gaseous isopropylamine: (A) Experimental; (B) simulated spectrum of T and G; enthalpy difference of 113 cm^{-1} at 25°C; (C) simulated spectrum of G conformer; (D) simulated spectrum of T conformer. 514

69. Raman spectra of the xenon solution (Top) and infrared spectra of the gaseous (Bottom) of isopropylamine (A) 1510 - 1310 cm^{-1}; (B) 1300 – 1100 cm-^{1}; (C) 900 – 700 cm^{-1}. 515

70. Spectra of isopropylamine (A) mid-infrared gas; (B) Raman Xe solution at -100°C. 517

71. Raman spectra of isopropylamine in xenon solution at different temperatures. 520

72. Five conformers of 2-cyanoethylamine. 535

73. Experimental and predicted infrared spectra of 2-cyanoethylamine: (A) gas; (B) amorphous solid; (C) simulated spectrum of mixture of Gg and Gt (ΔH = 75 cm^{-1}) conformers at 25°C; (D) simulated Gt conformer; (E) simulated Gg conformer. 538

74. Experimental and predicted Raman spectra of 2-cyanoethylamine: (A) liquid; (B) simulated spectrum of mixture of Gg and Gt (ΔH = 75 cm^{-1}) conformers at 25°C; (C) simulated Gt conformer; (D) simulated Gg conformer. 539

75. Potential function of rotation around the C-N bond (H_6-N_1-C_2-C_3 dihedral angle) for the gauche C-C-C-N heavy atom structure calculated using MP2(full) method with 6-311+G(2d,2p) basis set. 553

76. Ethanol showing atomic numbering. 564

77. Mid-infrared spectra of ethanol (A) gas; (B) Xe solution at -60 °C. 565

78. Comparison of experimental and predicted infrared spectra of ethanol: (A) Xe solution at -60 ºC; (B) simulated spectrum of mixture of trans and gauche conformers at -60ºC with ΔH = 62 cm^{-1}; (C) simulated spectrum of gauche conformer; (D) simulated spectrum of trans conformer. 574

79. Comparison of experimental and predicted Raman spectra of ethanol: (A) gas; (B) simulated spectrum of the mixture of trans and gauche conformers at 25ºC with ΔH = 62 cm^{-1}; (C) simulated spectrum of gauche conformer; (D) simulated spectrum of trans conformer A' block. 583

80. van't Hoff plot of –ln(I887/I879) as a function of 1/T. 584

81. Predicted (dotted curve, from MP2(full)/6-311+G(2d,2p)) and experimental (solid curve) potential function governing the hydroxyl torsion of ethanol. 590

82. Possible stable conformers of allyl thiol. 595

83. Comparison of experimental and calculated infrared spectra of allyl thiol: (A) observed spectrum of gas; (B) observed spectrum of xenon solution at -70°C, asterisk denotes location of impurity bands that develop soon after purification; (C) simulated spectrum of mixture of Gg, Cg ($\Delta H = 120$ cm^{-1}), Gg′ ($\Delta H = 337$ cm^{-1}), and Gt ($\Delta H = 360$ cm^{-1}) conformers at 25°C. 602

84. Comparison of experimental and calculated infrared spectra of solid allyl thiol: (A) simulated Gt conformer; (B) simulated Gg′ conformer; (C) simulated Cg conformer; (D) simulated Gg conformer; (E) observed spectrum. 603

85. Comparison of experimental and calculated Raman spectra of liquid allyl thiol: (A) observed spectrum; (B) simulated spectrum of mixture of Gg, Cg ($\Delta H = 120$ cm^{-1}), Gg′ ($\Delta H = 337$ cm^{-1}), and Gt ($\Delta H = 360$ cm^{-1}) conformers at 25°C; (C) simulated Gt conformer; (D) simulated Gg′ conformer; (E) simulated Cg conformer; (F) simulated Gg conformer. 607

86. Mid-infrared spectra of allyl thiol (A) gas; (B) Xe solution at -70°C, asterisk denotes location of impurity bands that develop soon after purification. 623

87. Fit of infrared spectra of xenon solution of allyl thiol. 625

88. Temperature (-60 to -100°C) dependent infrared spectrum of allyl thiol dissolved in liquid xenon. 626

89. Raman spectra (100-1700 cm^{-1}) showing the polarized and the depolarized bands for allyl thiol. 631

S1. Labeled cyclobutylsilane molecule. 654

S2. van't Hoff plot of ln(Iconf1/Iconf2) as a function of 1/T. 656

S3. Comparison of experimental and predicted infrared spectra of 2,2,3,3,3-pentafluoropropylamine-ND_2: (A) gas; (B) simulated spectrum of Tt and Tg; enthalpy difference of 280 cm^{-1} at 25°C; (C) simulated spectrum of Tg conformer; (D) simulated spectrum of Tt conformer. 657

S4. Comparison of experimental and predicted Raman spectra of 2,2,3,3,3-pentafluoropropylamine-ND_2: (A) liquid; (B) simulated spectrum of Tt and

Tg; enthalpy difference of 280 cm^{-1} at 25°C; (C) simulated spectrum of Tg conformer; (D) simulated spectrum of Tt conformer. 658

S5. Trans and gauche conformers of isopropylamine showing atomic numbering. 659

ACKNOWLEDGMENTS

I would like to thank my advising Professor James R Durig and my advising committee for all their help.

I would like to thank my fellow graduate students whom I have worked with on many occasions and spent many nights finishing publications with. Specifically Arindam Ganguly, Ikhlas Darkhalil, Savitha Panikar, Shaun Purohit, Bhushan Deodohar, and Dattatray Sawant.

I would also like to thank the Professors I have worked on my research with and under both from UMKC and other Universities. Specifically Prof. Todor, Prof. Groner, Prof. Wurrey, Prof. Tubergen, and Prof. Pate. Additionally I would like to thank the faculty of the Chemistry and Geosciences departments of UMKC for their teaching and help.

Finally, I would like to acknowledge the University of Missouri–Kansas City, for a Faculty Research Grant for partial financial support of this research. Additionally I would like to thank the department of Chemistry and PACE for their financial support in the form of GTA, GRA, and grader grants.

CHAPTER 1

INTRODUCTION

The study of natural phenomenon or natural philosophy was first concerned with the determination of identity. Another way of saying this is that science was originally interested in figuring out what things are. This began with the identification of the elements and phases of matter. Out of these experiments the science of chemistry was developed. As the understanding of the elements was increased molecules were identified and with this molecular bonds between the atoms. This new understanding of molecules and molecular bonding created the field of synthetic and analytical chemistry. Synthetic chemistry is the rearrangement of atoms from one molecule to another molecule. These molecules will have different chemical formula which can be determined using methods from analytical chemistry which is primarily concerned with identification of a sample.

The chemical formula determines many of the bulk properties of a molecule, however this does not give a complete understanding of these molecules and gives an even worse understanding of real world systems where these systems are usually composed of interacting molecules often of different chemical formulas. The understanding of any system was of course incomplete with only understanding a chemical formula. The intermolecular forces involved in the system exhibit strong influences on the bulk properties of a sample, hydrogen bonding being an iconic example. This same hydrogen bonding however also can occur within a molecule in which case it is an intramolecular hydrogen bonding. It therefore follows that even the molecular geometry of a molecule cannot be determined from the chemical formula

alone. There must be an understanding of the interaction of the molecule with the immediate environment of the molecule and the intramolecular forces acting upon the molecule. To understand these forces a quantitative method is needed for studying these systems.

Most molecules with more than four atoms have two or more conformational states that they can assume. The symmetry of the molecule can often cause some of these states to be degenerate in their zero-point energy. Where the conformational states are not degenerate they will have a potential function associated with them and an energy difference between the conformers. This will cause an order of stability which is influenced by the temperature of the system. The effects of this conformational interchange can be drastic as the second order structure of proteins and DNA are based on the conformation stabilities of the molecule and the temperature of the system. It is in changing the conformational stabilities of a protein or DNA that their secondary structure changes. Conformational geometry is also important for crystal structures which can change the bulk properties of the sample. Such properties as melting point, conductance, and hardness depend on the crystal structure which often depends on the conformational geometry.

The molecular structure is the orientation of the atoms of a molecule within three dimensional space. Conformational identity is part of molecular structure but molecular structure also includes the distance between atoms (this distance along a bond is a bond distance), the angles between three atoms (between two consecutive bonds is a bond angle), and the angles between a plane composed of three atoms and another atom (if these four atoms are bonded in three consecutive bonds they are a torsional angle). These

quantitative molecular structure elements such as the length of a bond distance can lead to important information such as the forces acting upon the bond. This can lead to important information about the molecule such as if the bond has been weakened due to a catalyst or the extent of intramolecular forces.

This analysis of structure can be further expanded to the geometry of a complex. The geometry of these complexes often determines how they interact with the world. This is well known in biochemistry where the difference in the binding geometry determines whether an enzyme will catalyze a reaction or not. The study of binding geometry has become a major focus of biochemical studies and material science studies as much of the bulk material properties and catalytic properties of these samples is determined from the geometry of the entire complex and the forces involved in the binding sites.

The study of the identity of a sample has led to the development of the field of spectroscopy which is defined [1] as the study of physical systems by the electromagnetic radiation with which they interact or that they produce. Spectrometry is the measurement of such radiations as a means of obtaining information about the systems and their components. In certain types of optical spectroscopy, the radiation originates from an external source and is modified by the system, whereas in other types, the radiation originates within the system itself. There are many types of spectroscopy which have been developed however the types of spectroscopy which we have found to be best suited to the study of molecular structure, conformational stability, and binding geometry are the spectroscopies dealing with the infrared, terahertz, and microwave spectral regions. The information which is determined in these spectroscopies is the vibrational and rotational energy levels.

The vibrational energy levels of molecules have been discussed in a number of books and reference manuals [2-4]. A complete discussion of this topic is beyond the limits of this dissertation and is the topic of many textbooks. The relevant part of this large wealth of knowledge about vibrational energy levels is that the forces and geometry of the molecule affect the spacing between these energy levels. The change in this energy level spacing is reflected in the spectra by a shift in band frequency. Therefore the vibrational energy levels can be used to determine bond length [5,6], binding [7-9], and chemical formula [10]. The intensity of a band is an expression of the dipole moment derivative (a temporary change in the dipole moment brought on by the change in molecular structure from the molecular vibration) and the population in the associated energy well. This allows you to determine the change in population if you can monitor the change in band intensity with temperature.

Rotational energy levels similar to vibrational energy levels are the topic of a number of reference manuals and textbooks [11,12]. The current theory of rotational energy levels involves the use of a rigid rotor model modified by distortion constants to help account for the non-rigid nature of molecules. The spacing of the rotational energy levels are based primarily on the moments of inertia and to a much lesser degree the quadruple coupling constants (in the case of fermions) and the distortion constants. The spacing of these energy levels and the transitions of populations between these energy levels is the rotational spectra. The moments of inertia are related to the distribution of mass across the molecular structure and so there is a large amount of information on the molecular structure [13,14] of the molecule in the rotational energy levels. There is also information on the structure of complexes [15] as they can act similar to a single

molecule and have their own moments of inertia. The intensity of transitions is based on the dipole moment (where a dipole moment of zero will have an intensity of zero) and the population involved in the transition. This does allow for monitoring the change in population to determine the change in populations similar to vibrational spectroscopy.

Spectroscopy in the infrared (12,820 to 500 cm^{-1}) and terahertz (500 to 3 cm^{-1}) regions of the electromagnetic spectrum includes absorption [1] and scattering [1]. Absorption spectroscopy in the infrared region is referred to as infrared spectroscopy whereas in the terahertz region can be referred to as far-infrared or terahertz spectroscopy. The most common form of scattering spectroscopy in the infrared and terahertz regions is Raman spectroscopy. These methods are commonly used to study vibrational energy levels however information on the rotational energy levels can be studied as well. This is normally referred to as vibrational spectroscopy as this region reveals a large amount of information about the vibrational energy levels of a sample. The state of matter that can be studied is very broad which allows samples in the amorphous solid, crystalline solid, matrices, liquid, solutions, and vapor states to be studied with the different forms of vibrational spectroscopy.

One of the forms of vibrational spectroscopy used in the research presented in this dissertation is the infrared or Raman spectra of the variable temperature rare gas solutions. There has been a significant amount of study on the use of vibrational spectroscopy of xenon solutions [16-20]. However its use for conformational determination is something that is relatively unique to only a few labs and use of the Raman spectra for these conformational studies is a recent development first used in some of the research presented in this dissertation. There are many advantages as well as

disadvantages for the utilization of liquid rare gases as solvents for enthalpy determinations. The ten advantages are: (1) The bands are very narrow. (2) Very accurate measurement of the temperature is possible. (3) The temperature range is fairly large. (4) There is normally little interaction of solvent with solute molecules. (5) Small enthalpy changes can be measured. (6) Band areas are easily measured. (7) Paths lengths for the liquids are long so very dilute solutions can be used. (8) The xenon solvent has no absorption bands. (9) Several conformer pairs can usually be measured. (10) The statistical uncertainty of the determined values is very low. The most common disadvantages are: (1) Limited solubility of many polar molecules. (2) It is difficult to have very dry xenon so water can interfere. (3) At low temperatures the sample may deposit on the window.

Spectroscopy in the microwave spectral region (1.6 to 30 GHz) is usually referred to as rotational spectroscopy as the information obtained is largely that of the rotational energy levels. Microwave spectroscopy is usually limited to the low pressure vapor state and low temperatures due to the complexity of the rotational spectra and large number of energy levels the sample population can be distributed among at high temperatures and high pressure vapor, liquid, or solid states. The current methodology of microwave spectroscopy utilizes jet propulsion nozzle(s) which has greatly improved its precision but has greatly reduced the control of the temperature of the sample (approx. ~4 kelvin in these systems) and limits microwave spectroscopy to diffuse vapor states.

The research in this dissertation is a series of theoretical and experimental studies of the vibrational fundamentals, rotational constants, distortion constants, quadrupole coupling constants, charge distribution, potential functions, intramolecular binding,

molecular structure, and enthalpy determinations. The techniques it involves are Møller-Plesset perturbation method [21] to the second order MP2 with full electron correlation and density functional theory by the B3LYP method calculations using the Gaussian computational program [22], Raman spectroscopy of the vapor, liquid, and rare gas solutions, infrared spectroscopy of the vapor, solid, and rare gas solutions, microwave spectroscopy of the vapor, and far-infrared spectroscopy of the vapor and solid. The results of these studies are reported herein.

CHAPTER 2

EXPERIMENTAL AND THEORETICAL METHODS

The mid-infrared spectra of the gas and solid are obtained from 4000 to 220 cm^{-1} on a Perkin-Elmer model 2000 Fourier transform spectrometer equipped with a Ge/CsI beamsplitter and a DTGS detector. Atmospheric water vapor was removed from the spectrometer housing by purging with dry nitrogen. The gas and solid spectra are obtained with a theoretical resolution of 0.5 cm^{-1} for the gas and 2 cm^{-1} for the solid with 128 interferograms added and truncated. Multiple annealings are required to obtain satisfactory spectra of the solid.

The mid-infrared spectra (4000 to 400 cm^{-1}) of the sample dissolved in liquefied xenon are recorded on a Bruker model IFS-66 Fourier transform spectrometer equipped with a globar source, a Ge/KBr beamsplitter and a DTGS detector. In all cases, 100 interferograms are collected at 1.0 cm^{-1} resolution, averaged, and transformed with a boxcar truncation function. For these studies, a specially designed cryostat cell is used. It consists of a copper cell with a path length of 4 cm with wedged silicon windows sealed to the cell with indium gaskets. The copper cell is enclosed in an evacuated chamber fitted with KBr windows. The temperature is maintained with boiling liquid nitrogen and monitored by two Pt thermo resistors.

The far infrared spectra (600 to 10 cm^{-1}) of the sample dissolved in liquid xenon is recorded on a Bruker model IFS 66 v/S Fourier transform spectrophotometer equipped with a Globar source, a 6.0 μm Mylar beamsplitter, and a liquid helium cooled Si

bolometer. The sample is contained in a 7 cm cell fitted with Si windows and the sample added as described for the mid-infrared studies. For all spectra 250 interferograms are collected at 0.5 cm^{-1} resolution, averaged, and transformed with a Blackman-Harris three term function.

The Raman spectra of the liquid are recorded from 4000 to 40 cm^{-1} on a Spex model 1403 spectrophotometer equipped with a Spectra-Physics model 2017 argon ion laser operating on the 514.5 nm line. The laser power used is 1.5 W with a spectral bandpass of 3 cm^{-1}. The spectra of the liquid are recorded with the sample sealed in a Pyrex glass capillary. The measurements of the Raman frequencies are expected to be accurate to $\pm$ 2 cm^{-1}.

Alternatively, Raman spectra of the liquid are collected in back-scattering geometry using the 514.532 nm line of an Argon ion laser as the excitation source, with ~ 22 mW incident on the diamond cell. A Semrock 514 nm edge filter is used to separate the laser line from the Raman scattered light. The scattered light is dispersed in a Spectra-pro 500i spectrograph and detected with a Spec-10 liquid nitrogen cooled CCD detector. Raman spectra are collected using a 2400 g/mm grating with a slit width of 100 μm, which gives spectral resolution of ~0.2 cm^{-1}.

The Raman spectra (4000 to 300 cm^{-1}) of the sample dissolved in liquefied xenon at five different temperatures (-60 to -100^{o}C) is recorded on a Trivista 557 spectrometer consisting of a double f = 50 cm monochromator equipped with a 2000 lines mm^{-1} grating, a f = 70 cm spectrograph equipped with a 2400 lines mm^{-1} grating, and a back-illuminated LN2-cooled PI Acton Spec-10:2 kB/LN 2048 x 512 pixel CCD detector. For all experiments, the 514.5 nm line of a 2017-Ar S/N 1665 Spectra-Physics argon ion laser

is used for Raman excitation, with the power set to 0.8 Watt. Signals related to the plasma lines are removed by using an interference filter. The frequencies are calibrated using Neon emission lines, and depending on the setup used, are expected to be accurate within 0.4 cm^{-1}. The experimental set-up used to investigate the solutions has been described before [23,24]. A home-built cell for liquids, equipped with four quartz windows at right angles, is used to record the spectra.

Microwave spectra are recorded by using a "mini-cavity" Fourier-transform microwave spectrometer [25,26] at Kent State University. The Fabry-Perot resonant cavity is established by two 7.5-inch diameter diamond-tip finished aluminum mirrors with a 30.5-cm spherical radius. The Fabry-Perot cavity resides inside a vacuum chamber formed by a 6-way cross and a 15-inch long, 8-inch diameter extension tube. The two cavity mirrors are nominally separated by 30 cm.

The sample is entrained in a 70:30 Ne-He carrier gas mixture at 2 atm and expanded into the cavity to attain 4K using a reservoir nozzle [26] made from a modified Series-9 General Valve. The reservoir nozzle is mounted in a recessed region of the mirror flange, external to the vacuum chamber, and the expansion passes through a 0.182-inch diameter hole into the resonant cavity. The center of the expansion is offset from the center of the mirror by 1 inch.

The sample is irradiated by microwave radiation generated by an Agilent Technologies E8247C PSG CW synthesizer; details of the irradiation and heterodyne detection circuitry can be found in Ref. [27] The vacuum system can accommodate pulse repetition rates of up to 15 s^{-1} while maintaining a pressure below 10^{-4} torr, and the instrument can scan 450 MHz in 6 hours while averaging 100 shots per scan segment.

Alternatively, the rotational spectra of the sample are studied by using a CP-FTMW spectrometer developed at the University of Virginia, operating in the 6.5 to 18 GHz range. The chirped pulse methods used in this study have been described in detail previously [28], so only the brief details relevant to this experiment are necessary.

The microwave source was a 24 GS/s arbitrary waveform generator, producing a 12-0.5 GHz linear frequency sweep in 1 μs. The pulse was upconverted to 6.5-18 GHz by a 18.95 GHz phase-locked resonant dielectric oscillator (PDRO), and then amplified by a pulsed 300 W traveling wave tube amplifier. The amplified pulse is then transmitted through free space between two standard-gain microwave horns, where it interacts with a molecular beam generated by five pulsed nozzles (General Valve Series 9) operating perpendicular to the propagation direction of the microwave pulse. On the detection end, the receiver is protected from the high power pulse by a combination of a PIN diode limiter and single-pole microwave switch. The resulting molecular free induction decay (FID) was then amplified and digitized directly on a 100 GS/s oscilloscope with 33 GHz of hardware bandwidth, with a 20 μs detection time per FID. Due to the speed of this excitation and detection process, a sequence of 10 excitation/detection cycles is possible per gas pulse, and all ten detected FIDs are collected and averaged together before the next valve injection cycle begins. Phase stability of this experiment over the course of many valve injection cycles is enabled by locking all the frequency sources and the oscilloscope to a 10 MHz Rb-disciplined quartz oscillator. For this experiment, approximately 78 000 valve injection cycles of the sample gas were completed at 3.3 Hz to create a time-averaged spectrum of 780 000 molecular FIDs (approximately 6.5 hours

of averaging). Additionally, the time domain resolution afforded by a 20 μs FID generates an average Doppler broadened linewidth of approximately 130 kHz at FWHM.

The entrained sample for spectral investigation was prepared by balancing the target molecule sample vapor with approximately 3.4 atm of Ne gas (GTS Welco) for a total sample concentration of approximately 0.1%. This afforded a frequency-domain dynamic range of approximately 4000:1 at 780 000 averages.

Ab initio and density functional theory (DFT) calculations are performed with the Gaussian 03 program [22] by using Gaussian-type basis functions. The energy minima with respect to nuclear coordinates are obtained by the simultaneous relaxation of all geometric parameters by the gradient method of Pulay [29]. A variety of basis sets, as well as, the corresponding ones with diffuse functions are employed with the Møller-Plesset perturbation method [21] to the second order MP2 with full electron correlation as well as with density functional theory by the B3LYP method.

In order to obtain descriptions of the molecular motions involved of the fundamental modes, a normal coordinate analysis is carried out. The force field in Cartesian coordinates is obtained with the Gaussian 03 program at the MP2(full) level with the 6-31G(d) basis set. The internal coordinates used to calculate the G and B matrices are given with the atomic numbering shown. By using the B matrix [30], the force field in Cartesian coordinates is converted to a force field in internal coordinates. Subsequently, one or two scaling factors are used to obtain the fixed scaled force constants and the resulting wavenumbers. A set of symmetry coordinates are used to determine the corresponding potential energy distributions (P.E.Ds) to described the fundamental vibrational modes.

The predicted scaled frequencies are used together with a Lorentzian function to obtain the simulated spectra. Infrared intensities are obtained based on the dipole moment derivatives with respect to Cartesian coordinates. The derivatives are transformed with respect to normal coordinates by $(\partial\mu_u/\partial Q_i) = \sum_j (\partial\mu_u/\partial X_j)L_{ij}$, where Q_i is the i^{th} normal coordinate, X_j is the j^{th} Cartesian displacement coordinate, and L_{ij} is the transformation matrix between the Cartesian displacement coordinates and the normal coordinates. The infrared intensities are then calculated by $(N\pi)/(3c^2)$ $[(\partial\mu_x/\partial Q_i)^2 + (\partial\mu_y/\partial Q_i)^2 + (\partial\mu_z/\partial Q_i)^2]$. A comparison may then be made of the experimental infrared spectra of the gas and simulated infrared spectra where the predictions of the isolated molecule are normally close to the values in the gas phase.

Additional support for the vibrational assignments is obtained from the simulated Raman spectra. The evaluation of Raman activity by using the analytical gradient methods has been developed [31-34] and the activity S_j can be expressed as: $S_j = g_j(45\alpha_j^2 + 7\beta_j^2)$, where g_j is the degeneracy of the vibrational mode j, α_j is the derivative of the isotropic polarizability, and β_j is the anisotropic polarizability. To obtain the Raman scattering cross sections, the polarizabilities are incorporated into S_j by multiplying S_j with $(1-\rho_j)/(1+\rho_j)$ where ρ_j is the depolarization ratio of the j^{th} normal mode. The Raman scattering cross sections and calculated wavenumbers obtained from the Gaussian 03 program are used together with a Lorentzian function to obtain the simulated Raman spectra. The average difference in band center due to going from gas to liquid is usually less than 3 cm^{-1}, and thus, there is usually little interaction between molecules in the liquid phase for the majority of the molecules studied. A comparison may therefore be made of the experimental Raman spectra of the liquid and predicted Raman spectra.

CHAPTER 3

THE r_0 STRUCTURAL PARAMETERS, CONFORMATIONAL STABILITY, AND VIBRATIONAL ASSIGNMENT OF EQUATORIAL AND AXIAL CYANOCYCLOBUTANE

INTRODUCTION

There has been interest in the conformational equilibrium of monosubstituted cyclobutanes for many years but from the initial microwave studies of flouro-[35], chloro-[35], bromo-[36], and cyanocyclobutane[37] only the single equatorial conformer was found. However, there was evidence from vibrational spectra that a second conformer was present at ambient temperature for some of the monosubstituted cyclobutanes[38-43]. Subsequent microwave studies of chloro-[44], fluoro-[45], and cyanocyclobutane[46] have resulted in the identification of the axial form for all three of these molecules. Additionally from the later study [44] of chlorocyclobutane significantly different values were obtained of the rotational constants for several of the isotopes originally reported[35] from which the structural parameters were obtained. In an attempt[47] to utilize the initially reported rotational constants for chlorocyclobutane to obtain the structural parameters it was not possible to obtain agreement with several of the values of the A rotational constants. However, with the newer A values it was possible to obtain the structural parameters from *ab initio* calculations with the microwave data for the complete structural determination of chlorocyclobutane[48] which was consistent with the corresponding parameters of chlorocyclobutane[44]. As a continuation of the determination of the structural parameters of monosubstituted

cyclobutanes we turned our attention to cyanocyclobutane. From the initial microwave investigations[49,37] of cyanocyclobutane, which appeared almost at the same time, only the spectrum of the equatorial conformation was assigned. These results were consistent with the previously reported[39] potential function for the ring-puckering mode of cyanocyclobutane which had a single well. However from further microwave studies[46] the spectrum of the axial conformer was identified and assigned from which the rotational constants were obtained. Additionally a new potential function governing the ring-puckering mode was proposed[46] with three bound states of the axial conformer with an enthalpy difference of 258 $\pm$ 50 cm^{-1}. Later an infrared and Raman study of cyanocyclobutane was reported[50] and the enthalpy difference of 402 $\pm$ 33 cm^{-1} for the liquid was obtained from the temperature variation of the Raman spectrum. Also the barrier to ring conversion was proposed[50] to be less than 418 cm^{-1} and assignments were made for twelve of the twenty A' normal modes of the equatorial conformer along with ten of the thirteen A" fundamentals. Thus, in addition to the structure parameters we were also interested in obtaining a complete vibrational assignment for the equatorial conformer as well as several of the axial fundamentals which would be supported by *ab initio* calculations for predictions of the barrier to ring inversion and fundamental frequencies for both conformers with infrared intensities and Raman activities. The results of these experimental and theoretical investigations of cyanocyclobutane are reported herein.

EXPERIMENTAL

The sample of cyanocyclobutane was purchased from Aldrich Chemical Co., with stated purity of 97%. The sample was further purified by low-temperature, low-pressure

fractionation column and the purity of the sample was verified by comparing the infrared spectrum with that previously reported[50].

The mid-infrared spectra of the gas and solid were obtained from 4000 to 220 cm^{-1} on a Perkin-Elmer model 2000 Fourier transform spectrometer equipped with a Ge/CsI beamsplitter and a DTGS detector. Atmospheric water vapor was removed from the spectrometer housing by purging with dry nitrogen. The theoretical resolution used to obtain the spectrum of the gas was 0.5 cm^{-1} and 2.0 cm^{-1} for the spectra of the solid. One hundred twenty eight interferograms were added and transformed with a boxcar truncation function. The frequencies for the predicted and observed fundamentals are listed in Tables 1 and 2.

TABLE 1. Observed[a] and calculated[b] frequencies for the *equatorial* conformer of cyanocyclobutane.

		Fundamental	ab initio	Fixed scaled[c]	IR int.	Raman act.	dp ratio	B3LYP	IR int.	Raman act.	dp ratio	IR gas	IR gas[d]	IR Xe	Raman liquid	Raman liquid[d]	IR solid	IR solid[d]	P.E.D.[e]	Band Contour		
																				A	B	C
A'	ν_1	β-CH_2 antisymmetric stretch	3213	3048	30.5	45.0	0.70	3144	49.7	44.0	0.65	3004	3004	3000	3003	2996	3001	2996	$65S_1,33S_2$	2	-	98
	ν_2	γ-CH_2 antisymmetric stretch	3195	3031	7.1	74.6	0.47	3120	12.5	102.3	0.33	2989	2989	2990	2994	2984	2994	2988	$63S_2,31S_1$	90	-	10
	ν_3	β-CH_2 symmetric stretch	3141	2980	3.5	59.5	0.25	3086	1.9	206.8	0.10	2974	2961	2971	2968	2950	2976	2956	$62S_3,37S_5$	12	-	88
	ν_4	γ-CH_2 symmetric stretch	3136	2975	15.0	215.8	0.10	3076	5.1	177.9	0.17	2962	2942	2965	2965	2934	2961	2942	$57S_4,26S_5,11S_3$	98	-	2
	ν_5	CH symmetric stretch	3134	2973	8.0	55.3	0.44	3073	32.6	71.7	0.32	2889	2889	2880	2874	2872	2865	2871	$35S_5,39S_4,26S_3$	68	-	32
	ν_6	CN stretch	2210	2097	0.04	61.9	0.29	2341	22.1	146.1	0.22	2249	2240	2242	2237	2239	2237	2227	$87S_6,13S_{16}$	15	-	85
	ν_7	β-CH_2 scissors	1575	1494	0.9	6.0	0.72	1535	1.0	3.3	0.74	1476	1478	1475	1472	1478	1471	1470	$63S_7,34S_8$	2	-	98
	ν_8	γ-CH_2 scissors	1550	1470	5.1	19.2	0.74	1510	3.7	16.2	0.74	1454	1453	1447	1448	1462	1442	1453	$65S_8,35S_7$	30	-	70
	ν_9	β-CH_2 wag	1405	1333	2.3	13.3	0.49	1371	2.2	13.4	0.46	1330	1327	1326	1328	1327	1329	1328	$68S_9,10S_{10}$	96	-	4
	ν_{10}	CH in-plane-bend	1318	1250	1.4	0.4	0.46	1292	0.7	0.5	0.63	1258	1250	1252	1254	1250	1252	1246	$76S_{10},10S_9$	35	-	65
	ν_{11}	β-CH_2 twist	1276	1211	0.1	10.1	0.70	1245	0.1	4.2	0.62	1216	~1219	1217	1214	1213	1211	1215	$75S_{11},12S_{12}$	69	-	31
	ν_{12}	β-CH_2 rock	1169	1109	2.2	2.7	0.05	1137	1.9	3.1	0.04	1101	1109	1108	1108	1108	1106	1097	$44S_{12},14S_{15},12S_{20}$	99	-	1
	ν_{13}	Ring breathing	1116	1059	0.1	11.8	0.13	1073	0.01	21.7	0.13	1064	-	1062	1048	1049	1053	1053	$32S_{13},28S_{16},16S_{14},14S_9$	84	-	16
	ν_{14}	γ-CH_2 rock	996	945	0.7	7.9	0.09	959	0.7	9.8	0.07	939	~940	941	940	937	944	942	$62S_{14},14S_{16},10S_{10}$	36	-	64
	ν_{15}	Ring deformation	940	892	2.1	2.6	0.27	899	1.7	2.2	0.10	883	~888	888	887	885	887	880	$19S_{15},35S_{17},17S_{12},16S_{13}$	99	-	1
	ν_{16}	C-CN stretch	780	740	1.3	2.8	0.20	758	1.8	2.3	0.15	744	743	744	749	749	747	748	$10S_{16},40S_{12},21S_{13},14S_{11}$	19	-	81
	ν_{17}	Ring deformation	597	566	0.8	2.1	0.59	594	0.8	1.4	0.57	582	~580	585	590	587	581	588	$53S_{17},20S_{15}$	14	-	86
	ν_{18}	Ring-CN in-plane-bend	527	500	0.7	2.4	0.22	526	0.9	3.9	0.13	492	~518	515	520	521	523	522	$33S_{18},31S_{19},16S_{16}$	100	-	-
	ν_{19}	CN in-plane-bend	286	271	1.1	1.4	0.74	262	1.7	2.1	0.75	-	-	-	262	265	266	257	$37S_{19},46S_{20}$	31	-	69
	ν_{20}	Ring puckering	146	139	3.4	1.3	0.62	124	3.1	1.0	0.55	-	-	-	142	~150	-	149	$37S_{20},39S_{18},22S_{19}$	12	-	88
A"	ν_{21}	β-CH_2 antisymmetric stretch	3205	3041	14.1	68.5	0.75	3136	14.2	93.2	0.75	2984	2975	2985	2985	2960	2986	2981	$99S_{21}$	-	100	-
	ν_{22}	β-CH_2 symmetric stretch	3137	2976	30.9	0.6	0.75	3082	54.8	1.5	0.75	2976	2871	2876	2874	-	2865	2975	$99S_{22}$	-	100	-
	ν_{23}	β-CH_2 scissors	1542	1463	1.9	5.9	0.75	1503	2.3	2.8	0.75	1448	1435	1444	1461	1446	1461	1440	$100S_{23}$	-	100	-
	ν_{24}	γ-CH_2 wag	1322	1254	2.7	5.5	0.75	1291	2.2	2.5	0.75	1253	1270	1248	1248	1279	1247	1249	$64S_{24},11S_{26},10S_{27}$	-	100	-

ν_{25}	CH out-of-plane bend	1293	1227	0.4	0.5	0.75	1269	0.1	0.6	0.75	1222	-	1220	1222	1232	1219	1234	$62S_{25},19S_{27},10S_{29}$	-	100	-
ν_{26}	β-CH_2 wag	1285	1219	0.1	5.7	0.75	1252	0.3	3.6	0.75	1214	-	1213	1212	-	1208	1219	$57S_{26},16S_{24},14S_{29}$	-	100	-
ν_{27}	γ-CH_2 twist	1240	1176	0.5	9.4	0.75	1216	0.5	5.0	0.75	1182	-	1178	1177	1185	1184	1192	$35S_{27},31S_{25},14S_{29},12S_{30}$	-	100	-
ν_{28}	β-CH_2 twist	1069	1014	0.002	1.5	0.75	1037	0.02	1.7	0.75	-	-	1027	1030	1016	1035	1017	$49S_{28},32S_{29}$	-	100	-
ν_{29}	Ring deformation	985	934	0.3	8.1	0.75	953	0.4	8.4	0.75	937	~940	935	935	937	938	947	$27S_{29},35S_{28},16S_{26},10S_{27}$	-	100	-
ν_{30}	Ring deformation	975	925	2.3	6.4	0.75	942	2.1	7.7	0.75	922	922	919	925	923	923	924	$70S_{30},10S_{24}$	-	100	-
ν_{31}	β-CH_2 rock	822	780	1.5	0.7	0.75	800	0.9	0.6	0.75	780	782	782	784	787	784	785	$76S_{31},12S_{27}$	-	100	-
ν_{32}	CN out-of-plane bend	527	500	0.008	0.3	0.75	537	0.003	0.3	0.75	-	~580	506	506	~530	512	534	$48S_{32}$, $37S_{33},11S_{28}$	-	100	-
ν_{33}	Ring-CN out-of-plane bend	177	168	4.5	2.8	0.75	180	5.0	3.5	0.75	-	-	-	192	191	-	190	$49S_{33}$, $49S_{32}$	-	100	-

[a] Observed spectra: gas, Xe, and solid are IR while liquid is Raman

[b] MP2(full)/6-31G(d) *ab initio* calculations, B3LYP/6-31G(d) *density functional theory* calculations, scaled frequencies, infrared intensities (km/mol), Raman activities ($Å^4$/u), depolarization ratios (dp) and potential energy distributions (P.E.D.s).

[c] Scaled frequencies with scaling factors of 0.90 for all modes.

[d] Frequencies listed are taken from reference [50].

[e] Symmetry coordinates with P.E.D. contribution less than 10% are omitted.

TABLE 2. Observed[a] and calculated[b] frequencies for the *axial* conformer of cyanocyclobutane.

		Fundamental	ab initio	Fixed scaled[c]	IR int.	Raman act.	Dp ratio	B3LYP	IR int.	Raman act.	Dp ratio	IR gas	IR Xe	Raman liquid	Raman liquid[d]	IR High pressure crystal[d]	P.E.D.[e]	Band Contour		
																		A	B	C
A'	ν_1	β-CH_2 antisymmetric stretch	3212	3047	30.6	51.8	0.74	3145	45.3	54.2	0.74						$59S_1,41S_2$	98	-	2
	ν_2	γ-CH_2 antisymmetric stretch	3195	3031	6.3	74.7	0.61	3119	11.2	88.4	0.48						$58S_2,39S_1$	2	-	98
	ν_3	CH symmetric stretch	3151	2989	9.2	137.9	0.11	3092	11.8	287.4	0.06						$90S_3,10S_5$	-	-	100
	ν_4	γ-CH_2 symmetric stretch	3138	2977	19.3	97.9	0.09	3080	8.2	94.7	0.27						$95S_4$	11	-	89
	ν_5	β-CH_2 symmetric stretch	3135	2974	6.5	110.9	0.31	3076	35.0	83.8	0.29						$86S_5$	20	-	80
	ν_6	CN stretch	2211	2098	0.4	50.4	0.29	2340	24.5	127.6	0.22						$87S_6,13S_{16}$	41	-	59
	ν_7	γ-CH_2 scissors	1573	1492	0.5	7.5	0.71	1532	0.4	5.1	0.75						$49S_7,49S_8$	11	-	89
	ν_8	β-CH_2 scissors	1550	1470	4.5	16.8	0.75	1509	2.6	14.8	0.74			1485			$50S_8,50S_7$	49	-	51
	ν_9	β-CH_2 wag	1393	1322	1.1	7.6	0.60	1360	2.1	8.7	0.50						$62S_9,17S_{11}$	92	-	8
	ν_{10}	CH in-plane-bend	1329	1261	2.9	1.0	0.33	1299	1.8	3.6	0.31						$83S_{10}$	1	-	99
	ν_{11}	β-CH_2 twist	1271	1206	0.2	10.5	0.72	1242	0.1	5.6	0.59						$58S_{11},16S_{17},12S_9$	99	-	1
	ν_{12}	β-CH_2 rock	1168	1108	1.9	1.4	0.42	1140	1.3	0.8	0.61	1113	1113	1118			$36S_{12},20S_9,11S_{17}$	20	-	80
	ν_{13}	Ring breathing	1080	1025	0.3	21.3	0.08	1039	0.4	28.5	0.07	1030	1028	1026	1025	1045	$45S_{13},33S_{14}$	99	-	1
	ν_{14}	γ-CH_2 rock	971	921	2.2	1.0	0.33	940	2.0	3.0	0.33						$51S_{14},18S_{13},11S_{10}$	99	-	1
	ν_{15}	Ring deformation	919	872	0.5	3.1	0.45	874	0.7	3.9	0.12	869	868	868	865	850	$44S_{15},29S_{17},11S_{12}$	68	-	32
	ν_{16}	C-CN stretch	835	792	0.8	4.5	0.24	786	0.4	3.4	0.16	791	791				$42S_{16},15S_{13},10S_{12}$	34	-	66
	ν_{17}	Ring deformation	694	658	1.9	1.1	0.29	688	2.0	0.8	0.22	671	673		~670	~680	$31S_{17},34S_{15},15S_{12}$	48	-	52
	ν_{18}	Ring-CN in-plane-bend	485	460	1.0	1.8	0.42	490	1.1	2.8	0.20	479	479	488	486	518	$32S_{18},35S_{19},13S_{15}$	25	-	75
	ν_{19}	CN in-plane-bend	278	264	1.1	1.9	0.50	247	2.1	2.7	0.54						$37S_{19},44S_{20}$	13	-	87
	ν_{20}	Ring puckering	136	129	2.7	1.3	0.73	100	2.1	1.4	0.75						$41S_{20},37S_{18},20S_{19}$	26	-	74
A"	ν_{21}	β-CH_2 antisymmetric stretch	3205	3041	8.7	59.0	0.75	3139	9.1	86.1	0.75						$98S_{21}$	-	100	-
	ν_{22}	β-CH_2 symmetric stretch	3135	2974	29.0	2.3	0.75	3081	48.9	9.1	0.75						$98S_{22}$	-	100	-
	ν_{23}	β-CH_2 scissors	1538	1459	2.9	7.1	0.75	1502	3.7	3.3	0.75		1431				$100S_{23}$	-	100	-
	ν_{24}	γ-CH_2 wag	1325	1257	2.4	0.4	0.75	1295	1.6	0.2	0.75						$68S_{24}$	-	100	-
	ν_{25}	CH out-of-plane bend	1295	1229	0.1	0.4	0.75	1275	0.01	0.2	0.75						$72S_{25},13S_{24}$	-	100	-
	ν_{26}	γ-CH_2 twist	1279	1213	2.3	14.2	0.75	1248	2.2	9.8	0.75						$42S_{26},36S_{27}$	-	100	-
	ν_{27}	β-CH_2 wag	1198	1137	0.1	4.9	0.75	1181	0.2	2.2	0.75	1160	1164				$35S_{27},21S_{28},15S_{25}$	-	100	-
	ν_{28}	Ring	1105	1048	0.01	1.9	0.75	1076	0.002	1.4	0.75						$53S_{28},15S_{31},12S_{26},10S_{30}$	-	100	-

	deformation													
ν_{29}	Ring deformation	984	934	0.3	15.4	0.75	956	0.5	16.9	0.75	$60S_{29},20S_{30}$	-	100	-
ν_{30}	β-CH_2 twist	960	911	2.9	0.8	0.75	932	2.2	1.4	0.75	$34S_{30},16S_{29},14S_{31},12S_{27},10S_{28}$	-	100	-
ν_{31}	β-CH_2 rock	804	763	0.2	0.2	0.75	773	0.03	0.2	0.75	$56S_{31},19S_{30},13S_{26}$	-	100	-
ν_{32}	Ring-CN out-of-plane bend	550	522	0.1	0.5	0.75	558	0.01	0.4	0.75	$42S_{32},47S_{33}$	-	100	-
ν_{33}	CN out-of-plane bend	191	181	3.4	2.5	0.75	194	3.9	3.5	0.75	$51S_{33},48S_{32}$	-	100	-

[a] Observed spectra: gas, Xe, and solid are IR while liquid is Raman

[b] MP2(full)/6-31G(d) *ab initio* calculations, B3LYP/6-31G(d) *density functional theory* calculations, scaled frequencies, infrared intensities (km/mol), Raman activities ($Å^4$/u), depolarization ratios (dp) and potential energy distributions (P.E.D.s).

[c] Scaled frequencies with scaling factors of 0.90 for all modes.

[d] Frequencies listed are taken from reference [50].

[e] Symmetry coordinates with P.E.D. contribution less than 10% are omitted.

The mid-infrared spectra (4000 to 400 cm^{-1}) of the sample dissolved in liquefied xenon (Fig. 1B) were recorded on a Bruker model IFS-66 Fourier transform spectrometer equipped with a globar source, a Ge/KBr beamsplitter and a DTGS detector. In all cases, 100 interferograms were collected at 1.0 cm^{-1} resolution, averaged and transformed with a boxcar truncation function. For these studies, a specially designed cryostat cell was used. It consists of a copper cell with a path length of 4 cm with wedged silicon windows sealed to the cell with indium gaskets. The copper cell was enclosed in an evacuated chamber fitted with KBr windows. The temperature was maintained with boiling liquid nitrogen and monitored by two Pt thermo resistors. A very small sample was introduced into the cell after cooling to the designated temperature. The system was then pressurized with the noble gases, which condensed in the cell, allowing the compound to dissolve.

The Raman spectrum (Fig. 2) was recorded on a Spex model 1403 spectrophotometer equipped with a Spectra-Physics model 2017 argon ion laser operating on the 514.5 nm line. The laser power used was 1.5 W with a spectral bandpass of 3 cm^{-1}. The spectrum of the liquid was recorded with the sample sealed in a Pyrex glass capillary. The measurements of the Raman frequencies are expected to be accurate to ±2 cm^{-1}. All of the observed fundamentals in the spectrum of the liquid with their proposed assignments are listed in Tables 1 and 2.

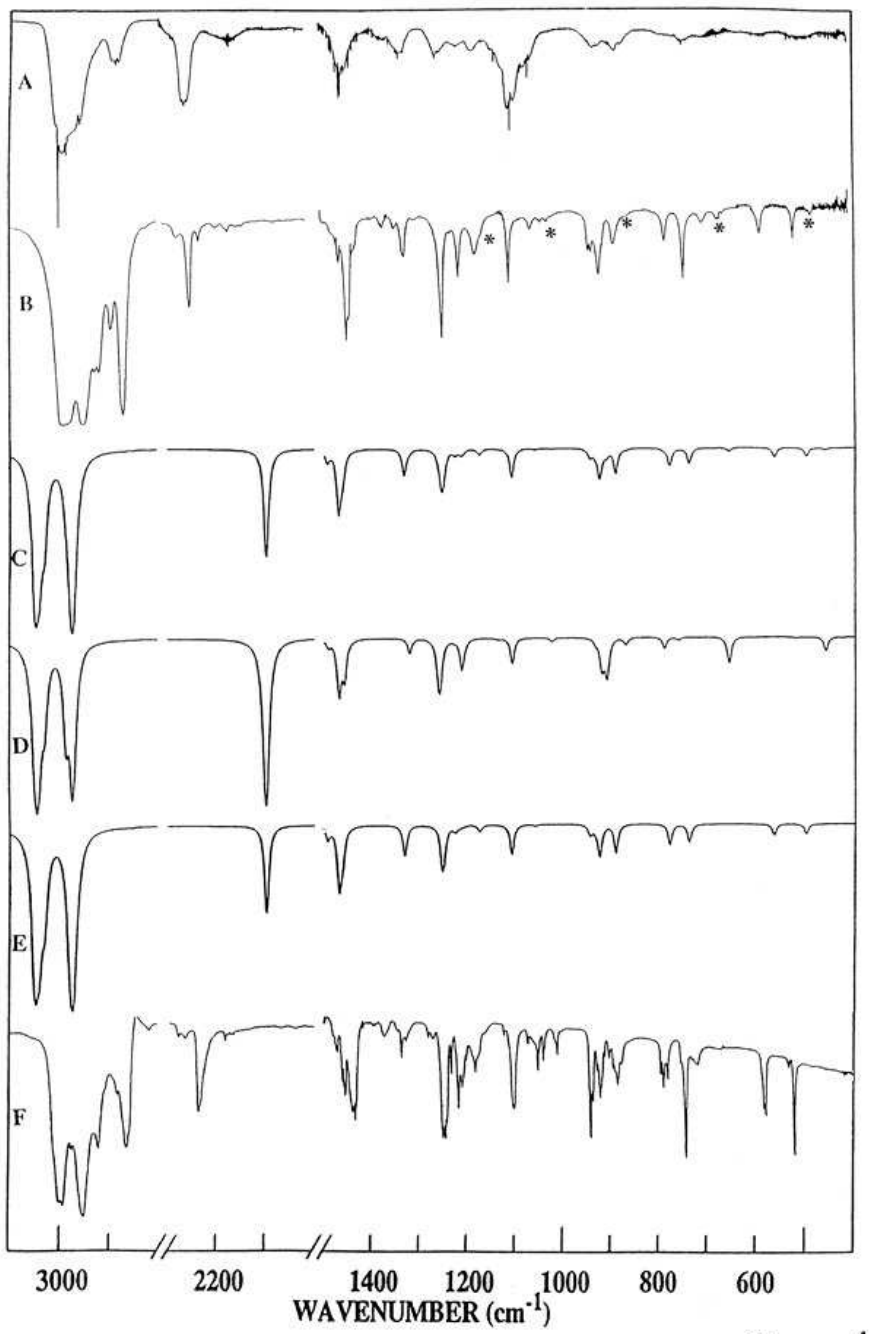

Figure 1. Comparison of experimental and predicted infrared spectra of cyanocyclobutane: (A) gas; (B) Xe solution at -70 ºC; (C) simulated spectrum of mixture of equatorial and axial conformers at -70^{o}C with ΔH = 254 cm^{-1}; (D) simulated spectrum of axial conformer; (E) simulated spectrum of equatorial conformer; (F) annealed solid.

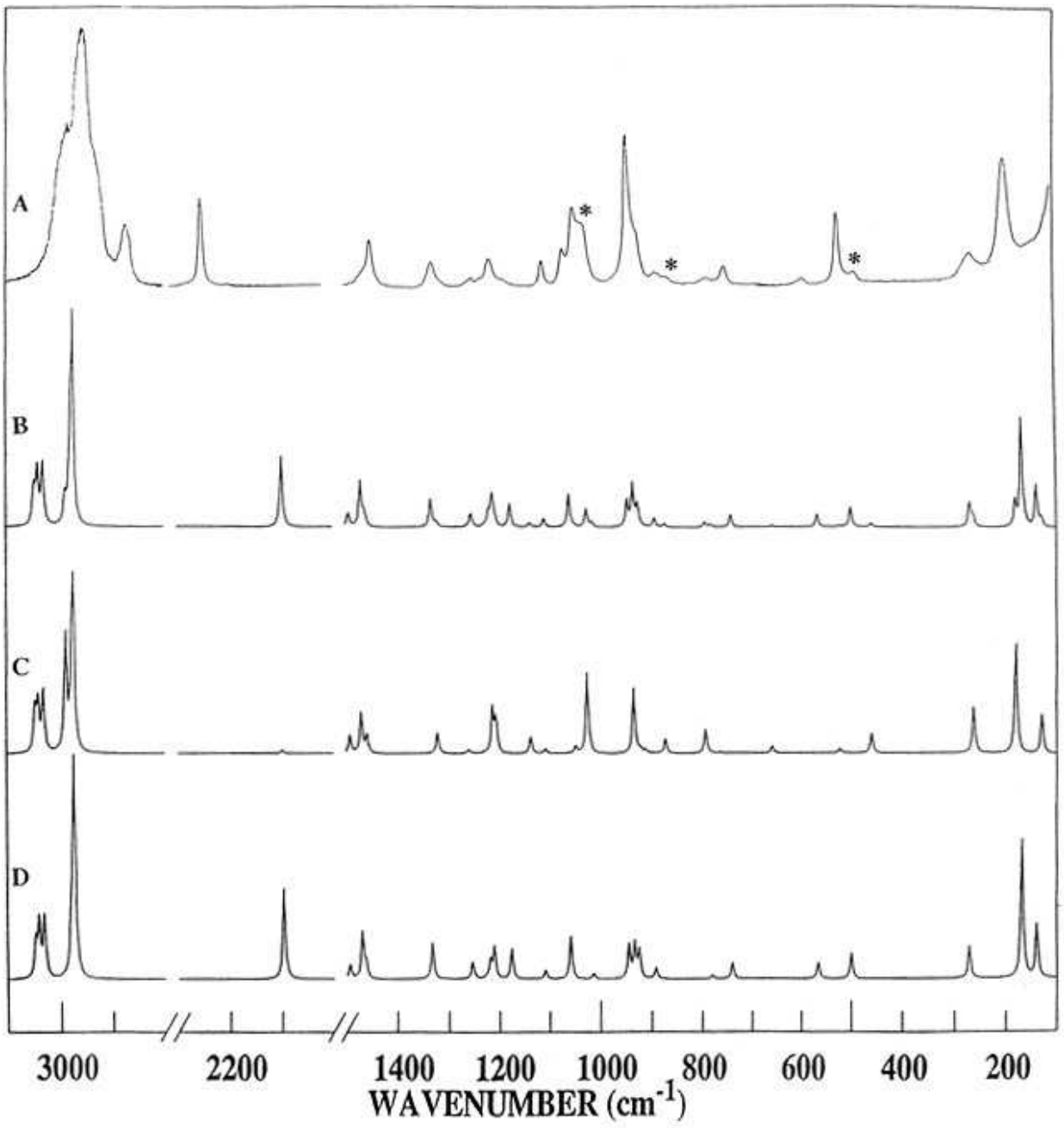

Figure 2. Comparison of experimental and predicted Raman spectra of cyanocyclobutane: (A) liquid; (B) simulated spectrum of the mixture of equatorial and axial conformers at 25ºC with ΔH = 254 cm^{-1}; (C) simulated spectrum of axial conformer; (D) simulated spectrum of equatorial conformer.

AB INITIO CALCULATIONS

The LCAO-MO-SCF restricted Hartree-Fock calculations were performed with the Gaussian-03 program[22] using Gaussian-type basis functions. The energy minima with respect to nuclear coordinates were obtained by the simultaneous relaxation of all geometric parameters using the gradient method of Pulay[29]. A variety of basis sets as well as the corresponding ones with diffuse functions were employed with the Møller-Plesset perturbation method[21] to the second order MP2(full) as well as with the density functional theory by the B3LYP method. The predicted conformational energy differences are listed in Table 3.

In order to obtain a complete description of the molecular motions involved in the fundamental modes of cyanocyclobutane, a normal coordinate analysis has been carried out. The force field in Cartesian coordinates was obtained with the Gaussian 03 program at the MP2(full) level with the 6-31G(d) basis set. The internal coordinates used to calculate the **G** and **B** matrices are given in Table 4 with the atomic numbering shown in Fig. 3. By using the **B** matrix[30], the force field in Cartesian coordinates was converted to a force field in internal coordinates. Subsequently, 0.90 for all coordinates were used, along with the geometric average of scaling factors for interaction force constants, to obtain the fixed scaled force field and resultant wavenumbers. A set of symmetry coordinates was used (Table S1) to determine the corresponding potential energy distributions (P.E.D.s). A comparison between the observed and calculated wavenumbers, along with the calculated infrared intensities, Raman activities,

depolarization ratios and potential energy distributions for the *equatorial* and *axial* conformers, which are given in Tables 1 and 2, respectively.

TABLE 3. Calculated energies (H) and energy differences (cm^{-1}) for the two conformers, transition state of cyanocyclobutane, and barrier to linearity of the $\angle C_\alpha CN$ angle.

Method/Basis Set	Energy[a], E	Energy Differences, Δ				
	equatorial	*axial*[b]	*planar ring*[b]	*planar ring*[c]	*eq*[b,d]	*ax*[c,d]
RHF/6-31G(d)	0.834294	317				
MP2(full)/6-31G(d)	1.659713	231	849	618	7	1
MP2(full)/6-31+G(d)	1.672605	239				
MP2(full)/6-31G(d,p)	1.716770	263				
MP2(full)/6-31+G(d,p)	1.728669	255				
MP2(full)/6-311G(d,p)	1.884198	227				
MP2(full)/6-311+G(d,p)	1.890060	223	1053	830	8	2
MP2(full)/6-311G(2d,2p)	1.948524	201				
MP2(full)/6-311+G(2d,2p)	1.953745	240				
MP2(full)/6-311G(2df,2pd)	2.042632	216	906	690	8	3
MP2(full)/6-311+G(2df,2pd)	2.046926	242	917	675	6	2
MP2(full)/aug-cc-pVTZ	2.056305	285				
Average MP2(full)	-	238 ± 23	931 ± 86	703 ± 78	7 ± 1	2 ± 1
B3LYP/6-31G(d)	2.455589	335	410	75	6	5
B3LYP/6-31+G(d)	2.465082	339				
B3LYP/6-311G(d,p)	2.521613	325				
B3LYP/6-311+G(d,p)	2.524852	327	391	64	6	5
B3LYP/6-311G(2d,2p)	2.529825	318				
B3LYP/6-311+G(2d,2p)	2.533238	332				
B3LYP/6-311G(2df,2pd)	2.537226	331	396	65	7	6
B3LYP/6-311+G(2df,2pd)	2.540307	341	399	58	6	5
B3LYP/aug-cc-pVTZ	2.547998	333				
Average B3LYP	-	331 ± 7	399 ± 8	65 ± 7	6 ± 0	5 ± 1

[a]Energy of conformer is given as –(E+247) H.
[b]Difference is relative to *equatorial* form and given in cm^{-1}.
[c]Difference is relative to *axial* form and given in cm^{-1}.
[d]Barrier to Linearity of the $\angle C_\alpha CN$ angle.

TABLE 4. Structural parameters (Å and degrees), rotational constants (MHz) and dipole moments (Debye) for *equatorial* and *axial cyano*cyclobutane.

Structural Parameters	Int. coor.	MP2(full)/ 6-311+G(d,p)		B3LYP/ 6-311+G(d,p)		Adjusted r_0[a]	
		Eq	Ax	Eq	Ax	Eq	Ax
rC≡N	R_1	1.175	1.175	1.154	1.154	1.160(3)	1.160(3)
rC_α-CN	R_2	1.454	1.458	1.452	1.455	1.461(3)	1.468(3)
rC_α-C_β,$C_{\beta'}$	R_3	1.553	1.558	1.563	1.568	1.557(3)	1.562(3)
rC_γ-C_β,$C_{\beta'}$	R_4	1.547	1.547	1.552	1.552	1.549(3)	1.550(3)
rC_α-H	r_1	1.094	1.093	1.093	1.092	1.094(2)	1.092(2)
rC_β-H_1, $C_{\beta'}$-H_1	r_2	1.093	1.091	1.091	1.090	1.093(2)	1.091(2)
rC_β-H_2, $C_{\beta'}$-H_2	r_3	1.091	1.093	1.090	1.091	1.091(2)	1.093(2)
rC_γ-H_1	r_4	1.091	1.093	1.090	1.092	1.091(2)	1.093(2)
rC_γ-H_2	r_5	1.093	1.091	1.092	1.090	1.094(2)	1.091(2)
∠C_αCN	ϕ_1	178.2	179.0	178.6	179.4	178.6(5)	179.9(5)
∠$C_\beta C_\alpha$CN	ϕ_2	118.7	111.9	118.6	113.9	118.0(5)	111.1(5)
∠$C_\beta C_\alpha C_\beta$	θ_1	87.60	87.28	88.22	88.10	88.3(5)	87.9(5)
∠$C_\gamma C_\beta C_\alpha$	θ_2	87.54	88.16	88.39	89.27	87.8(5)	89.1(5)
∠$C_\beta C_\gamma C_\beta$	θ_3	88.03	88.05	89.02	89.29	88.9(5)	88.8(5)
∠ H$C_\alpha C_\beta$	σ_1	110.2	117.5	110.6	115.8	110.5(5)	118.0(5)
∠ HC_αCN	σ_2	109.7	109.3	108.8	108.4	109.8(5)	109.3(5)
∠ $H_1C_\beta C_\alpha$	λ_1	110.2	117.5	111.1	116.6	110.1(5)	117.5(5)
∠ $H_1C_\beta C_\gamma$	λ_2	110.9	118.9	112.1	117.8	107.7(5)	121.6(5)
∠ $H_2C_\beta C_\alpha$	λ_3	117.4	109.3	116.5	116.6	117.4(5)	109.3(5)
∠ $H_2C_\beta C_\gamma$	λ_4	119.3	111.3	118.4	117.8	122.0(5)	107.5(5)
∠ $H_1C_\beta H_2$	λ_5	109.8	109.9	109.1	109.1	109.8(5)	109.9(5)
∠ $H_1C_\gamma C_\beta$	π_1	117.8	110.8	117.2	111.9	119.0(5)	108.5(5)
∠ $H_2C_\gamma C_\beta$	π_2	111.1	118.1	111.9	117.0	109.4(5)	119.9(5)
∠ $H_1C_\gamma H_2$	π_3	109.6	109.4	108.7	108.7	109.5(5)	109.4(5)
τ$C_\gamma C_\beta C_\beta C_\alpha$	τ_1	32.6	-30.7	26.1	-21.5	28.5(5)	-24.1(5)
τ NCC_αH	τ_2	180.0	180.0	180.0	180.0	180.0	180.0
A(MHz)		10015.6	7511.0	9707.5	7809.0	9761.7	7592.0
B(MHz)		2355.4	2710.3	2379.5	2615.5	2383.1	2681.8
C(MHz)		2084.2	2556.4	2099.2	2414.5	2105.4	2506.1
$\lvert\mu_a\rvert$		4.603	4.316	4.297	4.103		
$\lvert\mu_b\rvert$		0.000	0.000	0.000	0.000		
$\lvert\mu_c\rvert$		0.908	0.934	1.568	1.455		
$\lvert\mu_t\rvert$		4.692	4.416	4.574	4.353		

[a] adjusted parameters using the microwave data from reference [46] for the given ground states

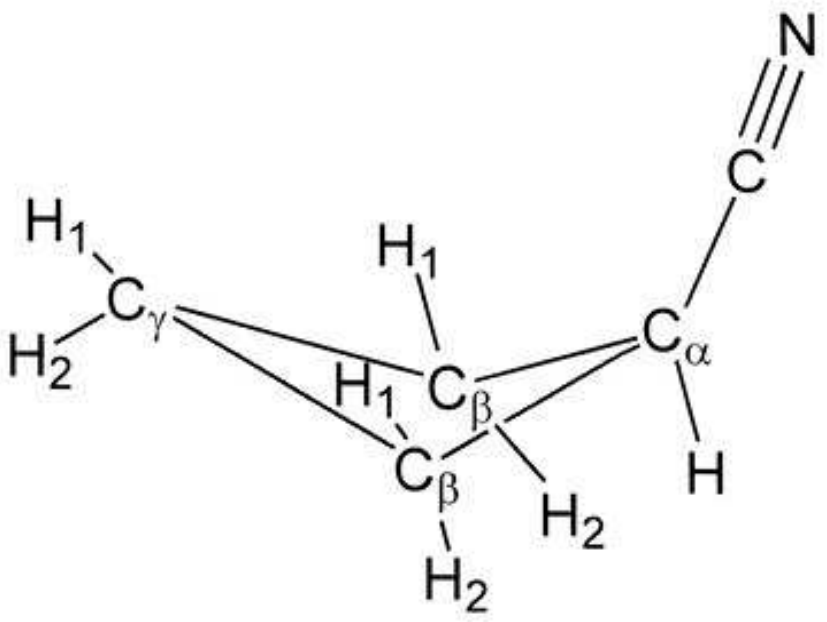

Figure 3. Cyanocyclobutane showing atomic numbering.

The infrared spectra were predicted from the MP2(full)/6-31G(d) calculations. The predicted scaled frequencies were used together with a Lorentzian function to obtain the calculated spectra. Infrared intensities determined from MP2(full)/6-31G(d) calculations were obtained based on the dipole moment derivatives with respect to Cartesian coordinates. The derivatives were transformed with respect to normal coordinates by $(\partial\mu_u/\partial Q_i) = \sum_j (\partial\mu_u/\partial X_j)\mathbf{L_{ij}}$, where Q_i is the i^{th} normal coordinate, X_j is the j^{th} Cartesian displacement coordinate, and $\mathbf{L_{ij}}$ is the transformation matrix between the Cartesian displacement coordinates and the normal coordinates. The infrared intensities were then calculated by $[(N\pi)/(3c^2)]\ [(\partial\mu_x/\partial Q_i)^2 + (\partial\mu_y/\partial Q_i)^2 + (\partial\mu_z/\partial Q_i)^2]$. In Fig. 1 a

comparison of the experimental and simulated infrared spectra of cyanocyclobutane is shown. Infrared spectrum of the cyanocyclobutane at ambient temperature (Fig. 1A) and the predicted infrared spectra for the pure *equatorial* (Fig. 1E) and *axial* (Fig. 7D) conformers, as well as the mixture (Fig. 1C) of the two conformers with relative concentrations calculated for the equilibrium mixture at ambient by using the experimentally determined enthalpy difference are presented. The predicted spectrum is in relatively good agreement with the experimental spectrum which indicates the utility of the scaled predicted frequencies and intensities for supporting the vibrational assignment.

Also to further support the vibrational assignments, we have simulated the Raman spectra from the *ab initio* MP2(full)/6-31G(d) results. The evaluation of Raman activity by using the analytical gradient methods has been developed[31-34]. The activity S_j can be expressed as: $S_j = g_j (45\alpha_j^2 + 7\beta_j^2)$, where g_j is the degeneracy of the vibrational mode j, α_j is the derivative of the isotropic polarizability, and β_j is that of the anisotropic polarizability. To obtain the polarized Raman scattering cross sections, the polarizabilities are incorporated into S_j by multiplying S_j with $(1-\rho_j)/(1+\rho_j)$, where ρ_j is the depolarization ratio of the j^{th} normal mode. The Raman scattering cross sections and calculated wavenumbers obtained from the Gaussian 03 program were used together with a Lorentzian function to obtain the simulated Raman spectra. Comparison of experimental Raman spectra of the liquid (Fig. 2A) and the predicted Raman spectra for the pure *equatorial* (Fig. 2D) and *axial* (Fig. 2C) conformers as well as the mixture (Fig. 2B) of the two conformers with relative concentrations calculated for the equilibrium mixture at 25ºC by using the experimentally determined enthalpy difference are shown.

The predicted spectrum of the mixture should be compared to that of the Raman spectrum of the liquid at room temperature, although there may be some difference between the predicted and that obtained experimentally due to the intramolecular forces in the liquid. Nevertheless, the predicted spectrum is in good agreement with the experimental spectrum which again indicates the utility of the scaled predicted frequencies and intensities of the Raman spectra for supporting the vibrational assignment.

VIBRATIONAL ASSIGNMENT

In order to obtain the best enthalpy values possible it is very important to assign as many of the conformer bands of the less stable conformer as possible to make wise decisions for their use in the ΔH determination. Additionally, all of the fundamentals of the most stable conformer should be assigned to assure a correct choice of the band pairs for the temperature study. Although there has been an extensive vibrational study[50] of cyanocyclobutane there were a number of the fundamentals which were not previously assigned for the gas from an infrared spectrum. Of particular importance is the region from 400 to 1000 cm^{-1} which will have the fewest numbers of overtone and combination bands possible and the fundamental frequencies in this region for the two different conformers will usually be the skeletal modes rather than the modes for the lighter atoms. The skeletal modes have the most pronounced differences for the conformers which makes them the most suitable for the enthalpy determinations. Therefore, the primary emphasis began with the assignment from 400 to 1000 cm^{-1} for each of the symmetry species for both conformers. After an extensive review of the assignments presented previously[50] there was only one assignment that was in error which is the CN torsion,

ν_{32}, which was originally assigned at 580 cm^{-1}. However it was clearly observed at 506 cm^{-1} even though it has a very small predicted infrared intensity.

Additionally, in the earlier study[50] there were a number of fundamentals for which no assignments were given for the gas although they were assigned from the spectra of the argon and nitrogen matrices, as well as, in the liquid and solid. In the A' block there is a fundamental C-C(N) stretch, which was predicted at 1059 cm^{-1} and observed at 1064 cm^{-1} but no assignment was given for it for the gas. Also three other fundamentals, ν_{25} through ν_{28}, from the A" block were also unassigned in the gas. All of these modes have very small predicted intensities ranging from a high value of 0.05 to 0.002 km/mol, which explains why they were not assigned earlier. Aided by the spectral study in xenon solution where weak bands are much easier to detect, made it possible to identify all but ν_{28} in the spectrum of the gas and their assignments are given in Table 1, along with the fundamental frequencies from the spectrum of the gas of the most stable conformer.

By utilizing the infrared spectrum for the xenon solution in comparison to the spectrum of the gas (Fig. 4) it was possible to obtain several bands of the second conformer which could be confidently assigned based upon the *ab initio* predicted frequencies, band contours, and/or relative intensities. There were eight fundamentals of the less stable conformer that could be confidently identified and their frequencies are listed in Table 2. From these eight fundamentals careful consideration was given to choose bands with reasonable intensities and without interference from bands from the major conformer which could be used to obtain the enthalpy difference for cyanocyclobutane.

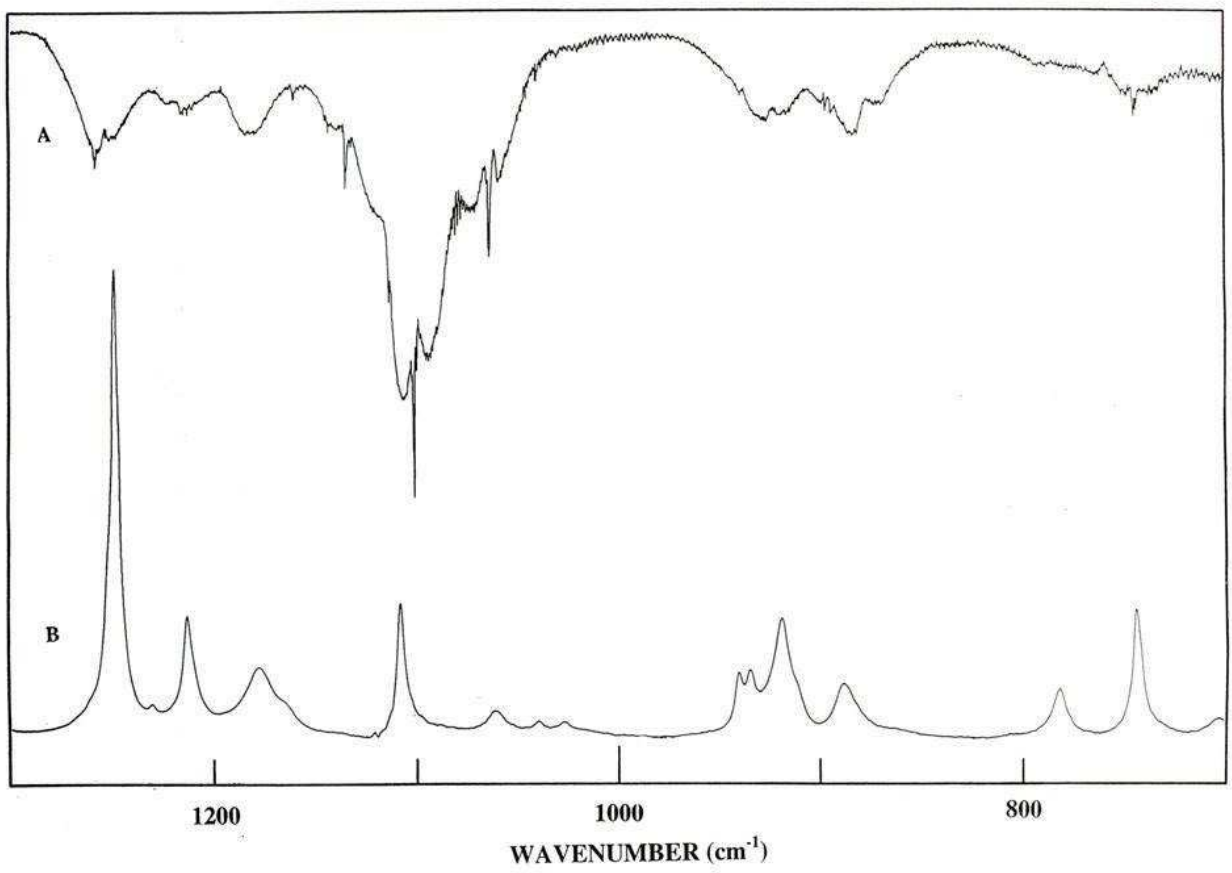

Figure 4. Mid-infrared spectra of cyanocyclobutane (A) gas; (B) Xe solution at -70°C.

STRUCTURAL PARAMETERS

We have[51] shown that *ab initio* MP2(full)/6-311+G(d,p) calculations predict the r_0 structural parameters for more than fifty carbon-hydrogen distances better than 0.002Å compared to the experimentally determined values from isolated CH stretching frequencies which are compared[5] to previously determined values from earlier microwave studies. Thus, all of the carbon-hydrogen parameters can be taken from the MP2(full)/6-311+G(d,p) predicted values for cyanocyclobutane. Also, we have found[14]

that we can obtain good structural parameters by adjusting the structural parameters from the *ab initio* calculations to fit the rotational constants obtained from the microwave experimental data. In order to reduce the number of independent variables, the structural parameters are separated into sets according to their types. Bond lengths in the same set keep their relative ratio which results in only three heavy atoms distances for cyanocyclobutane. Also, the bond angles and torsional angles in the same set keep their differences in degrees. This assumption is based on the fact that the errors from *ab initio* calculations are systematic. Additionally we have also shown that the differences in predicted distances and angles from the ab initio calculations for different conformers of the same molecule can usually be used as one parameter with the *ab initio* predicted differences except for some dihedral angles. Also the C≡N distance is nearly constant irrespective of the substitutions on it[52]. Thus, it is possible to reduce the number of independent structural parameters to six with one CC bond length, one C-CN distance, one CCC angle, one NCC angle, and two ring puckering angles. Therefore, if the CH parameters are taken from the MP2(full)/6-311+G(d,p) calculations, then it should be possible to obtain "adjusted r_0" structural parameters for the equatorial and axial conformers of cyanocyclobutane by utilizing the previously reported[46] six rotational constants from the microwave study.

These determined r_0 parameters are listed in Table 4 and the final fit of the rotational constants is shown in Table 5. The differences are quite small with the largest being 0.3 MHz for the B rotational constant of the equatorial form with the remaining rotational constants fit to 0.2 or better for both conformers. The largest adjustments are associated with the two ring puckering angles from 32.6° to 28.5° for the equatorial

conformer and from 30.7° to 24.1° for the axial conformer. Another change is for the C-CN bond distance which changed from 1.454 to 1.461 Å for the equatorial form and 1.458 to 1.468 Å for the axial form. The remaining changes were relatively small. It is somewhat difficult to estimate the uncertainties in these structural parameters, but it is believed those for the CH distances should be no more than $\pm$0.002 Å, the heavy atom distances $\pm$0.003 Å, and the angles $\pm$0.5°. These parameters are expected to be more accurate than those that could be obtained from an electron diffraction or microwave study alone.

TABLE 5. Comparison of rotational constants (MHz) obtained from modified *ab initio*, MP2(full)/6-311+G(d,p) structural parameters and the experimental values from the microwave spectra of cyanocyclobutane.

Isotopomer	Rotational constant	Experimental[a]	Calculated	$\lvert\Delta\rvert$
eq-C_4H_7CN	A	9761.88(3)	9761.69	0.2
	B	2383.396(4)	2383.11	0.3
	C	2105.118(3)	2105.37	0.2
ax-C_4H_7CN	A	7591.86(6)	7591.97	0.1
	B	2681.987(7)	2681.86	0.1
	C	2505.943(8)	2506.09	0.1

[a]Ref. [46].

CONFORMATIONAL STABILITY

To determine the enthalpy difference between the two conformers, the mid-infrared spectra of cyanocyclobutane dissolved in liquefied xenon as a function of temperature from -55 to -100°C were recorded. Only small interactions are expected to occur between the dissolved sample and the surrounding xenon atoms, and consequently, only small frequency shifts are anticipated when passing from the gas phase to the liquefied noble gas solutions[16-19]. A significant advantage of this study is that the conformer bands are better resolved in comparison with those in the infrared spectrum of the gas. From *ab initio* calculations, the dipole moments of the two conformers are predicted to have similar values and the molecular sizes of the two conformers are nearly the same, so the ΔH value obtained from the temperature dependent FT-IR study is expected to be close to that for the gas[16-20].

With eight fundamentals confidently identified for the axial conformer the major requirement was to determine which of these bands were sufficiently separated from other bands to obtain good intensity measurements. After careful analysis it was concluded only the two bands at 479 and 673 cm^{-1} could be used for confident intensity measurements for the axial conformer. The choice of the bands to be used for the equatorial was somewhat more difficult since the requirement it be sufficiently separated from any interfering bands and for best results it should have comparable intensity to the band being used for the axial conformer and in the lower frequency range. From the inspection of the various possible bands the fundamentals at 515, 585, 743, and 782 cm^{-1} were selected for the equatorial conformer to use in the determination of the enthalpy difference.

The intensities of the infrared bands were measured as a function of temperature and their ratios were determined (Fig. 5). By application of the van't Hoff equation $-\ln K = \Delta H/(RT) - \Delta S/R$, ΔH was determined from a plot of $-\ln K$ versus $1/T$, where $\Delta H/R$ is the slope of the line and K is substituted with the appropriate intensity ratios, *i.e.* $I_{equatorial} / I_{axial}$. It was assumed that ΔS and α are not a function of temperature in the temperature range studied.

By combining the two axial and the four equatorial conformer bands, eight pairs were utilized for the determination of the enthalpy difference, and the resulting values with statistical uncertainties are listed in Table 6. The statistical average obtained by using all eight pairs as a single set gives a value of 254 ± 12 cm^{-1} where the error limit is derived from the statistical standard deviation of one sigma of the measured intensity data. This error limit does not take into account small associations with the liquid xenon or the interference of overtones and combination bands in near coincidence with the measured fundamentals. The variations in the individual values are undoubtedly due to these types of interferences, but by taking several pairs, the effect of such interferences should cancel. The abundance of the less stable axial conformer present at ambient temperature is $23 \pm 1\%$.

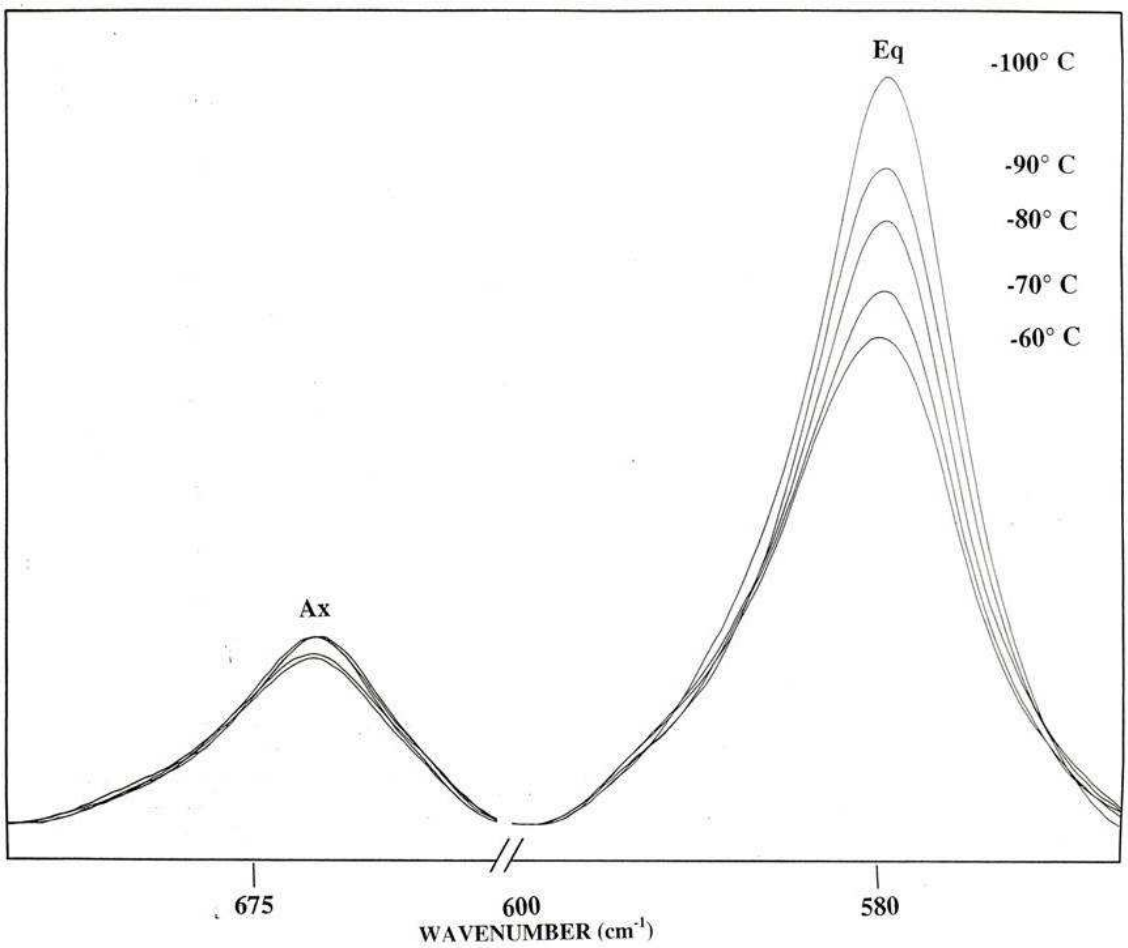

Figure 5. Infrared spectra of cyanocyclobutane, in Xe solution at different temperatures.

TABLE 6. Temperature and intensity ratios of the *equatorial* and *axial* bands of cyanocyclobutane.

	T(°C)	1/T ($\times 10^{-3}$ K^{-1})	I_{515} / I_{479}	I_{585} / I_{479}	I_{743} / I_{479}	I_{782} / I_{479}	I_{515}/ I_{673}	I_{585} / I_{673}	I_{743} / I_{673}	I_{782} / I_{673}
Liquid xenon	–55.0	4.584	4.098	3.262	10.312	3.555	3.288	2.618	8.276	2.853
	–60.0	4.692	5.066	4.052	12.417	4.313	3.516	2.813	8.618	2.993
	–65.0	4.804	4.500	3.691	11.398	3.983	3.493	2.865	8.849	3.092
	–70.0	4.923	4.763	3.886	12.203	4.322	3.638	2.968	9.320	3.301
	–75.0	5.047	4.729	3.936	11.912	4.064	3.721	3.097	9.373	3.197
	–80.0	5.177	5.382	4.290	13.485	4.606	3.883	3.096	9.731	3.323
	–85.0	5.315	5.832	4.757	14.956	5.088	4.197	3.424	10.764	3.662
	–90.0	4.460	5.331	4.426	14.223	4.661	4.006	3.326	10.689	3.503
	–95.0	5.613	6.867	5.531	18.152	6.066	4.689	3.777	12.395	4.142
	–100.0	5.775	7.095	6.038	19.052	6.303	4.482	3.814	12.036	3.982
ΔH^a			279 ± 45	301 ± 41	324 ± 41	289 ± 45	190 ± 20	212 ± 16	235 ± 18	200 ± 23

[a] Average value $\Delta H = 254 \pm 12$ cm^{-1} (3.03 ± 0.15 kJ mol^{-1}) with the equatorial conformer the more stable form and the statistical uncertainty (1σ) obtained by utilizing all of the data as a single set.

DISCUSSION

The predicted infrared intensities from the B3LYP calculations for the C≡N stretch are nearly four orders of magnitude greater than those predicted from the MP2 calculations. Similarly the Raman activities for this mode are about two and one-half times more intense. These large differences are the result of the MP2 predicted distance for the triple bond being nearly 0.021 Å longer than the value predicted from the B3LYP calculations, which are near the experimental r_0 value (Table 4). There are smaller predicted intensity differences for the γ-CH_2 and CH symmetric stretching modes where

the infrared intensities are predicted three times more intense for the γ-CH_2 symmetric stretch but one-fourth the intensity for the CH symmetric stretch, respectively, from the MP2 calculations compared to those from the B3LYP calculations.

In the earlier vibrational study of cyanocyclobutane the authors [50] only provided P.E.D.s for the modes below 1350 cm^{-1}; thus, we have compared them to those obtained in this study. We were particularly interested in the mixing of the ring motions with the CH_2 bends (twists and rocks). For example ν_{29} is a ring deformation (stretch) but there are significant contributions from four symmetry coordinates.

The conformational enthalpy difference of 254 $\pm$ 12 cm^{-1} (3.03 + 0.15 kJ/mol) is in agreement with the value of 258 $\pm$ 50 cm^{-1} obtained from the microwave study except the value obtained in the current study has a much smaller uncertainty. Also the MP2(full) average predicted value of 238 $\pm$ 23 cm^{-1} is in excellent agreement with the experimental value which is somewhat better than the difference obtained for chlorocyclobutane [48]. The predicted value had a larger variation (430 $\pm$ 40 cm^{-1}) compared to the experimentally determined value of 361 $\pm$ 17 cm^{-1}. The determination of the ΔH by several conformer pairs, i.e. eight in the current study and six in the chlorocyclobutane significantly decreases the uncertainty in the determined enthalpy value. Of particular interest would be the *ab initio* predicted energy difference between the two conformers of flourocyclobutane where experimental enthalpy differences of 413 $\pm$ 43 cm^{-1} for the gas and 400 $\pm$ 30 cm^{-1} for the liquid were obtained from variable temperature studies of the Raman spectra [53].

The barrier to linearity of the $\angle C_\alpha CN$ group is very small, i.e predicted to be 7 $\pm$ 1 cm^{-1} from the MP2(full) calculations as might be expected since the predicted angle is

178.2°. For the axial form the corresponding predicted angle is 179.0° so there is no reason to expect it to have any significant effect on fitting the rotational constants for this conformer. We have also calculated the barrier to planarity for which the *ab initio* MP2(full) predicts a value of 931 $\pm$ 86 cm^{-1} which is one-third larger than the value of 600 cm^{-1} obtained from the microwave study[54]. However, it should be noted that the B3LYP calculations give an average barrier of 399 $\pm$ 8 cm^{-1}, which of course is clearly too small. Four clear transitions have been observed at 138.3, 129.7, 118.0, and 113.2 cm^{-1} (Fig. 6) which are undoubtedly due to the ring puckering mode of the equatorial conformer. The frequencies of the fundamental and "hot bands" clearly indicate a barrier greater than 570 cm^{-1}. In the earlier study[55] a fifth transition was assigned at 109.2 cm^{-1} but the contour looks somewhat different (Fig. 6) than the first four assigned transitions. This difference could be due to it being near the top of the barrier or it being the fundamental of the ring puckering mode for the axial conformer.

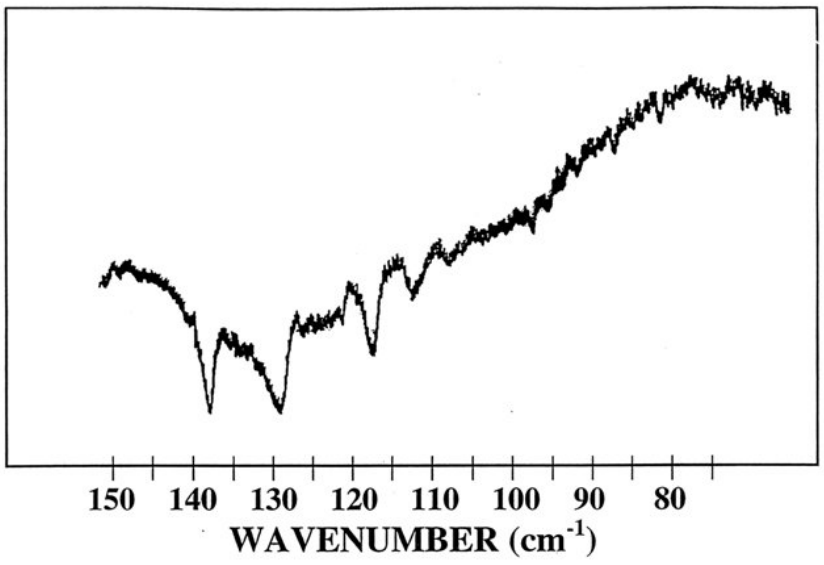

Figure 6. Far-infrared spectrum of gaseous cyanocyclobutane.

In the potential function previously proposed [54] the frequencies of the four transitions were used for the equatorial well along with the enthalpy difference from the microwave data which gave a barrier of planarity for the axial well of ~220 cm^{-1} which is consistent with the *ab initio* MP2(full) predicted barrier of 230 $\pm$ 11 cm^{-1} (Table 3) for this conformer. It should be noted that the *ab initio* predicted frequency for the ring puckering mode is 129 cm^{-1}. Therefore the high frequency shoulder on the second transition of the ring puckering mode of the equatorial conformer could possibly be the ν_{20} fundamental for the axial conformer. With the currently determined ΔH value along with the determined structural parameters for both conformers and observed transitions in both wells it should be possible to obtain a more definitive potential function governing the ring puckering vibration of cyanocyclobutane.

We have calculated the five quadratic centrifugal distortion constants, Δ_J, Δ_{JK}, Δ_K, δ_J, and δ_K, for the asymmetric reduced Hamiltonian for both the equatorial and axial conformers of cyanocyclobutane from the *ab initio* predicted force constants at the level of MP2(full) with two basis sets, i.e. 6-31G(d) and 6-311+G(d,p). Similar calculations were carried out by density functional theory by the B3LYP method with the same basis sets. These distortion constants were obtained from the latest microwave study [46] and both the predicted and experimental values are listed in Table 7. As expected there is little difference in the predicted values from the two basis sets for both the *ab initio* and density functional theory calculations since the force constants are very similar in value from these two basis sets. However there is a large difference in the predicted values between those obtained from the MP2(full) calculations and those from the B3LYP calculations. This difference is mainly due to the poor predicted C≡N bond distance from the MP2 calculations with the very long bond and the resulting smaller force constant compared to the value for this bond distance from the B3LYP method. As can be seen from the data in Table 7 the predicted values for Δ_J, Δ_{JK}, δ_J, and δ_K are in very good agreement with the experimental values obtained for both the equatorial and axial conformers from the B3LYP method. However the experimental value of Δ_K has a very large uncertainty (9.7 $\pm$ 2.1 and 8.7 $\pm$ 2.4 kHz for the equatorial and axial conformers, respectively) so the predicted value of 12.0 kHz for Δ_K for the equatorial conformer is near the maximum experimental value of 11.8 kHz for the equatorial form. However, the agreement for the predicted value for the Δ_K of the axial conformer is acceptable for the MP2 predicted value but unacceptable from the B3LYP calculations. This inordinately high value is apparently caused by a very small force constant for the ring puckering

vibrational mode which is predicted almost 50% lower than the frequency predicted by the MP2 calculation. Thus the MP2 calculations provide a reasonable value for the Δ_K constant. With this exception it is clear that the *ab initio* and density functional theory predicted distortion constants are excellent for checking the experimentally determined values.

The differences in the heavy atom parameters for cyclobutane and a limited number of monosubstituted cyclobutanes are listed in Table 9. For cyclobutane[56] the two different C-H distances were assumed to have the same value of 1.0910(6) Å, with the carbon-carbon distance of 1.555(2) Å, and a puckering angle of 28.58(9)°. Substitution of a chlorine atom causes the C_α-C_β to be reduced significantly, whereas the C_γ-C_β distance is essentially the same as the distance for the corresponding parameter for cyclobutane (Table 8). For cyanocyclobutane the C_α-CN distance is quite short [1.461(3) Å], whereas the C_α-C_β is essentially the same as the corresponding distance in cyclobutane, while, the C_γ-C_β seems a little shorter but within experimental errors of the corresponding cyclobutane distance.

It should be noted that the bond distance for the C≡N group is nearly constant irrespective of the attached species. For example this parameter is given for the methyl cyanide, ethyl cyanide, and cyanocyclopropane (Table 8) which is the same value obtained for this parameter for cyanocyclobutane. Also the C_α-CN distances are quite short whereas the C-C_α distances may be slightly longer which is consistent with the changes obtained for these parameters for cyanocyclobutane. It would be of interest to see if the ethynyl (-C≡C-) group would have similar effects on the carbon-carbon distances of the cyclobutane ring with the substitution of this group.

TABLE 7. Quadratic centrifugal distortion constants (kHz) for equatorial and axial conformers of cyanocyclobutane.

	equatorial					*axial*				
	MP2(full)/ 6-31G(d)	MP2(full)/ 6-311+G(d,p)	B3LYP/ 6-31G(d)	B3LYP/ 6-311+G(d,p)	Exp.[a]	MP2(full)/ 6-31G(d)	MP2(full)/ 6-311+G(d,p)	B3LYP/ 6-31G(d)	B3LYP/ 6-311+G(d,p)	Exp.[a]
Δ_J	0.33	0.32	0.37	0.38	0.35(1)	1.12	1.13	1.31	1.32	1.33(8)
Δ_{JK}	1.21	1.41	0.93	0.90	0.96(13)	-2.00	-1.88	-4.32	-4.50	-3.31(4)
Δ_K	10.8	10.8	12.1	12.0	9.7(21)	8.7	8.1	16.2	17.0	8.7(24)
δ_J	0.016	0.015	0.021	0.022	0.016(2)	-0.101	-0.094	-0.137	-0.138	-0.126(2)
δ_K	1.5	1.6	1.5	1.5	1.6(2)	0.68	0.54	1.06	1.09	0.91(18)

[a] Values taken from Ref [46].

TABLE 8. Structural parameters (Å and degree) for cyclobutane[a], cyanocyclobutane, chlorocyclobutane, cyclobutanol, cyanocyclopropane, cyclopropane, methyl cyanide, and ethyl cyanide.

Structural Parameters	cyanocyclobutane[b]		chlorocyclobutane[c]		cyclobutanol[d]	cyano-cyclopropane[e]	cyclopropane[f]	methyl cyanide[g]	ethyl cyanide[h]
	Eq	Ax	Eq	Ax	*eq*-trans				
$rC{\equiv}N$	1.160(3)	1.160(3)				1.161(4)		1.1583(6)	1.159(1)
rC_{α}-CN	1.461(3)	1.468(3)				1.420(6)		1.4594(6)	1.459(1)
rC_{α}-C_{β},$C_{\beta'}$	1.557(3)	1.562(3)	1.539(3)	1.547(3)	1.547(5)	1.529(5)	1.515321(75)		1.537(1)
rC_{γ}-C_{β},$C_{\beta'}$	1.549(3)	1.550(3)	1.558(3)	1.557(3)	1.552(5)	1.500(3)	1.515321(75)		
rC_{α}-H	1.094(2)	1.092(2)	1.092(2)	1.090(2)	1.093(2)	1.080*	1.07739(12)	1.0922(3)	1.094(1)
rC_{β}-H_1, $C_{\beta'}$-H_1	1.093(2)	1.091(2)	1.093(2)	1.091(2)	1.095(2)	1.080*	1.07739(12)		1.091(1)
rC_{β}-H_2, $C_{\beta'}$-H_2	1.091(2)	1.093(2)	1.092(2)	1.095(2)	1.091(2)	1.080*	1.07739(12)		1.091(1)
rC_{γ}-H_1	1.091(2)	1.093(2)	1.091(2)	1.091(2)	1.091(2)	1.080*	1.07739(12)		
rC_{γ}-H_2	1.094(2)	1.091(2)	1.093(2)	1.091(2)	1.093(2)	1.080*	1.07739(12)		
$\tau C_{\gamma}C_{\beta}C_{\beta}C_{\alpha}$	28.5 (5)	24.1(5)	30.7(5)	22.3(5)	32.7(5)				

[a] Structural parameters[38]; rC-C 1.555(2), rC-H 1.0910(6), and puckering angle 28.58(9).
[b] This study.
[c] Ref. [48] r_0 structural parameters
[d] Ref. [57] r_0 structural parameters
[e] Ref. [58] r_s structural parameters; asterisk indicates assumed value
[f] Ref. [55] r_0 structural parameters
[g] Ref. [59] r_0 structural parameters
[h] Ref. [60] r_s structural parameters

CHAPTER 4

THE r_0 STRUCTURAL PARAMETERS, CONFORMATIONAL STABILITY, AND VIBRATIONAL ASSIGNMENT OF EQUATORIAL AND AXIAL BROMOCYCLOBUTANE

INTRODUCTION

Very limited structural data has been obtained for monosubstituted cyclobutane and the first study using microwave spectra was for bromocyclobutane [36] with a more extensive one for chlorocyclobutane [35]. In this later investigation [35] only the equatorial conformer for the normal species and eight of its isotopomers were assigned. The isotopomers were β-^{13}C and 3 isotopomers with deuterium substitutions(d_1, d_2, and d_5) which were α-d and β-d_2, as well as α-d, β-d_2 and β'-d_2 for the ^{35}Cl isotope and only the three deuterium isotopomers for ^{37}Cl. In this study all fourteen structural parameters were determined assuming the equatorial and axial CH distances on the same carbon had the same values. However, the determined values for the CH distances ranged from 1.090 to 1.110Å which is a very large difference. A later effort [47] was made utilizing *ab initio* calculations and the experimentally determined rotational constants to determine the r_0 structural parameters more accurately by utilization of the diagnostic least squares method [61]. However a satisfactory fit of the A rotational constants for several of the isotopomers could not be achieved. In the same study [47] *ab initio* calculations were utilized to predict the structural parameters of the higher energy axial conformer which subsequently Caminati *et al*. [44] used to identify and assign the spectra of the axial conformer. In this new investigation, values of the A rotational constants for both the ^{35}Cl

and ^{37}Cl isotopomers of the equatorial conformer were reported which were significantly different from those initially reported [35]. Therefore, we recently used these new values to obtain [48] r_0 structural parameters for the equatorial and axial conformers by combining the rotational constants obtained from these experimental studies [44] coupled with the MP2(full)/6-311+G(d,p) *ab initio* calculations.

As a continuation of our conformational and structural determination of monosubstituted cyclobutanes [48,57,62,63] we have investigated the infrared and Raman spectra of bromocyclobutane. The microwave spectrum was recorded by Rothschild and Dailey [36] but only the spectrum of equatorial conformer was identified and assigned. However, Rothschild [64] later reported vibrational evidence for the axial conformer from temperature studies of the infrared spectrum from which a potential for the ring puckering mode was proposed. Since that time there have been extensive vibrational studies of bromocyclobutane with two of the investigations [65,66] emphasizing the vibrational assignment. In the first study [65], three different deuterated isotopes were utilized to distinguish the vibrations associated with the α-CH motions and the β-CH_2 motions and a complete assignment for the equatorial conformer was made. In the later vibrational study [66], the emphasis was on obtaining the normal modes of the equatorial and axial conformers utilizing a scaled *ab initio* force fields transferred from one derived for cyclobutane [67].

In another study [39] the focus was on the identification of the low frequency ring puckering vibration and the associated “hot bands” in the far infrared spectra. In this study [39] a potential function was reported but with a single well. This was followed by another study [68] where the enthalpy difference of bromocyclobutane was obtained from

the variable temperature Raman spectra of the gas but only an approximate value of ~350 cm^{-1} was obtained. In this study a two minima potential function was proposed by using this enthalpy difference. Since no potential function governing the ring puckering vibration has been reported with a reliable value of ΔH of the vapor, we initiated a study to determine the enthalpy difference by variable temperature studies in xenon solution which should provide a value close to that for the gas [16-20]. To obtain a reliable ΔH value, the correct vibrational assignment of the fundamentals of the axial conformer used for the ΔH determination is required. Therefore, we have again investigated the vibrational spectra of bromocyclobutane with the support of *ab initio* calculations to predict the harmonic force fields, infrared intensities, Raman activities, depolarization values, and vibrational frequencies.

Since the structural parameters proposed from the microwave study included an estimate of the C-Br distance, C-H distances, and all angles except for the heavy atom ring values, a determination of all structural parameters is desirable. Thus, a complete structure has been obtained by combining predicted values from MP2(full)/6-311+G(d,p) calculations with the previously reported rotational constants [36]. The results of these experimental and theoretical investigations of bromocyclobutane are reported herein.

EXPERIMENTAL

The sample of bromocyclobutane was purchased from Sigma-Aldrich Chemical Co., with stated purity of 96%. The sample was further purified by low-temperature, low-pressure fractionation column and the purity of the sample was verified by comparing the infrared spectrum with that previously reported [65].

The mid-infrared spectra of the gas and solid were obtained from 4000 to 220 cm^{-1} on a Perkin-Elmer model 2000 Fourier transform spectrometer equipped with a Ge/CsI beamsplitter and a DTGS detector. Atmospheric water vapor was removed from the spectrometer housing by purging with dry nitrogen. The theoretical resolution used to obtain the spectrum of the gas was 0.5 cm^{-1} and 2.0 cm^{-1} for the spectrum of the solid. One hundred twenty eight interferograms were added and transformed with a boxcar truncation function. The frequencies for the predicted and observed fundamentals are listed in Tables 9, 10, 11 and 12.

The mid-infrared spectra (4000 to 400 cm^{-1}) of the sample dissolved in liquefied xenon (Fig. 7A) were recorded on a Bruker model IFS-66 Fourier transform spectrometer equipped with a globar source, a Ge/KBr beamsplitter and a DTGS detector. In all cases, 100 interferograms were collected at 1.0 cm^{-1} resolution, averaged and transformed with a boxcar truncation function. For these studies, a specially designed cryostat cell was used. It consists of a copper cell with a path length of 4 cm with wedged silicon windows sealed to the cell with indium gaskets. The copper cell was enclosed in an evacuated chamber fitted with KBr windows. The temperature was maintained with boiling liquid nitrogen and monitored by two Pt thermo resistors.

The Raman spectra (Fig. 8) were recorded on a Spex model 1403 spectrometer equipped with a Spectra-Physics model 2017 argon laser operating on the 514.5 nm line. The laser power used was 0.5 W with a spectral bandpass of 3 cm^{-1}. The spectrum of the liquid was recorded with the sample sealed in a Pyrex glass capillary. The measurements of the Raman frequencies are expected to be accurate to $\pm$ 2 cm^{-1}. All of the observed

Raman bands with their proposed assignments and predicted depolarization values are listed in Tables 9 and 12.

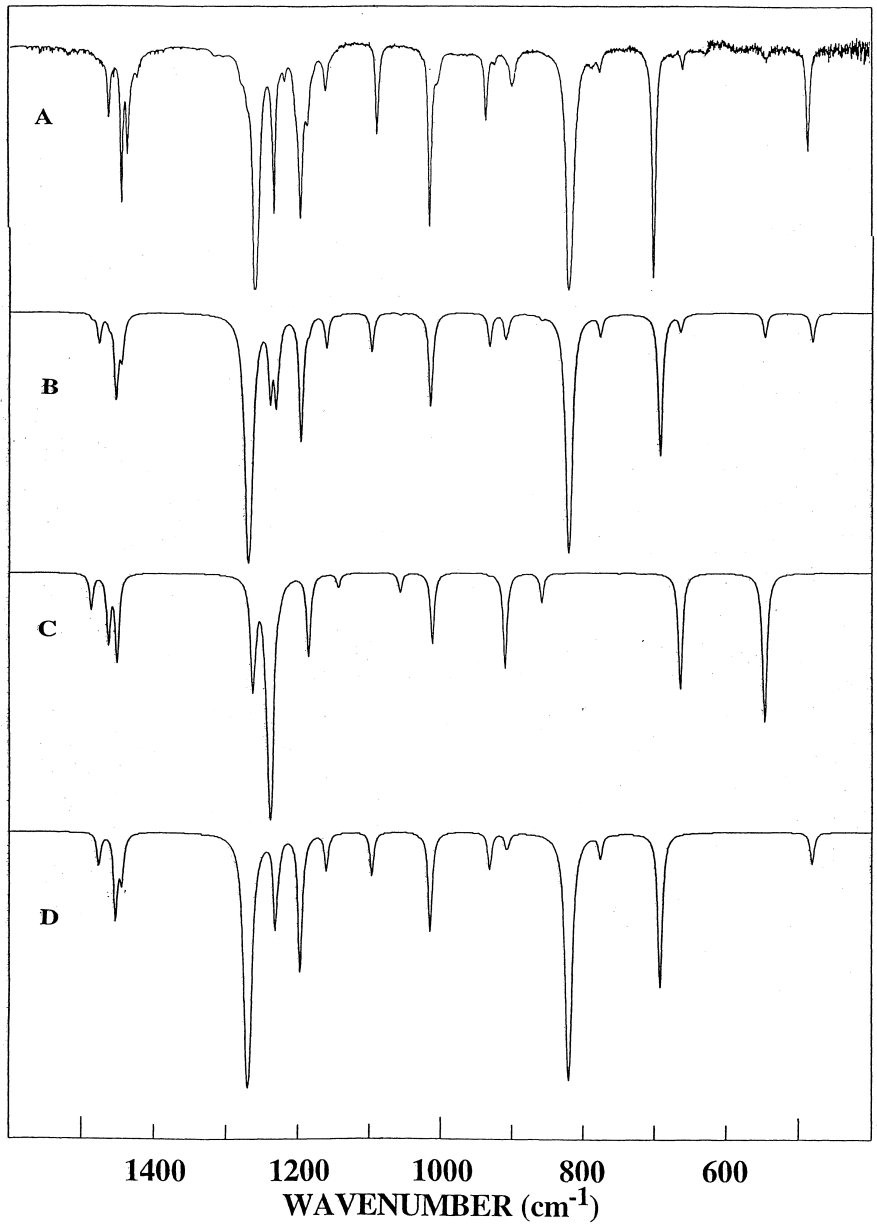

Figure 7. Comparison of experimental and predicted infrared spectra of bromocyclobutane: (A) Xe solution at -70 ºC; (B) simulated spectrum of mixture of equatorial and axial conformers at -70^{o}C with ΔH = 291 cm^{-1}; (C) simulated spectrum of axial conformer; (D) simulated spectrum of equatorial conformer.

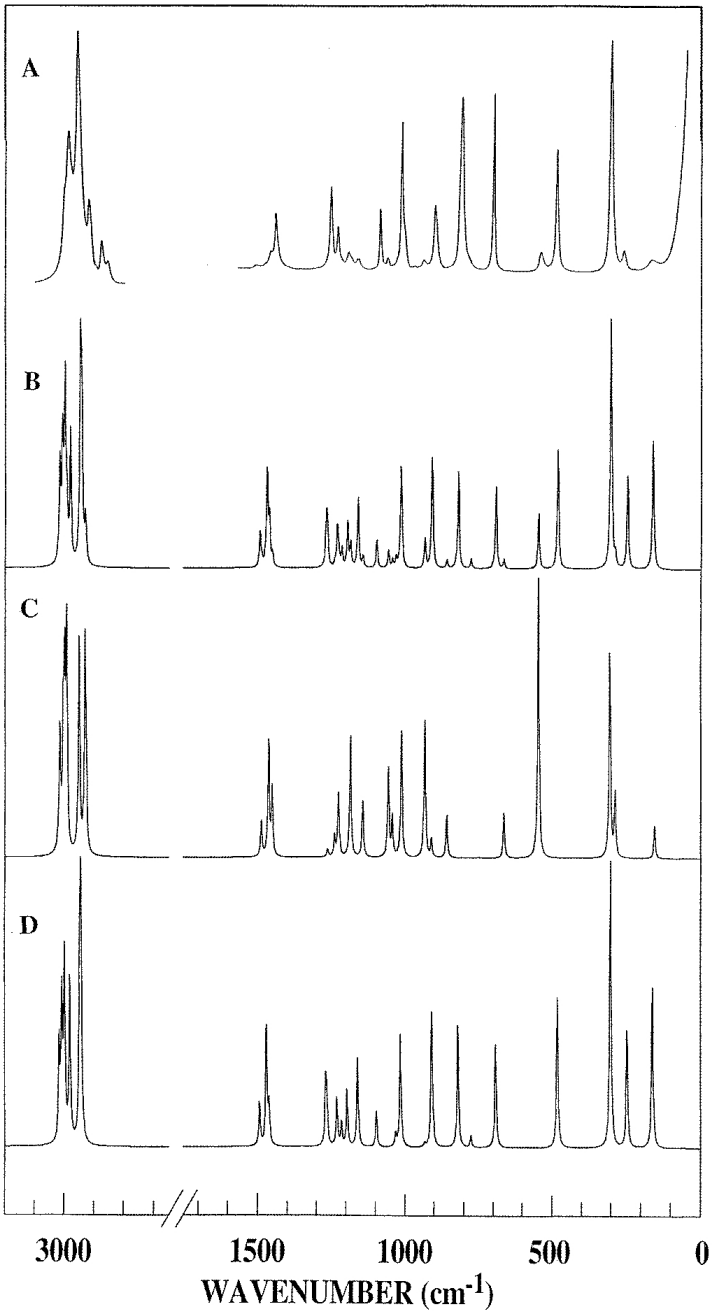

Figure 8. Comparison of experimental and predicted Raman spectra of bromocyclobutane: (A) liquid; (B) simulated spectrum of the mixture of equatorial and axial conformers at 25ºC with ΔH = 291 cm^{-1}; (C) simulated spectrum of axial conformer; (D) simulated spectrum of equatorial conformer.

TABLE 9. Observed[a] and calculated[b] frequencies for the *equatorial* conformer of bromocyclobutane.

		Fundamental	ab initio	Fixed scaled[c]	IR int.	Raman act.	dp ratio	IR gas	Raman gas[d]	IR Xe Soln.	Raman liquid[e]	IR solid	Raman solid[d]	P.E.D.[f]	Band Contour		
															A	B	C
A'	ν_1	β-CH_2 antisymmetric stretch	3215	3016	28.5	43.4	0.61	3005	-	2996	-	3003/2993	-	$66S_1,28S_2$	59	-	41
	ν_2	γ-CH_2 antisymmetric stretch	3196	2998	5.0	82.0	0.43	2996	-	-	-	-	2994	$70S_2,22S_1$	3	-	97
	ν_3	CH stretch	3177	2980	1.6	71.6	0.49	2988	-	-	-	-	2980	$87S_3,12S_1$	74	-	26
	ν_4	β -CH_2 symmetric stretch	3140	2946	4.7	199.0	0.05	2962	-	2950	2945	2950/2946	2945	$86S_4,12S_5$	-	-	100
	ν_5	γ -CH_2 symmetric stretch	3136	2942	22.9	67.7	0.44	2931	-	2918	2912	2916/2906	2906	$87S_5,13S_4$	96	-	4
	ν_6	β-CH_2 scissors	1574	1477	1.8	6.7	0.64	1476	~1470	1464	1460	1461/1459	1458	$64S_6,34S_7$	99	-	1
	ν_7	γ-CH_2 scissors	1549	1453	5.4	18.1	0.74	1452	1449	1445	1438	1441/1434	1443	$65S_7,34S_6$	16	-	84
	ν_8	β-CH_2 wag	1339	1270	50.0	7.4	0.62	1263	1262	1257	1252	1264/1254	1255	$50S_8,28S_9$	15	-	85
	ν_9	CH in-plane bend	1299	1232	5.9	5.8	0.74	1235	1234	1232	1227	1236/1232	1233	$22S_9,29S_8,28S_{10},10S_{13}$	100	-	-
	ν_{10}	β-CH_2 twist	1262	1197	10.3	6.6	0.75	1199	1204	1195	1190	1204/1194	1195	$46S_{10},18S_{15},11S_9$	59	-	41
	ν_{11}	β-CH_2 rock	1156	1097	2.5	3.7	0.21	1093	1091	1088	1084	1090/1085	1090	$33S_{11},25S_{12},13S_{17}$	73	-	27
	ν_{12}	Ring breathing	1070	1015	6.6	10.7	0.20	1017	1016	1014	1012	1016/1014	1016	$67S_{12},14S_{11}$	57	-	43
	ν_{13}	Ring deformation 1	955	906	0.5	2.0	0.42	900	-	900	-	906/902	905	$55S_{13},15S_{15},13S_8$	96	-	4
	ν_{14}	Ring deformation 2	864	820	39.4	8.9	0.17	827	824	818	808	811/802	803	$34S_{14},20S_{15},16S_{13},11S_{16}$	26	-	74
	ν_{15}	γ-CH_2 rock	729	692	12.2	6.1	0.24	701	701	700	698	702/699	701	$32S_{15},29S_{14},13S_{16}$	100	-	-
	ν_{16}	C-Br stretch	508	482	1.8	5.5	0.33	487	486	487	481	485/476	484	$26S_{16},22S_{14},17S_{11},12S_9,11S_{17}$	84	-	16
	ν_{17}	C-Br in-plane bend	318	302	3.9	5.4	0.29	302	301		298	299	303	$21S_{17},17S_{18},46S_{16}$	97	-	3
	ν_{18}	Ring puckering	170	161	0.6	1.1	0.28	-	150		150	-	175	$60S_{18},21S_{16},16S_9$	100	-	-
A"	ν_{19}	β-CH_2 antisymmetric stretch	3206	3007	15.1	62.5	0.75	2993		2986	2977	2983/2980	2971	$100S_{19}$	-	100	-
	ν_{20}	β -CH_2 symmetric stretch	3138	2944	28.2	2.2	0.75	2975		2963	-	2971/2969	2960	$100S_{20}$	-	100	-
	ν_{21}	β -CH_2 scissors	1540	1445	2.6	5.9	0.75	1442		1437	1438	1438/1425	1434	$99S_{21}$	-	100	-
	ν_{22}	CH out-of-plane bend	1334	1266	1.7	5.6	0.75	1280		1277	-	1271/1259	1270	$47S_{22},29S_{23},10S_{29}$	-	100	-
	ν_{23}	γ-CH_2 wag	1293	1227	0.8	0.3	0.75	1228		1228	1227	1227/1221	1226	$29S_{23},24S_{27},18S_{25},17S_{22},11S_{24}$	-	100	-
	ν_{24}	β-CH_2 wag	1282	1216	0.01	2.7	0.75	-		1218	-	-	1220	$43S_{24},20S_{23},19S_{25},12S_{22}$	-	100	-
	ν_{25}	γ-CH_2 twist	1224	1161	2.1	10.0	0.75	1161		1161	1160	1166/1160	1166	$29S_{25},39S_{24},11S_{26}$	-	100	-
	ν_{26}	Ring deformation 1	1087	1031	0.1	1.2	0.75	-		1030	1025	1031/1020	1034	$27S_{26},34S_{28},28S_{27}$	-	100	-
	ν_{27}	β -CH_2 twist	982	932	2.1	0.3	0.75	938		937	933	942/938	940	$34S_{27},21S_{22},20S_{26},16S_{25}$	-	100	-
	ν_{28}	Ring deformation 2	958	909	0.6	10.2	0.75	907		891	896	896/892	896	$58S_{28},24S_{26}$	-	100	-
	ν_{29}	β-CH_2 rock	818	776	1.3	0.8	0.75	786		778	785	785/778	779	$78S_{29},13S_{25}$	-	100	-
	ν_{30}	C-Br out-of-plane bend	259	246	0.2	1.6	0.75	245			249	249	255	$91S_{30}$	-	100	-

[a] Observed spectra: gas, Xe, and solid are IR while liquid is Raman.

[b] MP2(full)/6-31G(d) *ab initio* calculations, scaled frequencies, infrared intensities (km/mol), Raman activities ($Å^4$/u), depolarization ratios (dp) and potential energy distributions (P.E.D.s).

[c] Scaled frequencies with scaling factors of 0.88 for the CH stretches, β-CH_2 and γ-CH_2 scissors and 0.90 for all other modes.
[d] Frequencies listed are taken from reference [66].
[e] Frequencies listed are taken from reference [65].
[f] Symmetry coordinates with P.E.D. contribution less than 10% are omitted.

TABLE 10. Observed[a] and calculated[b] frequencies for the *equatorial* conformer of bromocyclobutane-d_1.

		Fundamental	ab initio	fixed scaled[c]	IR int.	Raman act.	dp ratio	IR gas[d]	Raman Liquid[d]	P.E.D.[e]	Band Contour		
											A	B	C
A'	ν_1	β-CH_2 antisymmetric stretch	3224	3024	25.1	53.5	0.74	3001	-	$64S_1,36S_2$	59	-	41
	ν_2	γ-CH_2 antisymmetric stretch	3206	3007	4.8	81.0	0.54	2989	-	$62S_2,36S_1$	2	-	98
	ν_4	β-CH_2 symmetric stretch	3152	2957	4.4	195.4	0.05	2962	2953	$87S_4,12S_5$	76	-	24
	ν_5	γ-CH_2 symmetric stretch	3148	2953	23.6	71.8	0.42	2936	2926	$87S_5,12S_4$	95	-	5
	ν_3	CD stretch	2351	2205	3.2	31.9	0.29	2237	2228	$98S_3$	99	-	1
	ν_6	β-CH_2 scissors	1579	1481	1.8	6.9	0.64	1459	-	$64S_6,34S_7$	15	-	85
	ν_7	γ-CH_2 scissors	1555	1459	5.3	18.2	0.74	1451	1442	$66S_7,34S_6$	9	-	91
	ν_8	β-CH_2 wag	1324	1256	19.0	2.2	0.37	1250		$84S_8,12S_{14}$	14	-	86
	ν_{10}	β-CH_2 twist	1274	1209	0.4	11.7	0.75	1210	1207	$81S_{10},10S_{15}$	95	-	5
	ν_{11}	β-CH_2 rock	1183	1122	19.1	1.7	0.40	1119	1116	$51S_{11},17S_{15},14S_9,12S_{18}$	46	-	54
	ν_{12}	Ring breathing	1108	1051	28.7	9.4	0.22	1045	1038	$80S_{12}$	99	-	1
	ν_9	CD in-plane bend	969	919	15.6	12.7	0.25	914	907	$17S_9,18S_{14},16S_{18},14S_{11},11S_{16},10S_{13}$	97	-	3
	ν_{13}	Ring deformation 1	948	899	17.6	3.0	0.24	896	899	$35S_{13},16S_{15},16S_{11},14S_{14},10S_9$	85	-	15
	ν_{14}	Ring deformation 2	804	763	7.3	1.3	0.22	762	759	$17S_{14},27S_{15},18S_9,17S_{16}$	99	-	1
	ν_{15}	γ-CH_2 rock	714	677	13.0	6.8	0.24	688	684	$21S_{15},33S_{13},17S_{17},14S_{16}$	87	-	13
	ν_{16}	C-Br stretch	501	475	2.0	5.7	0.31	478	478	$28S_{16},21S_{13},16S_{11},12S_{17},11S_9$	91	-	9
	ν_{17}	C-Br in-plane bend	318	302	3.8	5.3	0.29	295	300	$22S_{17},45S_{16},17S_{18}$	96	-	4
	ν_{18}	Ring puckering	169	160	0.6	1.1	0.28	-	150	$60S_{18},21S_{16},16S_9$	100	-	-
A"	ν_{19}	β-CH_2 antisymmetric stretch	3217	3018	15.2	63.0	0.75	-	-	$100S_{19}$	-	100	-
	ν_{20}	β -CH_2 symmetric stretch	3149	2954	28.4	2.2	0.75	2989	2985	$100S_{20}$	-	100	-
	ν_{21}	β -CH_2 scissors	1546	1450	2.6	5.9	0.75	1442	1463	$99S_{21}$	-	100	-
	ν_{23}	γ-CH_2 wag	1314	1247	2.1	2.4	0.75	~1250	1244	$74S_{23}$	-	100	-
	ν_{24}	β-CH_2 wag	1290	1224	0.1	2.0	0.75	-	1234	$54S_{24},32S_{25}$	-	100	-
	ν_{25}	γ-CH_2 twist	1228	1165	2.0	9.7	0.75	1167	1162	$26S_{25},40S_{24},12S_{27},12S_{26}$	-	100	-
	ν_{22}	CD out-of-plane bend	1158	1099	0.7	2.4	0.75	-	1095	$30S_{22},23S_{27},16S_{29},10S_{28}$	-	100	-
	ν_{26}	Ring deformation 1	1087	1031	0.04	1.5	0.75	-	1016	$22S_{26},39S_{27},28S_{28}$	-	100	-
	ν_{28}	Ring deformation 2	960	911	1.0	9.4	0.75	-	-	$51S_{28},32S_{26}$	-	100	-
	ν_{27}	β-CH_2 twist	867	823	0.01	0.1	0.75	-	810	$13S_{27},26S_{22},23S_{29},20S_{25},11S_{26}$	-	100	-
	ν_{29}	β-CH_2 rock	779	739	1.9	1.8	0.75	-	741	$50S_{29},42S_{22}$	-	100	-
	ν_{30}	C-Br out-of-plane bend	257	244	0.2	1.6	0.75	-	250	$91S_{30}$	-	100	-

[a] Observed spectra: gas, Xe, and solid are IR while liquid is Raman.

[b] MP2(full)/6-31G(d) *ab initio* calculations, scaled frequencies, infrared intensities (km/mol), Raman activities ($Å^4$/u), depolarization ratios (dp) and potential energy distributions (P.E.D.s).

[c] Scaled frequencies with scaling factors of 0.88 for the CH stretches, β-CH_2 and γ-CH_2 scissors and 0.90 for all other modes.

[d] Frequencies listed are taken from reference [65].

[e] Symmetry coordinates with P.E.D. contribution less than 10% are omitted.

TABLE 11. Observed[a] and calculated[b] frequencies for the *equatorial* conformer of bromocyclobutane-d_4.

		Fundamental	ab initio	Fixed scaled[c]	IR int.	Raman act.	dp ratio	IR gas[d]	Raman Liquid[d]	P.E.D.[e]	Band Contour		
											A	B	C
A'	ν_2	γ-CH_2 antisymmetric stretch	3212	3013	16.4	83.8	0.71	2990	2977	$99S_2$	57	-	43
	ν_3	CH stretch	3192	2994	5.3	70.8	0.24	~2990	~2977	$99S_3$	7	-	93
	ν_5	γ-CH_2 symmetric stretch	3148	2953	28.6	106.9	0.12	2966	2948	$99S_5$	16	-	84
	ν_1	β-CD_2 antisymmetric stretch	2392	2244	6.4	27.2	0.68	2203	2192	$99S_1$	99	-	1
	ν_4	β-CD_2 symmetric stretch	2294	2152	0.4	73.1	0.13	-	2154	$98S_4$	5	-	95
	ν_7	γ-CH_2 scissors	1563	1466	2.0	11.6	0.70	1460	1448	$99S_7$	56	-	44
	ν_9	CH in-plane bend	1299	1232	55.6	7.0	0.73	1222	1212	$62S_9,25S_{17}$	53	-	47
	ν_6	β-CD_2 scissors	1213	1138	3.8	5.4	0.25	1143	1134	$56S_6,30S_{12}$	94	-	6
	ν_8	β-CD_2 wag	1169	1109	3.4	3.9	0.37	1097	1088	$35S_8,42S_{14}$	-	-	100
	ν_{10}	β-CD_2 twist	1098	1042	1.9	5.1	0.59	-	-	$20S_{10},39S_{15},16S_{11}$	99	-	1
	ν_{12}	Ring breathing	1029	976	6.5	7.8	0.32	971	968	$34S_{12},20S_6,18S_{10}$	77	-	23
	ν_{11}	β-CD_2 rock	953	904	15.9	4.7	0.63	935	933	$16S_{11},22S_{10},20S_{12},10S_6$	82	-	18
	ν_{13}	Ring deformation 1	831	788	15.9	3.6	0.11	786	770	$44S_{13},18S_8,12S_{11},11S_{15}$	100	-	-
	ν_{14}	Ring deformation 2	784	744	19.4	12.0	0.18	751	740	$25S_{14},30S_8,18S_{17},14S_{13}$	99	-	1
	ν_{15}	γ-CH_2 rock	655	621	2.9	3.3	0.40	558	558	$30S_{15},29S_{10},11S_{11},10S_{13}$	96	-	4
	ν_{16}	C-Br stretch	442	419	2.0	5.7	0.34	430	422	$34S_{17},23S_{11},22S_{13}$	60	-	40
	ν_{17}	C-Br in-plane bend	294	279	3.1	3.9	0.29	275	280	$26S_{16},34S_{17},16S_{18}$	99	-	1
	ν_{18}	Ring puckering	158	150	0.5	0.9	0.27	-	-	$64S_{18},19S_{16},14S_9$	100	-	-
A"	ν_{19}	β-CD_2 antisymmetric stretch	2390	2242	7.4	29.9	0.75	2258	2244	$99S_{19}$	-	100	-
	ν_{20}	β-CD_2 symmetric stretch	2289	2147	15.1	1.4	0.75	2166	2170	$99S_{20}$	-	100	-
	ν_{22}	CH out-of-plane bend	1318	1250	2.5	6.3	0.75	1248	1240	$33S_{22},49S_{23}$	-	100	-
	ν_{23}	γ-CH_2 wag	1268	1203	0.2	3.3	0.75	-	-	$37S_{23},50S_{22}$	-	100	-
	ν_{25}	γ-CH_2 twist	1223	1160	0.1	4.3	0.75	-	1167	$64S_{25},12S_{26}$	-	100	-
	ν_{21}	β-CD_2 scissors	1147	1076	2.8	5.0	0.75	1050	1035	$72S_{21},14S_{25}$	-	100	-
	ν_{24}	β-CD_2 wag	1069	1014	0.8	0.3	0.75	-	1011	$33S_{24},59S_{28}$	-	100	-
	ν_{26}	Ring deformation 1	991	940	0.1	2.2	0.75	909	902	$47S_{26},17S_{21},14S_{24}$	-	100	-
	ν_{28}	Ring deformation 2	868	823	1.2	7.1	0.75	823	823	$30S_{28},46S_{24},15S_{26}$	-	100	-
	ν_{27}	β-CD_2 twist	759	720	0.3	1.6	0.75	-	704	$92S_{27}$	-	100	-

ν_{29}	β-CD_2 rock	656	622	1.0	0.2	0.75	626	626	$86S_{29}$	-	100	-
ν_{30}	C-Br out-of-plane bend	238	226	0.3	1.5	0.75	-	232	$89S_{30}$	-	100	-

[a] Observed spectra: gas, Xe, and solid are IR while liquid is Raman.

[b] MP2(full)/6-31G(d) *ab initio* calculations, scaled frequencies, infrared intensities (km/mol), Raman activities ($Å^4$/u), depolarization ratios (dp) and potential energy distributions (P.E.D.s).

[c] Scaled frequencies with scaling factors of 0.88 for the CH stretches, β-CD2 and γ-CH_2 scissors and 0.90 for all other modes.

[d] Frequencies listed are taken from reference [65].

[e] Symmetry coordinates with P.E.D. contribution less than 10% are omitted.

TABLE 12. Observed[a] and calculated[b] frequencies for the *axial* conformer of bromocyclobutane.

		Fundamental	ab initio	Fixed scaled[c]	IR int.	Raman act.	dp ratio	IR gas	IR gas[d]	IR Xe Soln.	Raman liquid[d]	P.E.D.[d]	Band Contour		
													A	B	C
A'	ν_1	γ-CH_2 antisymmetric stretch	3214	3015	24.8	53.4	0.74					$77S_1,22S_2$	78	-	22
	ν_2	β-CH_2 antisymmetric stretch	3197	2999	4.7	72.4	0.66					$66S_2,22S_1$	90	-	10
	ν_3	CH stretch	3190	2992	11.8	97.5	0.16					$96S_3$	1	-	99
	ν_4	γ -CH_2 symmetric stretch	3145	2950	21.6	93.2	0.14					$99S_4$	-	-	100
	ν_5	β -CH_2 symmetric stretch	3123	2930	12.9	179.5	0.16					$89S_5,10S_2$	44	-	56
	ν_6	γ-CH_2 scissors	1567	1470	2.0	5.4	0.51	1483		1480		$55S_6,43S_7$	47	-	53
	ν_7	β-CH_2 scissors	1542	1447	4.2	17.4	0.73	1459		1459		$56S_7,44S_6$	68	-	32
	ν_8	β-CH_2 wag	1332	1264	7.2	0.9	0.72	1264		1261		$80S_8,10S_{13}$	14	-	86
	ν_9	CH in-plane bend	1306	1239	42.4	2.5	0.24	1239		~1237		$34S_9,43S_{10},11S_{17}$	17	-	83
	ν_{10}	β-CH_2 twist	1250	1186	5.2	14.1	0.74	1187		1187		$31S_{10},20S_9,19S_{15},14S_{11}$	96	-	4
	ν_{11}	β-CH_2 rock	1114	1057	1.1	8.9	0.18	1064	-	1068	1061	$37S_{11},18S_{17},14S_{12},11S_{10}$	73	-	27
	ν_{12}	Ring breathing	1066	1011	4.4	12.0	0.24	1007	-	1006	1005	$79S_{12}$	90	-	10
	ν_{13}	Ring deformation 1	960	911	2.2	0.9	0.31					$67S_{13},15S_8$	94	-	6
	ν_{14}	Ring deformation 2	904	858	1.6	3.3	0.42	857		~856		$48S_{14},20S_{15},12S_{11}$	3	-	97
	ν_{15}	γ-CH_2 rock	700	664	8.1	2.5	0.52	676		661		$36S_{15},38S_{14},10S_{11}$	100	-	-
	ν_{16}	C-Br stretch	577	547	11.7	12.2	0.26	550	549	545	538	$67S_{16},12S_{11}$	86	-	14
	ν_{17}	C-Br in-plane bend	321	305	1.2	3.9	0.20	305				$22S_{17},31S_{18},27S_{16}$	97	-	3
	ν_{18}	Ring puckering	162	154	0.3	0.2	0.75					$50S_{18},25S_{17},19S_9$	84	-	16
A"	ν_{19}	β-CH_2 antisymmetric stretch	3202	3004	9.7	49.8	0.75					$90S_{19},10S_{20}$	-	100	-
	ν_{20}	β -CH_2 symmetric stretch	3119	2926	20.8	17.6	0.75					$90S_{20},10S_{19}$	-	100	-
	ν_{21}	β -CH_2 scissors	1529	1434	5.6	10.0	0.75	1424		1424		$100S_{21}$	-	100	-
	ν_{22}	γ-CH_2 wag	1328	1260	2.1	0.1	0.75	-		1254		$61S_{22},16S_{25},12S_{28}$	-	100	-
	ν_{23}	γ-CH_2 twist	1293	1227	0.2	7.0	0.75					$43S_{23},24S_{24},13S_{25}$	-	100	-
	ν_{24}	β-CH_2 wag	1290	1224	0.2	1.3	0.75					$48S_{24},31S_{25},17S_{22}$	-	100	-
	ν_{25}	CH out-of-plane bend	1206	1144	0.8	6.2	0.75	1130		~1133		$18S_{25},23S_{23},17S_{27},15S_{24},14S_{26},11S_{22}$	-	100	-
	ν_{26}	β -CH_2 twist	1099	1043	0.0	3.9	0.75					$59S_{26},13S_{29},11S_{23}$	-	100	-
	ν_{27}	Ring deformation 2	984	934	0.1	11.8	0.75					$70S_{27},10S_{24}$	-	100	-
	ν_{28}	Ring deformation 1	959	910	4.2	0.6	0.75	908		907		$54S_{28},12S_{29},10S_{26},10S_{25}$	-	100	-
	ν_{29}	β-CH_2 rock	791	750	0.02	0.04	0.75					$64S_{29},20S_{28},11S_{23}$	-	100	-
	ν_{30}	C-Br out-of-plane bend	302	287	0.1	1.1	0.75	289				$94S_{30}$	-	100	-

[a] Observed spectra: gas, Xe, and solid are IR while liquid is Raman.

[b] MP2(full)/6-31G(d) *ab initio* calculations, scaled frequencies, infrared intensities (km/mol), Raman activities ($Å^4$/u), depolarization ratios (dp) and potential energy distributions (P.E.D.s).
[c] Scaled frequencies with scaling factors of 0.90 for all modes.
[d] Frequencies listed are taken from reference [66].
[e] Symmetry coordinates with P.E.D. contribution less than 10% are omitted.

AB INITIO CALCULATIONS

The LCAO-MO-SCF restricted Hartree-Fock calculations were performed with the Gaussian-03 program [22] using Gaussian-type basis functions. The energy minima with respect to nuclear coordinates were obtained by the simultaneous relaxation of all geometric parameters using the gradient method of Pulay [29]. A variety of basis sets as well as the corresponding ones with diffuse functions were employed with the Møller-Plesset perturbation method [21] to the second order MP2 with full electron correlation as well as with the density functional theory by the B3LYP method. The predicted conformational energy differences are listed in Table 13.

TABLE 13. Calculated energies in (H) and energy differences (cm^{-1}) for the two conformers, and transition states of bromocyclobutane.

	Energy[a], E		Energy Differences	
Method/Basis Set	*equatorial*	*axial*[b]	*planar ring*[b]	*planar ring*[c]
MP2(full)/6-31G(d)	1.092514	354	1042	688
MP2(full)/6-31+G(d)	1.120535	555		
MP2(full)/6-31G(d,p)	1.150069	370		
MP2(full)/6-31+G(d,p)	1.177130	563		
MP2(full)/6-311G(d,p)	4.116611	578		
MP2(full)/6-311+G(d,p)	4.120547	586	1493	907
MP2(full)/6-311G(2d,2p)	4.178448	579		
MP2(full)/6-311+G(2d,2p)	4.178448	572		
MP2(full)/6-311G(2df,2pd)	4.178448	567	1224	657
MP2(full)/6-311+G(2df,2pd)	4.283381	576	1216	640
MP2(full)/aug-cc-pVTZ	4.098934	456		
Average[d]	-	560 ± 46	1244 ± 161	723 ± 107
B3LYP/6-31G(d)	3.323143	459	535	76
B3LYP/6-31+G(d)	3.347769	560		
B3LYP/6-311G(d,p)	5.805924	589		
B3LYP/6-311+G(d,p)	5.807273	605	622	17
B3LYP/6-311G(2d,2p)	5.808999	578		
B3LYP/6-311+G(2d,2p)	5.808999	590		

B3LYP/6-311G(2df,2pd)	5.808999	602	606	4
B3LYP/6-311+G(2df,2pd)	5.814938	612	610	-2
B3LYP/aug-cc-pVTZ	5.905011	599		
Average B3LYP predictions	-	569 ± 47	593 ± 39	24 ± 35

[a] Energy of conformer is given as –(E+2725) H.
[b] Difference is relative to *equatorial* form and given in cm^{-1}.
[c] Difference is relative to *axial* form and given in cm^{-1}.
[d] Average from the seven largest basis sets.

In order to obtain descriptions of the molecular motions involved in the fundamental modes of bromocyclobutane, a normal coordinate analysis has been carried out. The force field in Cartesian coordinates was obtained with the Gaussian 03 program at the MP2(full) level with the 6-31G(d) basis set. The internal coordinates used to calculate the **G** and **B** matrices are given in Table 14 with the atomic numbering shown in Fig. 9. By using the **B** matrix [30], the force field in Cartesian coordinates was converted to a force field in internal coordinates. Subsequently, 0.90 was used as scaling factor, along with the geometric average of scaling factors for interaction force constants, to obtain the fixed scaled force field and resultant wavenumbers. A set of symmetry coordinates was used (Table S2) to determine the corresponding potential energy distributions (P.E.D.s). A comparison between the observed and calculated wavenumbers, along with the calculated infrared intensities, Raman activities, depolarization ratios and potential energy distributions for the *equatorial* and *axial* conformers of bromocyclobutane, are given in Tables 9 and 12, respectively.

TABLE 14. Structural parameters (Å and degrees), rotational constants (MHz) and dipole moments (Debye) for *equatorial* and *axial* ^{79}*bromo*cyclobutane.

Structural Parameters	Int. coor.	MP2(full)/6-311+G(d,p)		Microwave[a]	Adjusted r_0 [b]	Predicted[c]
		Eq	Ax	Eq	Eq	Ax
rC_α-Br	R_1	1.938	1.948	1.939*	1.942(3)	1.952
rC_α-C_β,$C_{\beta'}$	R_2	1.535	1.542	1.540(3)	1.541(3)	1.548
rC_γ-C_β,$C_{\beta'}$	R_3	1.551	1.548	1.548(3)	1.552(3)	1.546
rC_α-H	r_1	1.092	1.090	1.096*	1.092(2)	1.090
rC_β-H_1, $C_{\beta'}$-H_1	r_2	1.093	1.091	1.096*	1.093(2)	1.091
rC_β-H_2, $C_{\beta'}$-H_2	r_3	1.092	1.095	1.096*	1.092(2)	1.095
rC_γ-H_1	r_4	1.091	1.092	1.096*	1.091(2)	1.092
rC_γ-H_2	r_5	1.093	1.092	1.096*	1.093(2)	1.092
$\angle C_\beta C_\alpha$Br	ϕ_1	118.9	111.8	118.0	118.4(5)	111.3
$\angle C_\beta C_\alpha C_{\beta'}$	θ_1	89.10	88.28	88.68(1)	89.7(5)	88.7
$\angle C_\gamma C_\beta C_{\alpha,}$	θ_2	86.35	88.13	91.61(1)	86.8(5)	88.7
$\angle C_\beta C_\gamma C_{\beta'}$	θ_3	87.93	87.82	88.10(1)	88.9(5)	88.8
$\angle$ $HC_\alpha C_\beta$	σ_1	111.4	119.3	109.6	111.8(5)	119.6
$\angle$ HC_αBr	σ_2	106.4	105.8	111	106.4(5)	105.8
$\angle$ $H_1C_\beta C_\alpha$	λ_1	110.4	118.0	115.8	110.4(5)	118.0
$\angle$ $H_1C_\beta C_\gamma$	λ_2	110.4	119.1	115.6	106.8(5)	121.7
$\angle$ $H_2C_\beta C_\alpha$	λ_3	117.9	109.2	115.9	117.9(5)	109.2
$\angle$ $H_2C_\beta C_\gamma$	λ_4	119.5	111.0	115.7	122.5(5)	107.6
$\angle$ $H_1C_\beta H_2$	λ_5	110.1	109.6	108.7	110.1(5)	109.7
$\angle$ $H_1C_\gamma C_\beta$	π_1	117.5	111.2	114.1	118.6(5)	109.3
$\angle$ $H_2C_\gamma C_\beta$	π_2	111.4	117.8	114.1	109.7(5)	119.1
$\angle$ $H_1C_\gamma H_2$	π_3	109.6	109.5	110.7*	109.6(5)	109.5
$\tau C_\gamma C_\beta C_\beta C_\alpha$	τ_1	34.4	-29.4	29.4(1)	29.8(5)	-24.0
A(MHz)		10208.3	7794.0	10003(13)	10003.4	7876.0
B(MHz)		1624.1	1904.4	1629.41(3)	1629.60	1882.4
C(MHz)		1485.1	1811.9	1488.48(3)	1488.33	1781.0
$\lvert\mu_a\rvert$		2.644	2.406		2.637	2.447
$\lvert\mu_b\rvert$		0.000	0.000		0.000	0.000
$\lvert\mu_c\rvert$		0.348	0.749		0.406	0.758
$\lvert\mu_t\rvert$		2.667	2.520		2.668	2.562

[a]Ref. [36]

[b]adjusted parameters using the microwave data from reference [36] for the given ground states.

[c]predicted parameters using the equatorial adjustments.

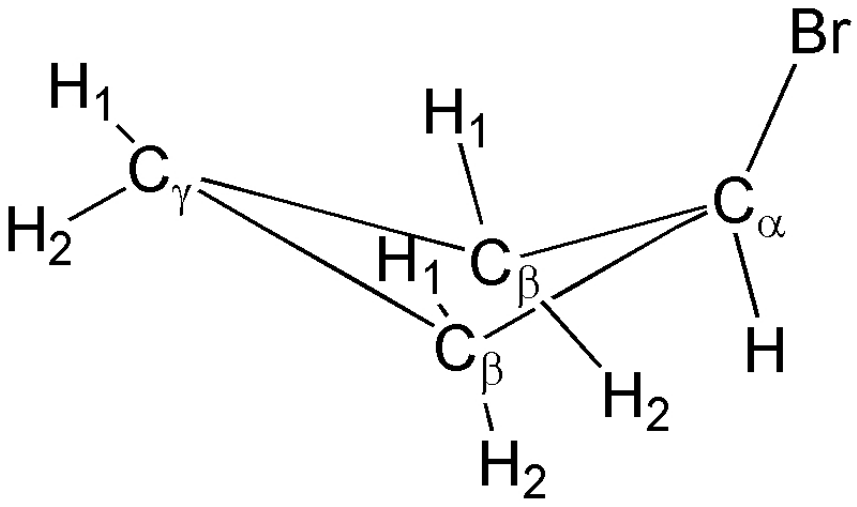

Figure 9. Bromocyclobutane showing atomic numbering.

The infrared spectra were predicted from the MP2(full)/6-31G(d) calculations. The predicted scaled frequencies were used together with a Lorentzian function to obtain the calculated spectra. Infrared intensities determined from MP2(full)/6-31G(d) calculations were obtained based on the dipole moment derivatives with respect to Cartesian coordinates. The derivatives were transformed with respect to normal coordinates by $(\partial\mu_u/\partial Q_i) = \sum_j (\partial\mu_u/\partial X_j)L_{ij}$, where Q_i is the i^{th} normal coordinate, X_j is the j^{th} Cartesian displacement coordinate, and L_{ij} is the transformation matrix between the Cartesian displacement coordinates and the normal coordinates. The infrared intensities were then calculated by $[(N\pi)/(3c^2)]\ [(\partial\mu_x/\partial Q_i)^2 + (\partial\mu_y/\partial Q_i)^2 + (\partial\mu_z/\partial Q_i)^2]$. In Fig. 7 a comparison of the experimental and simulated infrared spectra of bromocyclobutane is

shown for the spectral region from 400 to 1600 cm^{-1}. The predicted spectrum is in relatively good agreement with the experimental spectrum which indicates the utility of the scaled predicted frequencies and intensities for supporting the vibrational assignment.

To further support the vibrational assignments, we have simulated the Raman spectra from the *ab initio* MP2(full)/6-31G(d) results (Fig. 8). The evaluation of Raman activity by using the analytical gradient methods has been developed [34,31-33]. The activity S_j can be expressed as: $S_j = g_j (45\alpha_j^2 + 7\beta_j^2)$, where g_j is the degeneracy of the vibrational mode j, α_j is the derivative of the isotropic polarizability, and β_j is that of the anisotropic polarizability. To obtain the polarized Raman scattering cross sections, the polarizabilities are incorporated into S_j by multiplying S_j with $(1-\rho_j)/(1+\rho_j)$, where ρ_j is the depolarization ratio of the j^{th} normal mode. The Raman scattering cross sections and calculated wavenumbers obtained from the Gaussian 03 program were used together with a Lorentzian function to obtain the simulated Raman spectra. The predicted spectrum of the mixture should be compared to that of the Raman spectrum of the liquid (Fig. 8) and there is reasonable agreement with the relative intensities of the bands again this shows good utility of the scaled predicted frequencies and intensities of the Raman spectra for supporting the vibrational assignment.

STRUCTURAL PARAMETERS

We have [51] shown that *ab initio* MP2(full)/6-311+G(d,p) calculations predict the r_0 structural parameters for more than fifty carbon-hydrogen distances better than 0.002Å compared to the experimentally determined values from isolated CH stretching frequencies which are compared [5] to previously determined values from earlier microwave studies. Thus, all of the carbon-hydrogen r_0 parameters can be taken from the

MP2(full)/6-311+G(d,p) predicted values for bromocyclobutane. Also, we have found [14] that we can obtain good structural parameters by adjusting the structural parameters from the *ab initio* calculations to fit the rotational constants obtained from the microwave experimental data. In order to reduce the number of independent variables, the structural parameters are separated into sets according to their types. Bond lengths in the same set keep their relative ratio which results in only two heavy atoms distances, i.e. C-C and C-Br, for bromocyclobutane. Also, the bond angles and torsional angles in the same set keep their differences in degrees. This assumption is based on the fact that the errors from *ab initio* calculations are systematic. Thus, it is possible to reduce the number of heavy atom independent structural parameters to five with the CC and CBr bond lengths, and the angles of BrCC, CCC and the ring puckering angle. Therefore, if the CH parameters are taken from the MP2(full)/6-311+G(d,p) calculations, then it should be possible to obtain "adjusted r_0" structural parameters for the equatorial conformer of bromocyclobutane by utilizing the previously reported [36] six rotational constants from the microwave study.

These determined adjusted r_0 parameters are listed in Table 14 and the final fit of the rotational constants is shown in Table 15. The differences are quite small with those for the B and C rotational constants fit to better than 0.2 MHz. The largest adjustment for the angles is associated with the ring puckering angle which changes from 34.4° to 29.8° and the largest distance change is the C_α-C_β ($C_{\beta'}$) bond which increased from 1.535 to 1.541 Å. The remaining changes were relatively small. It is somewhat difficult to estimate the uncertainties in these structural parameters, but it is believed those for the CH distances should be no more than ±0.002 Å and for the heavy atom distances ±0.003

Å, whereas the uncertainties in the angles is estimated to be ±0.5°. These parameters are expected to be more accurate than those that could be obtained from electron diffraction or microwave study alone or a microwave study with all atoms substituted to obtain r_s parameters.

TABLE 15. Comparison of rotational constants (MHz) obtained from modified *ab initio*, MP2(full)/6-311+G(d,p) structural parameters and the experimental values from the microwave spectra of two isotopes of bromocyclobutane.

Isotopomers	Rotational constant	Experimental[a]	Calculated	|Δ|
eq-$C_4H_7{}^{79}Br$	A	10003.4 ± 13	10003.43	(0.03)[b]
	B	1629.41 ± 0.03	1629.60	0.19
	C	1488.48 ± 0.03	1488.33	0.15
eq-$C_4H_7{}^{81}Br$	A	10002.6 ± 13	10002.89	(0.29)[b]
	B	1615.14 ± 0.03	1615.27	0.13
	C	1476.50 ± 0.03	1476.38	0.12

[a]Ref. [36].
[b]Values in parenthesis are difference from mean value.

Because the A rotational constants previously reported [36] have large uncertainties of ±13 MHz, we investigated whether changing their values by the uncertainty amounts, i.e. by increasing of decreasing them 13 MHz. These modified values were used along with the reported values of B and C for both isotopomers and the heavy atom structural parameters were again determined. These changes were negligible for the structural parameters with bond distances changing by a maximum 0.0009Å and

usually less with angles changing by less than 0.06°. These results indicate that the uncertainties given for the structural parameters in our study will clearly include any new error limits obtained for the A rotational constants as long as they are within the reported values from the earlier microwave study [36].

VIBRATIONAL ASSIGNMENT

In the initial complete vibrational analysis [65] there was considerable reliance on deuterium substitution to distinguish the normal modes which arise from the α-CH, and β, β'-CH_2, modes along with the d_5-isotopomer which left the γ-CH_2 group not deuterated. This information along with the infrared gas phase band contours with B-type bands for the A" modes along with the corresponding Raman lines being depolarized made it possible to provide reasonable assignments for most of the fundamentals. In the second study [66] the frequencies of the fundamentals were predicted from transferred force constants from cyclobutane which resulted in a few of the initial assignments [65] for the fundamentals to be reassigned. In the current study we have *ab initio* predicted frequencies, infrared band contours and intensities, Raman activities and depolarization values for both conformers to aid in the vibrational assignment. With these additional data again only a few of the assignments have been changed for the equatorial form along with more confident assignments for some of the fundamentals for the axial conformer.

In the most recent study [66] the earlier assigned fundamental bands [65] at 633 and 963 cm^{-1} were suggested as probable impurities and we support this probable origin since neither one of these bands were observed in our spectrum. Since we believe our sample is very pure we concur that these two bands are due to impurities and there

assignments as fundamentals is in error and they have been replace by bands at 900 and 1218 cm^{-1}. Also the assigned fundamentals [65] at 808 and 1181 cm^{-1} have been replaced as fundamentals with bands at 1235 cm^{-1} and 1280 cm^{-1}. These latter two assigned bands agree with the more recent assignment [66] with fundamentals at 1234 and 1282 cm^{-1} and these assigned fundamentals are listed in Table 9.

To obtain the enthalpy difference between the two conformers we search the spectrum for bands arising from the axial conformer which are significantly separated from the fundamentals of the equatorial form. Fifteen bands (Fig. 10) were identified as arising from the axial conformer (Table 12) but several of them were shoulders on the equatorial fundamentals and, therefore, could not be used to obtain ΔH. Due to the low intensities and close proximity to equatorial fundamentals as can be observed for the 1006, 1261 and 1424 cm^{-1} bands (Fig. 10), only three fundamentals 545, 661 and 1187 cm^{-1} were possible for determination of ΔH. The 661 cm^{-1} band, with it being very close to the frequency of carbon dioxide, left us with only two bands which were eventually utilized for ΔH. It should be noted that the spectrum from the xenon solution makes it possible to observe bands which normally are doubtful in the spectrum of the gas.

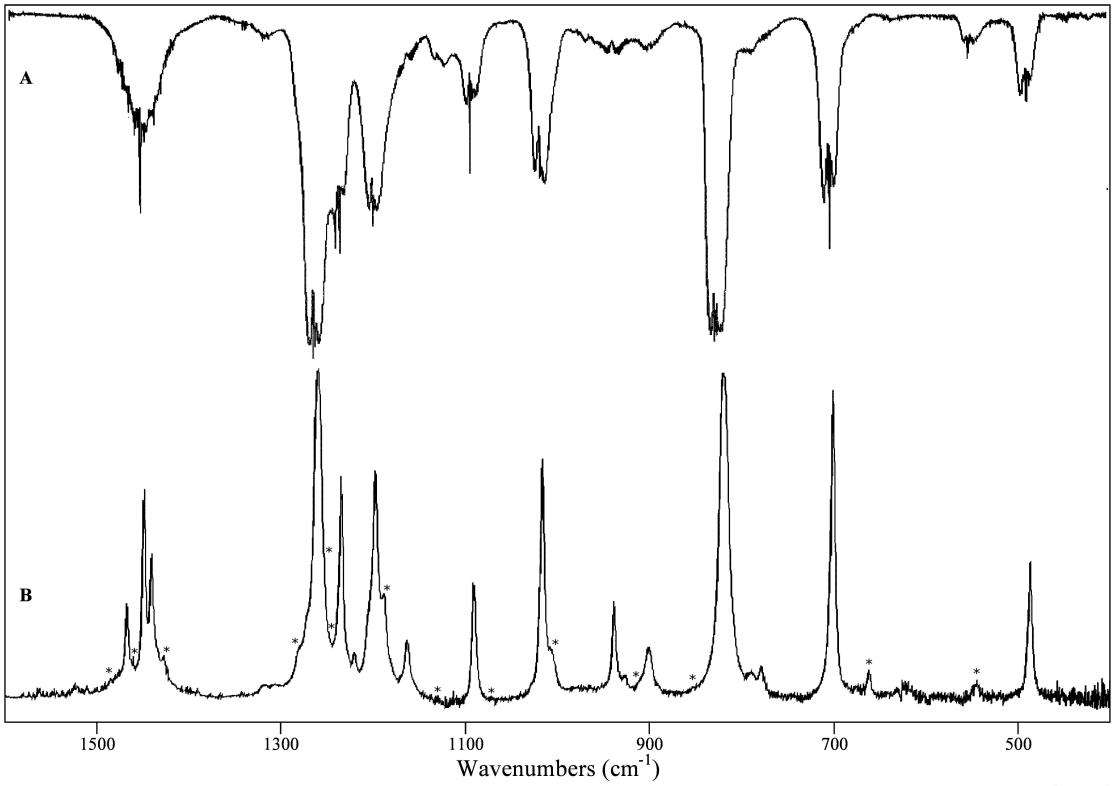

Figure 10. Mid-infrared spectra of bromocyclobutane (A) gas; (B) Xe solution at -70°C; asterisk denotes axial fundamentals.

CONFORMATIONAL STABILITY

To determine the enthalpy difference between the two conformers, the mid-infrared spectra of bromocyclobutane dissolved in liquefied xenon as a function of temperature from -55 to -100°C were recorded. Only small interactions are expected to occur between the dissolved sample and the surrounding xenon atoms, and consequently, only small frequency shifts are anticipated when passing from the gas phase to the

liquefied noble gas solutions. A significant advantage of this study is that the conformer bands are better resolved in comparison with those in the infrared spectrum of the gas. From *ab initio* calculations, the dipole moments of the two conformers are predicted to have similar values and the molecular sizes of the two conformers are nearly the same, so the ΔH value obtained from the temperature dependent FT-IR study is expected to be close to that for the gas [16-20].

As indicated earlier only the two bands at 545 and 1187 cm^{-1} could be used for intensity measurements for the axial conformer. The choice of the bands to be used for the equatorial conformer was somewhat more difficult since they must be sufficiently separated from any interfering bands. Also for best results they should have comparable intensity to the band being used for the axial conformer and preferably be in the lower frequency range to minimize interference of overtone and combination bands. From the inspection of the various possible bands the fundamentals at 487, 900, 1195, 1217, and 1232 cm^{-1} were selected for the equatorial conformer bands to be use in the determination of the enthalpy difference.

The intensities of the infrared bands were measured as a function of temperature (Fig. 11) and their ratios were determined. By application of the van't Hoff equation $-\ln K = \Delta H/(RT) - \Delta S/R$, ΔH was determined from a plot of $-\ln K$ versus 1/T, where ΔH/R is the slope of the line and K is substituted with the appropriate intensity ratios, *i.e.* $I_{equatorial} / I_{axial}$. It was assumed that ΔH, ΔS, and α are not a function of temperature in the temperature range studied.

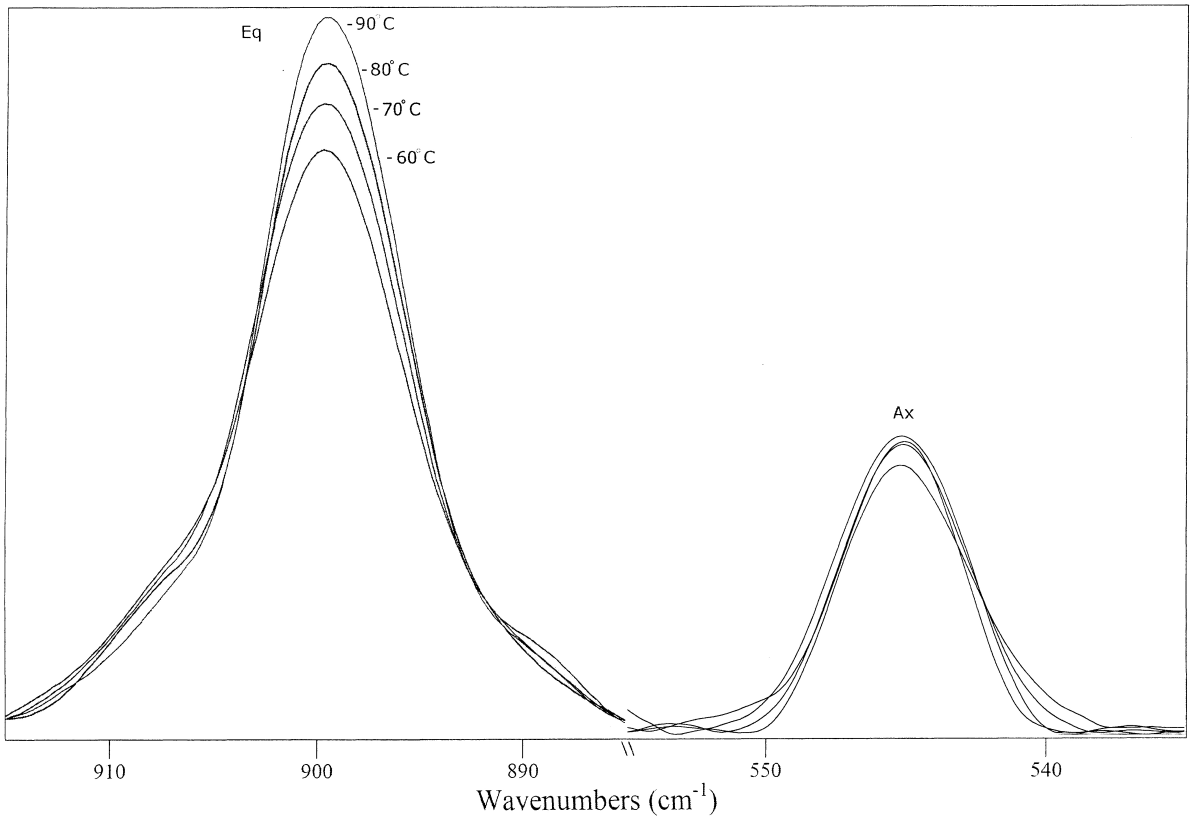

Figure 11. Infrared spectra of bromocyclobutane, in Xe solution at different temperatures.

By combining the two axial and the five equatorial conformer bands, ten pairs were found of which eight were utilized for the determination of the enthalpy difference, and the resulting values with statistical uncertainties are listed in Table 16. As can be seen from the data in this table there are a fair spread of values but each one has a relatively small uncertainty. However, this spread is expected when measuring band intensities for bands with shoulders and considerable potential for underlying overtones and combination bands. Nevertheless the statistical uncertainty is quite small and the

statistical average obtained by using all eight pairs as a single set gives a value of 291 ± 11 cm^{-1}. This error limit is derived from the statistical standard deviation of one sigma of the measured intensity data. This error limit does not take into account small associations with the liquid xenon or the interference of overtones and combination bands in near coincidence with the measured fundamentals. The variations in the individual values are undoubtedly due to these types of interferences, but by taking several pairs, the effect of such interferences should cancel. Nevertheless we expect the error is probably twice the statistical uncertainty obtained so we believe the determined ΔH value is 291 ± 22 cm^{-1}. Thus, the abundance of the less stable axial conformer present at ambient temperature is 20 ± 1%.

TABLE 16. Temperature and intensity ratios of the *equatorial* and *axial* bands of bromocyclobutane.

	T(°C)	1/T ($\times 10^{-3}$ K^{-1})	I_{487} / I_{545}	I_{900} / I_{545}	I_{1195} / I_{545}	I_{1232}/ I_{545}	I_{487} / I_{1187}	I_{900} / I_{1187}	I_{1195} / I_{1187}	I_{1217} / I_{1187}
Liquid	–60.0	4.692	9.862	2.769	21.295	16.465	2.432	0.683	5.251	0.197
xenon	–65.0	4.804	10.926	3.179	23.653	18.010	2.505	0.729	5.423	0.211
	–70.0	4.923	11.095	3.214	24.679	18.540	2.585	0.749	5.750	0.235
	–75.0	5.047	11.901	3.599	26.316	19.323	2.755	0.833	6.091	0.262
	–80.0	5.177	11.942	3.608	27.254	19.880	2.768	0.836	6.317	0.278
	–85.0	5.315	12.850	4.017	28.934	20.808	2.913	0.911	6.558	0.319
	–90.0	4.460	13.728	4.220	31.720	22.195	3.004	0.923	6.941	0.347
	–95.0	5.613	14.649	4.519	34.786	23.831	3.085	0.952	7.327	0.357
	–100.0	5.775	15.804	4.782	36.686	25.097	3.299	0.998	7.659	0.395
ΔH^a			280 ± 14	332 ± 21	337 ± 13	254 ± 11	188 ± 8	240 ± 20	245 ± 7	454 ± 23

[a] Average value $\Delta H = 291 \pm 11$ cm^{-1} (3.48 ± 0.13 kJ mol^{-1}) with the equatorial conformer the more stable form and the statistical uncertainty (1σ) obtained by utilizing all of the data as a single set.

DISCUSSION

The *ab initio* MP2(full)/6-31G(d) calculations with two scaling factors of 0.88 for the CH stretches and CH_2 scissors along with 0.90 for all other modes provides outstanding predictions for the frequencies of the fundamentals of bromocyclobutane. For the modes of A′ symmetry the average difference is 6 cm^{-1} which represents an error of 0.4% with the modes of A″ symmetry being predicted to within 7 cm^{-1} for an average error of 0.5%. These results are exceptionally good which aided considerably the search for the axial conformer fundamentals.

With these excellent predictions for the fundamentals we then predicted the infrared and Raman spectra for the α-d_1 and β,β′-d_4 isotopomers and have assigned the fundamentals (Tables 10 and 11). We were particularly interested in how the mixing would be affected by the deuteration of the α and β carbon-hydrogen bending modes. For the α-CH in-plane bend (ν_9) which is assigned at 1235 cm^{-1} there is only 22% S_9 contribution to this band with 29% S_8 and 28% S_{10} contributions along with 10% S_{13} contribution. There is 28% S_9 to the 1262 cm^{-1} band, 11% S_9 to the 1199 cm^{-1} band and 16% S_9 to the ring puckering mode. The α-CH out-of-plane mode (ν_{22}) is now assigned to the 1280 cm^{-1} rather than in the 900 cm^{-1} region as originally assigned [65] and it has 30% S_{22} with bands at 1228 and 1218 cm^{-1} having 17% and 12% S_{22} contributions, respectively. Several other bands in this general frequency region have contributions of a few percent, i.e. less than ten percent, which shows that the simple description of some of these modes does not give a very good indication of the molecular motions involved.

For the α-d_1 isotopomer the C-D in-plane bend at 914 cm^{-1} has 10% or more contributions from six symmetry coordinates (Table 10) with the corresponding out-of-

plane mode having contributions from four symmetry coordinates. Thus, the mixing is more extensive for the α-d_1 isotopomer than the normal molecule and the C-D in-plane contributions to both ring deformations one and two with 10% and 15% S_9 contributions, respectively. For the β,β'-d_4 isotopomer the mixing is even more extensive with many of the modes having only 20 to 30% contributions for the assigned vibrational descriptions. Nevertheless the *ab initio* predictions made the assignment of the fundamentals for the deuterated isotopomers relatively straight forward.

The determined ΔH value of 291 $\pm$ 22 cm^{-1} (3.48 $\pm$ 0.26 kJ/mol) is significantly lower than the *ab initio* predicted energy difference of 560 $\pm$ 46 cm^{-1} (6.70 $\pm$ 0.55 kJ/mol). Based on the significant number of fundamental bands observed for the axial conformer the lower experimental value seems very reasonable with the *ab initio* value predicted entirely too large. A similar problem was found for chlorocyclobutane where the *ab initio* predicted value is 646 $\pm$ 73 cm^{-1} whereas the experimentally determined value is 361 $\pm$ 17 cm^{-1} (4.32 $\pm$ 0.20 kJ.mol). It would be interesting to see if the similar problem exists for fluorocyclobutane. Also it should be noted that the energy difference predicted from the MP2(full)/aug-cc-pVTZ calculations was lower with a value of 456 cm^{-1} (5.46 kJ/mol) so it is possible higher level calculations could significantly improve the agreement with the experimentally determined ΔH value.

The determined structural parameters obtained in this study for the equatorial conformer are quite similar to the structural parameters provided by Rothschild [36]. The C-Br distance of 1.942(3)Å is within experimental error of the 1.939Å value assumed by Rothschild. The carbon-carbon distances of 1.541(3)Å for C_α-C_β ($C_{\beta'}$) and 1.552(3)Å for C_γ-C_β ($C_{\beta'}$) from this study is within experimental error of the values determined by

Rothschild [36] of 1.540(3)Å for C_α-C_β ($C_{\beta'}$) and 1.548(3)Å for C_γ-C_β ($C_{\beta'}$). The puckering angle of 29.8(5)° from this study is also within experimental error of the 29.4(1)° value determined by Rothschild [36].

It is interesting to compare the heavy atom parameters of bromocyclobutane with those of cyclobutane which were obtained from a microwave study [56] with the determined distances of: CC = 1.5555(2)Å and a ring puckering angle of 28.58(9)^o. The comparison indicates a reasonable reduction of the C_α-C_β ($C_{\beta'}$) distance where the bromine atom is attached with an insignificant reduction of the C_γ-C_β ($C_{\beta'}$) distance, with consistent CH distances and puckering angle. This is similar to the structural parameters obtained in the case of equatorial chlorocycobutane [48] with the exception of the C_γ-C_β ($C_{\beta'}$) bond distance which is almost unchanged in bromocyclobutane but elongates in chlorocyclobutane. There is a strong correlation of the C_α-C_β ($C_{\beta'}$) distance with the C-X bond length and the mass of the bromine atom could be the cause of this difference.

The C-Br distance varies over a very large range and we were interested on whether the MP2(full)/6-311+G(d,p) calculations would predict these large differences in the different molecules. Several C-Br distances were predicted and the values compared to the experimentally determined value (Table 17). As can be seen from the data the *ab initio* predicted value is frequently slightly smaller than the reported value but many of them do not give uncertainties. For some of the CC distances there appears to be an elongation of the CC bond such as for tert-butyl bromide. However, by using the reported rotational constants an excellent fit was obtained where the C-C bond was only elongated by 0.006 Å which is a value frequently found. It would be interesting to further evaluate the C-Br distance in organobromides.

TABLE 17. Structural parameters (Å and degrees) of cyclobutane[a] and some bromoalkanes and bromoalkenes.

Parameters	bromomethane		bromoethane		bromoethene		3-bromopropene		bromocyclopropane		isopropyl bromide	
	MP2[b]	Exp.[c]	MP2[b]	Exp.[d]	MP2[b]	Exp.[e]	MP2[b]	Exp.[f]	MP2[b]	Exp.[g]	MP2[b]	Exp.[h]
rC_α-Br	1.9319	1.9340	1.946	1.950(1)	1.884	1.884(1)	1.956	1.950	1.911	1.899(5)	1.961	1.962(6)
rC_α-C_β			1.516	1.519(1)			1.488	1.493	1.499	1.507(10)	1.518	1.518(10)
rC_γ-C_β									1.516	1.518(4)		
rC_α-H	1.0872	1.0823	1.089	1.087(1)	1.083	1.080(1)	1.090	1.094	1.082	1.080*	1.092	1.089(6)

Parameters	*trans*-1-bromopropane		*tert*-butyl bromide		*eq*-bromocyclobutane		*eq*-bromocyclopentane		*eq*-bromocyclohexane	
	MP2[b]	Exp.[i]	MP2[b]	Exp.[j]	MP2[b]	Exp.[k]	MP2[b]	Exp.[l]	MP2[b]	Exp.[m]
rC_α-Br	1.946	1.953	1.978	1.975(2)	1.938	1.942(3)	1.944	1.947	1.959	1.966(5)
rC_α-C_β	1.517	1.518	1.522	1.533(2)	1.535	1.541(3)	1.523	1.525	1.521	1.524(3)
rC_γ-C_β	1.528	1.530			1.551	1.552(3)	1.541	1.543	1.533	1.539(3)
rC_α-H	1.091	1.091			1.092	1.092(2)	1.094	1.095	1.095	1.095(2)

[a] Structural parameters[56]; rC-C 1.555(2), rC-H 1.0910(6), and puckering angle 28.58(9).
[b] From *ab initio* MP2(full)/6-311+G(d,p).
[c] Ref. [58] r_e structural parameters
[d] Ref. [69] r_s structural parameters
[e] Ref. [70] r_0 structural parameters
[f] Ref. [71] r_s structural parameters
[g] Ref. [72] r_0 structural parameters; asterisk indicates assumed parameter
[h] Ref. [73] r_s structural parameters
[I] Ref. [74] Adjusted r_0 structural parameters
[j] Ref. [75] r_0 structural parameters
[k] This study.
[l] Ref. [76] Adjusted r_0 structural parameters
[m] Ref. [77] Adjusted r_0 structural parameters

We have calculated the five centrifugal distortion constants from force constants predicted by *ab initio* MP2(full)/6-31G(d) calculations for several molecules and they usually agree very well with the experimentally determined values. In the most recent conformational stability determination of chlorocyclobutane [48] we obtained the values of Δ_J, Δ_{JK}, Δ_K, δ_J and δ_K for both the equatorial and axial forms for comparison to those obtained experimentally where only the Δ_J, Δ_{JK} and δ_J values were obtained. The predicted values were in excellent agreement with the experimental ones for the equatorial conformer of the ^{35}Cl isotopomer but differ significantly for the ^{37}Cl isotopomer where only the Δ_J and Δ_{JK} values were obtained. However, it was believed that the predicted values for the isotopomer were more consistent with the expected values than the ones reported from experiment where three of them were essentially assumed to be zero. For the axial conformer the agreement was satisfactory for Δ_J which was expected to be poorly determined from the microwave data. Since from the earlier microwave investigation [36] of bromocyclobutane the centrifugal distortion constants were not reported, we attempted to obtain them from the frequencies reported for 72 measured transitions of each isotopomer (Table 18). The frequencies observed by Rothschild and Dailey [36] were used to determine rotational, centrifugal distortion and quadrupole coupling constants with an exact Hamiltonian for the interaction with the quadrupole. The standard deviations of the fits for both isotopomer were rather high and the values of the centrifugal distortion constants obtained were very different from those predicted by the force field [41]. Therefore we used the theoretical values from the force constants from the MP2(full)/6-31G(d) calculation as fixed parameters in the fit and varied only the rotational and quadrupole coupling constants. Among the latter ones, the

very small off-diagonal element of the quadrupole coupling tensor was obtained, albeit with relatively large errors, confirming that the angle between the A principal inertia axis and the z-axis of the coupling tensor is only a few degrees. This means that the C-Br bond is almost parallel to the A principal inertia axis. The results of the fit and the resulting constants are listed in Table 19. Unfortunately, there seem to be rather large uncertainties in the frequency measurements which precluded the determination of more precise rotational, centrifugal distortion, and quadrupole coupling constants. Therefore it would be valuable to reinvestigate the microwave spectra of bromocyclobutane with much higher resolution.

TABLE 18. Rotational transition frequencies [a] and residuals (MHz) of bromocyclobutane-^{79}Br and ^{81}Br

	$^{79}BrC_4H_7$							
	$F = J+3/2$		$F = J+1/2$		$F = J-1/2$		$F = J-3/2$	
	ν_{obs}	res	ν_{obs}	res	ν_{obs}	res	ν_{obs}	res
6_{06} - 5_{05}	18643.85	-0.54	18643.37	-0.65	18649.61	0.45	18649.03	-0.47
6_{16} - 5_{15}	18268.18	0.01	18271.29	0.07	18274.39	-0.37	18271.29	-0.29
6_{15} - 5_{14}	19112.73	-0.01	19115.85	0.07	19119.92	0.02	19116.70	-0.02
6_{25} - 5_{24}	18693.63	0.16	18705.88	-0.06	18705.88	-0.43	18693.63	0.54
6_{24} - 5_{23}	18754.28	-0.25	18767.54	0.06	18767.54	-0.09	18754.28	0.01

6_{34} - 5_{33}	18704.92	0.12	18733.41	-0.17	18727.71	0.10	18698.22	-0.05
6_{33} - 5_{32}	18705.88	0.32	18736.14	1.79 [b]	18727.71	-0.67	18698.22	-0.81
6_{42} - 5_{41}	18693.63	-0.11	18744.35	-0.74	18729.83	-0.24	18677.89	-0.46
6_{51} - 5_{50}	18681.84	-0.12	18762.83	0.07	18736.14	0.40	18653.44	-2.34 [b]
7_{07} - 6_{06}	21726.73	0.51	21726.08	0.27				
7_{17} - 6_{16}	21307.54	-0.19	21309.27	-0.32	21312.09	-0.31	21310.24	-0.20
7_{16} - 6_{15}	22292.34	0.04	22293.64	-0.35	22297.32	-0.02	22295.04	-0.19
7_{26} - 6_{25}	21807.90	1.10	21814.83	-0.25	21814.83	-0.73	21807.90	-0.15
7_{25} - 6_{24}	21904.97	0.08	21913.07	-0.03	21913.83	-0.27	21905.73	0.12
7_{35} - 6_{34}	21831.12	0.10	21848.63	-0.35	21846.45	-0.32	21829.49	1.08
7_{34} - 6_{33}	21832.63	-0.11	21850.11	-0.61	21848.63	0.12	21831.12	0.98
7_{43} - 6_{42}	21820.68	-0.14	21852.83	0.00	21846.45	0.48	21814.50	0.98
7_{52} - 6_{51}	21813.23	1.63 [b]	21862.63	0.81	21850.41	1.59 [b]	21798.53	0.08
7_{61} - 6_{60}	21801.93	-0.11	21874.57	-0.17	21854.86	0.92	21781.64	-0.31
8_{18} - 7_{17}	24344.20	-0.09					24347.40	0.98

	$^{81}BrC_4H_7$							
	$F = J+3/2$		$F = J+1/2$		$F = J-1/2$		$F = J-3/2$	
$6_{06} - 5_{05}$	ν_{obs}	res	ν_{obs}	res	ν_{obs}	res	ν_{obs}	res
$6_{16} - 5_{15}$	18489.08	-0.07	18488.55	-0.20	18493.20	0.10	18493.58	-0.13
$6_{15} - 5_{14}$	18118.55	-0.04	18121.02	-0.08	18123.72	-0.20	18121.02	-0.29
$6_{25} - 5_{24}$	18949.35	0.06	18952.05	0.27	18955.43	0.13	18952.48	-0.20
$6_{24} - 5_{23}$	18537.57	0.24	18548.06	0.42	18548.06	0.07	18537.57	0.58
$6_{34} - 5_{33}$	18596.19	-0.28	18607.22	-0.09	18607.22	-0.20	18596.19	-0.08
$6_{33} - 5_{32}$	18549.16	-0.60	18573.34	0.36	18568.77	0.76	18543.90	0.22
$6_{42} - 5_{41}$	18549.16	-0.60	18573.34	-0.38	18568.77	0.02	18543.90	-0.51
$6_{51} - 5_{50}$	18539.46	0.04	18581.85	-0.23	18570.00	0.42	18526.19	-0.46
$7_{07} - 6_{06}$	18530.22	0.79	18596.19	-0.28	18573.34	-0.75	18508.24	0.64
$7_{17} - 6_{16}$	21545.02	-0.78	21545.02	-0.33	21548.52	0.20	21548.52	0.04
$7_{16} - 6_{15}$	21133.35	0.16	21135.26	0.56	21137.20	0.21	21135.21	-0.16
$7_{26} - 6_{25}$	22101.81	0.18	22103.01	0.05	22106.01	0.15	22103.99	-0.09
$7_{25} - 6_{24}$	21624.02	-0.13	21631.37	0.17	21631.77	0.45	21625.55	0.16
$7_{35} - 6_{34}$	21719.34	0.00	21726.35	0.11	21726.73	-0.33	21719.34	-0.58
$7_{34} - 6_{33}$	21648.94	0.67	21662.50	-0.71	21660.33	-1.02 [b]	21645.20	-0.92
$7_{43} - 6_{42}$	21648.94	-0.97	21665.06	0.19	21662.50	-0.51	21647.18	-0.58
$7_{52} - 6_{51}$	21639.12	0.05	21665.95	0.27	21660.33	0.37	21632.96	-0.08
$7_{61} - 6_{60}$	21631.37	0.30	21674.39	1.61 [b]	21662.50	0.54	21619.82	-0.32
$8_{18} - 7_{17}$	21623.18	0.23	21683.74	0.47	21666.95	0.91	21606.72	0.52

[a] Ref. [36]
[b] Not used in least-squares fit

TABLE 19. Rotational, centrifugal distortion and quadrupole coupling constants of bromocyclobutane.

	$^{79}BrC_4H_7$	$^{79}BrC_4H_7$	$^{79}BrC_4H_7$ [a]	$^{81}BrC_4H_7$	$^{81}BrC_4H_7$	$^{81}BrC_4H_7$ [a]
A / MHz	10010(14)	10014(14)	10003.4	9983.9(67)	9984.6(55)	10002.6
B / MHz	1629.419(17)	1629.397(17)	1629.41	1615.143(17)	1615.119(16)	1615.14
C / MHz	1488.491(17)	1488.474(16)	1488.48	1476.5(17)	1476.514(16)	1476.50

Δ_J / kHz	0.17122 [b]	0		0.16878 [b]	0	
Δ_{JK} / kHz	0.48763 [b]	0		0.47561 [b]	0	
Δ_K / kHz	7.50244 [b]	0		7.52240 [b]	0	
δ_J / kHz	0.01196 [b]	0		0.01169 [b]	0	
δ_k / kHz	0.70224 [b]	0		0.69284 [b]	0	
y / MHz [c]	-24(14)	-24(14)		-28(13)	-27(12)	
χ_{aa} / MHz	450.1(15)	450.1(15)	450.1	373.8(13)	373.9(13)	376
χ_{bb} / MHz [d]	-249(14)	-249(14)	-256.6	-215(13)	-214(12)	
χ_{cc} / MHz [d]	-201(14)	-201(14)	-193.5	-159(13)	-160(13)	
χ_{ac} / MHz	129(35)	128(34)		147(30)	144(29)	
n [f]	72	72		74	74	
s [g] / MHz	0.45	0.44		0.43	0.41	

[a] Ref. [36]
[b] Calculated from MP2(full)/6-31G(d) force field (uniform scale factor of force constants = 1)
[c] $y = \chi_{bb} - \chi_{cc}$
[d] Dependent parameters
[e] Standard uncertainty in units of the last digit in parentheses
[f] Number of transitions in least-squares fit
[g] Standard deviation

In the present study the enthalpy difference was determined to be much smaller at 291 cm^{-1} than the 361 cm^{-1} enthalpy used in the previous study [47] for determining the ring-puckering potential function. Further, the barrier to planarity is 596 cm^{-1} as compared to 636 cm^{-1} in the previous study [47]. With the lower and more reliable ΔH value, we have again obtained the potential function governing the conformational interchange for bromocyclobutane. The two lowest frequencies in the equatorial well can be confidently assigned and the ΔH value places a strong constraint on the energy level of the ground state for the axial level (Fig. 12). For an appropriate series in the equatorial well, it is possible to place the fourth energy levels to give a reasonable frequency for the third transition in the equatorial well. With the placement of these energy levels there is significant restriction on the fundamentals puckering frequency for the axial conformer.

The *ab initio* MP2(full)/6-31G(d) calculations predict this fundamental at 154 cm^{-1} compared to the predicted value of 161 cm^{-1} for the corresponding fundamental of the equatorial conformer. One expects a very poor prediction for the axial ring puckering fundamental since the predicted barrier between these conformers is 1042 cm^{-1} whereas the frequency differences of the "hot bands" series for the equatorial conformer indicate a barrier near 600 cm^{-1}. In the case of the axial conformer the fundamental ring puckering vibration is predicted with relatively less accuracy compared to the equatorial conformer. It is predicted at 154 cm^{-1} as compared to the observed value of 118.5 cm^{-1} from the Raman data. With these four initial assignments the remaining ones were then assigned (Table 20) and the potential function was determined. This potential function is somewhat different from the previous one [68] but the changes are relatively minor. It would be of interest to obtain the potential function of some of the other four member ring molecules when more accurate ΔH values are determined.

TABLE 20. Observed and calculated frequencies (cm^{-1}) for the ring-puckering vibrations of bromocyclobutane.

		Observed[a]				
Conformer	Transition	Infrared	Raman[c]	Calculated	Obs. – Calc.[b]	Weight
Equatorial	1 ← 0	149.45	149	148.61	0.84	1.0
	2 ← 1	140.45	140	138.08	2.37	1.0
	5 ← 2	124.50	125	128.03	-3.53	1.0
	7 ← 5		109.5	110.86	-1.36	1.0
	8 ← 5		(172)	171.86	0.14	0.0
	8 ← 7			60.99		
Axial	4 ← 3		118.5	119.76	-1.26	1.0
	6 ← 4		94.0	94.06	-0.06	1.0
	9 ← 6	136.50	136	137.12	-0.62	1.0

8 ← 6	(84)	81.78	2.22	0.0

[a] The infrared were utilized preferentially over the Raman in the calculations.
[b] Calculated by using a potential of the form V (cm^{-1}) = (7.02 ± 0.97) x 10^5X^4 + (3.87 ± 0.52) x 10^4X^3 – (3.42 ± 0.28) x 10^4X^2 with a reduced mass of 214 amu.
[c] Values in parenthesis were assigned for this paper.

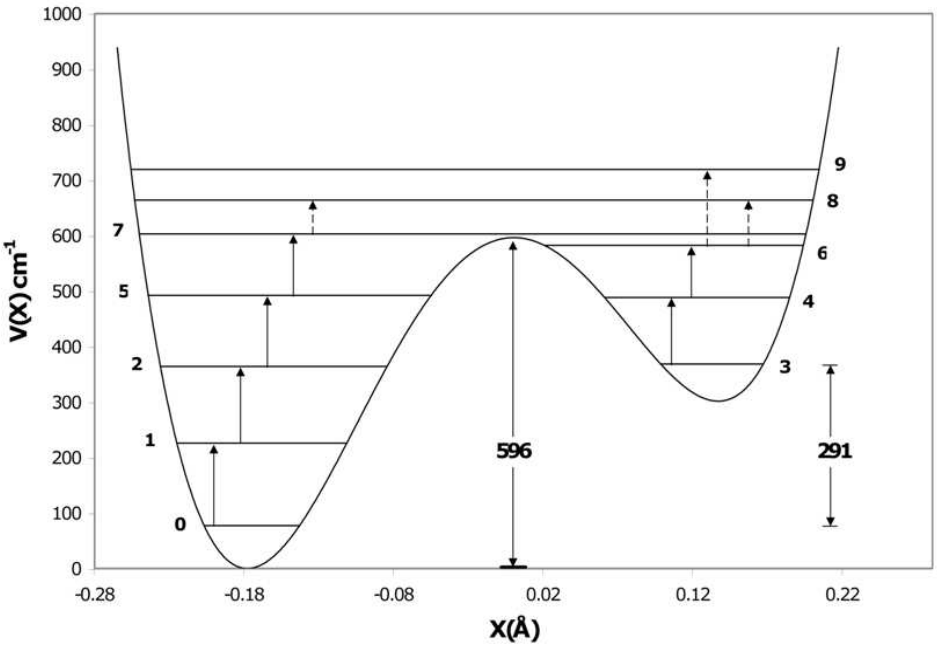

Figure 12. Potential function governing the ring-puckering vibration of bromocyclobutane. V (cm^{-1}) = (7.02 ± 0.97) x 10^5X^4 + (3.87 ± 0.52) x 10^4X^3 – (3.42 ± 0.28) x 10^4X^2 with a reduced mass of 214 amu.

CHAPTER 5

CONFORMATIONAL STABILITY, r_0 STRUCTURAL PARAMETERS, AND VIBRATIONAL ASSIGNMENTS OF MONO-SUBSTITUTED CYCLOBUTANES: FLUOROCYCLOBUTANE

INTRODUCTION

The cyclobutane molecule is puckered in the ground vibrational state which results from the steric forces being larger than the ring strain forces. The structural parameters of cyclobutane have been determined from a microwave investigation of four different deuterated isotopomers and the puckering angle was determined [78] to be $29.55(9)^{o}$. Prior to this study only the structural parameters of the equatorial chlorocyclobutane had been reported [35] from a microwave study but the reported A rotational constants were found to differ significantly from those parameters obtained by the weighted least-squares adjusted method from *ab initio* predicted values [47]. However, from a more recent microwave investigation of both the equatorial and axial conformers of chlorocyclobutane [44] it has been possible to obtain the complete structural parameters [48] from the revised rotational constants of the equatorial conformer along with those for axial conformer combined with those predicted from the *ab initio* MP2(full)/6-311+G(d,p) calculations. By utilizing the *ab initio* predicted parameters in combination with previously reported microwave rotational constants it has been possible to obtain complete r_0 structural parameters in addition to chlorocyclobutane for cyclobutylamine [62], bromocyclobutane [79], cyanocyclobutane [63], and

cyclobutanol [57]. All of these molecules have at least two conformers present at ambient temperature. By variable temperature infrared investigations of rare gas solutions [48,62,79,63,57] the enthalpy differences have been determined after confident vibrational assignments have been made by using *ab initio* predicted frequencies, infrared band contours and intensities, along with Raman activities and depolarization values. From far infrared and low frequency Raman spectra of the gases it has been possible to obtain the potential function governing the conformational interchange for many of these molecules. A comparison of the different values of the heavy atom structural parameters and the barrier to inversion and enthalpy differences has been made along with predicted energy differences.

As a continuation of our conformational and structural determination of monosubstituted cyclobutanes with halogen and pseudo-halogen substituents we have investigated the temperature dependent infrared spectra of fluorocyclobutane in xenon solutions to obtain the enthalpy difference between the two conformers. In the initial study [35] of the microwave spectrum of fluorocyclobutane the structural parameters could not be obtained from the three experimentally obtained rotational constants. Therefore, corresponding parameters from chlorocyclobutane were used for fluorocyclobutane along with an estimated C-F bond distance of 1.37 Å. These parameters were sufficient to provide rotational constants which satisfactorily agreed with the experimentally determined ones [35].

Later by weighted least-squares adjustment method the C-F distance and the angle of the fluorine atom to the plane of the ring were determined [53], by utilizing the three experimentally determined rotational constants from the initial microwave study [35]

along with the remaining parameters, to be the same as the corresponding parameters obtained for chlorocyclobutane [47]. Therefore, to obtain a more complete structural parameter determination for fluorocyclobutane we have combined the *ab initio* MP2(full)/6-311+G(d,p) predicted parameters with the six experimentally determined rotational constants [44] for the two forms to obtain the complete structural parameters for both conformers of fluorocyclobutane.

TABLE 21. Observed[a] and calculated[b] frequencies for the *equatorial* conformer of fluorocyclobutane.

		Fundamental	ab initio	Fixed scaled[c]	IR int.	Raman act.	dp ratio	gas[d]	gas[f]	gas	Xe	P.E.D.[h]	Band Contour		
													A	B	C
A'	ν_1	β-CH_2 antisymmetric stretch	3214	3015	38.3	41.5	0.74	3006	2992	3003	2995	$52S_1,47S_2$	-	-	100
	ν_2	γ-CH_2 antisymmetric stretch	3199	3001	5.3	81.8	0.51	2992	2970	2991	-	$50S_2,44S_1$	93	-	7
	ν_3	γ -CH_2 symmetric stretch	3141	2947	18.7	142.9	0.10	2950	2961	2947	2950	$90S_3$	88	-	12
	ν_4	β -CH_2 symmetric stretch	3138	2944	8.9	117.4	0.21	2912	2950	2910	2895	$92S_4$	27	-	73
	ν_5	CH stretch	3131	2937	27.1	83.7	0.28	2861*	2934	2892	2878	$91S_5$	17	-	83
	ν_6	β-CH_2 scissors	1578	1480	6.4	6.4	0.66	1472	1471	1473	1466	$56S_6,38S_7$	84	-	16
	ν_7	γ-CH_2 scissors	1553	1457	4.7	15.4	0.75	1453	1453	1454	1446	$60S_7,39S_6$	-	-	100
	ν_8	CH in-plane bend	1449	1375	44.8	8.3	0.66	1361	1361	1362	1358	$49S_8,27S_{17}$	100	-	-
	ν_9	β-CH_2 wag	1314	1247	16.4	2.5	0.74	1242	1242	1244	1240	$61S_9,16S_{14}$	96	-	4
	ν_{10}	β-CH_2 twist	1279	1213	3.1	9.2	0.74	1140	1221	1222	1218	$72S_{10},12S_{15}$	85	-	15
	ν_{11}	β-CH_2 rock	1199	1137	25.2	1.9	0.67	1098	1140	1141	1136	$41S_{11},16S_{17},15S_{12},15S_{15},11S_{18}$	83	-	17
	ν_{12}	C-F stretch	1168	1108	58.9	8.0	0.22	1079*	1098	1099	1090	$39S_{12},40S_{13}$	96	-	4
	ν_{13}	Ring breathing	1016	964	14.4	15.2	0.11	959	959	961	954	$46S_{13},17S_{12},14S_{16}$	79	-	21
	ν_{14}	Ring deformation 1	955	906	1.8	1.3	0.74	783*	851	914	911	$40S_{14},19S_{16},17S_{15},12S_9$	99	-	1
	ν_{15}	γ-CH_2 rock	792	751	3.5	1.9	0.32	750	750	750	750	$44S_{15},25S_{14},16S_{10}$	13	-	87
	ν_{16}	Ring deformation 2	618	586	2.3	3.0	0.49	599	599	599	599	$62S_{16},14S_{11},12S_{12}$	94	-	6
	ν_{17}	C-F in-plane bend	474	450	7.2	0.4	0.49	456	456	455	454	$32S_{17},27S_8,14S_{18},13S_{11}$	80	-	20
	ν_{18}	Ring puckering	202	192	1.6	0.1	0.02	166	166	(166)[g]	-	$72S_{18},13S_8,11S_{17}$	28	-	72
A"	ν_{19}	β-CH_2 antisymmetric stretch	3204	3006	20.1	61.6	0.75	2988	2988	2993	2986	$99S_{19}$	-	100	-
	ν_{20}	β -CH_2 symmetric stretch	3135	2941	29.4	0.1	0.75	2966*	2914*	2941	2940	$99S_{20}$	-	100	-

ν_{21}	β -CH_2 scissors	1537	1442	3.1	7.8	0.75	1441	1441	1441	1435	$99S_{21}$	-	100	-
ν_{22}	CH out-of-plane bend	1359	1289	1.4	3.7	0.75	1263	1246	1260	1257	$60S_{22},16S_{23}$	-	100	-
ν_{23}	γ-CH_2 wag	1294	1228	1.5	0.1	0.75	1221	1263	1223	1221	$58S_{23},17S_{27},16S_{22}$	-	100	-
ν_{24}	γ-CH_2 twist	1282	1216	0.3	5.0	0.75	1161	1216	1218	1215	$42S_{24},43S_{25}$	-	100	-
ν_{25}	β-CH_2 wag	1221	1158	0.3	8.6	0.75	1049	1161	1159	1161	$46S_{25},21S_{24}$	-	100	-
ν_{26}	Ring deformation 1	1102	1045	8.5	1.5	0.75	1057[e]	1026	1050	1048	$24S_{26},29S_{28},26S_{27},10S_{30}$	-	100	-
ν_{27}	β -CH_2 twist	974	924	2.8	1.1	0.75	921	921	926	921	$42S_{27},18S_{24},17S_{22},14S_{26}$	-	100	-
ν_{28}	Ring deformation 2	957	908	0.5	12.6	0.75	899	843	897	893	$57S_{28},26S_{26}$	-	100	-
ν_{29}	β-CH_2 rock	821	779	0.3	1.2	0.75	835*	783*	781	774	$79S_{29},13S_{24}$	-	100	-
ν_{30}	C-F out-of-plane bend	374	355	3.4	1.1	0.75	371	371	-	-	$81S_{30},12S_{26}$	-	100	-

[a] Observed spectra: gas and Xe are IR.

[b] MP2(full)/6-31G(d) *ab initio* calculations, scaled frequencies, infrared intensities (km/mol), Raman activities ($Å^4$/u), depolarization ratios (dp) and potential energy distributions (P.E.D.s).

[c] Scaled frequencies with scaling factors of 0.88 for the CH stretches, β-CH_2 and γ-CH_2 scissors and 0.90 for all other modes.

[d] Frequencies listed are taken from reference [80], values marked with an asterisk (*) are from the Raman spectrum, all others are from the IR spectrum of the gas.

[e] Frequency taken from the IR spectrum of the solid.

[f] Frequencies listed are taken from reference [53].

[g] Frequency taken from far infrared of the gas.

[h] Symmetry coordinates with P.E.D. contribution less than 10% are omitted.

TABLE 22. Observed[a] and calculated[b] frequencies for the *axial* conformer of fluorocyclobutane.

		Fundamental	ab initio	Fixed scaled[c]	IR int.	Raman act.	dp ratio	gas[d]	gas	Xe	P.E.D.[f]	Band Contour		
												A	B	C
A'	ν_1	γ-CH2 antisymmetric stretch	3217	3018	32.2	41.3	0.74				$69S_1,30S_2$	53	-	47
	ν_2	β-CH_2 antisymmetric stretch	3198	3000	4.9	71.6	0.62				$67S_2,30S_1$	-	-	100
	ν_3	CH stretch	3152	2957	45.1	179.1	0.07				$79S_3,17S_5$	19	-	81
	ν_4	γ -CH_2 symmetric stretch	3146	2951	41.8	62.1	0.15				$95S_4$	56	-	44
	ν_5	β -CH_2 symmetric stretch	3131	2937	3.0	121.6	0.37				$80S_5,16S_3$	98	-	2
	ν_6	γ-CH_2 scissors	1566	1469	3.1	5.8	0.65				$64S_6,34S_7$	100	-	-
	ν_7	β-CH_2 scissors	1538	1443	3.9	18.2	0.75				$64S_7,35S_6$	30	-	70
	ν_8	CH in-plane bend	1425	1352	27.6	2.6	0.72		1348	1348	$47S_8,29S_{17},11S_{10}$	98	-	2
	ν_9	β-CH_2 wag	1336	1267	11.7	1.4	0.55				$78S_9,14S_{13}$	81	-	19
	ν_{10}	β-CH_2 twist	1276	1211	5.8	16.4	0.74				$63S_{10},11S_{16}$	60	-	40
	ν_{11}	β-CH_2 rock	1194	1133	24.1	0.9	0.43				$35S_{11},23S_{15},15S_{17},15S_{16},12S_{18}$	38	-	62
	ν_{12}	Ring breathing	1095	1039	17.5	19.4	0.16		1039	1037	$70S_{12},13S_{15}$	89	-	11
	ν_{13}	Ring deformation 2	970	920	14.4	5.5	0.09				$36S_{13},19S_{15},15S_{12},10S_{10}$	72	-	28
	ν_{14}	Ring deformation 1	927	879	7.5	4.0	0.42				$26S_{14},26S_{16},20S_{13}$	98	-	2
	ν_{15}	C-F stretch	895	849	16.2	4.4	0.50	825	832	832	$27S_{15},28S_{14},20S_{11},10S_{13}$	45	-	55
	ν_{16}	γ-CH_2 rock	708	672	1.7	0.6	0.60				$39S_{16},27S_{14},16S_{11}$	10	-	90
	ν_{17}	C-F in-plane bend	403	382	1.8	0.3	0.14				$30S_{17},18S_8,16S_{18},15S_{11},13S_{14}$	100	-	-
	ν_{18}	Ring puckering	180	171	1.5	0.1	0.19	131	(131)[e]		$69S_{18},13S_8,10S_{17}$	60	-	40
A"	ν_{190}	β-CH_2 antisymmetric stretch	3204	3006	9.3	72.4	0.75				$97S_{19}$	-	100	-
	ν_{20}	β -CH_2 symmetric stretch	3131	2937	26.7	0.8	0.75				$97S_{20}$	-	100	-
	ν_{21}	β -CH_2 scissors	1523	1429	4.4	6.5	0.75				$99S_{21}$	-	100	-
	ν_{22}	CH out-of-plane bend	1344	1275	0.8	1.5	0.75				$46S_{22},29S_{23},19S_{28}$	-	100	-
	ν_{23}	γ-CH_2 wag	1303	1236	2.4	6.4	0.75				$31S_{23},33S_{25},15S_{26},11S_{22}$	-	100	-
	ν_{24}	β-CH_2 wag	1292	1226	0.3	0.1	0.75				$65S_{24},15S_{23},11S_{22}$	-	100	-
	ν_{25}	γ-CH_2 twist	1217	1155	5.2	5.5	0.75				$31S_{25},20S_{27},16S_{24},14S_{23}$	-	100	-
	ν_{26}	β -CH_2 twist	1098	1042	2.3	6.1	0.75				$63S_{26},10S_{25}$	-	100	-
	ν_{27}	Ring deformation 1	979	929	0.8	14.6	0.75				$64S_{27},13S_{24}$	-	100	-
	ν_{28}	Ring deformation 2	953	904	5.8	0.6	0.75				$57S_{28},10S_{22},10S_{29}$	-	100	-
	ν_{29}	β-CH_2 rock	779	739	0.2	0.2	0.75				$63S_{29},19S_{28},11S_{25}$	-	100	-
	ν_{30}	C-F out-of-plane bend	397	377	3.2	0.7	0.75				$83S_{30},10S_{29}$	-	100	-

[a] Observed spectra: gas, Xe, are IR.

[b] MP2(full)/6-31G(d) *ab initio* calculations, scaled frequencies, infrared intensities (km/mol), Raman activities ($Å^4$/u), depolarization ratios (dp) and potential energy distributions (P.E.D.s).
[c] Scaled frequencies with scaling factors of 0.88 for the CH stretches, β-CH_2 and γ-CH_2 scissors and 0.90 for all other modes.
[d] Frequencies listed are taken from reference [53].
[e] Frequency taken from far infrared of the gas.
[f] Symmetry coordinates with P.E.D. contribution less than 10% are omitted.

EXPERIMENTAL

The fluorocyclobutane sample was prepared by replacing the chlorine atom in chlorocyclobutane (Sigma-Aldrich Chemical Co., with stated purity of 97%) with a fluorine atom by allowing the chlorocyclobutane to drip onto powdered AgF_2 which had been dried under vacuum at 110° C for 24 h. The sample was purified by a low-temperature, low-pressure fractionation column and the purity of the sample was verified by comparing the infrared spectrum with that previously reported [80].

The mid-infrared spectrum of the gas (Fig. 13B) was obtained from 4000 to 250 cm^{-1} on a Perkin-Elmer model 2000 Fourier transform spectrometer equipped with a Ge/CsI beamsplitter and a DTGS detector. Atmospheric water vapor was removed from the spectrometer housing by purging with dry nitrogen. The theoretical resolution used to obtain the spectrum of the gas was 0.5 cm^{-1}. One hundred twenty eight interferograms were added and transformed with a boxcar truncation function. The frequencies for the predicted and observed fundamentals are listed in Tables 21 and 22.

The mid-infrared spectra (4000 to 400 cm^{-1}) of the sample dissolved in liquefied xenon (Fig. 13C) were recorded on a Bruker model IFS-66 Fourier transform spectrometer equipped with a globar source, a Ge/KBr beamsplitter and a DTGS detector. In all cases, 100 interferograms were collected at 1.0 cm^{-1} resolution, averaged and transformed with a boxcar truncation function. For these studies, a specially designed cryostat cell was used. It consists of a copper cell with a path length of 4 cm with wedged silicon windows sealed to the cell with indium gaskets. The copper cell was enclosed in an evacuated chamber fitted with KBr windows. The temperature was maintained with boiling liquid nitrogen and monitored by two Pt thermo resistors.

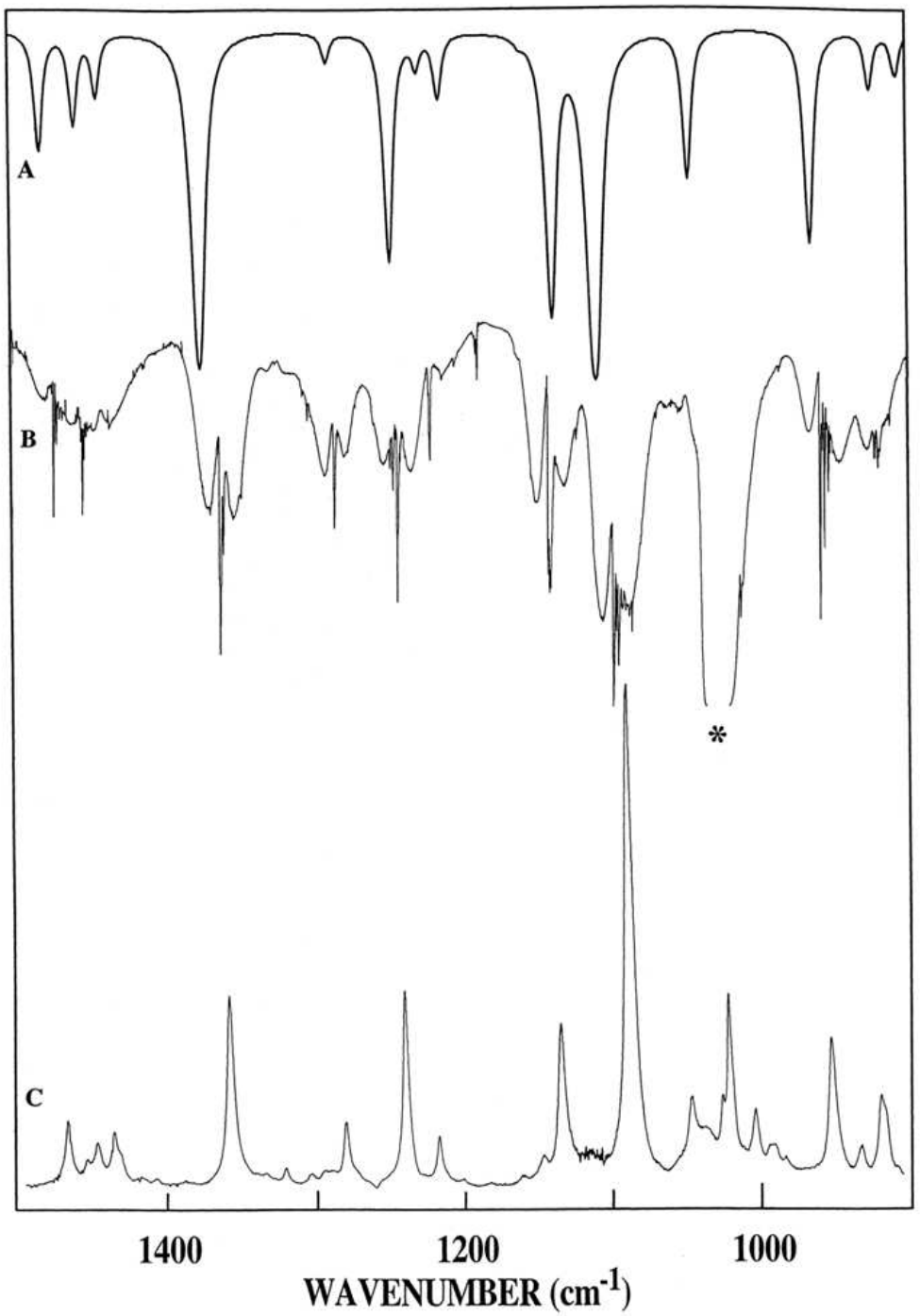

Figure 13. Comparison of experimental and predicted mid-infrared spectra of fluorocyclobutane: (A) simulated spectrum of equatorial conformer; (B) observed infrared spectrum of the gas, asterisk denotes an impurity; (C) Xe solution at -70 ºC.

AB INITIO CALCULATIONS

The *ab initio* calculations were performed with the Gaussian-03 program [22] using Gaussian-type basis functions. The energy minima with respect to nuclear coordinates were obtained by the simultaneous relaxation of all geometric parameters using the gradient method of Pulay [29]. A variety of basis sets as well as the corresponding ones with diffuse functions were employed with the Møller-Plesset perturbation method [21] to the second order MP2 with full electron correlation as well as with the density functional theory by the B3LYP method. The predicted conformational energy differences are listed in Table 23.

TABLE 23. Calculated energies in (H) and energy differences (cm^{-1}) for the two conformers, and transition state of fluorocyclobutane.

	Energy[a], E	Energy Differences, Δ		
Method/Basis Set	*equatorial*	*axial*[b]	*planar ring*[b]	*planar ring*[c]
RHF/6-31G(d)	0.952938	583		
MP2(full)/6-31G(d)	1.661929	658	1189	531
MP2(full)/6-31+G(d)	1.682782	668		
MP2(full)/6-31G(d,p)	1.719525	722		
MP2(full)/6-31+G(d,p)	1.739104	712		
MP2(full)/6-311G(d,p)	1.906145	779		
MP2(full)/6-311+G(d,p)	1.915779	793	1377	584
MP2(full)/6-311G(2d,2p)	1.976511	694		
MP2(full)/6-311+G(2d,2p)	1.984410	730		
MP2(full)/6-311G(2df,2pd)	2.065639	762	1279	516
MP2(full)/6-311+G(2df,2pd)	2.073066	794	1236	443
MP2(full)/aug-cc-pVTZ	2.087353	740		
Average MP2(full)	-	732 ± 47	1270 ± 69	518 ± 50
B3LYP/6-31G(d)	2.447881	643	659	15
B3LYP/6-31+G(d)	2.465403	585		
B3LYP/6-311G(d,p)	2.524013	600		
B3LYP/6-311+G(d,p)	2.531097	596	555	41
B3LYP/6-311G(2d,2p)	2.533492	577		

B3LYP/6-311+G(2d,2p)	2.539708	587		
B3LYP/6-311G(2df,2pd)	2.539411	612	584	29
B3LYP/6-311+G(2df,2pd)	2.545645	612	566	46
B3LYP/aug-cc-pVTZ	2.554573	605		
Average B3LYP	-	602 ± 20	591 ± 47	33 ± 14

[a]Energy of conformer is given as –(E+254) H.
[b]Difference is relative to *equatorial* form and given in cm^{-1}.
[c]Difference is relative to *axial* form and given in cm^{-1}.

In order to obtain descriptions of the molecular motions involved in the fundamental modes of fluorocyclobutane, a normal coordinate analysis was carried out. The force field in Cartesian coordinates was obtained with the Gaussian 03 program at the MP2(full) level with the 6-31G(d) basis set. The internal coordinates used to calculate the **G** and **B** matrices are given in Table 24 with the atomic numbering shown in Fig. 14. By using the **B** matrix [30], the force field in Cartesian coordinates was converted to a force field in internal coordinates. Subsequently, 0.88 was used as the scaling factor for the CH stretches and CH_2 scissors whereas 0.90 was used as the scaling factor for all other modes to obtain the fixed scaled force field and resultant wavenumbers. A set of symmetry coordinates was used similar to those used for chlorocyclobutane [48] to determine the corresponding potential energy distributions (P.E.D.s). A comparison between the observed and calculated wavenumbers, along with the calculated infrared intensities, Raman activities, depolarization ratios and potential energy distributions for the *equatorial* and *axial* conformers of fluorocyclobutane, are given in Tables 21 and 22, respectively.

Figure 14. Fluorocyclobutane showing atomic numbering.

TABLE 24. Structural parameters (Å and degrees), rotational constants (MHz) and dipole moments (Debye) for *equatorial* and *axial* fluorocyclobutane.

Structural Parameters	Int. coor.	MP2(full)/ 6-311+G(d,p)		B3LYP/ 6-311+G(d,p)		Microwave[a]	Adjusted r_0 [b]	
		Eq	Ax	Eq	Ax	Eq	Eq	Ax [c]
rC_α-F	R_1	1.386	1.398	1.398	1.407	1.386(2)	1.383(3)	1.407(3)
rC_α-C_β,$C_{\beta'}$	R_2	1.530	1.534	1.536	1.541	1.535	1.543(3)	1.546(3)
rC_γ-C_β,$C_{\beta'}$	R_3	1.551	1.552	1.557	1.557	1.548	1.554(3)	1.554(3)
rC_α-H	r_1	1.094	1.092	1.093	1.091	1.092	1.094(2)	1.092(2)
rC_β-H_1, $C_{\beta'}$-H_1	r_2	1.093	1.092	1.092	1.091	1.094	1.093(2)	1.092(2)
rC_β-H_2, $C_{\beta'}$-H_2	r_3	1.091	1.094	1.091	1.092	1.093	1.091(2)	1.094(2)
rC_γ-H_1	r_4	1.090	1.091	1.090	1.091	1.092	1.090(2)	1.091(2)
rC_γ-H_2	r_5	1.093	1.091	1.092	1.091	1.094	1.093(2)	1.091(2)
$\angle C_\beta C_\alpha F$	ϕ_1	117.3	109.6	116.6	111.2	116.9	117.4(5)	109.2(5)
$\angle C_\beta C_\alpha C_\beta$	θ_1	89.4	88.9	90.0	89.9	89.7	89.3(5)	89.2(5)
$\angle C_\gamma C_\beta C_\alpha$	θ_2	86.4	88.0	87.4	89.3	87.1	85.0(5)	89.2(5)
$\angle C_\beta C_\gamma C_\beta$	θ_3	87.8	87.6	88.4	88.7	88.7	88.6(5)	88.6(5)
$\angle HC_\alpha C_\beta$	σ_1	112.1	120.2	113.2	118.8	112.5	112.1(5)	120.4(5)
$\angle HC_\alpha F$	σ_2	107.7	107.2	106.7	106.4	107.7	107.7(5)	107.2(5)
$\angle H_1C_\beta C_\alpha$	λ_1	109.3	116.3	110.0	114.8	109.9	109.3(5)	116.3(5)
$\angle H_1C_\beta C_\gamma$	λ_2	110.4	119.1	111.3	117.6	109.7	112.8(5)	123.3(5)

$\angle H_2C_\beta C_\alpha$	λ_3	118.8	110.4	118.0	111.9	118.2	118.8(5)	110.4(5)
$\angle H_2C_\beta C_\gamma$	λ_4	119.6	111.4	119.0	113.1	117.9	118.5(5)	105.8(5)
$\angle H_1C_\beta H_2$	λ_5	110.2	109.9	109.4	109.0	109.3	110.2(5)	109.9(5)
$\angle H_1C_\gamma C_\beta$	π_1	117.7	111.3	117.1	112.7	116.1	116.4(5)	108.3(5)
$\angle H_2C_\gamma C_\beta$	π_2	111.4	117.8	112.2	116.5	111.2	112.4(5)	120.1(5)
$\angle H_1C_\gamma H_2$	π_3	109.4	109.6	108.8	108.6	108.6	109.4(5)	109.6(5)
$\tau C_\gamma C_\beta C_\beta C_\alpha$	τ_1	34.0	29.2	28.0	17.6	20	37.4(5)	20.7(5)
A(MHz)		10392.071	8463.98	10204.376	8762.20	10250.412(7)	10250.620	8628.79
B(MHz)		4271.121	4848.58	4247.106	4619.90	4274.930(3)	4275.419	4726.22
C(MHz)		3411.111	4109.91	3380.445	3815.67	3402.614(3)	3402.568	3939.20
$\|\mu_a\|$		1.968	1.819	2.066	1.802	1.870(5)		1.61(5)
$\|\mu_b\|$		0.000	0.000	0.000	0.000	0.000		0.000
$\|\mu_c\|$		0.553	1.314	0.599	1.116	0.52(2)		1.22(22)
$\|\mu_t\|$		2.044	2.244	2.151	2.120	1.94(1)		2.02(17)

[a] proposed structural parameters from reference [53], equatorial dipole moments from reference [35], rotational constants [44].
[b] adjusted parameters using the microwave data from reference [44] for the given ground states.
[c] experimental rotational constants A = 8628.77(7) MHz, B = 4726.25(6) MHz, and C = 3939.16(8) MHz and dipole moments taken from reference [44].

The infrared spectra were predicted from the MP2(full)/6-31G(d) calculations. The predicted scaled frequencies were used together with a Lorentzian function to obtain the calculated spectra. Infrared intensities determined from MP2(full)/6-31G(d) calculations were obtained based on the dipole moment derivatives with respect to Cartesian coordinates. The derivatives were transformed with respect to normal coordinates by $(\partial\mu_u/\partial Q_i) = \sum_j (\partial\mu_u/\partial X_j)L_{ij}$, where Q_i is the i^{th} normal coordinate, X_j is the j^{th} Cartesian displacement coordinate, and L_{ij} is the transformation matrix between the Cartesian displacement coordinates and the normal coordinates. The infrared intensities

were then calculated by $[(N\pi)/(3c^2)]\ [(\partial\mu_x/\partial Q_i)^2 + (\partial\mu_y/\partial Q_i)^2 + (\partial\mu_z/\partial Q_i)^2]$. In Fig. 13 a comparison of the experimental and simulated infrared spectra of fluorocyclobutane is shown for the spectral region from 900 to 1500 cm^{-1}. The predicted spectrum is in relatively good agreement with the experimental spectrum which shows the utility of the scaled predicted frequencies and intensities for supporting the vibrational assignment.

VIBRATIONAL ASSIGNMENT

In order to obtain the enthalpy difference between the two stable conformers of fluorocyclobutane it is necessary to confidently identify a vibrational mode for the axial conformer which is expected to be a very small percentage of the sample at ambient temperature. This requires confident assignments of all the fundamentals of the more stable equatorial conformer. There have been two extensive vibrational assignments [53,80] for fluorocyclobutane where in the earlier study [80] the assignment was made by using the infrared vapor phase band contours, Raman depolarization data, expected infrared and Raman intensities and "group frequencies". In the more recent study [53] *ab initio* calculations with the 3-21G(d) basis set with two scaling factors of 0.88 for stretches and 0.90 for the bends were used to predict frequencies for the fundamentals and potential energy distributions. These new data resulted in some significant changes in a few of the descriptions of the motions contributing to some of the bands. In particular, two ring deformations were reassigned to lower frequency bands. There was also a few major changes in the vibrational assignment where the C-H out-of-plane bend was reassigned as nearly accidently degenerate with the β-CH_2 wag at 1242 cm^{-1}. The more accurately predicted fundamental frequencies along with the predicted infrared intensities and Raman activities as well as the relatively sharp bands in the spectrum from the xenon

solution provides considerably more spectral information for making the vibrational assignment.

With the confident assignment for the fundamentals of the equatorial conformer a search was made for bands arising from the axial conformer. As expected the C-F stretch should be the most intense band in the spectral "fingerprint" region. Unfortunately there is mixing of this mode with both ring deformations along with the β-CH_2 rock. Nevertheless, the band at 832 cm^{-1} is quite pronounced and it can be assigned as a fundamental of the axial conformer. There is also a band at 1348 cm^{-1} which undoubtedly is due to the axial conformer. There is another band at 1037 cm^{-1} which is probably due to the axial conformer but it is partly overlaid by the equatorial band at 1048 cm^{-1}. Therefore, there are only two bands of the axial conformer which could be considered for the determination of the enthalpy difference for the two conformers.

CONFORMATIONAL STABILITY

To determine the enthalpy difference between the two conformers, the mid-infrared spectra of fluorocyclobutane dissolved in liquefied xenon as a function of temperature from -55 to -100°C were recorded. Only small interactions are expected to occur between the dissolved sample and the surrounding xenon atoms, and consequently, only small frequency shifts are anticipated when passing from the gas phase to the liquefied noble gas solutions. A significant advantage of this study is that the conformer bands are better resolved in comparison with those in the infrared spectrum of the gas. From *ab initio* calculations, the dipole moments of the two conformers are predicted to have similar values and the molecular sizes of the two conformers are nearly the same, so

the ΔH value obtained from the temperature dependent FT-IR study is expected to be close to that for the gas [16-20,5,51].

As indicated earlier only the two bands at 832 and 1348 cm^{-1} were confidently assigned for the axial conformer. The fundamental at 1348 cm^{-1} could not be resolved in the spectra of the xenon solution due to the close proximity of the ν_8 equatorial conformer fundamental. Therefore, only the band at 832 cm^{-1} could be used for intensity measurements for the axial conformer. The choice of the bands to be used for the equatorial conformer was also a little difficult since they must be sufficiently separated from any interfering bands. Also, for best results they should have comparable intensity to the band being used for the axial conformer and preferably be in the lower frequency range to minimize interference of overtone and combination bands. From the inspection of the various possible bands the fundamentals at 954, 1090, 1136, and 1240 cm^{-1} were selected for the equatorial conformer bands to be use in the determination of the enthalpy difference.

The intensities of the infrared bands were measured as a function of temperature and their ratios were determined. By application of the van't Hoff equation $-\ln K = \Delta H/(RT) - \Delta S/R$, ΔH was determined from a plot of $-\ln K$ versus 1/T, where ΔH/R is the slope of the line and K is substituted with the appropriate intensity ratios, *i.e.* $I_{equatorial} / I_{axial}$. It was assumed that ΔH, ΔS, and α are not a function of temperature in the temperature range studied.

By combining the axial band and the four equatorial conformer bands, four pairs were utilized for the determination of the enthalpy difference, and the resulting values with statistical uncertainties are listed in Table 25. As can be seen from the data in this

table there is a fair spread of values but each one has a relatively small uncertainty. However, this spread is expected when measuring band intensities for bands with shoulders and considerable potential for underlying overtones and combination bands. Nevertheless, the statistical uncertainty is quite small and the statistical average obtained by using all eight pairs as a single set gives a value of 496 ± 9 cm^{-1}. This error limit is derived from the statistical standard deviation of one sigma of the measured intensity data. This error limit does not take into account small associations with the liquid xenon or the interference of overtones and combination bands in near coincidence with the measured fundamentals. The variations in the individual values are undoubtedly due to these types of interferences, but by taking several pairs, the effect of such interferences should cancel. Nevertheless, we expect the error is probably significantly larger than the statistical uncertainty obtained so we believe the determined ΔH value is 496 $\underline{+}$ 40 cm^{-1}. Thus, the abundance of the less stable axial conformer present at ambient temperature is 8 ± 1%.

TABLE 25. Temperature and intensity ratios of the *equatorial* and *axial* bands of fluorocyclobutane.

	T(°C)	1/T ($\times 10^{-3}$ K^{-1})	I_{1240} / I_{832}	I_{1136} / I_{832}	I_{1090} / I_{832}	I_{954} / I_{832}
Liquid xenon	–55.0	4.584	28.047	21.816	73.347	20.196
	–60.0	4.692	30.335	22.479	82.453	21.944
	–65.0	4.804	34.427	25.001	91.191	24.540
	–70.0	4.923	37.342	26.659	99.334	25.717
	–75.0	5.047	42.126	30.737	107.541	29.125
	–80.0	5.177	45.832	31.483	120.126	32.373
	–85.0	5.315	51.851	36.427	132.261	35.535
	–90.0	5.460	55.804	37.080	144.495	39.539

	–95.0	5.613	64.312	42.029	156.716	43.091
	–100.0	5.775	69.057	44.885	176.726	47.951
ΔH^a (cm^{-1})			536 ± 14	439 ± 18	499 ± 14	508 ± 11

[a] Average value $\Delta H = 496 \pm 9$ cm^{-1} (5.93 ± 0.11 kJ mol^{-1}) with the equatorial conformer the more stable form and the statistical uncertainty (1σ) obtained by utilizing all of the data as a single set.

STRUCTURAL PARAMETERS

We have [51] shown that *ab initio* MP2(full)/6-311+G(d,p) calculations predict the r_0 structural parameters for more than fifty carbon-hydrogen distances better than 0.002 Å compared to the experimentally determined values from isolated CH stretching frequencies which are compared [5] to previously determined values from earlier microwave studies. Thus, all of the carbon-hydrogen r_0 parameters can be taken from the MP2(full)/6-311+G(d,p) predicted values for fluorocyclobutane. Also, we have found [14] that we can obtain good structural parameters by adjusting the structural parameters from the *ab initio* calculations to fit the rotational constants obtained from the microwave experimental data. In order to reduce the number of independent variables, the structural parameters are separated into sets according to their types. Bond lengths in the same set keep their relative ratio which results in only two heavy atoms distances, i.e. C-C and C-F, for fluorocyclobutane. Also, the bond angles and torsional angles in the same set keep their differences in degrees. This assumption is based on the fact that the errors from *ab initio* calculations are systematic. Thus, it is possible to reduce the number of heavy atom independent structural parameters to five with the CC and CF bond lengths, and the angles of FCC, CCC and the ring puckering angle. Therefore, if the CH parameters are taken from the MP2(full)/6-311+G(d,p) calculations, then it should be possible to obtain

"adjusted r_0" structural parameters for the equatorial and axial conformers of fluorocyclobutane by utilizing the previously reported [44] six rotational constants from the microwave study.

These determined adjusted r_0 parameters are listed in Table 24 and the final fit of the rotational constants is shown in Table 26. The differences are quite small with those for the B and C rotational constants fit to better than 0.5 MHz. The largest adjustment for the angles is associated with the ring puckering angle which changes from 34.0° to 37.4° for the equatorial conformer and from 29.2° to 20.7° for the axial conformer and the largest distance change is the C_α-C_β ($C_{\beta'}$) bond which increased from 1.530 to 1.543 Å for the equatorial conformer and 1.534 to 1.546 Å for the axial conformer. The C-F bond distance in the axial conformer also exhibits a significant change from 1.398 to 1.407 Å. The remaining changes were relatively small. It is somewhat difficult to estimate the uncertainties in these structural parameters, but it is believed those for the CH distances should be no more than ± 0.002 Å and for the heavy atom distances ± 0.003 Å, whereas the uncertainties in the angles is estimated to be ± 0.5°. These parameters are expected to be more accurate than those that could be obtained from electron diffraction or microwave study alone or a microwave study with all atoms substituted to obtain r_s parameters.

TABLE 26. Comparison of rotational constants (MHz) obtained from modified *ab initio*, MP2(full)/6-311+G(d,p) structural parameters and the experimental values from the microwave spectra of *equatorial* and *axial* fluorocyclobutane.

Isotopomers	Rotational constant	Experimental[a]	Calculated	$\|\Delta\|$
eq-C_4H_7F	A	10250.412 (7)	10250.620	0.208
	B	4274.930 (3)	4275.419	0.489
	C	3402.614 (3)	3402.568	0.046
ax-C_4H_7F	A	8628.77 (7)	8628.79	0.02
	B	4726.25 (6)	4726.22	0.03
	C	3939.16 (8)	3939.20	0.04

[a]Ref. [44].

DISCUSSION

The determined enthalpy difference of 496 ± 40 cm^{-1} is a reasonable value compared to the relative values obtained for bromocyclobutane (ΔH = 291 ± 22 cm^{-1} [79]) and chlorocyclobutane (ΔH = 361 ± 17 cm^{-1} [48]) as compared to the predicted values from the MP2(full) calculations with a relatively large number of basis sets. For the bromide the ΔE value was 560 ± 46 cm^{-1} and for the chloride the ΔE value was 646 ± 73 cm^{-1} where the calculations include basis sets up to aug-cc-pVTZ. Therefore, the *ab initio* calculations predicted considerably large energy differences than the experimentally determined enthalpy difference for both the chloride and bromide. For the fluoride the predicted energy difference is 732 ± 47 cm^{-1} which is about 230 cm^{-1} larger than the experimental determined enthalpy difference. However, from the microwave study of fluorocyclobutane [44] the energy difference was determined to be 620 ± 30 cm^{-1} which is significantly larger than the ΔH value obtained herein. Nevertheless it is clear that the

enthalpy difference for the fluoride is much larger than the value for the other two halocyclobutanes.

In the present study the experimentally determined enthalpy difference was larger at 496 cm^{-1} than the 413 cm^{-1} enthalpy difference used in the previous study [53] for determining the ring-puckering potential function. With the higher and more reliable ΔH value, we have again obtained the potential function governing the conformational interchange for fluorocyclobutane. By using the far infrared and low frequency Raman (Fig. 15) data the "hot bands" series for the equatorial conformer as well as the first transition in the axial well were assigned (Table 27) and the assignment used matches the previous spectral study [53]. With this assignment the potential function (Fig. 16) was determined to have a ΔH of 450 cm^{-1} with a barrier of 774 cm^{-1} as compared to the previous study where the potential function gave a barrier slightly smaller at 713 cm^{-1}. This ΔH value is on the low side of the experimentally determined value for this study. This potential function is not significantly different from the potential function from the previous study [53].

TABLE 27. Observed and calculated frequencies (cm^{-1}) for the ring-puckering vibrations of fluorocyclobutane.

		Observed[a]				
Conformer	Transition	Infrared	Raman	Calculated[b]	Obs. – Calc.	Weight
Equatorial	1 ← 0	166.44	167	166.92	-0.48	1.0
	2 ← 1	157.25	157	157.29	-0.04	1.0
	4 ← 2	146.50	147	145.51	0.99	1.0
	6 ← 4	129.04		129.46	-0.42	1.0
Axial	5 ← 3	130.94		132.03	-1.09	1.0

[a] The infrared were utilized preferentially over the Raman [10] in the calculations.
[b] Calculated by using a potential of the form V (cm^{-1}) = (8.46 ± 0.12) x 10^5X^4 – (4.05 ± 0.18) x 10^4X^2 + (6.01 ± 0.11) x 10^4X^3 with a reduced mass of 214 amu.

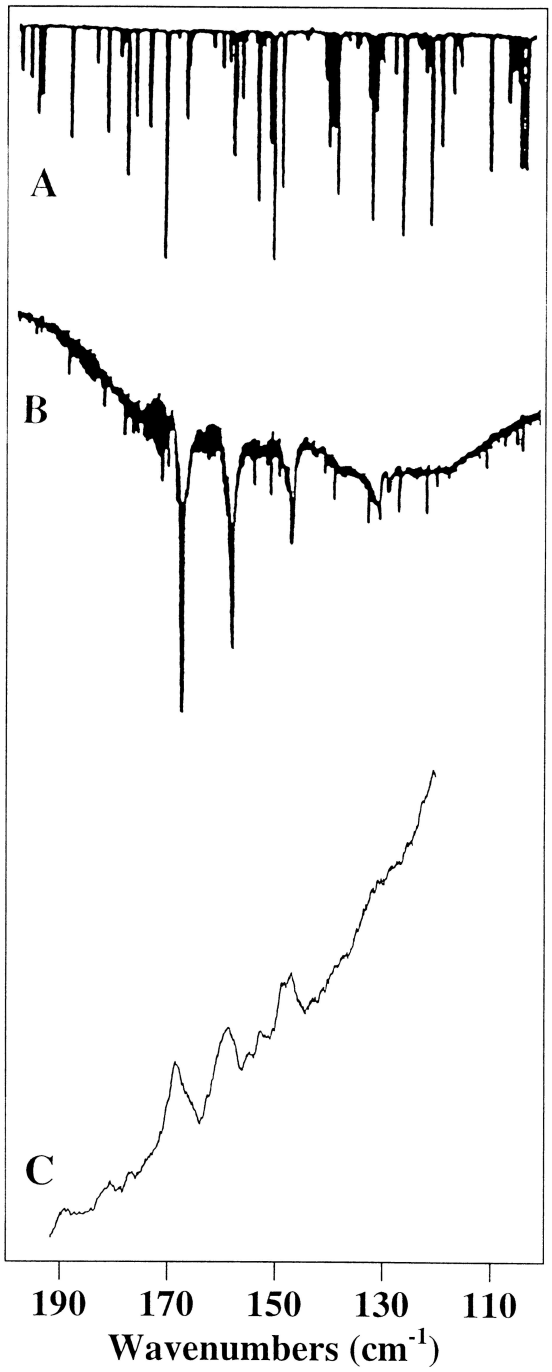

Figure 15. Low frequency spectra of gaseous fluorocyclobutane: (A) background; (B) far infrared; (C) Raman.

Figure 16. Potential function governing the ring-puckering vibration of fluorocyclobutane. $V\ (cm^{-1}) = (8.46 \pm 0.12) \times 10^5 X^4 - (4.05 \pm 0.18) \times 10^4 X^2 + (6.01 \pm 0.11) \times 10^4 X^3$ with a reduced mass of 214 amu.

The three parameters which show significant differences from the previous study [53] of this molecule are the puckering angle, as well as the C_α-C_β ($C_{\beta'}$) and C_γ-C_β ($C_{\beta'}$) bond distances. In the previous study these parameters were all assumed with values of 20°, 1.535 Å, and 1.548 Å respectively; however for this study we obtained values of 37.4(5)° for the puckering angle along with 1.543(3) and 1.554(3) Å for the C_α-C_β ($C_{\beta'}$) and C_γ-C_β ($C_{\beta'}$) bond distances in the equatorial conformer. We found that there are two parameters which were very sensitive to the A rotational constant, with those being the C_α-C_β ($C_{\beta'}$) bond distance and the puckering angle for the equatorial and axial

conformers. We also found that the C-F distance in the axial conformer was very sensitive to even small changes in the A rotational constant and to a lesser extent the B and C rotational constants so that even a relatively small change of 0.001 Å would change the fit of the rotational constants by one to two MHz for each rotational constant. This lead to the 1.407 Å C-F bond distance where even a small change would drastically alter the rotational constant fit. Therefore, the determined C-F distance has a very small uncertainty.

We have compared the heavy atom and C-F distances of a number of fluoroalkanes and alkenes (Table 28) in order to demonstrate the effect of fluorine atom on the structural parameters of a molecule. The *ab initio* MP2(full)/6-311+G(d, p) predicted C-F distances for all the fluoroalkanes and alkenes is predicted to be larger than the experimentally determined values. Whereas the C_{α}-C_{β} ($C_{\beta'}$) bond distance is on average predicted 0.010 Å shorter than its corresponding experimental value. It is also of interest that the C_{γ}-C_{β} ($C_{\beta'}$) distance for *gauche*-1-fluoropropene is predicted to be equal to the experimentally determined value.

TABLE 28. Structural parameters (Å and degrees) of cyclobutane[a] and some fluoroalkanes and fluoroalkenes.

Parameters	fluoromethane		fluoroethane		fluoroethene		*cis*-3-fluoropropene		isopropyl fluoride		*gauche*-1-fluoropropane	
	MP2[b]	Exp.[c]	MP2[b]	Exp.[d]	MP2[b]	Exp.[e]	MP2[b]	Exp.[f]	MP2[b]	Exp.[g]	MP2[b]	Exp.[h]
rC_α-F	1.387	1.383(1)	1.396	1.387(3)	1.346	1.342(4)	1.399	1.388(4)	1.406	1.398(13)	1.398	1.390(5)
rC_α-C_β			1.510	1.512(2)			1.492	1.495(4)	1.512	1.522(7)	1.512	1.506(2)
rC_γ-C_β											1.526	1.526(3)
rC_α-H	1.091	1.087(1)	1.093	1.094(1)	1.084	1.080*	1.094	1.098(2)	1.095	1.092*	1.093	1.097(1)

Parameters	*gauche*-1-fluoro-2-methylpropane		*eq*-fluorocyclobutane		*ax*-fluorocyclobutane		chair eq-fluorocyclohexane		chair ax-fluorocyclohexane	
	MP2[b]	Exp.[i]	MP2[b]	Exp.[j]	MP2[b]	Exp.[j]	MP2[b]	Exp.[k]	MP2[b]	Exp.[k]
rC_α-F	1.396	1.398(13)	1.386	1.383(3)	1.398	1.407(3)	1.403	1.399(2)	1.408	1.4021(14)
rC_α-C_β	1.515	1.525(5)	1.530	1.543(3)	1.534	1.546(3)	1.515	1.5346(1)	1.518	1.5348(1)
rC_γ-C_β	1.528	1.536*	1.551	1.554(3)	1.552	1.554(3)	1.532	1.5358(1)	1.530	1.5359(1)
rC_α-H			1.094	1.094(2)	1.092	1.092(2)				

[a] Structural parameters[78]; rC-C 1.555(2), rC-H 1.0910(6), and puckering angle 29.55(3).
[b] From *ab initio* MP2(full)/6-311+G(d,p).
[c] Ref. [81] r_e structural parameters
[d] Ref. [82] r_e structural parameters
[e] Ref. [83] r_0 structural parameters; value with asterisk is assumed
[f] Ref. [84] adjusted r_0 structural parameters
[g] Ref. [85] r_0 structural parameters; value with asterisk is from isolated C-H stretch
[h] Ref. [86] r_0 structural parameters
[i] Ref. [87] r_0 structural parameters; value with asterisk is assumed
[j] This study.
[k] Ref. [88] r_0 structural parameters

The heavy atom structural parameters for the halogen substituted four member rings also shows some interesting trends (Table 29). The C_γ-C_β ($C_{\beta'}$) distances for the conformers of chlorocyclobutane differ by only 0.001 Å and for the C_γ-C_β ($C_{\beta'}$) distance in fluorocyclobutane they are equal but 0.004 Å shorter than those for the chloride. The most pronounced effect of a substituent on four membered rings can be visualized by comparing the puckering angle between the conformers. The largest difference of ~16° is obtained for the case of fluorocyclobutane for the halogens. The C_α-C_β ($C_{\beta'}$) bond also exhibits interesting behavior in the presence of a halogen substituent as the bond is significantly shorter for the halogen substituted molecules than the corresponding bond for the cyclobutane without substitution. This bond also is significantly longer in the axial conformers of chlorocyclobutane and fluorocyclobutane than in their equatorial conformers.

TABLE 29. Structural parameters of the ring for a few four-membered ring molecules (Å and degree).

Structural Parameters	Cyclobutane[a]	Chlorocyclobutane[b]		Bromocyclobutane[c]		Fluorocyclobutane[d]	
		Equatorial	Axial	Equatorial	Axial	Equatorial	Axial
rC_{α}-X		1.783(5)	1.803(5)	1.942(3)	1.952	1.383(3)	1.407(3)
rC_{α}-C_{β}	1.5555(2)	1.539(3)	1.547(3)	1.541(3)	1.548	1.543(3)	1.546(3)
rC_{β}-C_{γ}	1.5555(2)	1.558(3)	1.557(3)	1.552(3)	1.546	1.554(3)	1.554(3)
Puckering angle	28.58(9)	30.7(5)	22.3(5)	29.8(5)	24.0	37.4(5)	20.7(5)

[a]Ref[78].
[b]Ref[48], X = Cl.
[c]Ref[79], X = Br.
[d]This study, X = F.

The centrifugal distortion constants obtained for the asymmetric reduced Hamiltonian for both conformers are listed in Table 30 along with the values obtained from the force constants that were predicted from the *ab initio* MP2(full)/6-31G(d) and 6-311+G(d, p) calculations and from the density functional theory calculations by the B3LYP method with both the 6-31G(d) and the 6-311+G(d,p) basis sets. In general the fit is much better with the larger basis set from the B3LYP calculations where the differences between the predicted and experimental values is quite small for all the constants for the equatorial conformer. However for the axial conformer the difference from the predicted values from the MP2(full) and B3LYP calculations are significantly different from the values reported from the microwave study [44]. The magnitude of the constants are in fair agreement but the signs of the constants are all different for the experimentally determined values compared to the predicted values.

TABLE 30. Quadratic centrifugal distortion constants (kHz) for *equatorial* and *axial* conformers of fluorocyclobutane.

	equatorial					*axial*				
	MP2(full)/ 6-31G(d)	MP2(full)/ 6-311+G(d,p)	B3LYP/ 6-31G(d)	B3LYP/ 6-311+G(d,p)	Exp.[a]	MP2(full)/ 6-31G(d)	MP2(full)/ 6-311+G(d,p)	B3LYP/ 6-31G(d)	B3LYP/ 6-311+G(d,p)	Exp.[a]
Δ_J	0.68	0.68	0.73	0.76	0.72(2)	2.6	2.6	3.7	5.4	-2.(2)
Δ_{JK}	1.93	1.967	1.59	1.388	1.74(7)	-6.0	-5.9	-12.2	-23.3	10.(1)
Δ_K	3.4	3.4	4.8	5.4	4.4(2)	8.9	8.9	18.5	37.3	-27.(1)
δ_J	0.122	0.124	0.131	0.135	0.138(4)	-0.02	-0.02	-0.2	-0.5	0.7(1)
δ_K	1.8	1.8	1.8	1.8	1.7(1)	1.3	1.3	1.9	3.5	-7.(3)

[a] Values taken from Ref [44].

We recently obtained the enthalpy difference for the equatorial and axial conformers of cyanocyclobutane [63] and the determined experimental value was 254 ± 12 cm^{-1} (3.03 ± 12 kJ/mol) with the equatorial conformer more stable, which indicates that there is 23 ± 1% of the axial form present at ambient temperature. This value is smaller than the corresponding values for the halocyclobutanes and the question arises what are the factors of the substitute species that control the relative amounts of the two forms. The *ab initio* MP2(full) calculations predicted an enthalpy difference for the cyanide of 238 ± 23 cm^{-1} which is consistent with the experimentally determined value. Thus it would be of interest to investigate the conformational stability of ethynylcyclobutane, as it is isoelectronic with cyanide, to determine the enthalpy difference for the two conformers for this molecule. Another molecule of interest is silylcyclobutane where the axial form is predicted more stable by *ab initio* MP2(full) calculations using relatively large basis sets, whereas, by using the smaller basis sets the equatorial form is predicted more stable. Also of interest would be the isocyanocyclobutane which is expected to have *trans* and *cis* forms in addition to the equatorial and axial conformers. Therefore, the conformational study of these and similar molecules might be used to determine the factors which control the relative stability of these types of molecules.

CHAPTER 6

CONFORMATIONAL AND STRUCTURAL STUDIES OF CYCLOBUTYLSILANE FROM TEMPERATURE DEPENDENT INFRARED SPECTRA OF XENON SOLUTIONS AND AB INITIO CALCULATIONS

INTRODUCTION

The structure of the cyclobutane molecule generated tremendous controversy whether it was a puckered or planar molecule. Several different techniques were used to try to obtain conclusive evidence of the structure of the molecule. However, by different methods both forms were reported to be the "correct" structure. This controversy continued for several years until finally an extensive vibrational study showed conclusively that the molecule was puckered [89]. These investigators referenced many papers where the conclusion clearly showed that the stable form of cyclobutane was the puckered form.

The structure of the monosubstituted cyclobutane was shown to be puckered earlier from studies of cyclobutyl chloride and bromide [38,64,65,90] where for both of these molecules the axial and equatorial conformers were identified. One of these investigators carried out a microwave investigation of cyclobutyl bromide [36] but the equatorial conformer was the only form identified. Also, from a subsequent microwave investigation of cyclobutyl chloride [35], where no evidence was found for the axial conformer, there was considerable doubt of the presence of the axial form for many monosubstituted cyclobutanes. However more recently the axial forms of both cyclobutyl chloride [44] and fluoride [45] were identified in the FT-microwave spectra; these studies

then lead to the determination of the structural parameters for these molecules [48,91] which were significantly different from the parameters previously reported [35,53].

Although the axial form of the cyclobutyl halides were not observed in the microwave spectra for nearly three decades from their reported presences from vibrational studies there were two microwave studies [92,93] of monosubstituted cyclobutanes where both the equatorial and axial conformers were observed. However from these studies only two structural parameters were obtained for the silane and five for the germane with the other parameters estimated from other sources. These microwave studies were followed by comprehensive vibrational studies [43,94] soon after. Therefore, we have embarked on a study of the monosubstituted cyclobutanes to obtain structural parameter values and more accurate enthalpy differences than those previously obtained for the two forms. Initially we determined the enthalpy differences for the cyclobutyl halides which have relatively small amounts of the axial forms at ambient temperatures. As a continuation of these studies we have investigated cyclobutylsilane.

To support the experimental studies we have obtained the harmonic force constants, infrared intensities, Raman activities, depolarization ratios, and vibrational frequencies for MP2(full)/6-31G(d) *ab intio* calculations with full electron correlation. To obtain predictions on the conformational stabilities we have carried out MP2(full) *ab intio* and density functional theory (DFT) calculations by B3LYP method utilizing a variety of basis sets. The r_0 structural parameters have been obtained by combining the MP2(full)/6-311+G(d,p) *ab initio* predicted parameters with the previously reported rotational constants obtained from the microwave study [92] and compared to those

obtained in the electron diffraction study [95]. The results of these spectroscopic, structural, and theoretical studies of cyclobutylsilane are reported herein.

2. Experimental and theoretical methods

The sample of cyclobutylsilane was prepared in two steps. Firstly, by preparing cyclobutyl magnesium bromide in dry ether under dry nitrogen. Secondly, the Grignard compound is cannulated drop wise to tetrachlorosilane in dry ether and then refluxed overnight under dry nitrogen. The precipitated salt of magnesium bromochloride was filtered under dry nitrogen and washed several times with dry pentane. The ether and pentane were distilled off by using a 25-cm vigreux column under reduced pressure. The product of cyclobutyl trichlorosilane was reduced with lithium aluminum hydride in dry dibutyl ether. The sample was checked with previously reported infrared spectra [43]. The sample was further purified by a low-temperature, low-pressure fractionation column and the purity of the sample was verified by comparing the infrared spectrum with that previously reported [43].

TABLE 31. Observed and calculated[a] frequencies (cm^{-1}) for Eq cyclobutylsilane.

	Vib. No.	Approximate Descriptions	ab initio	fixed scaled[b]	IR int.	Raman act.	dp ratio	IR Xe soln.	P.E.D. [c]	Band Contours[d] A	Band Contours[d] C
A′	ν_1	γ-CH_2 antisymmetric stretch	3192	2994	49.8	61.8	0.71	2971	$57S_1$, $42S_2$	-	100
	ν_2	β-CH_2 antisymmetric stretch	3173	2977	9.2	77.9	0.38	2960	$51S_2$, $42S_1$	94	6
	ν_3	γ-CH_2 symmetric stretch	3121	2928	36.5	141.0	0.07	2911	$91S_3$	96	4
	ν_4	β-CH_2 symmetric stretch	3116	2923	14.6	49.9	0.50	2911	$64S_4$, $28S_5$	17	83
	ν_5	CH stretch	3109	2917	1.6	135.3	0.23	2898	$69S_5$, $25S_4$	61	39
	ν_6	SiH_3 antisymmetric stretch	2300	2158	165.9	58.0	0.75	2148	$100S_6$	11	89
	ν_7	SiH_3 symmetric stretch	2291	2149	97.5	179.3	0.01	2148	$100S_7$	98	2
	ν_8	β-CH_2 deformation	1576	1484	1.0	7.2	0.68	1467	$71S_8$, $27S_9$	39	61
	ν_9	γ-CH_2 deformation	1549	1458	4.4	20.9	0.73	1444	$73S_9$, $28S_8$	16	84
	ν_{10}	β-CH_2 wag	1352	1285	0.5	5.4	0.54	1271	$52S_{10}$, $26S_{11}$	6	94
	ν_{11}	CH in-plane bend	1302	1238	4.1	5.2	0.72	1231	$34S_{11}$,$32S_{10}$, $20S_{12}$	44	56
	ν_{12}	β-CH_2 twist	1270	1209	3.5	8.2	0.73	1198	$45S_{12}$, $19S_{19}$, $11S_{13}$, $11S_{11}$	29	71
	ν_{13}	β-CH_2 rock	1138	1085	16.9	2.8	0.32	1062	$29S_{13}$, $28S_{14}$	54	46
	ν_{14}	Ring breathing	1057	1004	4.0	13.9	0.18	996	$59S_{14}$, $14S_{11}$, $11S_{13}$	7	93
	ν_{15}	SiH_3 antisymmetric deformation	987	937	55.3	23.6	0.72	943	$96S_{15}$	1	99
	ν_{16}	Ring deformation 1	972	926	185.8	5.8	0.42	922	$27S_{16}$, $42S_{17}$	97	3
	ν_{17}	SiH_3 symmetric deformation	954	915	103.6	10.8	0.74	922	$46S_{17}$, $30S_{16}$	96	4
	ν_{18}	Ring deformation 2	913	884	24.9	5.6	0.25	907	$40S_{18}$, $21S_{19}$, $10S_{17}$	100	-
	ν_{19}	γ-CH_2 rock	750	717	6.6	5.4	0.34	715	$32S_{19}$, $17S_{20}$, $13S_{21}$, $11S_{16}$	-	100
	ν_{20}	SiH_3 rock	659	631	30.4	5.4	0.58	641	$52S_{20}$, $19S_{18}$, $16S_{13}$	1	99
	ν_{21}	Si-C stretch	506	486	4.8	12.7	0.34	497	$46S_{21}$, $23S_{18}$, $15S_{20}$	94	6
	ν_{22}	Ring-SiH_3 bending	315	306	0.6	0.6	0.40	287*	$35S_{22}$, $38S_{23}$, $11S_{21}$	6	94
	ν_{23}	Ring puckering	158	156	0.3	0.3	0.04	124.8*	$46S_{23}$, $48S_{22}$	-	-
A″	ν_{24}	β-CH_2 antisymmetric stretch	3180	2983	22.6	68.7	0.75	2967	$96S_{24}$	-	-

ν_{25}	β-CH_2 symmetric stretch	3112	2920	43.9	1.3	0.75	2911	$96S_{25}$	-	-
ν_{26}	SiH_3 antisymmetric stretch	2299	2157	173.6	76.4	0.75	2148	$100S_{26}$	-	-
ν_{27}	β-CH_2 deformation	1546	1455	0.5	5.8	0.75	1444	$100S_{27}$	-	-
ν_{28}	γ-CH_2 wag	1322	1256	3.8	3.6	0.75	1247	$67S_{28}$	-	-
ν_{29}	β-CH_2 wag	1306	1239	0.3	0.4	0.75	1231	$47S_{29}$, $24S_{30}$, $19S_{32}$	-	-
ν_{30}	CH out-of-plane bend	1284	1219	0.0	6.7	0.75	1215	$35S_{30}$, $26S_{31}$, $15S_{28}$, $12S_{29}$	-	-
ν_{31}	γ-CH_2 twist	1233	1172	1.9	7.8	0.75	1173	$27S_{31}$, $35S_{29}$, $20S_{32}$	-	-
ν_{32}	β -CH_2 twist	1053	1006	2.7	3.5	0.75	~996	$30S_{32}$, $26S_{34}$, $19S_{35}$	-	-
ν_{33}	SiH_3 antisymmetric deformation	990	940	22.8	13.6	0.75	944	$51S_{33}$, $27S_{35}$	-	-
ν_{34}	Ring deformation 2	981	934	3.1	0.2	0.75	942	$39S_{34}$, $17S_{32}$, $15S_{30}$, $14S_{31}$	-	-
ν_{35}	Ring deformation 1	973	931	44.5	19.4	0.75	940	$42S_{35}$, $43S_{33}$	-	-
ν_{36}	β-CH_2 rock	820	779	7.9	1.2	0.75	777	$76S_{36}$, $11S_{31}$	-	-
ν_{37}	SiH_3 wag	642	611	27.7	11.7	0.75	626	$80S_{37}$	-	-
ν_{38}	Ring-SiH_3 bending	195	193	0.5	0.0	0.75	190*	$82S_{38}$	-	-
ν_{39}	SiH_3 torsion	129	123	0.0	0.0	0.75	124*	$91S_{39}$	-	-

[a] MP2(full)/6-31G(d) *ab initio* calculations, scaled frequencies, infrared intensities (km/mol), Raman activities ($Å^4$/amu), depolarization ratios and potential energy distributions (P.E.D.s)

[b] MP2(full)/6-31G(d) fixed scaled frequencies with factors of 0.88 for CH and SiH stretches and CH_2 deformations, 1.0 for heavy atom bends, and 0.90 for all other modes.

[*] Ref [43].

[c] Contributions less than 10% are omitted.

[d] A and C values in the last two columns are percentage infrared band contours.

TABLE 32. Observed and calculated[a] frequencies (cm^{-1}) for Ax cyclobutylsilane.

	Vib. No.	Approximate Descriptions	*ab initio*	fixed scaled[b]	IR int.	Raman act.	dp ratio	IR Xe soln.	P.E.D. [c]	Band Contours[d] A	Band Contours[d] C
A′	ν_1	γ-CH_2 antisymmetric stretch	3198	3000	40.3	57.7	0.52	2971	$88S_1$, $11S_2$	79	21
	ν_2	β-CH_2 antisymmetric stretch	3165	2970	22.9	64.2	0.63	2960	$86S_2$, $12S_1$	13	87
	ν_3	γ-CH_2 symmetric stretch	3133	2940	23.5	133.0	0.74	2935	$96S_3$	61	39
	ν_4	β-CH_2 symmetric stretch	3108	2916	6.2	107.5	0.10	2898	$72S_4$, $27S_5$	99	1
	ν_5	CH stretch	3118	2925	19.4	114.1	0.09	2911	$70S_5$, $25S_4$	12	88
	ν_6	SiH_3 antisymmetric stretch	2302	2159	160.8	52.5	0.36	2148	$99S_6$	21	79
	ν_7	SiH_3 symmetric stretch	2294	2152	93.1	174.0	0.75	2148	$99S_7$	95	5
	ν_8	β-CH_2 deformation	1580	1488	0.1	9.1	0.02	-	$71S_8$, $27S_9$	94	6
	ν_9	γ-CH_2 deformation	1553	1462	3.8	17.1	0.61	1448	$72S_9$, $28S_8$	1	99
	ν_{10}	β-CH_2 wag	1341	1274	1.5	1.7	0.75	1261	$56S_{10}$, $26S_{11}$	15	85
	ν_{11}	CH in-plane bend	1315	1253	1.8	3.3	0.36	1247	$20S_{11}$, $29S_{12}$, $27S_{10}$, $16S_{16}$	96	4
	ν_{12}	β-CH_2 twist	1253	1193	2.5	11.4	0.19	1182	$34S_{12}$, $23S_{19}$, $18S_{13}$, $15S_{11}$	94	6
	ν_{13}	β-CH_2 rock	1091	1039	6.1	8.4	0.73	1027	$32S_{13}$, $24S_{11}$, $10S_{12}$, $10S_{22}$	33	67
	ν_{14}	Ring breathing	1068	1014	2.8	15.3	0.51	1003	$79S_{14}$, $13S_{11}$	90	10
	ν_{15}	SiH_3 antisymmetric deformation	989	940	26.6	19.6	0.16	944	$69S_{15}$, $19S_{16}$	-	100
	ν_{16}	Ring deformation 1	969	929	35.0	4.5	0.69	922	$52S_{16}$, $27S_{15}$, $10S_{10}$	24	76
	ν_{17}	SiH_3 symmetric deformation	966	919	299.1	10.4	0.71	922	$97S_{17}$	91	9
	ν_{18}	Ring deformation 2	904	877	4.6	4.9	0.75	907	$53S_{18}$, $25S_{19}$, $10S_{13}$	25	75
	ν_{19}	γ-CH_2 rock	735	702	17.4	5.1	0.51	705	$24S_{19}$, $27S_{20}$, $20S_{21}$, $10S_{18}$	8	92
	ν_{20}	SiH_3 rock	561	535	13.3	11.9	0.20	546	$50S_{20}$, $30S_{21}$, $10S_{18}$	39	61
	ν_{21}	Si-C stretch	662	637	9.7	4.6	0.47	641	$26S_{21}$, $25S_{18}$, $24S_{13}$, $15S_{19}$	34	66
	ν_{22}	Ring-SiH_3 bending	282	278	0.7	1.6	0.45	257*	$47S_{22}$, $27S_{23}$	33	67
	ν_{23}	Ring puckering	172	168	0.0	0.0	0.14		$58S_{23}$, $38S_{22}$	97	3

								112.2*			
A″	ν_{24}	β-CH_2 antisymmetric stretch	3168	2972	5.7	70.9	0.75	2960	$100S_{24}$	-	-
	ν_{25}	β-CH_2 symmetric stretch	3109	2917	63.4	2.0	0.75	2898	$100S_{25}$	-	-
	ν_{26}	SiH_3 antisymmetric stretch	2302	2159	170.8	73.7	0.75	2148	$100S_{26}$	-	-
	ν_{27}	β-CH_2 deformation	1550	1459	1.2	8.0	0.75	1444	$100S_{27}$	-	-
	ν_{28}	γ-CH_2 wag	1324	1258	2.7	0.4	0.75	1247	$70S_{28}$, $10S_{34}$	-	-
	ν_{29}	β-CH_2 wag	1292	1226	2.0	4.7	0.75	1215	$51S_{29}$, $33S_{31}$	-	-
	ν_{30}	CH out-of-plane bend	1280	1216	1.3	6.9	0.75	1215	$43S_{30}$, $27S_{29}$, $16S_{31}$	-	-
	ν_{31}	γ-CH_2 twist	1212	1150	0.4	6.0	0.75	1156	$14S_{31}$, $27S_{30}$, $27S_{32}$, $13S_{29}$, $11S_{35}$	-	-
	ν_{32}	β -CH_2 twist	1082	1029	4.1	3.3	0.75	1023	$49S_{32}$, $14S_{36}$, $13S_{31}$	-	-
	ν_{33}	SiH_3 antisymmetric deformation	984	935	43.9	7.4	0.75	942	$52S_{33}$, $18S_{34}$, $14S_{35}$	-	-
	ν_{34}	Ring deformation 2	967	928	17.6	4.7	0.75	922	$38S_{34}$, $27S_{33}$	-	-
	ν_{35}	Ring deformation 1	996	945	4.2	21.8	0.75	944	$61S_{35}$, $19S_{33}$	-	-
	ν_{36}	β-CH_2 rock	814	776	0.0	0.1	0.75	777	$63S_{36}$, $16S_{34}$, $14S_{31}$	-	-
	ν_{37}	SiH_3 wag	661	629	33.2	10.6	0.75	641	$85S_{37}$	-	-
	ν_{38}	Ring-SiH_3 bending	201	200	0.4	0.0	0.75	-	$90S_{38}$	-	-
	ν_{39}	SiH_3 torsion	134	127	0.0	0.0	0.75	139*	$99S_{39}$	-	-

[a] MP2(full)/6-31G(d) *ab initio* calculations, scaled frequencies, infrared intensities (km/mol), Raman activities ($Å^4$/amu), depolarization ratios and potential energy distributions (P.E.D.s)

[b] MP2(full)/6-31G(d) fixed scaled frequencies with factors of 0.88 for CH and SiH stretches and CH_2 deformations, 1.0 for heavy atom bends, and 0.90 for all other modes.

[*] Ref [43].

[c] Contributions less than 10% are omitted.

[d] A and C values in the last two columns are percentage infrared band contours.

The mid-infrared spectrum of the gas (Fig. 13B) was obtained from 3500 to 220 cm-1 on a Perkin-Elmer model 2000 Fourier transform spectrometer equipped with a Ge/CsI beamsplitter and a DTGS detector. Atmospheric water vapor was removed from the spectrometer housing by purging with dry nitrogen. The spectrum of the gas was obtained with a theoretical resolution of 0.5 cm-1 with 128 interferograms added and truncated.

The mid-infrared spectra (3500 to 400 cm^{-1}) of the sample dissolved in liquefied xenon (Fig. 14B) were recorded on a Bruker model IFS-66 Fourier transform spectrometer equipped with a globar source, a Ge/KBr beamsplitter and a DTGS detector. In all cases, 100 interferograms were collected at 1.0 cm^{-1} resolution, averaged and transformed with a boxcar truncation function. For these studies, a specially designed cryostat cell was used. It consists of a copper cell with a path length of 4 cm with wedged silicon windows sealed to the cell with indium gaskets. The copper cell was enclosed in an evacuated chamber fitted with KBr windows. The temperature was maintained with boiling liquid nitrogen and monitored by two Pt thermo resistors. The observed bands in the infrared spectra of the xenon solutions along with their proposed assignments are listed in Tables 31 and 32 for the equatorial (Eq) and axial (Ax) conformers, respectively.

TABLE 33. Calculated energies in Hartrees (H) and energy differences (cm^{-1}) for the two conformers and transition state of cyclobutylsilane.

Method/Basis Set	Energy[a], E	Energy Differences, Δ		
	equatorial	*axial*[b]	*planar ring*[b]	*planar ring*[c]
RHF/6-31G(d)	0.171720	149	331	182
MP2(full)/6-31G(d)	0.803105	134	749	615

MP2(full)/6-31+G(d)	0.813383	98		
MP2(full)/6-31G(d,p)	0.886353	150		
MP2(full)/6-31+G(d,p)	0.895576	101		
MP2(full)/6-311G(d,p)	1.138075	87		
MP2(full)/6-311+G(d,p)	1.141072	88	959	871
MP2(full)/6-311G(2d,2p)	1.202438	23		
MP2(full)/6-311+G(2d,2p)	1.204210	27		
MP2(full)/6-311G(2df,2pd)	1.284749	22	704	683
MP2(full)/6-311+G(2df,2pd)	1.286123	27	700	673
MP2(full)/cc-pVTZ	1.197213	-20		
MP2(full)/aug-cc-pVTZ	1.231387	-24		
Average MP2(full)	-	29 $\pm$ 42	788 $\pm$ 148	759 $\pm$ 112
B3LYP/6-31G(d)	1.904645	200	303	103
B3LYP/6-31+G(d)	1.910717	190		
B3LYP/6-311G(d,p)	1.974495	157		
B3LYP/6-311+G(d,p)	1.975247	158	273	115
B3LYP/6-311G(2d,2p)	1.983402	147		
B3LYP/6-311+G(2d,2p)	1.983924	151		
B3LYP/6-311G(2df,2pd)	1.989251	162	271	109
B3LYP/6-311+G(2df,2pd)	1.989660	161	269	109
B3LYP/aug-cc-pVTZ	1.994867	154		
Average B3LYP	-	164 $\pm$ 18	279 $\pm$ 16	115 $\pm$ 5

[a] Energy of conformer is given as –(E+446) H.

[b] Difference is relative to Eq form and given in cm^{-1}.

[c] Difference is relative to Ax form and given in cm^{-1}.

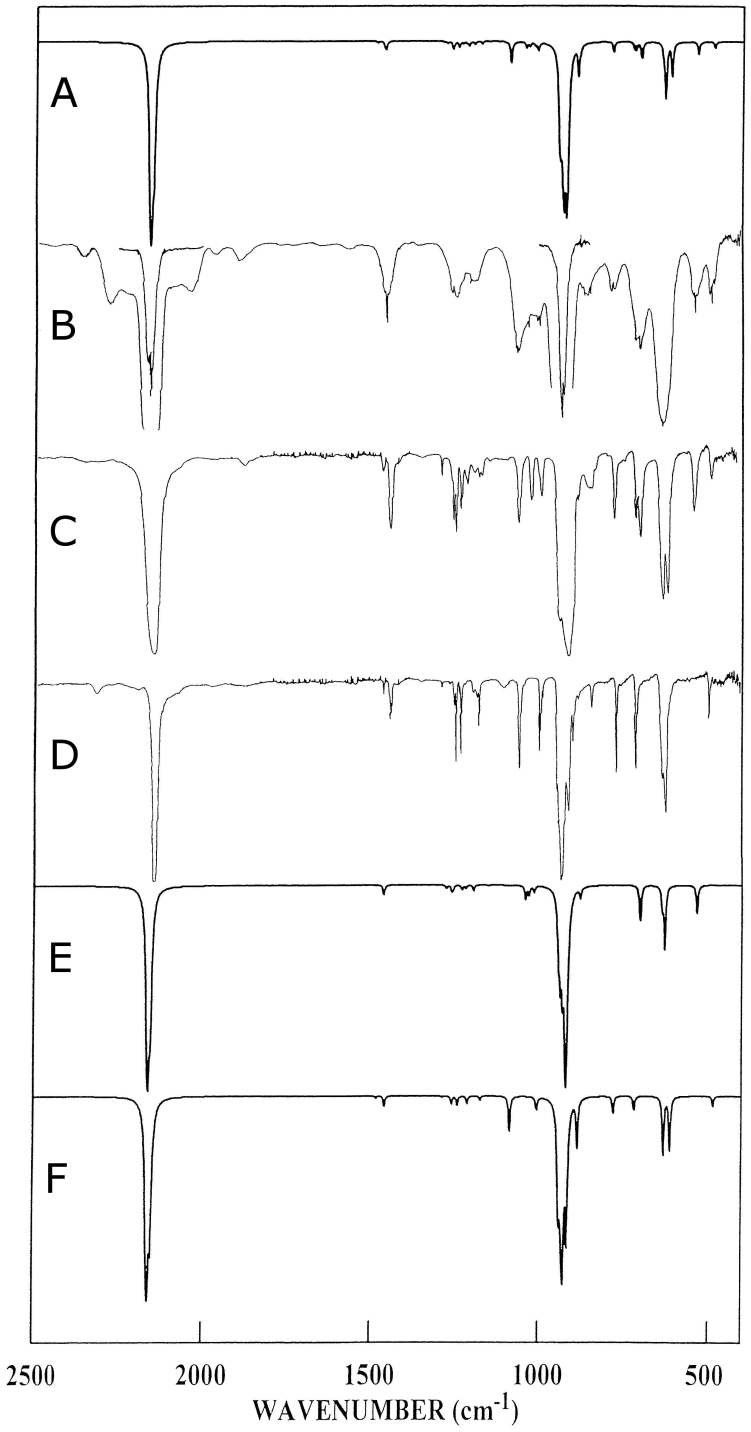

Figure 17. Experimental and predicted infrared spectra of cyclobutylsilane: (A) simulated spectrum of mixture of Eq and Ax (ΔH = 67 cm^{-1}) conformers at 25°C; (B) gas; (C) polycrystalline; (D) annealed solid; (E) simulated Ax conformer; (F) simulated Eq conformer.

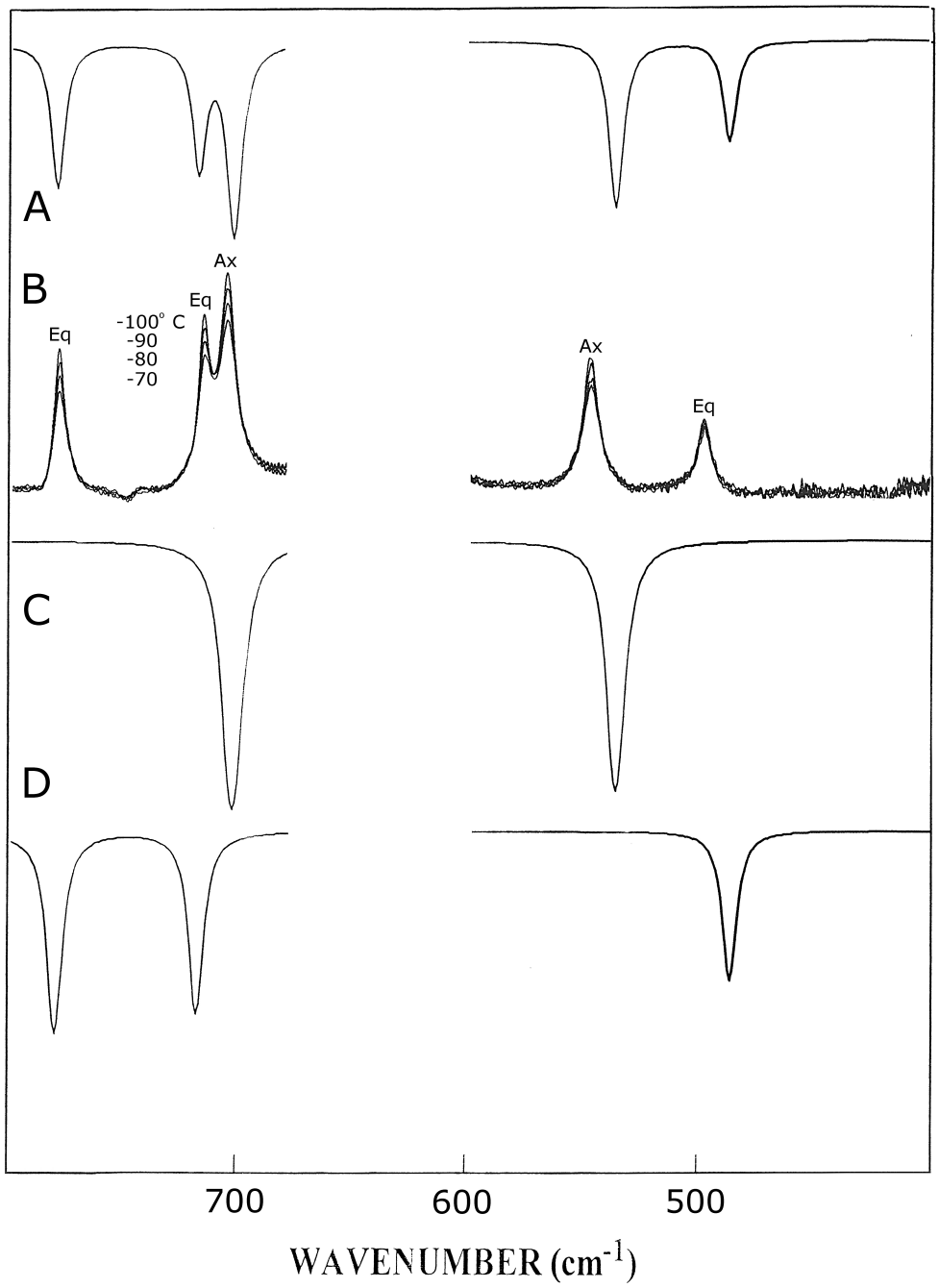

Figure 18. Experimental and predicted infrared spectra of cyclobutylsilane: (A) simulated spectrum of mixture of Eq and Ax (ΔH = 67 cm^{-1}) conformers at -70°C; (B) xenon solutions at various temperatures; (C) simulated Ax conformer; (D) simulated Eq conformer.

TABLE 34. Structural parameters (Å and degrees), rotational constants (MHz) and dipole moments (Debye) for Eq and Ax cyclobutylsilane.

Structural Parameters	Int. coor.	MP2(full)/ 6-311+G(d,p)		B3LYP/ 6-311+G(d,p)		ED[a]		Adjusted r_0[b]	
		Eq	Ax	Eq	Ax	Eq	Ax	Eq	Ax
rC_α-Si	R_1	1.875	1.879	1.886	1.888	1.873(3)	1.873(3)	1.879(3)	1.884(3)
rC_α-C_β,$C_{\beta'}$	R_2	1.559	1.559	1.566	1.566	1.573(4)	1.573(4)	1.562(3)	1.561(3)
rC_γ-C_β,$C_{\beta'}$	R_3	1.546	1.547	1.552	1.552	1.557(4)	1.557(4)	1.551(3)	1.553(3)
rC_α-H	r_1	1.097	1.096	1.095	1.094	1.126(8)	1.126(8)	1.097(2)	1.096(2)
rC_β-H_1, $C_{\beta'}$-H_1	r_2	1.096	1.094	1.094	1.093	1.126(8)	1.126(8)	1.096(2)	1.094(2)
rC_β-H_2, $C_{\beta'}$-H_2	r_3	1.093	1.094	1.092	1.093	1.126(8)	1.126(8)	1.093(2)	1.094(2)
rC_γ-H_1	r_4	1.093	1.093	1.092	1.092	1.126(8)	1.126(8)	1.093(2)	1.093(2)
rC_γ-H_2	r_5	1.094	1.092	1.093	1.092	1.126(8)	1.126(8)	1.094(2)	1.092(2)
rSi-H_1	r_6	1.480	1.480	1.489	1.489	1.474(9)	1.474(9)	1.480(3)	1.480(3)
rSi-H_2	r_7	1.480	1.479	1.489	1.489	1.474(9)	1.474(9)	1.480(3)	1.479(3)
$\angle C_\beta C_\alpha Si$	ϕ_1	119.7	114.3	119.6	115.4	118.6(19)	113.4(23)	118.6(5)	113.2(5)
$\angle C_\beta C_\alpha C_\beta$	θ_1	87.0	87.5	88.0	88.4	88.5(8)	88.5(8)	88.2(5)	88.4(5)
$\angle C_\gamma C_\beta C_\alpha$	θ_2	88.1	88.3	88.8	89.2	90.8	90.8	87.8(5)	88.9(5)
$\angle C_\beta C_\gamma C_\beta$	θ_3	87.9	88.4	89.0	89.4	89.7	89.7	88.9(5)	89.0(5)
$\angle HC_\alpha C_\beta$	σ_1	108.6	115.5	109.4	114.4			109.3(5)	116.2(5)
$\angle HC_\alpha Si$	σ_2	110.8	108.6	109.1	108.1			110.8(5)	108.8(5)
$\angle H_1C_\beta C_\alpha$	λ_1	111.0	118.7	112.2	117.9	112.5	112.5	111.0(5)	118.7(5)
$\angle H_1C_\beta C_\gamma$	λ_2	110.7	118.0	111.7	116.9	112.5	112.5	108.2(5)	120.2(5)
$\angle H_2C_\beta C_\alpha$	λ_3	117.9	110.8	117.0	111.7	112.5	112.5	117.9(5)	110.8(5)
$\angle H_2C_\beta C_\gamma$	λ_4	118.6	111.1	117.8	112.4	112.5	112.5	121.1(5)	108.0(5)
$\angle H_1C_\beta H_2$	λ_5	109.1	108.7	108.4	108.0	114.0(22)	114.0(22)	109.2(5)	108.8(5)
$\angle H_1C_\gamma C_\beta$	π_1	118.4	111.2	117.5	112.1	112.7	112.7	118.9(5)	109.2(5)
$\angle H_2C_\gamma C_\beta$	π_2	110.6	117.9	111.6	117.0	112.7	112.7	109.5(5)	119.4(5)

$\angle H_1C_\gamma H_2$	π_3	109.5	109.1	108.6	108.3	114.0(22)	114.0(22)	109.4(5)	109.1(5)
$\angle C_\alpha SiH_1$	η_1	108.6	110.1	109.6	110.4			108.5(5)	110.1(5)
$\angle C_\alpha SiH_2$	η_2	111.1	110.3	111.1	110.6			111.1(5)	110.3(5)
$\angle H_1SiH_2$	η_3	108.7	108.5	108.4	108.2	110.9(20)	110.9(20)	108.7(5)	108.5(5)
$\angle H_2SiH_2$	η_4	108.7	109.0	108.4	108.6	110.9(20)	110.9(20)	108.7(5)	109.0(5)
$\tau C_\gamma C_\beta C_\beta C_\alpha$	τ_1	31.6	29.0	24.8	20.9	31.8(30)	23.3(41)	29.0(5)	23.5(5)
$\tau H_1SiC_\alpha C_\gamma$	τ_2	0.0	0.0	0.0	0.0	0.0	0.0	0.0	0.0
A(MHz)		9177.758	7385.341	8952.620	7543.484	8984.388(10)	7404.909(90)	8984.922	7405.566
B(MHz)		2372.114	2692.022	2358.992	2593.878	2395.635(2)	2682.684(15)	2396.272	2682.397
C(MHz)		2086.276	2473.441	2069.387	2350.242	2101.061(1)	2445.930(14)	2100.394	2446.826
$\lvert\mu_a\rvert$		0.827	0.751	0.917	0.849	0.844(16)	0.806(10)		
$\lvert\mu_b\rvert$		0.000	0.000	0.000	0.000	0.000	0.000		
$\lvert\mu_c\rvert$		0.279	0.355	0.299	0.395	0.225(14)	0.397(20)		
$\lvert\mu_t\rvert$		0.873	0.831	0.965	0.936	0.873	0.898		

[a] Structural parameters from Ref. [95], rotational constants and dipole moments from Ref. [92].
[b] Adjusted parameters using the microwave data from Ref. [92] for the given ground states

The *ab initio* calculations were performed with the Gaussian 03 program [22] using Gaussian-type basis functions. The energy minima with respect to nuclear coordinates were obtained by the simultaneous relaxation of all geometric parameters using the gradient method of Pulay [29]. A variety of basis sets as well as the corresponding ones with diffuse functions were employed with the Møller-Plesset perturbation method [21] to the second order MP2 with full electron correlation as well as with the density functional theory by the B3LYP method. The predicted conformational energy differences are listed in Table 33.

In order to obtain descriptions of the molecular motions involved in the fundamental modes of cyclobutylsilane, a normal coordinate analysis was carried out. The force field in Cartesian coordinates was obtained with the Gaussian 03 program at the MP2(full) level with the 6-31G(d) basis set. The internal coordinates used to calculate the G and B matrices are given for both conformers in Table 34 with the atomic numbering shown in Fig. S1. By using the B matrix [30], the force field in Cartesian coordinates was converted to a force constant in internal coordinates. Subsequently, 0.88 was used as the scaling factor for the CH and SiH stretches and CH_2 deformations and 0.90 was used for all other modes excluding the heavy atom bends to obtain the fixed scaled force constants and the resulting wavenumbers. A set of symmetry coordinates was used (Table S3) to determine the corresponding potential energy distributions (P.E.Ds). A comparison between the observed and calculated wavenumbers, along with the calculated infrared intensities, Raman activities, depolarization ratios and P.E.D.s for the Eq and Ax conformers of cyclobutylsilane are given in Tables 31 and 32, respectively.

The vibrational spectra were predicted from the MP2(full)/6-31G(d) calculations. The predicted scaled frequencies were used together with a Lorentzian function to obtain the simulated spectra. Infrared intensities were obtained based on the dipole moment derivatives with respect to Cartesian coordinates. The derivatives were transformed with respect to normal coordinates by $(\partial\mu_u/\partial Q_i) = \sum_j (\partial\mu_u/\partial X_j)L_{ij}$, where Q_i is the i^{th} normal coordinate, X_j is the j^{th} Cartesian displacement coordinate, and L_{ij} is the transformation matrix between the Cartesian displacement coordinates and the normal coordinates. The infrared intensities were then calculated by $(N\pi)/(3c^2)$ $[(\partial\mu_x/\partial Q_i)^2 + (\partial\mu_y/\partial Q_i)^2 + (\partial\mu_z/\partial Q_i)^2]$. A comparison of the experimental spectra and simulated infrared spectra with relative concentrations calculated for the equilibrium mixture at 25ºC in Figs. 17 and 18. The spectrum of the mixture should be compared to that of the infrared spectrum of a molecule in isolation which is closest to that of the vapor at room temperature, therefore frequency and intensity changes are expected for the spectrum of the solid. The spectrum of the xenon solutions should be close to that of the vapor phase as there is little interaction between the xenon solvent and the sample. The predicted spectrum is mostly in good agreement with the experimental spectrum which shows the utility of the scaled predicted frequencies and predicted intensities for supporting the vibrational assignment.

Additional support for the vibrational assignments was obtained from the simulated Raman spectra. The evaluation of Raman activity by using the analytical gradient methods has been developed [31-34] and the activity S_j can be expressed as: $S_j = g_j(45\alpha_j^2 + 7\beta_j^2)$, where g_j is the degeneracy of the vibrational mode j, α_j is the derivative of the isotropic polarizability, and β_j is the anisotropic polarizability. To obtain the Raman scattering cross sections, the polarizabilities are incorporated into S_j by

multiplying S_j with $(1-\rho_j)/(1+\rho_j)$ where ρ_j is the depolarization ratio of the j^{th} normal mode. The Raman scattering cross sections and calculated wavenumbers obtained from the Gaussian 03 program were used together with a Lorentzian function to obtain the simulated Raman spectra. Comparison of experimental and predicted Raman spectra with relative concentrations calculated for the equilibrium mixture at 25ºC by using the experimentally determined enthalpy difference are shown in Figs. 19 and 20. The fundamentals in the A″ mode show up as nondescript bands in the gas phase Raman spectrum and hence the A″ mode bands were not used in the simulated spectra (Fig. 19C). The spectrum of the mixture should be compared to that of the Raman spectrum of a molecule in isolation which is closest to that of the vapor at room temperature, therefore frequency and intensity changes are expected for the spectrum of the liquid and solid. The predicted frequencies are in reasonable agreement with the experimental spectrum though the intensities are poorly predicted in several places. The utility of the predicted Raman spectra for supporting vibrational assignments is still demonstrated as the predicted frequencies are shown to be of significant use.

VIBRATIONAL ASSIGNMENT

The first comprehensive vibrational assignment for cyclobutylsilane [43] was made by utilizing the Raman spectra of the gas, liquid, and solid as well as the infrared spectra of the gas and solid for both conformers. The vibrational assignments were made mostly based on group frequencies along with existing assignments of corresponding vibrations of similar molecules. There were ten fundamentals that were assigned as arising from the Ax form. However, by the utilization of MP2(full)/6-31G(d) predicted vibrational wavenumbers along with *ab intio* predicted intensities, and depolarization

ratios along with infrared data from xenon solutions it has been possible to assign a significantly larger number of the fundamentals for the Ax conformer. This is important for obtaining the enthalpy difference since the fundamentals being used for the temperature study must be for a single confidently identified conformer. Therefore, we have attempted to assign all of the fundamentals for both conformers in the region from 1300 to 400 cm^{-1} where the number of overtone and combination bands are greatly reduced compared to those in the higher wavenumber region.

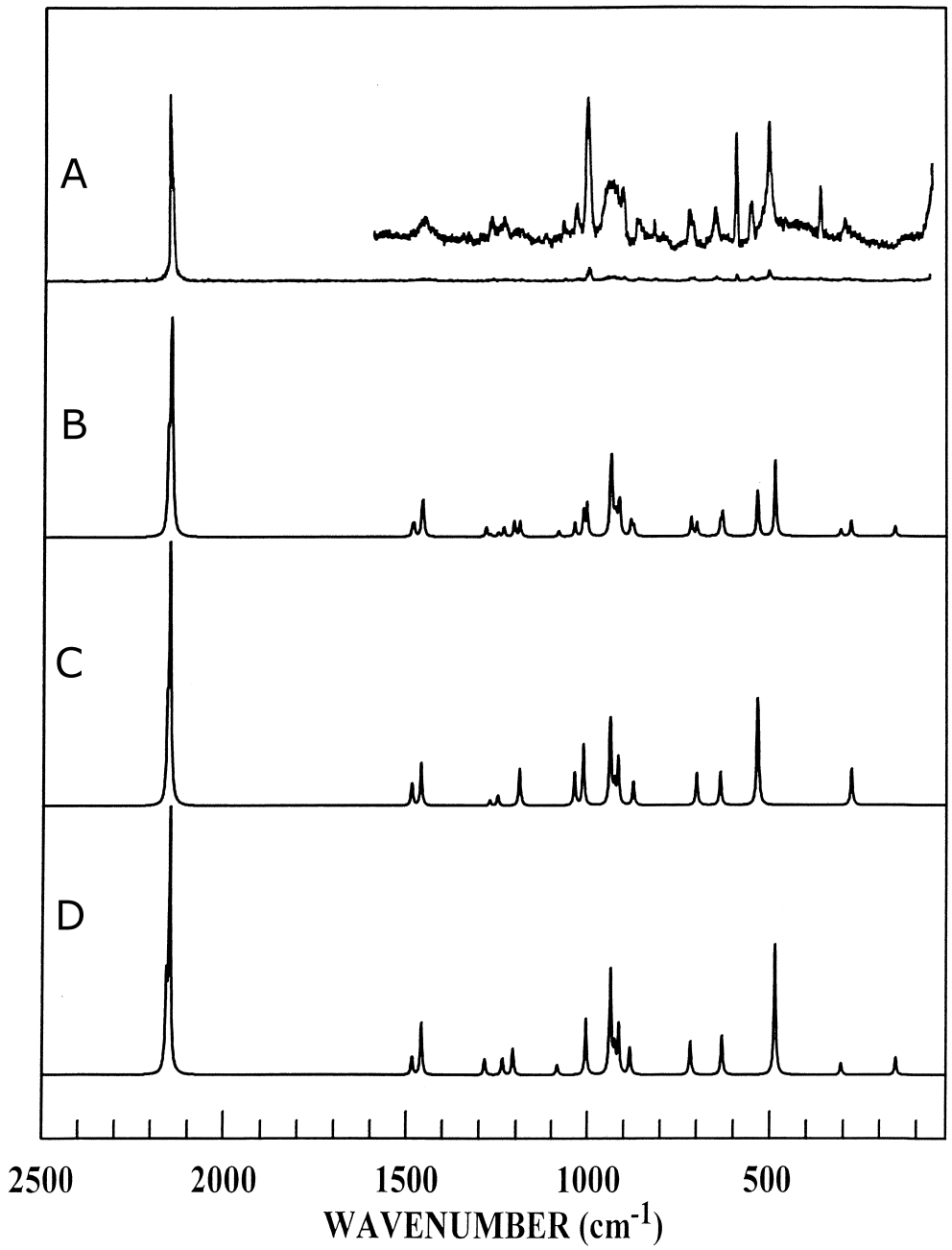

Figure 19. Experimental and predicted Raman spectra of cyclobutylsilane: (A) gas; (B) simulated spectrum of mixture of Eq and Ax (ΔH = 67 cm^{-1}) conformers at 25°C; (C) simulated Ax conformer; (D) simulated Eq conformer.

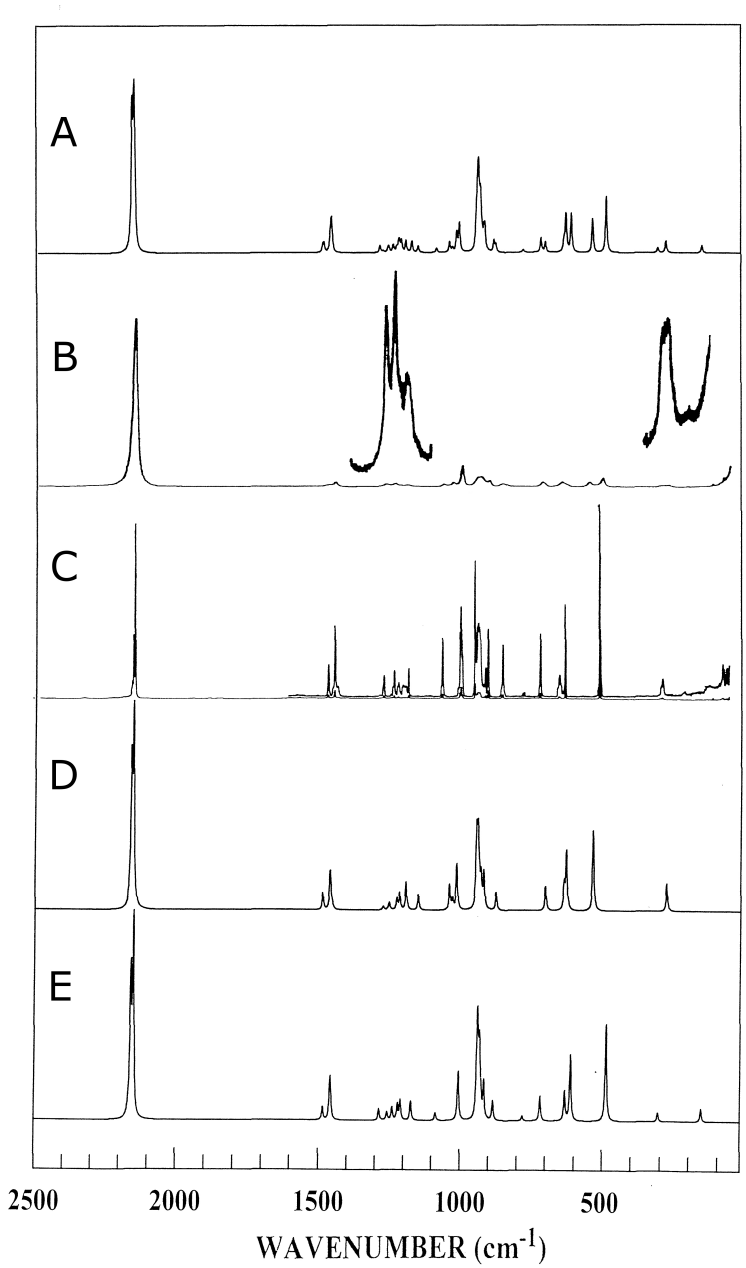

Figure 20. Experimental and predicted Raman spectra of cyclobutylsilane: (A) simulated spectrum of mixture of Eq and Ax (ΔH = 67 cm^{-1}) conformers at 25°C; (B) liquid; (C) solid; (D) simulated Ax conformer; (E) simulated Eq conformer.

For the previous vibrational assignment all of the fundamentals were assigned for the Eq form. Only 10 of the fundamentals were assigned for the Ax conformer; seven of which are assigned in the region from 1100 to 400 cm^{-1} and none of which come from the 1300 to 1100 cm^{-1} region. An effort must then be made to verify the assignment of the bands in the 1100 to 400 cm^{-1} region, to find any bands in the 1300 to 1100 cm^{-1} region that may be sufficient for the enthalpy determination, and to identify any additional Ax bands for the enthalpy determination.

The assignment for the 1100 to 400 cm^{-1} for the most part agrees with the current assignment. The region from 1100 to 1000 cm^{-1} agrees with the current assignment except for the addition of another Ax band at 1023 cm^{-1} in the current assignment which is resolved in the infrared spectra of the xenon solutions. The next region from 1000 to 900 cm^{-1} is dominated by several extremely intense modes which combine to form one broad and intense band at ~922 cm^{-1} which obscures most of that region in the infrared spectra of the xenon solutions. These modes are the two Eq fundamentals (ν_{16} and ν_{17}) with predicted intensities of 185.3 and 103.6 km/mol, respectively, and the Ax fundamental (ν_{17}') with a predicted intensity of 299.1 km/mol. This region is therefore unsuitable for use in the enthalpy determination. The next region from 900 to 400 cm^{-1} has two important changes from the previous assignment where the fundamentals ν_{17} and ν_{17}' from the previous study were assigned at 848 (shoulder) and 864 (weak) cm^{-1} in the infrared spectra of the gas which correspond to 858 cm^{-1} in the infrared spectra of the xenon solutions. This band however is an impurity that reduces in intensity upon further purification. The ν_{17} and ν_{17}' fundamentals are predicted at 915 and 919 cm^{-1} and these modes are reassigned to the broad band at 922 cm^{-1}. The other important change for this

region are the bands which have been assigned at 641 cm^{-1} in infrared spectra of the xenon solution which corresponds to 640 cm^{-1} in the infrared spectra of the gas. This band has contributions from three fundamentals which are predicted in near coincidence; ν_{20}, ν_{21}', and ν_{37}' at 631, 637, and 629 cm^{-1} respectively and appear as one single broad band in the infrared spectra of the xenon solutions. The assignment of the 1100 to 400 cm^{-1} region is then complete with all of the fundamentals for both conformers accounted for as shown in Tables 31 and 32. The utility of ab initio calculations to assist assignment of the infrared spectra is also shown as demonstrated by the data in Fig. 18.

The region from 1300 to 1100 cm^{-1} is very complex with 7 fundamentals for each conformer predicted. The spectra of the pure crystalline solid should show only one conformer thereby simplifying this problem; this single conformer is the Eq as can be verified from the data in Fig. 17. It should be noted that the most stable conformer in the fluid state need not be the same as that in the crystalline solid due to crystal packing factors which can play a major role in determining the conformer stability in the solid. The Eq form has seven bands in the region from 1300 to 1100 cm^{-1} which are predicted for the isolated molecule at 1285 (ν_{10}), 1256 (ν_{28}), 1239 (ν_{29}), 1238 (ν_{11}), 1219 (ν_{30}), 1209 (ν_{12}), and 1172 (ν_{31}) cm^{-1}. The bands observed in the infrared spectra of the pure crystalline solid for this region are 1266, 1252, 1246, 1236, 1230, 1219, 1196, 1185, and 1179 cm^{-1}. This means that there are 9 bands for 7 fundamentals each separated by 6 cm^{-1}. It can be observed however that there are several "groupings" which seem to follow a pattern with splits of 6 cm^{-1} and a weak (w) followed by strong (s) or medium (m) intensities. These "groupings" are the bands 1252(w) with 1246(s), 1236(w) with 1230(s), and 1185(w) with 1179(m) cm^{-1}. If each of these "groupings" can be assigned

for a single fundamental then the assignment of the Eq fundamentals would be 1266 (ν_{10}), 1252/1246 (ν_{28}), 1236/1230 (ν_{29} and ν_{11} which would be accidentally degenerate), 1219 (ν_{30}), 1196 (ν_{12}), and 1185/1179 (ν_{31}) cm^{-1} which is supported by the predicted intensities. This "grouping" would seem to indicate two molecules per cell. With the fundamentals for the Eq form assigned, the Ax fundamentals can be assigned using the relative frequency differences as predicted by ab initio calculations which are systematic in their errors. These assignments are given in Tables 31 and 32. With the reported assignments for this region the bands for use in the enthalpy determination can be selected. The complexity of the spectra in the 1300 to 1100 cm^{-1} region is such that curve fitting is insufficient for obtaining reliable band intensities or areas. The bands at 497, 715, 777, and 996 cm^{-1} for the Eq conformer and 546, 705, 1003, 1023, and 1027 cm^{-1} for the Ax form appear to be sufficiently resolved and of sufficient intensity for use in the enthalpy determination.

CONFORMATIONAL STABILITY

To determine the enthalpy differences among the two observed conformers of cyclobutylsilane, the sample was dissolved in liquefied xenon and the infrared spectra were recorded as a function of temperature from -65 to -100°C. Relatively small interactions are expected to occur between xenon and the sample. Therefore, only small wavenumber shifts are anticipated for the xenon interactions when passing from the gas phase to the liquefied xenon. A significant advantage of this study is that the conformer bands are better resolved in comparison with those in the infrared spectrum of the vapor. From *ab initio* calculations, the dipole moments of the two conformers are predicted to have similar values and the molecular sizes of the two conformers are nearly the same,

thus, the ΔH value obtained from the temperature dependent infrared study is expected to be near that for the gas [16-20].

Once confident assignments have been made for the fundamentals of both conformers the task was then to find pairs of bands from which the enthalpy difference could be obtained. The bands should be sufficiently resolved as to determine their intensities. The selection of the bands to use in the enthalpy determination was complicated in some cases due to the presence of broad high intensity bands but was significantly simplified in other cases by the relatively large frequency differences between the Eq and Ax fundamentals in the 1100 to 400 cm^{-1} region of the spectra (Fig. 18). Good examples of this are the fundamentals at 495 and 547 cm^{-1} for the Eq and Ax conformers where the bands are predicted at 486 and 535 cm^{-1}, respectively. The fundamentals at 495 and 715 cm^{-1} for the Eq conformer and those at 547, 705, 1003, 1023, and 1028 cm^{-1} for the Ax form were initially selected as they are confidently assigned, satisfactory resolved, and a limited number of overtone and combination bands are possible. The band at 778 cm^{-1} β-CH_2 rock was then selected for the Eq form as it was found that the predicted underlying Ax fundamental was not of sufficient intensity to significantly affect the intensity of the observed band. Additionally, the band at 996 cm^{-1} which is the Ring Breathing mode (ν_{14}) for the Eq conformer which was found not to be significantly affected by the underlying ν_{32} mode which is predicted to be nearly degenerate. With the use of curve fitting the contribution of this underlying mode was accounted for sufficiently to allow a reliable measurement of the intensity of the ν_{14} fundamental band. The band at 495 cm^{-1} appears to have a combination or an overtone

band underneath or near it. This keeps the intensity of the 495 cm^{-1} band from changing appropriately to give a reliably accurate enthalpy difference.

The intensities of the individual bands were measured as a function of temperature and their ratios were determined (Fig. 18). By application of the van't Hoff equation $-\ln K = \Delta H/(RT) - \Delta S/R$, the enthalpy difference was determined from a plot of $-\ln K$ versus 1/T, where $\Delta H/R$ is the slope of the line and K is substituted with the appropriate intensity ratios, *i.e.* $I_{conf\text{-}1} / I_{conf\text{-}2}$, etc. It was assumed that ΔS, and α are not functions of temperature in the range studied.

These eight bands, three Eq and five Ax, were utilized for the determination of the enthalpy difference by combining them to form 15 band pairs. The enthalpy difference was determined from these 15 band pairs with a value of 67 ± 4 cm^{-1} (Table 35). This error limit is derived from the statistical standard deviation of one sigma of the measured intensity data taken as a single data set, but it does not take into account small associations with the liquid xenon or the possible presence of overtones and combination bands in near coincidence of the measured fundamentals. The variations in the individual values are undoubtedly due to these types of interferences, but by taking several pairs, the effect of such interferences should cancel. However, this statistical uncertainty is probably better than can be expected from this technique and, therefore, an uncertainty of about 10% in the enthalpy difference is probably more realistic i.e. 67 ± 7 cm^{-1}. From the enthalpy difference the abundance of the Ax conformer present at ambient temperature is estimated to be 42 ± 1%.

TABLE 35. Temperature and intensity ratios of the Eq and Ax bands of cyclobutylsilane.

	T(°C)	1/T ($\times 10^{-3}$ K^{-1})	I_{715} / I_{546}	I_{715} / I_{705}	I_{715} / I_{1003}	I_{715}/ I_{1023}	I_{715} / I_{1027}	I_{777}/ I_{546}	I_{777}/ I_{705}	I_{777}/ I_{1003}
Liquid	-65	4.804	2.241	0.710	0.971	0.470	0.416	2.069	0.656	0.897
xenon	-70	4.922	2.287	0.697	0.984	0.464	0.414	2.104	0.641	0.906
	-75	5.047	2.216	0.688	0.961	0.443	0.398	2.169	0.673	0.940
	-80	5.177	2.150	0.696	0.991	0.447	0.404	2.039	0.660	0.940
	-85	5.315	2.234	0.729	1.034	0.470	0.426	2.123	0.693	0.983
	-90	5.460	2.315	0.729	1.064	0.475	0.427	2.232	0.703	1.025
	-95	5.613	2.321	0.717	1.058	0.476	0.428	2.279	0.704	1.039
	-100	5.775	2.400	0.748	1.112	0.491	0.454	2.284	0.711	1.058
ΔH[a]			45 ± 21	44 ± 15	100 ± 14	43 ± 22	65 ± 22	74 ± 20	72 ± 13	128 ± 9

	T(°C)	1/T ($\times 10^{-3}$ K^{-1})	I_{777} / I_{1023}	I_{777} / I_{1027}	I_{996} / I_{546}	I_{996}/ I_{705}	I_{996} / I_{1003}	I_{996}/ I_{1023}	I_{996}/ I_{1027}
Liquid	-65	4.804	0.434	0.384	0.615	1.950	2.667	1.290	1.143
xenon	-70	4.922	0.427	0.381	0.635	1.936	2.734	1.290	1.150
	-75	5.047	0.434	0.389	0.645	2.001	2.797	1.290	1.157
	-80	5.177	0.424	0.383	0.620	2.007	2.855	1.289	1.164
	-85	5.315	0.447	0.404	0.628	2.052	2.910	1.323	1.197
	-90	5.460	0.458	0.411	0.644	2.030	2.961	1.321	1.188
	-95	5.613	0.467	0.421	0.660	2.038	3.009	1.352	1.218
	-100	5.775	0.467	0.432	0.660	2.053	3.054	1.349	1.247
ΔH[a]			71 ± 15	93 ± 13	41 ± 14	40 ± 9	96 ± 5	39 ± 6	60 ± 6

[a] Average value $\Delta H = 67 \pm 4$ cm^{-1} (0.81 ± 0.05 kJ mol^{-1}) with the Eq conformer the more stable form and the statistical uncertainty (1σ) obtained by utilizing all of the data as a single set.

STRUCTURAL PARAMETERS

In the initial microwave study [96], the Eq conformer was observed and rotational constants were determined. This was followed by an electron diffraction (ED) study [95] where the structure was determined for both the Eq and Ax conformers. In this study the Ax conformer was found to be 41 ± 5 % in abundance. This led to another microwave study [92] from the same group as the previous microwave study where the Ax conformer was observed and the rotational constants, distortion constants, and barrier to internal rotation of the silyl group were published the same year as the ED study. There is no structure published utilizing the microwave roational constants and the structure from the ED work suffers from large uncertainties in the puckering and ∠Si-CCC angles. Therefore, we have determined the structural parameters for the two conformers by utilizing the rotational constants previously reported from the microwave study [92]. Only one isotopic species was studied for the two conformers and, thus, only three rotational constants are available for each conformer.

We [51] have shown that *ab initio* MP2(full)/6-311+G(d,p) calculations predict the carbon-hydrogen r_0 structural parameters for more than fifty hydrocarbons to at least 0.002 Å compared to the experimentally determined [5] values from isolated CH stretching frequencies which agree to previously determined values from earlier microwave studies. Therefore, all of the carbon-hydrogen parameters can be taken from the MP2(full)/6-311+G(d,p) predicted values for the Eq and Ax conformers of cyclobutylsilane.

We have found that good structural parameters for hydrocarbons and many substituted ones can be determined by adjusting the structural parameters obtained from

the *ab initio* MP2(full)/6-311+G(d,p) calculations to fit the rotational constants obtained from microwave experimental data by using a computer program "A&M" (*Ab initio* and Microwave) developed [14] in our laboratory. In order to reduce the number of independent variables, the structural parameters are separated into sets according to their types where bond distances in the same set keep their relative ratio, and bond angles and torsional angles in the same set keep their difference in degrees. This assumption is based on the fact that errors from *ab initio* calculations are systematic. Additionally, we have also shown that the differences in predicted distances and angles from the *ab initio* calculations for different conformers of the same molecule can usually be used as one parameter with the *ab initio* predicted differences except for some dihedral angles. Therefore, it should be possible to obtain "adjusted r_0" structural parameters for the five parameters of the five heavy atoms by utilizing the previously reported six rotational constants from the earlier microwave study [92]. Therefore we have obtained the complete structural parameters for the Eq and Ax forms of cyclobutylsilane.

The resulting adjusted r_0 parameters are listed in Table 34, where it is believed that the Si-C, C-C, and Si-H distances should be accurate to ± 0.003 Å, the C-H distances accurate to ± 0.002 Å, and the angles should be within ± 0.5°. The fit of the six determined rotational constants (Table 36) by the adjusted r_0 structural parameters for both conformers are good with the differences being less than 0.9 MHz. Therefore, it is believed that the suggested uncertainties are realistic values and the determined structural parameters are probably as accurate as can be obtained for the molecule in the gas phase by either electron diffraction or microwave substitution methods.

TABLE 36. Comparison of rotational constants (MHz) obtained from modified *ab initio*, MP2(full)/6-311+G(d,p) structural parameters and the experimental values from the microwave spectra of Eq and Ax cyclobutylsilane.

Isotopomers	Rotational constant	MP2(full)/ 6-311+G(d,p)	Experimental [a]	Adjusted r_0	$\|\Delta\|$
eq-$C_4H_7SiH_3$	A	9177.758	8984.388 (10)	8984.922	0.534
	B	2372.114	2395.635 (2)	2396.272	0.637
	C	2086.276	2101.061 (1)	2100.394	0.667
ax-$C_4H_7SiH_3$	A	7385.341	7404.909 (90)	7405.566	0.657
	B	2692.022	2682.684 (15)	2682.397	0.287
	C	2473.441	2445.930 (14)	2446.826	0.896

[a] Ref. [92].

DISCUSSION

The vibrational assignments reported herein are based on a significant amount of information with the infrared spectrum of the xenon solution and predictions of the fundamental frequencies from the scaled ab inito MP2(full)/6-31G(d) calculations as well as the predicted infrared bands contours and their intensities. For the Eq conformer the *ab inito* predicted frequencies for the A′ fundamentals are in error an average of 12 cm^{-1} which represent 0.8% error and for the A″ modes it is 8 cm^{-1} which is 0.6% error. The percent error for the predictions for the Ax conformer are nearly the same with the A′ fundamentals with 11 cm^{-1} or 0.7% error and the A″ modes 9 cm^{-1} which is 0.6% error . Thus the relatively small basis set of 6-31G(d) by the MP2(full) calculations with two scaling factors provides excellent predicted frequencies for aiding the vibrational assignments.

The adjusted r_0 structural parameters have been determined for both the Eq and Ax conformers. In the ED study [95] the structural parameters were determined for the heavy atom distances and the puckering and ∠SiCC angles. The C-Si distance determined in this study for the Eq conformer agrees with the value determined in the ED study within the combined error limits. However, the C-Si distance is 0.011 Å different than the value from the ED study for the Ax conformer which is a significant difference. The C_α-C_β distance is a large difference for both conformers where the values are 0.011 and 0.012 Å for the Eq and Ax conformers, respectively. The puckering and ∠SiCC angles both agree with the values from the current study to within the listed uncertainty from the ED study though the significance of this is minimal as the uncertainty of these angles is 2 to 4 degrees. Thus, the structural parameters reported in the current study are believed to be accurate to within the stated error limits.

It is of interest to compare the structural parameters of cyclobutane to that of cyclobutylsilane so that the effects of silane substitution on the ring parameters can be determined. In the microwave study [78] by Caminati et al. the r_0 structural parameters of cyclobutane were determined for the C-C bond distance to be 1.5549(5) Å and the puckering angle to be 28.32(23)°. The puckering angle in cyclobutylsilane for the Eq [Ax] form is 29.0(5) [23.5(5)]° upon addition of the silane group. This difference is relatively small for the Eq form but for the Ax conformer the difference is significant. The C-C bond distances for cyclobutylsilane are C_α-C_β,$C_{\beta'}$ = 1.562(3) and C_γ-C_β,$C_{\beta'}$ = 1.551(3) Å for the Eq form and C_α-C_β,$C_{\beta'}$ = 1.561(3) and C_γ-C_β,$C_{\beta'}$ = 1.553(3) Å for the Ax conformer. The C_γ-C_β distance agrees with that for cyclobutane within the stated

errors but the C_α-C_β distance differs by 0.007 for the Eq form and 0.006 Å for the Ax conformer.

The differences in the C_α-C_β bond distances for the two conformers of cyclobutylsilane with respect to the equivalent bond distance in cyclobutane indicate that the silane group causes some lengthening of the closest C-C bonds through either steric or electrostatic effects. It should be noted that the major structural change when comparing the Eq and Ax conformer is the orientation of the silane group away from the ring in the Eq form and above the ring in the Ax form. This orientation has little effect on the bond distances even the C_α-C_β bond distance where some affect would seem likely if steric interference were the reason for the increased bond length. The remaining C-C bond distance for C_γ-C_β shows no significant change for both conformers. This indicates the effect that shortens the C_α-C_β bond distance is short range as it does not affect the C_γ-C_β distance. There is a significant difference (6.5°) in the puckering angle between the Eq and Ax conformers. The Eq puckering angle is very close to that of cyclobutane so the effect of the silane on this angle is negligible. However the Ax conformer has a large difference for the puckering angle indicating that the effect of silane substitution in the Ax position is significant. These results would seem to indicate some form of steric interference between C_γ and the silane group.

The natural population analysis was carried out for the Eq and Ax conformers of cyclobutylsilane and for cyclobutane with the MP2(full) method at the 6-311+G(d,p) basis set. The C atoms for cyclobutane all carry a -0.337 charge. However the silane substitution of cyclobutane gives a charge distribution to the C-ring for the Eq [Ax] form of C_α = -0.676 [-0.672], C_β = -0.321 [-0.327], and C_γ = -0.332 [-0.340]. This indicates

that the lengthening of the C_α-C_β bond distances is in part an electrostatic effect which decreases rapidly further into the ring. There seems to be some increase in negative charge for the β and γ carbons but it is relatively small and probably not the deciding factor in the large difference in puckering angle between the Eq and Ax conformers. The steric effect is a significantly larger factor in the Ax conformer where the Si---C distance for the Eq conformer is 3.862(10) Å and for the Ax form is 3.366(10) Å which is a difference of 0.5 Å.

One of the major goals of this research was the determination of the enthalpy difference between the two conformers where there had been two significantly different values reported. From the ED study [95] a ΔG of 67 ± 33 cm^{-1} was reported which was supported by an *ab initio* calculation [95] where the energy difference was predicted to be 35 cm^{-1}. In contrast from the previous vibrational study [43] an enthalpy difference of 147 ± 50 cm^{-1} was determined from two band pairs in the Raman spectra of the gas and 231 ± 25 cm^{-1} from one band pair in the Raman spectra of the liquid. In the same vibrational study the potential function was determined with an enthalpy difference of 188 cm^{-1} and a barrier of 531 cm^{-1}. These values can be compared to the enthalpy difference in the present study of 67 ± 7 cm^{-1} from 15 band pairs in the infrared spectra of the xenon solutions. This value seems to match well with the value obtained from the ED study though this result is relatively insignificant since the ΔG value has an uncertainty of 50%. The vibrational value obtained from the Raman spectra of the gas is large even when the uncertainty of 50 cm^{-1} is taken into account. The large uncertainty with the small number of bands is probably due to the difficulty in measuring the intensities in the gas phase. The difference between the values in the liquid and vapor

phases is partly due to association of the sample in the liquid state as well as due to the previously mentioned difficulty.

To support the experimental values the *ab initio* energy differences have been determined by a variety of basis sets (Table 33). The results are interesting in that the MP2(full) method with basis sets of cc-pVTZ and aug-cc-pVTZ both predict the wrong conformer as being more stable with energy differences of ~20 cm^{-1}, whereas, the same method with much smaller basis sets predicts values much closer to that determined experimentally. The B3LYP method predicts significantly higher values than the values from the MP2(full) method with the same basis set and consistently predicts the correct conformer as stable though ~100 cm^{-1} too high in energy.

The barrier to conformer interchange is predicted by the MP2(full) method to be ~700 cm^{-1} and by the B3LYP method to be ~270 cm^{-1}. Both of these values are significantly different than the value of 531 cm^{-1} from the previously determined [43] potential function where the MP2(full) method is ~170 cm^{-1} too high and the B3LYP method is ~260 cm^{-1} too low.

TABLE 37. Quadratic centrifugal distortion constants (kHz) for Eq and Ax conformers of cyclobutylsilane.

	Eq			Ax		
	MP2(full)/ 6-311+G(d,p)	B3LYP/ 6-311+G(d,p)	Exp.[a]	MP2(full)/ 6-311+G(d,p)	B3LYP/ 6-311+G(d,p)	Exp.[a]
Δ_J	0.391	0.440	0.460(9)	0.8	1.1	0.8(3)
Δ_{JK}	0.94	-0.03	0.18(4)	-0.16	-2.4	-1.5(4)
Δ_K	4.8	8.6	7.3(8)	3	8	12(7)
δ_J	0.038	0.041	0.043(1)	-0.002	-0.04	-0.04(3)

δ_K	1.1	0.92	1.2(2)	0.6	1	3(3)

[a]Ref. [92]

In the most recent microwave study of cyclobutylsilane the quadratic centrifugal distortion constants were determined from the spectral data. We have obtained the quadratic centrifugal distortion constants from the MP2(full)/6-311+G(d,p) calculations as well as the density functional theory by the B3LYP method utilizing the same basis set. These data are given in Table 37 and as can be seen from the values of the quadratic centrifugal distortion constants, there is reasonable agreement with the predicted values for both calculations. Only the Δ_{JK} constant for the Eq conformer from the B3LYP method has an incorrect sign though the value is reasonably in scale. We have found in the past that the ab initio calculations usually predict fairly good distortion constants.

The r_0 structural parameters have not been determined for either cyclobutylmethane or cyclobutylgermane but the rotational constants have been determined for the germane. It would be of interest to obtain the adjusted r_0 structural parameters for these two molecules for comparison with those for cyclobutylsilane to obtain their effect on puckering angles.

CHAPTER 7

STRUCTURE AND CONFORMATION STUDIES FROM TEMPERATURE DEPENDENT INFRARED SPECTRA OF XENON SOLUTIONS AND AB INITIO CALCULATIONS OF CYCLOBUTYLGERMANE

INTRODUCTION

The stable conformation of cyclobutane generated a large amount of controversy whether it was a planar or puckered molecule. Many technologies were used to convince the scientific public that one or the other form was the more stable form but the controversy persisted for many years. Eventually an intensive study by using vibrational spectroscopy [89] settled the controversy that the stable form was the heavy atom puckered molecule. However the structure of monosubstituted cyclobutanes did not generate controversy but there were some interesting differences that arose from structural results from microwave studies and vibrational studies of the same molecule. The microwave studies did not provide evidence of a second conformer [35,36] whereas the vibration spectrum clearly showed the presence of the second conformer [38,64,65,90]. This difference persisted into the 1980's until the reported microwave investigation of cyclobutylsilane where spectra for both the axial and equatorial conformers were reported [43,92]. Following this study several more microwave investigations of spectra of monosubstituted molecules were reported which was helped by the development of FT-microwave instruments. Nevertheless only limited data has been provided on the structural parameter differences of the two conformers but there are

relatively large differences reported of the different enthalpies with some of them for the same molecules.

As a continuation of our interest in the structural parameters and conformational stabilities of three-, four-, five- and six membered rings, we have begun to study some four-membered rings to obtain structural parameters and enthalpy differences from xenon solutions which are expected to be more accurate than those previously obtained. We began these investigations with a study of the determination of the enthalpy differences of the cyclobutyl halides where there is a relatively small amount of the axial conformer. We have continued with cyclobutane carbonylchloride [97] which included recording microwave, infrared and Raman spectra. From these spectral data the structural parameters and the enthalpy differences were obtained. Three conformers were identified with the g-Eq the most stable conformer. Enthalpy differences of 91 ± 9 cm^{-1} were determined with g-Ax. As a continuation of these studies we have turned our attention to cyclobutylgermane.

To support the experimental studies we have obtained the harmonic force constants, infrared intensities, Raman activities, depolarization ratios, and vibrational frequencies for MP2(full)/6-31G(d) ab initio calculations with full electron correlation and has been compared to previous vibrational studies [94]. To obtain predictions on the conformational stabilities we have carried out MP2(full) ab initio and density functional theory (DFT) calculations by B3LYP method utilizing a variety of basis sets. The r_0 structural parameters have been obtained by combining the MP2(full)/6-311+G(d,p) ab initio predicted parameters with the previously reported rotational constants obtained from the microwave study [93] and compared to those obtained in the electron diffraction

study [98]. The results of these spectroscopic, structural, and theoretical studies of cyclobutylgermane are reported herein.

EXPERIMENTAL AND THEORETICAL METHODS

To a suspension of magnesium metal (646 mg, 26.6 mmol) in freshly distilled ether (22 mL) at 36 °C was added cyclobutylbromide (2.09 mL, 22.2 mmol) dropwise. After 1h the reaction was cooled to room temperature and then added, via cannula, to a solution of $GeCl_4$ (3.04 mL, 26.6 mmol) in ether (200mL) at 0 °C. After 24 h of stirring at room temperature under dry nitrogen the ether was distilled off and dry n-pentane was added and stirred for 1hr at room temperature. The reaction was filtered and the solid was washed two times with 5-mL dry n-pentane. The residual of ether and pentane were removed by distillation under reduced pressure. The sample of cyclobutylgermane was checked by infrared and nuclear magnetic resonance. The final purification was achieved by low pressure and low temperature fractionation column.

TABLE 38. Observed and calculated[a] frequencies (cm^{-1}) for Eq cyclobutylgermane.

	Vib. No.	Approximate Descriptions	ab initio	fixed scaled[b]	IR int.	Raman act.	dp ratio	IR Xe soln.	P.E.D. [c]	Band Contours* A	Band Contours* C
A′	ν_1	γ-CH_2 antisymmetric stretch	3192	2994	47.2	66.5	0.70	2974	$59S_1$, $40S_2$	-	100
	ν_2	β-CH_2 antisymmetric stretch	3173	2977	9.9	76.7	0.32	2970	$52S_2$, $40S_1$	97	3
	ν_3	CH stretch	3128	2935	12.8	43.2	0.63	2936	$92S_3$	3	97
	ν_4	γ-CH_2 symmetric stretch	3121	2928	38.3	144.8	0.10	2917	$96S_4$	99	1
	ν_5	β-CH_2 symmetric stretch	3112	2920	4.1	131.1	0.17	2917	$87S_5$	40	60
	ν_6	GeH_3 antisymmetric stretch	2085	2085	133.7	81.1	0.58	2072*	$97S_6$	26	74
	ν_7	GeH_3 symmetric stretch	2064	2064	72.7	189.9	0.01	2068*	$97S_7$	85	15
	ν_8	β-CH_2 deformation	1575	1483	1.4	7.4	0.65	1457*	$73S_8$, $24S_9$	20	80
	ν_9	γ-CH_2 deformation	1547	1457	4.3	20.3	0.73	1444	$75S_9$, $25S_8$	19	81
	ν_{10}	β-CH_2 wag	1355	1287	1.8	6.7	0.41	1280	$61S_{10}$, $16S_{11}$, $14S_{10}$	96	4
	ν_{11}	CH in-plane bend	1294	1231	4.4	6.4	0.63	1228	$30S_{11}$,$33S_{12}$, $23S_{10}$	1	99
	ν_{12}	β-CH_2 twist	1265	1205	2.6	9.0	0.64	1193	$32S_{12}$, $22S_{11,}$ $14S_{13}$	6	94
	ν_{13}	β-CH_2 rock	1139	1087	2.7	2.9	0.40	1065	$27S_{13}$, $31S_{14}$	80	20
	ν_{14}	Ring breathing	1052	1000	3.0	14.8	0.16	996	$58S_{14}$, $15S_{11,}$ $12S_{13}$	1	99
	ν_{15}	Ring deformation 1	949	916	1.7	2.5	0.35	897	$54S_{15,}$ $12S_{10}$	86	14
	ν_{16}	GeH_3 antisymmetric deformation	906	901	25.1	21.5	0.74	876	$87S_{16}$	6	94
	ν_{17}	Ring deformation 2	901	879	3.2	5.0	0.05	849	$44S_{17}$, $22S_{19}$	34	66
	ν_{18}	GeH_3 symmetric deformation	841	841	176.9	10.1	0.60	825	$100S_{18}$	97	3
	ν_{19}	γ-CH_2 rock	726	699	1.7	4.5	0.15	674	$37S_{19}$, $14S_{16}$	81	19
	ν_{20}	GeH_3 rock	606	598	18.5	2.1	0.75	590	$58S_{20}$, $16S_{18}$, $13S_{13}$	-	100
	ν_{21}	Ge-C stretch	459	446	13.8	10.3	0.35	436	$39S_{21}$, $30S_{20,}$ $15S_{16}$,	52	48

	ν_{22}	Ring-GeH_3 bending	284	277	1.9	1.0	0.18	262*	$27S_{22}$, $36S_{23}$, $23S_{21}$	13	87
	ν_{23}	Ring puckering	139	138	3.1	0.4	0.09	135*	$44S_{23}$, $50S_{22}$	3	97
A″	ν_{24}	β-CH_2 antisymmetric stretch	3179	2983	22.4	68.1	0.75	2970	$95S_{24}$	-	-
	ν_{25}	β-CH_2 symmetric stretch	3111	2919	39.4	1.9	0.75	2917	$96S_{25}$	-	-
	ν_{26}	GeH_3 antisymmetric stretch	2087	2087	124.0	89.0	0.75	2068*	$100S_{26}$	-	-
	ν_{27}	β-CH_2 deformation	1544	1453	0.7	5.2	0.75	1435	$100S_{27}$	-	-
	ν_{28}	γ-CH_2 wag	1324	1257	3.9	4.5	0.75	1257	$57S_{28,}$ $21S_{30}$	-	-
	ν_{29}	β-CH_2 wag	1319	1251	0.2	0.0	0.75	-	$42S_{29}$, $23S_{32}$, $13S_{30,}$ $12S_{31}$	-	-
	ν_{30}	CH out-of-plane bend	1286	1221	0.0	5.7	0.75	-	$35S_{30}$, $25S_{31}$, $17S_{28}$, $12S_{29}$	-	-
	ν_{31}	γ-CH_2 twist	1232	1171	2.3	8.0	0.75	1169	$28S_{31}$, $35S_{29}$, $18S_{32}$	-	-
	ν_{32}	β -CH_2 twist	1062	1016	3.7	2.4	0.75	1021	$31S_{32}$, $25S_{33}$, $23S_{34}$	-	-
	ν_{33}	Ring deformation 2	987	940	0.0	1.3	0.75	916	$19S_{33}$, $26S_{32,}$ $18S_{30,}$ $15S_{34}$ $15S_{31}$	-	-
	ν_{34}	Ring deformation 1	975	934	1.4	11.7	0.75	916	$47S_{34}$, $28S_{33}$, $12S_{28}$	-	-
	ν_{35}	GeH_3 antisymmetric deformation	902	900	33.0	19.7	0.75	876	$92S_{35}$	-	-
	ν_{36}	β-CH_2 rock	819	779	6.6	0.9	0.75	775	$77S_{36}$, $12S_{31}$	-	-
	ν_{37}	GeH_3 wag	556	554	30.8	6.4	0.75	555	$82S_{37}$	-	-
	ν_{38}	Ring-GeH_3 bending	189	189	0.4	0.0	0.75	262*	$79S_{38,}$ $11S_{39}$	-	-
	ν_{39}	GeH_3 torsion	117	117	0.1	0.0	0.75	-	$86S_{39}$	-	-

[a]MP2(full)/6-31G(d) *ab initio* calculations, scaled frequencies, infrared intensities (km/mol), Raman activities ($Å^4$/amu), depolarization ratios and potential energy distributions (P.E.D.s)

[b]MP2(full)/6-31G(d) fixed scaled frequencies with factors of 0.88 for CH and CH_2 deformations, 1.0 for heavy atom bends, GeH stretches and GeH bends, and 0.90 for all other modes.

[c]Calculated with MP2(full)/6-31G(d) and contributions of less than 10% are omitted.

[*]A and C values in the last two columns are percentage infrared band contours.

* Ref [94]

TABLE 39. Observed and calculated[a] frequencies (cm^{-1}) for Ax cyclobutylgermane.

	Vib. No.	Approximate Descriptions	ab initio	fixed scaled[b]	IR int.	Raman act.	dp ratio	IR Xe soln.	P.E.D. [c]	Band Contours* A	Band Contours* C
A′	ν_1	γ-CH_2 antisymmetric stretch	3196	2998	39.8	61.1	0.58	2974	$89S_1$, $11S_2$	87	13
	ν_2	β-CH_2 antisymmetric stretch	3164	2968	23.9	64.0	0.71	2958	$86S_2$, $11S_1$	16	84
	ν_3	γ-CH_2 symmetric stretch	3134	2940	5.6	170.3	0.07	2936	$70S_3$, $26S_4$	86	14
	ν_4	CH stretch	3130	2936	38.9	34.2	0.65	2936	$68S_4$, $27S_3$	27	73
	ν_5	β-CH_2 symmetric stretch	3107	2915	5.6	149.0	0.19	2917	$95S_5$	84	16
	ν_6	GeH_3 antisymmetric stretch	2088	2088	128.0	66.0	0.71	2072*	$100S_6$	30	70
	ν_7	GeH_3 symmetric stretch	2066	2066	70.0	191.8	0.01	2068*	$100S_7$	88	12
	ν_8	β-CH_2 deformation	1579	1486	0.5	8.3	0.57	1469	$67S_8$, $32S_9$	16	84
	ν_9	γ-CH_2 deformation	1552	1461	3.4	17.2	0.75	1466	$67S_9$, $33S_8$	1	99
	ν_{10}	β-CH_2 wag	1333	1267	5.0	0.5	0.59	1261	$82S_{10}$	21	79
	ν_{11}	CH in-plane bend	1310	1247	1.1	7.2	0.69	1247	$35S_{11}$, $46S_{12}$	75	25
	ν_{12}	β-CH_2 twist	1245	1186	1.0	11.9	0.68	1177	$28S_{12}$, $23S_{19}$, $20S_{13}$, $19S_{11}$	56	44
	ν_{13}	β-CH_2 rock	1085	1035	3.0	10.2	0.37	1029	$28S_{13}$, $26S_{14}$, $16S_{11}$	90	10
	ν_{14}	Ring breathing	1062	1009	1.4	13.1	0.21	1001	$61S_{14}$, $25S_{11}$	3	97
	ν_{15}	Ring deformation 1	968	935	1.7	1.8	0.19	916	$70S_{15}$, $13S_{10}$	87	13
	ν_{16}	GeH_3 antisymmetric deformation	908	903	6.6	6.9	0.53	876	$83S_{16}$	8	92
	ν_{17}	Ring deformation 2	887	864	20.4	17.2	0.73	849	$48S_{17}$, $24S_{19}$	11	89
	ν_{18}	GeH_3 symmetric deformation	843	823	164.6	8.2	0.59	825	$100S_{18}$	93	7
	ν_{19}	γ-CH_2 rock	701	681	3.1	1.5	0.60	660	$36S_{19}$, $25S_{16}$, $14S_{21}$	20	80
	ν_{20}	Ge-C stretch	630	609	17.7	5.9	0.16	598	$35S_{20}$, $21S_{21}$, $19S_{13}$, $13S_{17}$	19	81
	ν_{21}	GeH_3 rock	504	494	19.6	8.5	0.45	485	$51S_{21}$, $33S_{20}$	41	59
	ν_{22}	Ring-GeH_3 bending	252	248	1.2	1.7	0.11	-	$39S_{22}$, $31S_{24}$,$14S_{20}$	20	80
	ν_{23}	Ring puckering	157	156	0.3	0.1	0.45	-	$53S_{23}$, $43S_{22}$	6	94

A″	ν_{24}	β-CH_2 antisymmetric stretch	3166	2970	4.4	71.8	0.75	2958	$100S_{24}$	-	-
	ν_{25}	β-CH_2 symmetric stretch	3106	2914	59.0	4.2	0.75	2917	$100S_{25}$	-	-
	ν_{26}	GeH_3 antisymmetric stretch	2088	2088	122.2	84.1	0.75	2068*	$100S_{26}$	-	-
	ν_{27}	β-CH_2 deformation	1549	1458	2.2	8.4	0.75	1448	$100S_{27}$	-	-
	ν_{28}	γ-CH_2 wag	1322	1257	2.7	0.6	0.75	1257	$67S_{28}$, $11S_{34}$	-	-
	ν_{29}	β-CH_2 wag	1294	1228	1.2	3.1	0.75	1228	$63S_{29}$, $24S_{30}$	-	-
	ν_{30}	CH out-of-plane bend	1284	1219	1.6	8.2	0.75	1218	$44S_{30}$, $23S_{31}$, $13S_{29}$	-	-
	ν_{31}	γ-CH_2 twist	1216	1154	0.0	5.7	0.75	-	$16S_{31}$, $29S_{32}$, $24S_{30}$, $12S_{29}$, $10S_{33}$	-	-
	ν_{32}	β -CH_2 twist	1087	1036	4.2	2.7	0.75	1027	$46S_{32}$, $15S_{36}$, $13S_{30}$	-	-
	ν_{33}	Ring deformation 1	996	944	0.7	13.7	0.75	930	$71S_{33}$	-	-
	ν_{34}	Ring deformation 2	970	932	1.0	0.4	0.75	916	$54S_{34}$, $11S_{32}$, $10S_{31}$	-	-
	ν_{35}	GeH_3 antisymmetric deformation	900	899	31.4	17.8	0.75	876	$92S_{35}$	-	-
	ν_{36}	β-CH_2 rock	816	777	0.0	0.1	0.75		$65S_{36}$, $15S_{34}$, $14S_{30}$	-	-
	ν_{37}	GeH_3 wag	573	571	34.2	5.5	0.75	565	$83S_{37}$	-	-
	ν_{38}	Ring-GeH_3 bending	198	197	0.4	0.0	0.75	186*	$90S_{38}$	-	-
	ν_{39}	GeH_3 torsion	118	118	0.0	0.0	0.75	-	$99S_{39}$	-	-

[a]MP2(full)/6-31G(d) *ab initio* calculations, scaled frequencies, infrared intensities (km/mol), Raman activities ($Å^4$/amu), depolarization ratios and potential energy distributions (P.E.D.s)

[b]MP2(full)/6-31G(d) fixed scaled frequencies with factors of 0.88 for CH and CH_2 deformations, 1.0 for heavy atom bends, GeH stretches and GeH bends, and 0.90 for all other modes.

[c]Calculated with MP2(full)/6-31G(d) and contributions of less than 10% are omitted.

[*]A and C values in the last two columns are percentage infrared band contours.

* Ref [94]

The mid-infrared spectrum of the gas (Fig. 21B) was obtained from 3500 to 220 cm-1 on a Perkin-Elmer model 2000 Fourier transform spectrometer equipped with a Ge/CsI beamsplitter and a DTGS detector. Atmospheric water vapor was removed from the spectrometer housing by purging with dry nitrogen. The spectrum of the gas was obtained with a theoretical resolution of 0.5 cm-1 with 128 interferograms added and truncated.

The mid-infrared spectra (3500 to 400 cm-1) of the sample dissolved in liquefied xenon (Fig. 21A) were recorded on a Bruker model IFS-66 Fourier transform spectrometer equipped with a globar source, a Ge/KBr beamsplitter and a DTGS detector. In all cases, 100 interferograms were collected at 1.0 cm^{-1} resolution, averaged and transformed with a boxcar truncation function. For these studies, a specially designed cryostat cell was used. It consists of a copper cell with a path length of 4 cm with wedged silicon windows sealed to the cell with indium gaskets. The copper cell was enclosed in an evacuated chamber fitted with KBr windows. The temperature was maintained with boiling liquid nitrogen and monitored by two Pt thermo resistors. The observed bands in the infrared spectra of the xenon solutions along with their proposed assignments are listed in Tables 38 and 39 for the equatorial (Eq) and axial (Ax) conformers, respectively.

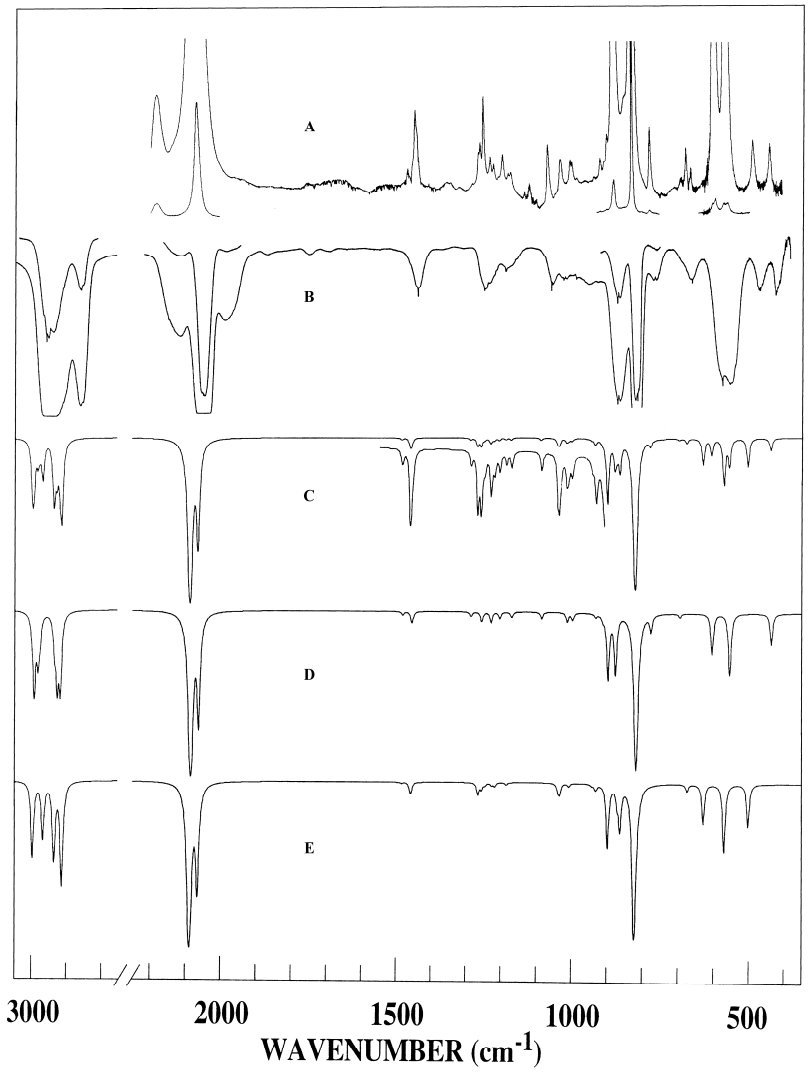

Figure 21. Experimental and predicted infrared spectra of cyclobutylgermane: (A) xenon solution at -70°C; (B) gas; (C) simulated spectrum of mixture of Eq and Ax (ΔH = 112 cm^{-1}) conformers at 25°C; (D) simulated Eq conformer; (F) simulated Ax conformer.

The ab initio calculations were performed with the Gaussian 03 program [22] using Gaussian-type basis functions. The energy minima with respect to nuclear

coordinates were obtained by the simultaneous relaxation of all geometric parameters using the gradient method of Pulay [29]. A variety of basis sets as well as the corresponding ones with diffuse functions were employed with the Møller-Plesset perturbation method [21] to the second order MP2 with full electron correlation as well as with the density functional theory by the B3LYP method. The predicted conformational energy differences are listed in Table S4.

In order to obtain descriptions of the molecular motions involved in the fundamental modes of cyclobutylgermane, a normal coordinate analysis was carried out. The force field in Cartesian coordinates was obtained with the Gaussian 03 program at the MP2(full) level with the 6-31G(d) basis set. The internal coordinates used to calculate the G and B matrices are given for both conformers in Tables 40 and 41 with the atomic numbering shown in Fig. 22. By using the B matrix [30], the force field in Cartesian coordinates was converted to a force constant in internal coordinates. Subsequently, 0.88 was used as the scaling factor for the CH stretches and CH_2 deformations and 0.90 was used for all other modes excluding the heavy atom bends and GeH_3 stretches and deformations to obtain the fixed scaled force constants and the resulting wavenumbers. A set of symmetry coordinates was used (Table S5) to determine the corresponding potential energy distributions (P.E.Ds). A comparison between the observed and calculated wavenumbers, along with the calculated infrared intensities, Raman activities, depolarization ratios and P.E.D.s for the Eq and Ax conformers of cyclobutylgermane are given in Tables 38 and 39, respectively.

TABLE 40. Structural parameters (Å and degrees), rotational constants (MHz) and dipole moments (Debye) for Eq cyclobutylgermane.

Structural Parameters	Int. coor.	MP2(full)/ 6-311+G(d,p)	B3LYP/ 6-311+G(d,p)	ED[a]	MW[b]	Adjusted r_0
rC_α-Ge	R_1	1.951	1.972	1.948 (4)	1.947	1.952 (5)
rC_α-$C_{\beta,\beta'}$	R_2, $R_{2'}$	1.555	1.561	1.557 (3)	1.553 (3)	1.557 (3)
rC_γ-$C_{\beta,\beta'}$	R_3, $R_{3'}$	1.547	1.553	1.558	1.553 (3)	1.551 (3)
rC_α-H	r_1	1.096	1.094	1.085 (4)	1.090*	1.096 (2)
$rC_{\beta,\beta'}$-H_1	r_2, $r_{2'}$	1.095	1.094	1.085 (4)	1.090*	1.095 (2)
$rC_{\beta,\beta'}$-H_2	r_3, $r_{3'}$	1.093	1.092	1.085 (4)	1.090*	1.093 (2)
rC_γ-H_1	r_4	1.093	1.092	1.085 (4)	1.090*	1.093 (2)
rC_γ-H_2	r_5	1.094	1.093	1.085 (4)	1.090*	1.094 (2)
rGe-H_2	r_6	1.525	1.542	1.513 (8)	1.529*	1.532 (2)
rGe-$H_{1,1'}$	r_7, $r_{7'}$	1.524	1.541	1.513 (8)	1.529*	1.531 (2)
$\angle C_{\beta,\beta'}C_\alpha$Ge	ϕ_1, $\phi_{1'}$	119.5	119.6	117.9 (6)	118.7 (4)	118.6 (5)
$\angle C_\beta C_\alpha C_\beta$	θ_1	87.3	88.3	89.6 (7)	88.9 (3)	88.3 (5)
$\angle C_\gamma C_{\beta,\beta'}C_\alpha$	θ_2, $\theta_{2'}$	87.9	88.6		87.9 (3)	87.8 (5)
$\angle C_\beta C_\gamma C_{\beta'}$	θ_3	87.9	88.8			88.7 (5)
$\angle HC_\alpha C_\beta$	σ_1	109.1	109.8			109.7 (5)
$\angle HC_\alpha$Ge	σ_2	110.2	108.3	103.7 (29)		110.2 (5)
$\angle H_{1,1'}C_\beta C_\alpha$	λ_1, $\lambda_{1'}$	111.1	112.3			111.1 (5)
$\angle H_{1,1'}C_\beta C_\gamma$	λ_2, $\lambda_{2'}$	110.6	111.5			108.1 (5)
$\angle H_{2,2'}C_\beta C_\alpha$	λ_3, $\lambda_{3'}$	118.0	117.2			118.0 (5)
$\angle H_{2,2'}C_\beta C_\gamma$	λ_4, $\lambda_{4'}$	118.7	117.9			121.1 (5)
$\angle H_1C_{\beta,\beta'}H_2$	λ_5, $\lambda_{5'}$	109.2	108.4	105.9 (32)	112*	109.2 (5)
$\angle H_1C_\gamma C_{\beta,\beta'}$	π_1, $\pi_{1'}$	118.3	117.4			118.9 (5)
$\angle H_2C_\gamma C_{\beta,\beta'}$	π_2, $\pi_{2'}$	110.7	111.7			109.6 (5)
$\angle H_1C_\gamma H_2$	π_3	109.5	108.6	105.9 (32)	110*	109.5 (5)
$\angle C_\alpha$Ge$H_{1,1'}$	η_2, $\eta_{2'}$	111.3	111.1	103.7 (29)	112.0 (2)	111.3 (5)
$\angle C_\alpha$GeH_2	η_1	108.2	109.1	103.7 (29)	112.0 (2)	108.2 (5)

$\angle H_1GeH_2$	η_3	108.6	108.5		106.8 (3)	108.6 (5)
$\angle H_1GeH_{1'}$	η_4	108.8	108.5		106.8 (3)	108.7 (5)
$\tau C_\gamma C_\beta C_\beta C_\alpha$	τ_1	31.9	25.4	25.3 (31)	27 (2)	29.1 (5)
$\tau H_2GeC_\alpha C_\gamma$	τ_2	0.0	0.0			0.0
A(MHz)		9082.77	8857.90		8900.60 (28)	8900.86
B(MHz)		1561.96	1542.93		1576.6562 (12)	1576.80
C(MHz)		1433.56	1414.57		1444.5428 (15)	1444.35
$\|\mu_a\|$		0.861	0.952			
$\|\mu_b\|$		0.000	0.000			
$\|\mu_c\|$		0.290	0.290			
$\|\mu_t\|$		0.908	0.995			
Δ_j		0.225[c]			0.220 (40)	

[a] Electron Diffraction (ED) data from Ref. [98]
[b] Microwave (MW) data from Ref. [93]
[c] Predicted value from MP2(full)/6-31G(d) calculation.
* Fixed parameters

TABLE 41. Structural parameters (Å and degrees), rotational constants (MHz) and dipole moments (Debye) for Ax cyclobutylgermane.

Structural Parameters	Int. coor.	MP2(full)/ 6-311+G(d,p)	B3LYP/ 6-311+G(d,p)	ED [a]	MW	Adjusted r_0 [b]
rC_{α}-Ge	R_1	1.955	1.975	1.948 (4)	1.947	1.950 (5)
rC_{α}-$C_{\beta,\beta'}$	R_2, $R_{2'}$	1.557	1.562	1.557 (3)	1.570 (3)	1.565 (3)
rC_{γ}-$C_{\beta,\beta'}$	R_3, $R_{3'}$	1.547	1.553	1.558	1.570 (3)	1.551 (3)
rC_{α}-H	r_1	1.095	1.093	1.085 (4)	1.090*	1.095 (2)
$rC_{\beta,\beta'}$-H_1	r_2, $r_{2'}$	1.094	1.093	1.085 (4)	1.090*	1.094 (2)
$rC_{\beta,\beta'}$-H_2	r_3, $r_{3'}$	1.095	1.093	1.085 (4)	1.090*	1.095 (2)
rC_{γ}-H_1	r_4	1.093	1.092	1.085 (4)	1.090*	1.093 (2)
rC_{γ}-H_2	r_5	1.092	1.092	1.085 (4)	1.090*	1.092 (2)
rGe-H_2	r_6	1.525	1.542	1.513 (8)	1.529*	1.532 (2)
rGe-$H_{1,1'}$	r_7, $r_{7'}$	1.524	1.541	1.513 (8)	1.529*	1.531 (2)
$\angle C_{\beta,\beta'}C_{\alpha}$Ge	ϕ_1, $\phi_{1'}$	113.9	115.0	114.9 (12)	112.4 (7)	113.4 (5)
$\angle C_{\beta}C_{\alpha}C_{\beta}$	θ_1	87.5	88.5	89.6 (0.7)	87.9 (2)	88.0 (5)
$\angle C_{\gamma}C_{\beta,\beta'}C_{\alpha}$	θ_2, $\theta_{2'}$	88.3	89.1		90.0 (6)	88.8 (5)
$\angle C_{\beta}C_{\gamma}C_{\beta'}$	θ_3	88.2	89.2			89.0 (5)
$\angle HC_{\alpha}C_{\beta}$	σ_1	116.0	115.2			116.3 (5)
$\angle HC_{\alpha}$Ge	σ_2	108.5	107.4	103.7 (2.9)		108.5 (5)
$\angle H_{1,1'}C_{\beta}C_{\alpha}$	λ_1, $\lambda_{1'}$	118.8	118.1			118.8 (5)
$\angle H_{1,1'}C_{\beta}C_{\gamma}$	λ_2, $\lambda_{2'}$	118.1	117.1			120.0 (5)
$\angle H_{2,2'}C_{\beta}C_{\alpha}$	λ_3, $\lambda_{3'}$	110.5	111.6			110.5 (5)
$\angle H_{2,2'}C_{\beta}C_{\gamma}$	λ_4, $\lambda_{4'}$	110.9	112.2			108.4 (5)
$\angle H_1C_{\beta,\beta'}H_2$	λ_5, $\lambda_{5'}$	108.7	107.9	105.9 (3.2)	112*	108.7 (5)
$\angle H_1C_{\gamma}C_{\beta,\beta'}$	π_1, $\pi_{1'}$	111.1	112.1		110*	109.5 (5)
$\angle H_2C_{\gamma}C_{\beta,\beta'}$	π_2, $\pi_{2'}$	118.0	117.0			119.1 (5)
$\angle H_1C_{\gamma}H_2$	π_3	109.1	108.4	105.9 (3.2)		109.1 (5)
$\angle C_{\alpha}$GeH$_{1,1'}$	η_2, $\eta_{2'}$	110.4	110.5	110	109.1 (9)	110.2 (5)
$\angle C_{\alpha}$GeH$_2$	η_1	109.8	110.1	110	109.1 (9)	109.7 (5)

$\angle H_1GeH_2$	η_3	108.5	108.4		109.8 (9)	108.7 (5)
$\angle H_1GeH_{1'}$	η_4	109.1	108.8		109.8 (9)	109.2 (5)
$\tau C_\gamma C_\beta C_\beta C_\alpha$	τ_1	29.3	21.5	20.4 (3.6)	21 (2)	25.1 (5)
$\tau H_2 GeC_\alpha C_\gamma$	τ_2	0.0	0.0			0.0
A(MHz)		7217.19	7355.96		7229.76(61)	7230.10
B(MHz)		1803.38	1722.47		1795.0825 (34)	1795.07
C(MHz)		1710.58	1619.21		1694.3280 (34)	1694.30
$\|\mu_a\|$		0.776	0.865			
$\|\mu_b\|$		0.000	0.000			
$\|\mu_c\|$		0.339	0.367			
$\|\mu_t\|$		0.847	0.940			
Δ_j		0.448[c]			0.510 (14)	

[a]Electron Diffraction (ED) data from Ref. [98]
[b]Microwave (MW) data from Ref. [93]
[c] Predicted value from MP2(full)/6-31G(d) calculation.
* Fixed parameters

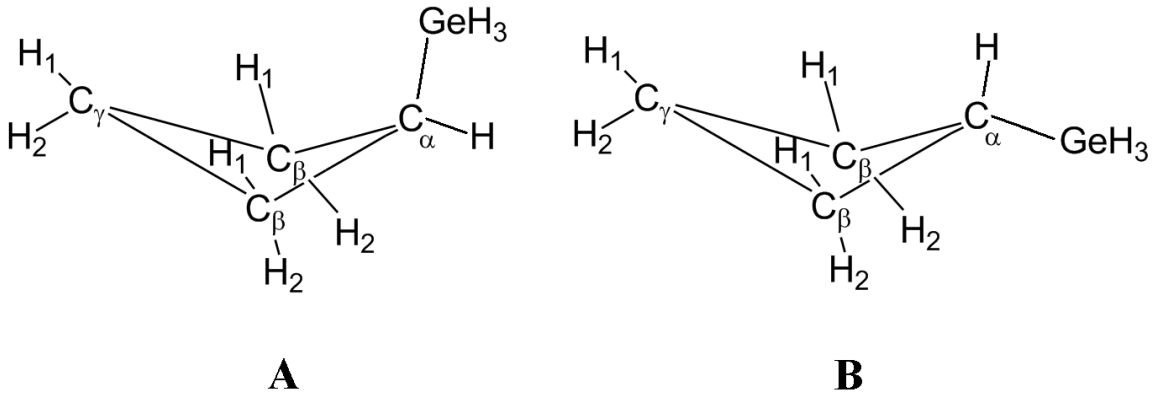

Figure 22. Labeled cyclobutylgermane molecule (A) Axial conformer; (B) Equitorial conformer.

The simulated infrared spectra were obtained from the scaled frequencies together with a Lorentzian function. Infrared intensities were obtained based on the dipole moment derivatives with respect to Cartesian coordinates. The derivatives were transformed with respect to normal coordinates by $(\partial\mu_u/\partial Q_i) = \sum_j (\partial\mu_u/\partial X_j)L_{ij}$, where Q_i is the i^{th} normal coordinate, X_j is the j^{th} Cartesian displacement coordinate, and L_{ij} is the transformation matrix between the Cartesian displacement coordinates and the normal coordinates. The infrared intensities were then calculated by $(N\pi)/(3c^2)$ $[(\partial\mu_x/\partial Q_i)^2 + (\partial\mu_y/\partial Q_i)^2 + (\partial\mu_z/\partial Q_i)^2]$. A comparison of the experimental spectra and simulated infrared spectra with relative concentrations calculated for the equilibrium mixture at 25ºC in Fig. 21. The spectrum of the mixture should be compared to that of the infrared spectrum of the isolated molecule which is closest to that of the vapor at room temperature, and

frequency and intensity changes are expected for the spectrum of the solid. The spectrum of the xenon solutions should be close to that of the vapor since there is little interaction between the xenon solvent and the sample. The predicted spectrum is in good agreement with the experimental spectrum which shows the utility of the scaled predicted frequencies and predicted intensities for supporting the vibrational assignment.

Additional support for the vibrational assignments was obtained from the simulated Raman spectra. The evaluation of Raman activity by using the analytical gradient methods has been developed [31-34] and the activity S_j can be expressed as: $S_j = g_j(45\alpha_j^2 + 7\beta_j^2)$, where g_j is the degeneracy of the vibrational mode j, α_j is the derivative of the isotropic polarizability, and β_j is the anisotropic polarizability. To obtain the Raman scattering cross sections, the polarizabilities are incorporated into S_j by multiplying S_j with $(1-\rho_j)/(1+\rho_j)$ where ρ_j is the depolarization ratio of the j^{th} normal mode. The Raman scattering cross sections and calculated wavenumbers obtained from the Gaussian 03 program were used along with a Lorentzian function to obtain the simulated Raman spectra. Comparison of experimental and predicted Raman spectra with relative concentrations calculated for the equilibrium mixture at 25ºC by using the experimentally determined enthalpy difference are shown in Fig. 23. The spectrum of the mixture should be compared to that of the Raman spectrum of the isolated molecule which is expected to be closest to that of the vapor at room temperature, but frequency and intensity changes are expected for the spectrum of the liquid and solid. It should however be noted that in the Raman spectra of the gas only modes from the A′ block will be observed. The predicted frequencies are in reasonable agreement with the experimental spectrum though the intensities are poorly predicted for several vibrations.

The utility of the predicted Raman spectra for supporting vibrational assignments is still demonstrated as the predicted frequencies are shown to be of significant use.

VIBRATIONAL ASSIGNMENT

The first comprehensive vibrational assignment for cyclobutylgermane [94] was made by utilizing the Raman spectra of the gas, liquid, and solid as well as the infrared spectra of the gas and solid for both conformers. The vibrational assignments were made mostly based on group frequencies along with existing assignments of corresponding vibrations of similar molecules. There were 11 fundamentals that were assigned as arising from the Ax form. However, by the utilization of MP2(full)/6-31G(d) predicted vibrational wavenumbers along with ab intio predicted intensities, and depolarization ratios along with infrared data from xenon solutions it has been possible to assign a significantly larger number of the fundamentals for the Ax conformer. This is important for obtaining the enthalpy difference since the fundamentals being used for the temperature study must be for a single confidently identified conformer. Therefore, we have attempted to assign all of the fundamentals for both conformers in the region from 1100 to 400 cm^{-1} where the number of overtone and combination bands are greatly reduced compared to those in the higher wavenumber region. An effort must then be made to verify the assignment of the bands in the 1100 to 400 cm^{-1} region and to identify any additional Ax bands for the enthalpy determination.

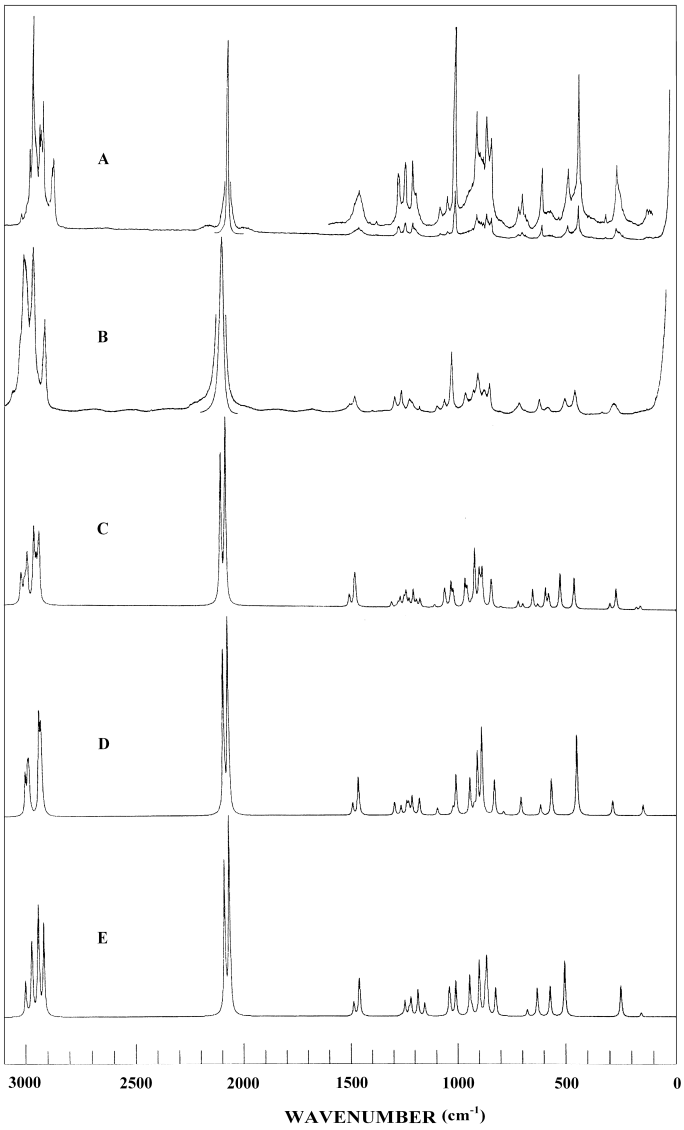

Figure 23. Experimental and predicted Raman spectra of cyclobutylgermane: (A) Gas; (B) liquid; (C) simulated spectrum of mixture of Eq and Ax (ΔH = 112 cm^{-1}) conformers at 25°C; (D) simulated Eq conformer; (F) simulated Ax conformer.

The region from 1100 to 800 cm^{-1} is fairly complex with ten predicted fundamentals for each of the Eq and Ax conformers. There are significant reassignments in this region based largely on the ab initio predicted band frequencies. The band at 1081 cm^{-1} in the infrared spectra of the solid which was assigned as the ν_{31} fundamental which has been reassigned to the band at 1169 cm^{-1} in the infrared spectra of the xenon solutions. The band at 1036 cm^{-1} in the Raman spectra of the gas was assigned for the $\nu_{13'}$ fundamental in the previous study. This band resolves into two bands at 1029 and 1027 cm^{-1} in the infrared spectra of the xenon solutions and they are assigned to the $\nu_{13'}$ and $\nu_{32'}$ fundamentals. The band at 1021 cm^{-1} in the infrared spectra of the xenon solutions is assigned as the ν_{32} fundamental and was previously assigned to the band at 940 cm^{-1} in the Raman spectra of the gas. The band at 930 cm^{-1} in the infrared spectra of the xenon solutions is assigned as the $\nu_{33'}$ fundamental and the band at 916 cm^{-1} in the infrared spectra of the xenon solutions is assigned to the $\nu_{15'}$, ν_{33}, ν_{34}, and $\nu_{34'}$ fundamentals where these fundamentals are predicted with intensities of 1.7 km/mol and less with predicted frequencies between 938 to 932 cm^{-1}. This assignment is tentative and based on the relative frequency predictions as the region is largely obscured by the broad band at 876 cm^{-1}. The band at 899 cm^{-1} in the Raman spectra of the gas was not assigned to any fundamental in the previous study. However this band corresponds to the band at 897 cm^{-1} in the infrared spectra of the xenon solutions and is assigned as the ν_{15} fundamental. The band at 876 cm^{-1} in the infrared spectra of the xenon solutions is a strong broad band which makes this region unsuitable for use in the enthalpy determination and as stated earlier there are a large number of fundamentals predicted in near coincidence with this band. The band appears to be primarily composed of four fundamentals of ν_{16}, $\nu_{16'}$, ν_{35}

and $\nu_{35'}$ which are predicted to be nearly degenerate. The band at 849 cm^{-1} in the infrared spectra of the xenon solutions corresponds to the band at 853 cm^{-1} in the Raman spectra of the gas and 843 cm^{-1} in the Raman spectra of the solid and it is assigned as the ν_{17} and $\nu_{17'}$ fundamentals. This broad spectral feature probably extends further under the broad very intense 825 cm^{-1} band and is probably a factor in the breadth of this band. The band at 825 cm^{-1} in the infrared spectra of the xenon solutions corresponds to the band at 828 cm^{-1} in the infrared spectra of the gas and is assigned to ν_{18} and $\nu_{18'}$ fundamentals in contrast to the previous assignment of ν_{17}. The complexity of the region with 14 predicted fundamentals as well as the two broad bands at 825 and 876 cm^{-1} make the bands in the region from 930 to 800 cm^{-1} unsuitable for use in the enthalpy determination.

The region from 800 to 400 cm^{-1} is much simpler with the current assignments mostly agreeing with those previously assigned. The bands at 708 and 692 cm^{-1} were assigned in the previous vibrational study as the $\nu_{18'}$ and ν_{18} fundamentals, respectively. It should be noted however in the current study these bands are assigned at 825 cm^{-1} and in the course of purification it was found that the bands at 708 and 692 cm^{-1} reduce in intensity with further purification. The bands at 675 and 566 cm^{-1} in the infrared spectra of the gas are visible as two bands each in the infrared spectra of the xenon solutions one Eq and one Ax. These bands are the bands at 674 and 660 cm^{-1} for the fundamentals ν_{19} and $\nu_{19'}$, respectively, and 565 and 555 cm^{-1} for the $\nu_{20'}$ and ν_{20} fundamentals. The band at 598 cm^{-1} in the infrared spectra of the xenon solutions was previously assigned to the fundamental ν_{19} but it has now been reassigned to the Ax conformer fundamental $\nu_{20'}$ on the basis of its relative frequency and temperature dependence. These assignments are listed in Tables 38 and 39 and the reported assignments from the region 800 to 400 cm^{-1}

are bands that can be used for the enthalpy determination. The complexity of the spectra in the 1100 to 800 cm^{-1} region is such that curve fitting is insufficient for obtaining reliable band intensities or areas. The bands at 436, 555, 590, 675, and 775 cm^{-1} for the Eq conformer and 485, 565, 598, and 661 cm^{-1} for the Ax form are resolved sufficiently and of appropriate intensity for use in the enthalpy determination.

CONFORMATIONAL STABILITY

To determine the enthalpy difference between the two observed conformers of cyclobutylgermane, the sample was dissolved in liquefied xenon and the infrared spectra were recorded as a function of temperature from -65 to -100°C. Relatively small interactions are expected to occur between xenon and the sample. Therefore, only small wavenumber shifts are anticipated for the xenon interactions when passing from the gas phase to the liquefied xenon. A significant advantage of this study is that the conformer bands are better resolved in comparison with those in the infrared spectrum of the vapor. From ab initio calculations, the dipole moments of the two conformers are predicted to have similar values and the molecular sizes of the two conformers are nearly the same. Thus, the ΔH value obtained from the temperature dependent infrared study is expected to be near that for the gas [16-20].

Once confident assignments have been made for the fundamentals of both conformers the task was then to find pairs of bands from which the enthalpy difference could be obtained. The bands should be sufficiently resolved in order to determine their intensities. The selection of the bands to use in the enthalpy determination was complicated due to the presence of two broad high intensity bands but was somewhat simplified by the relatively large frequency differences between the Eq and the

corresponding Ax fundamentals in the 800 to 400 cm^{-1} region of the spectra (Fig. 21). Good examples of this factor are the fundamentals at 435 and 485 cm^{-1} for the Eq and Ax conformers where the bands are predicted at 439 and 479 cm^{-1}, respectively. The fundamentals at 435, 555, 590, and 675 cm^{-1} for the Eq conformer and those at 485, 565, 600, and 660 cm^{-1} for the Ax form were initially selected as they are confidently assigned, satisfactory resolved, and a limited number of overtone and combination bands are possible. Additionally the band at 775 cm^{-1} (β-CH_2 rock) was also selected for the Eq form as it was found that the predicted underlying Ax fundamental was not of sufficient intensity to significantly affect the intensity of the observed band.

The intensities of the individual bands were measured as a function of temperature and their ratios were determined (Fig. 24). By application of the van't Hoff equation $-\ln K = \Delta H/(RT) - \Delta S/R$, the enthalpy difference was determined from a plot of $-\ln K$ versus 1/T, where $\Delta H/R$ is the slope of the line and K is substituted with the appropriate intensity ratios, *i.e.* $I_{conf\text{-}1} / I_{conf\text{-}2}$, etc. It was assumed that ΔS, and α are not functions of temperature in the relatively small range studied.

These nine fundamentals, five Eq and four Ax, were utilized for the determination of the enthalpy difference by combining them to form 20 band pairs. The enthalpy difference was determined from these 20 band pairs with a value of 112 ± 8 cm^{-1} (Table 42). This error limit is derived from the statistical standard deviation of two sigma of the measured intensity data taken as a single data set, but it does not take into account small associations with the liquid xenon or the possible presence of overtones and combination bands in near coincidence of the measured fundamentals. The variations in the individual values are undoubtedly due to these types of interferences, but by taking many pairs, the

effect of such interferences should cancel. However, this statistical uncertainty is probably better than can be expected from this technique and, therefore, an uncertainty of about 10% in the enthalpy difference is probably more realistic i.e. 112 ± 11 cm^{-1}. From the enthalpy difference the abundance of the Ax conformer present at ambient temperature is estimated to be 37 ± 1%.

Figure 24. Temperature (-70 to -100°C) dependent mid-infrared spectrum of cyclobutylgermane dissolved in liquid xenon.

Table 42. Temperature and intensity ratios of the Eq and Ax bands of cyclobutylgermane.

	T(°C)	1/T ($\times 10^{-3}$ K^{-1})	I_{436} / I_{485}	I_{436} / I_{565}	I_{436} / I_{598}	I_{436} / I_{661}	I_{555} / I_{485}	I_{555} / I_{565}	I_{555} / I_{598}	I_{555} / I_{661}	I_{590} / I_{485}	I_{590} / I_{565}
Liquid	-65	4.804	0.843	1.475	1.157	1.844	0.629	1.100	0.863	1.375	1.086	1.900
xenon	-70	4.922	0.861	1.531	1.192	1.879	0.653	1.160	0.904	1.424	1.111	1.975
	-75	5.047	0.865	1.561	1.185	1.882	0.662	1.195	0.907	1.441	1.122	2.024
	-80	5.177	0.846	1.590	1.158	1.833	0.667	1.253	0.912	1.444	1.122	2.108
	-85	5.315	0.877	1.651	1.214	1.972	0.679	1.279	0.940	1.528	1.117	2.105
	-90	5.460	0.880	1.622	1.237	1.921	0.699	1.289	0.983	1.526	1.157	2.133
	-95	5.613	0.887	1.620	1.231	1.910	0.726	1.326	1.008	1.564	1.190	2.174
	-100	5.775	0.898	1.681	1.264	1.975	0.716	1.340	1.008	1.575	1.193	2.234
ΔH^a			41 ± 8	79 ± 15	58 ± 12	42 ± 16	96 ± 10	135 ± 16	113 ± 11	97 ± 10	65 ± 9	104 ± 11

	T(°C)	1/T ($\times 10^{-3}$ K^{-1})	I_{590} / I_{598}	I_{590} / I_{661}	I_{675} / I_{485}	I_{675} / I_{565}	I_{675} / I_{598}	I_{675} / I_{661}	I_{775} / I_{485}	I_{775} / I_{565}	I_{775} / I_{598}	I_{775} / I_{661}
Liquid xenon	-65	4.804	1.490	2.375	0.800	1.400	1.098	1.750	0.871	1.525	1.196	1.906
	-70	4.922	1.538	2.424	0.826	1.469	1.144	1.803	0.931	1.654	1.288	2.030
	-75	5.047	1.537	2.441	0.838	1.512	1.148	1.824	0.932	1.683	1.278	2.029
	-80	5.177	1.535	2.431	0.859	1.614	1.175	1.861	0.949	1.783	1.298	2.056
	-85	5.315	1.547	2.514	0.864	1.628	1.197	1.944	0.975	1.837	1.350	2.194
	-90	5.460	1.627	2.526	0.904	1.667	1.271	1.974	1.012	1.867	1.424	2.211
	-95	5.613	1.653	2.564	0.964	1.761	1.339	2.077	1.036	1.891	1.438	2.231
	-100	5.775	1.680	2.625	0.977	1.830	1.376	2.150	1.091	2.043	1.536	2.400
ΔH^a			83 ± 11	67 ± 6	145 ± 12	184 ± 11	162 ± 13	146 ± 7	143 ± 11	181 ± 18	160 ± 15	144 ± 15

[a] Average value $\Delta H = 112 \pm 4$ cm^{-1} (1.34 ± 0.05 kJ mol^{-1}) with the Eq conformer the more stable form and the statistical uncertainty (1σ) obtained by utilizing all of the data as a single set.

STRUCTURAL PARAMETERS

The first determination of the molecular structure of cyclobutylgermane was an ED study [98] where most of the Eq parameters were determined and two of the Ax structural parameters were also obtained. Following the ED study was a microwave investigation [93] where the Eq and Ax conformers were observed and rotational constants were determined for the 74, 72, and 70 isotopes of germane. From these data a partial structure was determine from a diagnostic least-squares fit. The structure published from this microwave study is only a partial structure and the structural parameters obtained from the ED study suffers from large uncertainties in the puckering and ∠Ge-CCC angles. Therefore, we have determined the structural parameters for both conformers by utilizing the rotational constants previously reported from the microwave study [93]. Three isotopic species were investigated for the two conformers and, thus, nine rotational constants are available for each conformer.

We [51] have shown that ab initio MP2(full)/6-311+G(d,p) calculations predict the carbon-hydrogen r_0 structural parameters for more than fifty hydrocarbons to at least 0.002 Å compared to the experimentally determined [5] values from isolated CH stretching frequencies which agree to previously determined values from earlier microwave studies. Therefore, all of the carbon-hydrogen parameters can be taken from the MP2(full)/6-311+G(d,p) predicted values for the Eq and Ax conformers of cyclobutylgermane. The germane-hydrogen r_0 structural parameter values can be experimentally determined [5] from isolated GeH stretching frequencies. These values are listed in Tables 41 and 42 as determined from the assignments in Tables 38 and 39.

We have found that good structural parameters for hydrocarbons and many substituted ones can be determined by adjusting the structural parameters obtained from the ab initio MP2(full)/6-311+G(d,p) calculations to fit the rotational constants obtained from microwave experimental data by using a computer program "A&M" (Ab initio and Microwave) developed [14] in our laboratory. In order to reduce the number of independent variables, the structural parameters are separated into sets according to their types where bond distances in the same set keep their relative ratio, and bond angles and torsional angles in the same set keep their difference in degrees. This assumption is based on the fact that errors from ab initio calculations are systematic. Additionally, we have also shown that the differences in predicted distances and angles from the ab initio calculations for different conformers of the same molecule can usually be used as one parameter with the ab initio predicted differences except for some dihedral angles. Therefore, it should be possible to obtain "adjusted r_0" structural parameters for the five parameters of the five heavy atoms by utilizing the previously reported 18 rotational constants from the earlier microwave study [93]. Therefore we have obtained the complete structural parameters for both the Eq and Ax forms of cyclobutylgermane.

The resulting adjusted r_0 parameters are listed in Tables 41 and 42, where it is believed that the Ge-C distance should be accurate to ± 0.005 Å, the C-C distances accurate to ± 0.003 Å, and the C-H and Ge-H distances accurate to ± 0.002 Å, and the angles should be within ± 0.5°. The fit of the 18 determined rotational constants (Table 43) by the adjusted r_0 structural parameters for both conformers are good with the differences being less than 0.4 MHz. Therefore, it is believed that the suggested uncertainties are realistic values and the determined structural parameters are probably as

accurate as can be obtained for this molecule in the gas phase by either electron diffraction or microwave substitution methods.

Table 43. Comparison of rotational constants (MHz) obtained from modified *ab initio*, MP2(full)/6-311+G(d,p) structural parameters and the experimental values from the microwave spectra of Eq and Ax cyclobutylgermane.

Isotopomers	Rotational constant	MP2(full)/ 6-311+G(d, p)	Experimental[a]	Adjusted r_0[b]	$\|\Delta\|$
eq-$C_4H_7{}^{74}GeH_3$	A	9082.77	8900.60 (28)	8900.86	0.26
	B	1561.96	1576.6562 (12)	1576.80	0.14
	C	1433.56	1444.5428 (15)	1444.35	0.19
eq-$C_4H_7{}^{72}GeH_3$	A	9083.29	8901.34 (30)	8901.27	0.07
	B	1576.28	1591.0991 (15)	1591.27	0.17
	C	1.44561	1456.6449 (15)	1456.47	0.17
eq-$C_4H_7{}^{70}GeH_3$	A	9083.64	8901.33 (25)	8901.70	0.37
	B	1591.35	1606.2605 (13)	1606.47	0.20
	C	1458.27	1469.3315 (14)	1469.18	0.15
ax-$C_4H_7{}^{74}GeH_3$	A	7217.19	7229.76 (61)	7230.10	0.34
	B	1803.38	1795.0825 (34)	1795.07	0.01
	C	1710.58	1694.3280 (34)	1694.31	0.01
ax-$C_4H_7{}^{72}GeH_3$	A	7218.25	7231.47 (48)	7231.24	0.23
	B	1819.39	1811.0436 (21)	1811.04	0.00
	C	1724.91	1708.4659 (24)	1708.47	0.00
ax-$C_4H_7{}^{70}GeH_3$	A	7219.39	7232.56 (47)	7232.45	0.11
	B	1836.23	1827.7926 (21)	1827.81	0.01
	C	1739.98	1723.2957 (25)	1723.31	0.01

[a] Ref. [93].
[b] This Study.

DISCUSSION

The vibrational assignments reported herein are based on a significant amount of information with the infrared spectrum of the xenon solution and predictions of the fundamental frequencies from the scaled ab initio MP2(full)/6-31G(d) calculations as well as the predicted infrared band contours and their intensities. For the Eq conformer the ab initio predicted frequencies for the A′ fundamentals are in error an average of 13 cm^{-1} which represent 0.8% error and for the A″ modes it is 8 cm^{-1} which is 0.7% error excluding the GeH_3 deformations. The percent error for the predictions for the Ax conformer are nearly the same with the A′ fundamentals with 10 cm^{-1} or 0.6% error and the A″ modes 8 cm^{-1} which is 0.6% error again excluding the GeH_3 deformations. Thus the relatively small basis set of 6-31G(d) by the MP2(full) calculations with two scaling factors provides excellent predicted frequencies for aiding the vibrational assignments. Also there is no need to have multiple scaling factors.

It is of interest to compare the GeH_3 deformations from cyclobutylgermane to those of ethylgermane as these fundamentals show little change in frequency and are poorly predicted by the ab initio calculations where they are predicted nearly 30 cm^{-1} in error. Both the A′ and A″ GeH_3 antisymmetric deformations are predicted nearly degenerate and are observed as a band at 876 cm^{-1} in the infrared spectra of the xenon solutions. The GeH_3 symmetric deformation is observed at 825 cm^{-1} in the current study. In a previous vibrational study of ethylgermane [99] the Raman spectra of gaseous and solid phase ethylgermane, GeD_3-ethylgermane, and CD_3-ethylgermane were studied. The bands at 873 and 836 cm^{-1} clearly arise from the GeH_3 deformations and are very close in

frequencies to the cyclobutylgermane bands at 876 and 825 cm^{-1} in the infrared spectra of the xenon solutions. This seems to indicate that the GeH_3 moiety changes very little as the alkane is changed to the atom to which it is bonded.

The adjusted r_0 structural parameters have been determined for both the Eq and Ax conformers. From the ED study [98] the structural parameters were determined for four heavy atom parameters which are listed in Table 40 for the Eq conformer. The Ax form has in common all but three structural parameters with the Eq conformer. The majority of the heavy atom structural parameters determined for the Eq form in the ED study are within their error limits to the parameters determined in the current study with the determined puckering angle and constrained C_β-C_γ distance the only significant differences. However the difference in puckering angle is probably not meaningful as the error is very large. The constrained C_β-C_γ distance is probably a source of error in this structure and it is likely a contributor to the high error limits in the ED parameters. The Ax structure diverges significantly in two of the transferred Eq conformer parameters and two of the determined structural parameters. The C_β-C_γ distance is too large from the ED study. The C_α-C_β distance is much shorter in the ED investigation where the Eq conformer parameters were transferred to the Ax conformer which appears to contribute to the errors in the determined parameters. The $\angle$CCGe and puckering angles are both significantly different from those in the current study but differences are not very meaningful when the error limits are considered.

The structural parameters determined in the diagnostic least-squares microwave study [93] resulted in only four structural parameters determined by this technique for each conformer. For the Eq conformer there is agreement with the values for these except

the error limit on the puckering angle is very large which is a very important angle for the fit as it causes large changes in all three rotational constants. The Ax form has two parameters that are significantly different than those determined in the current study. The C_β-C_γ distance is 0.019 Å too long and the puckering angle is 4.1° too small from the microwave study. The puckering angle has a very large uncertainty which may be part of the reason for the much longer C_β-C_γ distance. A point of interest should be noted is the C_α-C_β distance from the microwave study agrees within the combined error limits with the value obtained in the current study.

It is of interest to compare the structural parameters of cyclobutane to that of cyclobutylgermane since the effect of germane substitution on the ring parameters can be determined. In the microwave study by Caminati et al. [78] the r_0 structural parameters of cyclobutane were determined for the C-C bond distance to be 1.5549(5) Å and the puckering angle to be 28.32(23)°. The puckering angle in cyclobutylgermane for the Eq form is 27 ± 2° compared to 29.1(5)° and for the Ax form 21 ± 2° compared to 25.1(5)° with addition of germane. This difference is relatively small for the Eq form but for the Ax conformer the difference is significant. The C-C bond distances for cyclobutylgermane are C_α-C_β,$C_{\beta'}$ = 1.557(3) and C_γ-C_β,$C_{\beta'}$ = 1.551(3) Å for the Eq form and C_α-C_β,$C_{\beta'}$ = 1.565(3) and C_γ-C_β,$C_{\beta'}$ = 1.551(3) Å for the Ax conformer. The C_γ-C_β distance agrees with that for cyclobutane within the stated errors but the C_α-C_β distance differs by 0.005 for the Eq form and 0.006 Å for the Ax conformer.

The differences in the C_α-C_β bond distances for the two conformers of cyclobutylgermane with respect to the equivalent bond distance in cyclobutane indicate that germane causes some lengthening of the closest C-C bonds through either steric or

electrostatic effects. It should be noted that the major structural change when comparing the Eq and Ax conformer is the orientation of the germane away from the ring in the Eq form and above the ring in the Ax form. This orientation has little effect on the C_γ-C_β bond distances but the C_α-C_β bond distance is significantly affected. The C_γ-C_β bond shows no significant change for both conformers when compared to each other and it is within error limits when compared to cyclobutane. This indicates the effect that lengthens the C_α-C_β bond distance is short range as it does not affect the C_γ-C_β distance. There is a significant difference (4°) in the puckering angle between the Eq and Ax conformers. The Eq puckering angle is very close to that of cyclobutane so the effect of the germane on this angle is negligible. However the Ax conformer has a large difference for the puckering angle indicating that the effect of germane substitution in the Ax position is significant. These results would seem to indicate some form of steric interference between C_γ and germane.

The natural population analysis (npa) was carried out for cyclobutane and cyclobutylmethane for comparison with that predicted for the Eq and Ax conformers of cyclobutylgermane by utilizing the MP2(full) method with the 6-311+G(d,p) basis set. The C atoms for cyclobutane all carry a -0.34 charge. However, germane substitution on cyclobutane gives a charge distribution to the C-ring for the Eq [Ax] form of C_α = -0.62 [-0.62], C_β = -0.33 [-0.33], and C_γ = -0.33 [-0.34] and for germane of +0.95 [+0.95]. These data indicate that the lengthening of the C_α-C_β bond distance is in part an electrostatic effect which decreases rapidly further into the ring. However it should be noted that the electrostatic forces of the molecule do not change significantly with the conformer change while the bond distance and puckering angle do. Also, there is no

significant change in the charge for the β and γ carbons and the C_γ-C_β distance for both conformers is close to that for cyclobutane. These two factors indicate that at least in the Ax conformer the steric interactions of germane with the ring may be the most significant factor determining the ring structure where the C_α-C_β bond distance and the ring puckering angle are both significantly different from the equivalent parameters found in cyclobutane. However, it should be noted that the steric effect is a significantly larger factor in the Ax conformer where the Ge-H---H-C distance for the Eq conformer is 4.72(1) Å and for the Ax form it is 3.67(1) Å which is a difference of 1.05 Å. Therefore for the Eq conformer the steric interaction of germane should play a much smaller role and the primary reason for the difference in the C_α-C_β bond distance difference as compared with cyclobutane may be solely the electrostatic forces. The adjusted r_0 structure of cyclobutylmethane is of interest where the npa predicts values of C_α = -0.19, C_β = -0.33, and C_γ = -0.34 for the ring parameters and so the steric effects of the substituent should be the primary reason for the changes in the ring structure as compared to cyclobutane.

One of the major goals of this research was the determination of the enthalpy difference between the two conformers where there had been several significantly different values previously reported. From the ED study [98] a ΔG of 259 ± 8 cm^{-1} was reported. This was followed by a vibrational study [94] were an enthalpy difference of <350 cm^{-1} was determined from the variable temperature Raman spectra of the gas. In the same vibrational study the potential function was determined with an enthalpy difference of 191 cm^{-1} with a barrier of 432 cm^{-1}. Finally from a more recent molecular mechanics study [100] an energy difference of 270 cm^{-1} was reported. These values can be

compared to the enthalpy difference in the present study of 112 ± 11 cm^{-1} from 20 band pairs in the infrared spectra of the xenon solutions. This value does not agree with the value obtained from the ED study though this result is relatively insignificant since the ED study is a ΔG value rather than a ΔH and the error limit is probably better than can be achieved through that method. The value from the Raman spectra of the gas agrees with the current value but this is not meaningful as it is any value from 350 to 0 cm^{-1}. The enthalpy difference from the potential function is much closer to the value found in the current study though still ~80 cm^{-1} and it is difficult to access how meaningful this difference may be since there was no error limit given and several of the "hot bands" fit for this potential function are relatively poorly fit with differences of 2.9 and 1.5 cm^{-1}.

To support the experimental values the ab initio energy differences have been determined by a variety of basis sets (Table S4). The results are interesting in that the MP2(full) method with basis sets of cc-pVTZ predict the wrong conformer as being more stable with energy differences of ~20 cm^{-1}. The same method with much smaller basis sets predicts the most stable conformer correctly as determined experimentally. However, the energy differences ranges drastically with the basis set. The B3LYP method predicts significantly higher values than the values from the MP2(full) method and consistently predicts the correct conformer as stable form but with ~90 cm^{-1} too high in energy which is similar to the silane [101].

The barrier to conformer interchange is predicted by the MP2(full) method to be ~750 cm^{-1} and by the B3LYP method to be ~330 cm^{-1}. Both of these values are significantly different than the value of 432 cm^{-1} from the previously determined [29] potential function where the MP2(full) method is ~320 cm^{-1} too high and the B3LYP

method is ~100 cm^{-1} too low. Interestingly the value predicted by the MP2(full) method with the aug-cc-pVTZ predicts the value within 22 cm^{-1} of the value determined [94] from the potential function.

From the microwave study [93] of cyclobutylgermane the quadratic centrifugal distortion constant Δ_J was determined from the spectral data for the 74, 72, and 70 isotopes of germane for both the Eq and Ax conformers. We have obtained the quadratic centrifugal distortion constants for the 74 isotope of germane from the MP2(full)/6-31G(d) calculation. For the Eq conformer this value is predicted to be 0.2251 kHz as compared to the experimental value of 0.2202(40) kHz and for the Ax form the predicted value is 0.448 kHz as compared to the experimental value of 0.510(14) kHz. These values are in excellent agreement and the 72 and 70 isotopes do not vary significantly. This result reconfirms our past findings that the ab initio calculations usually predict reasonably good distortion constants.

CONCLUSION

Initial determination [43] of the cyclobutylgermane fundamentals only those of equatorial (Eq) conformer were assigned and in the later investigation [94] there were only two fundamentals of the axial (Ax) conformer assigned. A few fundamentals of the equatorial conformer had some bands relatively close to the fundamentals that they were concluded to be excited state vibrations of the Eq conformer. In the current variable temperature study many of these bands were clearly shown to be fundamentals of the Ax conformer. This was possible from the low temperature inert gas solutions, where the bands are relatively sharp and it was easy to identify the Ax conformer bands and all but five of the fundamentals were assigned. Initial predictions for assignments were obtained

from the scaled ab initio MP2(full)/6-31G(d) calculations with two scaling factors which resulted for the Eq conformer and average error of 0.8% for the A′ fundamentals and 0.7% error for the A″ modes. Similar results were obtained for the Ax form. It should be noted that the GeH_3 deformations are relatively poorly predicted for both the A′ and A″ motions from the MP2 predictions and similar poor predictions are found for other germanium molecules.

Prior to these structural studies reported herein there were two previous structural investigations and the first was an electron diffraction study [98]. From this study it was assumed that the heavy atom distances would be the same for both Eq and Ax forms and all the angles except two were considered to be the same. Only the structural parameters were reported of major interest is the puckering angle which was reported as 25.3° for Eq form and 20.4° for the Ax form with uncertainties of ±3°. Structural parameters from the microwave study [93] were reported four years later and only four parameters were obtained by diagnostic least-square fit, with the remaining structures estimated from corresponding parameters from similar molecules. Of the four parameters for the Ax form the C_β-C_γ distance is 0.019 Å too long and the puckering angle too small by 4.1° relative to the determined parameters obtained in the current study. With the very limited structural information available for either the Eq or Ax conformers it is desirable to have the complete structural parameters for both conformers. Therefore, complete structural parameters were obtained by utilizing the carbon-hydrogen structural parameters from the isolated C-H stretching frequencies, the heavy atom structural parameters utilizing the 18 rotational constants from the previous microwave study to obtain the adjusted r_0 structural parameters. The determined heavy atom distances have uncertainties of ± 0.003

Å, and the puckering angle had uncertainties of ± 0.5°. The puckering angle for equatorial conformer is 29.1° and that of axial form is 25.1°. The equatorial puckering angle is very close to that of cyclobutane which indicates that germane does not affect this angle. The axial conformer has a large difference in the puckering angle indicating that the germane substitution in the axial position is significant.

The natural population analysis (npa) was carried out for cyclobutane and cyclobutylmethane for comparison with that predicted for the Eq and Ax conformers. The two major factors in determining the ring structure are the electrostatic forces and steric interactions. The steric interaction of the germane with the ring is an especially critical factor for the Ax form in determining the ring structure. For the Eq form the electrostatic charges predominate the ring C-C bond distances.

The third major goal of this research was the determination of the enthalpy difference between the two conformers where there had been several significant different values previously reported. From the ED study[98] the ΔH of 359 ± 8 cm^{-1} was reported which was followed by a vibrational study [94] where an enthalpy difference from the Raman spectrum of the gas was reported to be less than 350 cm^{-1}. In the same vibrational study the potential function was determined with an enthalpy difference of 191 cm^{-1} with a barrier of 432 cm^{-1}. Finally in a more recent molecular mechanics study [100] was reported in 1999 that an energy difference of 270 cm^{-1} was obtained. These values can be compared to the enthalpy difference in the present study of 112 ± 11 cm^{-1}, twenty band pairs in the infrared spectrum of the xenon solution. The utilization of twenty band pairs in this study were arising from combination or overtone bands lying under one of the fundamentals utilized for the enthalpy determination average out. The fact that the

statistical uncertainties at 2 cm^{-1} utilized the 10% as the more realistic uncertainty based upon possible factors arising from the interactions of the sample with the xenon solution or other associations with very small concentration of this sample.

To evaluate the ability of the ab initio calculations to predict the energy difference MP2(full) method was utilized with a large number of different basis sets. The largest basis set of cc-pVTZ predicts the wrong conformer as being the more stable energy difference of 20 cm^{-1}, same method with a smaller basis set predicts the more stable conformer correctly. The energy difference obtained by the B3LYP method utilizing similar basis sets consistently predicts the correct conformer as the stable form but the energies is approximately 90 cm^{-1} too high.

CHAPTER 8

MICROWAVE AND INFRARED SPECTRA, ADJUSTED r_0 STRUCTURAL PARAMETERS, CONFORMATIONAL STABILITIES, VIBRATIONAL ASSIGNMENTS AND THEORETICAL CALCULATIONS OF CYCLOBUTYLCARBOXYLIC ACID CHLORIDE

INTRODUCTION

Our interest in the conformational stabilities and structural parameters of small ring compounds, particularly monosubstituted four and five membered ring molecules, has led us to reinvestigate some of these molecules where there is considerably controversy of the most stable conformers. One such molecule is the monosubstituted four-membered ring cyclobutylcarboxylic acid chloride where there have been four different conformers/structure studies reported[1].These four possible conformers are the gauche-equatorial (g-Eq), gauche-axial (g-Ax), trans-equatorial (t-Eq), and trans-axial (t-Ax) where the three stable conformers (g-Eq, g-Ax and t-Eq) are shown in Fig. 25.

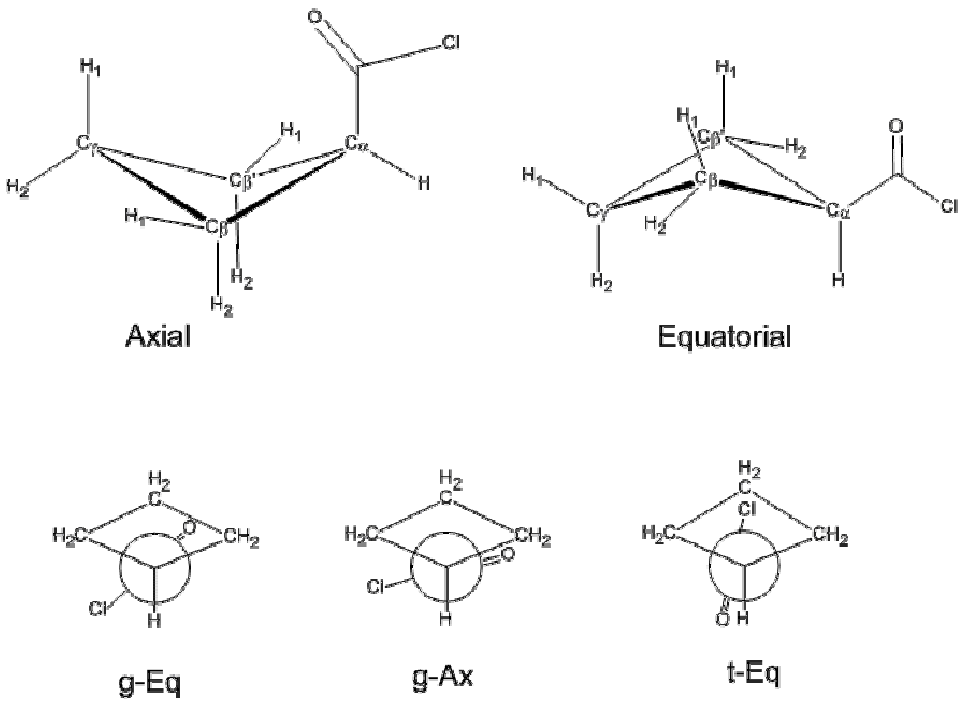

Figure 25. Labeled conformers of cyclobutylcarboxylic acid chloride with atomic numbering.

The earlier structural determination of this molecule in the vapor state was obtained by the electron diffraction technique by Adam and Bartell [102] in 1971. These scientists were interested in the structure and conformations of the series R-COX and concluded that the cyclobutyl derivative exists almost entirely as the gauche conformations. From this study it was concluded that there was coupling between the ring bending and torsional displacements based on the electron diffraction intensities. From these couplings it was observed that the gauche conformation aligned toward the cis side favored the equatorial puckered ring and those on the trans side favored the axial puckered ring. Bond lengths and bond angles were determined and it was concluded that

they were “normal” which indicates that they were similar to those obtained in “unstrained” alkyl carboxaldhydes [106-108] which is rather surprising since cyclobutyl compounds are moderately strained.

Following this initial structural investigation [102] there were three [103-105] additional structural investigations with two of them vibrational studies [103,104] and the other a microwave and vibrational study [105]. In the first vibrational study [103] the spectra were recorded of the condensed phases (liquid and solid) and it was concluded that there was a single conformer present in both phases and it was the same form.

A subsequent vibration investigation [104] was reported which included the infrared spectrum of the gas as well as the spectra of the liquid and solid and the Raman spectrum of the liquid. From this study there was clear evidence from the temperature dependence of the spectrum of the liquid that multiple conformers exist in the fluid state. For example, some bands increased where others decreased as the temperature was decreased and one band disappeared in the spectrum of the crystal. From these studies it was assumed that the proposed three conformers from the electron diffraction investigation were probably nearly equal concentrations.

From a later microwave and vibrational investigation [105] only the microwave spectrum of the ^{35}Cl isotope of the g-Eq form was assigned and there was no microwave data for the ^{37}Cl species or other conformers. From this microwave data a partial structure was reported for the g-Eq conformer. Also, in this study [105] an investigation of the Raman spectrum of the liquid was reported and the energy difference between the preferred g-Eq form and high energy (assumed to be t-Eq) conformer was determined to be 1.4 kcal mol^{-1} (490 cm^{-1}). Therefore from the four reported studies to date, there is at

least two and possibly three conformers present in the fluid phases but there is still a question which conformer is the most stable form and what are the energy differences, as well as, to assign the microwave spectral transitions of the ^{37}Cl isotopologue for the g-Eq form and determine a complete set of structural parameters from the microwave data. Thus, a microwave and vibration investigation has been initiated to answer these questions.

To aid in identifying the fundamental vibrations for the additional conformers and to assign fundamentals for the less stable conformers for use in determining the enthalpy differences ab initio calculations have been utilized. The harmonic force fields, infrared intensities, Raman activities, depolarization ratios, and vibrational frequencies were obtained from MP2/6-31G(d) ab initio calculations with full electron correlation. Additionally both MP2(full) ab initio and Density Functional Theory (DFT) calculations by the B3LYP method have been carried out with a variety of basis sets up to aug-cc-pVTZ as well as with diffuse functions to predict the conformational stabilities. The results of these spectroscopic, structural, and theoretical studies of cyclobutylcarboxylic acid chloride are reported herein.

EXPERIMENTAL AND THEORETICAL METHODS

The sample of cyclobutylcarboxylic acid chloride was purchased from Sigma-Aldrich Chemical Co., with stated purity of 98%. The sample was further purified by low-temperature, low-pressure fractionation column and the purity of the sample was verified by comparing the infrared spectrum with that previously reported [105].

Microwave spectra were recorded by using a “mini-cavity” Fourier-transform microwave spectrometer [25,26] at Kent State University. The Fabry-Perot resonant

cavity is established by two 7.5-inch diameter diamond-tip finished aluminum mirrors with a 30.5-cm spherical radius. The Fabry-Perot cavity resides inside a vacuum chamber formed by a 6-way cross and a 15-inch long, 8-inch diameter extension tube. The two cavity mirrors are nominally separated by 30 cm.

The sample was entrained in a 70:30 Ne-He carrier gas mixture at 2 atm and expanded into the cavity to attain 4K by using a reservoir nozzle [26] made from a modified Series-9 General Valve. The reservoir nozzle is mounted in a recessed region of the mirror flange, external to the vacuum chamber, and the expansion passes through a 0.182-inch diameter hole into the resonant cavity. The center of the expansion is offset from the center of the mirror by 1 inch.

The sample was irradiated by microwave radiation generated by an Agilent Technologies E8247C PSG CW synthesizer; details of the irradiation and heterodyne detection circuitry can be found in Ref. [27] The vacuum system can accommodate pulse repetition rates of up to 15 s^{-1} while maintaining a pressure below 10^{-4} torr, and the instrument can scan 450 MHz in 6 hours while averaging 100 shots per scan segment. The frequencies for the measured transitions in the region of 10,500 to 22,000 MHz are listed in Tables 44 and 45 along with their assignments.

The infrared spectrum of the gas (Fig. 26A) was obtained from 4000 to 220 cm^{-1} on a Perkin-Elmer model 2000 Fourier transform spectrometer equipped with a Ge/CsI beamsplitter and a DTGS detector. Atmospheric water vapor was removed from the spectrometer housing by purging with dry nitrogen. The spectrum of the gas was obtained with a theoretical resolution of 0.5 cm^{-1} for the gas with 128 interferograms added and truncated.

Table 44. Microwave spectrum for the g-Eq form of c-$C_4H_7C(O)^{35}Cl$. Observed frequencies of hyperfine components of rotational transitions (MHz) and deviations of calculated values (kHz).

Transition	2F'	2F''	obs (MHz)	Δ (kHz)	Transition	2F'	2F''	obs (MHz)	Δ (kHz)
$5_{05} \leftarrow 4_{04}$	11	9	12488.0928	0.0	$5_{23} \leftarrow 4_{22}$	11	11	13102.2947	-9.0
	7	5	12488.4513	0.0		11	9	13102.8295	0.0
	13	11	12488.8314	0.0		9	7	13102.9112	1.0
						13	11	13103.2076	0.0
$4_{23} \leftarrow 4_{04}$	7	5	12510.4984	-1.0		7	5	13103.2512	1.0
	5	5	12512.2725	-3.0		7	7	13103.7903	-3.0
	11	11	12513.7552	2.0					
	9	7	12515.6503	2.0	$6_{06} \leftarrow 5_{15}$	9	7	13298.0792	-2.0
						15	13	13298.7292	1.0
$5_{24} \leftarrow 5_{05}$	7	7	12801.0148	0.0		11	9	13299.1049	-2.0
	13	13	12801.9124	1.0		13	11	13299.7042	-1.0
	9	9	12804.5374	0.0					
	11	11	12805.6276	-3.0	$5_{14} \leftarrow 4_{13}$	11	9	13397.6336	-1.0
						9	7	13397.7486	2.0
$5_{42} \leftarrow 4_{41}$	11	9	12851.4369	1.0		13	11	13398.1012	0.0
	9	7	12852.8816	-1.0		7	5	13398.1832	1.0
	13	11	12854.9682	0.0					
	7	5	12856.3981	1.0	$8_{35} \leftarrow 8_{26}$	17	17	13543.8893	-1.0
						15	15	13544.1742	-1.0
$5_{41} \leftarrow 4_{40}$	11	9	12851.6285	1.0		19	19	13545.0002	-1.0
	9	7	12853.0725	-1.0		13	13	13545.0375	0.0
	13	11	12855.1571	-1.0					
	7	5	12856.5838	-3.0	$6_{33} \leftarrow 6_{24}$	13	13	14581.4210	-4.0
						11	11	14581.4906	-3.0
$5_{33} \leftarrow 4_{32}$	11	9	12866.4754	1.0		9	9	14581.5304	-1.0
	9	7	12867.4525	-2.0		15	15	14581.5809	2.0
	11	11	12868.2870	0.0					

			13	11	12868.6320	2.0	6_{06}	←	5_{05}	11	9	14837.8797	1.0
			7	5	12869.0708	1.0				13	11	14838.0792	1.0
5_{32}	←	4_{31}	11	9	12881.2035	3.0	4_{31}	←	4_{22}	5	5	15145.9291	3.0
			9	7	12881.7769	5.0				11	11	15146.7867	0.0
			13	11	12883.0272	4.0				7	7	15148.3560	2.0
			7	5	12883.7434	-2.0				9	9	15149.1610	1.0
9_{36}	←	9_{27}	19	19	12938.1931	2.0	10_{29}	←	10_{110}	23	23	16847.3301	0.0
			17	17	12938.3418	1.0				19	19	16850.9893	0.0
			21	21	12939.1964	1.0				21	21	16851.6156	0.0
			15	15	12939.3744	-2.0							
							7_{07}	←	6_{06}	13	11	17144.2289	1.0
7_{26}	←	7_{17}	11	11	13089.0202	-1.0				15	13	17144.3366	2.0
			13	13	13093.7375	2.0				11	9	17144.8521	-2.0
			15	15	13094.7280	0.0							

Table 45. Microwave spectrum for the g-Eq form of c-$C_4H_7C(O)^{37}Cl$. Observed frequencies of hyperfine components of rotational transitions (MHz) and deviations of calculated values (kHz).

Transition	2F'	2F''	obs (MHz)	Δ (kHz)	Transition	2F'	2F''	obs (MHz)	Δ (kHz)
$5_{15} \leftarrow 4_{14}$	9	7	11843.7145	0.0	$7_{26} \leftarrow 7_{17}$	11	11	12959.0087	-1.0
	7	5	11844.1191	-2.0		17	17	12959.7415	2.0
	11	9	11844.1191	6.0		13	13	12962.6624	0.0
	13	11	11844.3502	0.0		15	15	12963.4274	-1.0
	9	9	11845.9516	-1.0					
	7	7	11850.3009	0.0	$6_{06} \leftarrow 5_{15}$	9	7	12981.6414	-1.0
						15	13	12982.1523	1.0
$4_{14} \leftarrow 3_{03}$	9	9	11854.2267	-3.0		11	9	12982.4399	-1.0
	9	7	11858.5569	0.0		13	11	12982.9145	0.0
	7	5	11858.7653	-2.0					
	11	9	11860.5299	-1.0	$5_{14} \leftarrow 4_{13}$	11	9	13121.1218	-2.0
	5	3	11860.6000	5.0		9	7	13121.2000	6.0
						13	11	13121.4873	1.0
$5_{05} \leftarrow 4_{04}$	9	7	12246.1823	0.0		7	5	13121.5366	0.0
	11	9	12246.3667	1.0					
	7	5	12246.6679	-1.0	$6_{06} \leftarrow 5_{05}$	11	9	14554.8534	-2.0
	13	11	12246.8701	2.0		13	11	14554.9830	3.0
	9	9	12247.8543	-2.0		9	7	14555.3695	-2.0
	7	7	12251.4504	-2.0		15	13	14555.4882	2.0
$5_{24} \leftarrow 4_{23}$	11	9	12517.5782	-1.0	$6_{52} \leftarrow 5_{51}$	13	11	15104.3045	7.0
	9	7	12517.7214	1.0		11	9	15105.1831	3.0
	13	11	12518.4264	-1.0		15	13	15106.9214	2.0
	7	5	12518.5449	2.0		9	7	15107.7958	0.0
	7	7	12520.1200	-2.0					
					$6_{51} \leftarrow 5_{50}$	13	11	15104.3045	1.0
$5_{42} \leftarrow 4_{41}$	11	9	12588.5521	1.0		11	9	15105.1831	-4.0

			9	7	12589.7455	-2.0					15	13	15106.9214	-4.0
			13	11	12591.4810	-1.0					9	7	15107.7958	-6.0
			7	5	12592.6693	0.0								
							6_{43}	←	5_{42}	13	11	15119.1757	0.0
5_{41}	←	4_{40}	11	9	12588.7204	1.0				11	9	15119.6815	0.0
			9	7	12589.9163	0.0				15	13	15120.8317	1.0
			13	11	12591.6493	0.0				9	7	15121.3266	2.0
			7	5	12592.8426	6.0							
							6_{42}	←	5_{41}	13	11	15119.9299	-2.0
5_{33}	←	4_{32}	11	9	12602.7191	-1.0				11	9	15120.4393	2.0
			9	7	12603.3464	1.0				15	13	15121.5822	-1.0
			13	11	12604.3872	1.0				9	7	15122.0754	-1.0
			7	5	12604.8893	-1.0							
							6_{34}	←	5_{33}	13	11	15137.0321	-2.0
5_{32}	←	4_{31}	11	9	12616.1242	-1.0				11	9	15137.1476	0.0
			9	7	12616.5958	-2.0				15	13	15137.8741	0.0
			13	11	12617.6440	-2.0				9	7	15138.1516	-3.0
			7	5	12618.2493	0.0							
							6_{33}	←	5_{32}	13	11	15172.4394	1.0
5_{23}	←	4_{22}	11	11	12824.7289	-7.0				11	9	15172.6830	-2.0
			11	9	12825.2798	-2.0				15	13	15173.3002	1.0
			9	7	12825.3557	6.0				9	7	15173.4499	3.0
			13	11	12825.6322	-1.0							
			7	5	12825.6801	0.0							
			7	7	12826.2405	2.0							

The mid-infrared spectra (4000 to 400 cm^{-1}) of the sample dissolved in liquid xenon (Fig. 26B) were recorded on a Bruker model IFS-66 Fourier transform spectrometer equipped with a globar source, a Ge/KBr beamsplitter and a DTGS detector. In all cases, 100 interferograms were collected at 1.0 cm^{-1} resolution, averaged and transformed with a boxcar truncation function. For these studies, a specially designed cryostat cell was used. It consists of a copper cell with a path length of 4 cm with wedged silicon windows sealed to the cell with indium gaskets. The copper cell was enclosed in an evacuated chamber fitted with KBr windows. The temperature was maintained with boiling liquid nitrogen and monitored by two Pt thermo resistors. After cooling to the designated temperature, a small amount of the sample was condensed into the cell and the system was then pressurized with the noble gas, which condensed in the cell, allowing the compound to dissolve. All of the observed bands in the infrared spectra of the gas along with their proposed assignments of the g-Eq, g-Ax and t-Eq conformers are listed in Tables 46, 47 and 48, respectively.

Table 46. Observed[a] and predicted fundamental[b] frequencies for the g-Eq conformer of cyclobutylcarboxylic acid chloride.

	Fundamental	ab initio	fixed scaled[c]	IR int.	Raman act.	dp ratio	IR				Raman Liquid[d]	P.E.D.[f]	Band Contour		
							gas	Xe soln.	gas[d]	solid[d]			A	B	C
ν_1	β-CH_2 antisymmetric stretch	3213	3014	25.2	45.8	0.66	3003	3000	3004	3002	3004	$73S_1,25S_2$	-	16	84
ν_2	β-CH_2 antisymmetric stretch	3207	3008	13.2	62.4	0.75	2996	2994	2995	2995		$97S_2$	6	75	19
ν_3	γ-CH_2 antisymmetric stretch	3194	2996	7.7	78.1	0.48	2986	2984		2980	2984	$73S_3,23S_1$	70	-	30
ν_4	α-CH stretch	3147	2952	2.1	30.7	0.69	2961	2959	2964	2952	2956	$88S_4,11S_5$	45	16	39
ν_5	β-CH_2 symmetric stretch	3141	2946	12.9	122.0	0.09	2945	2944				$48S_5,42S_7$	23	65	12
ν_6	γ-CH_2 symmetric stretch	3134	2940	25.6	98.8	0.14	2943	2943				$93S_6$	76	24	-
ν_7	β-CH_2 symmetric stretch	3133	2939	14.4	54.1	0.24	2926	2926	2887	2866	2879	$51S_7,38S_5$	27	31	42
ν_8	C=O stretch	1853	1760	205.2	14.2	0.53	1807	1807	1808	1792	1805	$92S_8$	3	93	4
ν_9	β-CH_2 deformation	1575	1483	2.0	5.3	0.73	1470	1469		1467	1466	$62S_9,34S_{10}$	23	36	41
ν_{10}	γ-CH_2 deformation	1550	1459	5.2	17.8	0.74	1453	1453	1451	1446	1452	$64S_{10},34S_9$	8	42	50
ν_{11}	β-CH_2 deformation	1542	1452	2.3	5.6	0.74	1442	1442	1451[e]	1446[e]		$98S_{11}$	29	42	29
ν_{12}	α-CH in plane bend	1404	1337	17.9	8.9	0.56	1324	1322	1328	1319	1328	$56S_{12},11S_{20},10S_{14}$	94	5	1
ν_{13}	γ-CH_2 wag	1320	1254	5.0	5.5	0.73	1247	1246	1252	1246	1250	$63S_{13},10S_{16},10S_{21}$	6	82	12
ν_{14}	β-CH_2 wag	1315	1251	11.4	0.6	0.60	1245	1244	1252[e]	1242[e]	1250	$72S_{14},10S_{25}$	78	19	3
ν_{15}	β-CH_2 wag	1294	1229	0.9	4.3	0.73	1232	1232		1228[e]	1232[e]	$43S_{15},22S_{18},14S_{17},10S_{23}$	13	87	-
ν_{16}	α-CH out of plane bend	1282	1217	1.4	6.6	0.75	1213	1213	1209	1215	1217	$37S_{16},14S_{17},14S_{13},10S_{18},10S_{15}$	25	75	-
ν_{17}	β-CH_2 twist	1268	1205	4.8	5.9	0.72	1204	1201		1198	1208	$43S_{17},18S_{16},12S_{28},10S_{23}$	87	4	9
ν_{18}	γ-CH_2 twist	1239	1179	3.4	8.7	0.75	1177	1176		1176	1190	$31S_{18},39S_{15},10S_{21},10S_{23}$	53	45	2
ν_{19}	β-CH_2 rock	1170	1120	23.9	4.2	0.06	1110	1108	1110	1104	1109	$37S_{19},14S_{22},11S_{28},11S_{35}$	98	2	-
ν_{20}	C-C stretch	1127	1075	62.6	4.4	0.35	1069	1067	1071	1070	1071	$25S_{20},21S_{12},11S_{22}$	78	22	-

ν_{21}	Ring deformation	1078	1032	3.8	5.2	0.33	1027	1026	1030	1017	1025	$22S_{21},21S_{24},17S_{23},14S_{22},10S_{20}$	96	2	2
ν_{22}	Ring breathing	1013	970	52.9	9.7	0.07	960	958	955	954	962	$45S_{22},18S_{25},11S_{20}$	90	10	-
ν_{23}	β-CH_2 twist	994	946	0.9	2.5	0.72	946	946				$37S_{23},23S_{16},16S_{18},10S_{24},10S_{21}$	1	68	31
ν_{24}	Ring deformation	975	932	1.7	10.1	0.75	933	933		923	930[e]	$51S_{24},29S_{21},10S_{13}$	-	83	17
ν_{25}	Ring deformation	942	911	7.7	2.1	0.47	889	887	888	888	891	$33S_{25},24S_{30},13S_{28},11S_{19},10S_{14}$	46	51	3
ν_{26}	COCl scissors	847	823	152.8	2.4	0.30	809	807	810	799	804	$19S_{26},14S_{30},13S_{25},12S_{28}$	83	17	-
ν_{27}	β-CH_2 rock	818	779	7.3	0.9	0.72	778	776	775	779	784	$68S_{27},11S_{18}$	90	-	10
ν_{28}	γ-CH_2 rock	750	728	36.5	4.6	0.26	721	720	721	722	721	$30S_{28},13S_{29},12S_{33},10S_{17},10S_{32}$	86	14	-
ν_{29}	COCl wag	661	651	8.2	2.4	0.10	645	645	646	640	651	$48S_{29},11S_{30},11S_{19}$	69	2	29
ν_{30}	Ring deformation	591	578	6.9	3.7	0.14	569	569	570	566	572	$31S_{30},16S_{32},13S_{19},11S_{20}$	43	52	5
ν_{31}	C-Cl stretch	446	432	24.0	12.0	0.41	433	431	437	433	434	$61S_{31},35S_{26}$	41	56	3
ν_{32}	COCl rock	345	339	19.1	5.8	0.36	340	-	338	338	343	$11S_{32},22S_{26},19S_{31},19S_{34},11S_{20}$	78	22	-
ν_{33}	Ring-COCl bend	304	298	2.6	0.5	0.72	-	-	278	282	290	$26S_{33},35S_{35},13S_{32},12S_{29}$	82	-	18
ν_{34}	Ring-COCl bend	163	163	1.1	0.6	0.74	-	-	168	176	181	$55S_{34},33S_{32}$	21	45	34
ν_{35}	Ring puckering	145	144	1.7	0.4	0.42	-	-	-	153	-	$48S_{35},40S_{33}$	39	-	61
ν_{36}	COCl Assymetric torsion	47	47	0.0	1.0	0.73	-	-	-	83	-	$100S_{36}$	3	60	37

[a] Observed spectra: gas, Xe, and solid are IR while liquid is Raman.

[b] MP2(full)/6-31G(d) ab initio calculations, scaled frequencies, infrared intensities (km/mol), Raman activities ($Å^4$/u), depolarization ratios (dp) and potential energy distributions (P.E.D.s).

[c] Scaled frequencies with scaling factors of 0.88 for the CH stretches, β-CH_2 and γ-CH_2 deformations and 0.90 for all other modes except the heavy atom bending modes.

[d] Reference [105].

[e] Our Assignment

[f] Symmetry coordinates with P.E.D. contribution less than 10% are omitted.

Table 47. Observed[a] and predicted fundamental[b] frequencies for the g-Ax conformer of cyclobutylcarboxylic acid chloride.

	Fundamental	*ab initio*	fixed scaled[c]	IR int.	Raman act.	dp ratio	IR gas	IR Xe soln.	P.E.D.[e]	Band Contour		
										A	B	C
ν_1	β-CH_2 antisymmetric stretch	3214	3015	23.6	49.7	0.71	3012	3012	$48S_1,42S_3,10S_2$	47	43	10
ν_2	β-CH_2 antisymmetric stretch	3205	3007	8.9	62.8	0.66	3008	3007	$76S_2,21S_3$	74	6	20
ν_3	γ-CH_2 antisymmetric stretch	3195	2997	4.8	62.4	0.72	3002	2999	$35S_3,49S_1,13S_2$	18	2	80
ν_4	α-CH stretch	3165	2969	4.6	79.4	0.16	2963	2963	$96S_4$	38	5	57
ν_6	γ-CH_2 symmetric stretch	3142	2947	21.4	112.8	0.08	2945	2944	$96S_6$	61	-	39
ν_5	β-CH_2 symmetric stretch	3138	2944	14.7	84.8	0.23	2944	2943	$58S_5,35S_7$	23	6	71
ν_7	β-CH_2 symmetric stretch	3134	2940	18.8	41.9	0.23	2943	2943	$63S_7,34S_6$	5	86	9
ν_8	C=O stretch	1847	1754	189.8	10.1	0.49	1760	1759	$91S_8$	15	82	3
ν_{10}	γ-CH_2 scissors	1572	1480	2.8	7.6	0.72	1468	1468	$53S_{10},44S_9$	39	33	28
ν_9	β-CH_2 scissors	1550	1459	3.7	15.7	0.75	1458	1457	$47S_{10},44S_{10}$	3	54	43
ν_{11}	β-CH_2 scissors	1535	1445	5.2	7.2	0.75	1446	1443	$90S_{11},10S_9$	21	43	36
ν_{12}	α-CH in plane bend	1402	1334	24.9	3.8	0.61	1339	1337	$54S_{12},15S_{17},11S_{22}$	94	-	6
ν_{14}	β-CH_2 wag	1331	1266	2.8	0.4	0.29	1260	1259	$60S_{14},17S_{13},10S_{25}$	-	1	99
ν_{13}	γ-CH_2 wag	1322	1257	3.3	1.2	0.63	1251	1248	$49S_{13},20S_{14}$	1	99	-
ν_{15}	β-CH_2 wag	1293	1227	0.0	0.3	0.75			$70S_{15},14S_{13},10S_{16}$	44	15	41
ν_{18}	γ-CH_2 twist	1282	1219	3.6	15.3	0.75	1209	1208	$39S_{18},24S_{16},14S_{17},10S_{21}$	5	89	6
ν_{17}	β-CH_2 twist	1265	1203	3.9	9.8	0.71	1200	1199	$43S_{17},17S_{28},11S_{12},10S_{19}$	41	59	-
ν_{16}	α-CH out of plane bend	1207	1147	1.4	3.7	0.73	1145	1143	$27S_{16},18S_{23},16S_{15},13S_{24},11S_{18}$	17	83	-
ν_{19}	β-CH_2 rock	1155	1105	5.6	3.2	0.38	1090	1089	$30S_{19},17S_{12},17S_{33},10S_{20},10S_{28}$	22	61	17
ν_{23}	β-CH_2 twist	1117	1069	52.7	6.5	0.35	1065	1063	$37S_{23},10S_{27},10S_{22}$	92	8	-
ν_{22}	Ring breathing	1075	1022	31.0	14.0	0.08	1021	1020	$51S_{22},14S_{23},10S_{20}$	100	-	-

ν_{20}	C-C stretch	999	956	88.8	5.9	0.36	957	956	$10S_{20},26S_{25},23S_{22}$	98	2	-
ν_{24}	Ring deformation	985	938	22.9	11.1	0.75	940	938	$69S_{24}$	100	-	-
ν_{21}	Ring deformation	966	930	2.2	0.3	0.74	933[d]	932	$52S_{21},12S_{16},11S_{23},10S_{13},10S_{27}$	18	54	28
ν_{25}	Ring deformation	940	907	47.9	2.3	0.53	903	902	$32S_{25},16S_{28},15S_{30},10S_{14}$	87	8	5
ν_{26}	COCl scissors	896	872	47.5	1.4	0.70	875	873	$10S_{26},40S_{30},17S_{19},10S_{25}$	92	7	1
ν_{27}	β-CH_2 rock	804	767	0.9	0.3	0.08	773	773	$58S_{27},17S_{24},13S_{18}$	100	-	-
ν_{28}	γ-CH_2 rock	746	723	58.0	3.3	0.41	721[d]	719	$31S_{28},11S_{17},11S_{32},10S_{33}$	95	5	-
ν_{29}	COCl wag	669	654	18.7	4.7	0.08	662	660	$35S_{29},12S_{34},11S_{20,}10S_{32},10S_{27}$	71	23	6
ν_{30}	Ring deformation	635	623	14.5	2.1	0.38	625	624	$33S_{30},20S_{29},19S_{19},10S_{28}$	67	25	8
ν_{31}	C-Cl stretch	452	439	18.3	10.9	0.40	439	437	$52S_{31},44S_{26}$	54	43	3
ν_{32}	COCl rock	354	347	20.7	5.8	0.32	345		$11S_{32},25S_{31,}22S_{34},14S_{26}$	86	11	3
ν_{33}	Ring-COCl bend	300	297	1.2	0.8	0.50	293		$26S_{33},32S_{35},23S_{32},10S_{29}$	90	-	10
ν_{34}	Ring-COCl bend	200	200	0.7	0.7	0.65			$51S_{34},26S_{32,}12S_{29}$	4	34	62
ν_{35}	Ring puckering	153	150	1.5	0.2	0.68			$52S_{35},38S_{33}$	78	-	22
ν_{36}	COCl Assymetric torsion	55	55	0.0	1.2	0.74			$100S_{36}$	-	31	69

[a] Observed spectra: gas and Xe are IR.

[b] MP2(full)/6-31G(d) ab initio calculations, scaled frequencies, infrared intensities (km/mol), Raman activities ($Å^4$/u), depolarization ratios (dp) and potential energy distributions (P.E.D.s).

[c] Scaled frequencies with scaling factors of 0.88 for the CH stretches, β-CH_2 and γ-CH_2 deformations and 0.90 for all other modes except the heavy atom bending modes.

[d] This band is also assigned as a g-Eq conformer fundamental.

[e] Symmetry coordinates with P.E.D. contribution less than 10% are omitted.

Table 48. Observed[a] and predicted fundamental[b] frequencies for the t-Eq conformer of cyclobutylcarboxylic acid chloride.

		Fundamental	*ab initio*	Fixed scaled[c]	IR int.	Raman act.	dp ratio	IR gas	IR Xe soln.	P.E.D.[e]	Band Contour A	Band Contour B
A'	ν_1	β-CH_2 antisymmetric stretch	3217	3018	22.2	33.3	0.65	3014	3014	$79S_1,19S_2$	1	99
	ν_2	γ-CH_2 antisymmetric stretch	3195	2997	8.6	70.6	0.56	2997	2995	$79S_2,19S_1$	12	88
	ν_3	α CH stretch	3148	2953	3.3	54.2	0.52	2961	2960	$93S_3$	39	61
	ν_4	β-CH_2 symmetric stretch	3144	2949	1.8	198.7	0.07	2945	2944	$91S_4$	2	98
	ν_5	γ-CH_2 symmetric stretch	3135	2941	25.6	66.3	0.29	2924	2922	$94S_5$	99	1
	ν_6	C=O stretch	1841	1748	229.8	21.1	0.49	1750	1750	$92S_6$	98	2
	ν_7	β-CH_2 deformation	1574	1482	1.0	4.1	0.69	1468	1465	$52S_7,46S_8$	10	90
	ν_8	γ-CH_2 deformation	1550	1459	5.0	23.3	0.72	1453	1451	$53S_8,47S_7$	8	92
	ν_9	α CH in plane bend	1389	1320	1.0	6.6	0.64	1321	1320	$66S_9,14S_{10},10S_{15}$	30	70
	ν_{10}	β-CH_2 wag	1312	1248	0.8	1.1	0.66	1248	1245	$70S_{10},12S_9$	99	1
	ν_{11}	β-CH_2 twist	1282	1220	3.3	10.7	0.75	1222	1221	$73S_{11},13S_{16}$	56	44
	ν_{12}	β-CH_2 rock	1198	1149	84.7	2.5	0.38	1140	1137	$25S_{12},22S_{13},19S_{22},10S_{18},10S_{16}$	8	92
	ν_{13}	C-C stretch	1155	1101	50.1	9.4	0.08	1081	1079	$24S_{13},37S_{14},13S_{12}$	42	58
	ν_{14}	Ring breathing	1018	975	27.8	12.2	0.14	964	962	$46S_{14},19S_{15},10S_{12},10S_{10}$	80	20
	ν_{15}	Ring deformation 1	948	917	11.0	2.0	0.73	919	919	$31S_{15},26S_{17},15S_{12},12S_{16},10S_{10}$	69	31
	ν_{16}	γ-CH_2 rock	835	805	67.0	1.1	0.74	803	801	$30S_{16},16S_{15},13S_{11},11S_{20},10S_{17}$	19	81
	ν_{17}	Ring deformation 2	688	670	67.1	2.9	0.29	666	666	$32S_{17},23S_{16},14S_{12},13S_{20}$	46	54
	ν_{18}	COCl rock	527	517	0.2	4.0	0.30	~500	500	$17S_{18},34S_{22},21S_{20},10S_{12}$	35	65
	ν_{19}	C-Cl stretch	502	481	47.7	12.1	0.14	490	488	$47S_{19},17S_{17},16S_{13},10S_{12}$	46	54
	ν_{20}	COCl scissors	414	403	9.8	6.0	0.70	389		$29S_{20},37S_{19},10S_{18},10S_{13}$	24	76
	ν_{21}	Ring puckering	264	261	0.8	1.1	0.71			$39S_{21},33S_{18},11S_{20}$	2	98

	ν_{22}	Ring-COCl bend	137	136	0.7	0.6	0.57			$42S_{22},38S_{21},16S_{18}$	48	52
A"	ν_{23}	β'-CH_2 antisymmetric stretch	3211	3012	12.0	56.4	0.75	3014	3014	$100S_{23}$	-	-
	ν_{24}	β-CH_2 symmetric stretch	3142	2948	32.8	5.5	0.75	2945	2945	$100S_{24}$	-	-
	ν_{25}	β-CH_2 deformation	1539	1449	2.3	5.1	0.75			$100S_{25}$	-	-
	ν_{26}	γ-CH_2 wag	1324	1259	3.9	6.8	0.75			$53S_{26},23S_{27},10S_{33},10S_{29}$	-	-
	ν_{27}	α CH out of plane bend	1298	1233	0.0	2.0	0.75			$34S_{27},23S_{30},21S_{28},11S_{26},10S_{29}$	-	-
	ν_{28}	β-CH_2 wag	1289	1224	0.0	2.9	0.75			$40S_{28},21S_{29},19S_{26},14S_{27}$	-	-
	ν_{29}	γ-CH_2 twist	1241	1181	0.6	7.9	0.75			$33S_{29},33S_{28},14S_{30},10S_{31}$	-	-
	ν_{30}	β-CH_2 twist	1072	1029	0.6	0.9	0.75	1031	1029	$35S_{30},22S_{31},21S_{32},10S_{34},10S_{35}$	-	-
	ν_{31}	Ring deformation 2	988	944	0.8	0.7	0.75	946[d]	946[d]	$32S_{31},22S_{30},19S_{27},16S_{29}$	-	-
	ν_{32}	Ring deformation 1	977	931	1.5	13.7	0.75	933	932	$65S_{32},13S_{31},10S_{26}$	-	-
	ν_{33}	β-CH_2 rock	824	785	2.3	1.1	0.75	778	776[d]	$72S_{33},12S_{29}$	-	-
	ν_{34}	COCl wag	660	654	0.7	0.1	0.75			$61S_{34},14S_{31},13S_{35}$	-	-
	ν_{35}	Ring-COCl bend	217	217	2.1	0.6	0.75			$64S_{35},28S_{34}$	-	-
	ν_{36}	COCl torsion	54	54	0.6	1.0	0.75			$90S_{36},10S_{35}$	-	-

[a] Observed spectra: gas and Xe are IR

[b] MP2(full)/6-31G(d) ab initio calculations, scaled frequencies, infrared intensities (km/mol), Raman activities ($Å^4$/u), depolarization ratios (dp) and potential energy distributions (P.E.D.s).

[c] Scaled frequencies with scaling factors of 0.88 for the CH stretches, β-CH_2 and γ-CH_2 deformations and 0.90 for all other modes except the heavy atom bending modes.

[d] This band is also assigned as a g-Eq conformer fundamental.

[e] Symmetry coordinates with P.E.D. contribution less than 10% are omitted.

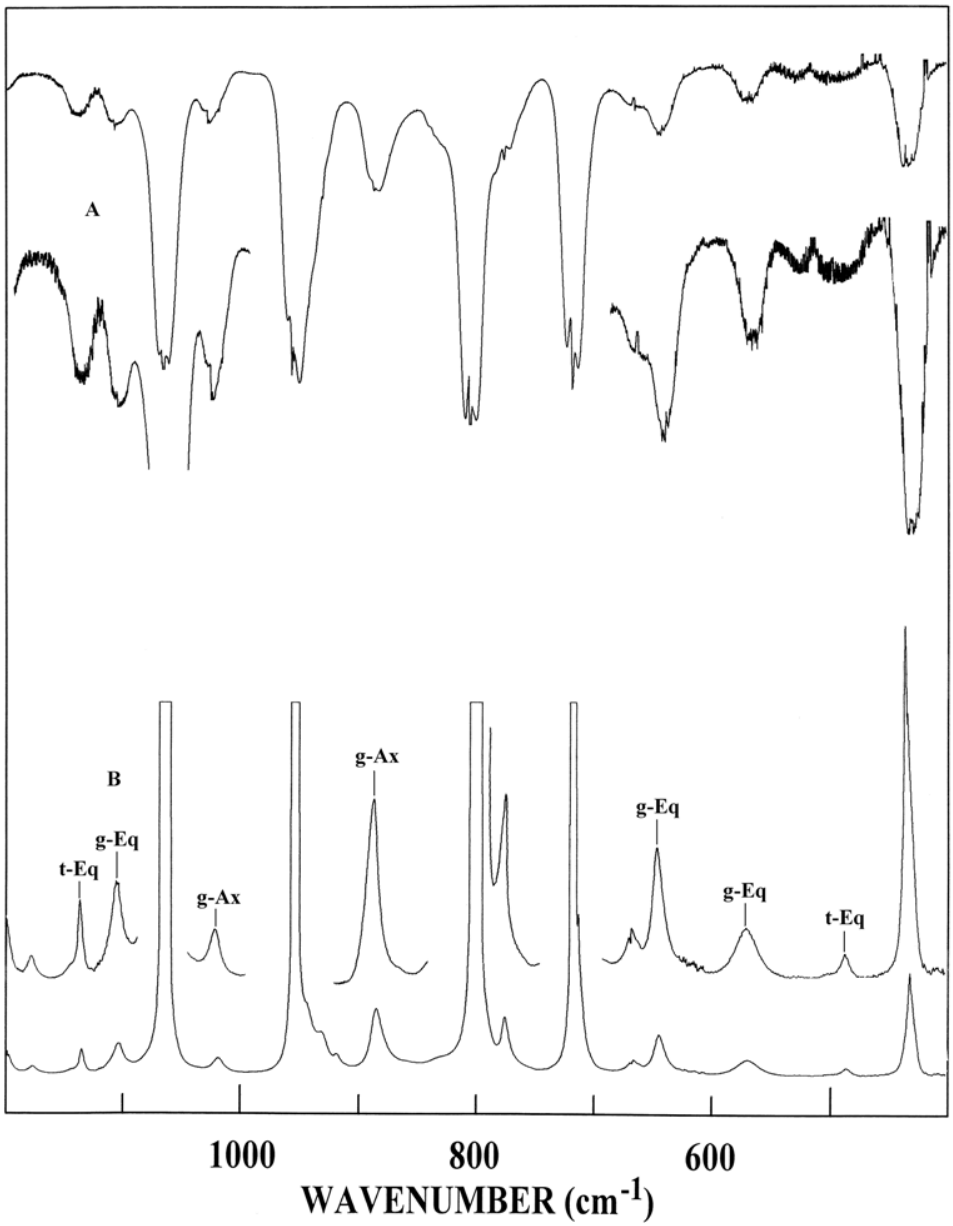

Figure 26. Mid-infrared spectra of cyclobutylcarboxylic acid chloride (A) spectrum of gas; (B) spectrum of xenon solution at -80°C with bands used in the enthalpy determination assigned on spectra.

The LCAO-MO-SCF restricted Hartree-Fock calculations were performed with the Gaussian-03 program [22] with Gaussian-type basis functions. The energy minima with respect to nuclear coordinates were obtained by the simultaneous relaxation of all geometric parameters by using the gradient method of Pulay [29]. Several basis sets as well as the corresponding ones with diffuse functions were employed with the Møller-Plesset perturbation method [21] to second order (MP2(full)) as well as with the density functional theory by the B3LYP method. The predicted conformational energy differences are listed in Table 49.

Table 49. Calculated energies[a] in (H) and energy differences (cm^{-1}) for the four possible conformers of cyclobutylcarboxylic acid chloride

		Energy Differences, Δ[b]		
Method/Basis Set	g-Eq	g-Ax	t-Eq	t-Ax[c]
RHF/6-31G(d)	-0.739087	287	551	952
MP2(full)/6-31G(d)	-1.729837	125	454	954
MP2(full)/6-31+G(d)	-1.748407	293	468	918
MP2(full)/6-31G(d,p)	-1.787077	153	433	1005
MP2(full)/6-31+G(d,p)	-1.804584	302	438	947
MP2(full)/6-311G(d,p)	-2.046919	120	509	1001
MP2(full)/6-311+G(d,p)	-2.058889	216	377	869
MP2(full)/6-311G(2d,2p)	-2.151748	83	425	834
MP2(full)/6-311+G(2d,2p)	-2.160468	171	310	702
MP2(full)/6-311G(2df,2pd)	-2.282393	82	383	818
MP2(full)/6-311+G(2df,2pd)	-2.290185	168	279	693
MP2(full)/aug-cc-pVTZ	-2.293038	149	213	550
B3LYP/6-31G(d)	-3.147955	288	396	775
B3LYP/6-31+G(d)	-3.159073	335	363	
B3LYP/6-311G(d,p)	-3.249426	280	525	863
B3LYP/6-311+G(d,p)	-3.255032	345	400	
B3LYP/6-311G(2d,2p)	-3.261525	284	513	866
B3LYP/6-311+G(2d,2p)	-3.266090	334	417	
B3LYP/6-311G(2df,2pd)	-3.270451	294	522	

B3LYP/6-311+G(2df,2pd)	-3.274864	326	416
B3LYP/aug-cc-pVTZ	-3.288942	320	410

[a] Energy of conformer is given as –(E+727) H.
[b] Difference is relative to g-Eq form and given in cm^{-1}.
[c] Blank energy differences optimize to t-Eq conformer when using that method/basis set.

In order to obtain a complete description of the molecular motions involved in the fundamental modes of cyclobutylcarboxylic acid chloride, a normal coordinate analysis has been carried out. The force field in Cartesian coordinates was obtained with the Gaussian 03 program [22] at the MP2(full) level with the 6-31G(d) basis set. The internal coordinates used to calculate the **G** and **B** matrices are given in Table 50 with the atomic numbering shown in Fig. 25. By using the **B** matrix [30], the force field in Cartesian coordinates was converted to a force field in internal coordinates. Subsequently, scaling factor of 0.88 for the CH stretches, β-CH_2 and γ-CH_2 deformations and 0.90 for all other modes excluding the heavy atom bending modes were used, along with the geometric average of the scaling factors for the interaction force constants, to obtain the fixed scaled force field and resultant wavenumbers. A set of symmetry coordinates was used for the g-Eq and g-Ax forms (Table S6) and another set for the symmetric t-Eq conformer (Table S7) to determine the corresponding potential energy distributions (P.E.D.s).

Table 50. Structural parameters (Å and degrees), rotational constants (MHz) and dipole moments (Debye) for g-Eq form of cyclobutylcarboxylic acid chloride.

Structural Parameters	Int. coor.	MP2(full)/ 6-311+G(d,p)	Microwave[a]	ED[c]	Adjusted r_0[e]
rC_α-C	R_1	1.492	1.509[b]	1.490(3)[d]	1.491(4)
rC=O	R_2	1.193	1.191[b]	1.195(13)	1.193(3)
rC_α-C_β	R_3	1.555	1.535[b]	1.540(3)[d]	1.553(4)
rC_α-$C_{\beta'}$	R_4	1.542	1.535[b]	1.540(3)[d]	1.540(4)
rC_γ-C_β	R_5	1.548	1.55[b]	1.540(3)[d]	1.547(4)
rC_γ-$C_{\beta'}$	R_6	1.548	1.55[b]	1.540(3)[d]	1.546(4)
rC-Cl	R_7	1.798	1.790[b]	1.793(6)[d]	1.801(3)
rC_α-H	r_1	1.094	1.10[b]	1.128(14)[d]	1.094(2)
rC_β-H_1	r_2	1.094	1.085[b]	1.128(14)[d]	1.094(2)
$rC_{\beta'}$-H_1	r_3	1.093	1.085[b]	1.128(14)[d]	1.093(2)
rC_β-H_2	r_4	1.091	1.085[b]	1.128(14)[d]	1.091(2)
$rC_{\beta'}$-H_2	r_5	1.091	1.085[b]	1.128(14)[d]	1.091(2)
rC_γ-H_1	r_6	1.091		1.128(14)[d]	1.091(2)
rC_γ-H_2	r_7	1.093		1.128(14)[d]	1.093(2)
$\angle C_\alpha CO$	ϕ_1	128.0	123.2(29)	127.0(15)	127.8(5)
$\angle ClCC_\alpha$	ϕ_2	111.1	112.7(15)	111.0(20)	110.8(5)
$\angle ClCO$	ϕ_3	120.8		122.0	121.2(5)
$\angle C_\beta C_\alpha C$	ϕ_4	116.6		112.8	117.5(5)
$\angle C_{\beta'} C_\alpha C$	ϕ_5	118.7		112.8	119.6(5)
$\angle C_{\beta'} C_\alpha C_\beta$	θ_1	88.4		90.9	87.4(5)
$\angle C_\gamma C_\beta C_\alpha$	θ_2	87.1		90.9	88.0(5)
$\angle C_\gamma C_{\beta'} C_\alpha$	θ_3	87.6		90.9	88.6(5)
$\angle C_{\beta'} C_\gamma C_\beta$	θ_4	88.4		90.9	87.5(5)
$\angle HC_\alpha C_\beta$	σ_1	109.9		116.2	107.6(5)
$\angle HC_\alpha C_{\beta'}$	σ_2	112.6		116.2	113.7(5)
$\angle HC_\alpha C$	σ_3	109.2	110.07[b]	107.5	109.2(5)
$\angle H_1C_\beta C_\alpha$	λ_1	110.3		116.2	110.3(5)
$\angle H_1C_{\beta'} C_\alpha$	λ_2	110.1		116.2	110.1(5)
$\angle H_1C_\beta C_\gamma$	λ_3	111.1		116.2	111.4(5)
$\angle H_1C_{\beta'} C_\gamma$	λ_4	111.4		116.2	111.7(5)
$\angle H_2C_\beta C_\alpha$	λ_5	117.5		116.2	117.3(5)
$\angle H_2C_{\beta'} C_\alpha$	λ_6	117.7		116.2	117.9(5)
$\angle H_2C_\beta C_\gamma$	λ_7	119.3		116.2	118.4(5)
$\angle H_2C_{\beta'} C_\gamma$	λ_8	118.8		116.2	117.9(5)
$\angle H_1C_\beta H_2$	λ_9	109.7		102.0	109.7(5)
$\angle H_1C_{\beta'} H_2$	λ_{10}	109.6		102.0	109.6(5)
$\angle H_1C_\gamma C_\beta$	π_1	117.7		116.2	118.1(5)
$\angle H_1C_\gamma C_{\beta'}$	π_2	118.0		116.2	118.3(5)
$\angle H_2C_\gamma C_\beta$	π_3	110.7		116.2	110.8(5)

$\angle H_2C_\gamma C_{\beta'}$	π_4	111.1		116.2	111.1(5)
$\angle H_1C_\gamma H_2$	π_5	109.5		102.0	109.5(5)
$\tau C_\gamma C_\beta C_{\beta'} C_\alpha$	τ_1	31.3	20.0(24)	21(5)	30.9(5)
$\tau HC_\alpha CO$	τ_2	127.5		123	130.0(5)
$\tau HC_\alpha CCl$	τ_3	55.0	61.1(24)	57(5)	55.0(5)
$\tau ClC_2C_\alpha O$	τ_4				
A(MHz)		4368.30	4349.86(17)		4350.60
B(MHz)		1411.29	1414.78(1)		1414.66
C(MHz)		1150.70	1148.24(1)		1148.28
$\lvert\mu_a\rvert$		3.049			
$\lvert\mu_b\rvert$		1.743			
$\lvert\mu_c\rvert$		0.848			
$\lvert\mu_t\rvert$		3.613			

[a] Proposed structural parameters, rotational constants, and dipole moments from reference [105].
[b] Assumed values.
[c] Proposed structural parameters from the electron diffraction study [102]
[d] C-C bond length values and all C-H distances are assumed to be the same.
[e] Adjusted parameters using the microwave data from ground states.

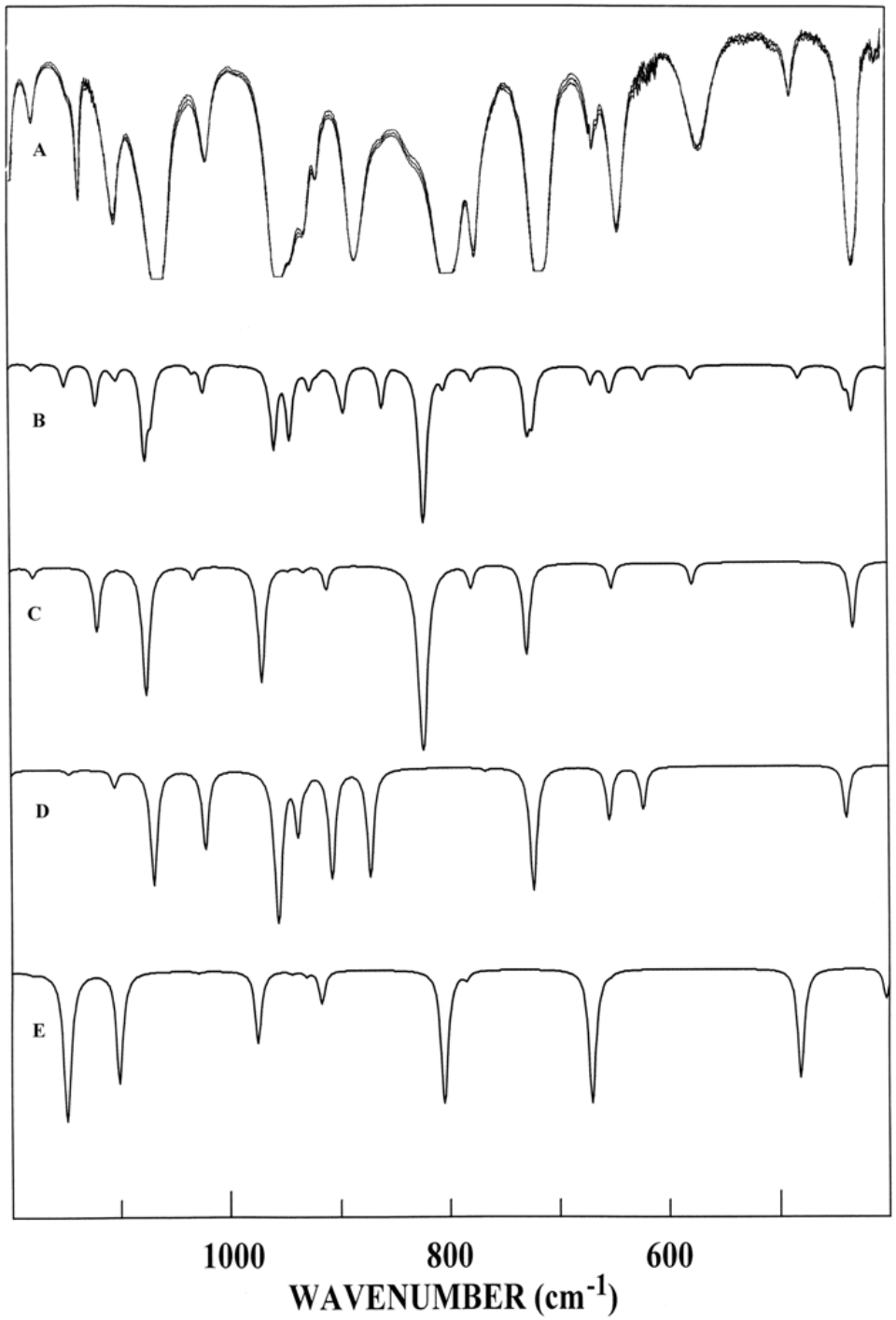

Figure 27. Experimental and predicted mid-infrared spectra of cyclobutylcarboxylic acid chloride: (A) observed spectra of xenon solutions at -80, -90, and -100°C; (B) simulated spectrum of mixture of g-Eq, g-Ax (ΔH = 91 cm^{-1}), and t-Eq (ΔH = 173 cm^{-1}) conformers at -80°C; (C) simulated g-Eq conformer; (D) simulated g-Ax conformer; (E) simulated t-Eq conformer.

The vibrational spectra were predicted from the MP2(full)/6-31G(d) calculations. The predicted scaled wavenumbers were used together with a Lorentzian function to obtain the simulated spectra. Infrared intensities were obtained based on the dipole moment derivatives with respect to Cartesian coordinates. The derivatives were transformed with respect to normal coordinates by $(\partial\mu_u/\partial Q_i) = \sum_j (\partial\mu_u/\partial X_j)L_{ij}$, where Q_i is the i^{th} normal coordinate, X_j is the j^{th} Cartesian displacement coordinate, and L_{ij} is the transformation matrix between the Cartesian displacement coordinates and the normal coordinates. The infrared intensities were then calculated by $(N\pi)/(3c^2)$ $[(\partial\mu_x/\partial Q_i)^2 + (\partial\mu_y/\partial Q_i)^2 + (\partial\mu_z/\partial Q_i)^2]$. The resulting simulated spectra are shown in Figure 27 and are compared to the infrared spectra of the xenon solutions at three different temperatures where the simulated spectrum of the mixture of conformers should be comparable to the experimental infrared spectra. It is interesting to note that whereas the band positions are reasonably predicted the band intensities are relatively poorly predicted.

MICROWAVE RESULTS

The Cl atom in Cyclobutylcarboxylic acid chloride contains a nucleus with a spin quantum number I = 3/2 and, therefore, a nuclear quadrupole moment which interacts with the electric field gradient created by the electrons of the rotating molecule. The quadrupole moments of ^{35}Cl and ^{37}Cl are not equal. The angular momentum J of the rotating molecule couples with the angular momentum I of the nuclear spin to create an overall angular momentum F whose quantum number F can assume any of the values F = J + I, J + I - 1, … |J - I|. Only F is an exact quantum number whereas J is only an approximate value. Therefore, a rotational level with quantum number J in the absence of quadrupole coupling splits into sublevels that can be labeled by the exact quantum

number F when a nuclear quadrupole is present. Each rotational level with J > 1 splits into 4 components (1 and 3 components for J = 0 and 1, respectively). The selection rules for rotational transitions are $\Delta F = 0, \pm 1$ and the strongest components are those given by $\Delta F = \Delta J$.

The frequencies of the components of the split rotational transitions were used in a least-squares fit to determine rotational, centrifugal distortional and quadrupole coupling constants. For that purpose, a computer program developed for molecules with one or two quadrupole nuclei in a plane of symmetry [109,110] was used. Of course, g-Eq cyclobutylcarboxylic acid chloride does not have a molecular symmetry plane. Because ab initio calculations performed by using the MP2(full) method with the 6-311+G(d,p) basis set predicted the full nuclear quadrupole coupling tensor with rather small values for the off-diagonal elements χac and χbc (a few MHz) but a significant χab (tens of MHz), fitting the spectrum with this program seemed worth a trial. The rotational and centrifugal distortion constants reported earlier [105] from conventional microwave spectroscopy for the Cl isotopologue together with quadrupole coupling constants from ab initio calculations were used to predict the spectrum for initial assignments. The final results of the least-squares fits (Table 51) justified the use of this program. The Fit 1 for the ^{35}Cl isotopologue of 69 components of 18 rotational transitions ended with a standard deviation of 2.2 kHz and for the Fit 2 included transitions from Ref. [105] and transition from this study where the hyperfine components could not be resolved. For the fit of the ^{37}Cl substituted species, 84 components of 19 transitions led to a standard deviation of 2.6 kHz. The frequencies of the assigned components of the observed transitions with their residuals in the least-squares fit are listed in Tables 44 and 45 and are excellent with

errors equal to or less than 4 kHz for ^{35}Cl and 7 kHz for the ^{37}Cl. With accurately determined rotational constants the adjusted r_0 structure may also be determined. It should, however, be noted that the fit of these rotational constants is probably better than the experimental data can achieve where the digital precision for instrument used is 2.5 kHz. Therefore, the rotational constants are reported for the ^{35}Cl [^{37}Cl] isotope; A = 4349.8429(25) [4322.0555(56)], B = 1414.8032(25) [1384.5058(25)], and C = 1148.2411(25) [1126.3546(25)] MHz.

Table 51. Rotational Constants (MHz), Quadratic centrifugal distortion constants (kHz) and quadrupole coupling constants (MHz) for the ^{35}Cl and ^{37}Cl isotopomers of the g-Eq conformer of cyclobutylcarboxylic acid chloride.

Isotopomer	c-$C_4H_7C(O)^{35}Cl$				c-$C_4H_7C(O)^{37}Cl$	
	MP2(full)/ 6-311+G(d,p)	Ref. [105]	Fit 1	Fit 2	MP2(full)/ 6-311+G(d,p)	Fit
A	4368.2065	4349.86(17)	4349.84294(48)	4349.8383(103)	4339.5884	4322.0555(56)
B	1411.2866	1414.78(1)	1414.80319(36)	1414.8038(18)	1381.0680	1384.50581(105)
C	1150.6863	1148.24(1)	1148.24114(18)	1148.2389(15)	1128.6613	1126.35465(101)
Δ_J	0.2999	0.25(2)	0.2786(40)	0.2811(85)	0.2925	0.2730(46)
Δ_{JK}	-1.1256	-2.44(49)	-0.9523(32)	-0.988(83)	-1.167	-1.001(21)
Δ_K	5.047		4.741(37)	4.52(97)	5.2	5.8(1)
δ_J	0.11171	0.088(16)	0.09685(96)	0.1034(32)	0.1092	0.0994(77)
δ_K	1.642		1.401(55)	1.61(26)	1.59	1.44(19)
χ_{aa}	-16.9372		-18.2005(43)	-18.17(13)	-14.0482	-15.0614(42)
χ_{ab}	-44.63		-46.21(11)	-46.3(32)	-35.08	-36.01(18)
χ_{bb}	-6.2552		-5.9667(49)	-5.88(14)	-4.2349	-3.9980(59)
χ_{cc}	23.1924		24.1672(56)	24.06(16)	18.2831	19.0594(52)
n		17	69	95		84
s		64	2.2	64		2.6
rsm(FT)		8		8		
rsm(MW)		114		114		

VIBRATIONAL ASSIGNMENT

An earlier vibrational assignment [105] for cyclobutylcarboxylic acid chloride was made by utilizing the Raman spectra of liquid and solid and the infrared spectra of the gas and solid for a complete assignment of the g-Eq conformer fundamentals and to assign two fundamentals for high energy conformer which could not be determined but it was assumed to be t-Eq. By the utilization of MP2(full)/6-31G(d) fundamental wavenumber predictions along with ab initio predicted intensities, and infrared data from xenon solutions it has been possible to assign nearly all of the fundamentals for the g-Eq conformer in the current study. Additionally, a nearly complete assignment of the fundamentals of the g-Ax form was made and a significant number of fundamentals for the t-Eq conformer were assigned. These assignments are important for obtaining the enthalpy differences since the fundamentals which are used in the variable temperature study need to be identified correctly for a single conformer. Therefore, an attempt was made to assign the fundamentals in the region from 1200 to 400 cm^{-1} for the three most stable conformers, where the overtone and combination bands are greatly reduced in this region compared to those possible in the higher wavenumber region. It is also interesting to determine what effect the acid chloride group will have on the fundamental frequencies particularly those which involve the ring modes. The vibrations of the CH_2 groups are expected to be very similar to those found in the usual four membered-ring molecules and a discussion of their assignments in detail is usually not necessary.

The most interesting assignments will be for the heavy atom fundamentals but these are in the region where the lower frequency CH_2 bending modes will undoubtedly interact with these heavy atom vibrations. Therefore, these modes are expected to have

contributions of three or four motions. For example, in the case of the β-CH_2 twist for the g-Eq form the band at 946 cm^{-1} in the infrared spectra of the gas has contributions from two of the heavy atom ring deformation modes.

Four membered carbon atom rings have well known ring deformations usually occurring in a pattern of one near 1000 cm^{-1} and three near 900 cm^{-1}. This pattern makes the assignment of these modes relatively simple for the g-Eq conformer where they are predicted at 1032, 932, and 911 cm^{-1} and observed at 1027, 933, and 889 cm^{-1} in the infrared spectra of the gas. The ring breathing mode usually occurs in this region as well and it is predicted at 970 cm^{-1} for the g-Eq form and assigned at 960 cm^{-1} in the infrared spectra of the gas. This mode was predicted to have a 'A' type band contour and the band in the spectra of the gas corresponds clearly to a 'A' type band contour and it was assigned based on this prediction.

For the g-Eq conformer there are some assignments necessary for bands in the infrared spectra of the gas since from the previous study [105] there were four fundamentals in the finger print region that were not assigned in the infrared spectra of the gas. Three of these fundamentals are CH_2 bending modes and they are now assigned based on frequencies observed in the spectra of the xenon solutions and are in agreement with the CH_2 bending modes of the usual four membered-ring molecules and the previous assignment from the infrared and/or Raman spectra of the liquid and solid. The ring deformation fundamental is predicted at 932 cm^{-1} and is now assigned at 933 cm^{-1} in the infrared spectra of the gas. This band has a predicted Raman activity of 10.1 and was previously assigned at 927 cm^{-1} in the Raman spectra of the liquid. This assignment is further away than expected and the previous assignment is for a shoulder of a much

stronger band, therefore, we have reassigned the band center to 930 cm^{-1} by using the previously reported [105] Raman spectra of the liquid.

It should be noted that most of the bands which are reassigned in the current study in the infrared spectra of the gas are within a few wavenumber differences from the previously reported assignments except for $\nu_{17,}$ the β-CH_2 twist. This fundamental is predicted at 1205 cm^{-1} but it was previously assigned at 1143 cm^{-1} in the infrared spectra of gas but it is now reassigned to the band at 1204 cm^{-1}. The band at 1143 cm^{-1} is now assigned as ν_{16}' for the g-Ax conformer based on the predicted band position and the temperature dependence in the infrared spectra of the xenon solutions.

The vibrational assignments were also made for the g-Ax conformer which is the second most abundant conformer. It should be noted that this conformer had not been mentioned in any of the previous reported vibrational studies [103-105]. Most of the fundamental frequencies assigned for this conformer are based on the spectra obtained from the xenon solutions. The C-C stretch from the g-Ax conformer is predicted with high intensity and assigned to the strong band at 957 cm^{-1} from the spectra of the gas and it is mainly attributed to this heavy atom stretch. The COCl scissoring motion for this conformer is predicted at 872 cm^{-1} which is 49 cm^{-1} higher frequency with respect to the corresponding mode of g-Eq conformer with approximately one-third the intensity and is therefore assigned at 875 cm^{-1}.

There are only a few of the vibrational assignments which could be made for the t-Eq conformer. This is not unexpected since the intensity predictions are low and this conformer is present at ambient temperature as only 12 ± 1% of the sample. Again from the spectra of the xenon solutions, it was possible to assign the ring breathing mode and

three of the ring deformational fundamentals and these fundamentals were observed at 964, 933, 919 and 672 cm^{-1}, respectively. Once these vibrations were observed in the xenon solutions, it was possible to assign them in the infrared spectra of the gas. The mode predicted at 975 cm^{-1} is observed at lower frequency than the corresponding modes of the two most abundant conformers and is now assigned to the band at 964 cm^{-1}. The ring deformation assignments at 933 and 919 cm^{-1} are in a good agreement with the corresponding vibrations of the other two conformers. However, the band at 666 cm^{-1} is assigned at a higher frequency compared to the band assignments of these fundamentals of the other two conformers. The fifth ring deformation, ν_{31}'', was not observed but it is believed to be at 946 cm^{-1} which is the same frequency for the corresponding mode for the g-Eq conformer.

CONFORMATIONAL STABILITY

To determine the enthalpy differences among the three observed conformers of cyclobutylcarboxylic acid chloride, the sample was dissolved in liquefied xenon and the infrared spectra were recorded as a function of temperature from -70 to -100°C. Relatively small interactions are expected to occur between xenon and the sample. Therefore, only small wavenumber shifts are anticipated for the xenon interactions when passing from the gas phase to the liquefied xenon which is confirmed with an average shift of 1 cm^{-1} for the fundamentals for the three observed conformers indicating this should not be a major influence on the enthalpy difference between the forms. A significant advantage of this study is that the conformer bands are better resolved in comparison with those in the infrared spectrum of the vapor. From ab initio calculations, the dipole moments of the three conformers are predicted to have similar values and the

molecular sizes of the three conformers are nearly the same, and thus, the ΔH value obtained from the temperature dependent infrared study is expected to be near that for the gas [14,17-20].

Once confident assignments have been made for the fundamentals of three observed conformers the task was then to find pairs of bands from which the enthalpy difference could be obtained. The bands should be sufficiently resolved for determining their intensities. The selection of the bands to use in the enthalpy determination was complicated due to the presence of three conformers with each having several broad intense bands however it was significantly simplified by the exceptionally good predictions of the relative band positions for the g-Eq, g-Ax, and t-Eq fundamentals in the 1200 to 400 cm^{-1} region of the spectra (Fig. 27) where there are a limited number of overtone and combination bands possible. Examples of this are the fundamentals at 1177 and 1021 cm^{-1} for the g-Eq and g-Ax forms where the bands are predicted at 1179 and 1022 cm^{-1}, respectively. The g-Eq band at 1177 cm^{-1} was found to not be significantly affected by the underlying t-Eq fundamental predicted at 1181 cm^{-1} with a predicted intensity of 0.6 km/mol. The bands at 1137 and 1143 cm^{-1} were assigned for the t-Eq and g-Ax fundamentals, respectively, where these assignments are based on their relative band positions and intensities. The g-Ax band at 1020 cm^{-1} predicted at 1022 cm^{-1} was found to not be significantly affected by the underlying t-Eq fundamental at 1029 cm^{-1} which has a predicted intensity of 0.6 km/mol. Finally the band at 1108 cm^{-1} was assigned to the g-Eq fundamental (β-CH_2 rock) predicted at 1120 cm^{-1} which was found to not be significantly affected by the broad band of the same conformer at 1066 cm^{-1} nor the two fundamentals located beneath the 1065 cm^{-1} band predicted at 1105 cm^{-1} for the

g-Ax conformer and 1101 cm^{-1} for the t-Eq form and assigned at 1089 and 1079 cm^{-1}, respectively.

The fundamentals at 569 cm^{-1} for the g-Eq conformer and 488 cm^{-1} for the t-Eq form are predicted to be free of any bands in near coincidence. The bands at 645, 660, and 666 cm^{-1} were selected for the g-Eq, g-Ax, and t-Eq conformers, respectively, which can be confidently assigned based on their relative frequencies from the ab initio calculations. These four g-Eq, three g-Ax, and three t-Eq bands were used for the enthalpy determination as they were each found to not be significantly affected by any nearby predicted fundamentals. The assignment of these bands is shown in Figure 26, where the conformer assigned is labeled above the band.

The intensities of the individual bands were measured as a function of temperature and their ratios were determined. An example set of assigned fundamental bands with one from the g-Eq (645 cm^{-1}), g-Ax (873 cm^{-1}), and t-Eq (1137 cm^{-1}) conformers each have been provided in Figure 28. The intensities of the g-Eq and t-Eq bands in the figure have been doubled to allow for better comparison of the bands, but this doubling in no way affects the enthalpy determination. With the measured intensity values of the conformer fundamentals the enthalpy values were obtained by application of the van't Hoff equation $-\ln K = \Delta H/(RT) - \Delta S/R$. The enthalpy difference was determined from a plot of $-\ln K$ versus $1/T$, where $\Delta H/R$ is the slope of the line and K is substituted with the appropriate intensity ratios, *i.e.* $I_{conf\text{-}1} / I_{conf\text{-}2}$, etc. It was assumed that ΔS, and α (thermal expansion constant) are not functions of temperature in the range studied.

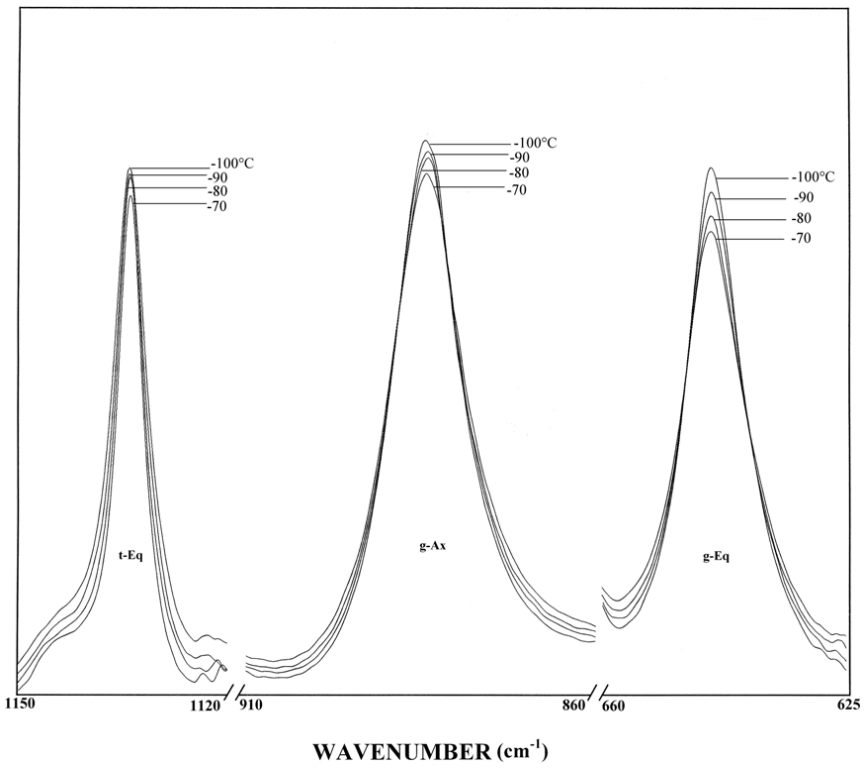

Figure 28. Temperature (-70 to -100°C) dependent mid-infrared spectrum of cyclobutylcarboxylic acid chloride dissolved in liquid xenon.

These bands were utilized for the determination of the enthalpy difference by combining them to form 12 independent band pairs each for the g-Eq to g-Ax and for the g-Eq to t-Eq independent enthalpy values and 9 band pairs for the g-Ax to t-Eq independent enthalpy values. These values are listed for each band pair in Table 52 and are within a relatively small range. The intensity data from each band pair is combined with the other band pairs to form a single data set for each conformer pair. From this single data set for each pair of conformers the enthalpy differences and error limits were determined to be 91 ± 4 cm^{-1} from the g-Eq to the g-Ax form, 173 ± 4 cm^{-1} from the g-Eq to the t-Eq conformer, and 82 ± 3 cm^{-1} from the g-Ax to the t-Eq conformer as listed in

Table 52. The error limit is derived from the statistical standard deviation of one sigma of the measured intensity data taken as a single data set, but it does not take into account small associations with the liquid xenon or the possible presence of overtones and combination bands in near coincidence of the measured fundamentals. The variations in the individual values are undoubtedly due to these types of interferences, but by taking several pairs, the effect of such interferences should cancel. However, this statistical uncertainty is probably better than can be expected from this technique and, therefore, an uncertainty of about 10% in the enthalpy difference is probably more realistic i.e. 91 ± 9 cm^{-1} from the g-Eq to the g-Ax conformer, 173 ± 17 cm^{-1} from the g-Eq to the t-Eq form, and 82 ± 8 cm^{-1} from the g-Ax to the t-Eq conformer. From the enthalpy differences the conformer abundance is estimated to be 54% g-Eq, 35 ± 1% g-Ax and 12 ± 1% t-Eq at ambient temperature.

Table 52A. Temperature and intensity ratios of the g-Eq and g-Ax bands of cyclobutylcarboxylic acid chloride.

	T(°C)	1/T ($\times 10^{-3}$ K^{-1})	I_{569} / I_{660}	I_{569} / I_{1020}	I_{569} / I_{1143}	I_{645} / I_{660}	I_{645} / I_{1020}	I_{645} / I_{1143}
Liquid	-70	4.922	1.250	0.816	1.860	1.406	0.918	2.093
xenon	-75	5.047	1.302	0.848	1.909	1.426	0.929	2.091
	-80	5.177	1.323	0.847	1.955	1.462	0.936	2.159
	-85	5.315	1.328	0.845	1.933	1.496	0.951	2.178
	-90	5.460	1.379	0.875	1.978	1.530	0.971	2.196
	-95	5.613	1.414	0.895	2.000	1.564	0.990	2.213
	-100	5.775	1.433	0.906	2.043	1.597	1.009	2.277
ΔH^a			107 ± 9	80 ± 11	67 ± 9	107 ± 3	78 ± 4	67 ± 7

	T(°C)	1/T ($\times 10^{-3}$ K^{-1})	I_{1108} / I_{660}	I_{1108} / I_{1020}	I_{1108} / I_{1143}	I_{1176} / I_{660}	I_{1176} / I_{1020}	I_{1176} / I_{1143}
Liquid	-70	4.922	1.328	0.867	1.977	1.359	0.888	2.023
xenon	-75	5.047	1.380	0.899	2.023	1.395	0.909	2.045
	-80	5.177	1.385	0.887	2.045	1.431	0.916	2.114
	-85	5.315	1.420	0.903	2.067	1.511	0.961	2.200
	-90	5.460	1.455	0.923	2.087	1.530	0.971	2.196
	-95	5.613	1.459	0.924	2.064	1.519	0.962	2.149
	-100	5.775	1.567	0.991	2.234	1.597	1.009	2.277
ΔH^a			115 ± 14	89 ± 17	75 ± 18	125 ± 16	97 ± 13	85 ± 19

[a] Average value $\Delta H = 91 \pm 4$ cm^{-1} (1.09 ± 0.05 kJ mol^{-1}) with the g-Eq conformer the more stable form and the statistical uncertainty (1σ) obtained by utilizing all of the data as a single set.

Table 52B. Temperature and intensity ratios of the g-Eq and t-Eq bands of cyclobutanecarbonyl chloride.

	T(°C)	1/T ($\times 10^{-3}$ K^{-1})	I_{569} / I_{488}	I_{569} / I_{666}	I_{569} / I_{1137}	I_{645} / I_{488}	I_{645} / I_{666}	I_{645} / I_{1137}
Liquid	-70	4.922	0.842	0.833	0.792	0.947	0.938	0.891
xenon	-75	5.047	0.884	0.878	0.840	0.968	0.961	0.920
	-80	5.177	0.915	0.901	0.860	1.011	0.995	0.950
	-85	5.315	0.926	0.915	0.870	1.043	1.030	0.980
	-90	5.460	0.989	0.959	0.919	1.098	1.065	1.020
	-95	5.613	1.022	0.994	0.949	1.130	1.099	1.051
	-100	5.775	1.043	1.018	0.980	1.163	1.134	1.092
ΔH^a			176 ± 12	159 ± 10	166 ± 11	176 ± 8	158 ± 4	166 ± 3

	T(°C)	1/T ($\times 10^{-3}$ K^{-1})	I_{1108} / I_{488}	I_{1108} / I_{666}	I_{1108} / I_{1137}	I_{1176} / I_{488}	I_{1176} / I_{666}	I_{1176} / I_{1137}
Liquid	-70	4.922	0.895	0.885	0.842	0.916	0.906	0.861
xenon	-75	5.047	0.937	0.930	0.890	0.947	0.940	0.900
	-80	5.177	0.957	0.943	0.900	0.989	0.974	0.930
	-85	5.315	0.989	0.977	0.930	1.053	1.040	0.990
	-90	5.460	1.043	1.012	0.970	1.098	1.065	1.020
	-95	5.613	1.054	1.025	0.980	1.098	1.068	1.020
	-100	5.775	1.141	1.113	1.071	1.163	1.134	1.092
ΔH^a			184 ± 12	167 ± 14	174 ± 16	194 ± 16	177 ± 16	184 ± 16

[a] Average value $\Delta H = 173 \pm 4$ cm^{-1} (2.07 ± 0.04 kJ mol^{-1}) with the g-Eq conformer the more stable form and the statistical uncertainty (1σ) obtained by utilizing all of the data as a single set.

Table 52C. Temperature and intensity ratios of the g-Ax and t-Eq bands of cyclobutanecarbonyl chloride.

	T(°C)	1/T ($\times 10^{-3}$ K^{-}	I_{660} /	I_{660} /	I_{660} /	I_{1020} /	I_{1020} /	I_{1020} /	I_{1143} /	I_{1143} /	I_{1143} /
Liquid	-70	4.922	0.674	0.667	0.634	1.032	1.021	0.970	0.453	0.448	0.426
xenon	-75	5.047	0.679	0.674	0.645	1.042	1.034	0.990	0.463	0.460	0.440
	-80	5.177	0.691	0.681	0.650	1.080	1.063	1.015	0.468	0.461	0.440
	-85	5.315	0.697	0.688	0.655	1.096	1.082	1.030	0.479	0.473	0.450
	-90	5.460	0.717	0.696	0.667	1.130	1.096	1.051	0.500	0.485	0.465
	-95	5.613	0.723	0.703	0.672	1.141	1.110	1.061	0.511	0.497	0.475
	-	5.775	0.728	0.710	0.684	1.152	1.124	1.082	0.511	0.498	0.480
ΔH^{a}			69 ± 5	51 ± 1	59 ± 3	97 ± 9	80 ± 6	87 ± 6	109 ± 10	91 ± 8	99 ± 8

[a] Average value $\Delta H = 82 \pm 3$ cm^{-1} (0.98 ± 0.04 kJ mol^{-1}) with the g-Ax conformer the more stable form and the statistical uncertainty (1σ) obtained by utilizing all of the data as a single set.

STRUCTURAL PARAMETERS

An electron diffraction (ED) study [102] was the first study performed on cyclobutylcarboxylic acid chloride where the structure was determined for the g-Eq conformer with a mean C-C distance of 1.540(3) Å for all the carbons in the ring and +0.05 (1.590) Å for the C-C distance outside the ring. The remaining structural parameters have very large errors which makes them somewhat meaningless for comparison with other structures. This was followed by a combined microwave and vibrational study [105] where the ^{35}Cl isotopologue of g-Eq conformer was observed and rotational constants were determined. In this microwave study the diagnostic least-squares adjusted structural parameters were determined by utilizing a combination of assumed parameters and parameters taken from the structure reported in the ED study [102]. The resulting extremely large uncertainties in the heavy atom angles determined are most likely a result of these assumed parameters and the parameters taken from the ED study. Therefore, we have determined the rotational constants for two isotopic species for the g-Eq conformer giving six constants available for the structural determination.

We have found that good structural parameters for hydrocarbons and many substituted ones can be determined by adjusting the structural parameters obtained from the ab initio MP2(full)/6-311+G(d,p) calculations to fit the rotational constants obtained from microwave experimental data by using a computer program "A&M" (Ab initio and Microwave) developed [51] in our laboratory.

We [5] have shown that ab initio MP2(full)/6-311+G(d,p) calculations predict the carbon-hydrogen r_0 structural parameters for more than fifty hydrocarbons to at least 0.002 Å compared to the experimentally determined [111] values from isolated CH

stretching frequencies which agree to previously determined values from earlier microwave studies. Therefore, all of the carbon-hydrogen parameters can be taken from the MP2(full)/6-311+G(d,p) predicted values for the g-Eq conformer of cyclobutylcarboxylic acid chloride. In order to further reduce the number of independent variables, the structural parameters are separated into sets according to their types where bond distances in the same set keep their relative ratio, and bond angles and torsional angles in the same set keep their difference in degrees. This assumption is based on the fact that errors from ab initio calculations are systematic. Therefore, it should be possible to obtain "adjusted r_0" structural parameters for the eleven parameters of the seven heavy atoms by adjusting the C-C distances as a single set and adjusting the ∠CCC angles as another set leaving seven sets of parameters to adjust. This structure however must be evaluated using parameters from similar molecules to help account for the relatively low number of rotational constants available and, thus, the –C(O)Cl parameters have a limited range that they change from the ab initio predicted values as has been reported in the literature. This is particularly true for the C=O bond distance which changes very little from its molecular environment.

The resulting adjusted r_0 parameters are listed in Table 50, where it is believed that the Cl-C and O=C distances should be accurate to ± 0.003 Å, the C-C distances accurate to ± 0.004 Å, the C-H distances accurate to ± 0.002 Å, and the uncertainties of the angles should be within ± 0.5°. The fit of the six determined rotational constants (Table 53) by the adjusted r_0 structural parameters are good with variations of the differences with values being less than 0.9 MHz. Therefore, it is believed that the suggested uncertainties are realistic values and the determined structural parameters are

probably as accurate as can be obtained for the molecule in the gas phase by either electron diffraction or microwave substitution methods. However with more rotational constants from further isotopic substitutions the accuracy of the adjusted r_0 parameter values could be improved.

Table 53. Comparison of rotational constants (MHz) obtained from modified ab initio MP2(full)/6-311+G(d,p) structural parameters and the experimental values from the microwave spectra of g-Eq conformer of cyclobutylcarboxylic acid chloride.

Isotopomers	Rotational constant	Fit 1	Adjusted r_0	$\|\Delta\|$
c-$C_4H_7C(O)^{35}Cl$	A	4349.8429(25)	4350.60	0.76
	B	1414.8032(25)	1414.66	0.14
	C	1148.2411(25)	1148.28	0.04
c-$C_4H_7C(O)^{37}Cl$	A	4322.0555(56)	4321.22	0.84
	B	1384.5058(25)	1384.54	0.04
	C	1126.3546(25)	1126.43	0.08

DISCUSSION

The vibrational assignments reported herein are based on a significant amount of information with the infrared spectrum of the xenon solutions, band contours in the infrared spectra of the gas, and predictions of the fundamental frequencies from the scaled ab initio MP2(full)/6-31G(d) calculations as well as the predicted intensities. For the g-Eq conformer the ab initio predicted frequencies differ by an average of 8 cm^{-1} which represents 0.6% error. The percent error for the predictions for the g-Ax conformer

is 4 cm^{-1} or 0.3% error. Thus the relatively small basis set of 6-31G(d) by the MP2(full) calculations with two scaling factors provides excellent predicted frequencies for aiding the vibrational assignments.

There are three repeated t-Eq frequencies which were assigned based on the most stable g-Eq conformer. These fundamentals are the C-C stretch which is now assigned at 1110 cm^{-1} in the infrared spectra of the gas and the second fundamental is the ring deformation which is assigned at 946 cm^{-1}. The third fundamental is the β-CH_2 rock which is assigned to the band at 776 cm^{-1} in the infrared spectra of the xenon solutions. The t-Eq –COCl wag motion is an interesting fundamental where this motion is predicted at 654 cm^{-1} with a low infrared intensity of 0.7 km/mol and was not observed in the infrared spectra of the gas unlike the other two forms where this motion was observed at 645 and 662 cm^{-1} for the g-Eq and g-Ax conformers, respectively. This is due to the low intensity of this fundamental as compared to the g-Eq fundamental with an intensity of 8.2 km/mol. These are several examples where the fundamentals of the g-Eq and g-Ax form have significantly different intensities than the same mode from the t-Eq conformer.

In general for the g-Eq conformer the mixing was extensive for the fundamentals starting at 1232 cm^{-1} and lower frequencies. Most of the fundamentals have extensive contributions from three or four symmetry coordinates and several of the descriptions are more for bookkeeping than an accurate description of the molecular motions. The g-Ax conformer is similar, with extensive mixing starting from the vibration at 1209 cm^{-1} and below. Similarly, several of the approximate descriptions for the fundamentals of the g-Ax form are again more for bookkeeping than providing descriptions of the molecular motions. Of significant note is the ν_{20}' fundamental where it has been assigned as S_{20} (C-

C stretch) despite only being 10% contribution and it has been described as such as any other placement results in several bookkeeping descriptions. However, for the t-Eq conformer, the descriptions are much more realistic than the other two conformers except for the ν_{18}'' fundamental described as the COCl rock which have only 17%S_{18}(COCl rock) with contributions of 34%S_{22}, 21%S_{20} and 10%S_{12} modes. The A″ modes are reasonably well described with no specific arbitrary descriptions necessary. This reduction of the mixing is largely due to the symmetry constraints due to the change from C_1 to C_v symmetry going from gauche to trans. Therefore, the approximate descriptions for the normal modes provide reasonable information on the molecular motions of vibrations with several modes described more for bookkeeping purposes than as a complete description. It should be noted that this large change in mixing due to the symmetry constraints may be at least partially responsible for the significant differences in the fundamental intensities noted above.

Because the measured information was just barely sufficient to determine all quartic centrifugal distortion constants, another fit was made for the ^{35}Cl isotopologue that included 13 frequencies involving higher rotational constants from the earlier microwave investigation [16]. Each of these represented a blend of unresolved hyperfine components; each blend's frequency was assigned to the two innermost components of the predicted hyperfine quartet. (Four transitions from the previous study [16] were omitted because their hyperfine pattern consisted of a widely spaced pair of narrow doublets.) Of course this fit (Fit 2 in Table 41) had a much larger standard deviation of 64 kHz, but the root mean square of the residuals for the FT data was only 8.0 kHz whereas the rms of the low-resolution measurements was 114 kHz. The difference of any constant

between Fit 1 and Fit 2 was smaller than the combined error limits except for ΔJ where the difference was only slightly larger.

The derived centrifugal distortion constants generally agree between the isotopic species and the ab initio predictions (Table 41). The same can be said for the quadrupole coupling constants, taking into account that the theoretical ratio $\chi(^{35}Cl)/\chi(^{37}Cl)$ for any coupling constant χ should be 1.269[26] provided there is no rotation of the principal inertial axes between the isotopologues.

The natural population analysis (NPA) was carried out for the g-Eq, g-Ax, and t-Eq conformers of cyclobutylcarboxylic acid chloride and for cyclobutane with the MP2(full) method at the 6-311+G(d,p) basis set. The C atoms for cyclobutane all carry a -0.34 charge. However the –C(O)Cl substitution of cyclobutane gives a charge distribution for the g-Eq form of C_α = -0.32, C_β = -0.31, $C_{\beta'}$ = -0.32, C_γ = -0.33, Cl = -0.12, O = -0.59, and C = 0.69. The difference in NPA predicted for the other two stable conformers are less than 0.01 from those listed for the g-Eq form. The majority of the ring has similar charges as those of cyclobutane indicating that –C(O)Cl has relatively little influence on the electron charge density in the ring.

Due to the relatively low number of rotational constants available for the g-Eq form of cyclobutylcarboxylic acid chloride the structural parameters must be evaluated for their accuracy and the number of parameters to change must be decreased. As stated in the structural parameters section the C-C distances were taken as a single set and the –C(O)Cl parameters were constrained within the limits determined from similar molecules. As can be seen in Table 54 the ab initio MP2(full) calculation at the 6-311+G(d,p) basis set does an excellent job predicting the bond distances and angles for

this moiety. The predicted structural parameter values for the methyl [14] and ethyl compounds [113] for the distances are usually within 0.001 Å and within 0.5° for the angles of the r_0 structural parameter values. The isopropyl molecule [56] shows larger differences between the predicted structural parameter values and the values from the r_0 structural parameters. The structure was determined for the g-Eq form of cyclobutylcarboxylic acid chloride and the parameters where allowed to change in fitting of the rotational constants. As can be seen from Table 50 the differences between the MP2(full)/6-311+G(d,p) and the adjusted r_0 structural parameter values for the –C(O)Cl bond distances and angles are less than the proposed experimental errors and are very close to the values for similar bond distances and angles in Table 54.

Table 54. Structural parameters[a] of a few acetyl chloride molecules of the form R-C(O)Cl (Å and degree).

Structural Parameters	R = CH_3[b]	R = CH_2CH_3[c]	R = $CH(CH_3)_2$[d]
		Cis	Cis
rC=O	1.192 [1.189(3)]	1.192 [1.192(3)]	1.193 [1.186(3)]
rC-Cl	1.795 [1.794(3)]	1.795 [1.796(4)]	1.798 [1.804(4)]
rC-C_α	1.500 [1.499(3)]	1.505 [1.506(3)]	1.510 [1.511(3)]
rC_α-C_β		1.522 [1.523(3)]	1.525 [1.534(3)]
rC_α-$C_{\beta'}$			1.535 [1.540(3)]
∠OCCl	120.6 [120.4(5)]	120.6 [120.7(6)]	120.3 [119.1(6)]
∠OCC	127.6 [127.2(5)]	127.4 [127.2(7)]	127.2 [127.3(7)]
∠ClCC	111.9 [112.4(5)]	111.9 [112.1(5)]	112.4 [113.6(5)]
∠C$C_\alpha C_\beta$		112.3 [112.4(8)]	110.1 [109.7(8)]
∠C$C_\alpha C_{\beta'}$			108.9 [109.9(8)]
∠$C_\beta C_\alpha C_{\beta'}$			111.7 [113.8(27)]

[a] MP2(full)/6-311+G(d,p) [Experimental]
[b] Adjusted r_0 parameters determined from rotational constants taken from reference [112]
[c] Ref [14]; adjusted r_0 parameters.
[d] Ref [113]; adjusted r_0 parameters.

The ring parameters are much more variable where the ring distances and angles for four-membered rings are often relatively sensitive to substitution as shown in Table 55. As the charges in the ring are fairly consistent with those for the cyclobutane molecule the ring structural parameters should be comparable between the two. It can be seen that the C_γ-C_β bond distances are ~0.008 Å shorter for the –C(O)Cl molecule as opposed to unsubstituted cyclobutane. These are probably not due to the electronic effects in the rings as these effects are predicted to be relatively small but rather due to the steric effects of the larger –C(O)Cl molecule's ring puckering angle. The C_α-C_β bond distances in the –C(O)Cl molecule are different from each other due to the oxygen group overlapping one of the C-C bonds, this bond distance is drastically reduced due to the steric effects of this overlap. The other C_α-C_β bond distance is much longer and is within the experimental error to the value from the cyclobutane r_0 structure. The ring structure of cyclobutylcarboxylic acid chloride is similar to that of cyclobutane as expected but with some logical departures brought on by the substitution of a –H with a –C(O)Cl group.

In this current study, the adjusted r_0 structural parameters have been determined for the g-Eq conformer these should be comparable to the previously reported ED study [102]. In the ED study the structural parameters were obtained for the g-Eq form from a least squares analysis of the anharmonic radial distribution function [61] in the interval $r \approx 0.0$ Å to $r \approx 1.95$ Å. All of the parameters have very large errors except the mean ring C-C, out of ring C-C, and the C-Cl distances which equal to 1.540(3), 1.590(3), and 1.793(6),

respectively. These values are in excellent agreement with the adjusted r_0 structural parameters obtained in this study. The remaining parameters with large uncertainties are not meaningful though due to these large uncertainties for the most part they agree within the stated errors to the adjusted r_0 structural parameters.

Table 55. Structural parameters[a] of a few four-membered ring molecules of the form c-C_4H_7X (Å and degree).

Structural Parameters	X = H[b]	X = OH[c]	X = Br[d]	X = F[e]		X = SiH_3[f]	
		t-Eq	Eq	Eq	Ax	Eq	Ax
rC_α-C_β	1.5478 [1.5555(2)]	1.542 [1.547(3)]	1.535 [1.541(3)]	1.530 [1.543(3)]	1.534 [1.546(3)]	1.559 [1.562(3)]	1.559 [1.561(3)]
rC_β-C_γ	1.5478 [1.5555(2)]	1.548 [1.556(3)]	1.551 [1.552(3)]	1.551 [1.554(3)]	1.552 [1.554(3)]	1.546 [1.551(3)]	1.547 [1.553(3)]
Puckering angle	32.34 [28.58(9)]	28.5 [31.3(10)]	34.4 [29.8(5)]	34.0 [37.4(5)]	29.2 [20.7(5)]	31.6 [29.0(5)]	29.0 [23.5(5)]

[a] MP2(full)/6-311+G(d,p) [Experimental]
[b] Ref [56]; r_0 parameters.
[c] Ref [114]; adjusted r_0 parameters.
[d] Ref [79]; adjusted r_0 parameters.
[e] Ref [79]; adjusted r_0 parameters.
[f] Ref [91]; adjusted r_0 parameters.

A decade later, a microwave and vibrational study followed [105] where one isotopomer of the g-Eq conformer was observed and the rotational constants were determined. The structural parameters were determined by fixing all but five parameters where these assumptions were in part informed by using the ED study structural parameters. The five parameters were then determined with a diagnostic least squares adjustment as described by Curl [61]. The structural parameters obtained have very large errors, which is partially due to the assumed parameters being off from the actual structure but also due to fitting three rotational constants with five parameters. The error is so large on these parameters that the ones that are far off from the adjusted r_0 structural parameters are probably not meaningful.

One of the major goals of this current study was the determination of the enthalpy difference between the conformers of the cyclobutylcarboxylic acid chloride where there had been different results reported. Fabregue [103] reported that the cyclobutylcarboxylic acid chloride exist in both the solid and liquid phases as the same nonsymmetrical isomer in which COCl group is in the equatorial position with respect to the ring. From the ED study [102] it was indicated that the molecule exist as a conformational equilibrium mixture of the *gauche*-like axial and a gauche-like equatorial conformers. A decade later, the vibrational spectra was reinvestigated [104] and it was found that the sample exists in a conformational equilibrium in the liquid and vapor phases. A few years later, the variable temperature Raman spectra of the liquid were studied [105] from which the enthalpy difference between the g-Eq and high energy (assumed t-Eq) conformations was determined to be 1.4 kcal mol^{-1} (490 cm^{-1}). The enthalpy value obtained in this study from the Raman spectra of the liquid would give a population of 4% t-Eq at room

temperature. This population is extremely small though with the assignment they propose it is not beyond reason. When compared to the vibrational assignment as determined in the current study it can be seen that this enthalpy value is far too large. In comparison the enthalpy determination between the g-Eq to t-Eq conformers is determined to be 173 ± 17 cm^{-1} in the current study where it was determined from 12 band pairs. This is nearly one-third of the value determined in the liquid state. However, enthalpy values determined from spectra of the liquid state are normally significantly higher than those determined for samples in the vapor state or in xenon solutions, and therefore, the difference in the determined enthalpy values may be largely due to the difference from the samples from which they were obtained.

The experimental values determined from the variable temperature infrared spectra of the xenon solutions should be near to those of the gas which should be similar to those of the isolated molecule. Therefore it can be useful to compare the ab initio and DFT energy differences shown in Table 49 with the experimental enthalpy differences. The order of stability is well predicted by the ab initio and DFT calculations where the correct order of stability is predicted by both the MP2 and B3LYP methods for all basis sets. The energy differences determined by the calculations approximately doubles for the g-Eq to g-Ax difference with addition of diffuse functions for the MP2 method, where the largest basis set without diffuse functions is very close to the experimental value. The B3LYP method for the same energy difference predicts the energy difference significantly higher and over three times the experimental value. The g-Eq to t-Eq energy difference is predicted significantly too large for all basis sets and both calculation methods. This is an interesting phenomenon where the addition of more functions into the ab initio basis sets

actually causes poorer results. However, as is previously stated the order of stability is predicted correctly for all the calculations attempted.

There are few molecular geometries of the carboxylic acid chloride derivatives determined in the literature, which lead to a scarcity of molecular structural parameters and conformational determinations with which the current molecule could be compared to. This would be an interesting topic to research and the five membered ring and open chain derivatives would be of particular interest.

CONCLUSIONS

The microwave spectra for the two isotopologues of g-Eq have been assigned and the rotational constants have been reported. From these rotational constants a complete structure has been determined which is made possible due to the reduction in the number of independent parameters as the C-H distances can be taken from the MP2(full)/6-311+G(d,p) structural parameters for substituted hydrocarbons.

The ring parameters appear to be largely determined due to steric effects rather than electrostatic effects. This is supported by the NPA predictions where the ring for cyclobutylcarboxylic acid chloride is nearly the same as cyclobutane in contrast to the significant difference in the ring puckering angle and C_α-C_β bond distances.

The observed fundamentals for the g-Eq, g-Ax, and t-Eq conformers have been assigned based upon the variable temperature infrared spectra of the xenon solutions. From the band intensities of several of these assigned fundamentals the enthalpy differences have been determined. The relative amounts at ambient temperature are 54% g-Eq, 35 ± 1% g-Ax and 12 ± 1% t-Eq forms. This relatively small difference in the amount of each conformer is in direct contrast to the results from previous studies [103-

105] where the g-Ax and t-Eq conformers went largely unassigned and were assumed to be either high energy or transition states.

CHAPTER 9

INFRARED AND RAMAN SPECTRA, AB INITIO CALCULATIONS, CONFORMATIONAL STABILITY AND VIBRATIONAL ASSIGNMENT OF 1-BROMO-1-SILACYCLOPENTANE

INTRODUCTION

Several monosubstituted cyclopentanes were determined to have two conformations at ambient temperature where the substituent occupies the *axial* and *equatorial* positions at the tip of the C_s-symmetric *envelope* form of the five-membered ring [116-120]. For many of the molecules the vibrational spectra were used to first identify the two forms before they were identified by microwave spectra and/or electron diffraction investigations. The monohalocyclopentanes are interesting examples where initially the fluoride, chloride, and bromide [116] were all reported to have these forms from analyses of their infrared spectra. Later, from an investigation of the Raman spectrum [121] of the liquid, it was concluded that there was only one conformer present in the fluid states and it was the *envelope-equatorial* conformer which was supported from the theoretical predictions [122] from CNDO predictions. More recently, we [123] have shown from the infrared spectra of the gas and variable temperature xenon solutions that there is, indeed, only one conformer in the fluid phases but it is the *twisted* (C_1 symmetry) form which was supported by structural parameters obtained from the rotational constants obtained from the microwave spectrum. For chlorocyclopentane there was only the *envelope-axial* conformer initially found from the microwave spectrum [124] and from a subsequent electron diffraction investigation [125] of it, the authors

indicated that the data could be explained equally well by either a mixture of *axial* and *equatorial* conformers or a dynamic model involving nearly free pseudorotation which lead to doubts about a second conformer. However, from a later re-investigation of the microwave spectrum of chlorocyclopentane [126], transitions for the *equatorial* conformer were observed and assigned.

There were no problems for bromocyclopentane concerning the early report [127] of the two forms since the observed microwave spectrum was assigned for the two conformers with estimated structural parameters consistent with the *axial* and *equatorial* forms. Therefore, we began our vibrational and conformational study of the corresponding five-membered rings with one of the carbon atoms replaced with a silicon atom which has a halogen atom attached, and for this study, the bromine atom, i.e. 1-bromo-1-silacyclopentane.

The infrared spectra (3500-300 cm^{-1}) of the gas and solid and the Raman spectrum (3500-60 cm^{-1}) of the liquid have been recorded of 1-bromo-1-silacyclopentane from which the conformational stability has been determined and a vibrational assignment of the fundamentals is reported. To support the conformational stability determination and aid in the vibrational assignment, *ab initio* MP2 with full electron correlation and density functional theory by the B3LYP method calculations have been carried out by using a variety of basis sets. The results of these spectroscopic and theoretical studies are reported herein.

EXPERIMENTAL AND THEORETICAL METHODS

The sample of 1-bromo-1-silacyclopentane was prepared in two steps. First, 1,1-dichloro-1-silacyclopentane was prepared by double Grignard of 1,4-dibromobutane and

coupled with tetrachlorosilane. The product 1,1-dichlro-1-silacyclopentane was reduced with lithium aluminum hydride in dry dibutyl ether. The product 1-silacyclopentane was brominated with boron tribromide at 0°C for 18 hr. to produce 1-bromo-1-silacyclopentane, which, was first purified using trap to trap distillation and finally by a low pressure, low temperature sublimation column. The sample was identified by IR and NMR spectroscopy.

The mid-infrared spectrum of the gas was obtained from 3500 to 300 cm^{-1} on a Perkin-Elmer model 2000 Fourier transform spectrometer equipped with a Ge/CsI beamsplitter and a DTGS detector. Atmospheric water vapor was removed from the spectrometer housing by purging with dry nitrogen. The theoretical resolution used to obtain the spectrum of the gas was 0.5 cm^{-1} and 128 interferograms were added and truncated with a boxcar function. For the spectrum of the solid the vapor was deposited on a CsI window cooled with boiling liquid nitrogen in a low temperature infrared cell. Typical spectra of the gas and solid are shown in
Fig. 29.

The Raman spectra (Fig. 30) were recorded on a Spex model 1403 spectrophotometer equipped with a Spectra-Physics model 2017 argon ion laser operating on the 514.5 nm line. The laser power used was 1.5 W with a spectral bandpass of 3 cm^{-1}. The spectrum of the liquid was recorded with the sample sealed in a Pyrex glass capillary. Depolarization measurements were obtained for the liquid sample using a standard Ednalite 35 mm camera polarizer with 38 mm of free aperture affixed to the Spex instrument. Depolarization ratio measurements were checked by measuring the state of polarization of the Raman bands of CCl_4 immediately before depolarization

measurements were made on the liquid sample. The measurements of the Raman frequencies are expected to be accurate to ± 2 cm^{-1}. All of the observed fundamental bands in the Raman spectrum of the liquid along with their proposed assignments and depolarization values are listed in Table 56.

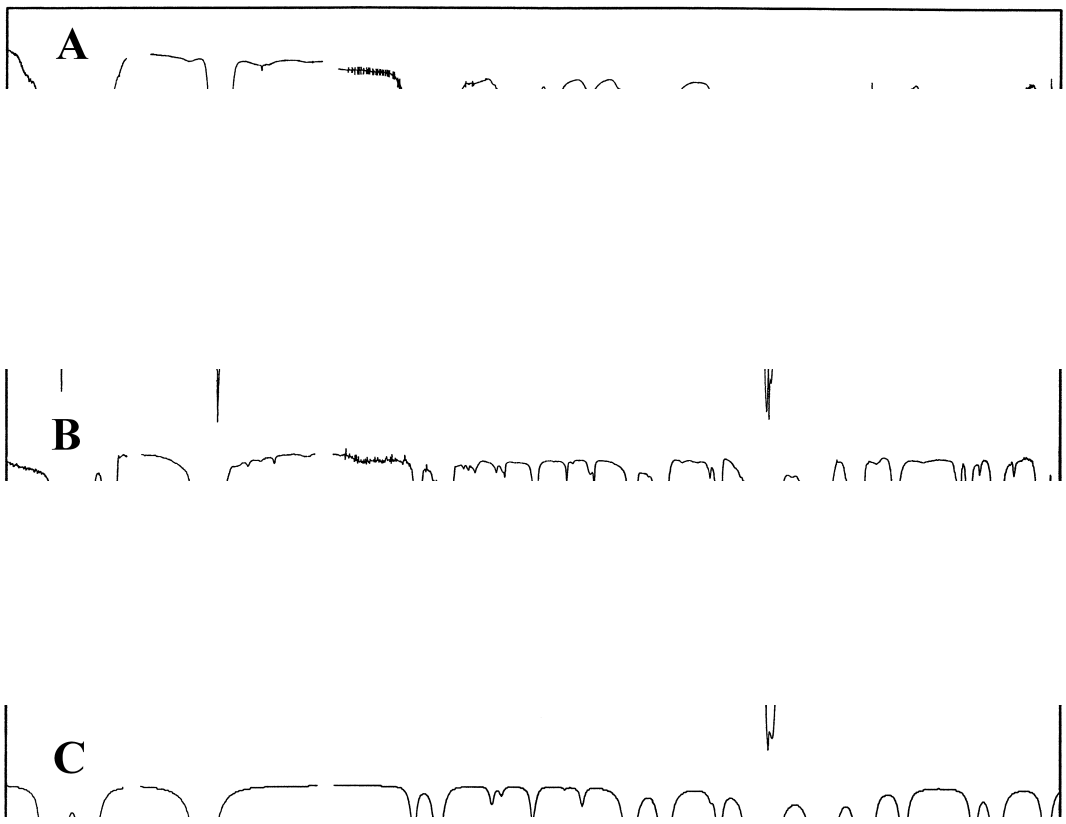

Figure 29. Comparison of experimental and calculated infrared spectra of 1-bromo-1-silacyclopentane: (A) observed infrared spectrum of gas; (B) observed infrared spectrum of solid; (C) simulated infrared spectrum of *twist* (C_1) conformer.

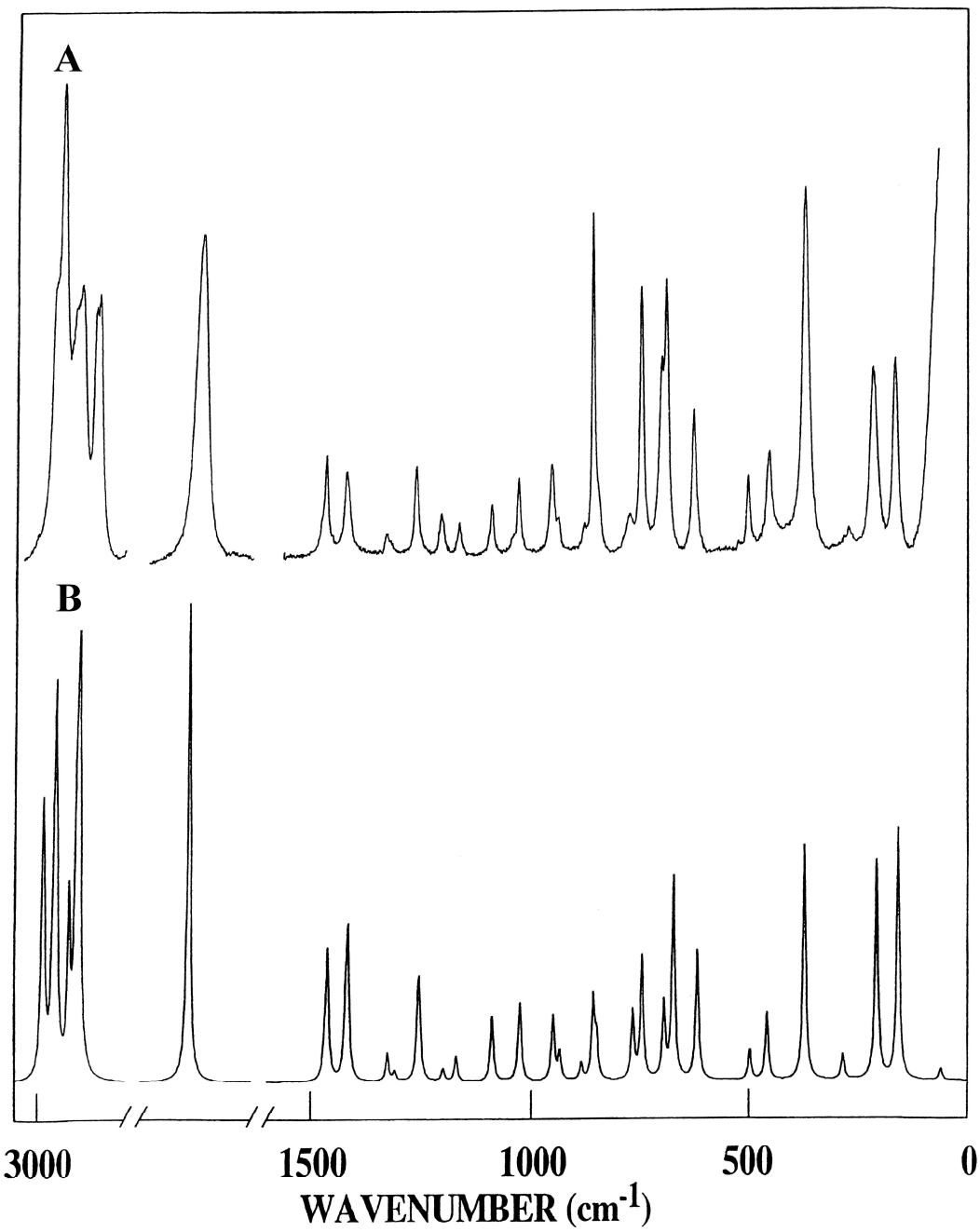

Figure 30. Comparison of experimental and calculated Raman spectra of 1-bromo-1-silacyclopentane: (A) observed Raman spectrum of the liquid; (B) simulated Raman spectrum of *twist* conformer (C_1).

TABLE 56. Calculated[a] and observed frequencies (cm^{-1}) for 1-bromo-1-silacyclopentane *twisted (C_1)* form.

Vib. No.	Approx. description	*ab initio*	fixed scaled[b]	IR int.	Raman act.	dp ratio	B3LYP [c]	IR int.	Raman act.	IR gas	Raman liquid	dp ratio	IR solid	P.E.D.[d]	Band Contour		
															A	B	C
ν_1	α-CH_2 antisymmetric stretch	3186	2988	6.8	60.0	0.63	3101	9.9	77.7	2989	2981	-	-	$47S_1,39S_2$	55	15	30
ν_2	α-CH_2 antisymmetric stretch	3182	2985	9.0	73.7	0.66	3095	15.2	88.3	2980	2972	-	-	$52S_2,42S_1$	13	16	71
ν_3	β-CH_2 antisymmetric stretch	3159	2963	27.0	57.8	0.74	3067	42.7	73.1	2968	2960	-	2957	$92S_3$	24	39	37
ν_4	β-CH_2 antisymmetric stretch	3153	2957	25.6	148.0	0.30	3062	38.3	259.5	2953	2944	-	2949	$85S_4,11S_8$	69	-	31
ν_5	α-CH_2 symmetric stretch	3119	2926	5.1	69.2	0.18	3045	11.1	75.6	2918	2915	-	-	$50S_5,46S_6$	35	62	3
ν_6	α-CH_2 symmetric stretch	3103	2911	10.6	68.7	0.28	3024	23.1	60.2	2906	2902	-	2911	$42S_6,39S_5$	-	2	98
ν_7	β-CH_2 symmetric stretch	3098	2906	20.4	47.7	0.38	3020	19.1	90.8	2882	2869	-	2900/2897	$88S_7$	12	36	52
ν_8	β-CH_2 symmetric stretch	3095	2903	22.9	146.4	0.09	3014	24.4	185.6	2875	2862	-	2864/2856	$82S_8,11S_4$	97	-	3
ν_9	Si-H stretch	2311	2193	153.7	125.1	0.17	2231	123.0	178.7	2176	2173	-	2197/2179	$100S_9$	2	3	95
ν_{10}	β-CH_2 deformation	1564	1470	0.5	3.3	0.43	1505	1.3	1.1	1470	1463	0.50	1456	$94S_{10}$	54	3	43
ν_{11}	β-CH_2 deformation	1556	1463	7.4	18.6	0.75	1496	6.8	11.1	1459	1452	0.67	1448/1446	$99S_{11}$	23	14	63
ν_{12}	α-CH_2 deformation	1513	1423	14.7	5.7	0.75	1456	10.4	4.6	1408	1407	0.70	1402	$78S_{12},19S_{13}$	1	74	25
ν_{13}	α-CH_2 deformation	1508	1418	4.9	19.8	0.74	1452	6.6	8.7	1403	1402	0.70	1395	$74S_{13},21S_{12}$	18	67	15
ν_{14}	β-CH_2 wag	1400	1329	2.1	3.5	0.74	1351	1.4	1.7	1327	1325	0.67	1353	$62S_{14},23S_{16}$	81	-	19
ν_{15}	β-CH_2 wag	1382	1312	1.0	1.2	0.74	1340	0.8	0.7	1316	1318	0.67	1316	$88S_{15}$	57	9	34
ν_{16}	β-CH_2 twist	1325	1259	3.6	6.1	0.69	(1284)	2.4	3.7	1266	1262	-	1250	$47S_{16},33S_{20}$	64	1	35
ν_{17}	β-CH_2 twist	1323	1255	1.1	9.3	0.75	(1280)	0.6	5.1	1253	1250	0.31	1244	$51S_{17},19S_{21},18S_{19}$	94	6	-
ν_{18}	α-CH_2 twist	1266	1202	0.3	1.4	0.24	1224	0.6	1.8	-	1195	0.05	1192	$36S_{18},32S_{24},12S_{20}$	2	82	16
ν_{19}	α-CH_2 wag	1230	1172	2.2	2.7	0.75	1184	1.9	2.0	1157	1153	0.75	1151/1144	$54S_{19},17S_{33},10S_{23},10S_{21}$	16	73	11
ν_{20}	α-CH_2 wag	1147	1089	41.5	6.4	0.73	1108	30.4	4.3	1080	1079	0.25	1078/1071	$39S_{20},21S_{16},10S_{31},10S_{14}$	82	-	18
ν_{21}	α-CH_2 twist	1084	1029	24.9	1.5	0.70	1056	25.9	0.8	1033	1033	0.50	1035/1026	$50S_{21},26S_{17}$	61	1	38
ν_{22}	ring deformation	1081	1026	11.4	6.2	0.68	1028	10.7	4.2	1019	1019	0.54	1018	$41S_{22},20S_{31},16S_{14}$	99	-	1

ν_{23}	ring deformation	996	950	0.8	5.4	0.75	957	0.4	4.5	-	945	0.75	941	$32S_{23},20S_{19},13S_{33},10S_{25}$	2	98	-
ν_{24}	β-CH_2 rock	985	935	9.4	2.2	0.63	949	8.2	1.9	932	930	0.50	927/921	$39S_{24},39S_{18}$	1	90	9
ν_{25}	ring deformation	923	885	21.1	1.3	0.72	882	26.8	1.6	871	870	0.50	873/870	$53S_{25},29S_{28}$	13	84	3
ν_{26}	ring breathing	898	857	17.8	5.9	0.08	(858)	1.5	9.2	851	851	0.07	849	$41S_{26},20S_{31},14S_{22}$	77	17	6
ν_{27}	α-CH_2 rock	891	849	120.3	2.8	0.64	(853)	126.5	1.6	843	840	0.24	840/832	$36S_{27},16S_{30},13S_{37}$	70	17	13
ν_{28}	β-CH_2 rock	805	764	87.2	4.3	0.73	776	74.2	4.4	767	765	0.58	761/754	$13S_{28},33S_{32},19S_{30},14S_{29}$	52	45	3
ν_{29}	α-CH_2 rock	780	743	23.5	7.5	0.11	744	25.3	8.1	737	738	0.05	736	$21S_{29},23S_{30},12S_{26},11S_{31}$	93	5	2
ν_{30}	Si-H parallel bend*	729	694	28.3	4.2	0.61	699	24.2	4.6	694	693	0.28	695/688	$19S_{30},22S_{27},14S_{23},10S_{32},10S_{33}$	11	70	19
ν_{31}	ring deformation	704	672	10.6	11.0	0.20	673	13.9	11.8	685	682	0.21	680/678	$21S_{31},22S_{26},17S_{25},10S_{23}$	68	13	19
ν_{32}	Si-H perpendicular bend*	649	618	14.7	6.3	0.57	619	14.8	7.4	620	621	0.38	620/617	$26S_{32},25S_{29},17S_{25},10S_{26}$	84	12	4
ν_{33}	ring deformation	512	498	12.3	1.1	0.37	499	8.8	1.1	493	496	0.23	495/493	$53S_{33},18S_{28},15S_{39},10S_{23}$	62	15	23
ν_{34}	ring deformation	471	459	32.6	2.2	0.36	453	38.3	2.3	452	449	0.18	439	$58S_{34},26S_{35}$	98	2	-
ν_{35}	Si-Br stretch	389	373	19.7	5.8	0.11	356	23.8	7.7	367	364	0.04	370	$51S_{35},20S_{34},12S_{37}$	52	1	47
ν_{36}	ring twist	298	285	0.3	0.4	0.48	269	0.2	0.4	-	268	0.40	-	$80S_{36}$	2	73	25
ν_{37}	Si-Br parallel bend*	215	208	0.7	2.2	0.39	205	0.8	3.1	-	210	0.30	-	$36S_{37},19S_{39},13S_{35},12S_{30}$	60	6	34
ν_{38}	Si-Br perpendicular bend*	159	158	1.1	1.6	0.75	150	1.0	2.1	-	160	0.83	-	$87S_{38}$	1	91	8
ν_{39}	ring puckering	63	60	0.5	0.8	0.69	61	0.5	1.0	-	-	-	-	$59S_{39},27S_{37}$	2	9	89

[a] MP2(full)/6-31G(d) *ab initio* calculations, B3LYP/6-311+G(d,p) density functional theory calculations, scaled frequencies, infrared intensities (km/mol), Raman activities ($Å^4$/u), depolarization ratios (dp), and potential energy distributions (P.E.D.s).

[b] Scaled frequencies with scaling factors of 0.88 for CH_2 stretches and deformations and 0.90 for all other modes except heavy atom bends.

[c] Values in parenthesis are reordered to match the MP2(full)/6-31G(d) *ab initio* values.

[d] Symmetry coordinates with P.E.D. contribution less than 10% are omitted.

* Bend parallel and perpendicular to the ring, respectively.

TABLE 57. Calculated electronic energies (hartree) and energy differences (cm^{-1}) for the *twisted* (C_1), *envelope-axial* (C_s), *envelope-equatorial* (C_s), and planar (C_s) forms of 1-bromo-1-silacyclopentane.

Method/Basis Set	# of Basis Functions	*Twist* (C_1)	*Axial* (C_s)[a]	*Equatorial* (C_s)[a]	Planar (C_s)[a]
RHF/6-31G(d)	127	-3015.591261	1364	1630	2319
RHF/6-31+G(d)	151	-3015.605360	1448	1569	2284
MP2(full)/6-31G(d)	127	-3016.363603	1364	1722	2778
MP2(full)/6-31+G(d)	151	-3016.386375	1351	1631	2606
MP2(full)/6-311G(d,p)	196	-3019.536273	1363	1694	2494
MP2(full)/6-311+G(d,p)	220	-3019.541142	1258	1667	2479
MP2(full)/6-311G(2d,2p)	253	-3019.619863	1233	1678	2659
MP2(full)/6-311+G(2d,2p)	277	-3019.622927	1187	1683	2643
MP2(full)/6-311G(2df,2pd)	340	-3019.744369	1254	1703	2637
MP2(full)/6-311+G(2df,2pd)	364	-3019.746926	1216	1715	2630
MP2(full) average			1252 ± 61	1690 ± 17	2590 ± 81
B3LYP/6-31G(d)	127	-3019.113573	1245	1453	2077
B3LYP/6-31+G(d)	151	-3019.131730	1310	1394	2012
B3LYP/6-311G(d,p)	196	-3021.616934	1221	1385	1860
B3LYP/6-311+G(d,p)	220	-3021.618264	1215	1381	1860
B3LYP/6-311G(2d,2p)	253	-3021.622659	1115	1288	1759
B3LYP/6-311+G(2d,2p)	277	-3021.624140	1170	1358	1831
B3LYP/6-311G(2df,2pd)	340	-3021.631479	1200	1363	1833
B3LYP/6-311+G(2df,2pd)	364	-3021.632497	1188	1363	1829
B3LYP/aug-cc-pVTZ	500	-3021.722449	1205	1367	1845
B3LYP average			1188 ± 36	1358 ± 32	1831 ± 34

[a] Energy differences are relative to the *twist* conformer.

The LCAO-MO-SCF restricted Hartree-Fock calculations were performed with the Gaussian-03 program [22] by using Gaussian-type basis functions. The energy minima with respect to nuclear coordinates were obtained with the simultaneous relaxation of all geometric parameters by using the gradient method of Pulay [29]. Several basis sets as well as the corresponding ones with diffuse functions up to the 6-311+G(2df,2pd) basis set were employed with the Møller-Plesset perturbation method [21] to the second order (MP2(full)) as well as with the density functional theory by the B3LYP method. The predicted conformational energy differences are listed in Table 57.

In order to obtain a complete description of the molecular motions involved in the fundamental modes of c-C_4H_8SiBrH, a normal coordinate analysis has been carried out. The force field in Cartesian coordinates was obtained with the Gaussian 03 program [22] at the MP2(full) level with the 6-31G(d) basis set. The internal coordinates used to calculate the **G** and **B** matrices are listed in Table 58 with the atomic numbering shown in Fig. 31. By using the **B** matrix [30], the force field in Cartesian coordinates was converted to a force field in internal coordinates. Subsequently, scaling factors of 0.88 for CH_2 stretches and deformations, and 0.90 for other coordinates except for the heavy atom bends were applied, along with the geometric average of the scaling factors for the interaction force constants, to obtain the fixed scaled force field and resultant wavenumbers. A set of symmetry coordinates was used (Table S8) to determine the corresponding potential energy distributions (P.E.D.s). A comparison between the observed and calculated wavenumbers, along with the calculated infrared intensities, Raman activities, depolarization ratios and potential energy distributions for the *twisted* conformer are listed in Table 56.

TABLE 58. Structural parameters (Å and degree), rotational constants (MHz) and dipole moment (debye) for 1-^{79}bromo-1-silacyclopentane *twisted* (C_1) form.

Structural Parameters	Internal Coordinates	RHF/ 6-31G(d)	MP2(full)/ 6-311+G(d, p)	B3LYP/ 6-311+G(d, p)	Estimated r_0
r (Si_1-C_2)	X_1	1.892	1.883	1.894	1.882(5)
r (Si_1-C_3)	X_2	1.889	1.878	1.892	1.877(5)
r (C_2-C_4)	Y_1	1.548	1.546	1.551	1.549(5)
r (C_3-C_5)	Y_2	1.546	1.543	1.549	1.546(5)
r (C_4-C_5)	Z	1.538	1.536	1.544	1.536(5)
r (Si_1-Br_6)	r_1	2.236	2.242	2.270	2.232(5)
r (Si_1-H_7)	r_2	1.471	1.474	1.483	1.482(2)
r (C_2-H_8)	r_3	1.086	1.095	1.094	1.095(2)
r (C_3-H_9)	r_4	1.089	1.098	1.097	1.098(2)
r (C_2-H_{10})	r_5	1.085	1.094	1.092	1.094(2)
r (C_3-H_{11})	r_6	1.084	1.092	1.092	1.092(2)
r (C_5-H_{12})	r_7	1.088	1.097	1.096	1.097(2)
r (C_4-H_{13})	r_8	1.088	1.097	1.097	1.097(2)
r (C_5-H_{14})	r_9	1.086	1.095	1.094	1.095(2)
r (C_4-H_{15})	r_{10}	1.085	1.094	1.094	1.094(2)
∠ $C_3Si_1C_2$	θ	96.5	96.5	96.5	96.8(5)
∠ $Si_1C_2C_4$	ψ_1	102.9	103.1	103.2	103.3(5)
∠ $Si_1C_3C_5$	ψ_2	102.7	102.1	103.1	102.3(5)
∠ $C_2C_4C_5$	φ_1	108.9	108.4	109.0	108.3(5)
∠ $C_3C_5C_4$	φ_2	108.6	107.7	108.8	107.6(5)
∠ $Br_6Si_1H_7$	α	105.5	106.1	105.2	106.1(5)
∠ $H_8C_2H_{10}$	γ_1	107.1	107.4	107.2	107.4(5)
∠ $H_9C_3H_{11}$	γ_2	107.2	107.8	107.3	107.8(5)
∠ $H_{13}C_4H_{15}$	ε_1	106.7	107.2	106.7	107.2(5)
∠ $H_{12}C_5H_{14}$	ε_2	106.9	107.3	106.8	107.3(5)
∠ $Br_6Si_1C_2$	β_1	112.3	111.2	112.0	111.2(5)
∠ $Br_6Si_1C_3$	β_2	112.7	110.9	112.6	110.9(5)
∠ $H_7Si_1C_3$	β_3	115.3	116.0	115.7	116.0(5)
∠ $H_7Si_1C_2$	β_4	114.9	116.2	115.0	116.2(5)
∠ $H_8C_2Si_1$	π_1	110.1	109.5	109.4	109.5(5)
∠ $H_9C_3Si_1$	π_5	109.2	109.5	108.5	109.5(5)
∠ $H_{10}C_2Si_1$	π_3	114.2	114.2	113.7	114.2(5)
∠ $H_{11}C_3Si_1$	π_7	115.1	114.5	114.5	114.5(5)
∠ $H_8C_2C_4$	π_2	110.2	110.1	110.6	110.1(5)
∠ $H_9C_3C_5$	π_6	110.0	109.5	110.3	109.5(5)
∠ $H_{10}C_2C_4$	π_4	112.3	112.5	112.7	112.5(5)
∠ $H_{11}C_3C_5$	π_8	112.6	113.2	113.0	113.2(5)
∠ $H_{13}C_4C_2$	σ_1	109.5	109.7	109.5	109.7(5)
∠ $H_{13}C_4C_5$	σ_2	108.9	108.5	109.0	108.5(5)
∠ $H_{15}C_4C_2$	σ_3	111.5	111.5	111.4	111.5(5)

$\angle H_{15}C_4C_5$	σ_4	111.3	111.5	111.2	111.5(5)
$\angle H_{12}C_5C_3$	σ_5	109.4	109.6	109.3	109.6(5)
$\angle H_{12}C_5C_4$	σ_6	109.2	109.0	109.1	109.0(5)
$\angle H_{14}C_5C_3$	σ_7	111.7	111.8	111.6	111.8(5)
$\angle H_{14}C_5C_4$	σ_8	111.2	111.4	111.1	111.4(5)
τ $Si_1C_2C_4C_5$	τ_1	-35.5	-34.6	-35.0	-34.6(5)
τ $C_2C_4C_5C_3$	τ_2	50.4	52.1	49.1	52.1(5)
A		4144.99	4197.99	4118.94	4039.24
B		972.91	1545.68	953.27	1000.16
C		904.20	1380.76	886.96	935.94
$\lvert\mu_a\rvert$		2.387	2.554	2.535	
$\lvert\mu_b\rvert$		0.038	0.071	0.022	
$\lvert\mu_c\rvert$		0.356	0.477	0.290	
$\lvert\mu_t\rvert$		2.414	2.599	2.552	

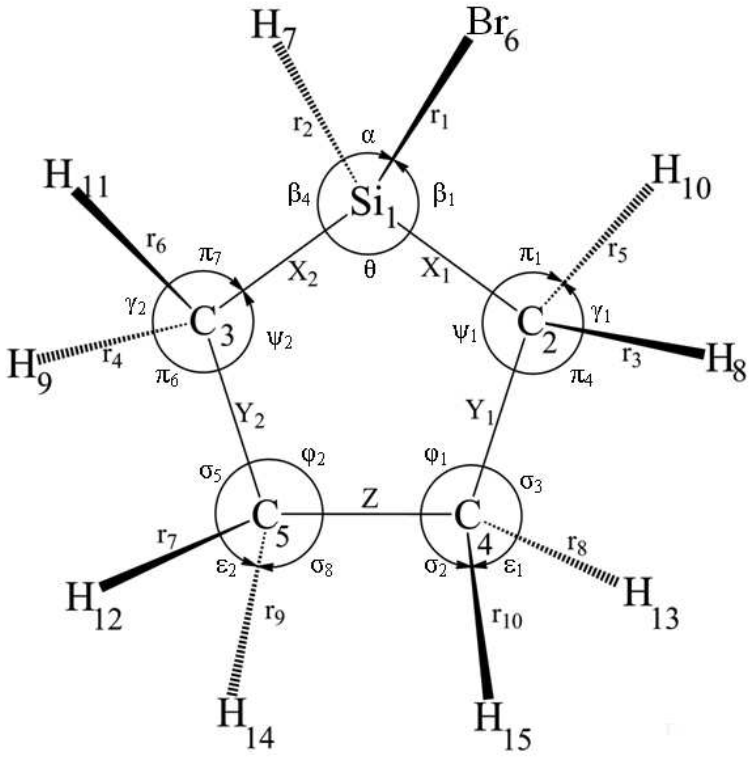

Figure 31. Planar (C_s) conformer of 1-bromo-1-silacyclopentane showing atom numbering and internal coordinates.

The vibrational spectra were predicted from the MP2(full)/6-31G(d) calculations. The predicted scaled frequencies were used together with a Lorentzian function to obtain the simulated spectra. Infrared intensities were obtained based on the dipole moment derivatives with respect to Cartesian coordinates. The derivatives were transformed with respect to normal coordinates by $(\partial\mu_u/\partial Q_i) = \sum_j (\partial\mu_u/\partial X_j)L_{ij}$, where Q_i is the i^{th} normal coordinate, X_j is the j^{th} Cartesian displacement coordinate, and L_{ij} is the transformation matrix between the Cartesian displacement coordinates and the normal coordinates. The

infrared intensities were then calculated by $(N\pi)/(3c^2)$ $[(\partial\mu_x/\partial Q_i)^2 + (\partial\mu_y/\partial Q_i)^2 + (\partial\mu_z/\partial Q_i)^2]$. A comparison of experimental and simulated infrared spectra of c-C_4H_8SiBrH is shown in Fig. 29. The predicted spectrum is in good agreement with the experimental spectrum which shows the utility of the scaled predicted frequencies and predicted intensities for supporting the vibrational assignment.

Additional support for the vibrational assignments was obtained from the simulated Raman spectrum. The evaluation of Raman activity by using the analytical gradient methods has been developed [31-34] and the activity S_j can be expressed as: $S_j = g_j(45\alpha_j^2 + 7\beta_j^2)$, where g_j is the degeneracy of the vibrational mode j, α_j is the derivative of the isotropic polarizability, and β_j is the anisotropic polarizability. To obtain the Raman scattering cross sections, the polarizabilities are incorporated into S_j by multiplying S_j with $(1-\rho_j)/(1+\rho_j)$ where ρ_j is the depolarization ratio of the j^{th} normal mode. The Raman scattering cross sections and calculated wavenumbers obtained from the Gaussian 03 program were used together with a Lorentzian function to obtain the simulated Raman spectra. Comparison of experimental Raman spectrum of the liquid and the predicted Raman spectrum are shown in Fig. 30.

CONFORMATIONAL STABILITY AND VIBRATIONAL ASSIGNMENT

To determine the conformational stabilities, we first determined whether there was more than one conformer present in the fluid states. A comparison of the infrared spectrum of the gas and solid indicated that there was only one conformer present in the gas since all of the bands observed in the spectrum of the gas were also present in the spectrum of the polycrystalline solid (Fig. 29) which was obtained by repeated annealing of the sample until no changes were observed in the spectrum. Also, a comparison of the

Raman spectrum of the liquid with that of the infrared spectra indicated that there were no Raman lines present which were not observed in the infrared spectrum. Once it was ascertained that there was only one conformer present in all of the physical states, the structure of this conformer was determined.

The predicted spectra were plotted for each of the three most likely conformers, i.e. *envelope-axial* (C_s), *envelope-equatorial* (C_s) and *twisted* form (C_1) with the assumption that the planar conformer would be a high energy form. The simulated spectra from *ab initio* MP2(full)/6-31G(d) calculations with two scaling factors were compared with the spectrum of the solid and are shown in Fig. 32. The most definitive spectral region for determining the conformer(s) present is the region from 400 to 1000 cm^{-1}, where five or six of the ring vibrations are expected. It is clear from these data that the predicted spectrum of the *twisted* (C_1) conformer is the best fit to the observed spectrum of the solid as well as that for the gas (Fig. 29). This conclusion is also supported by the *ab initio* calculations where both of the *envelope* forms are predicted to be saddle points by a negative frequency. Therefore, it is concluded that the conformer present in all of the physical states is the *twisted* form. Since both *envelope-axial* and -*equatorial* forms have predicted lower energies of ~1400 and ~900 cm^{-1}, respectively, than the planar form which shows that transitions from one *twisted* form to another will not be through the planar form.

Once the form of the stable conformer has been identified the vibrational assignment could be made which was aided significantly by the predicted information from the *ab initio* MP2(full)/6-31G(d) calculations. Of particular importance were the infrared band contours and intensities, the Raman activities and depolarization values,

and of course the fundamental frequencies which were obtained with only two scaling factors of 0.88 for the CH_2 stretches and deformations and 0.90 for the remaining vibrations except for the heavy atom bends. A significant number of the fundamental vibrations could be initially assigned from well known “group frequencies” particularly in the fingerprint region. The most uncertain assignments are for the CH_2 stretches where eight normal modes are “bunched” together with significant Fermi resonance expected. More confident assignments could be made in this spectral region by utilizing deuterium substitution for the α-CH_2 groups and then the β-CH_2 groups.

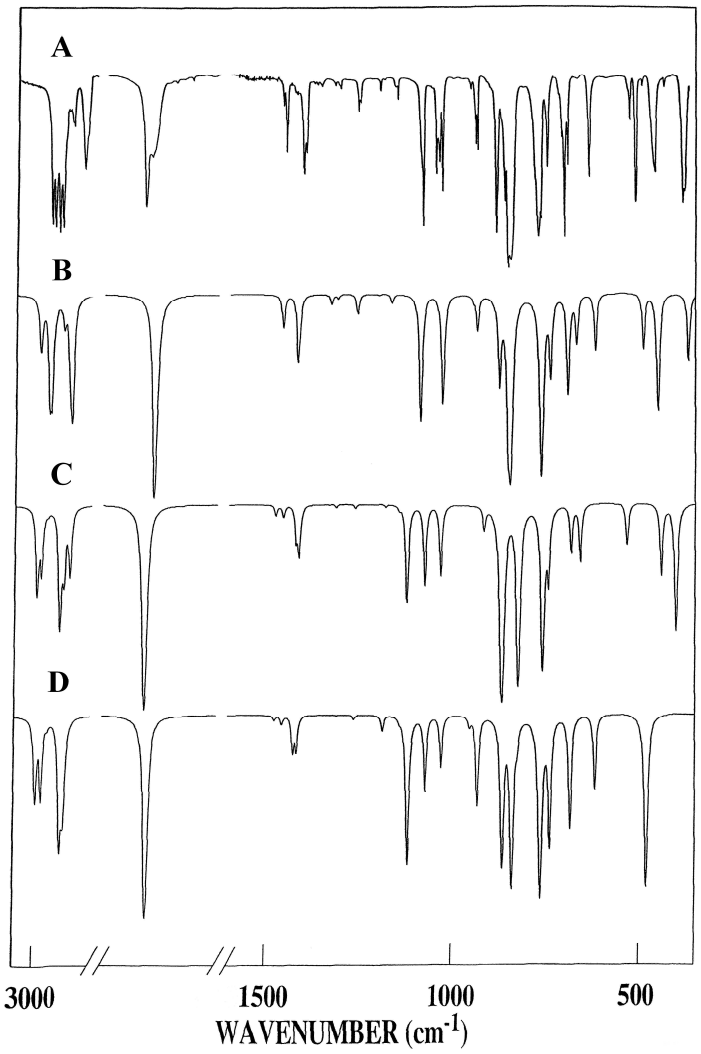

Figure 32. Comparison of experimental and calculated infrared spectra of 1-bromo-1-silacyclopentane: (A) observed infrared spectrum of solid; (B) simulated infrared spectrum of *twist* conformer; (C) simulated infrared spectrum of *envelope-axial* conformer; (D) simulated infrared spectrum of *envelope-equatorial* conformer.

Most of the CH_2 bending modes could be readily assigned with the predicted frequencies, band contours and intensities from the infrared spectra. The A-, C- or A/C-

and B-type bands could be observed in the spectrum (Fig. 33). For example, the band at 1157 cm^{-1} is obviously a B-type band and a fundamental is predicted at 1172 cm^{-1} with 73% B-type contour which is due to a relatively weak α-CH_2 wag. The band at 1080 cm^{-1} is clearly an A-type band (predicted 82% A and 18% C), where, the ν_{20} (α-CH_2 wag) fundamental is predicted to be at 1089 cm^{-1} with an intensity of 41.5 km/mol. The band at 1033 cm^{-1} has a pronounced shoulder at 1019 cm^{-1} with the latter one nearly a pure A-type band (99%) and the former one nearly an equal A/C type band (61% A and 38% C); these bands are due to ν_{21} (α-CH_2 twist, 50% S_{21}) and ν_{22} (ring deformation, 41% S_{22}, 20% S_{31}), respectively. These assignments illustrate how most of the CH_2 bends could be assigned but beginning at 1019 cm^{-1} and lower frequencies to 400 cm^{-1} the vibrations are due to heavy atom motions, the four CH_2 rocks, and two SiH bends. It is fairly easy to identify the fundamental frequencies but a significant number of them are extensively mixed with the CH_2 bends and heavy atom modes. Thus, the approximate descriptions are more for "bookkeeping" rather than the major molecular motion giving rise to the vibration.

The most interesting vibrations are the heavy atom modes particularly the ring vibrations. Four of these modes are expected to be between 850 and 1030 cm^{-1} and the other modes in this spectral range are CH_2 rocking modes. The ring deformation (ν_{25}) is predicted to have the largest infrared intensity of these modes and is assigned at 871 cm^{-1} with a weaker band (17.8 km/mol) at 851 cm^{-1} which is the ring breathing mode (41% S_{26}). In addition to the first ring mode assigned earlier there is another very weak one at 941 cm^{-1} (solid; 32% S_{23}, 13% S_{33}, 10% S_{25}, all ring modes). Three other ring deformations are expected in the region from 700 to 400 cm^{-1} and two of them could

readily be assigned at 493 (53% S_{33}) and 452 (58% S_{34}) cm^{-1} but the other one is difficult to assign although the band at 685 cm^{-1} (21% S_{31}) seems to be the best choice. The two SiH bends can be assigned at 620 and 694 cm^{-1} with the latter one having contributions from five symmetry coordinates with only 19% S_{30} and the former one with contributions from four symmetry coordinates with only 26% of S_{32}. Even though both of these modes are extensively mixed they are reasonable "group frequencies".

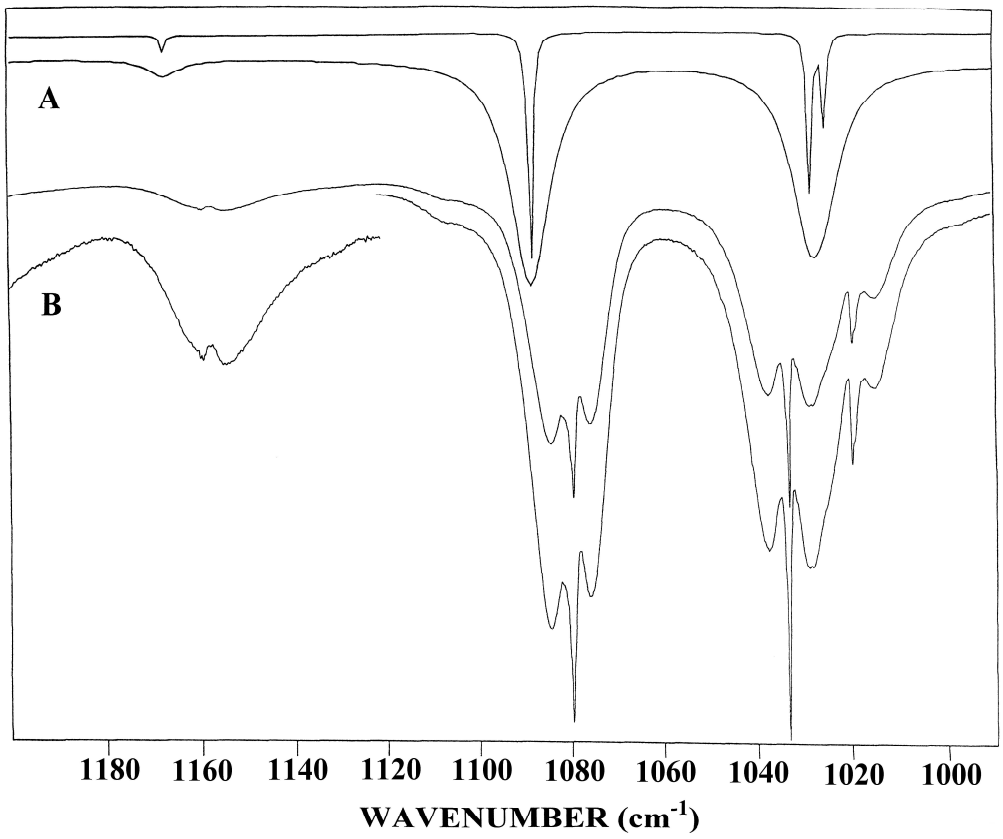

Figure 33. Comparison of experimental and calculated infrared spectra (990-1200 cm^{-1}) of 1-bromo-1-silacyclopentane: (A) simulated spectra of *twist* (C_1) conformer at 0.5 cm^{-1} and 4.0 cm^{-1} resolutions; (B) observed infrared spectrum of the gas

showing typical B-, A- and A/C-type band contours at 1157, 1080 and 1033 cm^{-1}, respectively, measured at 0.5 cm^{-1} resolution.

Three of the five fundamentals predicted below 400 cm^{-1} were observed in the Raman spectrum (Fig. 30) of the liquid with the ring twisting mode at 268 cm^{-1} (80% S_{36}) and the two SiBr bends are observed as distinct Raman lines at 210 and 160 cm^{-1} with predicted frequencies of 208 and 158 cm^{-1}, respectively. The ν_{37} mode is extensively mixed with contributions of greater than 10% from four symmetry coordinates.

DISCUSSION

We investigated the changes in the predicted intensities of the infrared bands and the Raman activities when the basis set was increased, from 6-31G(d) to 6-311+G(d,p), by the B3LYP density functional theory method. In Table S9 the values are reported and many have very small changes but a few of them have rather large differences for Raman activities. For example ν_8 has a Raman activity of 131.0 $Å^4$/u that increases to 185.6 $Å^4$/u when the basis set increases and for ν_9 (Si-H stretch) the Raman activity increases from 126.5 to 178.7 $Å^4$/u. There are also significant differences such as ν_{11} which drops ~50% from 20.1 to 11.1 $Å^4$/u and ν_{13} which decreases from 19.4 to 8.7 $Å^4$/u. However, as the vibrational frequencies decrease the differences decrease and are often nearly the same. The predicted intensities for the infrared bands are not nearly as varied as the Raman activities but they do follow the same trend to smaller differences at lower frequencies.

The predicted depolarization (dp) ratios do not vary significantly with the change in basis sets from B3LYP calculations and these are quite similar to the values obtained

from the MP2(full)/6-31G(d) calculations (Table S9). The P.E.D.s are very similar for both B3LYP predicted values, which, are also similar to those predicted from the MP2(full)/6-31G(d) calculations (Table S10).

The predicted dp ratios are quite good as compared to the experimental spectra (Fig. 34). The predicted depolarization ratios differ significantly for only four of the fundamentals, 1250 (ν_{17}), 1079 (ν_{20}), 840 (ν_{27}), and 693 (ν_{30}) cm^{-1}. The band at 1250 cm^{-1} assigned as the fundamental ν_{17} is predicted as having a dp ratio of 0.75 while the experimental ratio is 0.31, the fundamental can be described as a β-CH_2 twist (51%) with some α-CH_2 twist (19%) and α-CH_2 wag (18%) character. At 1079 cm^{-1} the ν_{20} (39% α-CH_2 wag and 21% β-CH_2 twist) fundamental has an experimental dp ratio of 0.25 as compared with 0.73 from the *ab initio* prediction. The fundamental at 840 cm^{-1} (ν_{27}) has a predicted dp ratio of 0.64 as compared to the experimentally determined ratio of 0.24, this band has 36% α-CH_2 rock character with contributions of 16% Si-H parallel bend and 13% Si-Br parallel bend while the remaining 35% is composed of smaller (less than 10%) contributions. The fundamental ν_{30} at 693 cm^{-1} is highly mixed with contributions from five different modes, it is described as the Si-H parallel bend (19%) but this should be considered "bookkeeping" rather than a meaningful description of this complex vibrational motion. The experimentally determined dp ratio is 0.28 compared to 0.61 from the *ab initio* predictions. This shows good utility for the *ab initio* predictions with the predicted depolarization ratios matching reasonably well with the experimentally observed depolarization ratios.

The *ab initio* predicted frequencies are in good agreement with the observed fundamentals of the *twist* form with an average difference of 8 cm^{-1} which is 0.5% error

where these errors arise mainly from the β-CH_2 symmetric stretches, α-CH_2 deformations, the α-CH_2 wag, and the ring deformations. The fundamental frequencies were also calculated using the B3LYP density functional theory method at two different basis sets. The 6-31G(d) and 6-311+G(d,p) basis sets were used and gave an average difference of 32 cm^{-1} (3.1% error) and 20 cm^{-1} (2.0% error), respectively, where the carbon-hydrogen stretching modes were not included as they differed by over a hundred wavenumbers from the observed frequencies. As noted the B3LYP calculations do significantly worse at predicting the fundamental frequencies. This is partially due to the B3LYP predicted frequencies having values that are sometimes higher and sometimes lower than the observed values so any effort to scale the predictions becomes complicated at best. This highlights the advantage of the *ab initio* MP2(full)/6-31G(d) predictions in that the predicted frequencies are usually higher than the observed values or relatively close to the observed values.

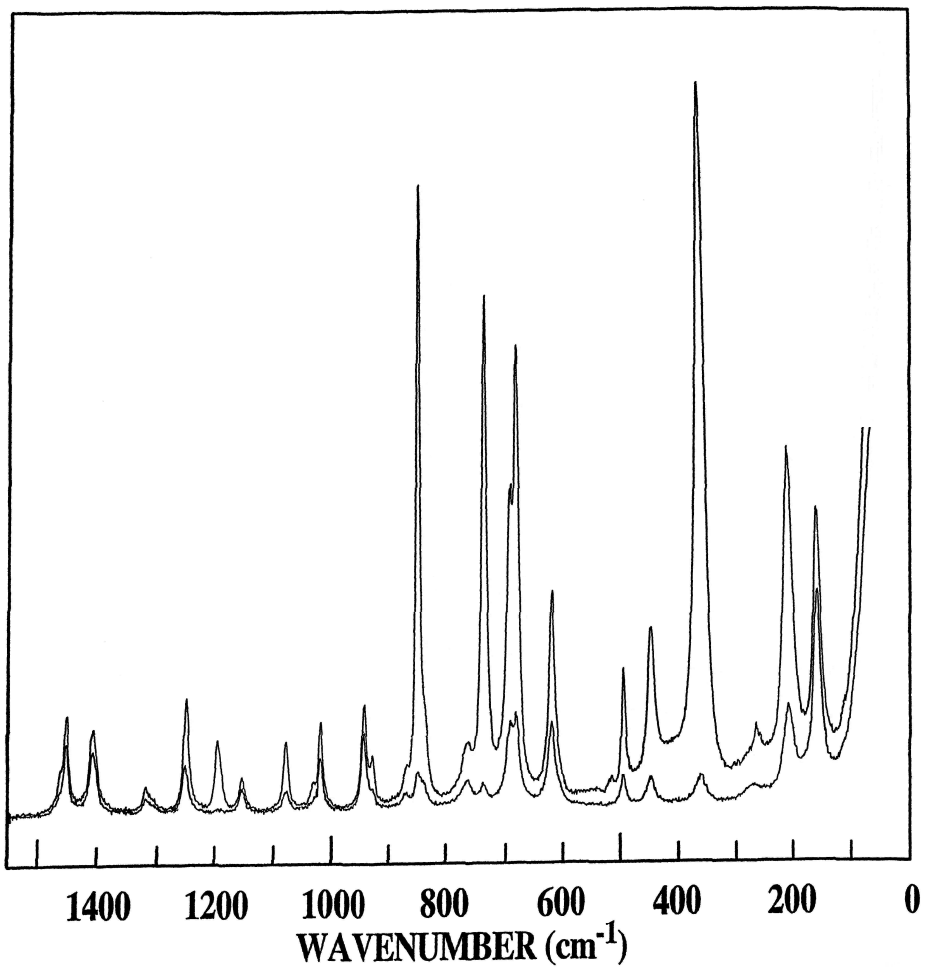

Figure 34. Raman spectra (0-1550 cm^{-1}) showing the polarized and the depolarized bands for 1-bromo-1-silacyclopentane.

The *twist* conformer is relatively rigid with the predicted energy difference to the *envelope-axial* form (saddle point) of 1216 cm^{-1} from the MP2 calculations by utilizing the largest basis set with a similar value of 1188 ± 36 cm^{-1} from the average of all the B3LYP calculations which agrees with the value of 1205 cm^{-1} from the B3LYP/aug-cc-pVTZ (500 basis functions). The next higher energy saddle point which is the *envelope-*

equatorial form, has a predicted value nearly 500 cm^{-1} greater than the *axial* form from the MP2 calculations with those from the B3LYP calculations only about 300 cm^{-1} higher. The energy difference at the planar position is about 900 cm^{-1} higher than the *equatorial* form from the MP2 calculations and about 500 cm^{-1} higher from the B3LYP calculations. These energy differences are relatively large compared to those of the corresponding carbon compounds. From the limited data that is currently available one would expect that 1-X-1-silacyclopentane molecules will have the *twisted* form as the most stable conformer for this molecule which is very different from the carbon analogues.

It should be possible to estimate structural parameters for the *twist* conformer of 1-bromo-1-silacyclopentane by adjusting the MP2(full)/6-311+G(d,p) calculated structural parameters using similar molecules as a guideline. The CH bond distances predicted by MP2(full)/6-311+G(d,p) *ab initio* calculations can be used as a good prediction without any adjustment as we [51] have shown that *ab initio* MP2/6-311+G(d,p) calculations predict the r_0 CH distances for more than fifty substituted hydrocarbons to better than ± 0.002 Å compared to the experimentally determined values from isolated CH stretching frequencies which were compared [5] to previously reported values from earlier microwave studies. Therefore, all of the carbon-hydrogen distances can be taken from the MP2(full)/6-311+G(d,p) predicted values for 1-bromo-1-silacyclopentane. The heavy atom ring parameters can be estimated by using the corresponding parameters in silacyclopentane [128] to adjust the MP2(full)/6-311+G(d,p) calculated parameters. For silacyclopentane the adjusted r_0 Si-C distance is 0.005 Å shorter than the predicted value whereas the two side C-C distances are 0.003 Å longer

and the unique "bottom" C-C distance has the same value as predicted. Therefore, we have predicted the two C-C distances for 1-bromo-1-silacyclopentane to be 0.003 Å longer than the *ab initio* predicted value with the same value for the "bottom" C-C distance as predicted. The Si-C distance for silacyclopentane, while interesting for comparison purposes to 1-bromo-1-silacyclopentane, was not used to find the estimated r_0 structural parameters as the parameters from trimethylbromide should give a more consistent value. The differences in the angle values with those obtained from the adjusted values to the predicted values for silacyclopentane were retained for the bromosubstituted molecule. This leaves the Si-Br and Si-C distances to be obtained from the values reported for trimethyl bromosilane [129] and bromosilane [130], while the Si-H distance can be obtained using the frequency of the isolated SiH stretching mode.

It has been shown that SiH distances can be obtained from the frequencies of the isolated SiH stretching modes [6]. Therefore, from the observed frequency of 2176 cm^{-1} for the SiH stretch we have obtained a value of 1.482 Å for the SiH distance (Table 58) which is 0.008 Å longer than the corresponding distance from the *ab initio* predicted parameter. We believe that this value has at most an uncertainty of ± 0.002 Å. This longer distance compared to the *ab initio* predicted value is the same difference found for many SiH distances in other organosilanes [131, 132].

In the microwave study [129] of trimethyl bromosilane the structure was determined though only the SiBr is a true r_s parameter while the carbon parameters are approximate r_s parameters. Therefore, we have again determined the structural parameters for trimethyl bromosilane by utilizing the three B rotational constants previously reported [129]. We have found that good structural parameters for

hydrocarbons and many substituted ones can be determined by adjusting the structural parameters obtained from the *ab initio* MP2(full)/6-311+G(d,p) calculations to fit the rotational constants obtained from microwave experimental data by using a computer program "A&M" (*Ab initio* and Microwave) developed [14] in our laboratory. In order to reduce the number of independent variables, the structural parameters are separated into sets according to their types where bond distances in the same set keep their relative ratio, and bond angles and torsional angles in the same set keep their difference in degrees. This assumption is based on the fact that errors from *ab initio* calculations are systematic. Therefore, we obtained "adjusted r_0" structural parameters using the previously reported rotational constants. The determined heavy atom structural parameters for trimethyl bromosilane are: the distances with MP2(full)/6-311+G(d,p) values in brackets (Å) Si-C = 1.863(3) [1.864], Si-Br = 2.244(3) [2.252], and the angle in degrees (°) ∠BrSiC = 106.9(5) [107.3]. These parameters give differences of -0.001 and -0.008 Å for the Si-C and Si-Br bonds, respectively, and -0.4° for the ∠BrSiC angle. The Si-C distances were then obtained using the MP2(full)/6-311+G(d,p) calculations and adjusting them by -0.001 Å. This leaves the Si-Br distance to be determined.

The microwave study of bromosilane [130] determined the r_0 structural parameters for Si-Br and Si-H to be 2.2123(1) and 1.4743(2) Å, respectively. The corresponding MP2(full)/6-311+G(d,p) parameters were predicted to be 2.225 and 1.468 Å from which the differences of -0.013 and 0.006 Å can be determined. The Si-H bond distance determined from the frequency of the SiH isolated stretching mode compares favorably with this prediction again showing the systematic nature of *ab initio* errors. The Si-Br value was adjusted using the average of the difference between the r_0 parameters

and the corresponding MP2(full)/6-311+G(d,p) parameter for bromosilane and trimethyl bromosilane. This average gives an adjustment of -0.010 Å, thereby, giving the bond distance listed in Table 58.

For the angles we retained the values from the *ab initio* calculation since the adjusted values of the angles of silacyclopentane differed by 0.3, 0.2, 0.1 and 0.1° and with the listed uncertainties of 0.5 we believe they should be within the experimentally determined values. All of these estimated parameters are listed in Table 58 along with those predicted from RHF/6-31G(d) and B3LYP/6-311+G(d,p) and those from the MP2 calculations from which the adjusted parameters were obtained. It should be noted that the predictions from the RHF calculation provided good estimates for the C-C distances but the Si-C distances are very long. The B3LYP predictions for the Si-C distances are even longer than those from the RHF calculation and those for the C-C are also slightly too long. It is believed that the estimated r_0 parameters reported herein for 1-bromo-1-silacyclopentane have listed uncertainty values that should be within the experimentally determined parameters. Thus, the listed rotational constants given in Table 58 for the ^{79}Br atom should make it relatively easy to assign the microwave spectrum from which the experimental parameters could be obtained.

It is clear that additional work to determine Si-Br distances would be of value where it would be interesting to see if the predicted parameter is consistent for several different types of Si-Br molecules. Also of interest would be a microwave study of a 5-membered ring which contains a silicon atom and four carbon atoms to obtain structural parameters by utilizing isotopic Si and ^{13}C data which should give accurate heavy atom distances of the 1-X-1-silacyclopentane molecules.

CONCLUSION

The vibrational spectra in the gas, liquid and solid indicate that the same conformer is present in all three physical states. By predicting the spectra from *ab initio* MP2(full)/6-31G(d) calculation for the *envelope-axial*, *envelope-equatorial* and *twisted* forms, a comparison was made of each of these spectra with the spectra observed in the three physical states. It is clear from these data that a single form is present and the comparison clearly indicated that it is the *twisted* form. Both MP2 and density functional theory calculations were used to predict the energy among the three potential conformers and it was found that the *twisted* form is lower in energy by ~1300 cm^{-1} (15.55 kJ/mol) than the *envelope-axial* form and the *envelope-equatorial* was only ~400 cm^{-1} (4.78 kJ/mol) higher and both of these were found to be saddle points. From the MP2 calculations the planar conformation is ~900 cm^{-1} (10.77 kJ/mol) higher in energy. Density functional theory calculations by the B3LYP method predicts slightly lower energies for the two *envelope* forms as well as for the planar conformer. The calculated heavy atom structural parameters for the present molecule suggest that the flexible form (C_1) is a rigid framework in silacyclopentanes.

By utilizing the MP2 calculations the force constants were obtained which were then scaled with only two scaling factors of 0.88 for the CH_2 stretches and deformations and 0.90 for the remaining force constants except for the heavy atom bends. The frequencies were obtained as well as the infrared intensities, Raman activities, band contours and depolarization ratios which supported the vibrational assignment. Of particular value for supporting the assignments were the band contours and infrared

intensities, as well as, depolarization values from the Raman effect which agreed with predictions except for four of the vibrations.

The r_0 structural parameters were estimated by utilizing MP2(full)/6-311+G(d,p) calculations and adjusting the C-C difference as normally found for this parameter from several other molecules and the Si-C distance adjusted from silyl compounds. The Si-H distance was obtained from the isolated Si-H stretching frequency. The Si-Br distance was obtained by comparing this distance from two other molecules where this parameter had been determined. However, it is clear that additional Si-Br distances should be determined where it would be helpful to see if this predicted parameter is consistent for several different types of Si-Br molecules. A microwave study of a 5-membered ring where the isotopic Si and ^{13}C will be utilized to obtain accurate structural parameters of the 1-X-1-silacyclopentane molecules would be of value.

CHAPTER 10

CONFORMATIONAL AND STRUCTURAL STUDIES OF ETHYNYLCYCLOPENTANE FROM TEMPERATURE DEPENDENT RAMAN SPECTRA OF XENON SOLUTIONS AND AB INITIO CALCULATIONS

INTRODUCTION

Mono-substituted cyclopentanes have been of interest for several decades since cyclopentane undergoes a ring vibration designated [133] as pseudorotation since there are two "out-of-plane" vibrational modes which are usually described qualitatively as ring-puckering and ring-twisting. After the initial prediction [133] of pseudorotation in saturated five-membered rings, a study followed [134] wherein the authors proposed that fluorocyclopentane as well as some other mono-substituted cyclopentanes should have the bent conformation (*envelope*) as the preferred form. Relatively complete vibrational [116,117] studies of the cyclopentyl halides (F, Cl, Br, and I) were carried out utilizing infrared and Raman spectra and it was concluded that the F, Cl, and Br compounds all had doublets for the carbon-halogen stretches arising from *equatorial* and *axial* conformers for the *envelope* form of these substituted cyclopentanes. We recently determined [76,135] the enthalpy differences between the two stable forms of the chloride and bromide by variable temperature studies of the infrared spectra of rare gas solutions with values of 145 ± 15 cm^{-1} (1.73 ± 0.18 kJ/mol) and 233 ± 23 cm^{-1} (2.79 ± 0.28 kJ/mol), respectively, with the *axial* conformer the more stable form for both molecules.

From the initial study [116,117] of fluorocyclopentane it was also concluded that both the *axial* and *equatorial* forms were present in the fluid phases. However from a later Raman study [121] it was concluded there was only a single conformer present in the fluid states and it was the *envelope-equatorial* (*Eq*) conformer. This conclusion was consistent with predictions from CNDO/2 calculations [122] that only the *Eq* conformer was a stable form. As a continuation of our studies of the conformational stabilities of mono-substituted cyclopentanes we reinvestigated the infrared and Raman spectra of fluorocyclopentane [123]. The results were quite interesting in that there is, in fact, a single stable conformer present in the fluid phases but it is neither the *envelope-axial* (*Ax*) nor *envelope-equatorial,* but the *twisted* form. These conclusions were based on infrared spectra of variable temperature xenon solutions, Raman spectra of the liquid and solid, and microwave spectrum which were supported by *ab initio* and density functional theory calculations. Therefore, as a continuation of these studies we have turned our attention to another mono-substituted cyclopentane, i.e. ethynylcyclopentane, c-C_5H_9CCH.

There has been a previous investigation of the conformational stability of ethynylcyclopentane from a microwave study [120] where the *Eq* conformer was reported to be more stable by 94 ± 24 cm^{-1} (1.12 ± 0.29 kJ/mol) than the *Ax* form. By transferring the parameters reported for cyanocyclopentane which were obtained from assumed parameters (four) transferred from analogous molecules and five parameters from the least squares fit of the two isotopic species of each conformer. The three parameters (angles) were reported for ethynylcyclopentane by fitting the experimental moments of inertia. However the heavy atom bond distances for cyanocyclopentane were reported not to be in error by more than 0.02 Å and the angles no more than 5°. Therefore

it is desirable to obtain a more accurate enthalpy difference between the two conformers and obtain more accurate structural parameters for ethynylcyclopentane, so as to compare them to the corresponding cyanocyclopentane parameters. Therefore we have investigated the vibrational spectrum of ethynylcyclopentane with a study of the infrared spectra of the gas and solid. Additionally we have investigated the Raman spectra of the liquid as well as spectra of the variable temperatures of xenon solutions. To support the vibrational study, we have carried out *ab initio* calculations with basis sets up to aug-cc-pVTZ as well as those with diffuse functions, i.e., 6-311+G(2df,2pd). We have also carried out density functional theory (DFT) calculations by the B3LYP method with the same basis sets. We have calculated optimized geometries, conformational stabilities, harmonic force fields, infrared intensities, Raman activities and depolarization ratios. The results of these spectroscopic, structural, and theoretical studies are reported herein.

EXPERIMENTAL AND THEORETICAL METHODS

The sample of c-C_5H_9CCH was purchased from GFS Chemicals, Columbus, OH with a stated purity of 95%. The sample was further purified by a low-temperature, low-pressure fractionation column and the purity of the sample was verified from the infrared spectra of the gas and NMR spectrum of the liquid.

The infrared spectrum of the gas (Fig. 35A) and solid (Fig. 35E) were obtained from 3500 to 220 cm^{-1} on a Perkin-Elmer model 2000 Fourier transform spectrometer equipped with a Ge/CsI beamsplitter and a DTGS detector. Atmospheric water vapor was removed from the spectrometer housing by purging with dry nitrogen. The spectra of the gas and solid were obtained with a theoretical resolution of 0.5 cm^{-1} for the gas and 2 cm^{-1} for the

solid with 128 interferograms added and truncated. Multiple annealings were required to obtain satisfactory spectra of the solid.

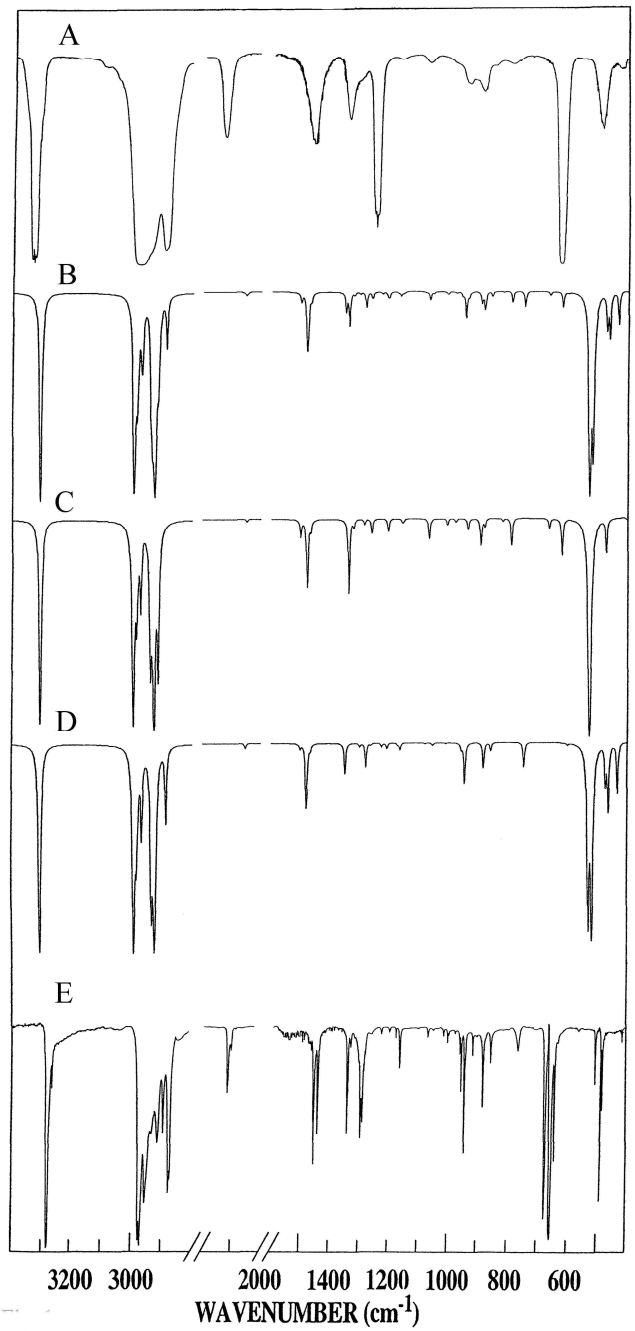

Figure 35. Comparison of experimental and calculated infrared spectra of ethynylcyclopentane: (A) observed spectrum of gas; (B) simulated spectrum of a mixture of *Eq* and *Ax* conformers (ΔH = 94 cm^{-1}) at 25°C; (C) simulated spectrum of *Ax* conformer; (D) simulated spectrum of *Eq* conformer; (E) observed spectrum of solid.

The Raman spectra of the liquid (Fig. 36A) obtained from 3400 to 60 cm^{-1} were recorded on a Spex model 1403 spectrophotometer equipped with a Spectra-Physics model 2017 argon ion laser operating on the 514.5 nm line. The laser power used was 1.5 W with a spectral bandpass of 3 cm^{-1}. The spectrum of the liquid was recorded with the sample sealed in a Pyrex glass capillary. The measurements of the Raman frequencies are expected to be accurate to ± 2 cm^{-1}. All of the observed bands in the Raman spectra of the liquid along with their proposed assignments and depolarization values are listed in Tables 59 and 60, for the *Eq* and *Ax* conformers, respectively.

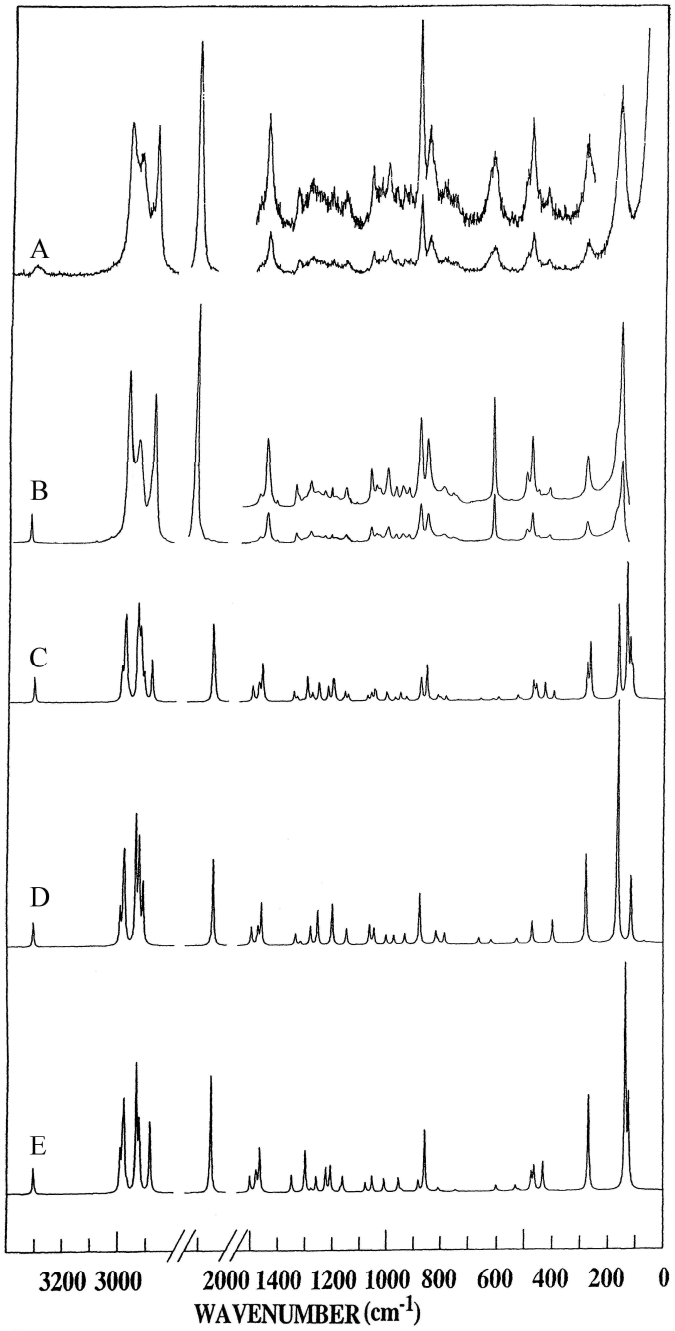

Figure 36. Comparison of experimental and calculated Raman spectra of ethynylcyclopentane: (A) observed spectrum of liquid; (B) observed spectrum of Xe solution at -60°C; (C) simulated spectrum of a mixture of *Eq* and *Ax* conformers (ΔH = 94 cm^{-1}) at -60°C; (D) simulated spectrum of *Ax* conformer; (E) simulated spectrum of *Eq* conformer.

Table 59. Calculated[a] and Observed Frequencies (cm^{-1}) for Ethynylcyclopentane *Eq* (*Cs*) Form.

	Vib. No.	Approx. description	*ab initio*	Fixed scaled[b]	IR int.	Raman act.	dp ratio	B3LYP	IR int.	Raman act.	Infrared		Raman		P.E.D.[c]	Band Contour		
											gas	solid	Xe soln.	liquid		A	B	C
A'	ν_1	C≡C-H stretch	3523	3307	57.1	46.3	0.25	3477	77.7	27.4	3329	3276/3274	3318	3308	$96S_1$	96	-	4
	ν_2	γ-CH_2 antisymmetric stretch	3189	2991	57.3	55.7	0.74	3101	76.8	65.0	2968	2968/2962	2965	2965	$65S_2,34S_3$	1	-	99
	ν_3	β-CH_2 antisymmetric stretch	3174	2977	1.7	119.5	0.45	3085	7.4	188.8	2968	2968/2962	2965	2965	$60S_3,32S_2$	94	-	6
	ν_4	γ-CH_2 symmetric stretch	3127	2933	30.9	179.9	0.04	3051	36.9	268.7	2934	2947	2927	2931	$92S_4$	99	-	1
	ν_5	β-CH_2 symmetric stretch	3116	2923	25.9	67.9	0.23	3043	38.8	63.7	2934	2947	2927	2931	$90S_5$	49	-	51
	ν_6	α-CH stretch	3075	2885	9.2	99.6	0.25	2997	8.5	135.1	2887	2869	2873	2873	$97S_6$	9	-	91
	ν_7	C≡C stretch	2166	2054	0.6	97.7	0.29	2208	18.1	286.1	2124	2115	2124	2117	$82S_7,14S_{16}$	100	-	-
	ν_8	γ-CH_2 deformation	1582	1488	0.5	8.5	0.68	1523	0.9	2.4	1474	1472	1476	1471	$72S_8,28S_9$	70	-	30
	ν_9	β-CH_2 deformation	1560	1467	6.3	8.6	0.72	1501	6.2	6.6	1456	1454	1448	1451	$72S_9,29S_8$	22	-	78
	ν_{10}	α-CH bend (in-plane)	1423	1354	3.4	7.7	0.48	1378	2.8	8.5	1340	1343	1343	1342	$37S_{10},40S_{12}$	96	-	4
	ν_{11}	γ-CH_2 wag	1371	1302	0.5	8.6	0.74	1328	0.9	2.9	~1300	1303	1290	1290	$58S_{11},23S_{13}$	88	-	12
	ν_{12}	β-CH_2 wag	1347	1279	2.3	2.1	0.70	1311	1.7	0.9	1247	1297	1249	1249	$27S_{12},29S_{10},26S_{14}$	67	-	33
	ν_{13}	β-CH_2 twist	1272	1212	0.5	10.2	0.73	1230	0.4	5.3	1218	1201	1214	1216	$47S_{13},19S_{11},12S_{18},10S_{17}$	84	-	16
	ν_{14}	γ-CH_2 twist	1225	1166	0.7	6.6	0.46	1190	0.4	3.5	1162	1167	1162	1168	$39S_{14},16S_{12},14S_{10}$	69	-	31
	ν_{15}	Ring deformation	1110	1058	0.3	5.5	0.69	1066	0.2	4.2	1052	1055	1050	-	$20S_{15},18S_{18},12S_{11},12S_{16}$	98	-	2
	ν_{16}	C-CC stretch	1063	1011	0.0	3.6	0.28	1020	0.0	6.3	-	1007	1007	1011	$33S_{16},32S_{15},14S_{19}$	99	-	1
	ν_{17}	β-CH_2 rock	1008	959	0.6	3.5	0.29	975	0.6	5.9	957	958	952	952	$32S_{17},29S_{14}$	3	-	97
	ν_{18}	Ring deformation	929	893	3.0	1.6	0.04	889	3.2	3.6	884	886	~887	~893	$47S_{18},20S_{15}$	98	-	2
	ν_{19}	Ring breathing	904	865	0.4	17.6	0.09	864	0.6	21.7	858	862	861	858	$53S_{19},12S_{17},11S_{22}$	95	-	5
	ν_{20}	γ-CH_2 rock	786	747	2.7	0.4	0.19	761	2.5	0.4	770	769	770	768	$81S_{20}$	3	-	97
	ν_{21}	C≡C-H linear bend (in-plane)	560	537	32.4	1.4	0.33	675	51.2	8.3	645	678	-	-	$55S_{21},13S_{25},11S_{23}$	11	-	89
	ν_{22}	Ring deformation	500	488	3.7	2.5	0.25	521	3.5	4.3	~505	510	505	508	$54S_{22},18S_{16},10S_{17}$	3	-	97
	ν_{23}	Ring-CCH bend (in-plane)	489	472	14.2	2.5	0.53	489	1.2	2.9	492	491	486	~490	$28S_{23},45S_{21}$	1	-	99
	ν_{24}	Ring puckering	285	284	0.2	5.0	0.74	284	2.8	4.8	282	292	286	288	$52S_{24},43S_{25}$	3	-	97
	ν_{25}	C-C≡C linear bend (in-plane)	133	132	0.0	4.1	0.73	133	0.1	2.3	-	-	-	-	$34S_{25},36S_{23},30S_{24}$	2	-	98
A"	ν_{26}	β-CH_2 antisymmetric stretch	3179	2982	13.7	73.0	0.75	3092	25.1	77.6	2968	2968/2962	2965	2965	$78S_{26},19S_{27}$	-	100	-
	ν_{27}	γ-CH_2 antisymmetric stretch	3162	2966	10.7	10.6	0.75	3069	22.7	23.5	2968	2968/2962	2965	2965	$78S_{27},16S_{26}$	-	100	-
	ν_{28}	γ-CH_2 symmetric stretch	3117	2924	26.8	25.3	0.75	3038	8.2	18.5	2934	2947	2927	2931	$91S_{28}$	-	100	-
	ν_{29}	β-CH_2 symmetric stretch	3113	2920	11.1	12.0	0.75	3037	30.6	31.2	2934	2947	2927	2931	$90S_{29}$	-	100	-
	ν_{30}	γ-CH_2 deformation	1557	1464	2.5	4.9	0.75	1499	4.5	1.7	1449	1447	1448	1451	$68S_{30},33S_{31}$	-	100	-
	ν_{31}	β-CH_2 deformation	1546	1454	0.5	22.4	0.75	1489	0.1	12.6	1449	-	1448	1451	$68S_{31},33S_{30}$	-	100	-
	ν_{32}	γ-CH_2 wag	1379	1310	0.0	0.0	0.75	1337	0.1	0.4	-	-	-	-	$52S_{32},17S_{34}10S_{36}$	-	100	-
	ν_{33}	α-CH bend (out-of-plane)	1370	1301	0.0	9.3	0.75	1321	0.0	4.7	~1300	1303	1290	1290	$51S_{33},19S_{32},12S_{36}$	-	100	-

ν_{34}	β-CH_2 wag	1328	1260	0.2	6.7	0.75	1294	0.0	4.0	~1266	1265	1266	1262	$31S_{34},33S_{35},17S_{32},15S_{33}$	-	100	-
ν_{35}	γ-CH_2 twist	1290	1227	0.4	10.1	0.75	1257	0.5	4.9	~1238	1259	1238	1239	$48S_{35},32S_{34}$	-	100	-
ν_{36}	β-CH_2 twist	1235	1175	0.2	1.3	0.75	1199	0.2	0.3	-	1180	1173	1175	$41S_{36},27S_{39},11S_{40}$	-	100	-
ν_{37}	Ring deformation	1136	1089	0.1	2.9	0.75	1078	0.2	5.1	1074	1073	1076	1073	$46S_{37},17S_{41},16S_{38}$	-	100	-
ν_{38}	Ring deformation	1006	962	0.7	1.9	0.75	980	0.7	0.6	957	958	952	952	$35S_{38},25S_{37},16S_{36}$	-	100	-
ν_{39}	γ-CH_2 rock	994	950	3.9	0.2	0.75	955	4.0	0.3	948	947	946	952	$24S_{39},20S_{40},16S_{38},16S_{33},13S_{36}$	-	100	-
ν_{40}	β-CH_2 rock	853	815	0.0	1.1	0.75	822	0.0	0.9	-	-	~803	~807	$44S_{40},19S_{39},16S_{41},11S_{37}$	-	100	-
ν_{41}	Ring deformation	635	620	0.2	1.1	0.75	673	51.4	8.9	~630	~658	~625	-	$59S_{41},17S_{40}$	-	100	-
ν_{42}	C≡C-H bend (out-of-plane)	548	546	45.6	0.3	0.75	630	0.1	1.0	627	660	-	-	$71S_{42},15S_{44}$	-	100	-
ν_{43}	Ring-CCH bend (out-of-plane)	457	455	5.7	3.1	0.75	509	7.9	1.9	457	485	464	466	$38S_{43},35S_{42},18S_{44}$	-	100	-
ν_{44}	C-C≡C (out-of-plane)	145	145	0.0	7.2	0.75	158	0.6	6.1	-	-	161	170	$64S_{44}$, $36S_{43}$	-	100	-
ν_{45}	Ring twisting	48	48	0.0	0.0	0.75	29	0.0	0.0	-	-	-	-	$93S_{45}$	-	100	-

[a] MP2(full)/6-31G(d) *ab initio* calculations, scaled frequencies, B3LYP/6-311+G(d,p) calculations, infrared intensities (km/mol), Raman activities ($Å^4$/u), depolarization ratios (dp) and potential energy distributions (P.E.D.s).

[b] Scaled frequencies with scaling factors of 0.88 for CH stretches and CH_2 deformations, 1.0 for heavy atom bends, and 0.90 for all other modes.

[c] Symmetry coordinates with P.E.D. contribution less than 10% are omitted.

Table 60. Calculated[a] and Observed Frequencies (cm^{-1}) for Ethynylcyclopentane *Ax* (*Cs*) Form.

	Vib. No.	Approx. description	*ab initio*	Fixed scaled[b]	IR int.	Raman act.	dp ratio	B3LYP	IR int.	Raman act.	Infrared gas	Raman		P.E.D.[c]	Band Contour		
												Xe soln.	liquid		A	B	C
A'	ν_1	C≡C-H stretch	3523	3307	53.1	46.1	0.25	3477	71.0	28.3	3329	3318	3308	$96S_1$	71	-	29
	ν_2	γ-CH_2 antisymmetric stretch	3192	2994	55.3	52.9	0.75	3104	66.9	69.6	2968	2965	2965	$79S_2,20S_3$	82	-	18
	ν_3	β-CH_2 antisymmetric stretch	3175	2978	0.9	120.8	0.54	3090	8.7	160.2	2968	2965	2965	$70S_3,20S_2$	32	-	68
	ν_4	γ-CH_2 symmetric stretch	3132	2938	23.4	184.8	0.04	3058	30.6	316.3	2934	2927	2931	$95S_4$	56	-	44
	ν_6	α-CH stretch	3120	2926	48.6	136.6	0.12	3047	69.9	158.9	2934	2927	2931	$64S_6,30S_5$	-	-	100
	ν_5	β-CH_2 symmetric stretch	3105	2913	10.8	74.6	0.50	3030	13.1	69.8	2887	2873	2873	$59S_5,35S_6$	56	-	44
	ν_7	C≡C stretch	2160	2048	0.3	73.5	0.28	2204	13.4	229.4	2124	2117	2107	$83S_7,13S_{16}$	77	-	23
	ν_8	γ-CH_2 deformation	1580	1486	1.7	10.1	0.70	1520	2.0	3.5	1474	1476	1471	$78S_8,22S_9$	56	-	44
	ν_9	β-CH_2 deformation	1557	1464	5.6	5.8	0.74	1499	6.1	4.2	1456	1448	1451	$78S_9,23S_8$	10	-	90
	ν_{10}	α-CH bend (in-plane)	1410	1341	9.0	6.0	0.55	1369	10.5	3.0	~1340	1334	1333	$44S_{10},26S_{13}$	95	-	5
	ν_{12}	β-CH_2 wag	1390	1322	0.7	1.2	0.38	1345	0.7	5.3	-	1313	1312	$54S_{12},29S_{11}$	11	-	89
	ν_{11}	γ-CH_2 wag	1352	1284	0.6	8.3	0.59	1309	0.2	6.0	1287	1283	1282	$29S_{11},24S_{14},14S_{10},10S_{12}$	21	-	69
	ν_{13}	β-CH_2 twist	1268	1207	1.3	16.1	0.74	1230	0.9	7.3	1212	1214	1216	$30S_{13},24S_{11},12S_{14}$	93	-	7
	ν_{14}	γ-CH_2 twist	1218	1160	0.4	0.6	0.10	1188	0.3	0.4	-	-	-	$30S_{14},30S_{10},10S_{13}$	5	-	95
	ν_{15}	Ring deformation	1106	1052	0.0	6.1	0.71	1057	0.0	6.0	1041	1039	1036	$32S_{15},22S_{18},13S_{11}$	79	-	21
	ν_{16}	C-CC stretch	1028	978	0.4	2.9	0.43	991	0.5	3.6	974	976	978	$22S_{16},22S_{14},15S_{15},13S_{13}$	8	-	92
	ν_{18}	Ring deformation	985	941	1.3	2.9	0.23	943	1.5	5.8	937	930	932	$32S_{18},27S_{17}$	97	-	3
	ν_{19}	Ring breathing	926	883	0.7	15.1	0.07	884	1.2	15.4	893	887	893	$61S_{19},13S_{15},12S_{18}$	48	-	52
	ν_{22}	Ring deformation	863	834	0.5	2.7	0.26	818	1.0	1.5	803	803	807	$30S_{22},20S_{15},13S_{23},12S_{17},10S_{16}$	70	-	30
	ν_{20}	γ-CH_2 rock	832	792	2.5	4.1	0.06	804	1.7	8.5	791	795	796	$51S_{20},19S_{16},11S_{19}$	95	-	5
	ν_{17}	β-CH_2 rock	700	673	0.9	1.4	0.06	682	5.5	2.0	~665	665	665	$12S_{17},32S_{20},19S_{22},15S_{16},10S_{18}$	8	-	92
	ν_{21}	C≡C-H linear bend (in-plane)	557	527	48.5	0.5	0.08	674	45.6	6.7	645	-	-	$100S_{21}$	45	-	55
	ν_{23}	Ring-CCH bend (in-plane)	422	418	0.2	2.5	0.72	430	4.1	3.0	423	423	432	$33S_{23},23S_{22},22S_{25},10S_{17}$	67	-	33
	ν_{24}	Ring puckering	295	294	0.8	5.2	0.66	284	2.7	3.2	282	286	288	$55S_{24},42S_{25}$	59	-	41
	ν_{25}	C-C≡C linear bend (in-plane)	124	123	0.1	4.0	0.72	120	0.2	4.1	-	-	-	$33S_{25},36S_{23},33S_{24}$	64	-	36
A"	ν_{26}	β-CH_2 antisymmetric stretch	3180	2983	11.7	68.5	0.75	3097	25.0	61.7	2968	2965	2965	$67S_{26},28S_{27}$	-	100	-

ν_{27}	γ-CH_2 antisymmetric stretch	3166	2970	10.3	7.7	0.75	3072	10.8	29.2	2968	2965	2965	$72S_{27},23S_{26}$	-	100	-
ν_{28}	γ-CH_2 symmetric stretch	3123	2930	21.3	27.4	0.75	3046	29.0	40.5	2934	2927	2931	$99S_{28}$	-	100	-
ν_{29}	β-CH_2 symmetric stretch	3106	2914	14.2	9.3	0.75	3032	15.5	14.8	2887	2873	2873	$89S_{29},10S_{26}$	-	100	-
ν_{30}	γ-CH_2 deformation	1555	1463	3.3	4.8	0.75	1496	6.3	2.2	1449	1448	1451	$77S_{30},24S_{31}$	-	100	-
ν_{31}	β-CH_2 deformation	1543	1452	1.0	21.7	0.75	1486	1.1	12.6	~1449	1448	1451	$77S_{31},24S_{30}$	-	100	-
ν_{32}	γ-CH_2 wag	1392	1323	0.2	0.4	0.75	1347	0.4	0.3	1320	1320	1318	$48S_{32},21S_{34},12S_{33}$	-	100	-
ν_{34}	β-CH_2 wag	1343	1274	0.0	0.1	0.75	1315	0.1	0.1	-	-	-	$51S_{34},39S_{32}$	-	100	-
ν_{35}	γ-CH_2 twist	1325	1259	1.4	15.1	0.75	1283	1.6	9.9	~1266	1266	1262	$54S_{35},24S_{33},12S_{36}$	-	100	-
ν_{39}	γ-CH_2 rock	1269	1206	0.0	1.4	0.75	1231	0.1	0.2	-	1214	1216	$22S_{39},31S_{35},27S_{36},10S_{33}$	-	100	-
ν_{33}	α-CH bend (out-of-plane)	1214	1159	0.3	6.4	0.75	1167	0.0	5.0	~1162	1150	1156	$18S_{33},27S_{36},22S_{37},11S_{41}$	-	100	-
ν_{36}	β-CH_2 twist	1122	1069	2.2	7.5	0.75	1087	2.3	3.8	1069	1069	1069	$22S_{36},22S_{40},17S_{39},13S_{37},11S_{33}$	-	100	-
ν_{37}	Ring deformation	1058	1006	0.8	3.4	0.75	1022	0.3	3.6	-	1002	1008	$36S_{37},22S_{39},15S_{34}$	-	100	-
ν_{38}	Ring deformation	941	904	3.0	0.3	0.75	899	3.9	0.5	895	-	-	$71S_{38},13S_{33}$	-	100	-
ν_{40}	β-CH_2 rock	855	817	0.0	0.9	0.75	817	0.1	0.8	-	~803	~807	$41S_{40},18S_{39},16S_{41},13S_{37}$	-	100	-
ν_{41}	Ring deformation	656	645	4.7	0.7	0.75	673	49.0	7.8	~629	625	630	$52S_{41},14S_{43},10S_{39}$	-	100	-
ν_{42}	C≡C-H bend (out-of-plane)	560	557	42.9	0.4	0.75	648	2.1	0.5	629	-	-	$86S_{42}$	-	100	-
ν_{43}	Ring-CCH bend (out-of-plane)	499	495	2.9	2.8	0.75	522	6.2	1.4	492	486	490	$37S_{43},45S_{44}$	-	100	-
ν_{44}	C-C≡C (out-of-plane)	177	177	0.2	6.1	0.75	186	1.1	5.7	-	180	181	$54S_{44},34S_{43}$	-	100	-
ν_{45}	Ring twisting	74	74	0.0	0.4	0.75	53	0.0	0.6	-	-	-	$90S_{45}$	-	100	-

[a] MP2(full)/6-31G(d) *ab initio* calculations, scaled frequencies, B3LYP/6-311+G(d,p) calculations, infrared intensities (km/mol), Raman activities ($Å^4$/u), depolarization ratios (dp) and potential energy distributions (P.E.D.s).

[b] Scaled frequencies with scaling factors of 0.88 for CH stretches and CH_2 deformations, 1.0 for heavy atom bends, and 0.90 for all other modes.

[c] Symmetry coordinates with P.E.D. contribution less than 10% are omitted.

The Raman spectra (3500 to 136 cm^{-1}) of the sample dissolved in liquefied xenon (Fig. 36B) at six different temperatures (-50 to -100°C) were recorded on a Trivista 557 spectrometer consisting of a double f = 50 cm monochromator equipped with a 2000 lines mm^{-1} grating, a f = 70 cm spectrograph equipped with a 2400 lines mm^{-1} grating, and a back-illuminated LN2-cooled PI Acton Spec-10:2 kB/LN 2048 x 512 pixel CCD detector. For all experiments, the 514.5 nm line of a 2017-Ar S/N 1665 Spectra-Physics argon ion laser was used for Raman excitation, with the power set to 0.8 Watt. Signals related to the plasma lines were removed by using an interference filter. The frequencies were calibrated using Neon emission lines, and depending on the setup used, are expected to be accurate within 0.4 cm^{-1}. The experimental set-up used to investigate the solutions has been described earlier [23,24]. A home-built liquid cell equipped with four quartz windows at right angles was used to record the spectra.

The *ab initio* and density functional theory calculations were performed with the Gaussian-03 program [22]. The energy minima with respect to nuclear coordinates were obtained by the simultaneous relaxation of all geometric parameters using the gradient method of Pulay [29]. Several basis sets as well as the corresponding ones with diffuse functions were employed with the Møller-Plesset perturbation method [21] to the second order (MP2(full)) as well as with the density functional theory by the B3LYP method. The predicted conformational energy differences are listed in Table 61.

Table 61. Calculated Electronic Energies (Hartree) for the *Eq* (C_s) and Energy Differences (cm^{-1}) for *Ax* (C_s), *Twisted* (C_1), and *Planar* (C_s) Forms of Ethynylcyclopentane.

			Energy Difference[b]		
Method/Basis Set	# Basis Set	*Equatorial* (C_s)[a]	*Axial* (C_s)	*Twist* (C_1)	*Planar* (C_s)
RHF/6-31G(d)	125	0.835565	187	403	2174
RHF/6-31+G(d)	153	0.842019	271	490	2182
MP2(full)/6-31G(d)	125	1.767393	-178	92	2406
MP2(full)/6-31+G(d)	153	1.782766	-40	246	2467
MP2(full)/6-311G(d,p)	186	1.849138	-149	49	2345
MP2(full)/6-311+G(d,p)	214	1.863058	-44	125	2333
MP2(full)/6-311G(2d,2p)	251	2.037352	-224	85	2475
MP2(full)/6-311+G(2d,2p)	279	2.043042	-152	95	2426
MP2(full)/6-311G(2df,2pd)	350	2.112982	-185	100	2524
MP2(full)/6-311+G(2df,2pd)	378	2.117227	-169	123	2493
MP2(full)/aug-cc-pVTZ	552	2.220728	-180		2342
MP2(full) average	-	-	-169 ± 32	96 ± 28	2420 ± 80
B3LYP/6-31G(d)	125	2.695951	248	384	1963
B3LYP/6-31+G(d)	153	2.707166	305	455	1916
B3LYP/6-311G(d,p)	186	2.771491	203	344	1847
B3LYP/6-311+G(d,p)	214	2.773979	253	392	1827
B3LYP/6-311G(2d,2p)	251	2.781992	226	360	1782
B3LYP/6-311+G(2d,2p)	279	2.784391	256	394	1772
B3LYP/6-311G(2df,2pd)	350	2.790001	238	374	1813
B3LYP/6-311+G(2df,2pd)	378	2.792043	263	400	1792
B3LYP/aug-cc-pVTZ	552	2.800208	268	411	1810
B3LYP average	-	-	251 ± 29	390 ± 32	1836 ± 64

[a] Energy of conformer is given as -(E + 270) H.
[b] Energy difference related to the *Eq* conformer.

The vibrational spectra were predicted from the MP2(full)/6-31G(d) calculations. The predicted scaled frequencies were used together with a Lorentzian function to obtain the simulated spectra. Infrared intensities were obtained based on the dipole moment derivatives with respect to Cartesian coordinates. The derivatives were transformed with respect to normal coordinates by $(\partial\mu_u/\partial Q_i) = \sum_j (\partial\mu_u/\partial X_j)L_{ij}$, where Q_i is the i^{th} normal coordinate, X_j is the j^{th} Cartesian displacement coordinate, and L_{ij} is the transformation matrix between the Cartesian displacement coordinates and the normal coordinates. The infrared intensities were then calculated by $(N\pi)/(3c^2)$ $[(\partial\mu_x/\partial Q_i)^2 + (\partial\mu_y/\partial Q_i)^2 + (\partial\mu_z/\partial Q_i)^2]$. The infrared spectra of the vapor, solid, and the predicted infrared spectra for the pure *Eq* and *Ax* conformers, as well as the mixture of the two conformers with relative concentrations calculated for the equilibrium mixture at 25ºC by using the experimentally determined enthalpy difference are shown in Fig. 35 (A-E), respectively. The predicted spectrum is in good agreement with the experimental spectrum which shows the utility of the scaled predicted frequencies and predicted intensities for supporting the vibrational assignment.

Additional support for the vibrational assignments was obtained from the simulated Raman spectra. The evaluation of Raman activity by using the analytical gradient methods has been developed [31-34] and the activity S_j can be expressed as: $S_j = g_j(45\alpha_j^2 + 7\beta_j^2)$, where g_j is the degeneracy of the vibrational mode j, α_j is the derivative of the isotropic polarizability, and β_j is the anisotropic polarizability. To obtain the Raman scattering cross sections, the polarizabilities are incorporated into S_j by

multiplying S_j with $(1-\rho_j)/(1+\rho_j)$ where ρ_j is the depolarization ratio of the j^{th} normal mode. The Raman scattering cross sections and calculated wavenumbers obtained from the Gaussian 03 program were used together with a Lorentzian function to obtain the simulated Raman spectra. Comparison of experimental Raman spectra of the liquid, xenon solutions, and the predicted Raman spectra for the pure *Eq* and *Ax* conformers, as well as, the mixture of the two conformers with relative concentrations calculated for the equilibrium mixture at -60°C by using the experimentally determined enthalpy difference are shown in Fig. 36(A-E). The spectrum of the mixture should be compared to that of the Raman spectra of the liquid and xenon solutions.

VIBRATIONAL ASSIGMENT

To determine the enthalpy differences between the two conformers it is necessary to assign the spectra for both conformers of ethynylcyclopentane. For use in the vibrational assignment *ab initio* predictions from MP2(full)/6-31G(d) calculations were carried out to obtain the force constants, frequencies, infrared intensities, band contours, Raman activities, and depolarization values for both conformers. These predicted quantities, as well as, the group frequencies were used to aid in the assignment of the infrared and Raman spectra.

In order to obtain a complete description of the molecular motions involved in the fundamental modes of c-C_5H_9CCH, a normal coordinate analysis has been carried out. The force field in Cartesian coordinates was obtained with the Gaussian 03 program [22] at the MP2(full) level with the 6-31G(d) basis set. The internal coordinates used to calculate the **G** and **B** matrices are given in Table 62 with the atomic numbering shown in Fig. 37. By using the **B** matrix [30], the force field in Cartesian coordinates was

converted to a force field in internal coordinates. Subsequently, scaling factors of 0.88 for CH stretches and CH_2 deformations and 0.90 for all other modes except heavy atom bends were applied, along with the geometric average of the scaling factors for the interaction force constants, to obtain the fixed scaled force field and resultant wavenumbers. A set of symmetry coordinates was used (Table S11) to determine the corresponding potential energy distributions (P.E.D.s). A comparison between the observed and calculated wavenumbers, along with the calculated infrared intensities, Raman activities, depolarization ratios and potential energy distributions for the *Eq* and *Ax* conformers are listed in Tables 59 and 60, respectively.

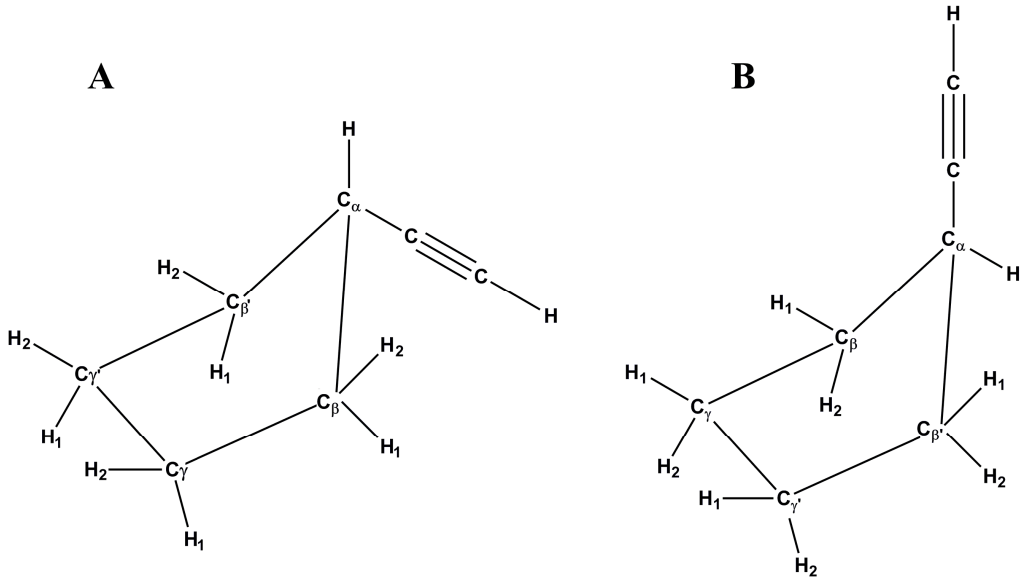

Figure 37. Conformers of ethynylcyclopentane (A) *Eq*; (B) *Ax*.

Table 62. Structural Parameters (Å and Degree), Rotational Constants (MHz) and Dipole Moment (Debye) for Ethynylcyclopentane *Eq* and *Ax* (C_s) Forms.

Structural Parameters	Int. coor.	MP2(full)/ 6-311+G(d,p)		B3LYP/ 6-311+G(d,p)		Microwave[a]		Adjusted r_0[c]	
		Eq	Ax	Eq	Ax	Eq	Ax	Eq	Ax
$rC{\equiv}C$	R_1	1.220	1.221	1.204	1.204	1.209[b]	1.209[b]	1.211(3)	1.211(3)
rC_α-$C{\equiv}C$	R_2	1.457	1.463	1.457	1.464	1.470	1.470	1.461(3)	1.467(3)
rC_α-C_β,$C_{\beta'}$	R_3	1.537	1.540	1.548	1.550	1.541	1.546	1.542(3)	1.542(3)
rC_β-C_γ, $rC_{\beta'}$-$C_{\gamma'}$	R_4	1.539	1.540	1.544	1.546	1.541	1.546	1.541(3)	1.542(3)
rC_γ-$C_{\gamma'}$	R_5	1.554	1.553	1.559	1.557	1.541	1.546	1.556(3)	1.555(3)
$rC{\equiv}C$-H	R_4	1.064	1.065	1.062	1.062	1.055[b]	1.055[b]	1.064(2)	1.065(2)
rC_α-H	r_1	1.099	1.095	1.098	1.095	1.100	1.100	1.099(2)	1.095(2)
rC_β-H_1, $C_{\beta'}$-H_1	r_2	1.096	1.093	1.094	1.091	1.100	1.100	1.096(2)	1.093(2)
rC_β-H_2, $C_{\beta'}$-H_2	r_3	1.093	1.096	1.092	1.095	1.100	1.100	1.093(2)	1.096(2)
rC_γ-H_1, $C_{\gamma'}$-H_1	r_4	1.093	1.093	1.092	1.092	1.100	1.100	1.093(2)	1.093(2)
rC_γ-H_2, $C_{\gamma'}$-H_2	r_5	1.094	1.093	1.093	1.092	1.100	1.100	1.094(2)	1.093(2)
$\angle C_\alpha$-$C{\equiv}C$	ϕ_1	179.8	179.6	179.6	179.9			179.4(5)	179.9(5)
$\angle C_\beta C_\alpha$-$C{\equiv}C$	ϕ_2	114.3	111.0	114.7	112.2	113	110	113.7(5)	111.5(5)
$\angle C_\beta C_\alpha C_{\beta'}$	θ_1	101.8	101.4	102.4	101.9	103.0	101.7	102.6(5)	102.1(5)
$\angle C_\alpha C_\beta C_\gamma$	θ_2	103.7	103.8	104.2	104.8	102	103	103.7(5)	103.7(5)
$\angle C_\beta C_\gamma C_{\gamma'}$	θ_3	105.7	105.6	106.0	106.0	106(5)	106(5)	106.0(5)	105.9(5)
$\angle$H-$C{\equiv}C$	σ	179.6	179.8	179.9	179.9			179.9(5)	179.6(5)
$\angle HC_\alpha$-$C{\equiv}C$	ψ	108.9	109.2	108.2	108.2	113.9	106.5	108.9(5)	109.2(5)
$\angle HC_\alpha C_\beta$	δ	108.6	112.0	108.3	111.1			108.8(5)	111.2(5)
$\angle H_1 C_\beta C_\alpha$	λ_1	108.2	112.9	108.6	112.6			108.2(5)	112.9(5)
$\angle H_1 C_\beta C_\gamma$	λ_2	110.7	113.2	110.8	113.2			109.1(5)	114.9(5)
$\angle H_2 C_\beta C_\alpha$	λ_3	112.8	108.1	112.4	108.0			112.8(5)	108.1(5)
$\angle H_2 C_\beta C_\gamma$	λ_4	113.4	110.4	113.3	110.4			114.9(5)	108.6(5)

$\angle H_1C_\beta H_2$	λ_5	107.9	108.3	107.4	107.7	109.5	109.5	107.9(5)	108.3(5)
$\angle H_1C_\gamma C_\beta$	π_1	111.5	110.0	111.4	110.2			111.5(5)	110.0(5)
$\angle H_1C_\gamma C_{\gamma'}$	π_2	112.2	110.2	112.2	110.2			112.8(5)	109.5(5)
$\angle H_2C_\gamma C_\beta$	π_3	110.1	111.4	110.4	111.3			110.1(5)	111.4(5)
$\angle H_2C_\gamma C_{\gamma'}$	π_4	110.3	112.2	110.3	112.3			109.3(5)	112.7(5)
$\angle H_1C_\gamma H_2$	π_5	107.1	107.4	106.7	106.9	109.5	109.5	107.1(5)	107.4(5)
$\tau C_\beta C_\alpha C_{\beta'} C_{\gamma'}$	τ_1	42.2	42.6	39.8	38.9	41(5)	39(5)	40.8(5)	41.6(5)
$\tau C_\beta C_\gamma C_{\gamma'} C_{\beta'}$	τ_2	0.0	0.0	0.0	0.0	0.0	0.0	0.0(5)	0.0(5)
A(MHz)		6417.27	4235.96	6339.43	4331.55	6349.37(40)	4264.82(43)	6350.25	4265.45
B(MHz)		1759.34	2191.33	1755.30	2117.51	1765.18(1)	2168.76(1)	1766.02	2169.63
C(MHz)		1477.47	2067.11	1469.16	1963.24	1480.55(1)	2032.08(1)	1479.74	2032.11
$\lvert\mu_a\rvert$		0.984	0.803	0.990	0.819				
$\lvert\mu_b\rvert$		0.000	0.000	0.000	0.000				
$\lvert\mu_c\rvert$		0.042	0.216	0.073	0.274				
$\lvert\mu_t\rvert$		0.985	0.832	0.993	0.864				

[a]Ref [120], values without uncertainties are taken from Ref [119].
[b]Value from Ref [136]
[c]Adjusted parameters using the microwave data from Ref [120] for the given ground states.

The C≡C modes are of significant note where the experimental and predicted frequencies are significantly different and so group frequencies and B3LYP predictions can be used to aid in the assignment of this fundamental. The approximate descriptions given in most cases are consistent with most of the "group frequencies" previously given for the similar mono-substituted cyclopentanes[5,6]. Fortunately there are nearly equal amounts of both conformers so a nearly complete assignment could be made for both conformers which gave a large number of fundamentals which could be chosen for enthalpy determinations. Careful consideration was given to choose bands with reasonable intensities and without interference from bands from the other conformer.

CONFORMATIONAL STABILITY

To determine the enthalpy differences among the two observed conformers of ethynylcyclopentane, the sample was dissolved in liquefied xenon and the Raman spectra were recorded as a function of temperature from -50 to -100°C. Relatively small interactions are expected to occur between xenon and the sample though the sample can associate with itself through van der Waals interactions. However, due to the very small concentration of sample (~10^{-4} molar) self association is greatly reduced. Therefore, only small frequency shifts are anticipated for the xenon interactions when passing from the gas phase to the liquefied xenon solutions (Fig. 38). A significant advantage of this study is that the conformer bands are better resolved in comparison with those in the infrared spectrum of the gas or the Raman spectra of the liquid. From *ab initio* calculations, the dipole moments of the two conformers are predicted to have similar values and the molecular sizes of the two conformers are nearly the same, so the ΔH value obtained

from the temperature dependent Raman study is expected to be close to that for the gas [16-20].

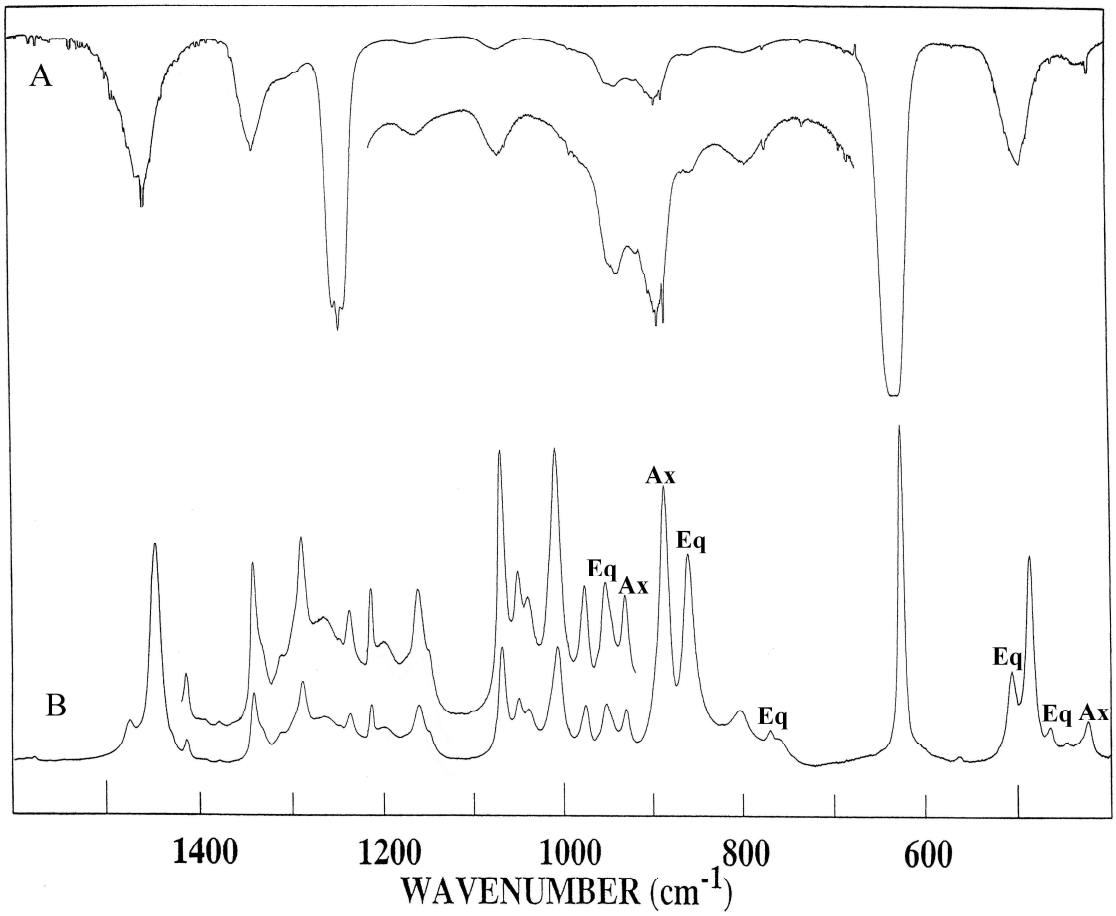

Figure 38. Infrared and Raman spectra of ethynylcyclopentane (A) observed mid-infrared spectrum of gas; (B) Raman spectrum of Xe solution at -60°C.

Once confident assignments have been made for the fundamentals of both conformers the task was then to find pairs of bands from which the enthalpy determination could be obtained. To minimize the effect of combination and overtone bands in the enthalpy determination it is desirable to have the lowest frequency pair(s) that is possible for the determination. The bands should also be sufficiently resolved so reproducible intensities can be obtained. The fundamentals at 464, 505, 770, 861, and 952 cm^{-1} were selected for the *Eq* conformer bands as they are free of interfering bands and in the lower frequency region of the spectrum. For the *Ax* form the fundamentals at 423 and 930 cm^{-1} are relatively free from interfering bands which allowed the determination of their band intensities to be confidently measured. The band at 887 cm^{-1} has an underlying *Eq* fundamental, though due to the high activity of the *Ax* fundamental and the low activity of the underlying *Eq* fundamental the band intensity is not significantly affected by the *Eq* fundamental.

The intensities of the individual bands were measured as a function of temperature and their ratios were determined (Fig. 39). By application of the van't Hoff equation $-\ln K = \Delta H/(RT) - \Delta S/R$, the enthalpy differences were determined from a plot of $-\ln K$ versus $1/T$, where $\Delta H/R$ is the slope of the line and K is substituted with the appropriate intensity ratios, *i.e.* $I_{conf\text{-}1} / I_{conf\text{-}2}$, etc. It was assumed that ΔH, ΔS, and α are not functions of temperature in the range studied.

These eight bands, five for *Eq* and three for *Ax*, were utilized for the determination of the enthalpy difference by combining them to form 15 band pairs where the enthalpy differences for each pair are given in Table 63. These 15 band pairs were combined to form a single data set and the enthalpy difference was determined with a

value of 94 ± 2 cm^{-1} (Table 63). This error limit is derived from the statistical standard deviation of one sigma of the measured intensity data taken as a single data set. This error determination does not take into account small associations with the liquid xenon or the interference of overtones and combination bands in near coincidence with the measured fundamental intensities. The variations in the individual values are undoubtedly due to these types of interferences, but by taking several pairs, the effect of such interferences should cancel. However, this statistical uncertainty is probably better than can be expected from this technique and, therefore, an uncertainty of about 10% in the enthalpy difference is probably more realistic i.e. 94 ± 9 cm^{-1}. From the enthalpy difference the abundance of the *Ax* conformer present at ambient temperature is estimated to be 39 ± 2%.

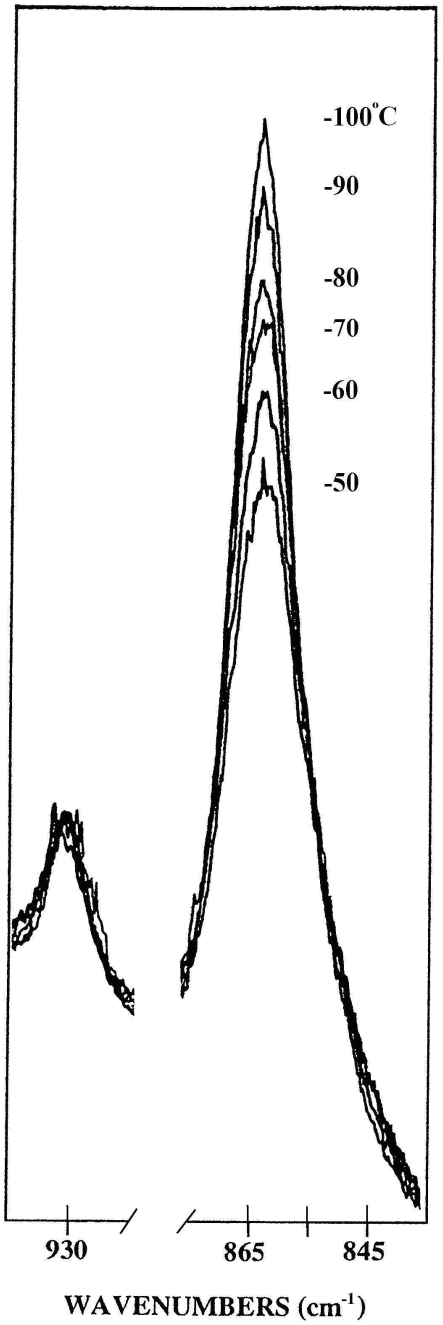

Figure 39. Temperature (-50 to -100°C) dependent Raman spectrum of ethynylcyclopentane dissolved in liquid xenon.

Table 63. Temperature and Activity Ratios of the *Eq* and *Ax* Bands of Ethynylcyclopentane.

	T(°C)	1/T ($\times 10^{-3}$ K^{-1})	I_{464} / I_{423}	I_{464} / I_{887}	I_{464} / I_{930}	I_{505} / I_{423}	I_{505} / I_{887}	I_{505} / I_{930}	I_{770} / I_{423}	I_{770} / I_{887}
Liquid xenon	–50.0	4.584	0.885	0.101	0.885	2.154	0.247	2.154	2.000	0.229
	–60.0	4.692	0.923	0.105	0.923	2.231	0.254	2.231	2.077	0.237
	–70.0	4.923	0.962	0.109	0.962	2.308	0.262	2.308	2.154	0.245
	–80.0	5.177	1.000	0.113	1.000	2.385	0.270	2.385	2.231	0.252
	–90.0	4.460	1.038	0.116	1.038	2.462	0.276	2.462	2.308	0.259
	–100.0	5.775	1.077	0.120	1.077	2.538	0.282	2.538	2.385	0.265
ΔH^a (cm^{-1})			105 ± 5	91 ± 6	105 ± 5	88 ± 4	72 ± 5	88 ± 4	94 ± 5	78 ± 6

	T(°C)	1/T ($\times 10^{-3}$ K^{-1})	I_{770} / I_{930}	I_{861} / I_{423}	I_{861} / I_{887}	I_{861} / I_{930}	I_{952} / I_{423}	I_{952} / I_{887}	I_{952} / I_{930}
Liquid xenon	–50.0	4.584	2.000	5.308	0.608	5.308	1.000	0.115	1.000
	–60.0	4.692	2.077	5.538	0.632	5.538	1.077	0.123	1.077
	–70.0	4.923	2.154	5.769	0.655	5.769	1.115	0.127	1.115
	–80.0	5.177	2.231	6.000	0.678	6.000	1.154	0.130	1.154
	–90.0	4.460	2.308	6.231	0.698	6.231	1.192	0.134	1.192
	–100.0	5.775	2.385	6.462	0.718	6.462	1.231	0.137	1.231
ΔH^a (cm^{-1})			94 ± 5	105 ± 5	89 ± 6	105 ± 5	104 ± 12	87 ± 12	104 ± 12

[a] Average value $\Delta H = 94 \pm 2$ cm^{-1} (1.12 ± 0.02 kJ/mol) with the *Eq* conformer the more stable form and the statistical uncertainty (1σ) obtained by utilizing all of the data as a single set.

STRUCTURAL PARAMETERS

In the microwave study [120], all but three of the structural parameters were assumed for the two identified conformers. The three parameters that were not assumed but were fitted were the $C_\beta C_\gamma C_{\gamma'}$ angle, the $C_\beta C_\alpha C_{\beta'} C_{\gamma'}$ and $C_\beta C_{\beta'} C_\alpha C{\equiv}C$ dihedral angles. Since the assumed structural parameters were common for both conformers, while the assumptions are reasonable they contribute significantly to the uncertainties of the structural parameters obtained in the initial microwave study. Therefore, we have determined the structural parameters for both rotamers by utilizing the rotational constants previously reported from the microwave study [120]. Only one isotopic species was studied for both conformers and, thus, only three rotational constants are available for each conformer.

We have found that good structural parameters for hydrocarbons and many substituted ones can be determined by adjusting the structural parameters obtained from the *ab initio* MP2(full)/6-311+G(d,p) calculations to fit the rotational constants obtained from microwave experimental data by using a computer program "A&M" (*Ab initio* and Microwave) developed [14] in our laboratory. In order to reduce the number of independent variables, the structural parameters are separated into sets according to their types where bond distances in the same set keep their relative ratio, and bond angles in the same set keep their difference in degrees. This assumption is based on the fact that errors from *ab initio* calculations are systematic. Additionally, we have shown that the differences in predicted distances and angles from the *ab initio* calculations for different conformers of the same molecule can usually be used as one parameter with the *ab initio* predicted differences except for some dihedral angles. Also it has been shown the C≡C

distance is nearly constant irrespective of the substitutions on it [52]. Therefore, it should be possible to obtain "adjusted r_0" structural parameters for both conformers of ethynylcyclopentane by utilizing the previously reported six rotational constants from the earlier microwave study [120] by fixing the C≡C distance and utilizing the sets as indicated.

We [51] have also shown that *ab initio* MP2(full)/6-311+G(d,p) calculations predict the r_0 structural parameters for more than fifty carbon-hydrogen distances to at least 0.002 Å compared to the experimentally determined values from isolated CH stretching frequencies which were compared [5] to previously determined values from earlier microwave studies. Therefore, all of the carbon-hydrogen distances can be taken from the MP2(full)/6-311+G(d,p) predicted values for *Eq* and *Ax* conformers of ethynylcyclopentane. The resulting adjusted r_0 parameters are listed in Table 62, where it is believed that the C-C distances should be accurate to ± 0.003 Å, the C-H distances should be accurate to ± 0.002 Å, and the angles should be within ± 0.5°.

The fit of the six determined rotational constants (Table 64) by the structural parameters for the *Eq* and *Ax* conformers is good with the differences being less than 1 MHz where the largest difference is 0.88 MHz. Therefore, it is believed that the suggested uncertainties are realistic values and the determined structural parameters are probably as accurate as can be obtained for the molecule in the gas phase by either electron diffraction or microwave substituted methods.

Table 64. Comparison of Rotational Constants (MHz) Obtained from *Ab Initio* MP2(full)/6-311+G(d,p) Predictions, Experimental Values[a] from Microwave Spectra, and Adjusted r_0 Structural Parameters for Ethynylcyclopentane.

Conformer	Rotational Constants	MP2(full)/ 6-311+G(d,p)	Experimental[a]	Adjusted r_0	$\|\Delta\|$
	A	6417.27	6349.37(40)	6350.25	0.88
Eq-C_5H_9CCH	B	1759.34	1765.18(1)	1766.02	0.84
	C	1477.47	1480.55(1)	1479.74	0.81
	A	4235.96	4264.82(43)	4265.45	0.63
Ax-C_5H_9CCH	B	2191.33	2168.76(1)	2169.63	0.87
	C	2067.11	2032.08(1)	2032.11	0.03

[a] Ref [120].

DISCUSSION

The predicted infrared intensities from the B3LYP calculations for the C≡C stretch are 18 times greater than those predicted from the MP2 calculations. Similarly the Raman activities for this mode are almost three times more intense. These large differences are the result of the MP2 predicted distance for the triple bond being nearly 0.016 Å longer than the value predicted from the B3LYP calculations, which are significantly closer to the experimental r_0 value (Table 62). There are smaller predicted intensity differences for the Ring-CCH and C≡C-H in-plane bending modes where the infrared intensities are predicted 1/12 as intense for the Ring-CCH bend but nearly twice the intensity for the C≡C-H bend, respectively, from the MP2 calculations compared to those from the B3LYP calculations.

The assignment was somewhat complicated by the nearly equal amounts of both conformers present. Therefore, significant reliance on the predicted wavenumbers was necessary to assign many of the modes with group frequencies also playing a significant role. Nevertheless the predicted wavenumbers for the *Eq* and *Ax* forms had average errors of 11 cm^{-1} which is 0.7% for the A′ modes and 9 cm^{-1} for the A″ modes which is 0.6% error. The C≡C stretch and C≡C-H bending modes were not included due to the poor *ab initio* predictions for these modes. A significant amount of the error is due to the predictions for the β-CH_2 rock and the γ-CH_2 wag but the assignments agree with previously reported group frequencies for these modes.

For the *Eq* conformer, the mixing of the normal modes is relatively minor for the A′ fundamentals except for the β-CH_2 twist and a ring deformation (ν_{15}), but for the A″ fundamentals there are three modes; β-CH_2 wag, γ-CH_2 rock, and β-CH_2 rock which have four or more symmetry coordinates contributing more than 10%. For the *Ax* conformer there is significantly more mixing of the modes. This indicates that many of these fundamentals are more complicated than the relatively simple descriptions they have been given.

When this study was initiated there was some question whether the *Eq* or *Ax* conformer is the more stable form. From the microwave study [120] the *Eq* conformer was reported to be more stable by 94 ± 24 cm^{-1} but *ab initio* calculations predict the *Ax* conformer more stable by approximately 180 cm^{-1}. Also it should be noted that cyanocyclopentane which is a very similar molecule to ethynylcyclopentane was reported [137] to have the *Ax* conformer the more stable form by 109 ± 37 cm^{-1}. Thus it was necessary to make a very definitive determination of the more stable conformer.

The process used was first to obtain the conformer which was the stable form in the crystal. The infrared spectrum of the solid (Fig. 35E) was obtained and the spectra was predicted of gaseous *Eq* (Fig. 35D) and *Ax* (Fig. 35C) ethynylcyclopentane. The spectra were compared and as can be seen from Fig. 35 the spectrum of the solid corresponds to that of the pure *Eq* conformer where the bands at 769, 1297, and 1343 cm^{-1} provide clear evidence of the stable form.

Next the variable temperature spectrum of the sample in liquefied xenon was obtained and the spectra were confidently assigned. The determined ΔH values conclusively showed that the *Eq* conformer was the more stable form. The value obtained for the enthalpy difference indicates that this is not an effect of one conformer associating with the xenon to form a more energetically stable complex.

With the confidence of the assignments of the lower wavenumber modes for the *Eq* and *Ax* conformers and the use of 15 band pairs as well as the statistical uncertainty the value for the enthalpy difference is believed to be well determined. The uncertainty of the value for each individual pair ranges from a high value of 12 cm^{-1} to a low of 4 cm^{-1}. This relatively small spread coupled with the fact that overtone and combination bands are not frequently observed in the Raman spectra indicates that there is little interference from overtones or combination bands having a significant effect on the determined enthalpy difference obtained in this study. The experimentally determined enthalpy difference between the more stable *Eq* conformer and the *Ax* form with the value of 94 ± 9 cm^{-1} is in excellent agreement with the previously reported value from the microwave study [120] of 94 ± 24 cm^{-1}.

The only way for a determination of the enthalpy difference that would not be altered by association would require the use of a sample in a very low pressure gaseous phase. It is doubtful that this would be an easy experiment to determine the enthalpy and, therefore, the value obtained from the xenon solution must be considered the best determined enthalpy difference at this time. The use of enthalpy determinations from 15 band pairs indicates the accuracy of the determination by this technique.

The reported enthalpy differences should be appropriate for comparison to *ab initio* predicted values or enthalpy differences obtained for other substituted cyclopentanes. The *ab initio* predicted energy difference from the MP2(full)/aug-cc-pVTZ (552 basis sets) calculation gave the *Ax* conformer more stable by 180 cm^{-1} (2.15 kJ/mol) than the *Eq* form. While the B3LYP/aug-cc-pVTZ (552 basis sets) calculation gave the *Eq* conformer as more stable by 268 cm^{-1} (3.20 kJ/mol) than the *Ax* form. These values are both far off in magnitude and the *ab initio* value even predicts the wrong conformer as being the more stable form. It is interesting to note for cyanocyclopentane [137] the *ab initio* and DFT calculations predict similar energy differences to those predicted in the current study.

The adjusted r_0 structural parameters have been determined for the *Eq* and *Ax* forms of ethynylcyclopentane. In the initial microwave study [120] only three parameters were determined for the *Eq* [*Ax*] form which were the angle (°) $\angle C_\beta C_\gamma C_{\gamma'}$ = 106(5) [106(5)], as well as, the dihedral angles (°) $\tau C_\beta C_\alpha C_{\beta'} C_{\gamma'}$ = 41(5) [39(5)] and $C_\beta C_{\beta'} C_\alpha C{\equiv}C$ = 130(5) [123(5)]. Due to the large error limits the values from the current study agree with those from the previous study.

It is also of interest to compare the structural parameters of ethynylcyclopentane with the corresponding parameters of other monosubstituted-cyclopentanes. The adjusted r_0 structure has been determined for the *Ax* [*Eq*] form of cyanocyclopentane [137] with the distances (Å) rC_α-C_β = 1.542(3) [1.543(3)], rC_β-C_γ = 1.542(3) [1.544(3)], rC_γ-$C_{\gamma'}$ = 1.559(5) [1.564(5)] and dihedral angle (°) $\tau C_\alpha C_\beta C_\gamma C_{\gamma'}$ = 25.8(5) [26.1(5)]. There is no significant difference between the cyano- and ethynyl-cyclopentane ring parameters as the differences are within the respective uncertainties. The adjusted r_0 structure has also been determined for the *Ax* [*Eq*] conformers of bromocyclopentane [76] with the distances (Å) rC_α-C_β = 1.526(5) [1.525(5)], rC_β-C_γ = 1.543(5) [1.543(5)], rC_γ-$C_{\gamma'}$ = 1.555(5) [1.559(5)] and dihedral angle (°) $\tau C_\beta C_\alpha C_{\beta'} C_{\gamma'}$ = 40.2(5) [44.0(5)]. The rC_α-C_β distance is significantly shorter and the $\tau C_\beta C_\alpha C_{\beta'} C_{\gamma'}$ dihedral angle is slightly more than 4° larger for the *Eq* conformer. The remaining parameters are within the respective uncertainties.

The *ab initio* and DFT calculations predict similar energy differences for cyanocyclopentane as those predicted for ethynylcyclopentane. However, the most recent study of cyanocyclopentane determined [137] the *Ax* conformer to be more stable than the *Eq* form. This is opposite of the order of stability of ethynylcyclopentane. This is of interest since there should be significant similarities between cyanocyclopentane and ethynylcyclopentane. However, it should be noted that the conformational determination of cyanocyclopentane was made from a single band pair and only five temperatures were used. The relation of the ethynyl- substituent to the conformational stability as compared to the cyano- group is explained by Klaebo et al. in their publication [138] for the six membered ring where the *Eq* conformer was determined to be the most stable form for

both ethynylcyclohexane and cyanocyclohexane in the liquid and gaseous phases however in the crystalline solid cyanocyclohexane is more stable in the *Ax* form while ethynylcyclohexane is most stable as the *Eq* conformer. This difference in conformational stability is according to Klaebo et al. "correlated with a high electronic density at the carbon bonded to the ring in ethynylcyclohexane lowered in the CCN due to the electronegative N atom with its lone pair orbital." A reinvestigation of the order of stability of cyanocyclopentane by using the variable temperature Raman spectra of the xenon solution is needed since it is doubtful that these two molecules will have significantly different conformer stabilities.

The cyanomethylcyclopropane [139] and ethynylmethylcyclopropane [140] molecules have significant differences of the effect on these molecules conformational differences due to the attached $-CH_2CN$ and $-CH_2C{\equiv}CH$ moieties. The carbon to the ring distances (Å) in the cyano molecule are 1.519 (cis) and 1.513 (gauche) and similar bonds of the ethynyl molecule are 1.522 (cis) and 1.516 (gauche) so that these distances are nearly the same. However, the experimental enthalpy difference for the ethynyl molecule is 147 ± 14 cm^{-1} with the cis conformer the more stable form, whereas for the cyano molecule the experimental enthalpy difference is 54 ± 4 cm^{-1} but the gauche conformer is the more stable form. For the ethynyl molecule *ab initio* MP2(full)6-311+G(2d,2p) calculations also predict the cis form the more stable ($\Delta E = 174$ cm^{-1}) conformer which is in agreement with the experimental results and similarly for the cyano compound the cis form again is predicted to be the more stable form by 134 cm^{-1} which does not agree with the experimental determination of the gauche conformer which is the more stable form.

The similarities of the ring parameters between cyanocyclopentane and ethynylcycplopentane and the necessity for experimental determination of the enthalpy difference between the *Eq* and *Ax* conformers of ethynylcyclopentane indicates the monosubstituted-cyclopentanes with triple bond substituents requires more study. The pseudo triple bond isocyanide substituent is currently an understudied moiety and may help to expand the understanding of this class of compounds. Also of interest are five membered rings where the substituent is in the ring i.e. pyrrolidine where the conformers at ambient temperature are the *Eq* and twist forms instead of *Eq* and *Ax*. The phosphorous compound (phospholane) is also of interest as it may have similar conformational stabilities and phosphorous compounds have a great degree of bioactivity. The large change in conformational stability due to differences in the substituent on (or in) the ring make the substituted five membered rings or interest.

CHAPTER 11

MICROWAVE, INFRARED, AND RAMAN SPECTRA, STRUCTURAL PARAMETERS, VIBRATIONAL ASSIGNMENTS AND THEORETICAL CALCULATIONS OF 1,3-DISILACYCLOPENTANE

INTRODUCTION

Considerable interest in the structure of cyclopentane resulted when it was proposed that the two low frequency bending modes could have nearly equal frequencies which resulted in a vibration that was described as pseudorotation [133]. However the concept of this motion for cyclopentane was not readily accepted particularly when the low frequency ring mode of this molecule appeared normal [141]. Also there was further reluctance to accept the pseudorotation motion of the puckering motion with the consequent indefiniteness of the mode [142,143]; however after two decades evidence was reported [144] from the CH_2 deformation of cyclopentane that the ring was undergoing pseudorotation which was nearly barrier free.

With the acceptance of pseudorotation there was a number of investigations on conformations of mono substituted cyclopentane molecules and the determination of the most stable structure. Some of the earliest conformational determinations were the halides, i.e. bromine, chlorine and fluorine. In the initial investigation [117,145] of these three molecules it was reported that all three had the envelope-equatorial conformer as the most stable forms in the fluid phases. A second conformer was also identified in the fluid phases as the envelope-axial forms. However from later studies [121] it was demonstrated that there was only one conformer present in the fluid phases of

fluorocyclopentane and it was the envelope-equatorial forms. Much later it was shown that the one form was not the envelope conformer but the twisted form [123]. Also it should be noted that incorrect conformational structures for five membered rings with another species, such as nitrogen instead of CH_2 have been initially reported [146,147] as the envelope form. From a later vibrational infrared study [148] it was shown that the conformer was the twisted form. Thus it is not easy to predict what the conformational structure will be for many different types of five membered rings. The conformational and structural studies of five membered rings continue to be of scientific interest because of these uncertainties.

Of particular interest are the heterocyclic five membered ring molecules where many important biomolecules are five membered ring heterocycles. The five membered rings of silicon and carbon have not been significantly studied. We recently began to investigate a number of mono-substituted 1-silacyclopentane compounds [149-151] of the form c-C_4H_8SiH-X where X has been several halogens. From these studies it was found that the twist conformer with no symmetry was the most stable form. However, only for the X = F molecule were the adjusted r_0 structural parameters determined. The 1,3- silacyclopentane compounds of the form c-$C_3H_6(SiX_2)_2$ where X= H and perhaps other halogens has largely not been studied due to difficulties in the synthesis of these compounds. The only previous publications of this compound are several synthesis studies [152-155] with only basic characterizations of these molecules. These compounds are of significant interest as the change from carbon to silicon significantly changes the physical and physiochemical properties of these molecules where the carbon analogue is normally stable in the equatorial and axial conformers. However, the single silicon

heterocycle molecule is [152] the twist form with only one stable conformer, whereas the structure of the double silicon molecule has not previously been determined. Therefore, we have initiated microwave, infrared and Raman spectroscopy studies to determine the stable conformer or conformers, the structural parameters, and vibrational fundamental frequencies which we expect to compare to the corresponding carbon compound.

To support the experimental studies we have obtained harmonic force constants, infrared intensities, Raman activities, depolarization ratios, and frequencies of the vibration fundamentals from MP2(full)/6-31G(d) ab initio calculations. To obtain predictions on the conformational stabilities we have carried out MP2(full) ab initio and density functional theory (DFT) calculations by the B3LYP method by utilizing a variety of basis sets. The r_0 structural parameters have been obtained by combining the MP2(full)/6-311+G(d,p) ab initio predicted parameters with the determined rotational constants obtained from this study. The results of these spectroscopic, structural, and theoretical studies of 1,3-disilacyclopentane (c-$C_3H_6Si_2H_4$) are reported herein.

EXPERIMENTAL AND THEORETICAL METHODS

The c-$C_3H_6Si_2H_4$ compound was prepared according to the method of Laane (personal communication) with modifications. The sample was first purified by trap-to-trap and was also further purified by a low-temperature, low-pressure fractionation column. The purity of the sample was checked by infrared and nuclear magnetic resonance spectroscopy.

The rotational spectrum of c-$C_3H_6Si_2H_4$ was obtained by using a CP-FTMW spectrometer developed at the University of Virginia, operating in the 6.5 to 18 GHz

range. The chirped pulse methods used in this study have been described in detail previously [28], so only the brief details relevant to this experiment are necessary.

The microwave source was a 24 GS/s arbitrary waveform generator, producing a 12-0.5 GHz linear frequency sweep in 1 μs. The pulse was upconverted to 6.5-18 GHz by a 18.95 GHz phase-locked resonant dielectric oscillator (PDRO), and then amplified by a pulsed 300 W traveling wave tube amplifier. The amplified pulse is then transmitted through free space between two standard-gain microwave horns, where it interacts with a molecular beam generated by five pulsed nozzles (General Valve Series 9) operating perpendicular to the propagation direction of the microwave pulse. On the detection end, the receiver is protected from the high power pulse by a combination of a PIN diode limiter and single-pole microwave switch. The resulting molecular free induction decay (FID) was then amplified and digitized directly on a 100 GS/s oscilloscope with 33 GHz of hardware bandwidth, with a 20 μs detection time per FID. Due to the speed of this excitation and detection process, a sequence of 10 excitation/detection cycles is possible per gas pulse, and all ten detected FIDs are collected and averaged together before the next valve injection cycle begins. Phase stability of this experiment over the course of many valve injection cycles is enabled by locking all the frequency sources and the oscilloscope to a 10 MHz Rb-disciplined quartz oscillator. For this experiment, approximately 78 000 valve injection cycles of the sample gas were completed at 3.3 Hz to create a time-averaged spectrum of 780 000 molecular FIDs (approximately 6.5 hours of averaging). Additionally, the time domain resolution afforded by a 20 μs FID generates an average Doppler broadened linewidth of approximately 130 kHz at FWHM.

The sample for spectral investigation was prepared by balancing c-$C_3H_6Si_2H_4$ vapor with approximately 3.4 atm of Ne gas (GTS Welco) for a total sample concentration of approximately 0.1%. This afforded a frequency-domain dynamic range of approximately 4000:1 at 780 000 averages, which enabled assignment of all common heavy atom single isotopologues (^{13}C, ^{29}Si, ^{30}Si) in natural abundance as well as a double isotopologue (^{29}Si / ^{30}Si). These assignments are listed in Tables 65-67 and the experimental analysis of c-$C_3H_6Si_2H_4$ was supplemented with ab initio electronic structure calculations for rotational constant and centrifugal distortion predictions (Table 68). These calculations were performed with the Gaussian 09 suite of programs [156].

Table 65. Rotational transition frequencies (MHz) of the ground vibrational state of c-$C_3H_6Si_2H_4$.

Transitions	ν_{obs}	$\Delta\nu^a$
$3_{1\,2} \leftarrow 3_{0\,3}$	6029.5499	0.002
$1_{1\,1} \leftarrow 0_{0\,0}$	6355.8855	-0.002
$5_{3\,2} \leftarrow 5_{2\,3}$	7271.7928	0.001
$2_{2\,1} \leftarrow 2_{1\,2}$	7438.3389	-0.003
$6_{3\,3} \leftarrow 6_{2\,4}$	7609.4435	-0.005
$5_{2\,3} \leftarrow 5_{1\,4}$	7697.0649	-0.001
$2_{0\,2} \leftarrow 1_{1\,1}$	7796.2244	0.004
$4_{3\,1} \leftarrow 4_{2\,2}$	7883.8794	-0.004
$4_{2\,3} \leftarrow 3_{3\,0}$	8765.6491	0.002
$3_{3\,0} \leftarrow 3_{2\,1}$	8847.0955	-0.001
$3_{2\,2} \leftarrow 3_{1\,3}$	9038.6740	-0.002
$4_{1\,3} \leftarrow 4_{0\,4}$	9163.4355	0.000
$8_{4\,4} \leftarrow 8_{3\,5}$	9613.0200	0.000
$7_{4\,3} \leftarrow 7_{3\,4}$	9839.0175	-0.002
$3_{3\,1} \leftarrow 3_{2\,2}$	10202.2062	-0.001
$2_{1\,2} \leftarrow 1_{0\,1}$	10232.3159	0.000
$6_{2\,4} \leftarrow 6_{1\,5}$	10780.1754	-0.001
$4_{3\,2} \leftarrow 4_{2\,3}$	10945.4142	0.000
$6_{4\,2} \leftarrow 6_{3\,3}$	10961.8345	-0.002

Transitions	ν_{obs}	$\Delta\nu$[a]
$5_{3\,3} \leftarrow 4_{4\,0}$	11040.7921	-0.001
$3_{1\,2} \leftarrow 2_{2\,1}$	11056.0749	0.004
$4_{2\,3} \leftarrow 4_{1\,4}$	11161.2729	-0.003
$5_{3\,3} \leftarrow 5_{2\,4}$	12218.9057	0.000
$5_{4\,1} \leftarrow 5_{3\,2}$	12263.4777	0.004
$4_{2\,2} \leftarrow 3_{3\,1}$	12380.1696	0.007
$3_{0\,3} \leftarrow 2_{1\,2}$	12464.8663	0.002
$5_{1\,4} \leftarrow 5_{0\,5}$	12642.8522	0.000
$4_{4\,0} \leftarrow 4_{3\,1}$	13167.9785	0.009
$4_{4\,1} \leftarrow 4_{3\,2}$	13633.0508	0.008
$3_{1\,3} \leftarrow 2_{0\,2}$	13780.9194	-0.001
$5_{4\,2} \leftarrow 5_{3\,3}$	13783.4088	0.010
$6_{3\,4} \leftarrow 6_{2\,5}$	14050.0729	0.007
$6_{4\,3} \leftarrow 6_{3\,4}$	14280.1935	0.007
$7_{2\,5} \leftarrow 7_{1\,6}$	14437.3442	-0.003
$2_{2\,1} \leftarrow 1_{1\,0}$	15191.2031	-0.003
$2_{2\,0} \leftarrow 1_{1\,1}$	16463.7296	-0.006
$4_{0\,4} \leftarrow 3_{1\,3}$	16765.1093	-0.010
$4_{1\,3} \leftarrow 3_{2\,2}$	16889.8728	-0.006
$6_{5\,2} \leftarrow 6_{4\,3}$	17262.7051	-0.013
$4_{1\,4} \leftarrow 3_{0\,3}$	17329.8483	0.006

[a] $\Delta\nu = \nu_{obs} - \nu_{calc}$ in MHz.

Table 66. Rotational transition frequencies (MHz) of the ground vibrational state of c-$C_3H_6Si_2H_4$.

^{29}Si			^{30}Si		
Transitions	ν_{obs}	$\Delta\nu$[a]	Transitions	ν_{obs}	$\Delta\nu$[a]
$1_{1\,1} \leftarrow 0_{0\,0}$	6335.7803	-1	$1_{1\,1} \leftarrow 0_{0\,0}$	6316.6031	-1
$5_{3\,2} \leftarrow 5_{2\,3}$	7392.4986	4	$5_{2\,3} \leftarrow 5_{1\,4}$	7473.4399	-7
$2_{2\,1} \leftarrow 2_{1\,2}$	7477.9138	2	$2_{2\,1} \leftarrow 2_{1\,2}$	7516.4809	0
$5_{2\,3} \leftarrow 5_{1\,4}$	7580.1960	2	$2_{0\,2} \leftarrow 1_{1\,1}$	7558.8852	-1
$6_{3\,3} \leftarrow 6_{2\,4}$	7626.8853	-5	$4_{3\,1} \leftarrow 4_{2\,2}$	8210.8749	4
$2_{0\,2} \leftarrow 1_{1\,1}$	7675.3853	1	$3_{2\,2} \leftarrow 3_{1\,3}$	9046.1478	2
$4_{3\,1} \leftarrow 4_{2\,2}$	8049.7378	2	$3_{3\,0} \leftarrow 3_{2\,1}$	9160.1439	9
$3_{3\,0} \leftarrow 3_{2\,1}$	9006.9139	-3	$2_{1\,2} \leftarrow 1_{0\,1}$	10127.7041	0
$4_{1\,3} \leftarrow 4_{0\,4}$	9024.6961	2	$3_{3\,1} \leftarrow 3_{2\,2}$	10409.0807	5
$3_{2\,2} \leftarrow 3_{1\,3}$	9041.9601	-3	$4_{2\,3} \leftarrow 4_{1\,4}$	11081.4784	-8
$2_{1\,2} \leftarrow 1_{0\,1}$	10178.9173	3	$4_{3\,2} \leftarrow 4_{2\,3}$	11089.4188	6
$3_{3\,1} \leftarrow 3_{2\,2}$	10307.2952	1	$3_{0\,3} \leftarrow 2_{1\,2}$	12175.8957	-4

^{29}Si			^{30}Si		
Transitions	ν_{obs}	$\Delta\nu^a$	Transitions	ν_{obs}	$\Delta\nu^a$
$3_{1\,2} \leftarrow 2_{2\,1}$	10789.0408	1	$3_{1\,3} \leftarrow 2_{0\,2}$	13614.9723	2
$4_{3\,2} \leftarrow 4_{2\,3}$	11017.9372	6	$2_{2\,1} \leftarrow 1_{1\,0}$	15138.6816	-5
$4_{2\,3} \leftarrow 4_{1\,4}$	11119.9144	0	$4_{1\,3} \leftarrow 3_{2\,2}$	16284.8693	27
$3_{0\,3} \leftarrow 2_{1\,2}$	12318.0859	4	$2_{2\,0} \leftarrow 1_{1\,1}$	16344.5281	-10
$5_{4\,1} \leftarrow 5_{3\,2}$	12513.7769	-3	$4_{0\,4} \leftarrow 3_{1\,3}$	16439.3333	-20
$4_{4\,0} \leftarrow 4_{3\,1}$	13375.2004	1	$4_{1\,4} \leftarrow 3_{0\,3}$	17086.2790	2
$3_{1\,3} \leftarrow 2_{0\,2}$	13696.1474	2			
$2_{2\,1} \leftarrow 1_{1\,0}$	15164.1798	-5			
$2_{2\,0} \leftarrow 1_{1\,1}$	16402.3518	-4			
$4_{1\,3} \leftarrow 3_{2\,2}$	16582.3751	-4			
$4_{0\,4} \leftarrow 3_{1\,3}$	16599.6488	1			
$4_{1\,4} \leftarrow 3_{0\,3}$	17205.3214	1			

[a] $\Delta\nu = \nu_{obs} - \nu_{calc}$ in kHz.

Table 67. Rotational transition frequencies (MHz) of the ground vibrational state of c-$C_3H_6Si_2H_4$.

$^{13}C_\beta$			$^{13}C_\alpha$		
Transitions	ν_{obs}	$\Delta\nu^a$	Transitions	ν_{obs}	$\Delta\nu^a$
$1_{1\,1} \leftarrow 0_{0\,0}$	6264.2017	4	$1_{1\,1} \leftarrow 0_{0\,0}$	6260.1739	15
$2_{0\,2} \leftarrow 1_{1\,1}$	7791.5602	2	$2_{0\,2} \leftarrow 1_{1\,1}$	7823.7598	6
$2_{1\,2} \leftarrow 1_{0\,1}$	10105.9171	1	$2_{1\,2} \leftarrow 1_{0\,1}$	10105.5467	8
$3_{0\,3} \leftarrow 2_{1\,2}$	12402.3824	1	$5_{4\,1} \leftarrow 5_{3\,2}$	11626.1524	-2
$3_{1\,3} \leftarrow 2_{0\,2}$	13623.2458	-10	$3_{0\,3} \leftarrow 2_{1\,2}$	12433.5927	5
$2_{2\,1} \leftarrow 1_{1\,0}$	14950.8533	5	$3_{1\,3} \leftarrow 2_{0\,2}$	13626.1160	10
$2_{2\,0} \leftarrow 1_{1\,1}$	16245.0166	-4	$2_{2\,0} \leftarrow 1_{1\,1}$	16245.0166	-4
$4_{1\,4} \leftarrow 3_{0\,3}$	17151.2461	4	$4_{0\,4} \leftarrow 3_{1\,3}$	16670.7003	-20
			$4_{1\,4} \leftarrow 3_{0\,3}$	17161.3089	-1

[a] $\Delta\nu = \nu_{obs} - \nu_{calc}$ in kHz.

Table 68. Experimental rotational and centrifugal distortion constants of the ground vibrational state of c-$C_3H_6Si_2H_4$ isotopologues.

	MP2(full)/ 6-311++G(d,p)	c-$C_3H_6Si_2H_4$	^{29}Si	^{30}Si[a]	$^{13}C_\beta$[a]	$^{13}C_\alpha$[a]
A (MHz)	4427.8194	4417.6710(7)	4414.2128(7)	4411.0525(10)	4343.3367(14)	4337.4673(25)
B (MHz)	2860.4216	2887.0548(6)	2851.5540(8)	2817.5636(8)	2877.0556(19)	2887.1237(25)
C (MHz)	1927.4735	1938.2171(6)	1921.5697(6)	1905.5525(6)	1920.8618(6)	1922.6925(11)
Δ_J (kHz)	0.40	0.41(2)	0.43(2)	[0.41]	[0.41]	[0.41]
Δ_{JK} (kHz)	-0.16	-0.17(3)	-0.11(6)	[-0.17]	[-0.17]	[-0.17]
Δ_K (kHz)	0.89	1.04(3)	0.87(6)	[1.04]	[1.04]	[1.04]
δ_J (kHz)	0.110	0.118(4)	0.13(1)	[0.118]	[0.118]	[0.118]
δ_K (kHz)	0.41	0.44(3)	0.38(6)	[0.44]	[0.44]	[0.44]
N[b]	-	40	24	18	8	9
σ_{fit} (kHz)[c]	-	3	2	7	3	6

[a] Distortion constants for all isotopologue are held fix to the normal species values.
[b] Number of frequencies fitted.
[c] Total RMS error of the observed-calculated frequencies for all N lines in fit.

Table 69. Observed and calculated[a] frequencies (cm^{-1}) and potential energy distributions (P.E.D.s) for the twist (C_2) conformer of c-$C_3H_6Si_2H_4$.

Sym. Block	Vib. No.	Approximate Description	*ab initio*	fixed scaled[b]	IR int.	Raman act.	IR Gas	Raman liquid	contour A	contour B	contour C	P.E.D.[c]
A	ν_1	β-CH_2 antisymmetric stretch	3155	2960	11.1	112.4	2940	2933	-	100	-	$90S_1,10S_3$
	ν_2	α-CH_2 symmetric stretch	3134	2940	0.5	85.7	2935	2924	-	100	-	$100S_2$
	ν_3	β-CH_2 symmetric stretch	3095	2903	5.4	145.0	2905	2893	-	100	-	$90S_3,10S_1$
	ν_4	SiH_2 antisymmetric stretch	2289	2172	23.4	219.8	2152	2155	-	100	-	$64S_4,36S_5$
	ν_5	SiH_2 symmetric stretch	2281	2163	0.7	226.2	2142	2144	-	100	-	$64S_5,36S_4$
	ν_6	β-CH_2 symmetric deformation	1525	1434	6.4	8.2	1424	1426	-	100	-	$100S_6$
	ν_7	α-CH_2 deformation	1479	1390	10.0	11.9	1364	1361	-	100	-	$100S_7$
	ν_8	β-CH_2 twist	1318	1251	2.5	3.8	1234	1235	-	100	-	$53S_8,32S_9,13S_{14}$
	ν_9	β-CH_2 wag	1147	1090	0.1	3.6	-	1070	-	100	-	$49S_9,28S_8,15S_{11}$
	ν_{10}	α-CH_2 twist	1045	992	6.6	3.8	1000	1000	-	100	-	$84S_{10}$
	ν_{11}	Ring deformation	1013	963	0.3	5.8	-	963	-	100	-	$63S_{11},10S_{16},10S_{12},11S_9$
	ν_{12}	SiH_2 symmetric deformation	998	947	6.3	28.1	952	955	-	100	-	$88S_{12},10S_{11}$
	ν_{13}	SiH_2 wag	949	901	268.8	1.5	899	~899	-	100	-	$50S_{13},30S_{14}$
	ν_{14}	β-CH_2 rock		841			833	835	-	100	-	$23S_{14},25S_{13},17S_{17},13S_{15},10S_{19},10S_8$

			884		109.4	3.6						
	ν_{15}	Ring deformation	681	649	0.3	5.9	-	660	-	100	-	$46S_{15},17S_{16},13S_{13},12S_{14},10S_{17}$
	ν_{16}	Ring breathing	668	638	0.6	26.8	655	656	-	100	-	$62S_{16},13S_{19},11S_{11}$
	ν_{17}	SiH_2 twist	633	602	0.1	3.2	609	613	-	100	-	$60S_{17},17S_{15},10S_{14},10S_{10}$
	ν_{18}	SiH_2 rock	519	494	0.1	5.1	503	503	-	100	-	$70S_{18},10S_{19},10S_{16},10S_{14}$
	ν_{19}	Ring deformation	346	340	0.0	3.2	334	332	-	100	-	$72S_{19},11S_{18},10S_{15}$
	ν_{20}	Ring twist	190	189	0.2	0.0	-	184	-	100	-	$93S_{20}$
B	ν_{21}	α-CH_2 antisymmetric stretch	3195	2997	0.9	66.0	2969	2964	2	-	98	$100S_{21}$
	ν_{22}	β-CH_2 antisymmetric stretch	3161	2965	14.7	74.5	2946	2939	42	-	58	$98S_{22}$
	ν_{23}	β-CH_2 symmetric stretch	3097	2905	18.6	34.8	2905	2895	38	-	62	$98S_{23}$
	ν_{24}	SiH_2 antisymmetric stretch	2289	2172	358.4	14.6	2152	2155	23	-	77	$94S_{24}$
	ν_{25}	SiH_2 symmetric stretch	2277	2160	317.7	7.0	2142	2144	79	-	21	$94S_{25}$
	ν_{26}	β-CH_2 antisymmetric deformation	1515	1424	8.3	19.1	1416	1411	2	-	98	$100S_{26}$
	ν_{27}	β-CH_2 antisymmetric wag	1303	1238	3.3	0.3	1221	-	100	-	-	$80S_{27}$, $10S_{38}$, $10S_{29}$
	ν_{28}	α-CH_2 wag	1101	1045	74.1	3.4	1038	1038	87	-	13	$53S_{28},31S_{29}$

ν_{29}	β-CH_2 twist	1090	1035	44.1	3.5	1027	1027	78	-	22	$51S_{29},35S_{28}$
ν_{30}	SiH_2 antisymmetric deformation	986	936	213.1	2.4	996/945	993/945	96	-	4	$98S_{30}$
ν_{31}	SiH_2 antisymmetric wag	872	831	63.5	11.4	825	823	97	-	3	$60S_{31},20S_{36},14S_{38}$
ν_{32}	α-CH_2 rock	831	791	62.6	9.8	781	777	5	-	95	$33S_{32},28S_{34},17S_{37},10S_{39},10S_{36}$
ν_{33}	Ring deformation	758	721	17.9	12.2	728	727	100	-	-	$42S_{33},23S_{35},12S_{31},10S_{34},10S_{28}$
ν_{34}	SiH_2 twist	741	704	35.1	8.6	715	714	13	-	87	$36S_{34},25S_{36},15S_{33},10S_{38},10S_{37}$
ν_{35}	Ring deformation	685	658	19.1	5.6	663	668	80	-	20	$42S_{35},25S_{38},19S_{31}$
ν_{36}	β-CH_2 rock	587	560	8.9	3.5	558	556	54	-	46	$19S_{36},26S_{33},21S_{35},15S_{34},13S_{32},11S_{37}$
ν_{37}	SiH_2 rock	515	491	15.0	0.5	491	494	14	-	86	$39S_{37},42S_{32},10S_{38},10S_{34}$
ν_{38}	Ring deformation	353	344	3.7	0.4	334	332	32	-	68	$39S_{38},15S_{37},15S_{36},12S_{39}$
ν_{39}	Ring puckering	55	55	2.4	0.0	56*	50	7	-	93	$79S_{39},14S_{38}$

[a] MP2(full)/6-31G(d) ab initio calculations, scaled frequencies, infrared intensities (km/mol), Raman activities ($Å^4$/u) and potential energy distributions (P.E.D.s)

[b] Scaled ab initio calculations with factors of 0.88 for CH_2 stretches and CH_2 deformations, 0.90 for all other modes.

[*] Ref [155].

[c] Symmetry coordinates with P.E.D. contribution less than 10% are omitted.

The infrared spectrum of the gas (Fig. 40) was obtained from 4000 to 220 cm^{-1} on a Perkin-Elmer model 2000 Fourier transform spectrometer equipped with a Ge/CsI beamsplitter and a DTGS detector. Atmospheric water vapor was removed from the spectrometer housing by purging with dry nitrogen. The spectrum of the gas was obtained with a theoretical resolution of 0.5 cm^{-1} with 128 interferograms added and truncated.

Raman spectrum (Fig. 41) of the liquid was collected in back-scattering geometry using the 514.532 nm line of an Argon ion laser as the excitation source, with ~ 22 mW incident on the diamond cell. A Semrock 514 nm edge filter was used to separate the laser line from the Raman scattered light. The scattered light was dispersed in a Spectra-pro 500i spectrograph and detected with a Spec-10 liquid nitrogen cooled CCD detector. Raman spectra were collected by using a 2400 g/mm grating with a slit width of 100 μm, which gives spectral resolution of ~ 0.2 cm^{-1}. The observed bands in the infrared spectrum of the gas and Raman spectrum of the liquid along with their proposed assignments are listed in Table 69.

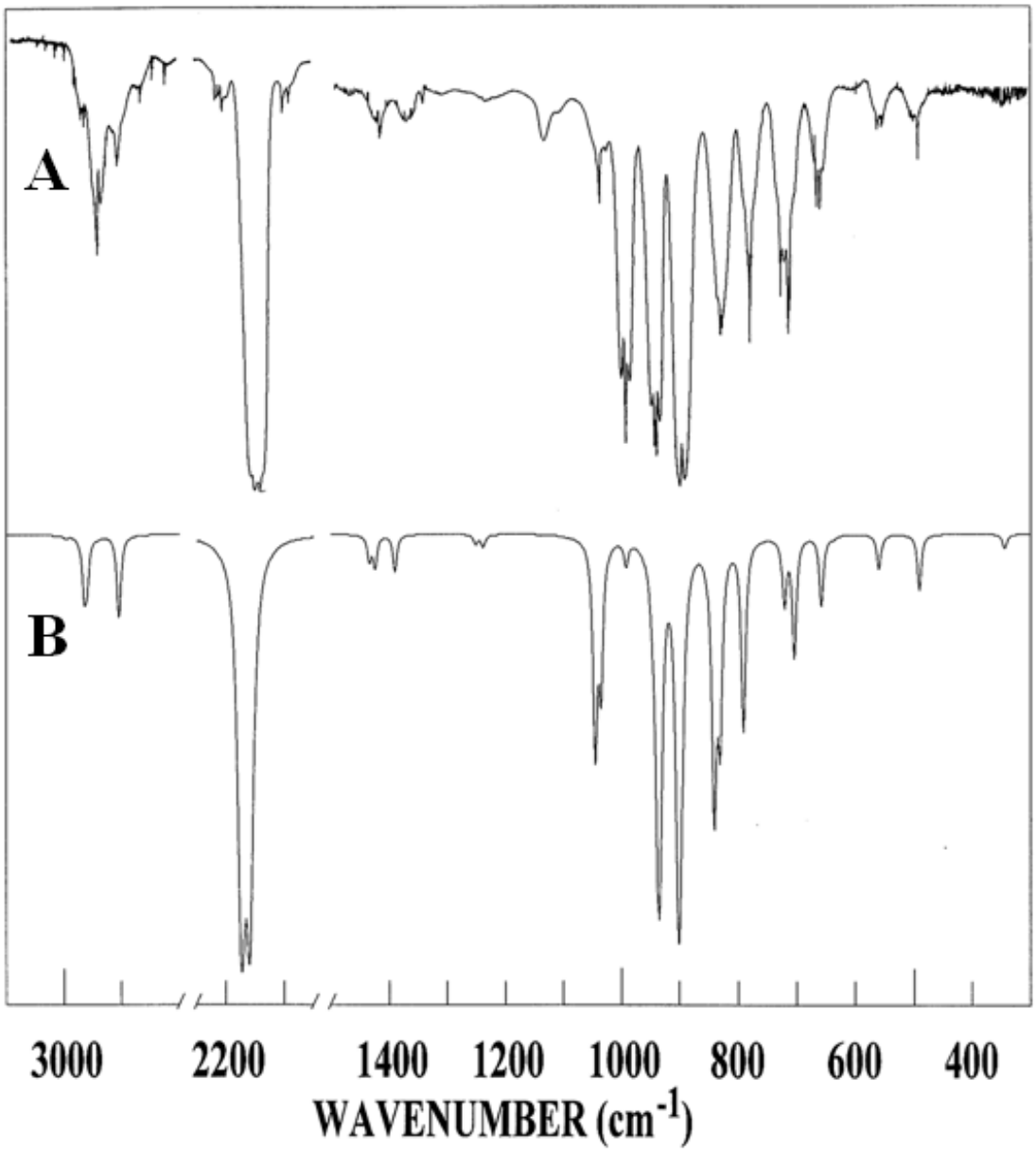

Figure 40. Comparison of experimental and calculated infrared spectra of c-$C_3H_6Si_2H_4$: (A) observed spectrum of gas; (B) simulated spectrum of twist conformer

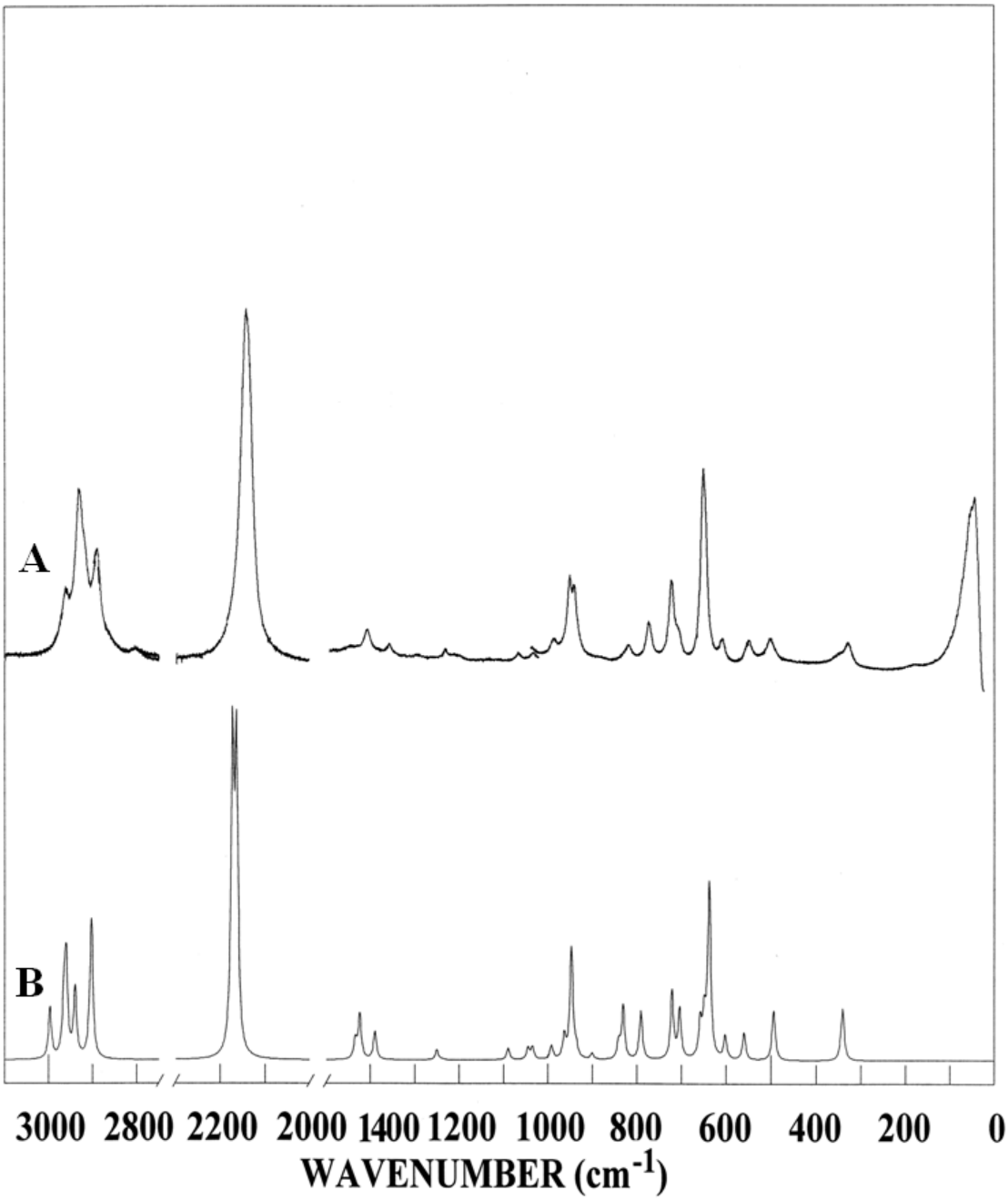

Figure 41. Comparison of experimental and calculated Raman spectra of c-$C_3H_6Si_2H_4$: (A) observed spectrum of liquid; (B) simulated spectrum of twist conformer

The ab initio calculations were performed with the Gaussian 03 program [22] by using Gaussian-type basis functions. The energy minima with respect to nuclear coordinates were obtained by the simultaneous relaxation of all geometric parameters by the gradient method of Pulay [29]. A variety of basis sets as well as the corresponding ones with diffuse functions were employed with the Møller-Plesset perturbation method [21] to the second order MP2 with full electron correlation as well as with density functional theory by the B3LYP method. The predicted conformational energy differences are listed in Table 70.

The predicted scaled frequencies were used together with a Lorentzian function to obtain the simulated spectra. Infrared intensities were obtained based on the dipole moment derivatives with respect to Cartesian coordinates. The derivatives were transformed with respect to normal coordinates by $(\partial\mu_u/\partial Q_i) = \sum_j (\partial\mu_u/\partial X_j)L_{ij}$, where Q_i is the i^{th} normal coordinate, X_j is the j^{th} Cartesian displacement coordinate, and L_{ij} is the transformation matrix between the Cartesian displacement coordinates and the normal coordinates. The infrared intensities were then calculated by $(N\pi)/(3c^2)$ $[(\partial\mu_x/\partial Q_i)^2 + (\partial\mu_y/\partial Q_i)^2 + (\partial\mu_z/\partial Q_i)^2]$. A comparison of the experimental infrared spectrum of the gas and simulated infrared spectrum of the isolated twist conformer is shown in Fig. 40.

Table 70. Calculated energies in Hartrees (H) and energy differences (cm^{-1}) for the three conformers of c-$C_3H_6Si_2H_4$.

Method/Basis Set	Energy[a], E	Energy Differences, Δ	
	Twist	Envelope[b]	Planar[b]
MP2(full)/6-31G(d)	0.858570	941	1391
MP2(full)/6-31+G(d)	0.869926	859	1292
MP2(full)/6-31G(d,p)	0.942927	950	1381
MP2(full)/6-31+G(d,p)	0.953429	877	1294
MP2(full)/6-311G(d,p)	1.309829	921	1267
MP2(full)/6-311+G(d,p)	1.313460	889	1260
MP2(full)/6-311G(2d,2p)	1.387107	927	1423
MP2(full)/6-311+G(2d,2p)	1.389146	916	1393
MP2(full)/6-311G(2df,2pd)	1.471870	924	1508
MP2(full)/6-311+G(2df,2pd)	1.473414	912	1492
MP2(full)/aug-cc-pVTZ	1.353673	935	1579
B3LYP/6-31G(d)	2.340691	689	940
B3LYP/6-31+G(d)	2.347209	699	932
B3LYP/6-31G(d,p)	2.354676	671	926
B3LYP/6-31+G(d,p)	2.360873	683	923
B3LYP/6-311G(d,p)	2.428704	685	913
B3LYP/6-311+G(d,p)	2.429736	687	905
B3LYP/6-311G(2d,2p)	2.439413	672	923
B3LYP/6-311+G(2d,2p)	2.439994	667	914
B3LYP/6-311G(2df,2pd)	2.446767	673	928
B3LYP/6-311+G(2df,2pd)	2.447263	670	925
B3LYP/aug-cc-pVTZ	2.451245	679	936

[a] Energy of conformer is given as –(E+697) H.

[b] Difference is relative to twist form and given in cm^{-1}.

Additional support for the vibrational assignments was obtained from the simulated Raman spectra. The evaluation of Raman activity by using the analytical gradient methods has been developed [31-34] and the activity S_j can be expressed as: $S_j = g_j(45\alpha_j^2 + 7\beta_j^2)$, where g_j is the degeneracy of the vibrational mode j, α_j is the derivative of the isotropic polarizability, and β_j is the anisotropic polarizability. To obtain the Raman scattering cross sections, the polarizabilities are incorporated into S_j by multiplying S_j with $(1-\rho_j)/ (1+\rho_j)$ where ρ_j is the depolarization ratio of the j^{th} normal mode. The Raman scattering cross sections and calculated wavenumbers obtained from the Gaussian 03 program were used together with a Lorentzian function to obtain the simulated Raman spectra. A comparison of the experimental Raman spectrum of the liquid and predicted Raman spectrum of the isolated twist form are shown in Fig 41. This comparison is reasonable as the average difference in band center due to going from gas to liquid is 3 cm^{-1}, and thus, there is little interaction between molecules in the liquid.

MICROWAVE RESULTS

An overview of the fit rotational parameters for c-$C_3H_6Si_2H_4$ and the comparison to ab initio results can be found in Table 68. The spectrum was satisfactorily fit (Tables 65-67) using a standard Watson semi-rigid rotor Hamiltonian of the A-reduction type in the Ir representation [157], with 12.1 kHz RMS error, better than the experimental uncertainty of approximately 20 kHz (line centers determined to ±10 kHz). As mentioned previously, the high dynamic range afforded in this experiment enabled assignment of all common heavy atom single isotopologue. Due to symmetry considerations, the silicons are spectroscopically equivalent, as well as the carbons in the Si-C-C-Si backbone. This

equivalence leads to doubling in intensity in the spectra of these isotopologue. A summary of these isotopologue fits can be found in Table 68.

This kind of isotopic determination enables direct structure determination of the heavy atom structure via Kraitchman's equations [13]. The Kraitchman r_s substitution structure, calculated using the freely available KRA program [158] and it is in reasonable agreement with the MP2/6-311++G(d,p) results.

STRUCTURAL PARAMETERS

With accurate rotational constants the adjusted r_0 structure can be determined for the twist conformer by utilizing the rotational constants reported herein from the microwave spectra. The rotational constants for five isotopic species were determined in the current study and are listed in Table 68. Therefore, 15 rotational constants are available for the determination of the structural parameter values of the twist conformer of c-$C_3H_6Si_2H_4$.

We [51] have shown that ab initio MP2(full)/6-311+G(d,p) calculations predict the carbon-hydrogen r_0 structural parameters for more than fifty hydrocarbons to at least 0.002 Å compared to the experimentally determined [5] values from isolated CH stretching frequencies which agree to previously determined values from earlier microwave studies. Therefore, all of the carbon-hydrogen parameters can be taken from the MP2(full)/6-311+G(d,p) predicted values for the twist conformer of c-$C_3H_6Si_2H_4$. The silicon-hydrogen r_0 structural parameter values can be experimentally determined [6] from isolated SiH stretching frequencies. These values are listed in Table 71 as determined from the assignments in Tables 69.

Table 71. Structural parameters (Å and degrees), rotational constants (MHz) and dipole moments (Debye) for twist conformer c-$C_3H_6Si_2H_4$.

Structural Parameters	Int. coor.	6-311+G(d,p)		6-311++G(d,p)		r_s	Adjusted r_0[a]
		MP2(full)	B3LYP	MP2	B3LYP		
rC_α-Si	R_1	1.891	1.902	1.893	1.902	1.886(15)	1.8856(1)
$rSi\text{-}C_\beta,C_{\beta'}$	R_2	1.892	1.905	1.895	1.905	1.8847(66)	1.8884(4)
$rC_\beta\text{-}C_{\beta'}$	R_3	1.550	1.554	1.552	1.554	1.5481(40)	1.5515(4)
$rSi\text{-}H_1$	R_4	1.482	1.490	1.482	1.490		1.4880(1)*
$rSi\text{-}H_2$	R_5	1.480	1.489	1.481	1.489		1.4860(1)*
rC_α-H	r_1	1.094	1.093	1.094	1.093		1.0938(1)
$rC_\beta\text{-}H_1$, $C_{\beta'}\text{-}H_1$	r_2	1.098	1.097	1.098	1.097		1.0977(1)
$rC_\beta\text{-}H_2$, $C_{\beta'}\text{-}H_2$	r_3	1.095	1.094	1.095	1.094		1.0946(1)
$\angle SiC_\alpha Si$	θ_1	104.5	104.5	104.6	104.5	103.84(20)	103.87(6)
$\angle C_\alpha SiC_\beta$	θ_2	101.6	102.1	101.6	102.1		102.20(6)
$\angle SiC_\beta C_{\beta'}$	θ_3	106.7	107.6	106.8	107.6	106.51(37)	106.37(6)
$\angle C_\alpha SiH_1$	σ_1	110.2	110.3	110.3	110.3		110.343(1)
$\angle C_\alpha SiH_2$	σ_2	113.5	113.3	113.3	113.3		113.053(1)
$\angle C_\beta SiH_1$	σ_3	109.7	110.3	109.8	110.4		109.451(1)
$\angle C_\beta SiH_2$	σ_4	113.1	112.7	113.1	112.6		113.143(1)
$\angle H_1SiH_2$	σ_5	108.5	108.1	108.6	108.1		108.519(1)
$\angle HC_\alpha Si$	λ_1	111.2	111.5	111.2	111.1		111.46(2)
$\angle HC_\alpha H$	λ_2	107.1	107.0	107.0	107.1		107.19(2)
$\angle H_1C_\beta Si$	λ_3	108.8	108.5	108.8	108.4		108.818(4)
$\angle H_2C_\beta Si$	λ_4	113.0	112.6	113.0	112.5		113.037(4)
$\angle H_1C_\beta C_{\beta'}$	λ_5	109.7	109.9	109.7	109.9		110.016(4)
$\angle H_2C_\beta C_{\beta'}$	λ_6	111.9	111.9	111.8	111.9		111.935(4)
$\angle H_1C_\beta H_2$	λ_7	106.7	106.4	106.6	106.4		106.645(4)
$\tau C_\beta SiC_\alpha Si$	τ_1	11.4	10.5	11.3	10.5	13.8(17)	11.46(3)
$\tau SiC_\beta C_{\beta'}Si$	τ_2	45.7	42.4	45.4	42.4	45.25(86)	45.60(3)
A(MHz)		4429.38	4361.66	4416.85	4361.12		4417.76
B(MHz)		2859.11	2824.45	2848.85	2824.79		2887.12
C(MHz)		1926.63	1891.26	1919.11	1891.43		1938.27
$\lvert\mu_a\rvert$		0.000	0.000	0.000	0.000		
$\lvert\mu_b\rvert$		0.146	0.247	0.146	0.243		
$\lvert\mu_c\rvert$		0.000	0.000	0.000	0.000		
$\lvert\mu_t\rvert$		0.146	0.247	0.146	0.243		

[a] Adjusted parameters using the microwave data reported in this study; Si-H distance determined from the isolated stretching frequency.

We have found that good structural parameters for hydrocarbons and many substituted ones can be determined by adjusting the structural parameters obtained from the ab initio MP2(full)/6-311+G(d,p) calculations to fit the rotational constants obtained from microwave experimental data by using a computer program "A&M" (Ab initio and Microwave) developed [14] in our laboratory. Therefore, it should be possible to obtain "adjusted r_0" structural parameters for the fourteen parameters, taking the C-H angles as a single set, by utilizing the experimentally determined fifteen rotational constants obtained from the microwave spectra reported in this study. Therefore we have obtained the complete structural parameters for the twist form of c-$C_3H_6Si_2H_4$.

The resulting adjusted r_0 parameters are listed in Table 71, where the precisions are listed. It is believed that these precisions are probably smaller than the accuracy this method can achieve, and therefore, for the C-Si and C-C distances the value listed should be accurate to ± 0.002 Å, the C-H and Si-H distances accurate to ± 0.002 Å, and the angles should be within ± 0.4°. The fit of the fifteen determined rotational constants (Table 72) by the adjusted r_0 structural parameters for the twist conformer is excellent with the largest difference of 0.18 MHz and an average of 0.06 MHz for the fits. Therefore, it is believed that the suggested uncertainties are realistic values and the determined structural parameters are probably as accurate as can be obtained for the molecule in the gas phase by either electron diffraction or microwave substitution methods.

Table 72. Comparison of rotational constants (MHz) obtained from experimental values from microwave spectra, and from the adjusted r_0 structural parameters for c-$C_3H_6Si_2H_4$.

Isotopomer	Rotational constant	Experimental	Adjusted r_0	$\|\Delta\|$
Normal Species	A	4417.6710(7)	4417.7765	0.1055
	B	2887.0548(6)	2887.1194	0.0646
	C	1938.2171(6)	1938.2759	0.0588
^{29}Si	A	4414.2128(7)	4414.3074	0.0946
	B	2851.5540(8)	2851.5317	-0.0223
	C	1921.5697(6)	1921.5868	0.0171
^{30}Si	A	4411.0525(10)	4411.1363	0.0838
	B	2817.5636(8)	2817.4596	-0.1040
	C	1905.5525(6)	1905.5304	-0.0221
$^{13}C_\alpha$	A	4337.4673(25)	4337.4049	-0.0624
	B	2887.1237(25)	2887.1194	-0.0043
	C	1922.6925(11)	1922.6450	-0.0475
$^{13}C_\beta$	A	4343.3367(14)	4343.1530	-0.1837
	B	2877.0556(19)	2877.0777	0.0221
	C	1920.8618(6)	1920.8820	0.0202

VIBRATIONAL ASSIGNMENT

In order to obtain descriptions of the molecular motions involved of the fundamental modes of c-$C_3H_6Si_2H_4$, a normal coordinate analysis was carried out. The force field in Cartesian coordinates was obtained with the Gaussian 03 program at the MP2(full) level with the 6-31G(d) basis set. The internal coordinates used to calculate the G and B matrices are given for the twist conformer in Table 71 with the atomic numbering shown in Fig. 42. By using the B matrix [30], the force field in Cartesian

coordinates was converted to a force field in internal coordinates. Subsequently, 0.88 was used as the scaling factor for the CH stretches, the SiH stretches, and the CH_2 deformations and 0.90 was used for all other modes to obtain the fixed scaled force constants and the resulting wavenumbers. A set of symmetry coordinates was used (Table S12) to determine the corresponding potential energy distributions (P.E.D.s). A comparison between the observed and calculated wavenumbers, along with the calculated infrared intensities, Raman activities, depolarization ratios and P.E.D.s for the twist conformer of c-$C_3H_6Si_2H_4$ are given in Table 69.

The major reason for carrying out a vibrational assignment of c-$C_3H_6Si_2H_4$ is to determine the frequencies of the fundamentals of the heavy atoms of the ring which should aid in future studies of the corresponding five membered rings with more complex additions. The vibrations of the CH_2 group are expected to be very similar to those found in the usual five membered rings with just carbon atoms so a discussion of their assignments is not necessary. Therefore, the assignments of the nine fundamentals of the ring will be provided first and this will be followed by the vibration assignments involving the SiH_2 modes.

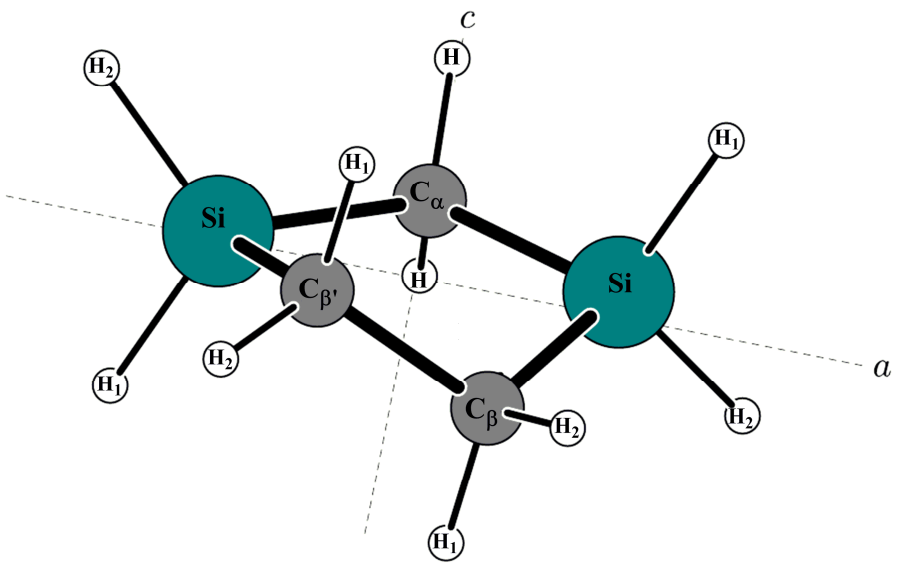

Figure 42. Model of c-$C_3H_6Si_2H_4$ showing atomic numbering

The heavy atom modes of the five membered rings result in a total of nine fundamentals with five of those in the 'A' block and the remaining four in the 'B' block. Five membered rings containing carbons have ring deformations occurring around 1000 cm^{-1} and the second ring deformation is usually around 200 cm^{-1} lower. For the molecule with the two silicon atoms these modes are at 963 cm^{-1} and significant lower at 660 cm^{-1} in the Raman spectra of the liquid. The ring breathing mode is observed at about the same frequency as the second deformation when the ring has carbon atoms and for the ring with the silicon atoms this mode is nearly the same frequency as the second deformation but both of them are about 158 cm^{-1} lower than those for the molecule with carbon.

For the vibrations in 'B' block the two ring deformations are fairly close in frequency at 728 cm^{-1} and 663 cm^{-1} with the third ring deformation at 334 cm^{-1} in the

infrared spectra of the gas. The corresponding mode in the 'A' block is predicted at nearly the same frequency i.e. 4 cm^{-1} difference so it is assumed that they are accidently degenerate. It should be noted that for this mode in the 'A' block it has a predicted IR intensity of 0.0 and a Raman activity of 3.2 whereas for this mode in the 'B' block the predicted IR intensity is 3.7 and the Raman activity is 0.4. The twisting mode and ring puckering modes are predicted at 189 cm^{-1} and 55 cm^{-1} and are assigned at 184 and 50 cm^{-1}, respectively, from the Raman spectra with both 0.0 predicted Raman intensity.

The four SiH_2 stretch modes are observed in the expected frequency region with those in the 'A' and 'B' blocks with the same frequencies. Also the two SiH_2 deformations are predicted to have similar frequencies of 947 'A' and 936 'B' cm^{-1} and they are relatively pure modes. However, the predicted intensities of these two modes are significantly different with infrared intensities of 6.3 'A' and 213.1 'B' km/mol and Raman activities of 28.1 'A' and 2.4 'B' $Å^4/u$. These relative Raman activities make assignment of the 'A' mode very simple where the Raman band at 955 cm^{-1} in the liquid is clearly the ν_{12} 'A' block SiH_2 symmetric deformation fundamental. The 'B' block fundamental is significantly more complex as there are two clear A-type fundamentals that appear in this region at 996 and 945 cm^{-1} in the infrared spectra of the gas, both of which have the same intensity and band contour. The band at 996 cm^{-1} is clearly not a band from impurities and is one of the three most intense bands in the spectra. These bands at 996 and 945 cm^{-1} appear to be due to a Fermi resonance of the ν_{30} 'B' SiH_2 antisymmetric deformation fundamental with a combination band in near coincidence. The two SiH_2 wags have significantly different frequencies of 899 'A' and 825 'B' cm^{-1} where their P.E.D.s are 50 and 59% but the remaining contributions are different. The two SiH_2 rocks are assigned

at 503 and 491 cm^{-1}, respectively, in the infrared spectra of the gas. However, the two SiH_2 twists are predicted to have bands separated by more than 100 cm^{-1} and they are observed at 609 and 715 cm^{-1} with the 715 cm^{-1} 'B' fundamental with only 36% contributions to this mode. This large difference is likely due to this significantly different mixing of these two fundamentals. With these assignments the remaining vibration modes are CH_2 modes which are easily assigned so the assignments for this molecule are concluded.

DISCUSSION

The ab initio energy differences of the possible forms have been determined by a variety of basis sets (Table 70). The MP2(full) method consistently predicts the twist form as the most stable conformer and the planar and envelope forms as not being stable species with all the basis sets and with only relatively small changes due to basis set selection. The B3LYP method agrees with the MP2(full) method as the identity of the most stable form but the magnitude of the energy differences are approximately two-thirds that of the MP2(full) method. However the B3LYP calculations still show the twist conformer as being the only stable form.

The vibrational assignments reported herein are based on a significant amount of information with the infrared and Raman spectrum of the xenon solution and predictions of the fundamental frequencies from the scaled ab initio MP2(full)/6-31G(d) calculations as well as the predicted infrared band contours and their intensities. For the twist conformer the fixed scaled ab initio predicted frequencies for the 'A' block fundamentals are in error with an average value of 11 cm^{-1} which represent an error of 0.80% and for the 'B' block modes it is 10 cm^{-1} which is 0.77% error. The largest errors are in the ring

deformations, which includes the ring breathing mode, and the SiH_2 bending modes. It should also be noted that these fundamentals are associated with the structural parameters which show the largest changes when comparing the ab initio MP2(full)/6-311+G(d,p) predicted structural parameters to the corresponding r_0 structures. It appears that ab initio calculations have some difficulties with predicting these parameters. Those errors are clearly observable but not necessarily so significant that the predictions lose value. Thus, the relatively small basis set of 6-31G(d) by the MP2(full) calculations with two scaling factors provides excellent predicted frequencies for aiding the vibrational assignments.

The identity of the combination band which interacts with the ν_{30} fundamental and produces the Fermi resonance at 996 and 945 cm^{-1} were determined by a few logical deductions. First the combination band must be of 'B' symmetry and in near coincidence to the ν_{30} fundamental energy level. Therefore, the combination band would have to be an 'A' + 'B' combination which gives a 'B' symmetry band. The energy of the ν_{30} fundamental would be 940 cm^{-1} determined from the predicted difference from the ab initio calculation applied to the 952 cm^{-1} assignment of the ν_{12} fundamental. This energy would be in near coincidence with the 943 ν_{38} (334) + ν_{17} (609) cm^{-1} combination band, which matches all the necessary criteria to cause the afore mentioned Fermi resonance band. The remaining possible combination bands are much less likely with energies above 990 or below 900 cm^{-1}. Therefore, this is the most logical candidate for the Fermi resonance bands at 996 and 945 cm^{-1}.

This Fermi resonance account for the two A-type bands at 996 and 945 cm^{-1} which otherwise could not be accounted for and are very good examples of A-type band contours. Furthermore, the band at 899 cm^{-1} is an excellent example of a B-type band

which aided considerably in the assignment of the spectra. The remaining bands in the spectra are somewhat nondescript Q-branches or broad bands indicating B-type but without the characteristic dip frequently associated with this band type. The Si-H fundamentals at 2152 and 2141 cm^{-1} are ,however, interesting as they are accompanied by the difference and combination bands at 2099 and 2089 cm^{-1} and 2212 and 2200 cm^{-1}, respectively. These differences and combination bands may be used to determine a frequency of 53 cm^{-1} for the ring puckering mode, which is observed in the Raman spectra of the liquid at 50 cm^{-1}. These data can be used along with a reduced mass calculation to determine ring puckering potential function which is part of the conformational interchange of the molecule.

It is of interest to compare the vibrational fundamentals and their assignments to similar molecules with corresponding fundamentals. This comparison is very limited in scope though for c-$C_3H_6Si_2H_4$ as there are no other 1,3-disilacyclopentanes vibrational assignments in the literature. The closest molecules to c-$C_3H_6Si_2H_4$ where vibrational data has been published are 1,3-disilacyclopent-4-ene (c-$CH=CHSi_2H_4CH_2$) and 1,1,3,3-tetrachloro-1,3-disilacyclopent-4-ene (c-$CH=CHSi_2Cl_4CH_2$) which have the planar ring conformation (C_{2v}) due to the double bond connecting the back carbons. These molecules were studied [155] with the Raman spectra of the liquid for both samples and the infrared spectra of the vapor for the 1,3-disilacyclopent-4-ene sample. It is of interest to compare and contrast the SiH_2 modes of c-$C_3H_6Si_2H_4$ with the corresponding modes in c-$CH=CHSi_2H_4CH_2$ where the SiH_2 stretching modes in both assignments are only ~3 cm^{-1} up-shifted by the proximity to the double bond indicating there is little change in the Si-H bond distance between these two molecules. The SiH_2 deformation (o.p.) and SiH_2

deformation (i.p.) modes are assigned at 999 and 948 cm^{-1}, respectively, for c-$CH=CHSi_2H_4CH_2$. The SiH_2 deformation (i.p.) mode is similar in description and energy to the SiH_2 symmetric deformation assigned at 952 cm^{-1} for c-$C_3H_6Si_2H_4$. However, the SiH_2 deformation (o.p.) mode is similar in description to the SiH_2 antisymmetric deformation but is considerably different in energy even when the Fermi resonance of the SiH_2 antisymmetric deformation band is taken into account. This difference is probably largely due to the change from planar to twist conformation and the resulting change from C_{2v} to C_2 symmetry.

Next, the SiH_2 wag (A_1) for c-$CH=CHSi_2H_4CH_2$ is similar in description to the ν_{13} fundamental described as a SiH_2 wag (A) for c-$C_3H_6Si_2H_4$ molecule and the bands for each are assigned at 868 and 899 cm^{-1}, respectively. This 31 cm^{-1} difference is probably due to the significant mixing of the ν_{13} fundamental which is only 50% SiH_2 wag (A) and 30% β-CH_2 rock. This mixing is actually related to going from a planar (C_{2v}) form to a twist (C_2) conformation as this mixing is not possible in the planar (C_{2v}) form. This is due to the symmetry constraints of the planar conformation where the two planes of symmetry divide these modes between two different symmetry blocks. No further SiH_2 fundamentals can be compared as the c-$CH=CHSi_2H_4CH_2$ study [155] did not assign the remaining 3 SiH_2 bending modes along with several other A_2 symmetry block modes. This is most likely due to the A_2 symmetry block not being infrared active. Finally, it is interesting to note the ring puckering modes for both molecules are very similar in energy at 48 and 53 cm^{-1} for c-$CH=CHSi_2H_4CH_2$ and c-$C_3H_6Si_2H_4$, respectively. This is somewhat unexpected since the puckering angle for the twist form of c-$C_3H_6Si_2H_4$ is only 11.5. It would be of interest to compare the vibrational studies of other 1,3-

disilacyclopentane molecules to evaluate how substitution affects the vibrational modes and to emphasize more ring modes which can be compared for these unique heterocyclic five-membered rings.

The r_s structural parameters determined by using the Kraitchman method can be compared with the corresponding parameters from the adjusted r_0 structural parameters, and the values are listed in Table 71. The r_s Si-C bond distance parameters match the r_0 structural parameters within error limits, but it is somewhat meaningless as the r_s parameters have very large uncertainties. The r_s angles $\angle SiC_{\alpha}Si$ and $\angle SiC_{\beta}C_{\beta'}$, are within their respective error limits as compared to the corresponding adjusted r_0 structural parameters and these parameters are well determined by both methods. The determined dihedral angles $\tau C_{\beta}SiC_{\alpha}Si$ and $\tau SiC_{\beta}C_{\beta'}Si$ are within the stated error limits to the adjusted r_0 structural parameters, but it is again somewhat meaningless as the r_s parameters again have very large uncertainties. These large uncertainties are due to the problem of the Kraitchman method when one or more of the atoms lie on a rotational axis. The remaining C_{β}-C_{β} parameter which can be determined has a small uncertainty and is within the combined error limits of the r_s and adjusted r_0 parameters. When the r_s structural parameters have small uncertainties they agree well with the corresponding adjusted r_0 structural parameters.

Recently there have been many scientific studies where the B3LYP method has been used to predict structural parameters. This can be a poor choice as can be observed in Table 71 where the MP2(full) method is in error from the r_0 structure an average of 0.003 ± 0.003 Å and $0.1 \pm 0.1°$ as compared to the B3LYP method of the same basis set where the error on average is 0.005 ± 0.007 Å and $0.7 \pm 1.1°$. This error is especially

large on the Si-C distances which are three times as large predicted as the same basis set MP2(full) method calculation. The basis set has relatively little effect on either method with no noticeable improvement at all for the B3LYP method with further diffuse functions added to it. Therefore, those who wish to obtain geometric parameters for a molecule the MP2 method should be used rather than a DFT B3LYP method for substituted hydrocarbons.

The natural population analysis was carried out for the twist conformer of c-$C_3H_6Si_2H_4$ with the MP2(full)6-311+G(d,p) calculation. The charge of the heavy atoms are; C_α = -1.36, Si = +1.30, C_β = -0.82, and $_{Si\text{-}}H$ = -0.22. The large charge on the silicon atom is of interest and could counteract some of the larger radius of the silicon atom than a carbon atom. These relatively large charges could also explain the larger than normal difference between the ab initio frequencies for the heavy atom bends and the experimental values, where normally no scaling factor is used a scaling factor of 0.9 had to be used for this molecule. Additionally, the atoms with charges of greater than one have significant differences between the predicted and adjusted r_0 structural parameters and the major structural changes for the adjusted r_0 structure are the Si-C and Si-H parameters. These quantum calculation problems with the silicon atoms are due to their large charges while being a neutral atom and are well known.

There is little information known about substituted cyclopentanes with silicons in the ring and no previously published structures for the disilacyclopentane molecules have been reported. Further study of these types of molecules would be of interest with several different substituents on the silicons so comparisons of these molecules structures, vibrational assignments, and conformational stabilities may be carried out.

CHAPTER 12

MICROWAVE, INFRARED, AND RAMAN SPECTRA, STRUCTURAL PARAMETERS, VIBRATIONAL ASSIGNMENTS AND THEORETICAL CALCULATIONS OF 1,1,3,3-TETRAFLUORO-1,3-DISILACYCLOPENTANE

INTRODUCTION

The saturated five-membered cyclic hydrocarbon ring molecule (cyclopentane) has two "out-of-plane" vibrational modes which are usually described as ring-puckering and ring-twisting modes. When the frequencies of these two modes are nearly equal, the cross terms in the potential function give rise to a vibrational motion which was initially described by Pitzer and colleagues as pseudorotation [133]. This motion was treated by these scientists for the two degenerate out-of-plane ring bending coordinates in terms of an amplitude coordinate q and a phase angle ø. However this concept for cyclopentane was questioned [141] when the low frequency ring mode of this molecule appeared normal but the fundamentals could not be assigned on the basis that cyclopentane had D_{5h} symmetry. The authors [141] stated that the spectral data were consistent with a rigid structure with C_s, C_2, or C_1 symmetry. Nevertheless these scientists [141] concluded that a decision among these three rigid models as well as pseudorotation could not be made. There was further reluctance [142,143] to accept the pseudorotation of the puckering motion and the consequent indefiniteness of the cyclopentane conformation persisted. However, a later infrared study [144] of the CH_2 deformation of cyclopentane clearly showed that the ring was undergoing pseudorotation which was nearly barrier free. Also

from this study an estimate of the value of the pseudorotational moment [159] of inertia was obtained from the spectral data.

With the acceptance of the pseudorotation motion there was a number of investigations on the possible conformations of mono substituted cyclopentane molecules and the determination of the most stable structures. Even before the acceptance of pseudorotation motion was reported in the scientific literature [134] Pitzer and his coworkers reported how one could predict the most stable structure of such molecules. Some of the earliest conformational determinations of the mono substituted cyclopentane molecules was for the halides i.e. bromine, chlorine and fluorine. In the initial studies [117,145] of these molecules it was concluded that all three had two conformers present in the fluid phases with the equatorial form the most stable. Later studies [121] of fluorocyclopentane demonstrated that there was only one form in the fluid phases and it was the envelope-equatorial forms. However several years later [123] it was shown correctly that there was only one form but it was not the envelope conformer but was the twisted form. There has been other reported incorrect conformational structures for five membered rings so it is not easy to predict what the conformational structure will be for many different types of five membered rings.

Recently some investigations of five membered rings [149-151] were initiated where instead of all five ring atoms being carbon one of them has been replaced by a silicon atom. There has been some limited studies of these molecules whether they are in the equatorial, axial or twisted forms or even possibly a planar form. As a continuation of these studies we have expanded the atoms in the ring instead of a single silicon atom to two silicon atoms. For the first molecule we studied [160] with two silicon atoms in the

ring, it included an oxygen atom between them instead of the carbon atoms since this molecule was available. For this study we were interested in the determination of the stable conformer which was found to be the twisted form as well as interested in the vibrational assignment of the fundamentals of the ring atoms. As a continuation of this initial study of the five membered rings with two silicon atoms we initiated a study with a carbon atom between the silicon atoms along with fluorine atoms on them i.e. 1,1,3,3-tetrafluoro-1,3-disilacyclopentane (c-$C_3H_6Si_2F_4$). With the fluorine atoms on the silicon atoms having largest electronegativity it could have a significant effect on the conformational stability of the heavy atom ring and the structural parameters. Additionally a very small fluorine atom should not have any steric effect. From this study we expected to determine the conformational form of the heavy atoms as well as all of the structural parameters of the molecule, and the frequencies of the fundamental vibrations. Additionally we carried out ab initio calculations to evaluate how well relatively small basis sets can predict the conformational stability and structural parameters of the five membered ring. The results of this microwave, infrared and Raman spectroscopic study along with the ab initio predicted values are reported herein.

EXPERIMENTAL AND THEORETICAL METHODS

The c-$C_3H_6Si_2F_4$ compound was prepared by the fluorination of 1,1,3,3-tetrachloro-1,3-dilacyclopentane [155] by freshly sublimed antimony trifluoride without solvent at room temperature for three hours. The sample was first purified by trap-to-trap distillation and finally by low pressure, low temperature sublimation. The purity of the sample was checked by infrared and nuclear magnetic resonance spectroscopy.

The rotational spectrum of c-$C_3H_6Si_2F_4$ was studied by using a CP-FTMW spectrometer developed at the University of Virginia, operating in the 6.5 to 18 GHz range. The chirped pulse methods used in this study have been described in detail previously [28], so only the brief details relevant to this experiment are necessary.

The microwave source was a 24 GS/s arbitrary waveform generator, producing a 12-0.5 GHz linear frequency sweep in 1 μs. The pulse was upconverted to 6.5-18 GHz by a 18.95 GHz phase-locked resonant dielectric oscillator (PDRO), and then amplified by a pulsed 300 W traveling wave tube amplifier. The amplified pulse is then transmitted through free space between two standard-gain microwave horns, where it interacts with a molecular beam generated by five pulsed nozzles (General Valve Series 9) operating perpendicular to the propagation direction of the microwave pulse. On the detection end, the receiver is protected from the high power pulse by a combination of a PIN diode limiter and single-pole microwave switch. The resulting molecular free induction decay (FID) was then amplified and digitized directly on a 100 GS/s oscilloscope with 33 GHz of hardware bandwidth, with a 20 μs detection time per FID. Due to the speed of this excitation and detection process, a sequence of 10 excitation/detection cycles is possible per gas pulse, and all ten detected FIDs are collected and averaged together before the next valve injection cycle begins. Phase stability of this experiment over the course of many valve injection cycles is enabled by locking all the frequency sources and the oscilloscope to a 10 MHz Rb-disciplined quartz oscillator. For this experiment, approximately 78 000 valve injection cycles of the sample gas were completed at 3.3 Hz to create a time-averaged spectrum of 780 000 molecular FIDs (approximately 6.5 hours

of averaging). Additionally, the time domain resolution afforded by a 20 μs FID generates an average Doppler broadened linewidth of approximately 130 kHz at FWHM.

The sample for spectral investigation was prepared by balancing c-$C_3H_6Si_2F_4$ vapor with approximately 3.4 atm of Ne gas (GTS Welco) for a total sample concentration of approximately 0.1%. This afforded a frequency-domain dynamic range of approximately 4000:1 at 780 000 averages, which enabled assignment of all common heavy atom single isotopologues (^{13}C, ^{29}Si, ^{30}Si) in natural abundance as well as a double isotopologue (^{29}Si / ^{30}Si). These assignments are listed in Tables 73-75 and the experimental analysis of c-$C_3H_6Si_2F_4$ was supplemented with ab initio electronic structure calculations for rotational constant and centrifugal distortion predictions (Table 76). These calculations were performed with the Gaussian 09 suite of programs [156].

The infrared spectrum of the gas (Fig. 43) was obtained from 4000 to 220 cm^{-1} on a Perkin-Elmer model 2000 Fourier transform spectrometer equipped with a Ge/CsI beamsplitter and a DTGS detector. Atmospheric water vapor was removed from the spectrometer housing by purging with dry nitrogen. The spectrum of the gas was obtained with a theoretical resolution of 0.5 cm^{-1} with 128 interferograms added and truncated.

Raman spectrum (Fig. 44) of the liquid was collected in back-scattering geometry using the 514.532 nm line of an Argon ion laser as the excitation source, with ~ 22 mW incident on the diamond cell. A Semrock 514 nm edge filter was used to separate the laser line from the Raman scattered light. The scattered light was dispersed in a Spectra-pro 500i spectrograph and detected with a Spec-10 liquid nitrogen cooled CCD detector. Raman spectra were collected using a 2400 g/mm grating with a slit width of 100 μm, which gives spectral resolution of ~ 0.2 cm^{-1}. The observed bands in the infrared

spectrum of the gas and Raman spectrum of the liquid along with their proposed assignments are listed in Table 77.

Table 73. Rotational transition frequencies (MHz) of the ground vibrational state of c-$C_3H_6Si_2F_4$.

c-$C_3H_6Si_2F_4$			c-$C_3H_6Si_2F_4$			c-$C_3H_6Si_2F_4$		
Transitions	ν_{obs}	$\Delta\nu^a$	Transitions	ν_{obs}	$\Delta\nu^a$	Transitions	ν_{obs}	$\Delta\nu^a$
$7_{1\,6} \leftarrow 6_{2\,4}$	6535.1069	0.0064	$7_{4\,4} \leftarrow 7_{3\,4}$	9510.5566	0.0315	$6_{3\,4} \leftarrow 5_{2\,4}$	15722.8977	0.0076
$9_{2\,7} \leftarrow 8_{3\,5}$	6626.8707	0.0105	$7_{4\,3} \leftarrow 7_{3\,5}$	9510.6425	-0.0134	$8_{2\,6} \leftarrow 7_{1\,6}$	15797.1394	0.0182
$13_{3\,11} \leftarrow 13_{2\,11}$	6677.9774	-0.0123	$6_{4\,3} \leftarrow 6_{3\,3}$	9510.9970	0.0220	$8_{2\,7} \leftarrow 7_{1\,7}$	16186.8760	0.0339
$12_{3\,10} \leftarrow 12_{2\,10}$	6708.3201	-0.0006	$5_{4\,2} \leftarrow 5_{3\,2}$	9511.2667	0.0144	$10_{1\,9} \leftarrow 9_{0\,9}$	16670.0780	-0.0550
$11_{3\,9} \leftarrow 11_{2\,9}$	6732.4364	-0.0161	$4_{4\,1} \leftarrow 4_{3\,1}$	9511.3859	-0.0243	$5_{4\,1} \leftarrow 4_{3\,1}$	16950.9792	0.0351
$10_{3\,8} \leftarrow 10_{2\,8}$	6751.1888	-0.0058	$11_{2\,10} \leftarrow 10_{3\,8}$	9551.3928	-0.0008	$7_{3\,4} \leftarrow 6_{2\,4}$	17203.9313	0.0443
$9_{3\,7} \leftarrow 9_{2\,7}$	6765.3359	-0.0158	$9_{1\,8} \leftarrow 8_{2\,6}$	9616.1991	0.0045	$7_{3\,5} \leftarrow 6_{2\,5}$	17212.2902	0.0467
$8_{3\,6} \leftarrow 8_{2\,6}$	6775.6965	-0.0044	$11_{2\,9} \leftarrow 10_{3\,7}$	9635.9327	0.0049	$9_{2\,7} \leftarrow 8_{1\,7}$	17240.4083	0.0466
$7_{3\,5} \leftarrow 7_{2\,5}$	6782.9645	-0.0076	$13_{3\,11} \leftarrow 12_{49}$	9840.9429	-0.0112	$9_{2\,8} \leftarrow 8_{1\,8}$	17734.2041	0.0516
$6_{3\,4} \leftarrow 6_{2\,4}$	6787.8277	-0.0059	$13_{3\,10} \leftarrow 12_{4\,8}$	9845.8772	0.0033			
$5_{3\,3} \leftarrow 5_{2\,3}$	6790.8723	-0.0082	$4_{2\,2} \leftarrow 3_{1\,2}$	9985.1545	-0.0079			
$4_{3\,2} \leftarrow 4_{2\,2}$	6792.6222	-0.0061	$4_{2\,3} \leftarrow 3_{1\,3}$	10072.3176	-0.0037			
$3_{3\,1} \leftarrow 3_{2\,1}$	6793.5023	-0.0065	$8_{0\,8} \leftarrow 7_{1\,6}$	10314.4550	-0.0063			
$3_{3\,0} \leftarrow 3_{2\,2}$	6794.1100	-0.0064	$10_{1\,10} \leftarrow 9_{2\,8}$	10386.0539	0.0009			
$4_{3\,1} \leftarrow 4_{2\,3}$	6794.4469	-0.0065	$6_{1\,5} \leftarrow 5_{0\,5}$	10444.0441	0.0026			
$5_{3\,2} \leftarrow 5_{2\,4}$	6795.1378	-0.0065	$12_{2\,11} \leftarrow 11_{3\,9}$	11030.5403	-0.0078			
$6_{3\,3} \leftarrow 6_{2\,5}$	6796.3666	-0.0061	$12_{2\,10} \leftarrow 11_{3\,8}$	11147.8743	-0.0012			
$7_{3\,4} \leftarrow 7_{2\,6}$	6798.3599	-0.0021	$10_{1\,9} \leftarrow 9_{2\,7}$	11160.8351	-0.0014			
$8_{3\,5} \leftarrow 8_{2\,7}$	6801.3714	-0.0061	$3_{3\,0} \leftarrow 2_{2\,0}$	11257.5551	-0.0088			
$9_{3\,6} \leftarrow 9_{2\,8}$	6805.7262	-0.0025	$3_{3\,1} \leftarrow 2_{2\,1}$	11257.6783	-0.0064			
$10_{3\,7} \leftarrow 10_{2\,9}$	6811.7705	-0.0016	$14_{3\,12} \leftarrow 13_{4\,10}$	11331.4508	0.0017			
$11_{3\,8} \leftarrow 11_{2\,10}$	6819.9203	0.0070	$14_{3\,11} \leftarrow 13_{4\,9}$	11339.0022	-0.0260			
$12_{3\,9} \leftarrow 12_{2\,11}$	6830.6024	-0.0076	$5_{2\,3} \leftarrow 4_{1\,3}$	11445.7429	-0.0078			
$13_{3\,10} \leftarrow 13_{2\,12}$	6844.3702	-0.0060	$5_{2\,4} \leftarrow 4_{1\,4}$	11589.7965	-0.0037			
$11_{3\,9} \leftarrow 10_{4\,7}$	6860.9769	-0.0207	$5_{4\,2} \leftarrow 6_{1\,6}$	11612.8264	-0.0232			
$11_{3\,8} \leftarrow 10_{4\,6}$	6862.8502	-0.0014	$9_{0\,9} \leftarrow 8_{1\,7}$	11731.0570	-0.0080			
$15_{3\,12} \leftarrow 15_{2\,14}$	6883.4665	-0.0034	$11_{1\,11} \leftarrow 10_{2\,9}$	11789.2550	-0.0006			
$16_{3\,13} \leftarrow 16_{2\,15}$	6910.0946	-0.0382	$7_{1\,6} \leftarrow 6_{0\,6}$	11986.3947	0.0011			

c-$C_3H_6Si_2F_4$			c-$C_3H_6Si_2F_4$			c-$C_3H_6Si_2F_4$		
Transitions	ν_{obs}	$\Delta\nu^a$	Transitions	ν_{obs}	$\Delta\nu^a$	Transitions	ν_{obs}	$\Delta\nu^a$
$2_{2\,0} \leftarrow 1_{1\,0}$	7044.8446	-0.0063	$14_{5\,10} \leftarrow 14_{4\,10}$	12223.3226	-0.0206			
$2_{2\,1} \leftarrow 1_{1\,1}$	7059.5546	-0.0049	$14_{5\,9} \leftarrow 14_{4\,11}$	12223.4900	0.0304			
$13_{4\,10} \leftarrow 12_{5\,8}$	7119.1018	0.0027	$13_{5\,9} \leftarrow 13_{4\,9}$	12224.7772	0.0026			
$4_{1\,3} \leftarrow 3_{0\,3}$	7384.6694	0.0000	$11_{5\,7} \leftarrow 11_{4\,7}$	12226.8317	0.0196			
$6_{0\,6} \leftarrow 5_{1\,4}$	7449.4537	-0.0039	$10_{5\,6} \leftarrow 10_{4\,6}$	12227.5115	0.0097			
$8_{1\,8} \leftarrow 7_{2\,6}$	7555.5886	-0.0003	$9_{5\,5} \leftarrow 9_{4\,5}$	12228.0248	0.0044			
$17_{6\,11} \leftarrow 16_{7\,9}$	7634.9756	-0.0320	$8_{5\,4} \leftarrow 8_{4\,4}$	12228.4189	0.0193			
$10_{2\,9} \leftarrow 9_{3\,7}$	8070.2200	0.0026	$7_{5\,3} \leftarrow 7_{4\,3}$	12228.6817	0.0145			
$8_{1\,7} \leftarrow 7_{2\,5}$	8073.9295	0.0056	$6_{5\,2} \leftarrow 6_{4\,2}$	12228.8390	-0.0090			
$10_{2\,8} \leftarrow 9_{3\,6}$	8129.1638	0.0073	$5_{5\,0} \leftarrow 5_{4\,2}$	12228.9894	0.0258			
$12_{3\,10} \leftarrow 11_{4\,8}$	8350.7954	-0.0071	$13_{2\,12} \leftarrow 12_{3\,10}$	12507.3288	-0.0087			
$12_{3\,9} \leftarrow 11_{4\,7}$	8353.8904	0.0047	$13_{2\,11} \leftarrow 12_{3\,9}$	12665.6940	0.0235			
$3_{2\,1} \leftarrow 2_{1\,1}$	8518.3533	-0.0073	$11_{1\,10} \leftarrow 10_{2\,8}$	12706.6446	-0.0184			
$3_{2\,2} \leftarrow 2_{1\,2}$	8562.2389	-0.0048	$4_{3\,1} \leftarrow 3_{2\,1}$	12745.1683	-0.0049			
$7_{0\,7} \leftarrow 6_{1\,5}$	8887.0220	-0.0045	$4_{3\,2} \leftarrow 3_{2\,2}$	12745.7720	-0.0040			
$5_{1\,4} \leftarrow 4_{0\,4}$	8910.2708	0.0012	$6_{2\,4} \leftarrow 5_{1\,4}$	12900.7440	-0.0067			
$9_{1\,9} \leftarrow 8_{2\,7}$	8974.8062	-0.0001	$6_{2\,5} \leftarrow 5_{1\,5}$	13114.6949	-0.0019			
$19_{4\,16} \leftarrow 19_{3\,16}$	9444.7055	-0.0073	$10_{0\,10} \leftarrow 9_{1\,8}$	13136.0844	-0.0089			
$18_{4\,15} \leftarrow 18_{3\,15}$	9459.3982	-0.0052	$12_{1\,12} \leftarrow 11_{2\,10}$	13184.3540	0.0076			
$17_{4\,14} \leftarrow 17_{3\,14}$	9471.3280	0.0113	$8_{1\,7} \leftarrow 7_{0\,7}$	13537.8178	0.0052			
$16_{4\,13} \leftarrow 16_{3\,13}$	9480.8782	-0.0098	$21_{6\,16} \leftarrow 20_{7\,14}$	13592.5927	0.0312			
$15_{4\,1} \leftarrow 15_{3\,12}$	9488.4987	-0.0020	$14_{2\,13} \leftarrow 13_{3\,11}$	13981.3797	-0.0229			
$14_{4\,1} \leftarrow 14_{3\,11}$	9494.4804	-0.0084	$5_{3\,2} \leftarrow 4_{2\,2}$	14232.3182	-0.0062			
$16_{4\,1} \leftarrow 16_{3\,14}$	9497.9125	0.0108	$5_{3\,3} \leftarrow 4_{2\,3}$	14234.1177	-0.0101			
$13_{4\,1} \leftarrow 13_{3\,10}$	9499.1396	-0.0017	$7_{2\,5} \leftarrow 6_{1\,5}$	14350.9095	-0.0057			
$15_{4\,1} \leftarrow 15_{3\,13}$	9500.1345	-0.0073	$11_{0\,11} \leftarrow 10_{1\,9}$	14528.7478	-0.0256			
$14_{4\,1} \leftarrow 14_{3\,12}$	9502.2529	0.0054	$7_{2\,6} \leftarrow 6_{1\,6}$	14647.0325	-0.0019			
$12_{4\,9} \leftarrow 12_{3\,9}$	9502.7047	-0.0013	$15_{6\,10} \leftarrow 15_{5\,10}$	14942.6553	-0.0015			
$13_{4\,9} \leftarrow 13_{3\,11}$	9504.1552	-0.0039	$14_{6\,8} \leftarrow 14_{5\,10}$	14943.6304	0.0581			

c-$C_3H_6Si_2F_4$			c-$C_3H_6Si_2F_4$			c-$C_3H_6Si_2F_4$		
Transitions	ν_{obs}	$\Delta\nu^a$	Transitions	ν_{obs}	$\Delta\nu^a$	Transitions	ν_{obs}	$\Delta\nu^a$
$11_{4\,8} \leftarrow 11_{3\,8}$	9505.3919	-0.0018	$13_{6\,8} \leftarrow 13_{5\,8}$	14944.3313	0.0145			
$12_{4\,8} \leftarrow 12_{3\,10}$	9505.8380	-0.0019	$12_{6\,7} \leftarrow 12_{5\,7}$	14944.8909	-0.0247			
$11_{4\,7} \leftarrow 11_{3\,9}$	9507.2569	-0.0157	$11_{6\,6} \leftarrow 11_{5\,6}$	14945.3672	-0.0215			
$10_{4\,7} \leftarrow 10_{3\,7}$	9507.3872	0.0046	$10_{6\,4} \leftarrow 10_{5\,6}$	14945.7256	-0.0297			
$10_{4\,7} \leftarrow 10_{3\,7}$	9507.3872	0.0046	$9_{6\,3} \leftarrow 9_{5\,5}$	14946.0129	-0.0200			
$10_{4\,6} \leftarrow 10_{3\,8}$	9508.4516	-0.0036	$8_{6\,2} \leftarrow 8_{5\,4}$	14946.2350	-0.0024			
$9_{4\,6} \leftarrow 9_{3\,6}$	9508.8200	-0.0016	$6_{6\,0} \leftarrow 6_{5\,2}$	14946.4569	-0.0259			
$9_{4\,5} \leftarrow 9_{3\,7}$	9509.3986	0.0000	$9_{1\,8} \leftarrow 8_{0\,8}$	15098.8363	-0.0180			
$8_{4\,5} \leftarrow 8_{3\,5}$	9509.8327	-0.0023	$4_{4\,0} \leftarrow 3_{3\,0}$	15463.0775	0.0033			
$8_{4\,4} \leftarrow 8_{3\,6}$	9510.1223	-0.0010	$6_{3\,3} \leftarrow 5_{2\,3}$	15718.6738	-0.0218			

[a] $\Delta\nu = \nu_{obs} - \nu_{calc}$ in mHz.

Table 74. Rotational transition frequencies (MHz) of the ground vibrational state of c-$C_3H_6Si_2F_4$.

^{29}Si			^{30}Si			$^{29}Si/^{30}Si$		
Transitions	ν_{obs}	$\Delta\nu^a$	Transitions	ν_{obs}	$\Delta\nu^a$	Transitions	ν_{obs}	$\Delta\nu^a$
$8_{3\,6} \leftarrow 8_{2\,6}$	6787.1087	9.6	$6_{3\,4} \leftarrow 6_{2\,4}$	6810.0547	-5.3	$2_{2\,0} \leftarrow 1_{1\,0}$	7037.7001	-11.8
$6_{3\,4} \leftarrow 6_{2\,4}$	6799.0530	0.4	$5_{3\,3} \leftarrow 5_{2\,3}$	6813.0094	-8.5	$2_{2\,1} \leftarrow 1_{1\,1}$	7052.1253	-7.6
$5_{3\,3} \leftarrow 5_{2\,3}$	6802.0549	0.6	$4_{3\,2} \leftarrow 4_{2\,2}$	6814.7074	-7.4	$4_{1\,3} \leftarrow 3_{0\,3}$	7335.3357	-8
$4_{3\,2} \leftarrow 4_{2\,2}$	6803.7724	-3.8	$3_{3\,1} \leftarrow 3_{2\,1}$	6815.5651	-4.6	$3_{2\,1} \leftarrow 2_{1\,1}$	8497.8651	-1.9
$3_{3\,1} \leftarrow 3_{2\,1}$	6804.6434	-0.3	$3_{3\,0} \leftarrow 3_{2\,2}$	6816.1554	-4.2	$3_{2\,2} \leftarrow 2_{1\,2}$	8540.8970	-0.7
$3_{3\,0} \leftarrow 3_{2\,2}$	6805.2385	-3.7	$4_{3\,1} \leftarrow 4_{2\,3}$	6816.4797	-6.9	$5_{1\,4} \leftarrow 4_{0\,4}$	8846.5483	-7.1
$4_{3\,1} \leftarrow 4_{2\,3}$	6805.5735	-0.7	$5_{3\,2} \leftarrow 5_{2\,4}$	6817.1537	-3.5	$4_{2\,2} \leftarrow 3_{1\,2}$	9951.4234	-6
$5_{3\,2} \leftarrow 5_{2\,4}$	6806.2541	-0.6	$6_{3\,3} \leftarrow 6_{2\,5}$	6818.3473	-2.1	$4_{2\,3} \leftarrow 3_{1\,3}$	10036.9146	4.4
$6_{3\,3} \leftarrow 6_{2\,5}$	6807.4613	-3.4	$8_{3\,5} \leftarrow 8_{2\,7}$	6823.2033	-2.6	$6_{1\,5} \leftarrow 5_{0\,5}$	10365.7674	7.9
$7_{3\,4} \leftarrow 7_{2\,6}$	6809.4267	2.6	$2_{2\,0} \leftarrow 1_{1\,0}$	7040.1189	-4.1	$3_{3\,0} \leftarrow 2_{2\,0}$	11249.9686	-5.9
$8_{3\,5} \leftarrow 8_{2\,7}$	6812.3889	-5.2	$2_{2\,1} \leftarrow 1_{1\,1}$	7054.6343	-6.5	$3_{3\,1} \leftarrow 2_{2\,1}$	11250.1030	12.9
$9_{3\,6} \leftarrow 9_{2\,8}$	6816.6805	0.7	$4_{1\,3} \leftarrow 3_{0\,3}$	7352.0001	-0.9	$5_{2\,3} \leftarrow 4_{1\,3}$	11398.8753	2.9
$11_{3\,8} \leftarrow 11_{2\,10}$	6830.6015	-47	$6_{0\,6} \leftarrow 5_{1\,4}$	7392.5881	5.7	$4_{3\,1} \leftarrow 3_{2\,1}$	12723.9606	-7.3
$2_{2\,0} \leftarrow 1_{1\,0}$	7042.4581	-3.3	$8_{1\,8} \leftarrow 7_{2\,6}$	7473.7892	13.4	$4_{3\,2} \leftarrow 3_{2\,2}$	12724.5416	-2.7
$2_{2\,1} \leftarrow 1_{1\,1}$	7057.0701	-3.4	$8_{1\,7} \leftarrow 7_{2\,5}$	7985.5776	7.3	$5_{3\,2} \leftarrow 4_{2\,2}$	14197.5039	-19
$4_{1\,3} \leftarrow 3_{0\,3}$	7368.1723	-0.6	$3_{2\,1} \leftarrow 2_{1\,1}$	8504.7848	-3.9	$5_{3\,3} \leftarrow 4_{2\,3}$	14199.2849	37.2
$6_{0\,6} \leftarrow 5_{1\,4}$	7420.7400	-3.9	$3_{2\,2} \leftarrow 2_{1\,2}$	8548.1017	-4.6	$1_{1\,0} \leftarrow 6_{1\,6}$	14568.5471	-1.7
$8_{1\,8} \leftarrow 7_{2\,6}$	7514.2952	7.8	$7_{0\,7} \leftarrow 6_{1\,5}$	8821.8846	6.7			
$8_{1\,7} \leftarrow 7_{2\,5}$	8029.3238	9.9	$5_{1\,4} \leftarrow 4_{0\,4}$	8868.0719	0.7			
$3_{2\,1} \leftarrow 2_{1\,1}$	8511.5030	-3	$11_{2\,10} \leftarrow 10_{3\,8}$	9430.6744	-6.1			
$3_{2\,2} \leftarrow 2_{1\,2}$	8555.1003	-2.7	$11_{2\,9} \leftarrow 10_{3\,7}$	9512.8399	38.8			
$7_{0\,7} \leftarrow 6_{1\,5}$	8854.1369	0.1	$9_{1\,8} \leftarrow 8_{2\,6}$	9518.2710	-29.9			
$5_{1\,4} \leftarrow 4_{0\,4}$	8888.9613	0.4	$9_{4\,6} \leftarrow 9_{3\,6}$	9539.7768	5.6			
$9_{1\,9} \leftarrow 8_{2\,7}$	8929.4253	7.6	$9_{4\,5} \leftarrow 9_{3\,7}$	9540.3195	-2.7			
$11_{4\,7} \leftarrow 11_{3\,9}$	9522.9108	3.9	$8_{4\,5} \leftarrow 8_{3\,5}$	9540.7461	-6.8			
$10_{4\,7} \leftarrow 10_{3\,7}$	9523.0314	4.1	$7_{4\,4} \leftarrow 7_{3\,4}$	9541.4291	7.3			

^{29}Si			^{30}Si			^{29}Si/^{30}Si		
Transitions	ν_{obs}	$\Delta\nu^a$	Transitions	ν_{obs}	$\Delta\nu^a$	Transitions	ν_{obs}	$\Delta\nu^a$
$10_{4\,6} \leftarrow 10_{3\,8}$	9524.0735	-1.8	$7_{4\,3} \leftarrow 7_{3\,5}$	9541.5399	-6.7			
$9_{4\,6} \leftarrow 9_{3\,6}$	9524.4387	-4.3	$6_{4\,3} \leftarrow 6_{3\,3}$	9541.8715	13.4			
$9_{4\,5} \leftarrow 9_{3\,7}$	9525.0211	14.2	$5_{4\,2} \leftarrow 5_{3\,2}$	9542.1412	14.1			
$8_{4\,5} \leftarrow 8_{3\,5}$	9525.4485	8	$4_{4\,1} \leftarrow 4_{3\,1}$	9542.2648	-15.7			
$8_{4\,4} \leftarrow 8_{3\,6}$	9525.7237	1.6	$4_{2\,2} \leftarrow 3_{1\,2}$	9962.8200	-2.8			
$7_{4\,3} \leftarrow 7_{3\,5}$	9526.2316	-16	$4_{2\,3} \leftarrow 3_{1\,3}$	10048.8654	-3.2			
$6_{4\,2} \leftarrow 6_{3\,4}$	9526.5990	-15	$8_{0\,8} \leftarrow 7_{1\,6}$	10241.2198	5.9			
$5_{4\,1} \leftarrow 5_{3\,3}$	9526.8667	13.9	$6_{1\,5} \leftarrow 5_{0\,5}$	10392.1951	1			
$4_{4\,0} \leftarrow 4_{3\,2}$	9526.9938	-1.8	$3_{3\,0} \leftarrow 2_{2\,0}$	11252.5247	-12.9			
$4_{2\,2} \leftarrow 3_{1\,2}$	9973.8781	-2.9	$3_{3\,1} \leftarrow 2_{2\,1}$	11252.6556	0.7			
$4_{2\,3} \leftarrow 3_{1\,3}$	10060.4755	-1.3	$5_{2\,3} \leftarrow 4_{1\,3}$	11414.7030	-2.6			
$8_{0\,8} \leftarrow 7_{1\,6}$	10277.4821	-1.9	$5_{2\,4} \leftarrow 4_{1\,4}$	11556.9320	-3.3			
$6_{1\,5} \leftarrow 5_{0\,5}$	10417.8618	1.8	$9_{0\,9} \leftarrow 8_{1\,7}$	11649.9281	15.7			
$3_{3\,0} \leftarrow 2_{2\,0}$	11255.0150	-7.2	$7_{1\,6} \leftarrow 6_{0\,6}$	11924.7668	0.3			
$3_{3\,1} \leftarrow 2_{2\,1}$	11255.1441	2.9	$9_{5\,4} \leftarrow 9_{4\,6}$	12267.7443	5			
$5_{2\,3} \leftarrow 4_{1\,3}$	11430.0721	-2	$10_{5\,5} \leftarrow 10_{4\,7}$	12267.2486	8.7			
$5_{2\,4} \leftarrow 4_{1\,4}$	11573.2027	-0.4	$8_{5\,4} \leftarrow 8_{4\,4}$	12268.1285	24			
$9_{0\,9} \leftarrow 8_{1\,7}$	11690.0975	-0.7	$7_{5\,2} \leftarrow 7_{4\,4}$	12268.3701	5.1			
$11_{1\,11} \leftarrow 10_{2\,9}$	11735.8591	-3.9	$6_{5\,1} \leftarrow 6_{4\,3}$	12268.5249	-15.6			
$7_{1\,6} \leftarrow 6_{0\,6}$	11955.2754	2	$5_{5\,1} \leftarrow 5_{4\,1}$	12268.6806	27.9			
$10_{5\,5} \leftarrow 10_{4\,7}$	12247.5813	18.4	$4_{3\,1} \leftarrow 3_{2\,1}$	12731.1236	-6			
$9_{5\,5} \leftarrow 9_{4\,5}$	12248.0739	7.6	$4_{3\,2} \leftarrow 3_{2\,2}$	12731.7152	0.4			
$8_{5\,4} \leftarrow 8_{4\,4}$	12248.4486	8.7	$6_{2\,4} \leftarrow 5_{1\,4}$	12861.0443	0.4			
$7_{5\,2} \leftarrow 7_{4\,4}$	12248.7171	12.9	$6_{2\,5} \leftarrow 5_{1\,5}$	13072.3198	-2.6			
$6_{5\,1} \leftarrow 6_{4\,3}$	12248.8932	11.1	$8_{1\,7} \leftarrow 7_{0\,7}$	13466.2604	-0.6			
$4_{3\,1} \leftarrow 3_{2\,1}$	12738.0816	2.9	$5_{3\,2} \leftarrow 4_{2\,2}$	14209.2793	2.5			
$4_{3\,2} \leftarrow 3_{2\,2}$	12738.6762	3.7	$5_{3\,3} \leftarrow 4_{2\,3}$	14211.0196	-8			

^{29}Si			^{30}Si			^{29}Si/^{30}Si		
Transitions	ν_{obs}	$\Delta\nu$[a]	Transitions	ν_{obs}	$\Delta\nu$[a]	Transitions	ν_{obs}	$\Delta\nu$[a]
$6_{2\,4} \leftarrow 5_{1\,4}$	12880.7007	-0.1	$7_{2\,5} \leftarrow 6_{1\,5}$	14302.5703	1.6			
$10_{0\,10} \leftarrow 9_{1\,8}$	13091.2487	4.1	$7_{2\,6} \leftarrow 6_{1\,6}$	14595.0490	-3.5			
$6_{2\,5} \leftarrow 5_{1\,5}$	13093.2980	0.2	$4_{4\,1} \leftarrow 3_{3\,1}$	15457.8457	5.3			
$8_{1\,7} \leftarrow 7_{0\,7}$	13501.6898	9.5	$6_{3\,3} \leftarrow 5_{2\,3}$	15686.6441	-22			
$5_{3\,2} \leftarrow 4_{2\,2}$	14220.6843	0.6	$6_{3\,4} \leftarrow 5_{2\,4}$	15690.7440	5			
$5_{3\,3} \leftarrow 4_{2\,3}$	14222.4573	-2.9						
$7_{2\,5} \leftarrow 6_{1\,5}$	14326.5038	0.6						
$7_{2\,6} \leftarrow 6_{1\,6}$	14620.7833	-0.4						
$9_{1\,8} \leftarrow 8_{0\,8}$	15057.6363	7.1						
$4_{4\,0} \leftarrow 3_{3\,0}$	15460.4318	5.9						
$6_{3\,3} \leftarrow 5_{2\,3}$	15702.5043	-16						
$6_{3\,4} \leftarrow 5_{2\,4}$	15706.6499	-2.7						
$8_{2\,7} \leftarrow 7_{1\,7}$	16155.6801	-9.8						
$5_{4\,1} \leftarrow 4_{3\,1}$	16943.7174	-21						

[a] $\Delta\nu = \nu_{obs} - \nu_{calc}$ in kHz.

Table 75. Rotational transition frequencies (MHz) of the ground vibrational state of c-$C_3H_6Si_2F_4$.

^{13}C-β/β′			^{13}C-α		
Transitions	ν_{obs}	$\Delta\nu$[a]	Transitions	ν_{obs}	$\Delta\nu$[a]
$2_{2\,0} \leftarrow 1_{1\,0}$	6976.4177	0.8	$2_{2\,0} \leftarrow 1_{1\,0}$	7004.2435	-0.2
$2_{2\,1} \leftarrow 1_{1\,1}$	6988.5518	2	$2_{2\,1} \leftarrow 1_{1\,1}$	7017.2495	-4.9
$4_{1\,3} \leftarrow 3_{0\,3}$	7335.0759	-0.1	$4_{1\,3} \leftarrow 3_{0\,3}$	7356.6206	-3.5
$6_{0\,6} \leftarrow 5_{1\,4}$	7468.2632	7.7	$6_{0\,6} \leftarrow 5_{1\,4}$	7466.7058	0.1
$1_{2\,8} \leftarrow 9_{3\,6}$	8178.7685	8.1	$3_{2\,1} \leftarrow 2_{1\,1}$	8477.7036	-5.1
$3_{2\,1} \leftarrow 2_{1\,1}$	8448.4280	-0.3	$3_{2\,2} \leftarrow 2_{1\,2}$	8516.5446	-4.7
$3_{2\,2} \leftarrow 2_{1\,2}$	8484.6601	0.5	$5_{1\,4} \leftarrow 4_{0\,4}$	8876.0991	-8
$5_{1\,4} \leftarrow 4_{0\,4}$	8849.9715	-0.6	$7_{0\,7} \leftarrow 6_{1\,5}$	8909.0007	3.1
$7_{0\,7} \leftarrow 6_{1\,5}$	8911.4741	-20.7	$4_{2\,2} \leftarrow 3_{1\,2}$	9945.1779	0.3
$5_{4\,2} \leftarrow 5_{3\,2}$	9367.2192	3.8	$4_{2\,3} \leftarrow 3_{1\,3}$	10022.3748	-4.9
$4_{2\,2} \leftarrow 3_{1\,2}$	9914.8230	5.1	$6_{1\,5} \leftarrow 5_{0\,5}$	10402.7330	-7.3
$4_{2\,3} \leftarrow 3_{1\,3}$	9986.8607	-1.3	$3_{3\,0} \leftarrow 2_{2\,0}$	11189.0574	0.8
$8_{0\,8} \leftarrow 7_{1\,6}$	10346.7302	-9.5	$3_{3\,1} \leftarrow 2_{2\,1}$	11189.1404	-11.4
$6_{1\,5} \leftarrow 5_{0\,5}$	10371.4973	-1.1	$5_{2\,3} \leftarrow 4_{1\,3}$	11407.0357	-4.1
$3_{3\,1} \leftarrow 2_{2\,1}$	11142.7882	-21.7	$5_{2\,4} \leftarrow 4_{1\,4}$	11534.7471	-4.9
$5_{2\,3} \leftarrow 4_{1\,3}$	11375.9305	4.2	$7_{1\,6} \leftarrow 6_{0\,6}$	11936.8419	-5.5
$5_{2\,4} \leftarrow 4_{1\,4}$	11495.1632	0.9	$4_{3\,1} \leftarrow 3_{2\,1}$	12675.0517	0.6
$7_{1\,6} \leftarrow 6_{0\,6}$	11899.9354	-2.8	$4_{3\,2} \leftarrow 3_{2\,2}$	12675.5218	-4.8
$4_{3\,1} \leftarrow 3_{2\,1}$	12626.4538	4.1	$6_{2\,4} \leftarrow 5_{1\,4}$	12863.7961	7.1
$4_{3\,2} \leftarrow 3_{2\,2}$	12626.8729	7.3	$6_{2\,5} \leftarrow 5_{1\,5}$	13053.6749	-4
$6_{2\,4} \leftarrow 5_{1\,4}$	12832.1895	5	$8_{1\,7} \leftarrow 7_{0\,7}$	13478.8260	11
$6_{2\,5} \leftarrow 5_{1\,5}$	13009.5686	-3.1	$5_{3\,2} \leftarrow 4_{2\,2}$	14160.6738	-9.1
$5_{3\,2} \leftarrow 4_{2\,2}$	14109.8586	3.2	$5_{3\,3} \leftarrow 4_{2\,3}$	14162.1113	4.9
$5_{3\,3} \leftarrow 4_{2\,3}$	14111.1132	13.1	$7_{2\,5} \leftarrow 6_{1\,5}$	14316.0182	-1.2
$7_{2\,5} \leftarrow 6_{1\,5}$	14284.1405	27.7	$7_{2\,6} \leftarrow 6_{1\,6}$	14579.1945	15
$4_{4\,0} \leftarrow 3_{3\,0}$	15303.0869	18	$4_{4\,0} \leftarrow 3_{3\,0}$	15367.5008	20.9
$6_{3\,3} \leftarrow 5_{2\,3}$	15592.6958	-24.7			
$5_{4\,1} \leftarrow 4_{3\,1}$	16786.9472	-22.9			

[a] $\Delta\nu = \nu_{obs} - \nu_{calc}$ in kHz.

Table 76. Experimental rotational and centrifugal distortion constants of c-$C_3H_6Si_2F_4$ isotopologues

	c-$C_3H_6Si_2F_4$		^{29}Si [b]	^{30}Si [b]	^{29}Si/^{30}Si [b]	^{13}C-β/β′[b]	13C-α[b]
	MP2(full)/ 6-31G(d)	Experimental					
A (MHz)	2058.3427	2102.74026(68)	2102.68742(51)	2102.63717(55)	2102.5846(20)	2080.16608(98)	2089.2035(12)
B (MHz)	744.6153	751.34319(32)	749.01578(33)	746.73383(32)	744.3835(12)	748.05599(53)	749.64852(57)
C (MHz)	725.8189	736.51478(31)	734.28573(27)	732.09979(25)	729.8480(25)	735.84108(49)	736.54375(70)
D_J (kHz)	0.02379	0.03236(77)					
D_{JK} (kHz)	0.3310	0.0638(39)					
D_K (kHz)	0.423	0.190(14)					
d_J (kHz)	0	[0]					
d_K (kHz)	-0.17	-0.41(9)					
N [a]		142	67	59	17	28	26
σ (kHz)		16.6	9.14	10.8	12.0	10.9	7.43

[a] Number of frequencies fitted.
[b] Distortion constants are fixed to that of the normal species for all isotopologues.

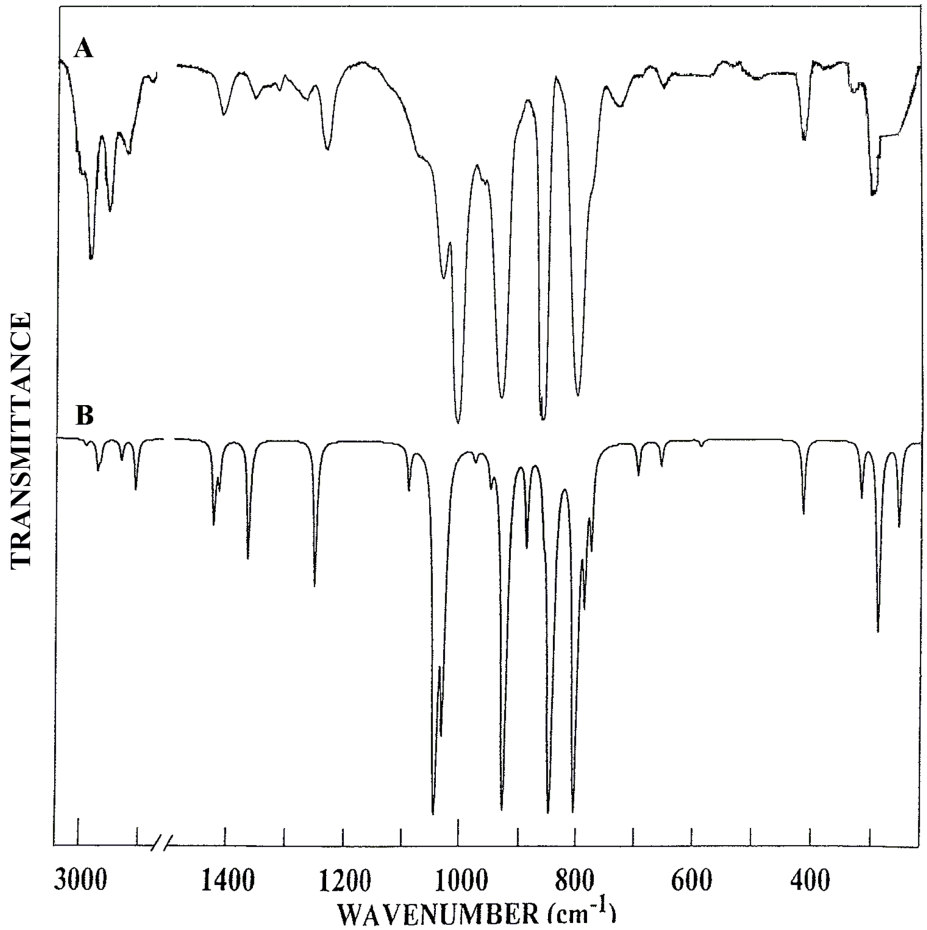

Figure 43. Comparison of experimental (path length = 9.5 cm & gas pressure = 400 mTorr) and calculated infrared spectra of c-$C_3H_6Si_2F_4$: (A) observed spectrum of gas; (B) simulated spectrum of twist conformer.

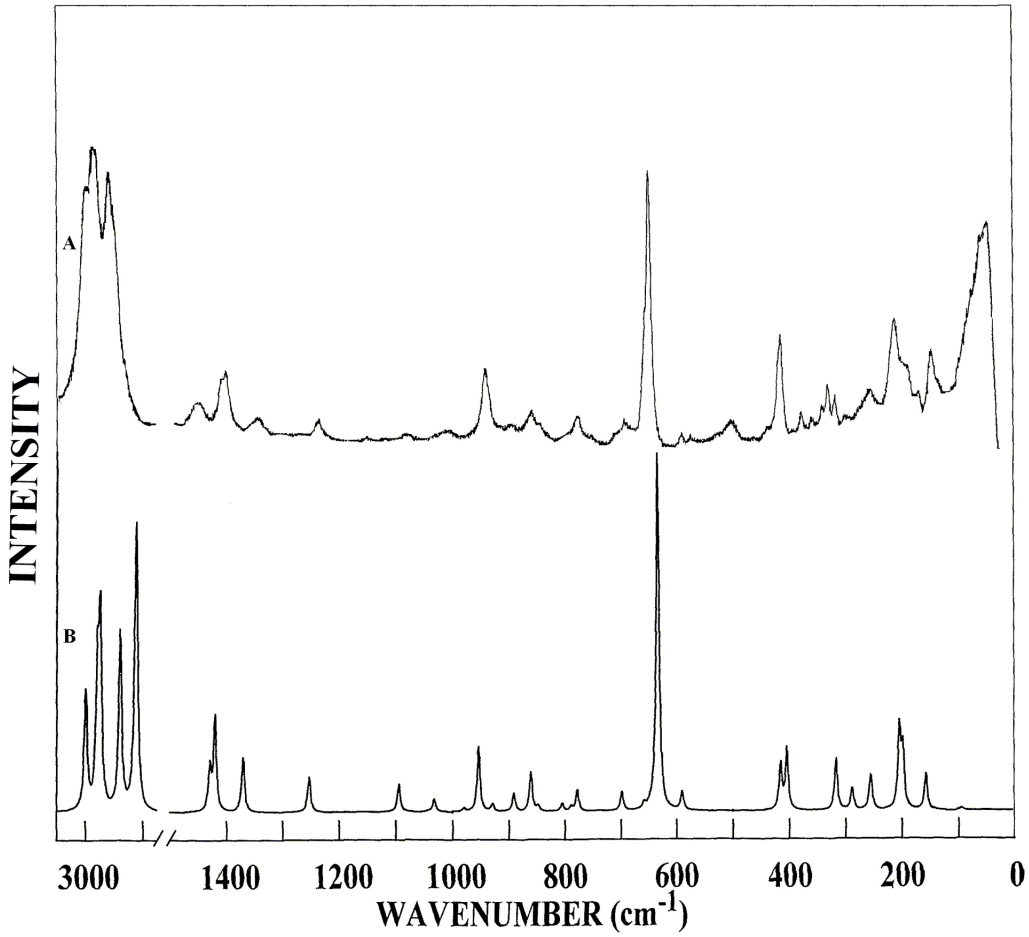

Figure 44. Comparison of experimental and calculated Raman spectra of c-$C_3H_6Si_2F_4$: (A) observed spectrum of liquid; (B) simulated spectrum of twist conformer.

Table 77. Calculated[a] and observed frequencies (cm^{-1}) for the twist form of c-$C_3H_6Si_2F_4$ (C_2).

	Vib. No.	Approx. description	ab initio	fixed scaled[b]	IR int.	Raman act.	dp ratio	IR gas	Raman liquid	P.E.D.[c]	Band Contour		
											A	B	C
A	ν_1	β-CH_2 antisymmetric stretch	3171	2975	3.2	100.8	0.42	2979	2980	$88S_1$, $12S_3$	-	-	100
	ν_2	α-CH_2 symmetric stretch	3134	2940	4.1	95.4	0.11	2958	2958	$100S_2$	-	-	100
	ν_3	β-CH_2 symmetric stretch	3105	2912	0.0	140.3	0.08	2917	2920	$89S_3$, $12S_1$	-	-	100
	ν_4	β-CH_2 deformation	1521	1430	17.8	8.0	0.61	1435	1438	$100S_4$	-	-	100
	ν_5	α-CH_2 symmetric deformation	1458	1371	27.2	9.5	0.74	1353	1349	$100S_5$	-	-	100
	ν_6	β-CH_2 twist	1321	1254	9.8	5.0	0.73	1240	1241	$52S_6$, $32S_7$, $13S_{13}$	-	-	100
	ν_7	β-CH_2 wag	1153	1095	9.2	3.7	0.72	1080	1079	$52S_7$, $30S_6$, $13S_9$	-	-	100
	ν_8	SiF_2 asymmetric stretch	1032	980	2.8	0.4	0.74	970		$41S_8$, $41S_{11}$	-	-	100
	ν_9	ring deformation	1003	954	6.1	7.1	0.48		944	$74S_9$, $13S_7$	-	-	100
	ν_{10}	SiF_2 symmetric stretch	938	891	21.0	1.8	0.63	897	897	$60S_{10}$,$15S_8$, $11S_{14}$	-	-	100
	ν_{11}	α-CH_2 twist	908	861	9.1	3.8	0.74	~861	861	$44S_{11}$, $35S_8$, $17S_{10}$	-	-	100
	ν_{12}	ring deformation	844	805	248.3	0.7	0.66	801	800	$47S_{12}$, $22S_{13}$, $16S_{16}$	-	-	100
	ν_{13}	β-CH_2 rock	816	778	19.3	1.8	0.58	789	778	$44S_{13}$, $16S_{12}$, $12S_6$	-	-	100
	ν_{14}	ring breathing	665	634	0.1	23.5	0.04	648	650	$64S_{14}$, $12S_{18}$	-	-	100
	ν_{15}	SiF_2 symmetric deformation	418	405	0.0	2.2	0.24	420	421	$40S_{15}$, $37S_{18}$	-	-	100

	ν_{16}	SiF_2 wag	301	289	27.4	0.2	0.68		298	$50S_{16}$, $18S_{14}$	-	-	100
	ν_{17}	SiF_2 rock	267	256	16.8	0.5	0.52		257	$33S_{17}$, $23S_{16}$, $13S_{15}$	-	-	100
	ν_{18}	ring deformation	214	205	1.9	1.0	0.42		214	$23S_{18}$, $41S_{15}$, $10S_{16}$	-	-	100
	ν_{19}	SiF_2 twist	166	158	0.5	0.3	0.73		151	$68S_{19}$, $21S_{17}$	-	-	100
	ν_{20}	ring twist	97	95	0.7	0.1	0.73		92	$56S_{20}$, $28S_{17}$, $16S_{19}$	-	-	100
B	ν_{21}	α-CH_2 antisymmetric stretch	3198	3000	1.1	65.6	0.75	2989	2993	$100S_{21}$	-	100	-
	ν_{22}	β-CH_2 antisymmetric stretch	3177	2980	5.6	71.7	0.75	2981	2979	$95S_{22}$	58	42	-
	ν_{23}	β-CH_2 symmetric stretch	3107	2915	10.4	24.3	0.75	2913	2920	$95S_{23}$	47	53	-
	ν_{24}	β-CH_2 asymmetric deformation	1511	1421	8.8	17.0	0.75	1418	1412	$100S_{24}$	3	97	-
	ν_{25}	β-CH_2 wag	1321	1255	26.4	0.4	0.75	1244	1241	$79S_{25}$, $29S_{28}$	99	1	-
	ν_{26}	α-CH_2 wag	1098	1044	262.7	0.1	0.75	1036		$73S_{26}$, $17S_{32}$	100	-	-
	ν_{27}	β-CH_2 twist	1087	1032	91.2	1.5	0.75	1009	1008	$73S_{27}$	14	86	-
	ν_{28}	SiF_2 asymmetric stretch	979	929	237.1	0.8	0.75	936	938	$79S_{28}$	-	100	-
	ν_{29}	SiF_2 symmetric stretch	892	848	257.4	0.5	0.75	865	867	$77S_{29}$, $10S_{26}$, $10S_{32}$	98	2	-
	ν_{30}	β-CH_2 rock	824	789	32.0	0.4	0.75	789		$23S_{30}$, $28S_{31}$, $26S_{34}$	98	2	-
	ν_{31}	ring deformation	734	698	6.9	1.4	0.75	698	696	$32S_{31}$, $19S_{33}$, $19S_{30}$	3	97	-
	ν_{32}	ring deformation	688	658	5.4	0.4	0.75	660	657	$34S_{32}$, $22S_{33}$, $15S_{34}$	17	83	-
	ν_{33}	α-CH_2 rock	619	590	1.3	1.1	0.75	597	593	$29S_{33}$, $36S_{30}$,	99	1	-

									$13S_{32}$, $11S_{31}$			
ν_{34}	ring deformation	427	416	15.9	1.7	0.75	416	416	$35S_{34}$, $17S_{31}$, $15S_{32}$, $11S_{36}$	96	4	-
ν_{35}	SiF_2 wag	333	317	11.6	1.3	0.75		319	$90S_{35}$	97	3	-
ν_{36}	SiF_2 asymmetric deformation	303	288	25.9	0.3	0.75		282	$75S_{36}$, $12S_{30}$	86	14	-
ν_{37}	SiF_2 rock	266	254	2.5	0.2	0.75		254	$38S_{37}$, $20S_{33}$, $20S_{38}$, $12S_{39}$	83	17	-
ν_{38}	SiF_2 twist	208	199	0.6	0.7	0.75		197	$68S_{38}$, $12S_{37}$	64	36	-
ν_{39}	ring puckering	33	33	3.6	0.0	0.75			$71S_{39}$, $13S_{34}$, $13S_{37}$	4	96	-

[a] MP2(full)/6-31G(d) *ab initio* calculations, scaled frequencies, infrared intensities (km/mol), Raman activities ($Å^4$/u), depolarization ratios (dp) and potential energy distributions (P.E.D.s).
[b] Scaled frequencies with scaling factors of 0.88 for CH_2 stretches and CH_2 deformations and 0.90 for all other modes.
[c] Symmetry coordinates with P.E.D. contribution less than 10% are omitted.
[*] Bend perpendicular and parallel to the ring, respectively.

Additional ab initio calculations were performed with the Gaussian 03 program [22] by using Gaussian-type basis functions. The energy minima with respect to nuclear coordinates were obtained by the simultaneous relaxation of all geometric parameters by the gradient method of Pulay [29]. A variety of basis sets as well as the corresponding ones with diffuse functions were employed with the Møller-Plesset perturbation method [21] to the second order MP2 with full electron correlation as well as with density functional theory by the B3LYP method. The predicted conformational energy differences are listed in Table 78.

Table 78. Calculated energies in Hartrees (H) and energy differences (cm^{-1}) for the two conformers and transition state of c-$C_3H_6Si_2F_4$.

Method/Basis Set	Energy[a], E	Energy Differences, Δ	
	Twist	Envelope[b]	Planar[b]
RHF/3-21G	0.007559	670	670
MP2(full)/6-31G(d)	1.297743	912	956
MP2(full)/6-31+G(d)	1.344176	785	820
MP2(full)/6-31G(d,p)	1.347648	917	974
MP2(full)/6-31+G(d,p)	1.392907	799	845
MP2(full)/6-311G(d,p)	1.993979	850	960
MP2(full)/6-311+G(d,p)	2.016998	792	891
MP2(full)/6-311G(2d,2p)	2.202762	848	896
MP2(full)/6-311+G(2d,2p)	2.218807	861	950
MP2(full)/6-311++G(2d,2p)	2.219499	868	957
MP2(full)/6-311G(2df,2pd)	2.382396	899	1069
MP2(full)/6-311+G(2df,2pd)	2.397520	899	1062
MP2(full)/6311++G(2df,2pd)	2.398050	897	1058
MP2(full)/6-311G(3df,3pd)	2.486937	938	1159
MP2(full)/6-311+G(3df,3pd)	2.497203	946	1180
MP2(full)/6311++G(3df,3pd)	2.497466	941	1183
MP2(full)/aug-cc-pVTZ	2.311046	893	1167
B3LYP/6-31G(d)	3.584387	619	625

B3LYP/6-31+G(d)	3.617723	510	512
B3LYP/6-31G(d,p)	3.594313	608	615
B3LYP/6-31+G(d,p)	3.627284	503	507
B3LYP/6-311G(d,p)	3.787429	570	586
B3LYP/6-311+G(d,p)	3.800665	524	535
B3LYP/6-311G(2d,2p)	3.828197	472	476
B3LYP/6-311+G(2d,2p)	3.837634	517	528
B3LYP/6-311++G(2d,2p)	3.837866	522	534
B3LYP/6-311G(2df,2pd)	3.845567	546	558
B3LYP/6-311+G(2df,2pd)	3.855744	552	567
B3LYP/6-311++G(2df,2pd)	3.855938	550	565
B3LYP/aug-cc-pVTZ	3.877661	565	567

[a] Energy of conformer is given as –(E+1093) H.
[b] Difference is relative to twist form and given in cm^{-1}.

In order to obtain descriptions of the molecular motions involved of the fundamental modes of c-$C_3H_6Si_2F_4$, a normal coordinate analysis was carried out. The force field in Cartesian coordinates was obtained with the Gaussian 03 program at the MP2(full) level with the 6-31G(d) basis set. The internal coordinates used to calculate the G and B matrices are given for the twist conformer in Table 78 with the atomic numbering shown in Fig. 45. By using the B matrix [30], the force field in Cartesian coordinates was converted to a force field in internal coordinates. Subsequently, 0.88 was used as the scaling factor for the CH stretches, the SiH stretches, and the CH_2 deformations and 0.90 was used for all other modes to obtain the fixed scaled force constants and the resulting wavenumbers. A set of symmetry coordinates was used (Table S13) to determine the corresponding potential energy distributions (P.E.Ds). A comparison between the observed and calculated wavenumbers, along with the calculated

infrared intensities, Raman activities, depolarization ratios and P.E.D.s for the twist conformer of c-$C_3H_6Si_2F_4$ are given in Table 77.

The predicted scaled frequencies were used together with a Lorentzian function to obtain the simulated spectra. Infrared intensities were obtained based on the dipole moment derivatives with respect to Cartesian coordinates. The derivatives were transformed with respect to normal coordinates by $(\partial\mu_u/\partial Q_i) = \sum_j (\partial\mu_u/\partial X_j)L_{ij}$, where Q_i is the i^{th} normal coordinate, X_j is the j^{th} Cartesian displacement coordinate, and L_{ij} is the transformation matrix between the Cartesian displacement coordinates and the normal coordinates. The infrared intensities were then calculated by $(N\pi)/(3c^2)$ $[(\partial\mu_x/\partial Q_i)^2 + (\partial\mu_y/\partial Q_i)^2 + (\partial\mu_z/\partial Q_i)^2]$. A comparison of the experimental infrared spectrum of the gas and simulated infrared spectrum of the isolated twist conformer is shown in Fig. 43.

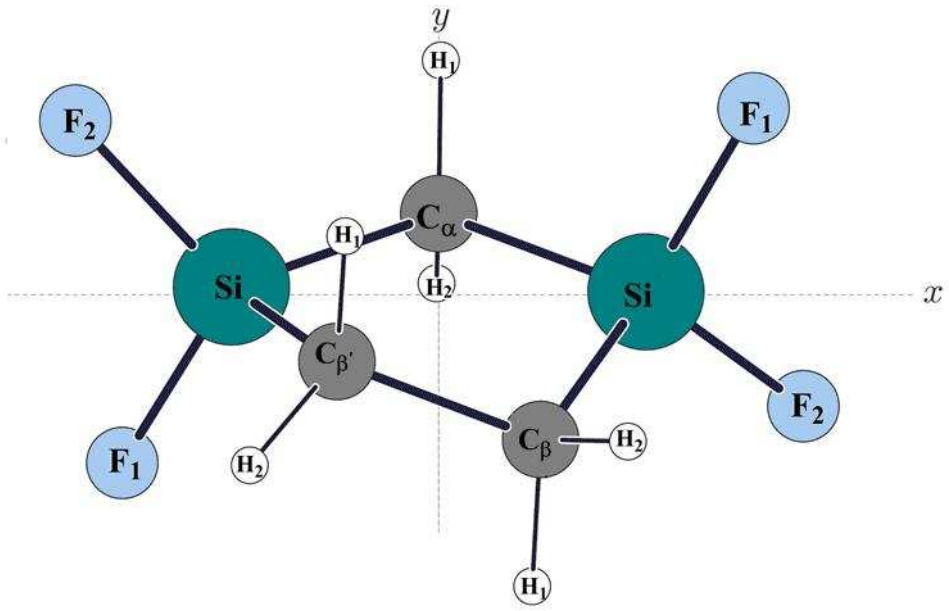

Figure 45. Model of c-$C_3H_6Si_2F_4$ showing atomic numbering.

Additional support for the vibrational assignments was obtained from the simulated Raman spectra. The evaluation of Raman activity by using the analytical gradient methods has been developed [31-34] and the activity S_j can be expressed as: $S_j = g_j(45\alpha_j^2 + 7\beta_j^2)$, where g_j is the degeneracy of the vibrational mode j, α_j is the derivative of the isotropic polarizability, and β_j is the anisotropic polarizability. To obtain the Raman scattering cross sections, the polarizabilities are incorporated into S_j by multiplying S_j with $(1-\rho_j)/(1+\rho_j)$ where ρ_j is the depolarization ratio of the j^{th} normal mode. The Raman scattering cross sections and calculated wavenumbers obtained from the Gaussian 03 program were used together with a Lorentzian function to obtain the simulated Raman spectra. A comparison of the experimental Raman spectrum of the liquid and predicted Raman spectrum of the isolated twist form are shown in Fig. 44.

This comparison is reasonable as the average difference in band center due to going from gas to liquid is 3 cm^{-1}, and thus, there is little interaction between molecules in the liquid.

MICROWAVE RESULTS

An overview of the fitted rotational parameters for c-$C_3H_6Si_2F_4$ and the comparison to ab initio results can be found in Table 76. The spectrum was fit by using a standard Watson semi-rigid rotor Hamiltonian of the A-reduction type in the I^r representation with the individual transitions fit as shown in Tables 73-75. As mentioned previously, the high dynamic range afforded in this experiment enabled assignment of all common heavy atom single isotopologues, as well as a double silicon isotopologue. Due to symmetry considerations, the silicons are equivalent, as well as the carbons in the Si-C-C-Si backbone. This equivalence leads to doubling in intensity in the spectra of these isotopologues, as well as with the double ^{29}Si – ^{30}Si isotopologue. A summary of these isotopologue fits can be found in Table 76. The fit also includes centrifugal distortion constants shown in Table 76. The fit is reasonable and they are in satisfactory agreement with the ab initio predicted centrifugal distortion constants. Utilization of a larger basis set would be beneficial.

The Kraitchman r_s substitution structure, calculated via Kraitchman's equations [13] by using the freely available KRA program [158] are good agreement with the MP2/6-311++g(d,p) results. Since the ring is nearly planar in the *ac* plane, the determination of a nonzero *b* coordinate of the Si-C-C-Si carbons, or at least a nonzero $\Delta|b|$ between the two types of carbons, confirms the twisted conformation over the planar form. Although some r_s coordinates could not be determined due to their close proximity to one of the principal axes, the derived r_s structural parameters are in general in good

agreement with the ab initio structure. A full summary of these parameters, for all of the bond lengths and angles, can be found in Table 79.

Table 79. Structural parameters (Å and degrees), rotational constants (MHz) and dipole moments (Debye) for twist conformer c-$C_3H_6Si_2F_4$.

Structural Parameters	Int. coor.	6-311+G(d,p)		6-311++G(d, p)		r_s[a]	Adjusted r_0[a]
		MP2(full)	B3LYP	MP2	B3LYP		
rC_α-Si	R_1	1.8600	1.8708	1.8625	1.8708	1.860(13)	1.8589(1)
$rSi-C_\beta,C_{\beta'}$	R_2	1.8633	1.8743	1.8659	1.8742	1.856(17)	1.8636(1)
$rC_\beta-C_{\beta'}$	R_3	1.5582	1.5640	1.5607	1.5641	1.5510(39)	1.5592(1)
$rSi-F_1$	R_4	1.6142	1.6209	1.6147	1.6210		1.5826(1)
$rSi-F_2$	R_5	1.6100	1.6175	1.6104	1.6174		1.5781(1)
rC_α-H	r_1	1.0940	1.0935	1.0946	1.0935		1.0940(1)
$rC_\beta-H_1$, $C_{\beta'}-H_1$	r_2	1.0972	1.0961	1.0979	1.0961		1.0972(1)
$rC_\beta-H_2$, $C_{\beta'}-H_2$	r_3	1.0932	1.0926	1.0939	1.0926		1.0932(1)
$\angle SiC_\alpha Si$	θ_1	102.75	102.77	102.77	102.74	102.21(63)	102.78(2)
$\angle C_\alpha SiC_\beta$	θ_2	104.22	104.86	104.22	104.85	104.68(28)	104.28(2)
$\angle SiC_\beta C_{\beta'}$	θ_3	106.60	107.64	106.60	107.60	106.47(22)	106.60(2)
$\angle C_\alpha SiF_1$	σ_1	109.58	109.80	109.58	109.77		109.55(2)
$\angle C_\alpha SiF_2$	σ_2	113.37	113.04	113.37	113.07		113.41(2)
$\angle C_\beta SiF_1$	σ_3	110.17	110.64	110.15	110.57		110.28(2)
$\angle C_\beta SiF_2$	σ_4	113.04	112.49	113.05	112.55		112.72(2)
$\angle F_1SiF_2$	σ_5	106.48	106.08	106.48	106.10		106.63(2)
$\angle HC_\alpha Si$	λ_1	111.30	111.39	111.30	111.36		111.29(2)
$\angle HC_\alpha H$	λ_2	108.01	107.70	107.98	107.73		108.01(2)
$\angle H_1C_\beta Si$	λ_3	108.37	108.00	108.38	108.05		108.37(2)
$\angle H_2C_\beta Si$	λ_4	113.34	112.91	113.33	112.88		113.34(2)
$\angle H_1C_\beta C_{\beta'}$	λ_5	109.75	109.96	109.76	109.98		109.63(2)
$\angle H_2C_\beta C_{\beta'}$	λ_6	111.86	111.72	111.87	111.72		111.98(2)
$\angle H_1C_\beta H_2$	λ_7	106.86	106.53	106.86	106.56		106.86(2)
$\tau C_\beta SiC_\alpha Si$	τ_1	10.71	9.52	10.71	9.57		10.67(2)
$\tau SiC_\beta C_{\beta'}Si$	τ_2	41.05	36.57	41.04	36.74	41.71(42)	40.85(2)
A(MHz)		2061.4092	2035.6232	2058.2277	2035.8908		2102.7784
B(MHz)		742.8442	731.0688	741.2055	731.3494		751.3680
C(MHz)		724.1462	714.6206	722.8103	714.8816		736.5361
$\lvert\mu_a\rvert$		0.0	0.0	0.0	0.0		
$\lvert\mu_b\rvert$		0.0	0.0	0.0	0.0		
$\lvert\mu_c\rvert$		1.279	1.322	1.271	1.315		
$\lvert\mu_t\rvert$		1.279	1.322	1.271	1.315		

[a] Determined using the microwave data reported in this study.

STRUCTURAL PARAMETERS

The adjusted r_0 structural parameters can be determined for the twist conformer by utilizing the rotational constants reported herein from the microwave spectra. The rotational constants for six isotopic species were determined in the current study and they are listed in Table 76 with their respective fits in Tables 73-75; therefore, 18 rotational constants are available for the determination of the structural parameter values of the twist conformer of c-$C_3H_6Si_2F_4$.

We [51] have shown that ab initio MP2(full)/6-311+G(d,p) calculations predict the carbon-hydrogen r_0 structural parameters for more than fifty hydrocarbons to at least 0.002 Å compared to the experimentally determined [5] values from isolated CH stretching frequencies which agree to previously determined values from earlier microwave studies. Therefore, all of the carbon-hydrogen parameters can be taken from the MP2(full)/6-311+G(d,p) predicted values for the twist conformer of c-$C_3H_6Si_2F_4$.

We have found that good structural parameters for hydrocarbons and many substituted ones can be determined by adjusting the structural parameters obtained from the ab initio MP2(full)/6-311+G(d,p) calculations to fit the rotational constants obtained from microwave experimental data by using a computer program "A&M" (*Ab initio* and Microwave) developed [14] in our laboratory. In order to reduce the number of independent variables, the structural parameters are separated into sets according to their types where bond distances in the same set keep their relative ratio, and bond angles and torsional angles in the same set keep their difference in degrees. This assumption is based on the fact that errors from ab initio calculations are systematic. It also should be noted that the C_2 symmetry reduces the number of independent parameters. Therefore, it should

be possible to obtain "adjusted r_0" structural parameters for the 16 independent parameters, taking the C-H distances as a single set, by utilizing the 18 experimentally determined rotational constants listed in Table 76. Therefore we have obtained the complete structural parameters for the twist form of c-$C_3H_6Si_2F_4$.

The resulting adjusted r_0 parameters are listed in Table 79, where the precisions are listed. It is believed that these precisions are probably smaller than the accuracy this method can achieve, and therefore, for the C-Si and Si-F distances the value listed should be accurate to ± 0.002 Å, the C-C distance accurate to ± 0.003 Å, the C-H distances accurate to ± 0.002 Å, and the angles should be within ± 0.3°. The fit of the 18 determined rotational constants (Table 80) by the adjusted r_0 structural parameters for the twist conformer is excellent with the differences being less than 0.04 MHz. Thus, it is believed that the suggested uncertainties are realistic values and the determined structural parameters are probably as accurate as can be obtained for the molecule in the gas phase by either electron diffraction or microwave substitution methods where all of the atoms are substituted.

Table 80. Comparison of rotational constants (MHz) obtained from experimental values from microwave spectra, and from the adjusted r_0 structural parameters for c-$C_3H_6Si_2F_4$.

Isotopomer	Rotational constant	Experimental	Adjusted r_0	$\|\Delta\|$
c-$C_3H_6Si_2F_4$	A	2102.74026(68)	2102.7784	0.0382
	B	751.34319(32)	751.3680	0.0248
	C	736.51478(31)	736.5361	0.0213
^{29}Si	A	2102.68742(51)	2102.7030	0.0155
	B	749.01578(33)	749.0241	0.0083
	C	734.28573(27)	734.2919	0.0061
^{30}Si	A	2102.63717(55)	2102.6292	0.0080
	B	746.73383(32)	746.7263	0.0075
	C	732.09979(25)	732.0914	0.0084
^{29}Si / ^{30}Si	A	2102.5846(20)	2102.5540	0.0306
	B	744.3835(12)	744.3588	0.0247
	C	729.8480(25)	729.8237	0.0243
$^{13}C_\alpha$	A	2089.2035(12)	2089.2114	0.0079
	B	749.64852(57)	749.6286	0.0199
	C	736.54375(70)	736.5361	0.0076
$^{13}C_\beta$	A	2080.16608(98)	2080.1431	0.0230
	B	748.05599(53)	748.0751	0.0191
	C	735.84108(49)	735.8545	0.0135

VIBRATIONAL ASSIGNMENT

The major reason for carrying out a vibrational assignment of c-$C_3H_6Si_2F_4$ is to determine the effect of the fluorine atoms on the fundamentals. It is expected that the fluorine atoms will have the largest effect on the vibrations involving silicon atoms of the

ring which is expected to provide modes that are strongly mixed with the ring vibrations. Additionally the ring parameters are expected to be affected since they would be quite different from those found in silicon atoms compared to the ones involving non polar groups [160]. The vibrations of the CH_2 group are expected to be very similar to those found in the usual five membered rings and so a discussion of their assignments is not necessary. Therefore the assignments of nine fundamentals of the ring will be provided first and this will be followed by the vibrations involving the SiF_2 modes.

The heavy atom modes of the five membered rings result in a total of nine fundamentals with five of those in 'A' block and the remaining four in the 'B' block. Five membered rings containing carbons have ring deformations occurring around 1000 cm^{-1}. The second ring deformation is usually around 200 cm^{-1} lower and for our molecule we have frequencies (800 cm^{-1}) which are consistent with the one observed in silicon. Ring breathing is observed at 650 cm^{-1} with deformations at 214 cm^{-1} and the twist at 92 cm^{-1}. For the vibrations in 'B' block it has the two ring deformations fairly close in frequency at 696 cm^{-1} and 657 cm^{-1} with the third ring deformation at 416 cm^{-1}. The ring puckering mode is predicted at 33 cm^{-1} but this vibration is not observed. It is rather interesting that the frequencies for most of the ring modes of c-$C_3H_6Si_2F_4$ are very similar to those of the silicon containing oxygen atom molecule [160] substituted with non polar methyl groups.

With the assignments of ring vibrations completed the other modes of interest are the ones of the SiF_2 group. In the 'A' block the antisymmetric stretch is observed at 970 cm^{-1} and the symmetric one at 897 cm^{-1} and the corresponding vibration in 'B' block are slightly lower in frequency at 936 cm^{-1} and 848 cm^{-1}, respectively. The SiF_2 deformations

in the ‘A’ block is observed at 801 cm^{-1} and the other deformation at 282 cm^{-1} which is considerably lower. The other SiF_2 bending modes are mainly the wag, rock and the twist which are observed at 298 cm^{-1}, 257 cm^{-1} and 151 cm^{-1} and in the the ‘B’ block the corresponding vibrations have similar frequencies of 319 cm^{-1}, 254 cm^{-1} and 197 cm^{-1} respectively.

These assignments are relatively easy to make since the predicted frequencies from ab initio calculations in most cases, have little questions concerning their frequencies even though P.E.D.s are somewhat different. This effect due to presence of SiF_2 groups will be further addressed in the discussion.

DISCUSSION

The ab initio energy differences of the possible forms have been determined by a variety of basis sets (Table 77). The MP2(full) method consistently predicts the twist form as the most stable conformer and the planar and envelope forms as not being stable conformers with all the basis sets and with only relatively small changes due to basis set selection. The B3LYP method agrees with the MP2(full) method as to the identity of the most stable form but the magnitude of the energy differences are approximately half that of the MP2(full) method. However the B3LYP calculations still shows the twist conformer as being the only stable form.

The vibrational assignments reported herein are based on a significant amount of information with the infrared and Raman spectrum of the xenon solution and predictions of the fundamental frequencies from the scaled ab initio MP2(full)/6-31G(d) calculations as well as the predicted infrared bands contours and their intensities. For the twist conformer the fixed scaled ab inito predicted frequencies for the ‘A’ block fundamentals

are in error with an average value of 9 cm^{-1} which represent 0.87% error and for the 'B' block modes it is 5 cm^{-1} which is 0.43% error. The largest errors are in the SiF_2 deformations and several of the ring deformations which includes the ring breathing mode. This is interesting as these modes show significant mixing with each other which is likely due to the large masses of the SiF_2 groups. Thus, the relatively small basis set of 6-31G(d) by the MP2(full) calculations with two scaling factors provides excellent predicted frequencies for aiding the vibrational assignments.

In the 'A' symmetry block there are only two modes which have less than 40% contribution from the vibrational description used. These are the low frequency ν_{17} and ν_{18}. For ν_{17} the largest contribution is 33% of S_{17} (SiF_2 rock) with the other two significant contributions from the SiF_2 wag and deformation. However for ν_{18} (ring deformation) there is only 23% S_{18} with 41% S_{15} for the SiF_2 deformation which is assigned at 420 cm^{-1} with 40% S_{15} and 37% S_{18} the ring deformation. Thus there is significant mixing of the SiF_2 vibrational modes with ring vibrations as might be expected with the similar mass values.

In the 'B' block there are five modes (ν_{30} through ν_{34}) which have less than 40% for the main contribution and only one of them (ν_{33}) which has 29% S_{33} has a greater contribution from another mode (36% S_{30}). These five modes are three ring deformations and two CH_2 rocks. This is not surprising that these fundamentals are extensively mixed. Nevertheless the vibrational assignments were relatively easy to make with confidence.

The r_s structural parameters determined using the Kraitchman method can be compared with the corresponding parameters from the adjusted r_0 structural parameters, and both of these structures can be found in Table 79. The r_s Si-C bond distance

parameters match the r_0 structural parameters within error limits, but it is somewhat meaningless as the r_s parameters have very large uncertainties. These large uncertainties are clearly due to the problem the Kraitchman method has determining parameters in which one or more atoms lie on a rotational axis. The r_s angle structural parameters i.e. $\angle SiC_\alpha Si$, $\angle C_\alpha SiC_\beta$, and $\angle SiC_\beta C_{\beta'}$, are within their respective error limits as compared to the corresponding adjusted r_0 structural parameters and these parameters are well determined by both methods. The two remaining parameters which can be determined have good uncertainties, but they are significantly different than the corresponding r_0 structural parameters. It is believed that the r_0 parameters are the more accurate determined as the back C_β-C_β distance is normally [123] predicted by the MP2(full) calculations as smaller than the experimental value as determined from the adjusted r_0 structure. The predicted structural parameters were also obtained from the B3LYP calculations with the same 6-311+G(d,p) basis set as those obtained from the MP2 calculations. The C_α-Si predicted distance is 0.108 Å longer from the MP2 and the C_β-C_β distance is predicted longer by 0.018 Å and hence the structure predictions with B3LYP calculations are not very satisfactory. From such predicted distances it is not possible to obtain a fit of the experimentally determined rotational constants. However the predicted angles obtained from the B3LYP calculations are reasonably similar to those obtained from the MP2 calculation.

The natural population analysis was carried out for the twist conformer of c-$C_3H_6Si_2F_4$ with the MP2(full) method at the 6-311+G(d,p) basis set. The charge of the heavy atoms are; Cα = -1.50, Si = +2.30, C_β = -0.90, and F = -0.68. The large charge on the silicon atom is of interest and could counteract some of the larger radius of the silicon

atom than a carbon atom. Comparison of this structure with 1,3-disilacyclopentane or tetrafluorocyclopentane would be of interest to determine the effects these different substituents on their corresponding ring structures.

It would be of interest to compare c-$C_3H_6Si_2F_4$ with similar molecules to elucidate the underlying physical causes for the molecular geometry observed in this study. However, there are currently no previously reported experimentally determined structures for the 1,3-disilacyclopentane moiety.

The closest structure in terms of chemical properties and molecular geometry is 1-fluoro-1-silacyclopentane (c-C_4H_9SiF) which has been previously studied [149] where an adjusted r_0 structure was reported. The first difference which is to be expected is the difference between a singly fluorinated sila-alkane and a difluorinated sila-alkane where the Si-F distances in the difluorinated sila-alkane are ~0.02 Å shorter. This difference is due to the increasing positive charge on the silane which means a smaller electron cloud which corresponds with the fluorines needing to be closer to bond with the silane. Similarly this explains the significantly shorter Si-C distances, which are ~0.01 Å shorter in the difluorinated sila-alkane, where the more positive silane causes the shorter bonds. These shorter bonds in this case are actually counterintuitive where the silane groups are normally larger than carbon groups. As c-C_4H_9SiF has only one silane group in the ring and c-$C_3H_5Si_2F_4$ by this logic a trend toward an increasing ring size and thereby longer bonds in the ring might be expected. The in ring bond angles are fairly similar with differences of less than 1-2 degrees and there appears to be a common trend for overall smaller angles in the c-$C_3H_5Si_2F_4$ ring which seems counterintuitive if the normal silane group versus alkane group size trend is considered. The back C_β-C_β distance in the ring is

~0.02 Å shorter for c-$C_3H_5Si_2F_4$ than the corresponding parameter in c-C_4H_9SiF. This difference stems from the more negatively charged carbons in the c-$C_3H_5Si_2F_4$ ring rather than a steric effect, due to the C_β atoms in this molecule which have a nearly full electron unit charge as discussed above. Finally, the ring torsional angles are significantly smaller in the c-$C_3H_5Si_2F_4$ ring than the corresponding torsional angles in the c-C_4H_9SiF where difference in the $\tau SiC_\beta C_{\beta'}Si$ angle is ~9° and the other torsional angles range from 1 to 4° smaller for c-$C_3H_5Si_2F_4$. This difference causes the c-$C_3H_5Si_2F_4$ ring to be much "flatter" than the c-C_4H_9SiF ring which is clearly reflected in the predicted energy differences between the planar and twist conformations where the MP2(full) ab initio calculation performed with the aug-cc-pVTZ basis set predicts the c-C_4H_9SiF energy difference as ~600 cm^{-1} larger in amplitude than the same prediction for the c-$C_3H_5Si_2F_4$ molecule. As can be seen there are many significant differences between the c-C_4H_9SiF and c-$C_3H_5Si_2F_4$ molecules, and therefore, it would be of interest to study more 1,3-disilacyclopentane type molecules where the molecular geometries, vibrational fundamentals, and conformational stabilities for a better understanding of the observed differences.

CHAPTER 13

CONFORMATIONAL AND STRUCTURAL STUDIES OF 2,2-DIFLUOROETHYLAMINE FROM TEMPERATURE DEPENDENT INFRARED SPECTRA OF XENON SOLUTION AND AB INITIO CALCULATIONS

INTRODUCTION

We recently initiated a study of the conformational stability and determined the structural parameters of several organoamines. In these studies we have been utilizing variable temperature infrared spectra of rare gas solution to obtain the enthalpy differences of the conformers. For the structural values we have obtained adjusted r_0 structural values by utilizing *ab initio* MP2(full)/6-311+G(d,p) predicted parameters for the heavy atoms which are then adjusted to agree with the microwave determined rotational constants. The parameters for the hydrogen atoms are taken from the *ab initio* calculations. By this method we [161] obtained the conformational stability of ethylamine which was determined to have the *trans* conformer more stable by 54 ± 4 cm^{-1} (0.65 ± 0.05 kJ/mol) than the *gauche* form. This value was in agreement with earlier determined values of 107 ± 70 cm^{-1}(1.28 ± 0.84 kJ/mol) from electron diffraction study [162], 110 ± 50 cm^{-1}(1.32 ± 0.60 kJ/mol) from a microwave investigation [163], and 100 ± 10 cm^{-1}(1.20 ± 0.12 kJ/mol) from an infrared study of ethylamine in an argon matrix [164]. However, several of the earlier studies [165-168] reported the *gauche* conformer as the more stable form, and it is rather interesting that MP2(full)/6-311+G(2d,2p) calculations predict [161] the *gauche* conformer to be the more stable form by 66 cm^{-1} (0.79 kJ/mol). However, without

the diffuse functions the *trans* form is predicted to be the more stable conformer by 32 cm^{-1}(0.38 kJ/mol).

These results clearly indicate that the enthalpy difference between the *gauche* and *trans* conformers of the NH_2 moiety will need to be determined experimentally rather than theoretical predictions for organoprimary amines. Nevertheless, it is of scientific interest to determine the effect of substituting one or more of the hydrogen atoms on β-carbon. One of the earliest molecules of this type studied was n-propylamine, $CH_3CH_2CH_2NH_2$ [169] for which the conformational stability was determined. The most stable conformer was determined to be the *Tt* form but this determination was for the solid. However the most stable conformer in the gas or the liquid need not be the same as found in the solid so it would be of interest to obtain the relative stabilities of the conformers of n-propylamine in the gaseous state. However, we have determined the conformational stabilities of all five of the conformers of 2-fluoroethylamine [170] where the fluorine atom might be expected to have a significant effect on the carbon-carbon distance.

For $FCH_2CH_2NH_2$, the most stable conformer was the *Gg′* form with the *Gt* conformer the second most stable form with an enthalpy difference of 62 ± 8 cm^{-1} (0.74 ± 0.10 kJ/mol), where the first indicator is the NCCF dihedral angle (G = *gauche* or T = *trans*) and the second one (g = *gauche* or t = *trans*) is the relative position of the lone pair of electrons on the nitrogen atom with respect to the β-carbon atom [Gg′ is noted by the N-H eclipsing the fluoride]. The third, fourth, and fifth conformers in relative energy are the *Tg* (262 ± 26 cm^{-1}), *Tt* (289 ± 45 cm^{-1}), and *Gg* (520 ± 50 cm^{-1}), respectively, where it was not possible to determine whether the *Tg* or *Tt* were the more stable one. Thus the

fluorine atom appears to have an effect on the conformer stability of the ethylene group so we have continued our investigations of substitutions on the β-carbon atom of ethylamine with the determination of the conformational stabilities and structural parameters of 2,2-diflouroethylamine. For these conformational and structural studies of 2,2-difluoroethylamine, $F_2CHCH_2NH_2$, we have recorded variable temperature mid-infrared spectra of xenon solutions. To support these experimental studies we have also obtained the harmonic force fields, infrared intensities, Raman activities, depolarization ratios, and vibrational frequencies from MP2(full)/6-31G(d) *ab initio* calculations with full electron correlation. To obtain predictions on the conformational stabilities we have carried out MP2(full) *ab initio* and density functional theory (DFT) calculations by the B3LYP method by utilizing a variety of basis sets. The r_0 structural parameters have been obtained by combining the MP2(full)/6-311+G(d,p) *ab initio* predicted parameters with the previously reported rotational constants obtained from the microwave study [171]. The results of these spectroscopic, structural and theoretical studies of 2,2-difluoroethylamine are reported herein.

EXPERIMENTAL AND THEORETICAL METHODS

The sample of $F_2CHCH_2NH_2$ was prepared by the reduction of 2,2-difluoroacetamide (Oakwood Chemical Co.) with lithium aluminum hydride in dry dibutyl ether. The volatile material was collected in a tube immersed in liquid nitrogen and first purified by trap-to-trap distillation and then finally by using a low-pressure, low-temperature purification column.

The mid-infrared spectrum of the gas (Fig. 46A) and solid (Fig. 47A) were obtained from 3500 to 300 cm^{-1} on a Perkin-Elmer model 2000 Fourier transform spectrometer

equipped with a Ge/CsI beamsplitter and a DTGS detector. Atmospheric water vapor was removed from the spectrometer housing by purging with dry nitrogen. The theoretical resolution used to obtain the spectrum of the gas was 0.5 cm^{-1} and 128 interferograms were added and transformed with a boxcar truncation function. For the spectrum of the solid theoretical resolution of 2 cm^{-1} was used with 128 interferograms added and truncated. Multiple annealings were required to obtain satisfactory spectra of the solid.

Figure 46. Mid-infrared spectra of 2,2-difluoroethylamine (A) gas; (B) Xe solution at -65°C.

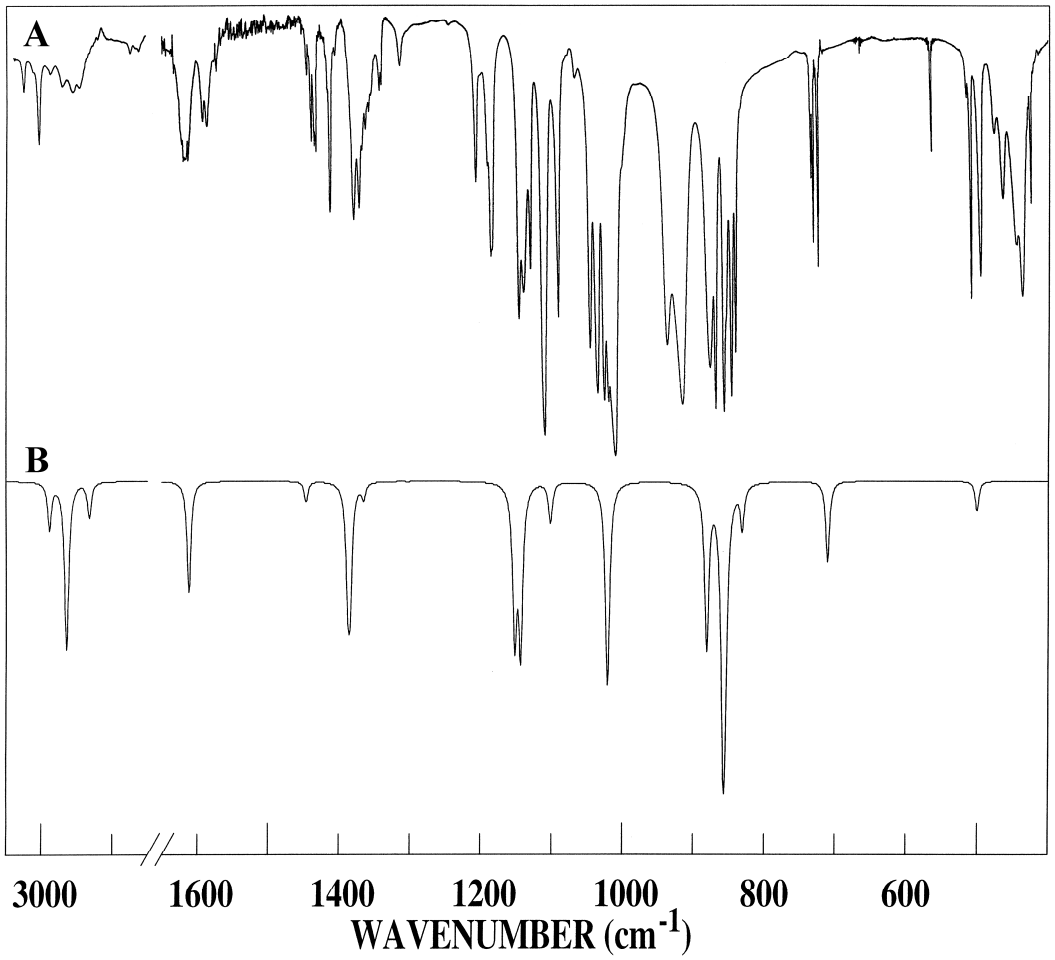

Figure 47. Comparison of experimental and predicted infrared spectra of 2,2-difluoroethylamine: (A) infrared spectra of the solid; (B) simulated spectrum of *Tt* conformer.

The mid-infrared spectra (3500 to 400 cm^{-1}) of the sample dissolved in liquefied xenon (Fig. 46B) at ten different temperatures (-55°C to -100°C) were recorded on a Bruker model IFS-66 Fourier transform spectrometer equipped with a globar source, a Ge/KBr beamsplitter and a DTGS detector. In all cases, 100 interferograms were

collected at 1.0 cm^{-1} resolution, averaged and transformed with a boxcar truncation function. For these studies, a specially designed cryostat cell was used. It consists of a copper cell with a path length of 4 cm with wedged silicon windows sealed to the cell with indium gaskets. The temperature was maintained with boiling liquid nitrogen and monitored by two Pt thermoresistors. After cooling to the designated temperature, a small amount of the sample was condensed into the cell and the system was then pressurized with the noble gas, which condensed in the cell, allowing the compound to dissolve. A typical spectrum is shown in Fig. 46B.

The Raman spectra (Fig. 48) were recorded on a Spex model 1403 spectrophotometer equipped with a Spectra-Physics model 2017 argon ion laser operating on the 514.5 nm line. The laser power used was 1.5 W with a spectral bandpass of 3 cm^{-1}. The spectrum of the liquid was recorded with the sample sealed in a Pyrex glass capillary. The measurements of the Raman frequencies are expected to be accurate to ± 2 cm^{-1}. All of the observed bands in the Raman spectra of the liquid along with their proposed assignments and depolarization values are listed in Tables 81, 82 and 83, for the *Tt*, *Gg* and *Gt* conformers, respectively. The first indicator (*G* = *Gauche* or *T* = *Trans*) is for the rotation around the C-C bond (dihedral angle NCCH) and the second one (*g* = *gauche* or *t* = *trans*) is for the rotation around the N-C bond which indicates the relative position of the lone pair of electrons on the nitrogen with respect to the β-carbon atom.

Figure 48. Comparison of experimental and predicted Raman spectra of 2,2-difluoroethylamine: (A) observed spectrum of the liquid; (B) simulated spectrum of a mixture of *Tt*, *Gg* (ΔH = 83 cm^{-1}), *Gt* (ΔH = 235 cm^{-1}) conformers at 25°C; (C) simulated spectrum of *Gt* conformer; (D) simulated spectrum of *Gg* conformer; (E) simulated spectrum of *Tt* conformer.

TABLE 81. Observed and calculated[a] frequencies for the *Trans-trans* conformer of 2,2-difluoroethylamine.

		Fundamentals	*ab initio*	fixed scale[b]	IR int.	Raman act.	dp ratio	IR			Raman liquid	P.E.D.[d]	Band Contours		
								gas	Xe soln	solid[c]			A	B	C
A′	ν_1	NH_2 symmetric stretch	3525	3344	1.5	72.8	0.11	3356	3348	3373	3336	$100S_1$	10	-	90
	ν_2	C-H stretch	3160	2964	62.4	105.6	0.17	2969	2963	3001	2968	$96S_2$	25	-	75
	ν_3	CH_2 symmetric stretch	3126	2932	10.6	72.8	0.18	2906	2914	2954	2914	$96S_3$	13	-	87
	ν_4	NH_2 deformation	1737	1611	36.9	7.2	0.69	1624	1621	1621	1619	$84S_4,14S_{11}$	31	-	69
	ν_5	CH_2 deformation	1538	1446	5.9	9.5	0.75	1447	1443	1440	1448	$99S_5$	36	-	64
	ν_6	H-C-C in-plane bend	1454	1384	37.0	5.0	0.75	1375	1371	1377	1371	$55S_6,25S_7,10S_{10}$	90	-	10
	ν_7	CH_2 wag	1437	1365	4.5	2.7	0.67	1361	1360	1347	1348	$81S_7,12S_{10}$	12	-	88
	ν_8	CF_2 symmetric stretch	1207	1143	63.3	6.2	0.47	1155	1149	1144	1148	$36S_8,25S_9,14S_{10}$	19	-	81
	ν_9	C-N stretch	1161	1101	12.2	1.6	0.74	1095	1095	1095	1100	$40S_9,20S_8,16S_{12},12S_{14}$	5	-	95
	ν_{10}	C-C stretch	908	881	60.7	2.9	0.18	875	873	872	870	$38S_{10},29S_{11},12S_8,10S_6$	100	-	-
	ν_{11}	NH_2 rock	984	857	181.7	6.6	0.16	824	819	834	853	$25S_{11},33S_9,12S_{10},10S_6$	90	-	10
	ν_{12}	CF_2 rock	749	711	25.2	4.3	0.46	718	716	727	727	$24S_{12},21S_{11},20S_8,16S_{14}$	26	-	74
	ν_{13}	CF_2 deformation	504	500	8.7	1.7	0.75	507	508	500	511	$85S_{13},10S_8$	3	-	97
	ν_{14}	C-C-N bend	266	261	17.2	0.2	0.34	266	-	269	243	$58S_{14},20S_{12},14S_6$	67	-	33
A″	ν_{15}	NH_2 antisymmetric stretch	3625	3439	4.6	42.5	0.75	3415	3415	3389	3389	$100S_{15}$	-	100	-

ν_{16}	CH_2 antisymmetric stretch	3187	2988	14.0	58.3	0.75	2989	~2990	3022	3000	$100S_{16}$	-	100	-
ν_{17}	H-C-C out-of-plane bend	1466	1387	31.8	0.6	0.75	1380	1380	1385	1384	$60S_{17},21S_{22},16S_{18}$	-	100	-
ν_{18}	CH_2 twist	1423	1302	0.1	17.5	0.75	1307	1303	1318	1306	$56S_{18},20S_{19},10S_{21}$	-	100	-
ν_{19}	NH_2 twist	1246	1151	57.7	1.3	0.75	1181	1182	1189	1187	$23S_{19},28S_{21},25S_{20},17S_{22}$	-	100	-
ν_{20}	CF_2 antisymmetric stretch	1105	1021	81.5	2.1	0.75	1035	1036	1030	1029	$58S_{20,}25S_{19},18S_{18}$	-	100	-
ν_{21}	CH_2 rock	901	831	13.0	2.2	0.75	814	814	830	825	$50S_{21},31S_{19},14S_{20}$	-	100	-
ν_{22}	CF_2 twist	417	397	8.1	0.8	0.75	398	-	442	427	$39S_{22},28S_{17},17S_{23}$	-	100	-
ν_{23}	NH_2 torsion	301	263	64.4	1.8	0.75	271	-	284	255	$82S_{23}$	-	100	-
ν_{24}	torsion	140	140	0.9	0.1	0.75	-	-	-	139	$92S_{24}$	-	100	-

[a]MP2(full)/6-31G(d) *ab initio* calculations, scaled frequencies, infrared intensities (km/mol), Raman activities ($Å^4$/amu), depolarization ratios and potential energy distributions (P.E.D.s)

[b]Scaled *ab initio* calculations with factors of 0.88 for CH stretches and CH_2 deformation, 0.70 for NH_2 bends (excluding deformation) and 0.90 for all other modes except torsions and heavy atom bends

[c]Frequencies may be significantly shifted due to hydrogen bonding.

[d]Values less than 10% are omitted.

TABLE 82. Observed and calculated[a] frequencies for the *Gauche-gauche* conformer of 2,2-difluoroethylamine.

	Fundamental	*ab initio*	fixed scale[b]	IR int.	Raman act.	dp ratio	IR		Raman liquid	P.E.D.[c]	Band Contours		
							gas	Xe soln			A	B	C
ν_1	NH_2 antisymmetric stretch	3642	3455	5.2	56.7	0.72	3432	3424	3413	$100S_1$	19	79	2
ν_2	NH_2 symmetric stretch	3541	3359	1.8	87.7	0.12	3360	3354	3346	$100S_2$	23	35	42
ν_3	C-H stretch	3190	2993	47.2	63.2	0.33	2994	~2990	3000	$86S_3,11S_4$	-	2	98
ν_4	CH_2 antisymmetric stretch	3173	2976	8.4	64.2	0.40	2986	2980	2988	$65S_4,22S_5,13S_3$	-	100	-
ν_5	CH_2 symmetric stretch	3068	2878	39.3	99.8	0.18	2881	2879	2872	$76S_5,24S_4$	21	12	66
ν_6	NH_2 deformation	1723	1597	42.2	7.5	0.70	1608	1606	1602	$83S_6,15S_{18}$	46	5	49
ν_7	CH_2 deformation	1562	1469	4.4	12.1	0.73	1458	1454	1460	$99S_7$	79	17	4
ν_8	H-C-C in-plane bend	1514	1429	24.2	3.5	0.37	1424	1422	1431	$25S_8,37S_{10},16S_{13},10S_{21}$	60	38	2
ν_9	H-C-C out-of-plane bend	1458	1385	28.8	4.8	0.74	1370	1368	1361	$54S_9,20S_{20}$	4	96	-
ν_{10}	CH_2 wag	1408	1318	16.4	4.9	0.75	1335	1330	1333	$30S_{10},23S_8,11S_9,11S_{20},10S_{21}$	99	1	-
ν_{11}	CH_2 twist	1346	1259	13.2	8.1	0.61	1279	1276	1277	$64S_{11},11S_{21}$	63	2	35
ν_{12}	NH_2 twist	1242	1148	37.4	3.2	0.73	1150	1149	1148	$20S_{12},31S_{17},16S_{16},10S_{20}$	28	62	10
ν_{13}	C-C stretch	1199	1138	58.6	5.0	0.73	1134	1132	1133	$35S_{13},15S_{14},14S_8$	13	78	9

ν_{14}	CF_2 symmetric stretch	1160	1104	113.1	3.7	0.32	1095	1095	1100	$40S_{14},30S_{16}$	79	14	7
ν_{15}	C-N stretch	1128	1072	25.5	6.3	0.11	1079	1073	1062	$71S_{15}$	73	26	1
ν_{16}	CF_2 antisymmetric stretch	1099	1005	49.2	4.9	0.69	1005	1001	1006	$28S_{16},38S_{12},11S_{11}$	-	98	2
ν_{17}	CH_2 rock	917	840	17.1	3.3	0.75	856	856	860	$29S_{17},21S_{13},21S_{12},14S_{14}$	6	32	62
ν_{18}	NH_2 rock	897	791	179.6	3.0	0.22	772	772	779	$75S_{18},13S_6$	19	14	67
ν_{19}	CF_2 deformation	583	565	5.7	2.0	0.35	578	576	576	$40S_{19},18S_{14},16S_{21}$	3	2	95
ν_{20}	CF_2 twist	494	483	6.7	0.8	0.69	485	482	484	$20S_{20},25S_{22},13S_{21},12S_8$	78	17	5
ν_{21}	CF_2 rock	445	439	4.9	1.2	0.46	439	439	439	$15S_{21},45S_{19},13S_{13}$	67	13	21
ν_{22}	C-C-N bend	305	273	36.8	1.2	0.75	280	-	266	$27S_{22},39S_{23},16S_{20},12S_9$	58	42	-
ν_{23}	NH_2 torsion	246	231	32.6	1.1	0.75	-	-	-	$56S_{23},19S_{22},11S_{20}$	34	64	2
ν_{24}	torsion	150	149	5.7	0.1	0.75	-	-	-	$93S_{24}$	47	45	9

[a]MP2(full)/6-31G(d) *ab initio* calculations, scaled frequencies, infrared intensities (km/mol), Raman activities ($Å^4$/amu), depolarization ratios and potential energy distributions (P.E.D.s)

[b]Scaled *ab initio* calculations with factors of 0.88 for CH stretches and CH_2 deformation, 0.70 for NH_2 bends (excluding deformation) and 0.90 for all other modes except torsions and heavy atom bends

[c]Values less than 10% are omitted.

TABLE 83. Observed and calculated[a] frequencies for the *Gauche-trans* conformer of 2,2-difluoroethylamine.

	Fundamental	*ab initio*	fixed scale[b]	IR int.	Raman act.	dp ratio	IR		Raman liquid	P.E.D.[c]	Band Contours		
							gas	Xe soln.			A	B	C
ν_1	NH_2 antisymmetric stretch	3631	3445	3.8	44.6	0.75	3421	3421	3402	$100S_1$	1	70	29
ν_2	NH_2 symmetric stretch	3528	3346	1.2	77.8	0.12	3358	3350	3354	$100S_2$	-	100	-
ν_3	CH_2 antisymmetric stretch	3196	2998	18.5	47.5	0.72	2992	~2990	3000	$97S_3$	1	26	73
ν_4	C-H stretch	3146	2951	49.1	67.6	0.36	2956	2953	2943	$96S_4$	-	2	98
ν_5	CH_2 symmetric stretch	3132	2938	12.4	100.9	0.08	2926	2932	2928	$98S_5$	21	71	8
ν_6	NH_2 deformation	1730	1603	33.2	7.2	0.69	1632	1630	1631	$83S_6,15S_{18}$	-	63	37
ν_7	CH_2 deformation	1540	1447	3.7	10.4	0.75	1447	1443	1448	$99S_7$	5	58	37
ν_8	H-C-C in-plane bend	1483	1409	28.2	3.3	0.73	1398	1400	1403	$38S_8,26S_{10},14S_{21},11S_{16}$	86	14	-
ν_9	H-C-C out-of-plane bend	1458	1386	30.1	4.5	0.75	1377	1375	1372	$57S_9,20S_{20},10S_{10}$	2	98	-
ν_{10}	CH_2 wag	1378	1310	11.4	11.3	0.75	1317	1309	1315	$45S_{10},14S_{11},12S_{20},11S_8$	99	1	-
ν_{11}	CH_2 twist	1422	1297	3.2	2.3	0.73	1307	1302	1298	$52S_{11},17S_{12},11S_{10},10S_{21}$	80	4	16
ν_{12}	NH_2 twist	1255	1162	13.4	1.3	0.57	1197	1193	1199	$23S_{12},32S_{17},17S_{21},13S_{16}$	26	6	68

ν_{13}	CF_2 symmetric stretch	1183	1126	67.5	5.7	0.60	1126	1124	1122	$36S_{13},24S_{16},12S_{14}$	11	71	18
ν_{14}	CF_2 antisymmetric stretch	1165	1102	49.8	2.4	0.48	1095	1095	1100	$31S_{14},30S_{15},12S_{23},10S_{20},10S_{13}$	55	43	2
ν_{15}	C-N stretch	1152	1095	107.8	3.4	0.57	1087	1087	1090	$50S_{15},32S_{14},13S_{13}$	65	31	4
ν_{16}	C-C stretch	1053	966	27.4	1.4	0.42	980	978	980	$17S_{16},31S_{12},15S_{11},11S_{13},10S_{14}$	26	65	9
ν_{17}	CH_2 rock	864	835	72.6	2.0	0.21	847	845	840	$31S_{17},23S_{12},17S_{18}$	79	19	2
ν_{18}	NH_2 rock	930	782	163.1	5.7	0.22	744	743	748	$54S_{18},10S_{17},10S_6,10S_{16}$	93	-	7
ν_{19}	CF_2 deformation	573	557	3.4	2.0	0.36	576	572	572	$46S_{19},19S_{13},12S_{21}$	44	2	54
ν_{20}	CF_2 twist	502	487	11.5	1.9	0.67	475	475	477	$19S_{20},23S_{23},13S_{21},12S_8,10S_{17}$	13	73	14
ν_{21}	CF_2 rock	436	429	12.5	2.1	0.45	431	430	435	$17S_{21},40S_{19},15S_{16},10S_8$	86	13	1
ν_{22}	NH_2 torsion	328	282	62.5	2.4	0.75	289	-	276	$80S_{22},10S_{23}$	4	21	75
ν_{23}	C-C-N bend	246	242	15.6	0.1	0.68	-	-	-	$39S_{23},24S_{20},21S_9,13S_{22}$	11	73	16
ν_{24}	torsion	143	143	1.2	0.1	0.75	-	-	139	$94S_{24}$	96	4	-

[a]MP2(full)/6-31G(d) *ab initio* calculations, scaled frequencies, infrared intensities (km/mol), Raman activities ($Å^4$/amu), depolarization ratios and potential energy distributions (P.E.D.s)

[b]Scaled *ab initio* calculations with factors of 0.88 for CH stretches and CH_2 deformation, 0.70 for NH_2 bends (excluding deformation) and 0.90 for all other modes except torsions and heavy atom bends

[c]Values less than 10% are omitted.

The LCAO-MO-SCF restricted Hartree-Fock calculations were performed with the Gaussian-03 program [22] using Gaussian-type basis functions. The energy minima with respect to nuclear coordinates were obtained by the simultaneous relaxation of all geometric parameters using the gradient method of Pulay [29]. Several basis sets as well as the corresponding ones with diffuse functions were employed with the Møller-Plesset perturbation method [21] to the second order (MP2(full)) as well as with the density functional theory by the B3LYP method. The predicted conformational energy differences are listed in Table 84.

TABLE 84. Calculated energies in (H) and energy differences (cm^{-1}) for the five conformers of 2,2-difluoroethylamine.

Method/Basis Set	Energy[a], E	Energy Differences[b], Δ			
	Trans-trans	*Gauche-gauche*	*Gauche-trans*	*Trans-gauche*	*Gauche-gauche′*
MP2(full)/6-31G(d)	0.743275	229	347	1074	1203
MP2(full)/6-31+G(d)	0.776801	58	307	942	1251
MP2(full)/6-311G(d,p)	1.037072	175	231	1001	1203
MP2(full)/6-311+G(d,p)	1.055675	96	261	855	1077
MP2(full)/6-311G(2d,2p)	1.130822	131	237	908	1028
MP2(full)/6-311+G(2d,2p)	1.146119	63	213	828	1026
MP2(full)/6-311G(2df,2pd)	1.232509	101	217	862	984
MP2(full)/6-311+G(2df,2pd)	1.247411	72	205	817	868
MP2(full)/6-311++G(2df,2pd)	1.247731	63	202	808	938
MP2(full)/aug-cc-pVTZ	1.266963	72	209	813	988
Average MP2(full)	-	93 ± 38	222 ± 20	862 ± 65	1014 ± 99
B3LYP/6-31G(d)	1.643218	259	220	1074	1285[c]
B3LYP/6-31+G(d)	1.671849	77	166	937	1094[c]
B3LYP/6-311G(d,p)	1.753232	183	173	1048	1209[c]
B3LYP/6-311+G(d,p)	1.767451	103	178	897	1039[c]
B3LYP/6-311G(2d,2p)	1.764692	179	175	962	1154[c]
B3LYP/6-311+G(2d,2p)	1.777312	99	152	860	991[c]
B3LYP/6-311G(2df,2pd)	1.772253	139	156	916	1092[c]
B3LYP/6-311+G(2df,2pd)	1.785325	90	142	839	957[c]

B3LYP/aug-cc-pVTZ	1.797705	90	137	818	927[c]
B3LYP/aug-cc-pVQZ	1.822513	93	136	821	924[c]
Average B3LYP	-	131 ± 38	164 ± 25	917 ± 90	1067 ± 123

[a]Energy of *Trans-trans* conformer is given as –(E+332) H.
[b]Differences are relative to *Trans-trans* form.
[c]The dihedral angle $\tau H_9N_3C_2C_1$ was fixed to 63° in order to calculate B3LYP energies of this conformer

In order to obtain a complete description of the molecular motions involved in the fundamental modes of $F_2CHCH_2NH_2$, a normal coordinate analysis has been carried out. The force field in Cartesian coordinates was obtained with the Gaussian 03 program [22] at the MP2(full) level with the 6-31G(d) basis set. The internal coordinates used to calculate the **G** and **B** matrices are given in Table 85 with the atomic numbering shown in Fig. 49. By using the **B** matrix [30], the force field in Cartesian coordinates was converted to a force field in internal coordinates. Subsequently, scaling factors of 0.88 for CH stretches and CH_2 deformation, 0.70 for NH_2 bends (excluding deformation) and 0.90 for all other modes except torsions and heavy atom bends were applied, along with the geometric average of the scaling factors for the interaction force constants, to obtain the fixed scaled force field and resultant wavenumbers. A set of symmetry coordinates was used (Table S14) to determine the corresponding potential energy distributions (P.E.D.s). A comparison between the observed and calculated wavenumbers, along with the calculated infrared intensities, Raman activities, depolarization ratios and potential energy distributions for the *trans-trans*, *gauche-gauche* and *gauche-trans* conformers are listed in Tables 81, 82, and 83, respectively.

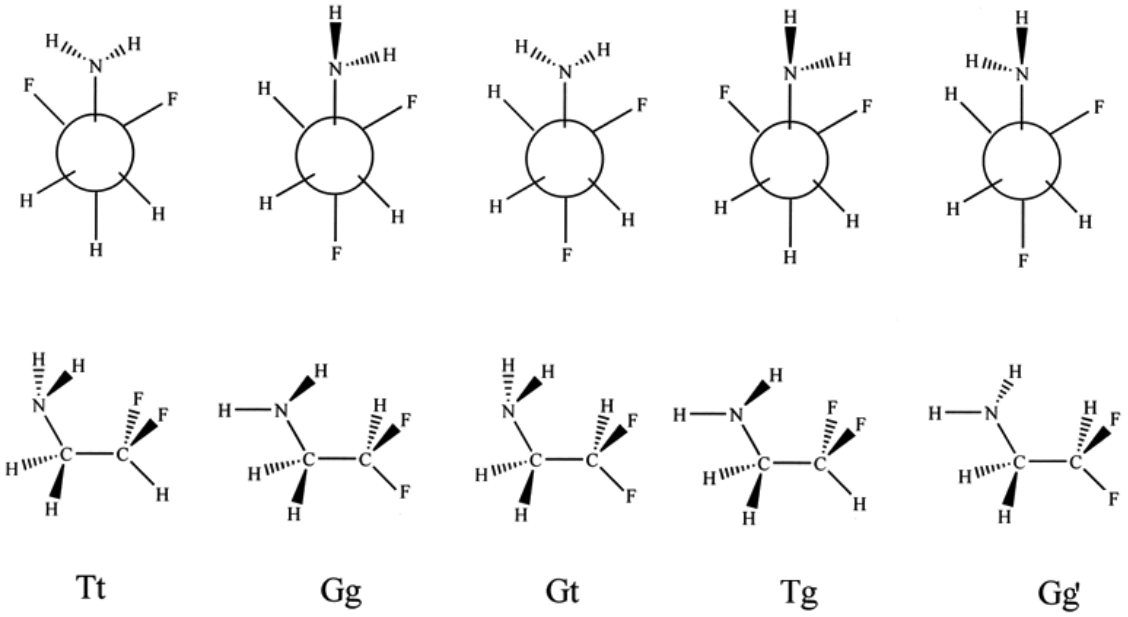

Figure 49. Possible stable conformers of 2,2-difluoroethylamine.

TABLE 85. Structural parameters (Å and degree), rotational constants (MHz), and dipole moment (Debye) for *Trans-trans*, *Gauche-gauche* and *Gauche-trans* forms of 2,2-difluoroethylamine .

Structural Parameters		MP2(full)/6-311+G(d,p)			MW[a]			Adjusted r_0 parameters		
		Trans-trans	*Gauche-gauche*	*Gauche-trans*	*Trans-trans*	*Gauche-gauche*	*Gauche-trans*	*Trans-trans*	*Gauche-gauche*	*Gauche-trans*
r C_1-C_2	R_1	1.513	1.506	1.512	1.530*	1.530*	1.530*	1.514(3)	1.507(3)	1.512(3)
r C_2-N_3	R_2	1.451	1.458	1.453	1.469*	1.469*	1.469*	1.452(3)	1.458(3)	1.453(3)
r C_1-F_4	R_3	1.369	1.370	1.369	1.350*	1.350*	1.350*	1.368(3)	1.370(3)	1.369(3)
r C_1-F_6	R_4	1.369	1.365	1.366	1.350*	1.350*	1.350*	1.368(3)	1.365(3)	1.366(3)
r C_1-H_5	r_1	1.092	1.090	1.093	1.093*	1.093*	1.093*	1.092(2)	1.090(2)	1.093(2)
r C_2-H_7	r_2	1.094	1.098	1.093	1.093*	1.093*	1.093*	1.094(2)	1.098(2)	1.093(2)
r C_2-H_8	r_3	1.094	1.092	1.093	1.093*	1.093*	1.093*	1.094(2)	1.092(2)	1.093(2)
r N_3-H_9	r_4	1.014	1.014	1.014	1.017*	1.017*	1.017*	1.014(2)	1.014(2)	1.014(2)
r N_3-H_{10}	r_5	1.014	1.013	1.014	1.017*	1.017*	1.017*	1.014(2)	1.013(2)	1.014(2)
∠ $N_3C_2C_1$	θ	115.1	108.6	114.7	114.0(10)	109.0(10)	114.0(10)	115.0(5)	108.8(5)	114.8(5)
∠ $F_4C_1C_2$	ρ_1	109.9	109.2	109.6	110.0*	110.0*	110.0*	110.3(5)	109.3(5)	109.7(5)
∠ $F_6C_1C_2$	ρ_2	109.9	109.9	109.9	110.0*	110.0*	110.0*	110.3(5)	110.0(5)	109.9(5)
∠ $F_4C_1H_5$	δ_1	107.9	107.8	107.4	109.2*	109.2*	109.2*	107.7(5)	108.1(5)	107.4(5)
∠ $F_6C_1H_5$	δ_2	107.9	108.8	108.2	109.20*	109.20*	109.20*	107.7(5)	108.5(5)	108.2(5)
∠ $F_4C_1F_6$	α	106.8	107.2	107.3	108.94*	108.94*	108.94*	106.5(5)	107.0(5)	107.1(5)
∠ $H_5C_1C_2$	μ	113.9	113.5	114.0	109.48*	109.48*	109.48*	113.9(5)	113.5(5)	114.0(5)
∠ $H_7C_2C_1$	π_1	107.6	107.5	107.2	109.48*	109.48*	109.48*	107.6(5)	107.5(5)	107.2(5)
∠ $H_8C_2C_1$	π_2	107.6	107.6	108.0	109.48*	109.48*	109.48*	107.6(5)	107.6(5)	108.0(5)
∠ $H_7C_2H_8$	β	107.5	108.3	107.7	109.48*	109.48*	109.48*	107.5(5)	108.3(5)	107.7(5)
∠ $H_9N_3C_2$	ε_1	110.4	110.3	110.7	109.48*	109.48*	109.48*	110.3(5)	110.3(5)	110.7(5)
∠ $H_{10}N_3C_2$	ε_2	110.4	110.6	111.4	109.48*	109.48*	109.48*	110.3(5)	110.6(5)	111.4(5)
∠ $H_{10}N_3H_9$	γ	107.3	107.5	107.9	109.48*	109.48*	109.48*	107.3(5)	107.5(5)	107.9(5)
τ F_4CCN	τ_1	58.6	64.0	63.1	60.0(0)	60.0(20)	60.0(20)	58.6(5)	64.5(5)	61.2(5)
τ F_6CCN	τ_2	-58.6	-178.5	-179.4	-	-	-	-58.6(5)	-178.1(5)	178.8(5)
τ H_9NCC	τ_3	-59.2	-72.1	-63.1	-	-	-	-59.2(5)	-72.13(5)	-56.6(5)

τ H_{10}NCC	τ_4	59.2	169.0	60.0	60.0*	0.0*	60.0*	59.2(5)	69.0(5)	63.5(5)
A		7106.51	8985.18	8888.13	7125.17	8987.27	8900.80	7125.34	8987.29	8900.72
B		4201.62	3714.28	3650.35	4185.89	3699.88	3646.84	4186.69	3700.08	3646.80
C		3444.26	2836.48	2808.35	3441.17	2828.92	2807.57	3440.48	2829.14	2807.65
$\lvert\mu_a\rvert$		0.060	2.382	1.194	0.090(20)	2.042(15)	1.073(14)			
$\lvert\mu_b\rvert$		0.000	1.231	0.315	0.0	1.101(29)	0.22(23)			
$\lvert\mu_c\rvert$		1.660	0.357	1.774	1.427(28)	~0.0	1.483(26)			
$\lvert\mu_t\rvert$		1.661	2.705	2.161	1.430(30)	2.320(27)	1.844(57)			

[a]Ref. [171]; asterisk indicates assumed values.

The vibrational spectra were predicted from the MP2(full)/6-31G(d) calculations. The predicted scaled frequencies were used together with a Lorentzian function to obtain the simulated spectra. Infrared intensities were obtained based on the dipole moment derivatives with respect to Cartesian coordinates. The derivatives were transformed with respect to normal coordinates by $(\partial\mu_u/\partial Q_i) = \sum_j (\partial\mu_u/\partial X_j)L_{ij}$, where Q_i is the i^{th} normal coordinate, X_j is the j^{th} Cartesian displacement coordinate, and L_{ij} is the transformation matrix between the Cartesian displacement coordinates and the normal coordinates. The infrared intensities were then calculated by $(N\pi)/(3c^2)$ $[(\partial\mu_x/\partial Q_i)^2 + (\partial\mu_y/\partial Q_i)^2 + (\partial\mu_z/\partial Q_i)^2]$. A comparison of the experimental spectra of the solid and simulated infrared spectra of *trans-trans* $F_2CHCH_2NH_2$ is shown in Fig. 47. The infrared spectra of the xenon solution and the predicted infrared spectra for the pure *trans-trans*, *gauche-gauche*, and *gauche-trans* conformers, as well as the mixture of the three conformers with relative concentrations calculated for the equilibrium mixture at -65ºC by using the experimentally determined enthalpy difference are shown in Fig. 50 (A-E), respectively. The predicted spectrum is in good agreement with the experimental spectrum which shows the utility of the scaled predicted frequencies and predicted intensities for supporting the vibrational assignment.

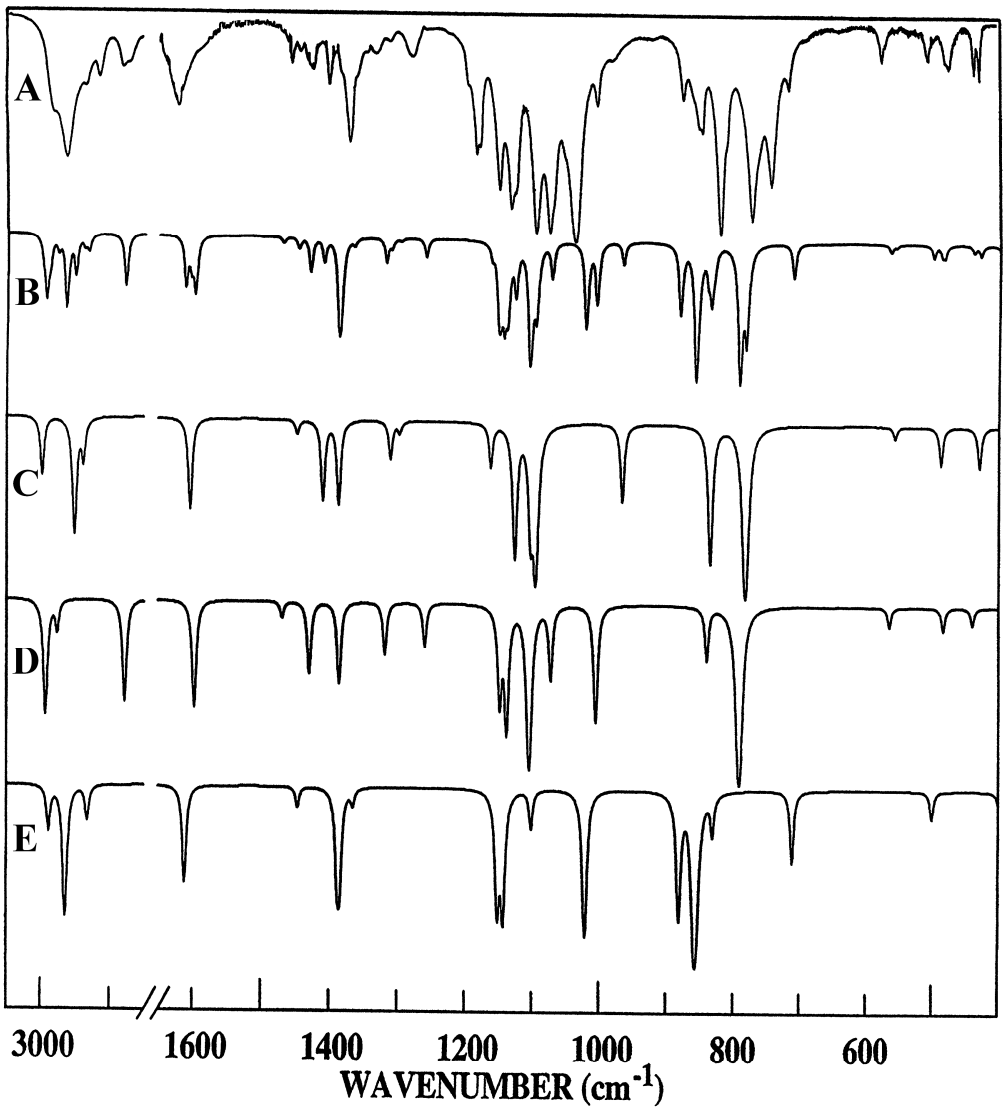

Figure 50. Comparison of experimental and predicted infrared spectra of 2,2-difluoroethylamine: (A) observed spectrum of Xe solution at -65°C; (B) simulated spectrum of mixture of *Tt*, *Gg* ($\Delta H = 83$ cm^{-1}), *Gt* ($\Delta H = 235$ cm^{-1}) conformers at -65°C; (C) simulated spectrum of *Gt* conformer; (D) simulated spectrum of *Gg* conformer; (E) simulated spectrum of *Tt* conformer.

Additional support for the vibrational assignments was obtained from the simulated Raman spectra. The evaluation of Raman activity by using the analytical gradient methods has been developed [31-34] and the activity S_j can be expressed as: $S_j = g_j(45\alpha_j^2 + 7\beta_j^2)$, where g_j is the degeneracy of the vibrational mode j, α_j is the derivative of the isotropic polarizability, and β_j is the anisotropic polarizability. To obtain the Raman scattering cross sections, the polarizabilities are incorporated into S_j by multiplying S_j with $(1-\rho_j)/(1+\rho_j)$ where ρ_j is the depolarization ratio of the j^{th} normal mode. The Raman scattering cross sections and calculated wavenumbers obtained from the Gaussian 03 program were used together with a Lorentzian function to obtain the simulated Raman spectra. Comparison of experimental Raman spectra of the liquid and the predicted Raman spectra for the pure *trans-trans*, *gauche-gauche,* and *gauche-trans* conformers as well as the mixture of the three conformers with relative concentrations calculated for the equilibrium mixture at 25°C by using the experimentally determined enthalpy difference are shown in Fig. 48(A-E). The spectrum of the mixture should be compared to that of the Raman spectrum of the liquid at room temperature. The predicted spectrum is in reasonable agreement with the experimental spectrum which shows the utility of the predicted Raman spectra for the supporting vibrational assignments.

VIBRATIONAL ASSIGNMENT

To be able to determine the enthalpy differences between the conformers it is necessary to assign the spectra for each of the three conformers which were previously identified from the microwave spectra of 2,2-difluoroethylamine. To begin the assignments of these conformers *ab initio* predictions from MP2(full)/6-31G(d) calculations were carried out to obtain the force constants, frequencies, infrared

intensities, band contours, Raman activities, and depolarization values for all three of the previously identified conformers. Most of these predicted quantities are listed in Tables 81, 82, and 83 for the *Tt*, *Gg*, and *Gt* conformers, respectively, and in addition to the frequencies, the infrared intensities and band contours were very valuable to make the initial assignments for the fundamentals for the spectral region from 400 to 1000 cm^{-1}.

The frequencies for the fundamentals of the *Gg* and *Gt* are very similar since the difference is only the position of the NH_2 group so they come as pairs. Thus for these two conformers the pairs for ν_{21}, ν_{20}, and ν_{19} are observed at 430, 439: 475, 482: 572, 576 cm^{-1}, respectively, in the xenon solution with the lower frequency for all three cases arising from the *Gt* form. These three modes are CF bends which are extensively mixed but best described as the CF_2 rock, CF_2 twist, and CF_2 deformation for ν_{21}, ν_{20}, and ν_{19}, respectively. It is interesting that there is only one fundamental predicted in the gas in this region at 500 cm^{-1} for the *Tt* conformer and observed at 507 cm^{-1} as a clear C-type contour with a predicted 97% C-type. For this conformer this CF_2 bend is primarily a CF_2 deformation (85% S_{13}). The next higher frequency fundamental for the *Tt* conformer is predicted at 711 cm^{-1} and observed at 718 cm^{-1} which has nearly 20% contribution from four symmetry coordinates with the CF_2 rock as the largest amount (24% S_{12}). The three quite strong bands at 743, 772 and 819 cm^{-1} are undoubtedly the NH_2 rocks of the *Gt*, *Gg* and *Tt* conformers, respectively, which are always observed at a significantly lower frequency than predicted from MP2(full)/6-31G(d) calculations. In addition to their intensities the observed infrared band contours are exactly as predicted so the assignments for these three NH_2 has been confidently made. However, the assignments for the CH_2 rocks is relatively difficult to make since their frequencies, intensities, and

band contours are significantly dependent on their mixing with the NH_2 rock as well as possibly heavy atom motions. The predicted frequencies for this mode (CH_2 rock) for the *Tt*, *Gg*, and *Gt* forms are 831, 840 and 835 cm^{-1}, respectively, and the pair of bands at 856 and 847 cm^{-1} are consistent with expected relative intensities and contours for the *Gg* and *Gt* conformers, respectively and are assigned accordingly. The best candidate for the CH_2 rock for the *Tt* form is the band at 814 cm^{-1} or obscured by the NH_2 rock at 824 cm^{-1}. The correct assignment of the fundamentals discussed so far is very important since it is desirable to use lower frequency fundamentals for the enthalpy determination. Most of the remaining fundamentals in the "fingerprint" region were assigned based on "group frequencies", *ab initio* predicted frequencies, band contours, intensities, and changes of intensities with the variable temperatures. These assignments are all listed in Tables 81, 82 and 83 along with those for the CH and NH stretches. These tables also include the frequencies observed from the Raman spectrum of the liquid which is expected to have some significant frequency shifts due to dimerization as a result of hydrogen bonding of the amino group.

CONFORMATIONAL STABILITY

To determine the enthalpy differences among the three conformers of 2,2-difluoroethylamine, the sample was dissolved in liquefied xenon and the mid-infrared spectra were recorded as a function of temperature from -55 to -100°C. Relatively very small interactions are expected to occur between xenon and the sample though the sample can associate with itself forming a dimmer, trimer or higher order complex. However, due to the very small concentration of sample (~10^{-4} molar) self association is greatly reduced. Therefore, only small frequency shifts are anticipated for the xenon interactions

when passing from the gas phase to the liquefied xenon solutions. A significant advantage of this study is that the conformer bands are better resolved in comparison with those in the infrared spectrum of the gas. From *ab initio* calculations, the dipole moments of the two conformers are predicted to have similar values and the molecular sizes of the two conformers are nearly the same, so the ΔH value obtained from the temperature dependent FT-IR study is expected to be close to that for the gas [16-20].

Once confident assignments have been made for the fundamentals of the three most abundant conformers the task was then to find a pair or pairs of bands from which the enthalpy determination could be obtained. To minimize the effect of combination and overtone bands in the enthalpy determination it is desirable to have the lowest frequency pair(s) that is possible to use for the determination. The bands should also be sufficiently resolved as to determine their intensities. The selection of the bands to use in the enthalpy determination was complicated due to the presence of all three conformers nearly in equal amounts. The fundamentals at 508 and 819 cm^{-1} were selected for the *Tt* conformer band as they are free of interfering bands and in the lower frequency region of the spectrum. For the *Gg* and *Gt* conformers the selection of the bands it was more difficult since there are few bands resolved sufficiently to determine their intensities. The fundamentals at 439, 772 cm^{-1} for the *Gg* form and 430, 743 cm^{-1} for the *Gt* conformer are relatively free from interfering bands which allowed the determination of their band intensities to be measured.

The intensities of the individual bands were measured as a function of temperature and their ratios were determined (Fig. 51). By application of the van't Hoff equation $-\ln K = \Delta H/(RT) - \Delta S/R$, the enthalpy difference was determined from a plot of

–lnK versus 1/T, where ΔH/R is the slope of the line and K is substituted with the appropriate intensity ratios, *i.e.* $I_{conf\text{-}1}$ / $I_{conf\text{-}2}$, etc. It was assumed that ΔH, ΔS, and α are not functions of temperature in the range studied.

Figure 51. Temperature (-60 to -100°C) dependent mid-infrared spectrum in the 725-835 cm^{-1} region of 2,2-difluoroethylamine dissolved in liquid xenon.

These six bands, two for each conformer, were utilized for the determination of the enthalpy difference by combining them to form 12 band pairs. By using the four band pairs for the *trans-trans* and *gauche-gauche* conformers the enthalpy difference was determined with a value of 83 ± 8 cm^{-1} (Table 86). Then the four band pairs for the *Tt* and *Gt* forms were used to obtain the enthalpy difference of 235 ± 11 cm^{-1}. To determine the enthalpy difference for the *Gg* and *Gt* conformers the four corresponding band pairs were used for which a value of 152 ± 13 cm^{-1} was obtained. These values are consistent with the corresponding predicted values from *ab initio* calculations with large basis sets (Table 84). This error limit is derived from the statistical standard deviation of one sigma of the measured intensity data taken as a single data set, but it does not take into account small associations with the liquid xenon or the interference of overtones and combination bands in near coincidence with the measured fundamentals. From these enthalpy differences abundance of the *Tt* conformer present at ambient temperature is estimated to be 34 ± 1%, with the remainder values of 45 ± 1% for the *Gg* conformer and 22 ± 1% for the *Gt* form.

TABLE 86. Temperature and intensity ratios of the *Trans-trans*, *Gauche-gauche*, and *Gauche-trans* bands of 2,2-difluoroethylamine.

			Tt → *Gg*				*Tt* → *Gt*				*Gg* → *Gt*			
	T(°C)	1/T ($\times 10^{-3}$ K^{-1})	I_{508} / I_{439}	I_{508} / I_{772}	I_{819} / I_{439}	I_{819} / I_{772}	I_{508} / I_{430}	I_{508} / I_{743}	I_{819} / I_{430}	I_{819} / I_{743}	I_{439} / I_{430}	I_{439} / I_{743}	I_{772} / I_{430}	I_{772} / I_{743}
Liquid xenon	-60	4.692	6.499	1.463	6.174	1.390	6.094	2.449	5.789	2.327	0.938	3.768	4.164	1.673
	-65	4.804	7.029	1.477	6.596	1.386	6.496	2.600	6.096	2.440	0.924	3.699	4.397	1.760
	-70	4.923	7.080	1.500	6.772	1.435	6.270	2.664	5.997	2.548	0.886	3.763	4.180	1.776
	-75	5.047	7.000	1.490	6.808	1.449	6.934	2.808	6.744	2.731	0.991	4.011	4.654	1.885
	-80	5.177	7.238	1.462	7.143	1.442	6.508	2.912	6.422	2.874	0.899	4.023	4.453	1.992
	-85	5.315	7.258	1.455	7.348	1.473	6.750	2.963	6.834	3.000	0.930	4.083	4.641	2.037
	-90	4.460	7.581	1.542	7.331	1.492	7.331	3.273	7.089	3.165	0.967	4.318	4.753	2.122
	-95	5.613	7.596	1.565	7.440	1.532	7.834	3.464	7.672	3.393	1.031	4.560	5.007	2.214
	-100	5.775	7.879	1.582	7.582	1.522	8.424	3.786	8.106	3.643	1.069	4.805	5.324	2.393
ΔH (cm^{-1})			100 ± 13	46 ± 14	120 ± 15	65 ± 6	186 ± 28	264 ± 14	206 ± 20	284 ± 5	86 ± 30	161 ± 16	141 ± 21	219 ± 9
ΔH (cm^{-1})[a]			83 ± 8				235 ± 11				152 ± 13			

[a] Average valuę and statistical uncertainty (1σ) obtained by utilizing all of the data as a single set.

STRUCTURAL PARAMETERS

In the microwave study [171], all but two of the structural parameters were assumed for the three identified conformers. The two parameters that were not assumed but fitted instead were the CCN angle and the FCCN dihedral angle, where the fluorine atom is involved in hydrogen bonding. Since the assumed structural parameters were common for all three conformers, it is likely that they are not very reliable from the microwave study. Therefore, we have again determined the structural parameters for the three rotamers by utilizing the rotational constants previously reported from the microwave study [171]. Only one isotopic species was studied for the three conformers and, thus, only three rotational constants are available for each conformer.

We have found that good structural parameters for hydrocarbons and many substituted ones can be determined by adjusting the structural parameters obtained from the *ab initio* MP2/6-311+G(d,p) calculations to fit the rotational constants obtained from microwave experimental data by using a computer program "A&M" (*Ab initio* and Microwave) developed [14] in our laboratory. In order to reduce the number of independent variables, the structural parameters are separated into sets according to their types where bond distances in the same set keep their relative ratio, and bond angles and torsional angles in the same set keep their difference in degrees. This assumption is based on the fact that errors from *ab initio* calculations are systematic. Additionally, we have also shown that the differences in predicted distances and angles from the *ab initio* calculations for different conformers of the same molecule can usually be used as one parameter with the *ab initio* predicted differences except for some dihedral angles.

Therefore, it should be possible to obtain "adjusted r_0" structural parameters for all three conformers of 2,2-difluoroethylamine by utilizing the previously reported nine rotational constants from the earlier microwave study [171] since there are only seven heavy atom parameters to be determined.

We [51] have shown that *ab initio* MP2(full)/6-311+G(d,p) calculations predict the r_0 structural parameters for more than fifty carbon-hydrogen distances to at least 0.002 Å compared to the experimentally determined values from isolated CH stretching frequencies which were compared [5] to previously determined values from earlier microwave studies. Therefore, all of the carbon-hydrogen distances can be taken from the MP2(full)/6-311+G(d,p) predicted values for *Tt*, *Gg* and *Gt* conformers of 2,2-difluoroethylamine. The resulting adjusted r_0 parameters are listed in Table 85, where it is believed that the N-C and C-C distances should be accurate to ± 0.003 Å, the C-H and N-H distances should be accurate to ± 0.002 Å, and the angles should be within ± 0.5°.

The fit of the nine determined rotational constants (Table 87) by the structural parameters for the *Tt*, *Gg* and *Gt* conformers is remarkably good with the biggest differences being 0.80, 0.69 and the smaller ones of 0.22, 0.20, 0.17 and the remaining less than 0.1 MHz. Therefore, it is believed that the suggested uncertainties are realistic values and the determined structural parameters are probably as accurate as can be obtained for the molecule in the gas phase by either electron diffraction or microwave substituted methods.

TABLE 87. Comparison of rotational constants obtained from *ab initio* MP2(full)/6-311+G(d,p) predictions, experimental values[a] from microwave spectra, and adjusted r_0 structural parameters for 2,2-difluoroethylamine.

Conformer	Rotational constants	MP2(full)/ 6-311+G(d,p)	Experimental[a]	Adjusted r_0	$\|\Delta\|$
Trans-trans	A	7106.51	7125.17	7125.34	0.17
	B	4201.62	4185.89	4186.69	0.80
	C	3444.26	3441.17	3440.48	0.69
Gauche-gauche	A	8985.18	8987.27	8987.29	0.02
	B	3714.28	3699.88	3700.08	0.20
	C	2836.48	2828.92	2829.14	0.22
Gauche-trans	A	8888.13	8900.80	8900.72	0.09
	B	3650.35	3646.84	3646.80	0.04
	C	2808.35	2807.57	2807.65	0.08

[a] Ref. [171].

DISCUSSION

The vibrational assignment in the lower frequency region could be made relatively easy but the assignments for the bands in the spectral region from 1000 to 1400 cm^{-1} was much more difficult. It should be noted that the approximate description for ν_{13}, ν_{14} and ν_{16} for the *Gg* and *Gt* conformers differ significantly but ν_{16} for the *Gt* form has only 17% S_{16} but 31% S_{12}. However, the NH_2 twist (23% S_{12}) is better placed at 1197 cm^{-1} where the largest contribution is from the CH_2 rock (32% S_{17}). Therefore, for many cases the approximate descriptions are more for "bookkeeping" than conveying the major

molecular motions. This is particularly needed when seven of the fundamentals have contributions of 10% or more from four symmetry coordinates and three that have five symmetry coordinates contributing 10% or more to the P. E. D. Nevertheless, it should be noted that the MP2(full)6-31G(d) predicted frequencies with three scaling factors which had average differences of 8.7 cm^{-1} and 9.9 cm^{-1} for the modes with A' and A" symmetry for the *Tt* form excluding the NH_2 rock which represents percentage error of 0.6% for both species.

The predicted Raman spectrum by using the isolated molecule predictions gives a reasonable simulated spectrum (Fig. 52) for the liquid where there must be a significant self association of the molecules. We also predicted and measured the depolarization of the three deformations are depolarized as predicted with similar results for the bands in the 1300 cm^{-1} region. The band at 1199 cm^{-1} has a predicted depolarization value of 0.57 which is consistent with the observed values. Most of the bands below this frequency are strongly polarized but with the presence of three conformers it appears that the predicted depolarization values are in satisfactory agreement with the observed values.

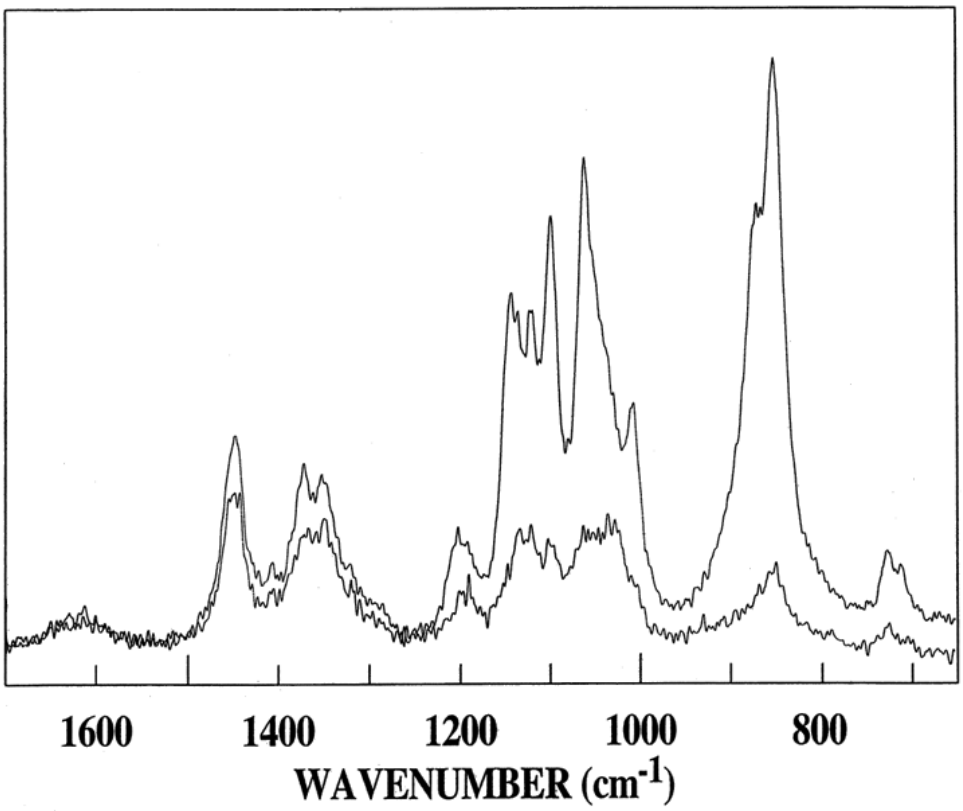

Figure 52. Raman spectra (650-1700 cm^{-1}) showing the polarized and the depolarized bands for 2,2-difluoroethylamine.

To determine the conformational stabilities we initially used the bands at 508 (*Tt*), 439 (*Gg*) and 430 (*Gt*) which are mainly heavy atom motions which should not be significantly affected by molecular association. As can be seen from the data in Table 86 the enthalpy difference between the *Tt* and *Gg* form is 100 ± 13 cm^{-1} (1.20 ± 0.16 kJ/mol). Normally, we would not use the fundamentals associated with NH_2 group since they can be significantly affected by molecular association as the temperature is decreased. However, there did not appear to be a significant decrease in the association as

the temperature was lowered from -60 to -100°C so we also then used the relatively strong band from the NH_2 rocks which were well separated and had excellent signal-to-noise ratios. Therefore, by using four pairs for the determination of this enthalpy difference and the data as a single set the enthalpy difference was determined to be 83 ± 8 cm^{-1} (0.99 ± 0.10 kJ/mol). Considering the uncertainties the two values agree but the value obtained from four pairs is expected to be a better value since the problem of overtone and combination bands contributing to the intensities of either fundamental should average out. Therefore, the reported enthalpy differences should be appropriate for comparison to *ab initio* predicted values or enthalpy differences obtained for other substituted organoamines. The *ab initio* predicted energy difference from the MP2(full)/aug-cc-pVTZ (345 basis sets) calculation gave a value of 72 cm^{-1} (0.86 kJ/mol) with the *Tt* form more stable than the *Gg* form. Similarly the *Gt* conformer energy difference between it and the *Tt* form was predicted to be 209 cm^{-1} (2.50 kJ/mol) which is in excellent agreement with the experimental enthalpy difference of 235 ± 11 cm^{-1} (2.81 ± 0.13). However, the density functional theory calculations by the B3LYP method gave a similar value of 93 cm^{-1} (1.11 kJ/mol) for the energy difference between the *Tt* and *Gg* forms but the predicted energy value for the *Tt* and *Gg* was a much smaller value of 136 cm^{-1} (1.63 kJ/mol). Nevertheless, the predicted values must be considered to be in excellent agreement with the experimental values.

In the earlier microwave study the quadratic centrifugal distortion constants were determined for all three of the conformers and we have predicted the values from the predicted force constants from the *ab initio* MP2(full) calculations with two different basis sets. Similar calculations have also been carried out by density functional theory

calculations by the B3LYP method with the same basis sets. For the *Tt* conformer the predicted values from the MP2 calculations do not differ significantly between the two basis sets. This is also true of the predictions from the B3LYP except for the δ_K constant which is predicted more than one-half the value with the larger basis set (Table 88). In general, the predicted values are in good agreement with the experimental determined values except for δ_K from the B3LYP calculations. However, for the *Gg* conformer there is a significantly value for Δ_K by both calculations where the value is quite large compared to the experimentally determined value. A similar problem also is found for the *Gt* form where the predicted values with the smaller basis set are more than twice the experimental values. Even with the large basis set the predicted values are ~ 20% and ~ 30% larger than the predicted values from the MP2 and B3LYP calculations, respectively. At this time the reason for these unusually poor values for only the Δ_K constant is not understood.

TABLE 88. Quadratic centrifugal distortion constants (kHz) for conformers of 2,2-difluoroethylamine.

			Trans-trans		
	MP2(full)/ 6-31G(d)	MP2(full)/ 6-311+G(d,p)	B3LYP/ 6-31G(d)	B3LYP/ 6-311+G(d,p)	Exp.[a]
Δ_J	1.9	1.9	2.0	2.0	1.0(5)
Δ_{JK}	7.03	7.19	9.15	9.28	8.34(10)
Δ_K	-5.94	-5.96	-7.99	-7.92	-6.59(36)
δ_J	0.2599	0.2541	0.2698	0.2636	0.2420(58)
δ_K	1.54	1.40	2.45	1.08	1.53(15)
			Gauche-gauche		
	MP2(full)/ 6-31G(d)	MP2(full)/ 6-311+G(d,p)	B3LYP/ 6-31G(d)	B3LYP/ 6-311+G(d,p)	Exp.[a]
Δ_J	0.7995	0.8318	0.8322	0.8823	0.9455(49)

Δ_{JK}	6.122	6.623	5.898	6.622	7.294(15)
Δ_K	1.562	1.016	1.804	1.150	0.838(14)
δ_J	0.1828	0.1915	0.1938	0.2087	0.2089(16)
δ_K	3.709	4.002	3.736	4.124	4.793(61)

Trans-gauche					
	MP2(full)/ 6-31G(d)	MP2(full)/ 6-311+G(d,p)	B3LYP/ 6-31G(d)	B3LYP/ 6-311+G(d,p)	Exp.[a]
Δ_J	0.7661	0.7993	0.7962	0.8383	0.8440(10)
Δ_{JK}	5.633	6.175	5.539	6.180	6.576(11)
Δ_K	1.7336	1.0622	1.9238	1.2894	0.8284(37)
δ_J	0.17023	0.17916	0.17864	0.19142	0.19209(68)
δ_K	3.359	3.612	3.439	3.751	3.979(15)

[a] Ref [171]

One of the major goals of this research was the determination of the r_0 structural parameters for the three conformers which has been done for the six heavy atom parameters. In the microwave study [171] only two parameters for each conformer were determined which were the $\angle N_3C_2C_1$ and τF_4CCN and the heavy atom distances were assumed to have the same values for the three conformers. The values obtained earlier for the $N_3C_2C_1$ angle with an uncertainty of 1.0 degree are in excellent agreement with the corresponding parameters obtained in this study. However, the determined dihedral angle does not agree with the values obtained for this angle in the current study, where, for the *Gg* form the value of 60 ± 2° is reported in the microwave work [171], whereas, the value from this study is 64.5 ± 0.5°. For the *Gt* conformer the value of 61.2 ± 0.5° is in agreement with the value given earlier [171] of 60 ± 2° but the value of exactly 60° for this dihedral angle for the *Tt* form is not in agreement with the value of 58.6 ± 0.5° from our results. The assumption that the heavy atom distances are the same [171] is a good

one for the *Tt* and *Gt* conformers where the differences are 0.001 Å for C_1-F_4 and C_2-N_3, and 0.002 Å for the C_1-C_2 and C_1-F_6 from the current study. However, for the *Gg* conformer the C_1-C_2 is shorter by 0.005 and 0.007 Å than the *Gt* and *Tt* forms, respectively but for the C_2-N_3 distance it is longer by 0.005 and 0.006 Å for these conformers, respectively. However, the major differences between the values reported earlier and those obtained herein is with the C-F distances which were estimated to be shorter by an average distance of 0.017 Å and for the C-N and C-C bonds where the average distances are too long by 0.015 and 0.019 Å, respectively. There is also a significant difference between the assumed FCF angle and the value obtained in this study which is nearly 2° smaller. With these exceptions many of the other estimated parameters are in acceptable agreement with those obtained in the current study.

It is also interesting to compare the heavy atom parameters of 2-fluoroethylamine [170] and 2,2,2-trifluoroethylamine [170] with the corresponding ones obtained in the current study of 2,2-difluoroethylamine. It should be noted that the C-C bond is smaller by an average of 0.003 Å for each substitution of fluorine on β-carbon which is within the experimental error of ± 0.003 Å for the heavy atom bond distances in each r_0 determination. When one compares the C-N bond distance, the change is considerable with the addition of the second fluorine atom the distance decreases by an average of 0.008 Å and with the addition of a further fluorine atom decreases by 0.005 Å. However, the parameter which shows the greatest change due to fluorine substitution on β-carbon is the C-F bond distance(s) which drastically reduces by ~ 0.030 Å each time a fluorine atom is added. Thus for 2-fluoroethylamine the average C-F distance is 1.399(3) Å, for

2,2-difluoroethylamine 1.368(3) Å and for 2,2,2-trifluoroethylamine 1.342(3) Å. Such large changes have a significant effect on some of the other parameters.

It is well known that intramolecular hydrogen bonding can be a stabilizing factor for the orientation of molecular coformers. This is important in the case of the fluoride substituted ethylamine where the fluorine atom(s) and the amine hydrogens have the possibility to form an intramolecular hydrogen bond. This is observed with 2-fluoroethylamine [170] where the most stable conformer (*Gg'*) has the amine hydrogen eclipsing the fluorine atom on the β-carbon atom and has the least distance separating the hydrogen and fluorine atoms of any of the possible conformers. The second stable conformer (*Gt*) likewise has the hydrogen and fluorine in the eclipsed positions but has a greater distance between them. The energy distances increase greatly in the conformers where no hydrogen bonding is possible. In the current study of 2,2-difluoroethylamine there are two fluorine atoms so the most stable conformer (*Tt*) allows two intramolecular hydrogen bonds. The second most stable conformer (*Gg*) only allows one hydrogen bond but has a shorter distance between the hydrogen and fluorine atoms. The third most stable conformer (*Gt*) then allows for a hydrogen bond but at an increased distance. In the case of 2,2,2-trifluoroethylamine the three fluorines allow for two intramolecular hydrogen bonds like in the diflouro- species so the most stable conformer is the *Trans* conformer where two hydrogen bonds may be formed. Clearly intramolecular hydrogen bonding plays a significant role in the conformational stabilities of these molecules and it would be of interest to see how other halogen substituents might affect this stability. Also this is a very small sample so it would be of interest to study other substituents on the β-carbon to evaluate other factors that affect the conformer stability of the other organoamines.

CHAPTER 14

CONFORMATIONAL AND STRUCTURAL STUDIES OF N-PROPYLAMINE FROM TEMPERATURE DEPENDENT RAMAN AND FAR INFRARED SPECTRA OF XENON SOLUTIONS AND AB INITIO CALCULATIONS

INTRODUCTION

Many organoamines and alcohols are very important biochemicals which play important roles in many areas. Their conformations and structures have been investigated over the years by several different techniques particularly microwave, infrared, and Raman spectra as well as electron diffraction data. A significant number of these studies for the enthalpy difference determinations between conformers was done in solution by infrared and/or Raman spectra. However, both amines and alcohols readily form dimers or larger associated species. Therefore, it is necessary to carry out these studies in very dilute solutions or in the gas phase to obtain reproducible results when varying the temperatures for enthalpy difference determinations, but variable temperature measurements in the gas phase results in very difficult experiments. However, we have found that we can overcome many of the difficulties by using rare gas solutions with very long liquid cells, i.e. 8 cm long, and the infrared technique. We have now extended this technique to the Raman spectra.

Recently, we have been investigating the conformation stability and determined the structural parameters of several organoamines [161,170,172-174] and alcohols [114,175,176]. One of the first amines studies was ethylamine [161] which was

determined to have the *trans* conformer more stable by 54 ± 4 cm^{-1} (0.65 ± 0.05 kJ/mol) than the *gauche* form. This value was in agreement with earlier determined values of 107 ± 70 cm^{-1}(1.28 ± 0.84 kJ/mol) from electron diffraction study [162], 110 ± 50 cm^{-1}(1.32 ± 0.60 kJ/mol) from a microwave investigation [177], and 100 ± 10 cm^{-1}(1.20 ± 0.12 kJ/mol) from an infrared study of ethylamine in an argon matrix [164]. However, several of the earlier studies [165-168] reported the *gauche* conformer as the more stable form, and it is rather interesting that MP2(full)/6-311+G(2d,2p) calculations predict [161] the *gauche* conformer to be the more stable form by 66 cm^{-1} (0.79 kJ/mol). However, without the diffuse functions the *trans* form is predicted to be the more stable conformer by 32 cm^{-1}(0.38 kJ/mol).

These results clearly indicate that the enthalpy difference between the *gauche* and *trans* conformers of the NH_2 moiety will need to be determined experimentally rather than by theoretical predictions for organoprimary amines. It is of scientific interest to determine the effect of substituting one or more of the hydrogen atoms on β-carbon. One of the earliest molecules of this type studied was n-propylamine, $CH_3CH_2CH_2NH_2$ [169] for which the conformational stability was determined. The conformers are designated according to the relative position of the amine group (T = *trans* or G = *gauche*) to the methyl group (rotation around the C-C bond) and the second one (t = *trans*, g = *gauche*, g′ = *gauche′*) to the relative position of the NH_2 rotor i.e. rotation around the N-C bond. These combinations result in five possible conformers i.e. the *trans-trans (Tt), trans-gauche (Tg), gauche-gauche (Gg), gauche-gauche' (Gg'), and gauche-trans (Gt)* conformers shown in Fig. 53. The most stable conformer was determined to be the *Tt* form but this determination was for the solid. However, the most stable conformer in the gas or the

liquid need not be the same as found in the solid so it is of interest to obtain the relative stabilities of the conformers of n-propylamine in the gaseous state.

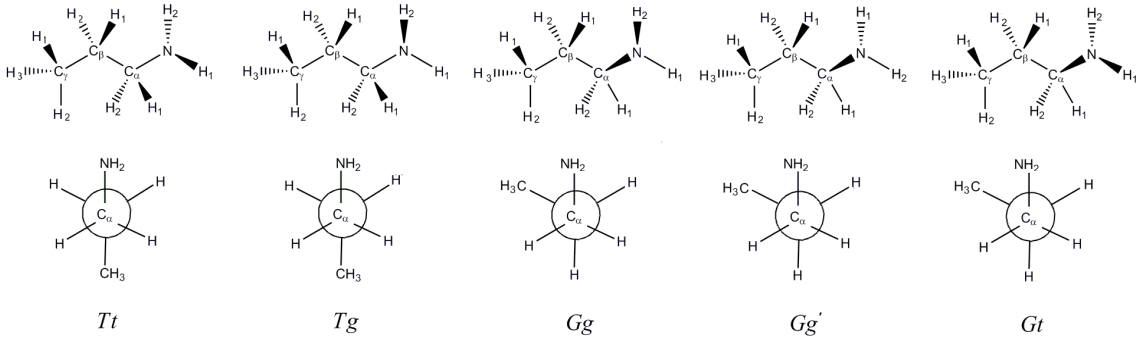

Figure 53. Five conformers of n-propylamine showing atomic numbering.

Prior to our earlier relatively complete vibrational study [169] of n-propylamine two vibrational studies were reported [178,179]. In the earliest of these studies [178] three even earlier studies were cited [180-182] but in none of these investigations was there any discussion of rotational isomers. In this early study [178] the investigators recorded the infrared spectra of $CH_3CH_2CH_2NH_2$ of the gas and a low temperature Ar matrix which was supported by *ab initio* calculations with basis set 4-31G(N*). By utilizing the NH_2 bending modes in the 700 cm^{-1} region and the NH_2 torsion it was concluded that all five conformers were present in the spectrum taken at ambient temperature. A similar study was reported [179] a year later where Raman spectrum of the liquid was utilized to identify conformers and *ab initio* calculations with a similar

basis set 3-21G(N*). These different investigators identified three conformers *Tt*, *Gt*, and one of the *gauche* forms in the Raman spectrum along with the predicted *ab initio* relative conformer stabilities with their relative populations. Therefore, from significantly larger basis sets and higher level calculations it is desirable for further evaluation of the potential utilization of *ab initio* calculations for conformational studies of organoamines.

As a continuation of our conformational studies of organoamines we initiated variable temperature (-60 to -100 °C) studies of xenon solutions of n-propylamine by recording Raman spectra from 1175 to 625 cm^{-1} and infrared spectra from 600 to 40 cm^{-1}. To support the spectroscopic studies we have carried out more extensive *ab initio* calculations by utilizing a variety of basis sets. To support the experimental studies we have also obtained the harmonic force constants, infrared intensities, Raman activities, depolarization ratios, and vibrational wavenumbers from MP2(full)/6-31G(d) *ab intio* calculations. To obtain predictions on the conformational stabilities we have carried out MP2(full) *ab intio* and density functional theory (DFT) calculations by the B3LYP method utilizing a variety of basis sets. The results of these spectroscopic, structural, and theoretical studies of n-propylamine are reported herein.

EXPERIMENTAL

The sample of n-propylamine was purchased from Sigma-Aldrich Chemical Co., with stated purity of ≥99%. The sample was further purified by low-temperature, low-pressure fractionation column and the purity of the sample was verified by comparing the infrared spectrum with that previously reported [169].

The mid-infrared spectrum of the gas (Fig. 54A) and solid (Fig. 54H) were obtained from 4000 to 220 cm^{-1} on a Perkin-Elmer model 2000 Fourier transform spectrometer

equipped with a Ge/CsI beamsplitter and a DTGS detector. Atmospheric water vapor was removed from the spectrometer housing by purging with dry nitrogen. The spectra of the gas and solid were obtained with a theoretical resolution of 0.5 cm^{-1} for the gas and 2 cm^{-1} for the solid with 128 interferograms added and truncated. Multiple annealings were required to obtain satisfactory spectra of the crystalline solid and the solid was cooled to liquid nitrogen temperatures. The observed fundamental bands with their assignments are listed in Table 89 for the *Tt*, *Tg*, *Gg*, *Gg'* and *Gt* conformers.

The far infrared spectra (600 to 10 cm^{-1}) of the sample dissolved in liquid xenon was recorded on a Bruker model IFS 66 v/S Fourier transform spectrophotometer equipped with a Globar source, a 6.0 μm Mylar beamsplitter, and a liquid helium cooled Si bolometer. The sample was contained in a 7 cm cell fitted with Si windows and the sample added as described for the mid-infrared studies. For all spectra 250 interferograms were collected at 0.5 cm^{-1} resolution, averaged and transformed with a Blackman-Harris three term function. A portion of the spectrum is shown in (Fig. 55B).

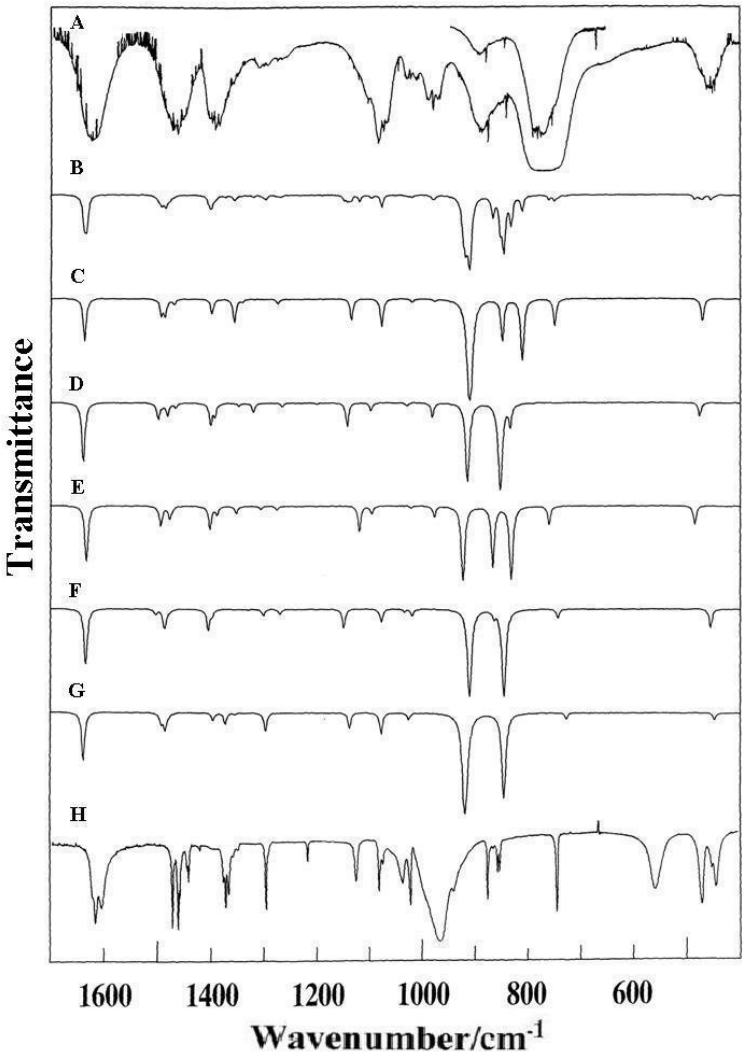

Figure 54. Experimental and predicted infrared spectra of n-propylamine: (A) gas; (B) simulated spectrum of mixture of *Tt*, *Tg* (ΔH = 79 cm^{-1}), *Gg* (ΔH = 91 cm^{-1}), *Gg′* (ΔH = 135 cm^{-1}), and Gt (ΔH = 143 cm^{-1}) conformers at 25°C.; (C) simulated *Tt* conformer; (D) simulated *Tg* conformer; (E) simulated *Gg* conformer; (F) simulated *Gg′* conformer; (G) simulated *Gt* conformer; (H) solid.

Table 89. Observed and predicted wavenumbers (cm^{-1}) for conformers of n-propylamine.

Vib. No.[a]	Approximate Descriptions	*Tt*		*Tg*		*Gg*		*Gg′*		*Gt*	
		fixed scaled[b]	IR Gas	fixed scaled	IR Gas	fixed scaled	IR Gas	fixed scaled	IR Gas	fixed scaled	IR Gas
ν_{20}	NH_2 antisymmetric stretch	3422	3417	3424	3417	3425	3417	3432	3417	3433	3417
ν_1	NH_2 symmetric stretch	3326	3345	3329	3345	3328	3345	3339	3345	3333	3345
ν_2	CH_3 antisymmetric stretch	2998	2966	2998	2966	3024	2979	3001	2966	2998	2966
ν_{21}	CH_3 antisymmetric stretch	2994	2958	2994	2958	2991	2958	2991	2958	2993	2958
ν_{22}	CH_2 antisymmetric stretch	2963	2937	2967	2937	2949	2913	2966	2937	2962	2937
ν_{23}	CH_2 antisymmetric stretch	2937	2903	2934	2903	2937	2903	2948	2913	2943	2913
ν_3	CH_3 symmetric stretch	2913	2888	2911	2888	2916	2888	2912	2888	2912	2888
ν_4	CH_2 symmetric stretch	2909	2878	2905	2878	2898	2858	2910	2888	2909	2878
ν_5	CH_2 symmetric stretch	2895	2858	2837	2839	2845	2839	2836	2839	2896	2858
ν_6	NH_2 symmetric deformation	1638	1624	1634	1624	1633	1624	1639	1624	1637	1624
ν_7	CH_3 antisymmetric deformation	1493	1470	1503	1470	1498	1470	1499	1470	1494	1470
ν_{24}	CH_3 antisymmetric deformation	1486	1463	1489	1463	1494	1470	1492	1470	1487	1463
ν_8	CH_2 deformation	1480	1455	1486	1463	1478	1455	1482	1455	1473	1446
ν_9	CH_2 deformation	1471	1446	1461	1455	1473	1446	1467	1446	1470	1446
ν_{10}	CH_3 symmetric deformation	1396	1401	1406	1401	1402	1401	1401	1401	1399	1401
ν_{11}	CH_2 wag	1373	1373	1398	1401	1389	1392	1393	1392	1361	1357
ν_{25}	CH_2 twist	1355	1357	1329	1308	1352	1350	1348	1350	1356	1357
ν_{12}	CH_2 wag	1297	1292	1301	1300	1306	1300	1320	1308	1341	1340
ν_{26}	CH_2 twist	1296	1292	1270	1274	1276	1274	1266	1274	1275	1274
ν_{27}	CH_3 rock	1224	1209[c]	1222	1209[c]	1220	1209[c]	1200	1209[c]	1213	1209[c]
ν_{13}	CH_3 rock	1139	1126	1150	1133	1120	1103	1144	1133	1136	1126
ν_{14}	CN stretch	1078	1074	1078	1074	1096	1084	1098	1084	1078	1074
ν_{15}	CCC antisymmetric stretch	1026	1022	1034	1022	1020	1029	1030	1022	1020	1029

ν_{28}	NH_2 twist	1011	1029	1019	1029	977	979	981	988	977	979
ν_{16}	NH_2 wag	918	786	910	771	922	786	914	782	910	771
ν_{17}	CCC symmetric stretch	845	865	864	876	866	890	852	854	848	865
ν_{29}	CH_2 rock	844	841	845	865	831	854	833	854	810	835
ν_{30}	CH_2 rock	726	736	742	749	759	760	754	760	748	749
ν_{18}	CCN bend	448	449	455	452	484	470	475	464	470	464
ν_{31}	NH_2 torsion	298	282[c]	291	282[c]	327	328[c]	335	328[c]	339	328[c]
ν_{19}	CCC bend	270	270[c]	257	255[c]	255	255[c]	286	282[c]	294	282[c]
ν_{32}	CH_3 torsion	228	213[c]	229	213[c]	226	213[c]	226	213[c]	235	213[c]
ν_{33}	CCC asymmetric torsion	134	145[c]	127	-	136	145[c]	137	145[c]	133	145[c]

[a] With respect to *Tt* conformer.

[b] MP2(full)/6-31G(d) fixed scaled wavenumbers with factors of 0.88 for CH stretches, 1.0 for heavy atom bends, and 0.90 for all other modes.

[c] Data from the Raman spectra of xenon solutions.

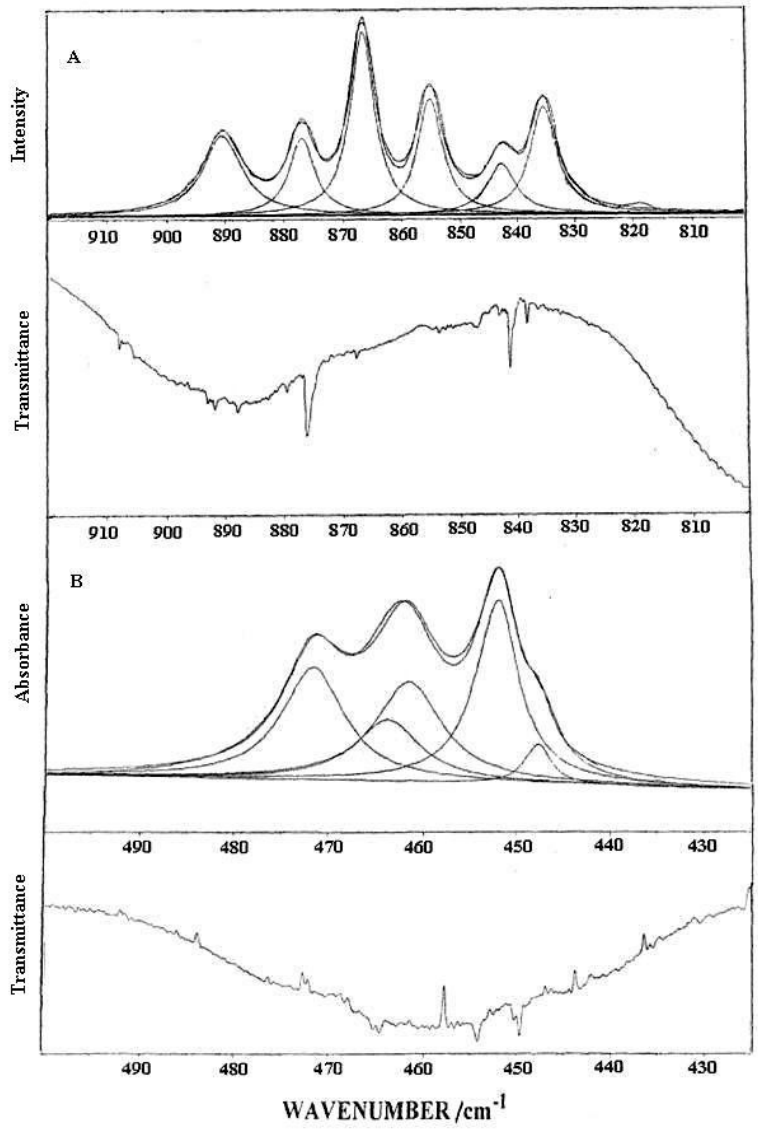

Figure 55. Raman spectra of the xenon solution (Top) and infrared spectra of the gaseous vapor (Bottom) of n-propylamine (A) 920 - 800 cm^{-1}; (B) 500 – 425 cm^{-1}.

The Raman spectra (3500 to 10 cm^{-1}) of the sample dissolved in liquefied xenon (Fig. 56A) at three different temperatures (-60 to -100^{o}C) were recorded on a Trivista 557

spectrometer consisting of a double f = 50 cm monochromator equipped with a 2000 lines mm^{-1} grating, a f = 70 cm spectrograph equipped with a 2400 lines mm^{-1} grating, and a back-illuminated LN2-cooled PI Acton Spec-10:2 kB/LN 2048 x 512 pixel CCD detector. For all experiments, the 514.5 nm line of a 2017-Ar S/N 1665 Spectra-Physics argon ion laser was used for Raman excitation, with the power set to 0.8 Watt. Signals related to the plasma lines were removed by using an interference filter. The wavenumbers were calibrated using Neon emission lines, and depending on the setup used, are expected to be accurate within 0.4 cm^{-1}. The experimental set-up used to investigate the solutions has been described before [23,24]. A home-built liquid cell equipped with four quartz windows at right angles was used to record the spectra. A comparison between the observed and calculated wavenumbers, along with the calculated infrared intensities, Raman activities, depolarization ratios and potential energy distributions for the *Tt, Tg, Gg, Gg', and Gt* conformers of the $CH_3CH_2CH_2NH_2$ are listed in Tables S15, S16, S17, S18 and S19, respectively.

AB INITIO CALCULATIONS

The LCAO-MO-SCF restricted Hartree-Fock calculations were performed with the Gaussian-03 program [22] with Gaussian-type basis functions. The energy minima with respect to nuclear coordinates were obtained by the simultaneous relaxation of all geometric parameters using the gradient method of Pulay [29]. Several basis sets as well as the corresponding ones with diffuse functions were employed with the Møller-Plesset perturbation method [21] to second order (MP2(full)) as well as with the density functional theory by the B3LYP method. The predicted conformational energy differences are listed in Table 90.

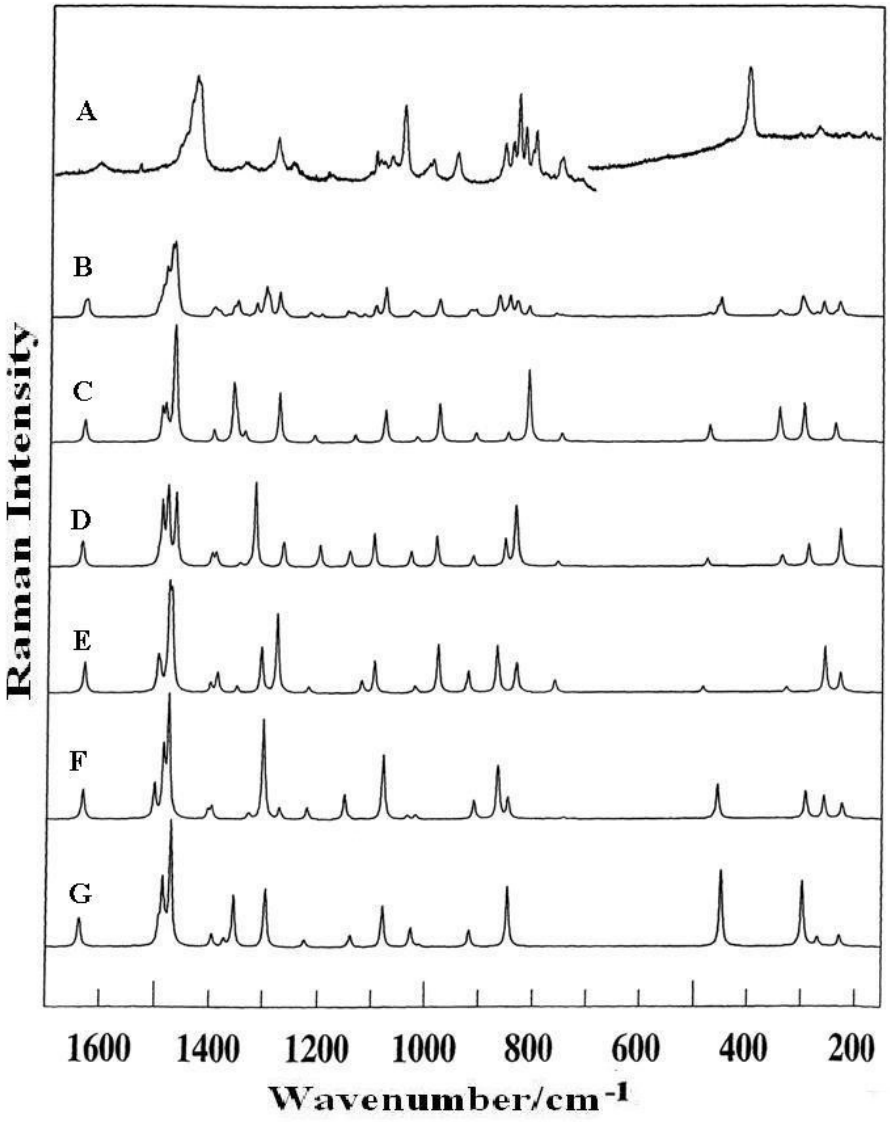

Figure 56. Experimental and predicted Raman spectra of n-propylamine: (A) xenon solution at -100°C; (B) simulated spectrum of mixture of *Tt*, *Tg* (ΔH = 79 cm^{-1}), *Gg* (ΔH = 91 cm^{-1}), *Gg′* (ΔH = 135 cm^{-1}), and Gt (ΔH = 143 cm^{-1}) conformers at -100°C.; (C) simulated *Tt* conformer; (D) simulated *Tg* conformer; (E) simulated *Gg* conformer; (F) simulated *Gg′* conformer; (G) simulated *Gt* conformer.

Table 90. Calculated energies in (H) and energy differences (cm^{-1}) for the five conformers of n-propylamine.

Method/Basis Set	# basis set	Energy[a], E	Energy Differences, Δ[b]			
		Tt	*Tg*	*Gg*	*Gg′*	*Gt*
RHF/6-31G(d)	78	0.282475	0	55	198	180
MP2(full)/6-31G(d)	78	0.858792	115	41	172	68
MP2(full)/6-31+G(d)	94	0.870987	-13	7	13	101
MP2(full)/6-31G(d,p)	105	0.936882	128	43	179	70
MP2(full)/6-31+G(d,p)	121	0.947888	-11	8	19	108
MP2(full)/6-311G(d,p)	126	1.057176	139	-16	26	26
MP2(full)/6-311+G(d,p)	142	1.063612	3	5	93	93
MP2(full)/6-311G(2d,2p)	173	1.111371	66	-79	80	2
MP2(full)/6-311+G(2d,2p)	189	1.116751	-14	14	17	82
MP2(full)/6-311G(2df,2pd)	246	1.181788	62	-66	88	0
MP2(full)/6-311+G(2df,2pd)	262	1.186816	-4	34	35	88
MP2(full)/aug-cc-pVTZ	391	1.193848	-14	43	15	93
MP2 Average		-	34 ± 58	-9 ± 48	51 ± 35	55 ± 44
B3LYP/6-31G(d)	78	1.484593	180	327	327	116
B3LYP/6-31+G(d)	94	1.494156	57	195	201	178
B3LYP/6-311G(d,p)	126	1.541266	141	120	274	79
B3LYP/6-311+G(d,p)	142	1.545868	36	145	179	153
B3LYP/6-311G(2d,2p)	173	1.549595	118	92	247	81
B3LYP/6-311+G(2d,2p)	189	1.553939	36	168	183	166
B3LYP/6-311G(2df,2pd)	246	1.553714	103	81	244	78
B3LYP/6-311+G(2df,2pd)	262	1.558014	35	173	191	172
B3LYP/aug-cc-pVTZ	391	1.562699	34	187	187	173
B3LYP Average		-	82 ± 55	165 ± 73	226 ± 51	133 ± 44

[a]Energy of conformer is given as –(E+173) H.
[b]Difference is relative to *trans-trans* form and given in cm^{-1}.

In order to obtain a complete description of the molecular motions involved in the fundamental modes of n-propylamine, a normal coordinate analysis has been carried out. The force field in Cartesian coordinates was obtained with the Gaussian 03 program [22] at the MP2(full) level with the 6-31G(d) basis set. The internal coordinates used to

calculate the **G** and **B** matrices are given in Table S20 with the atomic numbering shown in Fig. 53. By using the **B** matrix [30], the force field in Cartesian coordinates was converted to a force field in internal coordinates. Subsequently, scaling factor of 0.88 for CH stretches, 0.90 for all other modes excluding the heavy atom bends were applied, along with the geometric average of the scaling factors for the interaction force constants, to obtain the fixed scaled force field and resultant wavenumbers. A set of symmetry coordinates was used (Table S21) to determine the corresponding potential energy distributions (P.E.D.s).

The vibrational spectra were predicted from the MP2(full)/6-31G(d) calculations. The predicted scaled wavenumbers were used together with a Lorentzian function to obtain the simulated spectra. Infrared intensities were obtained based on the dipole moment derivatives with respect to Cartesian coordinates. The derivatives were transformed with respect to normal coordinates by $(\partial\mu_u/\partial Q_i) = \sum_j (\partial\mu_u/\partial X_j)L_{ij}$, where Q_i is the i^{th} normal coordinate, X_j is the j^{th} Cartesian displacement coordinate, and L_{ij} is the transformation matrix between the Cartesian displacement coordinates and the normal coordinates. The infrared intensities were then calculated by $(N\pi)/(3c^2)$ $[(\partial\mu_x/\partial Q_i)^2 + (\partial\mu_y/\partial Q_i)^2 + (\partial\mu_z/\partial Q_i)^2]$.

Additional information on the vibrational assignments was obtained from the simulated Raman spectra. The evaluation of Raman activity by using the analytical gradient methods has been developed [31-34] and the activity S_j can be expressed as: $S_j = g_j(45\alpha_j^2 + 7\beta_j^2)$, where g_j is the degeneracy of the vibrational mode j, α_j is the derivative of the isotropic polarizability, and β_j is the anisotropic polarizability. To obtain the Raman scattering cross sections, the polarizabilities are incorporated into S_j by

multiplying S_j with $(1-\rho_j)/(1+\rho_j)$ where ρ_j is the depolarization ratio of the j^{th} normal mode. The Raman scattering cross sections and calculated wavenumbers obtained from the Gaussian 03 program were used together with a Lorentzian function to obtain the simulated Raman spectra.

VIBRATIONAL ASSIGNMENT

In order to determine the enthalpy difference between the five stable conformers it was essential to have a confident assignment for all of the fundamentals of the most stable conformer and identify vibrations which cannot be assigned to this form. These additional modes must be overtones, combination bands, or fundamentals of the other conformers. In the initial complete vibrational assignment [169] of n-propylamine that was made for the *Tt* conformer with most of the observed vibrational bands assigned to this conformer as fundamentals except for the C-N stretch ($1097cm^{-1}$) as a Gg′ mode and several bands which begin at 842 cm^{-1} and below. These bands were assigned for the other conformers.

In this study the complete vibrational assignment for the most stable conformer was made by utilizing the wavenumbers predicted from the *ab initio* calculations along with the predicted band contours, the infrared intensities, Raman activities and the well-known group wavenumbers for the amine group. First the assignment was made for the most stable form in the infrared spectrum of the crystalline solid which was annealed several times to verify the observed bands arose from a single conformer. This conformer was shown to be the *Tt* form as can be verified from the data in Fig. 54. It should be noted that the most stable conformer in the fluid state need not be the same as that in the crystalline solid due to crystal packing factors which can play a major role in determining

the conformer stability in a the solid. This form was later shown to be the most stable form in the fluid state and the scientific evidence is explained later. The region below 1000 cm^{-1} is of particular interest since the spectrum of the vapor is complex but it is this spectral region where the bands for the conformational determination will be taken. However, this spectral region is greatly simplified in the spectrum of the solid which allows confident assignments of the *Tt* conformer fundamentals.

These assignments should be compared to the previous vibrational assignment [169] where the wavenumbers were predicted with *ab initio* calculations by the restricted HF method with a basis set of 3-21G*. In comparison, for the current study fixed scaled *ab initio* predicted wavenumbers were utilized which provided data that allowed for the reassignment of five previously assigned fundamentals. Firstly the band at 980 and 941 cm^{-1} in the infrared spectra of the gas and solid, respectively, was assigned as ν_{13} in the previous study. However, in the current study this band at 979 cm^{-1} in the gas is assigned as resulting from two accidently degenerate fundamentals of the *Gg* and *Gt* conformers whereas the 941 cm^{-1} band in the spectra of solid is likely a result of the NH_2 wag mode from the dimer or trimer. It is clear from the data in Table S15 that there is no *Tt* conformer fundamental predicted in the spectral region from 1000 to 900 cm^{-1} other than the NH_2 wag, which is assigned to the bands 786 (gas) and 967 (solid) cm^{-1} based on well-known group wavenumbers and relative infrared intensities (and agrees with the previous assignment). The band at 1292 (gas) and 1295 (solid) cm^{-1} in the current study is assigned as the accidentally degenerate fundamentals ν_{12} and ν_{26} due to the *ab initio* predicted difference in their wavenumbers of 1 cm^{-1}. This is differs from the previous assignment where the ν_{12} fundamental is assigned at 1349 cm^{-1} (gas and solid) and ν_{26} is

assigned at 1301 cm^{-1} in the gas and shifts to 1294 cm^{-1} in the spectrum of the solid. The band at 1217 which is observed in the infrared spectra of the solid in both the current and previous studies but it was not assigned in the previous study. It is now assigned as ν_{27} in the current study based on the predicted scaled wavenumber and the Raman spectra of the xenon solutions. The assignment of the bands from 900 to 800 cm^{-1} was of particular interest since it is where the CCC symmetric stretching modes are expected and they are predicted to have sufficient separation to be observed in the Raman spectra of the xenon solutions. In the previous study the band at 876 cm^{-1} in the infrared spectra of the gas was assigned as the CCC symmetric stretch. However, in the current study this mode is assigned to the band at 865 cm^{-1} in the infrared spectra of the gas which corresponds to the 866 cm^{-1} band in the Raman spectra of the xenon solutions. Finally the band at 750 cm^{-1} in the infrared spectra of the gas previously assigned as ν_{30} is now reassigned to the band at 736 cm^{-1} in the current study based on the *ab initio* fixed scaled wavenumbers.

With all of the fundamentals assigned for the most stable *Tt* conformer in the solid the *ab initio* predicted differences were used to assign many of the fundamentals for the other conformers. These assigned fundamentals (Table 89) were verified by using the spectra of the variable temperature xenon solutions along with the predicted band contours, intensities, and depolarization values.

Two regions of the spectra are of significant interest due to their complexity and the predicted spectra which can be observed in Fig. 54 and 56 where the bands for the different conformers are predicted to be sufficiently separated to determine band intensities for use in obtaining the energy differences. The bands at 877 and 447 cm^{-1} in the infrared spectra of the solid which correspond to the bands at 866 and 448 cm^{-1} in the

Raman spectra of Xenon solutions are assigned as ν_{15} and ν_{18} for the *Tt* conformer, respectively. By utilizing the *ab initio* predicted wavenumber differences the bands for the remaining conformers were assigned, and they were verified using their band contours and relative intensities.

CONFORMATIONAL STABILITY

To determine the enthalpy differences among the five observed conformers of n-propylamine, the sample was dissolved in liquefied xenon and the Raman and far infrared spectra were recorded as a function of temperature from -60 to -100°C and -70 to -100°C, respectively. Relatively small interactions are expected to occur between xenon and the sample though the sample can associate with itself forming a dimmer, trimer or higher order complex. However, due to the very low concentration of sample self-association is greatly reduced. Therefore, only small wavenumber shifts are anticipated for the xenon interactions when passing from the gas phase to the liquefied xenon solutions except for the NH_2 modes. A significant advantage of this study is that the conformer bands are better resolved in comparison with those in the Raman spectrum of the liquid or far infrared spectra of the gas. From *ab initio* calculations, the dipole moments of the five conformers are predicted to have similar values and the molecular sizes of the five conformers are nearly the same, so the ΔH value obtained from the temperature dependent Raman study is expected to be near to that for the gas [16-20].

Once confident assignments have been made for the fundamentals of the observed conformers the task was then to find a pair or pairs of bands from which the enthalpy determination could be obtained. The bands should be sufficiently resolved as to determine their intensities. The selection of the bands to use in the enthalpy determination

was complicated due to the presence of all five conformers nearly in equal amounts. The fundamentals at 448, 452, 472, 464, and 461 cm^{-1} were initially selected for the *Tg, Tg, Gg, Gg'* and *Gt* conformers, respectively, as they are confidently assigned, satisfactory resolved (Fig. 55B), and a limited number of overtone and combination bands are possible. The fundamentals at 866 cm^{-1} for the *Tt*, 876 cm^{-1} for the *Tg*, and 835 cm^{-1} for the *Gt* were then selected in the Raman spectra (Fig. 55A) as it was found that the band intensities were not significantly affected by the underlying NH_2 bending modes which are weak in the Raman effect. The intensities of the individual bands were measured as a function of temperature and their ratios were determined. By application of the van't Hoff equation, $-\ln K = \Delta H/(RT) - \Delta S/R$, the enthalpy differences were determined from a plot of $-\ln K$ versus 1/T (Fig. S2), where $\Delta H/R$ is the slope of the line and K is substituted with the appropriate intensity ratios, *i.e.* $I_{conf\text{-}1} / I_{conf\text{-}2}$, etc. It was assumed that ΔH, ΔS, and α are not functions of temperature in the range studied.

These bands, i.e. two for *Tt*, two for *Tg*, one for *Gg*, one for *Gg'*, and two for *Gt*, were utilized for the determination of the enthalpy difference by combining them to form the band pairs given in Table 91. By using the two band pairs for the *Tt* and *Tg* conformers the enthalpy difference was determined to be 79 ± 9 cm^{-1} (Table 91). The band pair for the *Tt* and *Gg* forms was used to obtain the enthalpy difference of 91 ± 26 cm^{-1}. To determine the enthalpy difference for the *Tt* and *Gg'* conformers the one band pair was used form which a value of 135 ± 21 cm^{-1} was obtained. Then the two band pairs for the *Tt* and *Gt* forms were used to obtain the enthalpy difference of 143 ± 11 cm^{-1}. This error limit is derived from the statistical standard deviation of one sigma of the measured intensity data taken as a single data set, but it does not take into account small

associations with the liquid xenon or the possible presence of overtones and combination bands in near coincidence of the measured fundamentals. From these enthalpy differences abundance of the *Tt* conformer present at ambient temperature is estimated to be 18 ± 1%, with the remaining values of 24 ± 1% for the *Tg* conformer, 23 ± 3% for the *Gg* conformer, 18 ± 1% for the *Gg'* conformer and 18 ± 1% for the *Gt* form. These values indicate that there are nearly equal amounts of all five conformers! Though the Tt conformer is clearly the most stable form the other forms are gauche conformers and each have a degeneracy factor of two, this means that the *Tt* (18%) conformer is 50% more abundant than a single *Tg* (12%) and *Gg* (11%) conformer.

STRUCTURAL PARAMETERS

It should be possible to estimate r_0 structural parameters for the all five conformers of n-propylamine by adjusting the MP2(full)/6-311+G(d,p) calculated structural parameters by using structural parameters from similar molecules as a guideline. The CH bond distances predicted by MP2(full)/6-311+G(d,p) *ab initio* calculations can be used without any adjustment as we [51] have shown that *ab initio* MP2(full)/6-311+G(d,p) calculations predict the r_0 CH distances for more than fifty substituted hydrocarbons to better than ± 0.002 Å compared to the experimentally determined values from isolated CH stretching wavenumbers. The heavy atom parameters can be estimated by using the corresponding parameters in ethylamine [161] and 1-chloropropane [183] to adjust the corresponding MP2(full)/6-311+G(d,p) calculated parameters. It is believed that the estimated r_0 parameters reported herein for n-propylamine have listed uncertainty values that should be within the experimentally determined parameters. Thus, the listed rotational constants given in Table S20 should

make it relatively easy to assign the microwave spectrum from which the experimental parameters could be obtained.

Table 91. Temperature and intensity ratios of the *Tt*, *Tg*, *Gg*, *Gg'*, and *Gt* bands of n-propylamine.

	T(°C)	1/T ($\times 10^{-3}$ K^{-1})	*Tt* → *Tg*		*Tt* → *Gg*	*Tt* → *Gg'*	*Tt* → *Gt*	
			I_{448} / I_{452}	I_{866} / I_{876}	I_{448} / I_{472}	I_{448} / I_{464}	I_{448} / I_{461}	I_{866} / I_{835}
Liquid	–60.0	4.692		2.149				1.391
xenon	–70.0	4.923	0.206		0.324	0.598	0.366	
	–80.0	5.177	0.216	2.265	0.350	0.652	0.396	1.527
	–90.0	4.460	0.226		0.357	0.673	0.425	
	–100.0	5.775	0.228	2.415	0.365	0.712	0.441	1.721
ΔH (cm^{-1})			84 ± 19	75 ± 1	91 ± 26	135 ± 21	153 ± 22	137 ± 1
ΔH (cm^{-1})[a]			79 ± 9				143 ± 11	

[a] Average value and statistical uncertainty (1σ) obtained by utilizing all of the data as a single set.

DISCUSSION

The vibrational assignments reported herein are based on a significant amount of information with the Raman spectra of the xenon solution, infrared spectra of the solid, and predictions from scaled force constant(s) by *ab initio* MP2(full)/6-31G(d) calculations as well as the predicted infrared band contours. The *ab initio* predicted Raman and infrared band intensities were also used but they seemed to be the least

reliable of the data utilized. One of the possible reasons for significant difference in predicted and observed intensities could be the results of the association of the amine portion of the molecule with xenon. The evidence for the van der Waals molecules was the significant decreases in the NH stretching wavenumbers from the gas to the solutions i.e. 17 cm^{-1} lower for the A' mode for the *Tt* form as well as 22 cm^{-1} for the A" mode for this same conformer. However, for the other fundamentals the difference between the wavenumbers in the gas and xenon solution averages two wavenumbers except for the CH_3 rock (ν_{13}), NH_2 twist (ν_{28}), and NH_2 symmetric deformation (ν_6) which had difference of 11, 8, and 7 cm^{-1}, respectively. Finally, it should be noted that there is a very, very small amount of the dimer present in the xenon solution as evidence by the very low intensity of the bands which are present at approximately 3288 cm^{-1} in xenon solutions.

For the *Tt* conformer the fixed scaled *ab initio* predicted wavenumbers was an average of 16 cm^{-1} in error for the A′ fundamentals, except for the NH_2 wag, which represent 0.95% error. If all the fundamental wavenumbers are included the percent error increases to 1.36% since the NH_2 wag is poorly predicted. The predicted wavenumber for the NH_2 wag is too high with 0.9 scaling but it can be corrected with a scaling factor of 0.7. However, if this value is used it usually results in two or three unacceptable P.E.D. values. Since the NH_2 wag gives rise to a very intense infrared band with well-known group wavenumbers, it is usually better to use 0.9 as the scaling factor so the other fundamentals have “normal” P.E.D.s. The predicted errors for the A″ modes have larger errors compared to the A′ modes with average predicted wavenumbers of 16 cm^{-1} which represent 1.04% error. Thus the relatively small basis set of 6-31G(d) by the MP2(full)

calculations with two or three scaling factors for the force constants provides good predicted wavenumbers for aiding the vibrational assignments.

For the *Tt* form the mixing is relatively small for the A′ modes except for ν_{13} which has only 26%S_{13} and five other symmetry coordinates with 15%S_{18} being the largest value of this group. For the A″ modes only ν_{27} (CH_3 rock) and ν_{28} (NH_2 twist) have relatively small percentage values where ν_{27} has 30%S with 28%S_{30} (CH_2 rock) and 10% of four other symmetry coordinates. The NH_2 twist 35%S_{28} with 22%S_{25} (CH_2 twist) and the three other coordinates of 14% and less. Therefore, the approximate descriptions for the normal modes provide reasonable information on the molecular motions of the vibrations.

The estimated structural parameters have been obtained (Table S20) in the current study and should be of considerable value for assigning the microwave spectrum for the conformers of n-propylamine. These parameters should be accurate to within ± 0.005 Å and 1° for the heavy atom bond distances and angles, respectively. The quadratic centrifugal distortion constants and quadrupole coupling constants (Table S22) have also been predicted to further aid in a possible study of the microwave spectrum. Such a study could be useful in determining the structure of n-propylamine for comparison to other n-propyl-X molecules and biologically active amines.

To support the experimental values the *ab initio* energy differences have been determined by a variety of basis sets (Table 90) which can be compared to the experimentally determined enthalpy differences listed in Table 91. The order of stability is not well predicted by the *ab initio* MP2(full) calculations as the order of stability changes from one basis set to another. The DFT calculations by the B3LYP method gives

somewhat better results by identifying the *Tt* as being the most stable conformer, but the order of stability changes for the rest of the conformers depending on the size of the basis set.

In the two previous conformational studies [178,179] all five conformers were observed in the experimental spectra and their order of stability was predicted by using *ab initio* calculations. These predictions have the *Tt* conformer as the most stable form and the carbon skeleton *Gauche* conformers are predicted as being the predominate fraction at room temperature. However, from neither study were reliable order of stability predicted for the four conformers. In the later investigation [169] the spectra of the solid showed the *Tt* conformer as the most stable form and reconfirmed that all five conformers are observed in both the Raman and infrared spectra of the vapor. In the most recent conformational study [184] again the *Tt* conformer was identified as being the most stable form and the enthalpy difference was obtained from the variable temperature Raman spectra of n-propylamine-ND_2 in the liquid phase with a value of 142 cm^{-1} (1.7 kJ/mol) between the *Tt* and *Gt* forms. This value is in excellent agreement with the value obtained in the current study, which is surprising since the value for enthalpy differences determined from the spectra of liquids is usually significantly higher.

It would be interesting to obtain the enthalpy differences for 3-aminopropionitrile to determine the effects of substitution on the 3- position of n-propylamine. It would also be of interest to see how different 1- position substituents affect the conformational stability of n-propyl-X, i.e. namely if there are nearly equal amounts of all five conformers for these similar molecules (-PH_2, -OH, -SH). A good example of one of these molecules is n-propylphophine [185] where the *Tt* form was found to be most

stable. The *Gt* conformer was determined to be the second most stable form and an enthalpy difference was obtained from the variable temperature Raman spectra of the gas of 140 ± 5 cm^{-1} (1.68 ± 0.06 kJ/mol) and 351 ± 20 cm^{-1} (4.2 ± 0.2 kJ/mol) for the liquid relative to the *Tt* conformer. The three remaining conformers were observed but in much lower fractions and their enthalpy differences were not determined. The n-propyl alcohol and thiol have both been studied. The propanol molecule has been studied [186-188] extensively and the Gt and Gg conformers have both been identified in the rotational and vibrational spectra but the enthalpy difference has not been determined in the gas. The propanthiol molecule has been studied [189] and the Tt and Gt conformers have been identified in the infrared spectra of the gas, liquid, and solid and the Raman spectrum of the liquid. Again the enthalpy difference has not been determined in the gas and it would be interesting to obtain the enthalpy difference for comparison with the corresponding propyl -amine and -phosphine molecules.

CHAPTER 15

CONFORMATIONAL AND STRUCTURAL STUDIES OF 2,2,2-TRIFLUOROETHYLAMINE FROM TEMPERATURE DEPENDENT RAMAN SPECTRA OF XENON SOLUTIONS AND AB INITIO CALCULATIONS

INTRODUCTION

There are a very large number of amines which are important biochemical molecules and therefore have generated a very large amount of scientific interest. Of particular interest has been the energy or enthalpy difference for molecular amines which have two or more conformers present at ambient temperature. Many different techniques have been used but vibrational spectroscopy was initially one of the most popular techniques for several decades but there has been a significant number of problems. Initially, most of the enthalpy difference determinations were made by infrared spectra of solutions such as carbon tetrachloride but there were problems with the amines forming dimers and higher forms of association. For some of the very small amines there were a few investigations in the gas phase with both infrared and Raman spectral studies but most of these studies included a single band pair for the enthalpy difference determination. In general, where there were multiple determinations for the same molecule there were large variations of the reported values from the different techniques.

In addition to self association there can be significant interaction of the amine with the solvent. To reduce both types of interaction we initiated studies using xenon or krypton as the solvents. These are very excellent solvents since very long paths can be used with these liquids so the solutions can be extremely dilute which greatly reduces the

interaction between the molecules. Other advantages due to the low temperature results in the narrow band contours. There is very accurate measurement of the temperature and the temperature range is large. Additionally, it is usually possible to obtain a relatively large number of band pairs.

More recently *ab initio* calculation has been used to predict the enthalpy differences for several molecules and for some molecules the predicted values give reasonable agreement with the experimentally determined values. From the conformational stability of ethylamine [161] the *trans* form was determined to be more stable by 54 ± 4 cm^{-1} (0.65 ± 0.05 kJ/mol) than the *gauche* form. However, *ab initio* calculations at the MP2 level with full electron correlation with diffuse functions predict the *gauche* conformer as the more stable form by approximately 200 cm^{-1} whereas, the correct conformer stability is predicted from the same basis set without diffuse functions.

For aminomethylcyclopropane c–$C_3H_5CH_2NH_2$ [190] the opposite result is obtained where the basis set with the diffuse functions give the correct conformer stability. Enthalpy determinations from variable temperature infrared spectra of rare gas solutions give an enthalpy difference of 109 ± 11 cm^{-1} (1.30 ± 0.13 kJ/mol) between the most stable *gauche–gauche* (*Gg*) conformer (the first *gauche* designation, with capital G, for the heavy atom conformation around the C–C bond, and the second *gauche* designation, with lower case g, is for the amino torsion, around the C–N bond) and the second most stable conformation, *gauche–trans* (*Gt*). For this molecule the MP2(full)/6-311+G(d,p) calculations predict *Gg* form to be more stable by 36 cm^{-1} whereas the MP2(full)/6-311G(d,p) calculations predict the *Gt* rotamer to be more stable by 135 cm^{-1}.

These results show the limitations in utilizing *ab initio* calculations to predict the most stable conformer of these organoamines.

To obtain more enthalpy differences of some significantly different amines we began a study of 2-fluoroethylamine where the molecule had been investigated by microwave spectra. From this investigation [191] two of the possible conformers were identified where the *Gg*' form was determined to be more stable than the *Gt* conformer. An enthalpy difference of 35 ± 105 cm^{-1} (0.42 ± 1.25 kJ/mol) was obtained but this very large uncertainty (which is three times the enthalpy difference) raises the question which form is the more stable conformer.

Since the value obtained from the microwave study provided a questionable stability of which conformer is more stable we initiated the conformational and structural studies of 2-fluorethylamine molecule, where five possible conformations could be present. We recorded variable temperature mid-infrared spectra of xenon solutions as well as the far infrared spectra of krypton solutions. From these data, all five possible conformations were identified and their relative stabilities obtained. The enthalpy differences were determined among the most stable *Gg'* conformer and the second stable form, *Gt*, to be 62 ± 8 cm^{-1} (0.74 ± 0.10 kJ/mol), the third stable conformer, *Tg*, the enthalpy difference of 262 ± 26 cm^{-1} (3.14 ± 0.3 kJ/mol), the fourth most stable conformer, *Tt*, to be 289 ± 45 cm^{-1} (3.46 ± 0.5 kJ/mol), and the fifth most stable conformer, *Gg* to be 520 ± 50 cm^{-1} (6.24 ± 0.6 kJ/mol) was obtained. These results clearly showed that the variable temperature studies (-55 to -131 ºC) provided excellent enthalpy differences for this molecule.

In order to improve the determination of the enthalpy difference of the amines we decided to utilize the Raman effect with xenon or krypton solutions to obtain the enthalpy difference. A particular interest was the 2,2,2 trifluoroethylamine since there was a large variation in the predicted energy difference for this molecule from the *ab initio* calculations which we carried out. Since there are only two conformers for 2,2,2 trifluoroethylamine it was felt that this molecule would be a good example as the enthalpy difference could be determined without the complicating problems associated with multiple conformers. Another factor in choosing this molecule was the fact that the *ab initio* calculations indicated that the energy difference would be about ~626 cm^{-1} (7.49 kJ/mol) which of course should make it really difficult to observe the second conformer. However, it has been shown that the *ab initio* predictions do not provide very meaningful energy difference for these amines. From a previous vibrational assignment [192] there was evidence for the second conformer from the observation of two fundamentals and the large energy difference value is probably way over estimated.

To support the experimental studies reported herein we have obtained the harmonic force constants, infrared intensities, Raman activities, depolarization ratios, and vibrational frequencies from MP2(full)/6-31G(d) *ab initio* calculations. To obtain predictions on the conformational stabilities we have carried out MP2(full) *ab initio* and density functional theory (DFT) calculations by the B3LYP method by utilizing a variety of basis sets. The r_0 structural parameters have been obtained by combining the MP2(full)/6-311+G(d,p) *ab initio* predicted parameters with the previously reported rotational constants obtained from the microwave studies [193,194]. The results of these

spectroscopic, structural, and theoretical studies of 2,2,2 trifluoroethylamine are reported herein.

EXPERIMENTAL AND THEORETICAL METHODS

The sample of 2,2,2 trifluoroethylamine was purchased from Sigma-Aldrich Chemical Co., with stated purity of ≥99.5%. The sample was used with no further purifications.

The Raman spectra (4000 to 300 cm^{-1}) of the sample dissolved in liquefied xenon (Fig. 57) at five different temperatures (-60 to -100^{o}C) was recorded on a Trivista 557 spectrometer consisting of a double f = 50 cm monochromator equipped with a 2000 lines mm^{-1} grating, a f = 70 cm spectrograph equipped with a 2400 lines mm^{-1} grating, and a back-illuminated LN2-cooled PI Acton Spec-10:2 kB/LN 2048 x 512 pixel CCD detector. For all experiments, the 514.5 nm line of a 2017-Ar S/N 1665 Spectra-Physics argon ion laser was used for Raman excitation, with the power set to 0.8 Watt. Signals related to the plasma lines were removed by using an interference filter. The frequencies were calibrated using Neon emission lines, and depending on the setup used, are expected to be accurate within 0.4 cm^{-1}. The experimental set-up used to investigate the solutions has been described before [23,24]. A home-built cell for liquids was equipped with four quartz windows at right angles was used to record the spectra. The infrared and Raman bands chosen as fundamentals along with their proposed assignments and depolarization values are listed in Tables 92 and 93, respectively.

The LCAO-MO-SCF restricted Hartree-Fock calculations were performed with the Gaussian-03 program [22] by using Gaussian-type basis functions. The energy minima with respect to nuclear coordinates were obtained by the simultaneous relaxation

of all geometric parameters by the gradient method of Pulay [29]. Several basis sets as well as the corresponding ones with diffuse functions were employed with the Møller-Plesset perturbation method [21] to the second order (MP2(full)) as well as with the DFT by the B3LYP method. The predicted conformational energy differences are listed in Table 94.

Figure 57. Experimental and predicted Raman spectra of 2,2,2 trifluoroethylamine: (A) xenon solution at -100°C; (B) simulated spectrum of *Trans* and *gauche;* enthalpy difference of 267 cm^{-1} at -100°C; (C) simulated spectrum of *gauche* conformer; (D) simulated spectrum of *Trans* conformer.

Table 92. Observed and calculated[a] wavenumbers (cm^{-1}) for *trans* 2,2,2 trifluoroethylamine.

	Vib. No.	Approximate Descriptions	*ab initio*	fixed scaled[b]	IR int.	Raman act.	dp ratio	IR		Raman			IR	P.E.D.[e]	Band Contours	
								Gas[c]	Gas[d]	Xenon	gas[d]	liquid[c]	Solid[c]		A*	B*
A′	ν_1	NH_2 symmetric stretch	3533	3352	2.5	72.9	0.12	3371	3370	3357	3372	3358	3270	$100S_1$	2	98
	ν_2	CH_2 symmetric stretch	3141	2947	11.6	84.0	0.08	2957	2958	2949	2957	2954	2965	$100S_2$	20	80
	ν_3	NH_2 scissor	1734	1645	34.5	6.6	0.70	1636	1636	1635	1635	1626	1625	$76S_3,23S_9$	-	100
	ν_4	CH_2 deformation	1536	1453	4.7	10.0	0.74	1446	1445	1440	1444	1445	1445	$100S_4$	16	84
	ν_5	CH_2 wag	1458	1389	40.9	0.5	0.55	1398	1380	1381	1368	1371	1391	$60S_5,19S_6,10S_{10}$	96	4
	ν_6	CC stretch	1339	1288	137.2	1.1	0.47	1277	1278	1272	1271	1272	1277	$22S_6,22S_5,19S_{10},19S_{11},10S_7$	25	75
	ν_7	CF_3 antisymmetric stretch	1241	1190	220.6	2.5	0.71	1172	1173	1162	1172	1149	1150	$58S_7,12S_5,10S_{12}$	60	40
	ν_8	CN stretch	1178	1122	13.7	2.4	0.44	1114	1124	1122	-	1113	1115	$74S_8,12S_9$	7	93
	ν_9	NH_2 wag	951	904	233.6	1.0	0.15	762	761	828	761	-	900	$49S_9,17S_3,15S_8$	94	6
	ν_{10}	CF_3 symmetric stretch	831	790	28.8	7.1	0.04	838	838	836	836	812	809	$53S_{10},24S_6,,10S_9$	77	23
	ν_{11}	CF_3 deformation	659	648	14.0	2.8	0.69	645	645	646	645	650	655	$39S_{11},15S_{14},12S_7,11S_{10},10S_{13}$	7	93
	ν_{12}	CF_3 deformation	547	539	5.8	1.8	0.45	545	545	543	542	543	548	$48S_{12},20S_{11},13S_6,12S_7$	28	72
	ν_{13}	CF_3 rock	420	416	11.3	2.1	0.46	413	414	414	410	417	422	$22S_{13},34S_{12},18S_{14},11S_6$	92	8
	ν_{14}	CCN deformation	231	229	7.9	0.1	0.52	-	236	-	240	239	-	$47S_{14},50S_{13}$	70	30
A″	ν_{15}	NH_2 antisymmetric stretch	3634	3448	6.5	42.9	0.75	3438	3438	3425	-	3414	3385	$100S_{15}$	-	-
	ν_{16}	CH_2 antisymmetric	3204	3006	7.5	54.2	0.75	2984	2983	3077	-	2979	2987	$100S_{16}$	-	-

	stretch														
ν_{17}	CH_2 twist	1440	1371	14.8	10.1	0.75	1362	1362	1363	-	1330	1361	$53S_{17},37S_{19}$	-	-
ν_{18}	CF_3 antisymmetric stretch	1320	1266	130.4	0.2	0.75	1251	1251	1245	-	1245	1246	$27S_{18},23S_{20,}21S_{19}$	-	-
ν_{19}	NH_2 twist	1141	1084	80.0	2.1	0.75	1088	1088	1083	-	1087	1095	$23S_{19,}37S_{18},37S_{17}$	-	-
ν_{20}	CH_2 rock	910	868	17.9	1.9	0.75	873	873	873	-	873	936	$58S_{20,}19S_{18,}19S_{19}$	-	-
ν_{21}	CF_3 deformation	532	526	0.0	0.6	0.75	543	543	536	-	543	535	$72S_{21,}13S_{18}$	-	-
ν_{22}	CF_3 rock	396	387	24.3	1.4	0.75	373	374	372	-	383	351	$46S_{22},29S_{23},16S_{21}$	-	-
ν_{23}	NH_2 torsion	304	293	52.1	1.4	0.75	269	269	-	-	-	-	$69S_{23},29S_{22}$	-	-
ν_{24}	CF_3 torsion	130	128	0.0	0.1	0.75	-	-	-	-	130	-	$97S_{24}$	-	-

[a] MP2(full)/6-31G(d) *ab initio* calculations, scaled wavenumbers, infrared intensities (km/mol), Raman activities ($Å^4$/amu), depolarization ratios and potential energy distributions (P.E.D.s)

[b] MP2(full)/6-31G(d) fixed scaled wavenumbers with factors of 0.88 for CH stretches, 1.0 for heavy atom bends, and 0.90 for all other modes.

[c] Ref [195]

[d] Ref [192]

[e] Calculated with MP2(full)/6-31G(d) and contributions of less than 10% are omitted.

[*] A, B and C values in the last three columns are percentage infrared band contours.

Table 93. Observed and calculated[a] wavenumbers (cm^{-1}) for *gauche* 2,2,2 trifluoroethylamine.

Vib. No.	Approximate Descriptions	*ab initio*	fixed scaled[b]	IR int.	Raman act.	dp ratio	IR	Raman		P.E.D.[d]	Band Contours		
							gas[c]	gas[c]	Xenon		A*	B*	C*
ν_1	NH_2 antisymmetric stretch	3649	3561	6.7	55.8	0.72			-	$100S_1$	20	49	31
ν_2	NH_2 symmetric stretch	3547	3365	2.6	86.2	0.11		3382	3367	$100S_2$	57	6	37
ν_3	CH_2 antisymmetric stretch	3187	2989	9.0	58.2	0.48			2975	$75S_3,25S_4$	2	13	85
ν_4	CH_2 symmetric stretch	3074	2884	39.5	90.5	0.19			2865	$75S_4,25S_3$	15	40	45
ν_5	NH_2 scissor	1725	1637	41.5	7.5	0.70			1626	$75S_5,24S_{15}$	70	-	30
ν_6	CH_2 deformation	1557	1472	6.2	11.2	0.72			1460	$100S_6$	78	22	-
ν_7	CH_2 wag	1513	1440	34.9	1.7	0.42			1429	$51S_7,21S_9,11S_{13}$	61	35	4
ν_8	CH_2 twist	1396	1331	79.7	8.3	0.66			1325	$52S_8,13S_{10},10S_{13}$	2	2	96
ν_9	CC stretch	1342	1288	124.7	1.6	0.64			1272	$20S_9,19S_{16},18S_7,19S_{17}$	32	66	2
ν_{10}	CF_3 antisymmetric stretch	1320	1266	111.9	0.9	0.69			1245	$21S_{10},28S_{13},19S_{14}$	8	33	59
ν_{11}	CF_3 antisymmetric stretch	1239	1188	211.1	3.3	0.55			1162	$49S_{11},10S_{18}$	66	23	11
ν_{12}	CN stretch	1160	1103	64.8	5.1	0.43			1111	$39S_{12},21S_8,16S_{10},12S_{13}$	25	39	36
ν_{13}	NH_2 twist	1122	1066	32.0	4.7	0.64			1062	$19S_{13},42S_{12},12S_7$	8	73	19
ν_{14}	CH_2 rock	1005	958	115.5	6.6	0.44			968	$41S_{14},22S_{10},13S_{15}$	2	14	84
ν_{15}	NH_2 wag	888	845	120.6	4.4	0.24			757	$40S_{15},21S_{14},12S_5$	7	67	26
ν_{16}	CF_3 symmetric stretch	832	791	27.7	3.5	0.07	828	822	836	$53S_{16},24S_9,13S_{15}$	35	18	47
ν_{17}	CF_3 deformation	650	638	19.7	0.8	0.61			635		88	4	8

								$38S_{17},16S_{22},11S_{11},10S_{20},10S_{16}$			
ν_{18}	CF_3 deformation	552	545	6.2	1.6	0.49	546	$46S_{18},20S_{17},13S_9,12S_{11}$	58	37	5
ν_{19}	CF_3 deformation	536	531	2.1	0.9	0.74	526	$73S_{19},13S_{10}$	11	11	78
ν_{20}	CF_3 rock	427	423	1.0	1.4	0.48	432	$22S_{20},35S_{18},19S_{22}$	31	-	69
ν_{21}	CF_3 rock	371	368	2.1	0.1	0.72	-	$70S_{21},15S_{19}$	95	3	2
ν_{22}	CCN deformation	248	243	16.0	1.0	0.72	-	$35S_{22},40S_{20},20S_{23}$	41	27	32
ν_{23}	NH_2 torsion	222	213	40.2	1.4	0.74	-	$73S_{23},12S_{22}$	40	34	26
ν_{24}	CF_3 torsion	131	129	4.2	0.2	0.75	-	$97S_{24}$	3	63	34

[a] MP2(full)/6-31G(d) *ab initio* calculations, scaled wavenumbers, infrared intensities (km/mol), Raman activities ($Å^4$/amu), depolarization ratios and potential energy distributions (P.E.D.s)

[b] MP2(full)/6-31G(d) fixed scaled wavenumbers with factors of 0.88 for CH stretches, 1.0 for heavy atom bends, and 0.90 for all other modes.

[c] Ref [192]

[d] Calculated with MP2(full)/6-31G(d) and contributions of less than 10% are omitted.

[*] A, B and C values in the last three columns are percentage infrared band contours.

Table 94. Calculated energies (hartree) and energy differences (cm^{-1}) for the two conformers of 2,2,2 trifluoroethylamine.

		Energy[a], E	Energy Differences, Δ
Method/Basis Set	# *basis set*	*trans*	*gauche*[b]
MP2(full)/6-31G(d)	98	0.7890437	828
MP2(full)/6-31+G(d)	122	0.8270485	694
MP2(full)/6-31G(d,p)	110	0.8249888	843
MP2(full)/6-31+G(d,p)	134	0.8620344	669
MP2(full)/6-311G(d,p)	132	1.1505005	783
MP2(full)/6-311+G(d,p)	156	1.1722942	651
MP2(full)/6-311G(2d,2p)	174	1.2694876	731
MP2(full)/6-311+G(2d,2p)	198	1.2874767	648
MP2(full)/6-311G(2df,2pd)	236	1.3958022	694
MP2(full)/6-311+G(2df,2pd)	260	1.4132769	642
MP2(full)/cc-pVTZ	236	1.3895263	681
MP2(full)/aug-cc-pVTZ	368	1.4399636	626
Average MP2(full)			708 ± 72
B3LYP/6-31G(d)	98	1.8960965	887
B3LYP/6-31+G(d)	122	1.9284823	741
B3LYP/6-31G(d,p)	110	1.9054581	887
B3LYP/6-31+G(d,p)	134	1.9376615	741
B3LYP/6-311G(d,p)	132	2.0350608	898
B3LYP/6-311+G(d,p)	156	2.0506047	728
B3LYP/6-311G(2d,2p)	174	2.0487408	805
B3LYP/6-311+G(2d,2p)	198	2.0628198	698
B3LYP/6-311G(2df,2pd)	236	2.0593206	764
B3LYP/6-311+G(2df,2pd)	260	2.0741500	680
B3LYP/aug-cc-pVTZ	368	2.0908799	665
B3LYP Average			772 ± 85

[a] Energy of conformer is given as –(E+431) H.
[b] Difference is relative to *trans* form and given in cm^{-1}.

In order to obtain a complete description of the molecular motions involved in the fundamental modes of $F_3CCH_2NH_2$, a normal coordinate analysis has been carried out. The force field in Cartesian coordinates was obtained with the Gaussian 03 program [22] at the MP2(full) level with the 6-31G(d) basis set. The internal coordinates used to

calculate the **G** and **B** matrices are given in Table 95 with the atomic numbering shown in Fig. 58. By using the **B** matrix [30], the force field in Cartesian coordinates was converted to a force field in internal coordinates. Subsequently, scaling factors of 0.88 for CH stretches and CH_2 deformation and 0.90 for all other modes except heavy atom bends were applied, along with the geometric average of the scaling factors for the interaction force constants, to obtain the fixed scaled force field and resultant wavenumbers. A set of symmetry coordinates was used (Table S23) to determine the corresponding potential energy distributions (P.E.D.s). A comparison between the observed and calculated wavenumbers, along with the calculated infrared intensities, Raman activities, depolarization ratios and potential energy distributions for the *trans* and *gauche* conformers are listed in Tables 92 and 93, respectively.

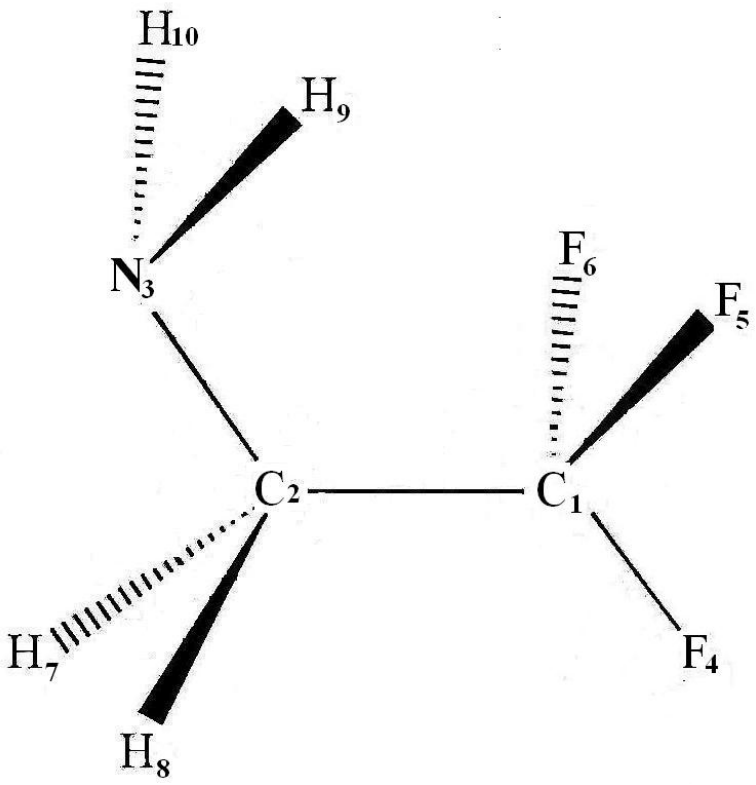

Figure 58. 2,2,2 trifluoroethylamine molecule showing atomic numbering.

Table 95. Structural parameters[a], rotational constants, and dipole moments for *trans* and *gauche* 2,2,2 trifluoroethylamine.

		trans				*gauche*		
Parameter	Int. Coor.	MP2(full)/ 6-311+G(d,p)	B3LYP/ 6-311+G(d,p)	MW[b]	adjusted r_0	MP2(full)/ 6-311+G(d,p)	B3LYP/ 6-311+G(d,p)	Predicted r_0
r C_1-C_2	R_1	1.513	1.524	1.530*	1.513(3)	1.509	1.519	1.509
r C_2-N_3	R_2	1.447	1.448	1.474*	1.447(3)	1.452	1.453	1.452
r C_1-F_4	R_3	1.344	1.352	1.335*	1.344(3)	1.347	1.356	1.347
r C_1-F_5	R_4	1.347	1.355	1.335*	1.347(3)	1.348	1.356	1.348
r C_1-F_6	R_5	1.347	1.355	1.335*	1.347(3)	1.337	1.344	1.337
r C_2-H_7	r_1	1.092	1.093	1.093*	1.092(2)	1.092	1.092	1.092
r C_2-H_8	r_2	1.092	1.093	1.093*	1.092(2)	1.098	1.099	1.098
r N_3-H_9	r_3	1.013	1.014	1.01(2)	1.013(3)	1.012	1.011	1.012
r N_3-H_{10}	r_4	1.013	1.014	1.01(2)	1.013(3)	1.013	1.013	1.013
rN-H---F		2.655	2.711	2.65(2)	2.655(5)	2.649	2.708	2.652
$\angle C_1C_2N_3$	A_1	115.0	115.6	113.8(10)	115.2(5)	109.9	110.7	110.1
$\angle F_4C_1C_2$	A_2	111.4	111.4	111.03*	111.4(5)	110.4	110.3	110.4
$\angle F_5C_1C_2$	A_3	111.6	111.9	111.03*	111.6(5)	110.9	111.3	110.9
$\angle F_6C_1C_2$	A_4	111.6	111.9	111.03*	111.6(5)	112.9	113.2	112.9
$\angle F_4C_1F_6$	A_5	107.5	107.3	108.5*	107.6(5)	107.5	107.3	107.6
$\angle F_4C_1F_5$	A_6	107.5	107.3	108.5*	107.6(5)	107.3	107.0	107.4
$\angle F_5C_1F_6$	A_7	106.9	106.8	108.5*	106.9(5)	107.5	107.3	107.5
$\angle H_7C_2H_8$	β	107.9	107.4	109.5*	107.9(5)	108.2	107.7	108.2
$\angle H_7C_2C_1$	σ_1	107.0	106.9	109.5*	107.0(5)	106.8	106.6	106.8
$\angle H_8C_2C_1$	σ_2	107.0	106.9	109.5*	107.0(5)	106.5	106.3	106.5
$\angle H_7C_2N_3$	π_1	109.8	109.8		109.7(5)	109.6	109.6	109.5
$\angle H_8C_2N_3$	π_2	109.8	109.8		109.7(5)	115.5	115.5	115.4
$\angle H_9N_3H_{10}$	γ	108.0	108.5	110.8(10)	108.0(5)	108.0	108.7	108.0

∠ $H_9N_3C_2$	α_1	111.0	112.0	110(20)	111.0(5)	110.6	111.5	110.6
∠ $H_{10}N_3C_2$	α_2	111.0	112.0	110(20)	111.0(5)	111.0	112.0	111.0
τ FCCN	τ_1	180.0	180.0		180.0	176.5	176.4	176.5
τ FCCH	τ_2	-57.7	-57.4		-57.7(5)	-64.7	-64.5	-64.7
τ CCNH	τ_3	60.1	61.1		60.1(5)	-76.5	-77.1	-76.5
τ HCNH	τ_4	-60.7	-59.9		-60.7(5)	166.4	165.6	166.4
A		5249.99	5196.94	5295(16)	5249.74	5282.71	5227.04	5282.84
B		2786.83	2745.49	2785.69(1)	2785.38	2808.87	2766.51	2807.59
C		2766.09	2723.22	2762.55(1)	2763.10	2779.67	2735.01	2777.59
$\|\mu_a\|$		0.86	1.29	1.13(3)		2.65	2.55	
$\|\mu_b\|$		0.17	0.27	0.28(3)		1.91	1.77	
$\|\mu_c\|$		0.00	0.00	0.00(5)		1.24	1.08	
$\|\mu_t\|$		0.88	1.32	1.16(5)		3.49	3.29	

[a] Bond distances in Å, bond angles in degrees, rotational constants in MHz, and dipole moments in Debye.
[b] Ref [193]; * are the assumed structural parameters

Additional support for the vibrational assignments was obtained from the simulated Raman spectra. The evaluation of Raman activity by using the analytical gradient methods has been developed [31-34] and the activity S_j can be expressed as: $S_j = g_j(45\alpha_j^2 + 7\beta_j^2)$, where g_j is the degeneracy of the vibrational mode j, α_j is the derivative of the isotropic polarizability, and β_j is the anisotropic polarizability. To obtain the Raman scattering cross sections, the polarizabilities are incorporated into S_j by multiplying S_j with $(1-\rho_j)/ (1+\rho_j)$ where ρ_j is the depolarization ratio of the j^{th} normal mode. The Raman scattering cross sections and calculated wavenumbers obtained from the Gaussian 03 program were used together with a Lorentzian function to obtain the simulated Raman spectra.

VIBRATIONAL ASSIGNMENT

The first comprehensive vibrational assignment for 2,2,2 trifluoroethylamine from Wolff et al. [195] was made by utilizing the infrared spectra of the NH_2, NHD and ND_2 isotopomers for the gas and crystalline solid. Additionally, the Raman spectra of the NH_2 and ND_2 isotopomers for the liquid. This was followed by another vibrational study from Kalasinsky and Anjarla [192] where both the 2,2,2 trifluoroethylamine and 2,2,2 trifluoroethanol were studied with the infrared and Raman spectra of the gas. The vibrational assignments were made mostly based on group frequencies along with existing assignments of corresponding vibrations of similar molecules. In the first study of the vibrational assignments [195] no bands were assigned for the *gauche* form but all of the fundamentals for the *trans* conformer were assigned. For the later study of the vibrational assignments [192] again all of the fundamentals were assigned for the *trans* conformer but only two fundamentals were assigned for the *gauche* form. This

assignment is reasonable based on the ΔH value of 1014 cm^{-1} obtained by these investigators' study of the enthalpy difference. This result indicates that the *gauche* form would be less that 1% abundance with this large enthalpy difference. However, by the utilization of MP2(full)/6-31G(d) predicted vibrational wavenumbers, *ab initio* predicted intensities, and depolarization ratios along with Raman data from xenon solutions it has been possible to assign a significantly larger number of the fundamentals for the *gauche* conformer. The relatively large number of bands and their relative intensities observed in the current study indicate an enthalpy difference much lower than that reported in the earlier study. Our study indicates that the ΔE value from the *ab initio* calculations appears to be larger than that expected based on the abundance of the *gauche* conformer. A reliable assignment of the fundamentals for both the *trans* and *gauche* conformer is important for obtaining the enthalpy difference since the bands being used for the temperature study must be for a single confidently identified conformer. Therefore, we have attempted to assign all of the fundamentals for both conformers in the region from 1300 to 400 cm^{-1} where the number of overtone and combination bands are significantly reduced compared to those in the higher wavenumber region.

In the current study, the fundamentals ν_6, ν_{18} , ν_7 and ν_{19} are assigned to the bands at 1272, 1245, 1162 and 1083 cm^{-1} ,respectively, in the Raman spectra of the Xenon solutions based on the *ab initio* predictions and the Raman activities but in the previous vibrational studies ν_6 was assigned to the band at 1278 cm^{-1}, ν_{18} was assigned to the band at 1251 cm^{-1}, ν_7 was assigned to the band at 1173 cm^{-1}, and ν_{19} was assigned to the band at 1088 cm^{-1}. The differences of 6, 11 and 5 cm^{-1} probably arise from the fact that these bands are broad in the spectra of the gas which makes the determinations of the band

center difficult to identify rather than from differences due to xenon solutions. Two of these bands are mixed B-type so their frequencies are frequently higher than the actual center. It is extremely difficult to correctly assign band center of B-type fundamental particularly for bands that have excited states on the low frequency side of the fundamental

The next band to be assigned is the fundamental ν_8, the CN stretch, where it is assigned at 1122 cm^{-1}. This band is a clearly resolved band in the Raman spectra of the Xenon solutions. In the first vibrational assignment [195] this fundamental was assigned at 1114 cm^{-1} but it is clearly an incorrect assignment based on the *ab initio* prediction as well as the results from previous studies of similar molecules. However, in the second vibrational assignment [192] it was reassigned to the band at 1124 cm^{-1} which agrees with our current assignment.

The next fundamental to be assigned is the NH_2 wag (ν_9) which is identified in the Raman spectra of the xenon solutions as the band at 828 cm^{-1} as the *trans* conformer. This corresponding band was previously reported [192] as the band at 828 cm^{-1} in the infrared spectra of the gas and 822 cm^{-1} in the Raman spectra of the gas for the *gauche* conformer. The band at 757 cm^{-1} is assigned as a *gauche* NH_2 wagging fundamental. This corresponding band was previously reported in the first vibrational study [195] at 762 cm^{-1} from the infrared spectra of the gas for the *trans* form as the NH_2 wagging fundamental. Also, in the second vibrational assignment study [192], the band at 761 cm^{-1} was also assigned to the NH_2 wagging mode from the infrared and Raman spectra of the gas which correspond as well to the band at 757 cm^{-1} in the Raman spectra of the xenon solutions assigned to the *gauche* form.

In the current study, the bands at 536 and 543 cm^{-1} are assigned as the ν_{21} and ν_{12} fundamentals, respectively, supported by their predicted frequencies and the relative intensities. It is interesting to note that both of the previous vibrational assignment studies [192,195] had bands at 543 and 545 cm^{-1} in the infrared spectra of the gas as the *trans* CF_3 deformations ν_{21} and ν_{12}, respectively, which rather surprisingly that both of the studies had the same frequencies for these assignments.

The assignments of the remaining bands of the *trans* conformer $\nu_{5,}$ $\nu_{10,}$ $\nu_{11,}$ $\nu_{13,}$ $\nu_{17,}$ and ν_{22} agree with the assignments previously reported since they are assigned within one or two wavenumbers. The fundamentals for the *gauche* form have been assigned in the current study and were largely not reported in the previous study though several of the bands proposed as components of *trans* fundamentals have now been assigned as *gauche* fundamentals.

With these complete and accurate assignments of the *trans* and *gauche* fundamentals in the region from 1300 to 400 cm^{-1} there are a significant number of bands that are suitable for the determination of the enthalpy difference between the conformers.

CONFORMATIONAL STABILITY

To determine the enthalpy differences between the two observed conformers of 2,2,2 trifluoroethylamine, the sample was dissolved in liquid xenon and the Raman spectra were recorded as a function of temperature from -60 to -100°C. Only relatively small interactions are expected to occur between xenon and the sample though the sample can associate with itself forming a dimmer, trimer or higher order complex. Therefore, only small wavenumber shifts are anticipated for the xenon interactions when passing from the gas phase to the liquid xenon solutions except for the NH_2 modes. A significant

advantage of this study is that the conformer bands are better resolved in comparison with those in the Raman spectrum of the liquid. From *ab initio* calculations, the dipole moments of the two conformers are predicted to have similar values and the molecular sizes of the two conformers are nearly the same, so the ΔH value obtained from the temperature dependent Raman study is expected to be near to that for the gas [16-20].

Once confident assignments have been made for the fundamentals of both conformers the task was then to find a pair or pairs of bands from which the enthalpy determination could be obtained. The bands should be sufficiently resolved so their intensities can be determined. The fundamentals at 646 cm^{-1} for the *trans* and 968 and 635 cm^{-1} for the *gauche* conformer were initially selected as they are confidently assigned, satisfactory resolved, and a limited number of overtone and combination bands are possible to contribute to them. The band at 1082 cm^{-1} was selected next for the *trans* conformer as it was found that the predicted underlying *gauche* fundamental was not of sufficient intensity to significantly affect the intensity of the observed band. The band at 3367 cm^{-1} was selected for the *gauche* form as it was satisfactory resolved which allowed the determination of it's intensity to be measured. Finally, the bands at 828 and 757 cm^{-1} (NH_2 wagging modes) were also used for the *trans* and *gauche* conformers, respectively. Whether these bands would be used to determine the enthalpy difference depends on whether the results were consistent with the values obtained from the initially chosen pairs.

The intensities of the individual bands were measured as a function of temperature (Fig. 59) and their ratios were determined. By application of the van't Hoff equation $-\ln K = \Delta H/(RT) - \Delta S/R$, the enthalpy difference was determined from a plot of

–lnK versus 1/T, where ΔH/R is the slope of the line and K is substituted with the appropriate intensity ratios, *i.e.* $I_{conf\text{-}1}$ / $I_{conf\text{-}2}$, etc. It was assumed that ΔS and α are not functions of temperature in the range studied.

These seven bands, three *trans* and four *gauche*, were utilized for the determination of the enthalpy difference by combining them to form 12 band pairs. The enthalpy difference was determined to have a value of 267 ± 5 cm^{-1} (Table 96). This error limit is derived from the statistical standard deviation of one sigma of the measured intensity data taken as a single data set, but it does not take into account small associations with the liquid xenon or the possible presence of overtones and combination bands in near coincidence of the measured fundamentals. The variations in the individual values are undoubtedly due to these types of interferences, but by taking several pairs, the effect of such interferences should cancel. However, this statistical uncertainty is probably better than can be expected from this technique and, therefore, an uncertainty of about 10% in the enthalpy difference is probably more realistic i.e. 267 ± 27 cm^{-1}. From the enthalpy difference the abundance of the *gauche* conformer present is estimated to be 35 ± 3% at ambient temperature.

Figure 59. Raman spectra of 2,2,2 trifluoroethylamine in xenon solution at different temperatures.

Table 96. Temperature and intensity ratios of the *trans* and *gauche* bands of 2,2,2 trifluoroethylamine.

	T(°C)	1/T ($\times 10^{-3}$ K^{-1})	I_{1083} / I_{3367}	I_{1083} / I_{968}	I_{1083} / I_{757}	I_{1083} / I_{635}	I_{828} / I_{3367}	I_{828} / I_{968}	I_{828} / I_{757}	I_{828} / I_{635}
Liquid	–60.0	4.692	3.500	1.400	0.500	3.500	7.000	2.800	1.000	7.000
xenon	–70.0	4.923	4.000	1.600	0.571	4.000	7.500	3.000	1.071	7.500
	–80.0	5.177	4.500	1.800	0.643	4.500	8.000	3.200	1.143	8.000
	–90.0	4.460	5.000	2.000	0.714	5.000	9.000	3.600	1.286	9.000
	-100.0	5.775	5.500	2.200	0.786	5.500	10.500	4.200	1.500	10.500
ΔH^a			287 ± 21	287 ± 21	288 ± 21	287 ± 21	257 ± 20	257 ± 20	257 ± 20	257 ± 20

	T(°C)	1/T ($\times 10^{-3}$ K^{-1})	I_{646} / I_{3367}	I_{646} / I_{968}	I_{646} / I_{757}	I_{646} / I_{635}
Liquid	–60.0	4.692	4.000	1.600	0.571	4.000
xenon	–70.0	4.923	4.500	1.800	0.643	4.500
	–80.0	5.177	5.000	2.000	0.714	5.000
	–90.0	4.460	5.500	2.200	0.786	5.500
	–100.0	5.775	6.000	2.400	0.857	6.000
ΔH^a			258 ± 18	258 ± 18	258 ± 18	258 ± 18

[a] Average value $\Delta H = 267 \pm 5$ cm^{-1} (3.20 ± 0.02 kJ mol^{-1}) with the *trans* conformer the more stable form and the statistical uncertainty (1σ) obtained by utilizing all of the data as a single set.

STRUCTURAL PARAMETERS

Initial structural parameters for the 2,2,2 trifluoroethylamine were proposed from a microwave study [193] where a partial structure of the *trans* conformer (Table 95) was determined. In this microwave study [193], all but four of the structural parameters were assumed for the *trans* conformer. The four parameters that were fitted were the NH bond distance and the angles CCN, CNH, HNH. This was followed by another microwave study [194] two decades later where the rotational constants were determined for the *trans* conformer for 2,2,2 trifluoroethylamine as well as isopropylamine and aminoethanol but no structural parameters were reported for any of these molecules. We have again determined the structural parameters by utilizing the rotational constants previously reported from the microwave studies [193,194].

We [51] have shown that *ab initio* MP2(full)/6-311+G(d,p) calculations predict the carbon-hydrogen r_0 structural parameters for more than fifty carbon-hydrogen distances to at least 0.002 Å compared to the experimentally determined [5] values from isolated CH stretching frequencies which agree to previously determined values from earlier microwave studies. Therefore, all of the carbon-hydrogen parameters can be taken from the MP2(full)/6-311+G(d,p) predicted values for the *trans* conformer of 2,2,2 trifluoroethylamine.

We have also found that good structural parameters for hydrocarbons and many substituted ones can be determined by adjusting the structural parameters obtained from the *ab initio* MP2(full)/6-311+G(d,p) calculations to fit the rotational constants obtained from microwave experimental data by using a computer program "A&M" (*Ab initio* and Microwave) developed [5] in our laboratory. In order to reduce the number of

independent variables, the structural parameters are separated into sets according to their types where bond distances in the same set keep their relative ratio, and bond angles and torsional angles in the same set keep their difference in degrees. This assumption is based on the fact that errors from *ab initio* calculations are systematic. Therefore, it should be possible to obtain "adjusted r_0" structural parameters for the six heavy atoms by utilizing the previously reported six rotational constants from the earlier microwave studies [193,194]. Therefore, we have obtained the complete heavy atom structural parameters for the *trans* form of 2,2,2 trifluoroethylamine.

The resulting adjusted r_0 parameters are listed in Table 95, where it is believed that the N-C, C-C, and C-F distances should be accurate to ± 0.003 Å, the C-H distances are accurate to ± 0.002 Å, and the angles should be within ± 0.5°. The fit of the six determined rotational constants (Table 97) by the structural parameters for the *trans* conformer are good with the differences being less than 0.8 MHz for both B and C rotational constants. The fact that this is a symmetric molecule where κ value is equal to -0.9814 does not permit an accurate determination of the A rotational constant. Therefore, it is believed that the suggested uncertainties are realistic values and the determined structural parameters are probably as accurate as can be obtained for the molecule in the gas phase by microwave substituted methods.

Table 97. Comparison of rotational constants obtained from experimental values from microwave spectra and adjusted r_0 structural parameters for *trans* 2,2,2 trifluoroethylamine.

Conformer	Rotational constants	Experimental[a]	Adjusted r_0	$\|\Delta\|$
$CF_3CH_2NH_2$[a]	A	5308(14)	5249	
	B	2785.722(3)	2785.378	0.34
	C	2762.578(3)	2763.103	0.52
$CF_3CH_2ND_2$[a]	A	5216(39)	5147	
	B	2628.714(2)	2627.977	0.74
	C	2617.842(2)	2618.638	0.80
CF_3CH_2NHD[b]	A	5247(22)	5199	
	B	2706.27(1)	2706.16	0.11
	C	2685.00(1)	2685.59	0.59

[a]Ref. [194].
[b]Ref. [193].

Additionally, we have also shown that the differences in predicted distances and angles from the *ab initio* calculations for different conformers of the same molecule can usually be used as one parameter with the *ab initio* predicted differences except for some dihedral angles. Therefore, we have predicted structural parameters for the *gauche* form of 2,2,2 trifluoroethylamine by applying the corresponding adjustments from the *trans* conformer to the MP2(full)/6-311+G(d,p) predicted parameters for the *gauche* form. These parameters should be close to the actual values.

DISCUSSION

The vibrational assignments reported herein are based on a significant amount of information with the Raman spectrum of the xenon solutions and predictions from the scaled *ab initio* MP2(full)/6-31G(d) calculations. The *ab initio* Raman band intensities were also used but they seemed to be the least reliable of the data utilized. One of the possible reasons for the significant difference in predicted and observed intensities could be the results of the association of the amine portion of the molecule with xenon. The evidence for the van der Waals molecules was the significant decreases in the NH stretching frequencies from the gas to the solutions i.e. 13 cm^{-1} for the *trans* conformer and 15 cm^{-1} for the *gauche* form. However, for the other fundamentals the difference between the frequencies in the gas and xenon solutions is less than ten wavenumbers except for the CF_3 antisymmetric stretch where the difference is eleven and CH_2 rock where the difference is thirteen wavenumbers for the *trans* conformer.

For the *trans* conformer the average *ab initio* predicted frequencies for A′ fundamentals with all the fundamentals, except for the NH_2 wag was 11 cm^{-1} which represent 0.9% error. The predicted frequency for the NH_2 wag was too high with 0.9 scaling but it can be corrected with a scaling factor of 0.7. However, if this value is used it usually results in two or three unacceptable P.E.D. values. Since the NH_2 wag gives rise to a very intense infrared band and it is readily assigned, it is usually better to use 0.9 as the scaling factor so the other fundamentals are “normal”. The percent error for the A″ modes for the *trans* form have similar errors to that of the A′ modes of the predicted frequencies. Thus, the relatively small basis set of 6-31G(d) by the MP2(full) calculations

with two scaling factors provides excellent predicted frequencies for aiding the vibrational assignments.

For the *trans* form the mixing is relatively small for the A′ modes except for ν_6 (CC stretch) which has only 22%S_6 with 22%S_5 of the CH_2 wag, ν_{11} (CF_3 deformation) which has 39%S_{11} with 15%S_{14} of the CCN deformation, and ν_{13} (CF_3 rock) which has 22%S_{13} with 34%S_{12} of the CF_3 deformation. For the A″ modes only ν_{18} (CF_3 antisymmetric stretch) of 27%S_{18} with 23%S_{20} of the CH_2 rock and ν_{19} (NH_2 twist) 23%S_{19} with 37%S_{18} of the CF_3 antisymmetric stretch have relatively small percentage. Therefore, the approximate descriptions for the normal modes provide reasonable information on the molecular motions of vibrations. However, for the *gauche* conformer there is significantly more mixing with the vibration at 1062 cm^{-1} assigned as the NH_2 twist with only 19%S_{13} and 42%S_{12} (CN stretch). Therefore, several of the approximate descriptions for the fundamentals of the *gauche* form are more for bookkeeping than providing descriptions of the molecular motions.

One of the major goals of this research was the determination of the enthalpy difference between the two conformers where there has been only a single value reported. In the previous vibrational study [192] an enthalpy difference of 1014 cm^{-1} was determined from a variable temperature study for the gas phase. This value is significantly different than the value obtained from the current study and as can be seen from the data in Table 96 the enthalpy difference between the *trans* and *gauche* form is 267 ± 27 cm^{-1}.

Normally, we would not use the fundamentals associated with the NH_2 group since they can be significantly affected by molecular association as the temperature is

decreased. However, there did not appear to be a significant change in the association as the temperature was lowered from -60 to -100°C so we used the NH_2 wag bands which gave excellent enthalpy results. Therefore, by using twelve pairs for the determination of this enthalpy difference and the data as a single set the enthalpy difference was determined to be 267 ± 5 cm^{-1}. This statistical uncertainty value is clearly smaller than the method is expected to provide.

The enthalpy value obtained from the xenon solutions must be considered the most confident enthalpy difference at this time as it is doubtful that any other experiments would give an enthalpy value with such a low uncertainty as the one determined in this study. The use of enthalpy determinations from 12 band pairs provides excellent accuracy of the determination by this technique.

In the most recent microwave study of 2,2,2 trifluoroethylamine the quadrupole coupling constants and the quartic centrifugal distortion constants were determine from the spectral data. We have predicted the quadratic centrifugal distortion constants and the quadrupole coupling constants from the MP2(full)/6-311+G(d,p) calculations as well as the DFT by the B3LYP method by utilizing the same basis set. These data are given in Table 98 and as can be seen from the values of the quadrupole coupling constants there is reasonable agreement with the predicted values from both techniques as well as the experimental values. However, the experiment centrifugal distortion constants are very different from those predicted by both calculation methods. We have found in the past that the *ab initio* calculations usually provide reasonably good centrifugal distortion constants and we expected reasonable agreement. Therefore, we believed this disagreement should be explored.

Table 98. Quadratic centrifugal distortion constants (kHz) and quadrupole coupling constants (MHz) for conformers of 2,2,2 trifluoroethylamine.

	Trans			*Gauche*	
	MP2(full)/ 6-311+G(d,p)	B3LYP/ 6-311+G(d,p)	Exp.[a]	MP2(full)/ 6-311+G(d,p)	B3LYP/ 6-311+G(d,p)
Δ_J	0.455	0.429	0.560(45)	0.446	0.464
Δ_{JK}	2.80	2.66	1.99(66)	2.78	3.16
Δ_K	-1.9548	-1.8128	2.648(47)	-1.9207	-2.2941
δ_J	-0.0004	-0.0004	0.0033(39)	0.0024	0.0044
δ_K	4	4	124(36)	1	1
χ_{aa}	-1.485	-1.526	-1.375(3)	2.609	2.752
χ_{bb}	-0.367	-0.527	-0.261(3)	0.160	-0.055
χ_{cc}	1.852	2.053	1.636(3)	-2.770	-2.697

[a]Ref [194]

An inspection of the microwave data from which the experimental data was taken to obtain the centrifugal distortion constants gives only fourteen J transitions and the values for the K_a are three with 0, nine with 1 and only two with 2. These excludingly small differences in the K_a values are not sufficient to obtain meaningful values for Δ_k and δ_k centrifugal distortion constants. The value of 1.99(66) kHz for Δ_{JK} with the listed uncertainty also indicates the probability although with the extremely large uncertainty it does agree with the theoretical predicted values. Also it should be noted that the experimentally reported values of 0.033(39) kHz has an uncertainty larger than the value and the value of 0.560(45) kHz for Δ_J has a much larger uncertainty than usually obtained for the distortion constants. However, it is believed that the theoretical predicted centrifugal distortion constants have a value within 10% of the correct experimental values.

In the previous microwave investigation [193], all but four of the structural parameters were assumed for the *trans* conformer. The four parameters that were not assumed but fitted instead were the NH bond and the CCN, CNH, HNH angles. The four determined values with their uncertainties (Table 95) are in agreement with the values obtained in this study. The values obtained earlier for the $N_3C_2C_1$ angle with an uncertainty of 1.0 degree are in excellent agreement with the corresponding parameters obtained in this study. However, the major differences between the values reported earlier and those obtained herein is with the C-F distances which were estimated to be shorter by an average distance of 0.009 Å and for the C-N and C-C bonds where the average distances are longer by 0.027 and 0.017 Å, respectively. The difference between the assumed FCF angle and the value obtained in this study is nearly 1° smaller. With these exceptions many of the other estimated parameters are in acceptable agreement with those obtained in the current study.

The predicted r_0 structural parameters for the *gauche* form have been predicted as shown in Table 95. It is interesting to note that the change from *trans* to *gauche* conformer causes several large structural changes. The heavy atom parameters with significant differences and their respective predicted structural changes are the -0.010 Å change in the C_1-F_6 distance and the -5.1° change in the CCN angle. These structural parameter differences are interesting in that the reduced CCN angle would seem to decrease the N-H---F distance yet this distance is not significantly changed in the overall structures. The difference in the C_1-F_6 distance is very interesting as this is the distance corresponding with the fluorine that would overlap the nitrogen lone pairs. The reduction in this distance would seem then to correspond to the reduction of the steric strain from

the nitrogen and fluorine lone pairs. It would be very interesting to determine the rotational constants for use in determining the adjusted r_0 structure of the *gauche* form so as to evaluate this comparsion.

It is also interesting to compare the heavy atom parameters of 2-fluoroethylamine [170] and 2,2-difluoroethylamine [172] with the corresponding ones obtained in the current study of 2,2,2 trifluoroethylamine. It should be noted that the C-C bond is smaller by an average of 0.002 Å for substitution of additional fluorine on β-carbon which is within the experimental error of ± 0.003 Å for the heavy atom bond distances in each r_0 determination. When we compare the C-N bond distance, the change is considerable with the addition of the second fluorine atom the distance decreases by an average of 0.009 Å and with the addition of a further fluorine atom decreases by 0.005 Å. However, the parameter which shows the greatest change due to fluorine substitution on β-carbon is the C-F bond distance(s) which reduces by ~0.030 Å each time a fluorine atom is added. Thus for 2-fluoroethylamine the average C-F distance is 1.398(3) Å, for 2,2-difluoroethylamine 1.368(3) Å and for 2,2,2 trifluoroethylamine 1.344(3) Å. Such large changes have a significant effect on some of the other parameters.

The natural population analysis (npa) calculations have been carried out for 2,2,2 trifluoroethylamine, 2,2-difluoroethylamine, and 2-fluoroethylamine for comparison by utilizing the MP2(full) method at the 6-311+G(d,p) basis set. The *trans* [*gauche*] conformers population analysis for 2,2,2 trifluoroethylamine for the heavy atoms are; C_1 = 1.18 [1.19], C_2 = -0.20 [-0.20], N = -0.84 [-0.84], F_4 = -0.40 [-0.41], F_5 = -0.41 [-0.41], and F_6 = -0.41 [-0.40]. As can be seen there is no significant change in atomic charges going from the *trans* to the *gauche* form. This is interesting when compared to the

predicted structure as discussed above where there are significant differences in the predicted structure of the *gauche* conformer this indicates that these changes are due to steric effects rather than electronic effects. The corresponding parameters from 2,2-difluoroethylamine [2-fluoroethylamine] are C_1 = 0.71 [0.16], C_2 = -0.18 [-0.16], N = -0.84 [-0.84], F_5 = -0.43 [-0.45], and F_6 = -0.43. The differences in the C_2, F_5, and F_6 charges are likely insignificant and there is no difference at all in the N charges among the three npa. The C_1 charge changes by 0.5 each time a fluorine atom is added. This change in charge is likely the cause of the change in the fluorine distances as they must come closer to the carbon atom to allow for bonding to its shrinking electron density.

From the microwave spectrum [193] only the *trans* form of 2,2,2,-trifluoroethylamine molecule has been reported. This conformer is a near prolate top which does not permit an accurate determination of the A rotational constant. Rotational constants for three isotopomers have been reported with the normal species, the NHD species and the ND_2 species, where the uncertainties on the A rotational constants are listed as 14 MHz and 39 MHz for the normal and deuterated species, respectively. The fit of the rotational constants are reported in Table 97.

It is well known that intramolecular hydrogen bonding can be a stabilizing factor for the orientation of molecular conformers. This is important in the case of the fluoride substituted ethylamine where the fluorine atom(s) and the amine hydrogens have the possibility to form an intramolecular hydrogen bond. This is observed with 2,2,2 trifluoroethylamine where the three fluorine atoms allow for two intramolecular hydrogen bonds so the most stable conformer is the *trans* conformer where two hydrogen bonds may be formed. Clearly intramolecular hydrogen bonding plays a significant role in the

conformational stabilities of such molecules and it would be of interest to see how other halogen or other substituents might affect the stability of other organoamines.

CHAPTER 16

CONFORMATIONAL, VIBRATIONAL, AND STRUCTURAL STUDIES OF 2,2,3,3,3-PENTAFLUOROPROPYLAMINE FROM RAMAN AND INFRARED SPECTRA OF GAS, LIQUID, XENON SOLUTIONS, AND SOLID SUPPORTED BY AB INITIO CALCULATIONS

INTRODUCTION

The conformational stability and the structural parameters of organoamines have been of scientific interest for several decades**.** This interest has arisen, in part, because of the importance of organoamines in biochemistry and many life processes. However**,** the determination of the enthalpy differences for many of the molecules studied has varied significantly depending on the techniques utilized to obtain the experimental value, i.e. infrared, Raman, NMR, and microwave spectroscopy as well as electron diffraction data. Because many of the enthalpy determinations were made from variable temperature studies of dilute solutions there have been problems with molecular association due to hydrogen bonding of the amines. To significantly reduce this problem we have utilized rare gas solutions where the pathlengths can be four to eight centimeters so the solutions can be very dilute, i.e. ~10^{-4} M. Since the association of the amine with the rare gas is relatively small the enthalpy difference in these solutions is similar to the value for the gas [16-20].

By this technique trans-ethylamine was determined [161] to be more stable by 54 ± 4 cm^{-1} (0.65 ± 0.05 kJ/mol) than the *gauche* form. This value was in agreement with earlier electron diffraction [162] determined value of 107 ± 70 cm^{-1} (1.28 ± 0.84 kJ/mol),

a microwave determined [177] value 110 ± 50 cm^{-1} (1.32 ± 0.60 kJ/mol), and IR matrix value [164] of 100 ± 10 cm^{-1} (1.20 ± 0.12 kJ/mol) from an infrared study of ethylamine in an argon matrix [164]. Earlier studies [165-168] reported the *gauche* conformer more stable. The MP2(full)/6-311+G(2d,2p) calculations predict [161] the *gauche* form more stable by 66 cm^{-1} (0.79 kJ/mol), but without diffuse functions the *trans* form is 32 cm^{-1} (0.38 kJ/mol) more stable. The enthalpy difference between the *gauche* and *trans* conformers of the NH_2 moiety need to be determined experimentally.

It is of scientific interest to determine the effect of substituting one or more of the hydrogen atoms on the β-carbon of the ethylene moiety. The first molecule investigated 2-fluoroethylamine [170], $FCH_2CH_2NH_2$, had been previously investigated in a microwave study [191] and the heavy atom skeleton was reported to be in the *gauche* form for the two conformers identified. The gauche form of the amine group was more stable by 35 ± 105 cm^{-1} (0.42 ± 1.26 kJ/mol) than the *trans* form. Our vibrational investigation [196] in xenon solutions identified all five conformers where the experimentally determined order of stability is *Gg′* > Gt [62 ± 8 cm^{-1} (0.74 ± 0.10 kJ/mol)] > *Tg* (262 ± 26 cm^{-1}) ≥ *Tt* (289 ± 45 cm^{-1}) > *Gg* (520 ± 50 cm^{-1}).

The next molecule investigated in this series of studies was the 2,2-difluoroethylamine [172] where the *trans-trans* conformer was found to be the most stable form. The first indicator is the NCCH dihedral angle and the second one is the relative position of the lone pair of electrons on nitrogen with respect to the β-carbon. The experimentally determined order of stability for the three identified conformers is *Tt* > *Gg* [83 ± 8 cm^{-1} (0.99 ± 0.10 kJ/mol)] > *Gt* [235 ± 11 cm^{-1} (2.81 ± 0.13 kJ/mol)]. In addition to the enthalpy differences, the r_0 structural parameters were obtained for the Gg′

and Gt conformers by utilizing the previously reported rotational constants from the microwave study [171].

As a continuation of these conformational and structural studies of the substituted ethylamines we chose the molecule where the H atom on the β-carbon of 2,2-difluoroethylamine was replaced by the trifluoromethyl moiety, $CF_3CF_2CH_2NH_2$. The vibrational study was carried out by utilizing the Raman spectra of the gas and liquid as well as the infrared spectra of the gas, variable temperature xenon solutions, and solid. Additionally to investigate the mixing of the NH_2 motions with the other atom motions of 2,2,3,3,3-pentafluoropropyl the Raman and infrared spectra of the corresponding ND_2 molecule were also recorded. These studies were for determining the conformational stabilities, identify the most stable forms, obtain predicted r_0 structural parameters, and provide vibrational assignments for both molecules.

To support the vibrational study, we have carried out *ab initio* calculations with basis sets up to aug-cc-pVTZ as well as those with diffuse functions, i.e., 6-311+G(2df,2pd). We found that there can be significant differences in the predicted stabilities of the ethylamine molecules with the size of basis set as well as with the inclusion of diffuse functions at the MP2 level. We have also carried out density functional theory (DFT) calculations by the B3LYP method with the same basis sets. We have calculated optimized geometries, conformational stabilities, harmonic force fields, infrared intensities, Raman activities and depolarization ratios. The results of these spectroscopic and theoretical studies are reported herein.

EXPERIMENTAL

The sample of 2,2,3,3,3-pentafluoropropylamine was prepared by the reaction of aqueous ammonia and 1,1,3-trihydrotetrafluoropropyl-p-toluenesulfonate in the presence of sodiumethylbenzene sulfonate as surfactant as previously reported [197]. The reaction mixture was heated for 24 hrs. at 175° C with continuous stirring. The compound was verified by infrared and nuclear magnetic resonance spectroscopy.

The mid-infrared spectrum of the gas phase of $CF_3CF_2CH_2NH_2$ (Fig. 60A) and $CF_3CF_2CH_2ND_2$ (Fig. S3A) and the solid (Fig. 60D) phase of $CF_3CF_2CH_2NH_2$ were obtained from 3600 to 400 cm^{-1} on a Perkin-Elmer model 2000 Fourier transform spectrometer equipped with a Ge/CsI beamsplitter and a DTGS detector. Atmospheric water vapor was removed from the spectrometer housing by purging with dry nitrogen. The theoretical resolution used to obtain the spectrum of the gas was 0.5 cm^{-1} and 128 interferograms were added and transformed with a boxcar truncation function. For the spectrum of the solid theoretical resolution of 2 cm^{-1} was used with 128 interferograms added and truncated. Multiple annealings were required to obtain satisfactory spectra of the solid.

The far infrared spectra (380 to 30 cm^{-1}) of the gas phase of $CF_3CF_2CH_2NH_2$ and $CF_3CF_2CH_2ND_2$ were obtained at a resolution of 0.10 cm^{-1} on a Nicolet model 8000 interferometer equipped with a vacuum bench and a liquid-helium cooled Ge bolometer containing a wedged sapphire filter and polyethylene windows. A 12.5 μ Mylar beam splitter was employed and the sample was contained in a 1-m cell. Interferograms for both the reference and sample cells were recorded 250 times, averaged, and transformed using a boxcar apodization.

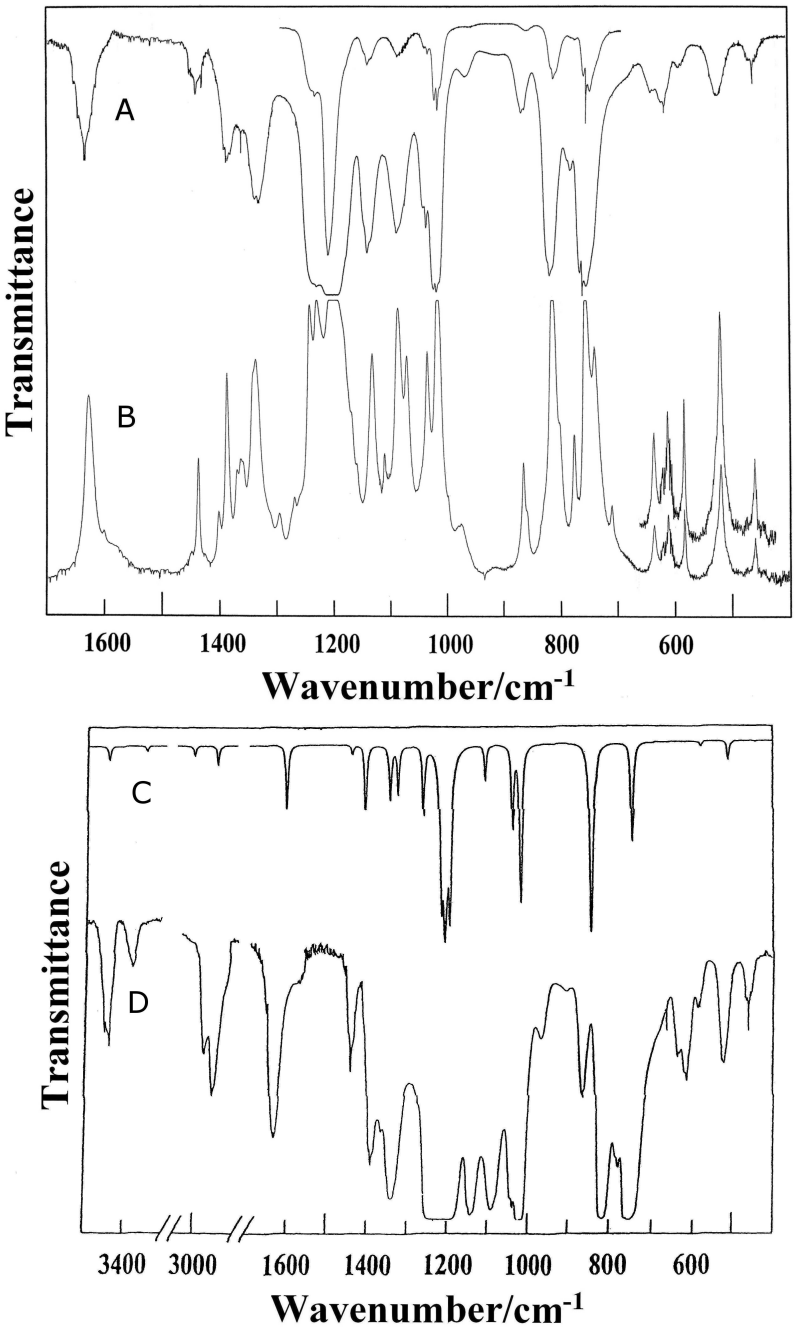

Figure 60. Mid-infrared spectra of normal 2,2,3,3,3-pentafluoropropylamine (A) gas; (B) Xe solution at -70°C; (C) simulated spectrum of *Tt* conformer; (D) infrared spectra of the solid.

The mid-infrared spectra (3600 to 400 cm^{-1}) of $CF_3CF_2CH_2NH_2$ dissolved in liquefied xenon (Fig. 60B) at ten different temperatures (-55 to -100°C) were recorded on a Bruker model IFS-66 Fourier transform spectrometer equipped with a globar source, a Ge/KBr beamsplitter and a DTGS detector. In all cases, 100 interferograms were collected at 1.0 cm^{-1} resolution, averaged and transformed with a boxcar truncation function. For these studies, a specially designed cryostat cell was used. It consists of a copper cell with a path length of 4 cm with wedged silicon windows sealed to the cell with indium gaskets. The temperature was maintained with boiling liquid nitrogen and monitored by two Pt thermoresistors. After cooling to the designated temperature, a small amount of the sample was condensed into the cell and the system was then pressurized with the noble gas, which condensed in the cell, allowing the compound to dissolve.

The Raman spectra were recorded on a Cary model 82 spectrophotometer equipped with a Spectra-Physics model 171 argon ion laser operating on the 5145 Å line. The spectra of the gas, $CF_3CF_2CH_2NH_2$ (Fig. 61A) and $CF_3CF_2CH_2ND_2$ (Fig. 62A), were recorded by using a standard Cary multipass accessory, and the laser power at the sample was 1 W. The spectra of the liquid phase, $CF_3CF_2CH_2NH_2$ (Fig. 63A) and $CF_3CF_2CH_2ND_2$ (Fig. S4A), were recorded from the sample sealed in a glass capillary. The measurements of the Raman wavenumbers are expected to be accurate to ± 2 cm^{-1}. All of the observed bands in the Raman spectra of the gas and liquid along with their proposed assignments and depolarization values are listed in Tables 99 (*Tt*) and 100 (*Tg*) for $CF_3CF_2CH_2NH_2$ and Tables S24 (*Tt*) and S25 (*Tg*) for $CF_3CF_2CH_2ND_2$. The first indicator is the NCCC dihedral angle (*G* = *gauche* or *T* = *trans*) and the second one (*g* =

gauche or *t* = *trans*) is the relative position of the lone pair of electrons on nitrogen with respect to β-carbon.

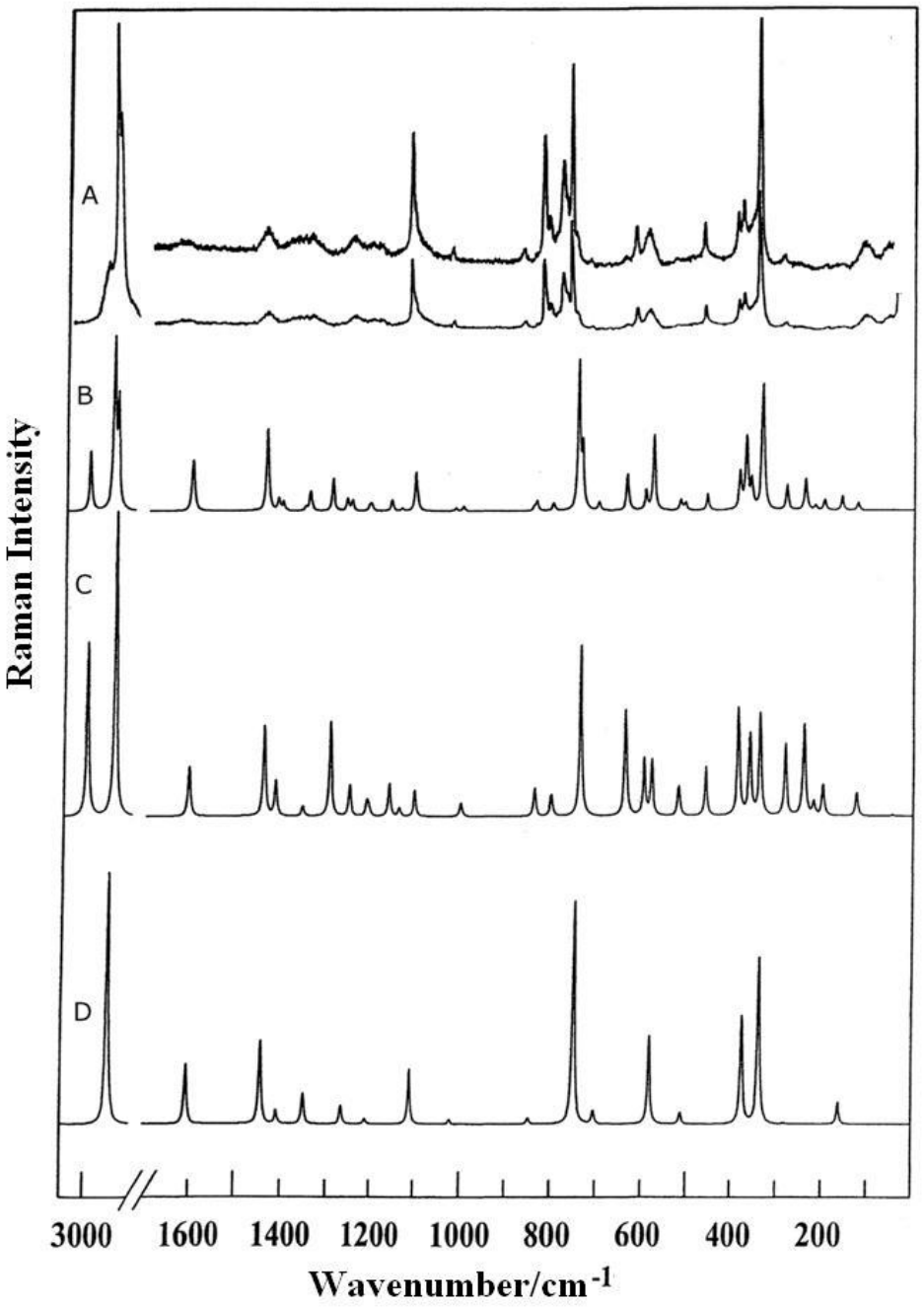

Figure 61. Comparison of experimental and predicted Raman spectra of 2,2,3,3,3-pentafluoropropylamine: (A) gas; (B) simulated spectrum of *Tt* and *Tg;* enthalpy difference of 280 cm^{-1} at 25°C; (C) simulated spectrum of *Tg* conformer; (D) simulated spectrum of A′ modes of *Tt* conformer.

Figure 62. Comparison of experimental and predicted Raman spectra of 2,2,3,3,3-pentafluoropropylamine-ND_2: (A) gas; (B) simulated spectrum of *Tt* and *Tg*; enthalpy difference of 280 cm^{-1} at 25°C; (C) simulated spectrum of *Tg* conformer; (D) simulated spectrum of A′ modes of *Tt* conformer.

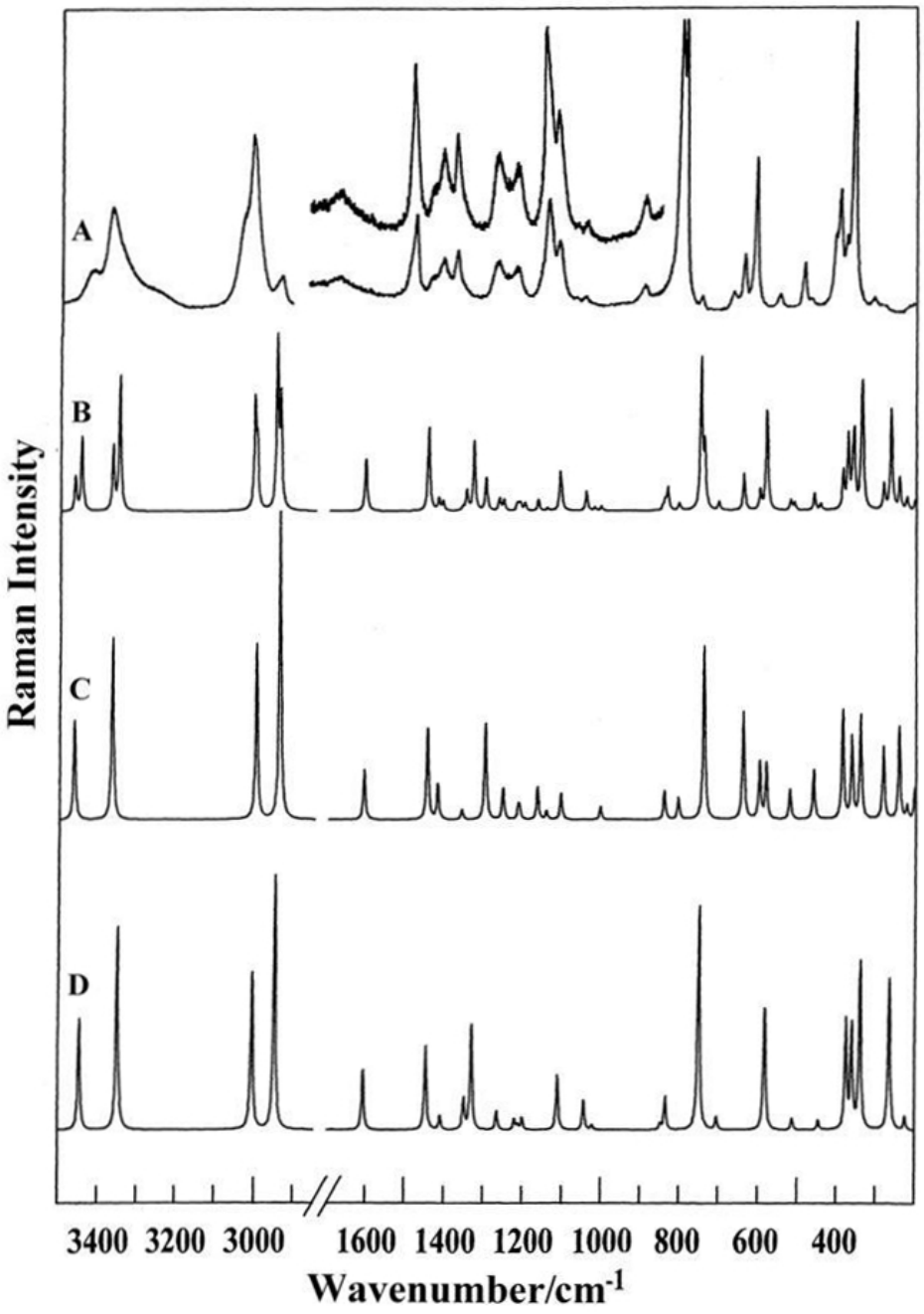

Figure 63. Comparison of experimental and predicted Raman spectra of 2,2,3,3,3-pentafluoropropylamine: (A) liquid; (B) simulated spectrum of *Tt* and *Tg*; enthalpy difference of 280 cm^{-1} at 25°C; (C) simulated spectrum of *Tg* conformer; (D) simulated spectrum of *Tt* conformer.

Table 99. Observed and calculated[a] wavenumbers (cm^{-1}) for *trans-trans* 2,2,3,3,3-pentafluoropropylamine.

	Vib. No.	Fundamental	*ab initio*	fixed scaled[b]	IR int.	Raman act.	dp ratio	IR Gas	Raman gas	Raman liquid	xenon solution	IR Solid	P.E.D.[c]	Band Contours A*	Band Contours B*
A′	ν_1	NH_2 symmetric stretch	3530	3349	2.7	71.5	0.11	3371	3372	3360	3354	3374	$100S_1$	26	74
	ν_2	CH_2 symmetric stretch	3142	2948	9.0	71.0	0.08	2962	2961	2954	2949	2960	$100S_2$	44	56
	ν_3	NH_2 symmetric deformation	1733	1606	36.5	6.7	0.69	1637	1634	1632	1628	1637/1634	$83S_3,15S_{11}$	2	98
	ν_4	CH_2 symmetric deformation	1538	1445	4.5	8.1	0.75	1450	1449	1445	1439	1447	$98S_4$	18	82
	ν_5	CCC antisymmetric stretch	1469	1409	38.2	1.3	0.10	1395	1394	1391	1389	1393	$31S_5,22S_6$	96	4
	ν_6	CH_2 wag	1413	1349	28.1	2.7	0.48	1350	1349	1343	1338	1341	$60S_6,16S_{17}$	84	16
	ν_7	CF_2 symmetric stretch	1308	1265	37.2	1.5	0.75	1270	1271	1270	1271	1278	$13S_7,29S_8,13S_{19},12S_{16}$	33	67
	ν_8	CF_3 antisymmetric stretch	1270	1211	284.3	0.4	0.30	1206	1207	1196	1206	1203	$44S_8,19S_7,13S_5$	-	100
	ν_9	CN stretch	1174	1110	18.0	3.8	0.38	1095	1095	1087	1089	1090	$63S_9,10S_{18}$	73	27
	ν_{10}	CF_2 wag	1064	1022	133.2	0.3	0.29	1023	1022	1017	1019	1022	$17S_{10},24S_{12},17S_9,14S_5,10S_{13}$	100	-
	ν_{11}	NH_2 wag	949	847	227.3	0.3	0.69	865	863	868	867	869	$47S_{11},11S_7,11S_9,10S_3,$	79	21
	ν_{12}	CF_3 symmetric stretch	796	750	59.9	9.4	0.06	781	780	779	777	760	$25S_{12},22S_7,17S_{11},17S_{17}$	100	-
	ν_{13}	CF_3 symmetric deformation	725	704	0.3	0.5	0.73	720	718	724	712	720	$28S_{13},25S_{12},13S_{10},10S_{11}$	65	35
	ν_{14}	CF_3 antisymmetric deformation	592	582	1.8	2.7	0.68	585	587	588	585	621/615	$25S_{14},15S_8,12S_{16},10S_5$	50	50
	ν_{15}	CF_2 symmetric deformation	516	512	9.0	0.3	0.63	526	527	526	521	527/522	$44S_{15},39S_{14}$	17	83
	ν_{16}	CF_3 symmetric rock	378	375	7.1	1.8	0.59	-	375	378	-	373	$22S_{16},24S_{15},23S_{14}$	100	-
	ν_{17}	CCC symmetric stretch	348	339	5.9	2.4	0.26	338	340	344	-	338	$38S_{17},25S_{13},12S_{18}$	100	-
	ν_{18}	CCN bend	284	282	10.1	0.0	0.34	280	282	287	-	-	$31S_{18},32S_{16},31S_{10}$	95	5
	ν_{19}	CCC bend	163	163	1.0	0.1	0.72	160	158	154	-	-	$57S_{19},22S_{16},14S_{18}$	20	80

A″	ν_{20}	NH_2 antisymmetric stretch	3632	3446	6.6	41.3	0.75	3440	-	3420	3422	3437	$100S_{20}$	-	-
	ν_{21}	CH_2 antisymmetric stretch	3205	3006	4.8	45.6	0.75	2988	-	2982	2975	2985	$100S_{21}$	-	-
	ν_{22}	CH_2 twist	1442	1330	24.8	9.1	0.75	1337	-	1338	1338	1341	$76S_{22},12S_{24}$	-	-
	ν_{23}	CF_3 antisymmetric stretch	1298	1220	133.0	0.8	0.75	1236	-	1232	1231	1231	$64S_{23},12S_{27}$	-	-
	ν_{24}	NH_2 twist	1268	1200	173.4	0.9	0.75	1148	-	1134	1134	1145	$22S_{24},28S_{26},26S_{25},12S_{23}$	-	-
	ν_{25}	CF_2 antisymmetric stretch	1136	1043	46.6	1.9	0.75	1041	-	1039	1036	1040	$41S_{25},32S_{24},23S_{22}$	-	-
	ν_{26}	CH_2 rock	904	834	7.4	1.6	0.75	~821	-	812	804	817	$51S_{26},33S_{24},13S_{25}$	-	-
	ν_{27}	CF_3 deformation	593	584	0.9	1.4	0.75	585	-	588	585	585/590	$39S_{27},24S_{23},15S_{30},12S_{28},$	-	-
	ν_{28}	CF_2 rock	453	446	0.4	0.2	0.75	464	-	465	462	462	$35S_{28},40S_{27},11S_{31}$	-	-
	ν_{29}	CF_2 twist	374	360	10.6	1.6	0.75	359	-	360	-	358	$55S_{29},13S_{30},12S_{31}$	-	-
	ν_{30}	NH_2 torsion	301	265	55.7	1.5	0.75	271	-	270	-	-	$82S_{30},12S_{29}$	-	-
	ν_{31}	CF_3 wag	224	224	5.3	0.1	0.75	226	-	220	-	-	$49S_{31},26S_{28},23S_{29}$	-	-
	ν_{32}	CCC asymmetric torsion	108	108	0.02	0.1	0.75	108	-	108	-	-	$100S_{32}$	-	-
	ν_{33}	CF_3 torsion	68	68	0.02	0.0	0.75	78	-	78	-	-	$100S_{33}$	-	-

[a] MP2(full)/6-31G(d) *ab initio* calculations, scaled wavenumbers, infrared intensities (km/mol), Raman activities ($Å^4$/amu), depolarization ratios and potential energy distributions (P.E.D.s)

[b] MP2(full)/6-31G(d) fixed scaled wavenumbers with factors of 0.88 for CH stretches and deformations, 0.7 for NH bends (excluding deformation), 1.0 for heavy atom bends, and 0.90 for all other modes.

[c] Calculated with MP2(full)/6-31G(d) and contributions of less than 10% are omitted.

[*] A, B and C values in the last three columns are percentage infrared band contours.

Table 100. Observed and calculated[a] wavenumbers (cm^{-1}) for *trans-gauche* 2,2,3,3,3-pentafluoropropylamine.

Vib. No.	Fundamental	*ab initio*	fixed scaled[b]	IR int.	Raman act.	dp ratio	IR gas	Raman gas	Raman liquid	xenon solution	P.E.D.[c]	Band Contours		
												A*	B*	C*
ν_{20}	NH_2 antisymmetric stretch	3651	3463	8.5	37.3	0.74	3440	3441	3430	3437	$99S_{20}$	29	45	26
ν_1	NH_2 symmetric stretch	3548	3366	3.7	65.6	0.11	3382	3383	3372	3366	$99S_1$	2	22	76
ν_{21}	CH_2 antisymmetric stretch	3198	3000	5.3	51.1	0.74	2983	2984	2982	2975	$97S_{21}$	26	29	45
ν_2	CH_2 symmetric stretch	3133	2939	10.0	86.1	0.09	2954	2953	2954	2949	$97S_2$	1	62	37
ν_3	NH_2 symmetric deformation	1737	1608	36.6	5.6	0.70	1637	1634	1632	1628	$82S_3,16S_{11}$	20	14	66
ν_4	CH_2 symmetric deformation	1537	1446	14.5	8.8	0.71	1450	1449	1445	1439	$88S_4$	62	6	32
ν_5	CCC antisymmetric stretch	1483	1420	17.5	3.3	0.59	1411	1409	1405	1404	$21S_5,13S_{22},11S_{13},11S_{17},11S_4,10S_{19}$	94	-	6
ν_6	CH_2 wag	1436	1359	4.8	0.9	0.75	1365	1366	1372	1364	$70S_6,10S_5$	35	-	65
ν_{22}	CH_2 twist	1411	1299	24.3	8.1	0.74	1298	1294	1308	1298	$57S_{22},16S_{24}$	92	4	4
ν_8	CF_3 antisymmetric stretch	1309	1254	42.4	2.5	0.73	1243	1245	1242	1244	$33S_8,10S_{19},10S_{16},10S_6$	38	56	6
ν_{23}	CF_3 antisymmetric stretch	1271	1215	227.9	1.1	0.74	1215	1215	1215	1215	$73S_{23},13S_{27}$	7	9	84
ν_7	CF_2 symmetric stretch	1264	1211	238.6	0.6	0.26	1206	1207	1196	1206	$16S_7,38S_8,12S_5,10S_{17}$	17	43	40
ν_{25}	CF_2 antisymmetric stretch	1236	1165	110.9	2.4	0.51	1182	1184	1180	1180	$35S_{25},10S_{26},10S_{24},10S_6$	53	15	32
ν_{13}	CF_3 symmetric deformation	1200	1142	153.1	0.6	0.52	1148	1146	1134	1134	$11S_{13},18S_{25},15S_{12},12S_{26},11S_{24}$	10	80	10
ν_9	CN stretch	1172	1106	10.1	1.8	0.39	1115	1115	1114	1112	$77S_9$	39	28	33
ν_{24}	NH_2 twist	1083	1005	47.8	0.8	0.74	1005	1004	1006	1001	$29S_{24},18_{22},15S_7,10S_{12}$	54	30	165
ν_{26}	CH_2 rock	935	841	104.0	1.4	0.74	821	819	812	815	$31S_{26},20S_{24},19S_{11},10S_7$	64	27	9
ν_{11}	NH_2 wag	888	805	176.1	1.0	0.26	750	749	746	741	$41S_{11},18S_{26},10S_3$	79	21	-
ν_{12}	CF_3 symmetric stretch	775	741	35.2	7.2	0.03	761	760	768	756	$47S_{12},22S_{13},13S_{17}$	89	10	1
ν_{18}	CCN bend	658	641	22.2	3.7	0.75	640	640	640	638	$15S_{18},10S_{10},10S_{25},10S_8,10S_{28},10S_{16},10S_{14}$	5	67	28
ν_{17}	CCC symmetric stretch	614	600	14.3	1.8	0.12	617	616	616	612	$14S_{17},22S_{13},19S_{15},19S_7,10S_{26},10S_{10}$	66	28	6
ν_{27}	CF_3 antisymmetric deformation	593	583	0.5	1.7	0.66	585	587	588	585	$34S_{27},21S_{23},12S_{31},10S_{28}$	64	32	4
ν_{14}	CF_3 antisymmetric	527	522	2.3	0.8	0.66	536		540	537	$52S_{14},10S_{27},10S_8$	9	1	90

	deformation						536							
ν_{28}	CF_2 rock	467	462	7.4	1.1	0.24	464	462	465	462	$15S_{28},24S_{27},17S_{15},10S_{10},10S_{17}$	57	19	24
ν_{15}	CF_2 deformation	393	388	7.0	1.9	0.60	-	386	387	-	$21S_{15},17S_{29},17S_{27},14S_{31},10S_{18}$	14	86	-
ν_{26}	CF_3 symmetric rock	373	364	4.8	1.3	0.75	360	359	360	-	$16S_{26},22S_{29},18S_{15},15S_{14}$	37	26	37
ν_{10}	CF_2 wag	357	342	11.2	1.5	0.49	345	340	344	-	$20S_{10},17S_{13},15S_5,14S_{17},13S_{30}$	16	62	22
ν_{30}	NH_2 torsion	309	284	28.4	0.8	0.66	283	282	287	-	$47S_{30},22S_{16},12S_{10}$	27	54	19
ν_{29}	CF_2 twist	250	243	16.5	0.8	0.70	241	249	247	-	$28S_{29},25S_{18},24S_{30},10S_{16}$	27	17	56
ν_{31}	CF_3 wag	223	222	8.2	0.1	0.69	218	216	220	-	$47S_{31},36S_{28},10S_{29}$	33	1	66
ν_{19}	CCC bend	202	202	4.8	0.2	0.65	192	193	192	-	$50S_{19},16S_{26},10S_{18}$	17	62	21
ν_{32}	CCC asymmetric torsion	128	127	1.1	0.2	0.75	114	115	117	-	$71S_{32},23S_{33}$	23	60	17
ν_{33}	CF_3 torsion	47	47	0.3	0.1	0.74	48	49	-	-	$76S_{33},23S_{32}$	7	15	78

[a] MP2(full)/6-31G(d) *ab initio* calculations, scaled wavenumbers, infrared intensities (km/mol), Raman activities ($Å^4$/amu), depolarization ratios and potential energy distributions (P.E.D.s)

[b] MP2(full)/6-31G(d) fixed scaled wavenumbers with factors of 0.88 for CH stretches and deformations, 0.7 for NH bends (excluding deformation), 1.0 for heavy atom bends, and 0.90 for all other modes.

[c] Calculated with MP2(full)/6-31G(d) and contributions of less than 10% are omitted.

[*] A, B and C values in the last three columns are percentage infrared band contours.

Table 101. Calculated energies in (H) and energy differences (cm^{-1}) for the five conformers of 2,2,3,3,3-pentafluoropropylamine.

Method/Basis Set	# *basis set*	Energy[a], E *trans-trans*	Energy Differences, Δ *trans-gauche*[b]	*gauche-gauche 2*[b]	*gauche-trans*[b]	*gauche-gauche 1*[b]
MP2(full)/6-31G(d)	143	-0.008200	183	667	931	1046
MP2(full)/6-31+G(d)	179	-0.065322	306	717	833	2220
MP2(full)/6-31G(d,p)	155	-0.044232	203	712	945	1994
MP2(full)/6-31+G(d,p)	191	-0.100233	309	714	799	2099
MP2(full)/6-311G(d,p)	186	-0.550388	256	699	907	1563
MP2(full)/6-311+G(d,p)	222	-0.583713	344	753	780	991
MP2(full)/6-311G(2d,2p)	243	-0.733475	235	749	835	1482
MP2(full)/6-311+G(2d,2p)	279	-0.760487	317	770	777	1405
MP2(full)/6-311G(2df,2pd)	326	-0.923402	215	713	787	1252
MP2(full)/6-311+G(2df,2pd)	362	-0.949598	315	767	765	1218
MP2(full)/aug-cc-pVTZ	506	-0.992809	293	702	727	1233
Average MP2(full)		-	282 ± 48	736 ± 30	797 ± 58	1306 ± 193
B3LYP/6-31G(d)	143	-1.676532	139	797	1008	1799
B3LYP/6-31+G(d)	179	-1.723617	292	804	895	2321
B3LYP/6-311G(d,p)	186	-1.885836	158	756	975	1960
B3LYP/6-311+G(d,p)	222	-1.908429	294	805	858	1994
B3LYP/6-311G(2d,2p)	243	-1.907176	179	813	913	1776
B3LYP/6-311+G(2d,2p)	279	-1.927345	301	832	838	1770
B3LYP/6-311G(2df,2pd)	326	-1.923258	169	769	863	1632
B3LYP/6-311+G(2df,2pd)	362	-1.944548	300	814	815	1678
B3LYP/aug-cc-pVTZ	506	-1.970696	313	801	800	1776
B3LYP Average		-	238 ± 74	799 ± 23	885 ± 70	1856 ± 210

[a]Energy of conformer is given as –(E+669) H.
[b]Difference is relative to *trans-trans* form and given in cm^{-1}.

AB INITIO CALCULATIONS

The LCAO-MO-SCF restricted Hartree-Fock calculations were performed with the Gaussian-03 program [22] using Gaussian-type basis functions. The energy minima with respect to nuclear coordinates were obtained by the simultaneous relaxation of all geometric parameters using the gradient method of Pulay [29]. Several basis sets as well as the corresponding ones with diffuse functions were employed with the Møller-Plesset perturbation method [21] to the second order (MP2(full)) as well as with the density functional theory by the B3LYP method. The predicted conformational energy differences are listed in Table 101.

In order to obtain a complete description of the molecular motions involved in the fundamental modes of 2,2,3,3,3-pentafluoropropylamine, a normal coordinate analysis has been carried out. The force field in Cartesian coordinates was obtained with the Gaussian 03 program [22] at the MP2(full) level with the 6-31G(d) basis set. The internal coordinates used to calculate the **G** and **B** matrices are given in Table 102 with the atomic numbering shown in Fig. 64. By using the **B** matrix [30], the force field in Cartesian coordinates was converted to a force field in internal coordinates. Subsequently, scaling factors of 0.88 for CH stretches and CH_2 deformation, 0.70 for NH_2 bends (excluding deformation) and 0.90 for all other modes except torsions and heavy atom bends were applied, along with the geometric average of the scaling factors for the interaction force constants, to obtain the fixed scaled force field and resultant wavenumbers. A set of symmetry coordinates was used (Table S26) to determine the corresponding potential energy distributions (P.E.D.s). A comparison between the observed and calculated wavenumbers, along with the calculated infrared intensities, Raman activities,

depolarization ratios and potential energy distributions for the *trans-trans* and *trans-gauche* conformers of the $CF_3CF_2CH_2NH_2$ and $CF_3CF_2CH_2ND_2$ molecules are listed in Tables 99, 100, S24, and S25, respectively.

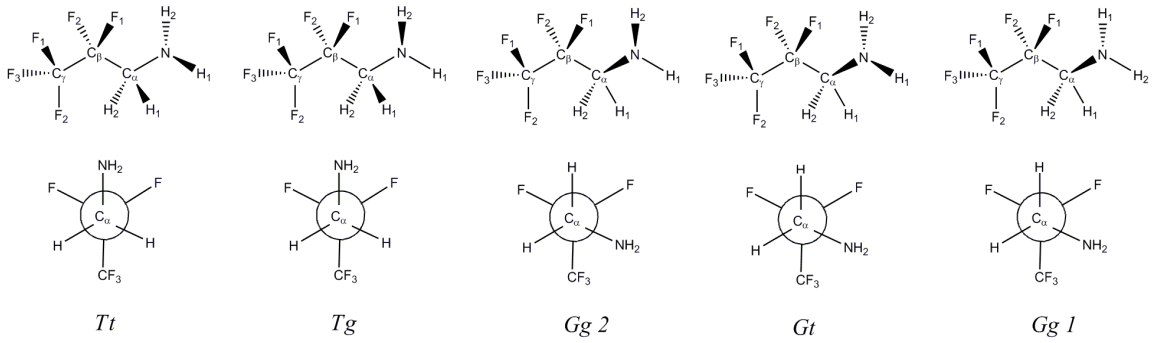

Figure 64. Five conformers of 2,2,3,3,3-pentafluoropropylamine showing atomic numbering.

Table 102. Structural parameters (Å and degree), rotational constants (MHz) and dipole moment (debye) for 2,2,3,3,3-pentafluoropropylamine *trans-trans* (C_s) and *trans-gauche* (C_1) forms.

Parameter	Int. Coor.	*MP2(full)/ 6-311+G(d, p)*		*B3LYP/ 6-311+G(d, p)*		Estimated r_0	
		Tt	*Tg*	*Tt*	*Tg*	*Tt*	*Tg*
r H---F		2.596	2.586	2.647	2.650	2.602(5)	2.585(5)
r C_α-N	X_1	1.448	1.453	1.448	1.453	1.448(5)	1.453(5)
r C_α-C_β	Y_1	1.519	1.514	1.532	1.526	1.517(5)	1.512(5)
r C_β-C_γ	Y_2	1.533	1.535	1.549	1.552	1.531(5)	1.533(5)
r C_β-F_1	Z_1	1.361	1.362	1.368	1.370	1.360(5)	1.363(5)
r C_β-F_2	Z_2	1.361	1.351	1.368	1.358	1.360(5)	1.352(5)
r C_γ-F_1	Z_3	1.330	1.329	1.336	1.335	1.331(5)	1.330(5)

r C_γ-F_2	Z_4	1.338	1.338	1.345	1.346	1.332(5)	1.332(5)
r C_γ-F_3	Z_5	1.338	1.339	1.345	1.346	1.332(5)	1.333(5)
r N-H_1	b_1	1.014	1.012	1.014	1.012	1.014(2)	1.012(2)
r N-H_2	b_2	1.014	1.013	1.014	1.013	1.014(2)	1.013(2)
r C_α-H_1	r_1	1.092	1.098	1.092	1.098	1.092(2)	1.098(2)
r C_α-H_2	r_2	1.092	1.092	1.092	1.092	1.092(2)	1.092(2)
$\angle$ $NC_\alpha C_\beta$	θ	114.0	109.0	114.5	109.8	114.0(5)	109.0(5)
$\angle$ $C_\alpha C_\beta C_\gamma$	χ	114.5	113.6	114.6	113.7	114.5(5)	113.6(5)
$\angle$ $C_\alpha C_\beta F_1$	ρ_1	110.2	109.9	110.3	110.0	110.6(5)	109.9(5)
$\angle$ $C_\alpha C_\beta F_2$	ρ_2	110.2	111.5	110.3	111.6	110.6(5)	111.5(5)
$\angle$ $C_\gamma C_\beta F_1$	ρ_3	107.2	106.9	107.2	106.8	107.6(5)	106.9(5)
$\angle$ $C_\gamma C_\beta F_2$	ρ_4	107.2	107.0	107.2	107.0	107.6(5)	107.0(5)
$\angle$ $F_1 C_\beta F_2$	ρ_5	107.2	106.9	107.7	107.4	106.9(5)	106.6(5)
$\angle$ $C_\beta C_\gamma F_1$	ρ_6	111.4	111.1	111.8	111.4	112.1(5)	111.8(5)
$\angle$ $C_\beta C_\gamma F_2$	ρ_7	109.9	110.4	110.1	110.6	110.3(5)	110.8(5)
$\angle$ $C_\beta C_\gamma F_3$	ρ_8	109.9	109.8	110.1	110.1	110.3(5)	110.2(5)
$\angle$ $F_1 C_\gamma F_2$	α_1	108.6	108.5	108.4	108.3	108.0(5)	108.1(5)
$\angle$ $F_1 C_\gamma F_3$	α_2	108.6	108.7	108.4	108.4	108.0(5)	108.1(5)
$\angle$ $F_2 C_\gamma F_3$	α_3	108.4	108.2	108.0	107.9	108.0(5)	107.8(5)
$\angle$ $C_\alpha NH_1$	β_1	110.9	110.3	111.9	111.4	110.9(5)	110.3(5)
$\angle$ $C_\alpha NH_2$	β_2	110.9	110.9	111.9	112.0	110.9(5)	110.9(5)
$\angle$ $H_1 NH_2$	γ	107.8	108.0	108.4	108.7	107.8(5)	108.0(5)
$\angle$ $NC_\alpha H_1$	δ_1	110.9	115.1	109.6	115.1	110.9(5)	115.1(5)
$\angle$ $NC_\alpha H_2$	δ_2	110.9	109.3	109.6	109.3	110.9(5)	109.3(5)
$\angle$ $C_\beta C_\alpha H_1$	ε_1	107.8	107.5	107.7	107.3	107.8(5)	107.5(5)
$\angle$ $C_\beta C_\alpha H_2$	ε_2	107.8	107.3	107.7	107.2	107.8(5)	107.3(5)
$\angle$ $H_1 C_\alpha H_2$	η	108.1	108.3	107.5	107.8	108.1(5)	108.3(5)
τ NCCC	τ_1	180.0	-175.5	180.0	-176.1	180.0(5)	-175.5(5)
τ $CCCF_1$	τ_2	180.0	-178.5	180.0	-178.7	180.0(5)	-178.5(5)
τ $CCNH_1$	τ_3	59.9	-164.6	61.0	-161.2	59.9(5)	-164.6(5)
τ $CCNH_2$	τ_4	-59.9	75.8	-61.0	76.7	-59.9(5)	75.8(5)
A		2538.1	2539.8	2510.5	2512.0	2552.2	2551.2
B		1236.8	1244.5	1216.5	1223.7	1237.2	1247.2
C		1199.7	1205.4	1177.8	1182.7	1197.9	1208.3
$\lvert\mu_a\rvert$		1.207	1.990	1.257	1.952		
$\lvert\mu_b\rvert$		0.696	3.026	0.612	2.782		
$\lvert\mu_c\rvert$		0.00	0.609	0.00	0.555		
$\lvert\mu_t\rvert$		1.393	3.673	1.398	3.444		

The vibrational spectra were predicted from the MP2(full)/6-31G(d) calculations. The predicted scaled wavenumbers were used together with a Lorentzian function to obtain the simulated spectra. Infrared intensities were obtained based on the dipole moment derivatives with respect to Cartesian coordinates. The derivatives were transformed with respect to normal coordinates by $(\partial\mu_u/\partial Q_i) = \sum_j (\partial\mu_u/\partial X_j)L_{ij}$, where Q_i is the i^{th} normal coordinate, X_j is the j^{th} Cartesian displacement coordinate, and L_{ij} is the transformation matrix between the Cartesian displacement coordinates and the normal coordinates. The infrared intensities were then calculated by $(N\pi)/(3c^2)$ $[(\partial\mu_x/\partial Q_i)^2 + (\partial\mu_y/\partial Q_i)^2 + (\partial\mu_z/\partial Q_i)^2]$. A comparison of the infrared spectra of the solid phase and the predicted infrared spectra for the pure *trans-trans* conformer are shown in Fig. 60 and the corresponding figure of the $–ND_2$ molecule with the infrared spectra of the vapor phase and the predicted infrared spectra for the pure *trans-trans* and *trans-gauche* conformers, as well as, the mixture of the two conformers with relative concentrations calculated for the equilibrium mixture at 25ºC by using the experimentally determined enthalpy difference are shown in Fig. S3. The predicted spectrum is in good agreement with the experimental spectrum which shows the utility of the scaled predicted wavenumbers and predicted intensities for supporting the vibrational assignment.

Additional support for the vibrational assignments was obtained from the simulated Raman spectra. The evaluation of Raman activity by using the analytical gradient methods has been developed [31-34] and the activity S_j can be expressed as: $S_j = g_j(45\alpha_j^2 + 7\beta_j^2)$, where g_j is the degeneracy of the vibrational mode j, α_j is the derivative of the isotropic polarizability, and β_j is the anisotropic polarizability. To obtain the Raman scattering cross sections, the polarizabilities are incorporated into S_j by

multiplying S_j with $(1-\rho_j)/(1+\rho_j)$ where ρ_j is the depolarization ratio of the j^{th} normal mode. The Raman scattering cross sections and calculated wavenumbers obtained from the Gaussian 03 program were used together with a Lorentzian function to obtain the simulated Raman spectra. Comparison of experimental Raman spectra of the liquid or gas phases of $CF_3CF_2CH_2NH_2$ and $CF_3CF_2CH_2ND_2$ with the respective predicted Raman spectra for the pure *trans-trans* and trans-*gauche* conformers as well as the mixture of the two conformers with relative concentrations calculated for the equilibrium mixture at 25°C by using the experimentally determined enthalpy difference are shown in Fig. 61, 62, 63, and S3. The spectrum of the mixture should be compared to that of the Raman spectrum of the liquid and/or vapor at room temperature. The predicted spectrum is in reasonable agreement with the experimental spectrum which shows the utility of the predicted Raman spectra for the supporting vibrational assignments.

VIBRATIONAL ASSIGNMENT

There is a very large amount of information available in addition to the predicted fundamental wavenumbers for both the conformers for the "normal" species and the ND_2 isotopomers which includes band contours, Raman activities and infrared intensities and depolarization values. These data for both isotopomers are listed in Tables 99, 100, S24, and S25 for the *Tt* and *Tg* conformers. Additionally, the Raman spectra of the gas has been obtained which usually provides mainly the A′ bands for molecules which have a plane of symmetry and the data are more definitive than the depolarization values. Also, the "group wavenumbers" for the various parts of the molecules, i.e., CF_3, NH_2, ND_2, CH_2, and CF_2, are well known so vibrational assignments for the more stable *Tt* conformer could be made with significant confidence. However, the fundamental wavenumbers for

the *Tg* form might be expected to be very similar to those for the *Tt* conformer since the difference is only the position of the NH_2 (ND_2) group. Thus many of the modes could be nearly in pairs except when the P.E.D differ extensively. Since one of the primary goals of this research is the conformational determination the assignments in the "finger print" region are the most critical for obtaining this information.

The NH_2 and CH_2 stretches were readily assigned as were the deformations and the CH_2 wag. However beginning in the thirteen hundred region there was extensive mixing and the description of the molecular motion was sometimes rather arbitrary. It became particularly difficult to assign the fundamentals in the twelve hundred to one thousand wavenumbers where the bands are very intense in the infrared spectrum but rather weak in the Raman spectrum with extensive overlap of the bands for the second conformer. Therefore, we emphasized the spectral region from 400 to 1000 cm^{-1} for assigning all the modes for both conformers so appropriate conformer pairs could be identified to obtain the enthalpy difference.

Most of these modes are primarily CF motions with the significantly poorer predicted wavenumbers than compared to those for CH motions. Most of these bands have contributions from at least three symmetry coordinates with many of them with contributions (10% or more) from four coordinates. Although many of the descriptions are more for bookkeeping than describing the molecular motions the choice of the bands for the fundamentals of the two conformers were distinguishable for most cases.

The fundamentals below 800 cm^{-1} are mainly CF bands which were not scaled and they are predicted quite well. These include the CF_3 symmetric deformation (ν_{13}, 720

cm^{-1}), 2 CF_3 antisymmetric deformations (ν_{14} and ν_{27}, 585 cm^{-1}), CF_2 deformation (ν_{15}, 526 cm^{-1}) and the CF_2 twist (ν_{29}, 359 cm^{-1}) for the *Tt* conformer.

One might expect similar wavenumbers for these modes for the *Tg* conformer and for some modes the wavenumbers are relatively close. For example the CF_3 antisymmetric deformations at 585 and 536 cm^{-1} for the *Tg* form are comparable to the assignment of 585 cm^{-1} for both of these modes for the *Tt* form but the CF_2 twist is observed at 241 cm^{-1} for the *Tg* conformer rather than near to this mode at 359 cm^{-1} for the *Tt* form. However, the CF_2 wag for the *Tg* conformer is observed at 345 cm^{-1} but there are five symmetry coordinates with the largest one 20% contributing to this vibration. Therefore, there is relatively little correspondence between the vibrational modes of the carbon-fluorine bending modes for the *Tt* and *Tg* conformers as can be observed from the data in Tables 99, 100, S24, and S25.

CONFORMATIONAL STABILITY

To determine the enthalpy differences among the two observed conformers of 2,2,3,3,3-pentafluoropropylamine, the sample was dissolved in liquefied xenon and the mid-infrared spectra were recorded as a function of temperature from -55 to -100°C. Relatively small interactions are expected to occur between xenon and the sample though the sample can associate with itself forming a dimmer, trimer or higher order complex. However, due to the very small concentration of sample (~10^{-4} molar) self association is greatly reduced. Therefore, only small wavenumber shifts are anticipated for the xenon interactions when passing from the gas phase to the liquefied xenon solutions. A significant advantage of this study is that the conformer bands are better resolved in comparison with those in the infrared spectrum of the gas. From *ab initio* calculations,

the dipole moments of the two conformers are predicted to have similar values and the molecular sizes of the two conformers are nearly the same, so the ΔH value obtained from the temperature dependent FT-IR study is expected to be close to that for the gas [16-20].

Once confident assignments have been made for the fundamentals of both conformers the task was then to find a pair or pairs of bands from which the enthalpy determination could be obtained. To minimize the effect of combination and overtone bands in the enthalpy determination it is desirable to have the lowest wavenumber pair(s) that is possible to use for the determination. The bands should also be sufficiently resolved as to determine their intensities. The selection of the bands to use in the enthalpy determination was complicated due to the presence of high intensity bands for both conformers and the near overlap of many modes. The fundamentals at 521 and 867 cm^{-1} were selected for the *Tt* conformer band as they are free of interfering bands and in the lower wavenumber region of the spectrum. The band at 585 cm^{-1} was also selected for the *Tt* form as the predicted interfering bands are estimated to be of very low intensity and the fundamental is in the lower region of the spectrum. For the *Tg* conformer the selection of the bands was more difficult since there are few bands with sufficient separation from the corresponding *Tt* fundamentals to determine their intensities. The fundamentals at 462 and 638 cm^{-1} are relatively free from interfering bands which allowed the determination of their band intensities to be measured.

The intensities of the individual bands were measured as a function of temperature and their ratios were determined (Fig. 65). By application of the van't Hoff equation $-\ln K = \Delta H/(RT) - \Delta S/R$, the enthalpy difference was determined from a plot of

–lnK versus 1/T, where ΔH/R is the slope of the line and K is substituted with the appropriate intensity ratios, *i.e.* $I_{conf\text{-}1}$ / $I_{conf\text{-}2}$, etc. It was assumed that ΔH, ΔS, and α are not functions of temperature in the range studied.

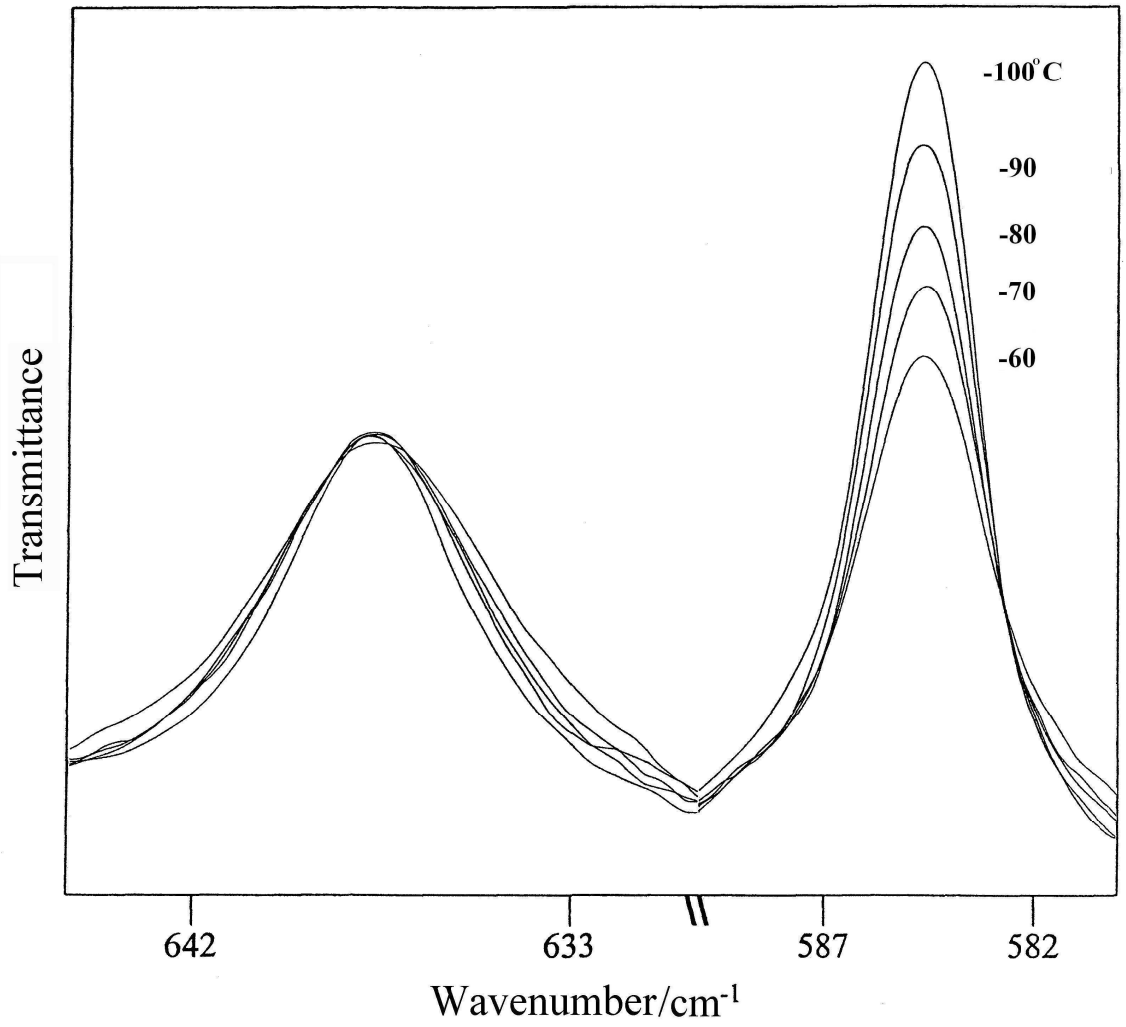

Figure 65. Infrared spectra of 2,2,3,3,3-pentafluoropropylamine in xenon solution at different temperatures.

These five bands, three for *Tt* and two for *Tg*, were utilized for the determination of the enthalpy difference by combining them to form 6 band pairs. The enthalpy difference was determined from these six band pairs with a value of 280 ± 6 cm^{-1} (Table 103). This value is in excellent agreement with the corresponding predicted values from *ab initio* calculations with large basis sets (Table 101). This error limit is derived from the statistical standard deviation of one sigma of the measured intensity data taken as a single data set, but it does not take into account small associations with the liquid xenon or the interference of overtones and combination bands in near coincidence with the measured fundamentals. The variations in the individual values are undoubtedly due to these types of interferences, but by taking several pairs, the effect of such interferences should cancel. However, this statistical uncertainty is probably better than can be expected from this technique and, therefore, an enthalpy difference of 280 ± 14 cm^{-1} is probably more realistic. From the enthalpy difference the abundance of the *Tg* conformer present at ambient temperature is estimated to be 34 ± 2%.

Table 103. Temperature and intensity ratios of the *trans-trans* and *trans-gauche* bands of 2,2,3,3,3-pentafluoropropylamine.

	T(°C)	1/T ($\times 10^{-3}$ K^{-1})	I_{521} / I_{462}	I_{585} / I_{462}	I_{867} / I_{462}	I_{521} / I_{638}	I_{585}/ I_{638}	I_{867} / I_{638}
Liquid xenon	–55.0	4.584	2.547	1.447	2.558	1.946	1.106	1.955
	–60.0	4.692	2.459	1.470	2.492	2.009	1.201	2.035
	–65.0	4.804	2.656	1.560	2.701	2.090	1.227	2.125
	–70.0	4.923	2.758	1.644	2.813	2.175	1.296	2.218
	–75.0	5.047	2.859	1.715	2.971	2.308	1.385	2.398
	–80.0	5.177	3.114	1.882	3.137	2.482	1.500	2.500
	–85.0	5.315	3.138	1.982	3.227	2.536	1.602	2.607
	–90.0	4.460	3.209	1.944	3.262	2.711	1.642	2.756
	–95.0	5.613	3.731	2.347	3.849	2.870	1.806	2.961
	–100.0	5.775	3.795	2.358	3.828	3.088	1.919	3.115
ΔH^a			254 ± 19	301 ± 19	259 ± 19	272 ± 6	318 ± 9	276 ± 6

[a]Average value $\Delta H = 280 \pm 6$ cm^{-1} (3.35 ± 0.08 kJ mol^{-1}) with the *trans-trans* conformer the more stable form and the statistical uncertainty (1σ) obtained by utilizing all of the data as a single set.

STRUCTURAL PARAMETERS

It should be possible to estimate structural parameters for the *Tt* and *Tg* conformers of 2,2,3,3,3-pentafluoropropylamine by adjusting the MP2(full)/6-311+G(d,p) calculated structural parameters using similar molecules as a guideline. The CH bond distances predicted by MP2(full)/6-311+G(d,p) *ab initio* calculations can be used as a good prediction without any adjustment as we [51] have shown that *ab initio* MP2(full)/6-311+G(d,p) calculations predict the r_0 CH distances for more than fifty substituted hydrocarbons to better than ± 0.002 Å compared to the experimentally determined values from isolated CH stretching wavenumbers. The heavy atom and NH_2

parameters can be estimated by using the corresponding parameters in 2,2-difluoroethylamine [172] and 2,2,2-trifluoroethylamine [170] to adjust the corresponding MP2(full)/6-311+G(d,p) calculated parameters. It is believed that the estimated r_0 parameters reported herein for 2,2,3,3,3-pentafluoropropylamine have listed uncertainty values that should be within the experimentally determined parameters. Thus, the listed rotational constants given in Table 102 should make it relatively easy to assign the microwave spectrum from which the experimental parameters could be obtained.

DISCUSSION

The assignments of the fundamentals for the *Tt* conformer could be made rather straight forwardly since they are in such a large proportion (66 ± 2%). However, the assignments for the *Tg* conformer was much more difficult than would be expected since change of the conformers is due to only the rotation of the NH_2 group. Nevertheless, the rotation of the NH_2 results in a very significant structural change since there is undoubtedly hydrogen bonding with both hydrogen atoms on the amine with the two fluorine atoms on the β-carbon atom. These result in drastic changes in the wavenumbers for the modes of the *Tg* conformer compared to the corresponding modes of the *Tt* form. Therefore, significant reliance on the predicted wavenumbers was necessary to assign many of the modes of the *Tg* conformer. Nevertheless the predicted wavenumbers for the *Tt* form had an average error of 11 cm^{-1} which is 0.9% for the A′ modes and 11 cm^{-1} for the A″ modes, which is 1% error. This value is slightly larger than normally obtained with MP2(full)/6-31G(d) predictions for hydrocarbons. Similarly, the *Tg* form had an average error of 10 cm^{-1} which is 1.0%. The predictions of the wavenumbers for the two ND_2 molecules are 0.8% for *Tt* and 1.1 % for *Tg*. A significant amount of the error is due

to the prediction for the NH_2 (ND_2), CH_2, and the symmetric CF_3 stretches along with either the NH_2 twist or wag. However, the assignments for the ND_2 isotopomers give reasonable agreement with the Teller-Redlich product rule which supports the assignments.

Because of the large amount of mixing it was difficult in some cases to give a distinct description of the vibration. This is particular true for several of the vibrations for the *Tg* conformer which has no symmetry elements, i.e. $\nu_{5,}$ $\nu_{13,}$ ν_{17} and ν_{18} where this last one had contributions from 7 symmetry coordinates with 6 of them with 10% and the other one 15%. The description of these vibrations is more for bookkeeping than to provide descriptions for the major atom motions. For the *Tt* form with a plane-of-symmetry there is still extensive mixup particularly with the CF_2 modes as shown by the CF_2 symmetry stretch (1270 cm^{-1}) with only $13S_7$ but $29S_8$ for the CF_3 antisymmetric stretch which is assigned at 1206 cm^{-1} in the $44S_8$. Similar mixup is found for the CF_2 wag (1023 cm^{-1}) with $17S_{10}$ and $24S_{12}$ which is the CF_3 symmetric stretch (781 cm^{-1}) with $25S_{12}$ which is the largest value of the four contributions of 10% or more. These values are representative of the P.E.D.s for many of the CF motions in the A′ block as well as many of the modes for the *Tg* conformer. Similar mixing is also found for the N-deuterated molecules.

With the confidence of the assignments of the lower wavenumber modes for the *Tt* and *Tg* conformers and the use of 6 band pairs as well as the statistical uncertainty the value for the enthalpy difference is believed to be well determined. The uncertainty of the value for each individual pair ranging from a high of 19 cm^{-1} to a low of 6 cm^{-1}. This small spread is a strong indication that there is little interference from overtones or

combination bands having a significant effect on the determined enthalpy difference obtained in this study. Usually we expect an error of ten percent based on this method for obtaining the enthalpy value but we have reduced the estimated error to only 5% because of the small variations of the individual statistical uncertainties. Also the degeneracy of the *Tg* conformer aided the study since a significant amount of this conformer was present (34 ± 2%) which made the assignment of the fundamentals for it more confidently made.

The experimentally determined enthalpy difference between the more stable *Tt* conformer and the *Tg* form with the value of 280 ± 14 cm^{-1} is much larger than expected for the simple rotation of the NH_2 from the *trans* to the *gauche* position where such a change for the $CH_3CH_2NH_2$ molecule has a value of 54 ± 4 cm^{-1} [161]. However the *ab initio* and density functional theory calculations for $CF_3CF_2CH_2NH_2$ give similar energy differences with the largest basis set or with the average of all the values from the basis sets utilized. This very large value is undoubtedly due to the intramolecular hydrogen bonding of the amine hydrogens with the fluorine atoms of the β-carbon atom. This effect is clearly demonstrated by the $HCF_2CH_2NH_2$ molecule where the most stable conformer is the *Tt* form and with the rotation of the NH_2 moiety the *Tg* predicted energy difference is 813 cm^{-1} from the MP2(full)/aug-cc-pVTZ calculations. Therefore the value of 280 ± 14 cm^{-1} for the $CF_3CF_2CH_2NH_2$ molecule is a reasonable enthalpy difference which is undoubtedly affected by the steric effect of the perfluormethyl group.

The estimated structural parameters obtained in the current study should be of considerable value for assigning the microwave spectrum for both the *Tt* and *Tg* conformers. Such a study could be very useful to determine the role of hydrogen bonding

contributing to the relatively large enthalpy difference between the *Tt* and *Tg* forms. Since there are no naturally occurring isotopes of fluorine there are a rather small number of molecules containing fluorine atoms where the structures have been determined from the microwave data.

It is interesting to compare the conformation stability of n-propylamine with 2,2,3,3,3-pentafluoropropylamine to evaluate the effect of the fluorine on two of the carbon atoms. In our earlier study [169] of the normal molecule the Raman spectra were used to show the presence of a least two conformers in the fluid phases. Also it was concluded that the *trans-trans (Tt)* form was the conformer present in the solid state and the *trans-gauche (Tg)* form was the second most stable conformer in the fluid phases and it had nearly equal energy to the *trans-trans* form from *ab intio* MP2/6-31G(d) calculations. However from the potential function obtained from the observed wavenumbers for the asymmetric torsion transitions it was calculated that the enthalpy of 251 cm^{-1} (3.35 kJ/mol) was the difference between the *Tt* and *Tg* forms. This value is not significantly smaller than the value of 280 ±14 cm^{-1} for the pentafluoride molecule. It would be of interest to obtain the enthalpy difference of n-propylamine by a variable temperature study of the Raman spectra in a rare gas solution. Similarly the determinations of the enthalpy differences of $CH_3CF_2CH_2NH_2$ and $HCF_2CH_2NH_2$ would be of interest to assess the effect of the fluorine atoms on the enthalpy differences of these amines.

CHAPTER 17

CONFORMATIONAL AND STRUCTURAL STUDIES OF ISOPROPYLAMINE FROM TEMPERATURE DEPENDENT RAMAN SPECTRA OF XENON SOLUTIONS AND AB INITIO CALCULATIONS

INTRODUCTION

Many organoamine molecules are extremely important biomaterials including pharmaceuticals, pesticides, cleaners, food additives, etc. Recently there has also been a great deal of interest in organoamines in the material sciences and nano-technology fields where organoamines are used for organic light emitting diodes (OLED) and solar cells, as well as, simple nano-machine structures and molecular scaffolding for precision nano-engineering.

Many of these molecules have been extensively studied to determine their most stable conformation and to obtain the energy or enthalpy differences between or among the conformers present at ambient temperature. Additionally, there has been significant interest in the structural parameters for many of the small organoamines and for some of them the carbon-nitrogen or nitrogen-hydrogen bond distances are reported significantly different. Since the organoamines are such important molecules we embarked again on the infrared, Raman and microwave studies of several of them which have been supported by *ab inito* calculations and rare gas solutions to determine the enthalpy differences between or among the conformers identified. We began this study [161] with a vibrational spectroscopic investigation of ethylamine in which it was determined to

have the *trans* conformer more stable by 54 ± 4 cm^{-1} (0.65 ± 0.05 kJ mol^{-1}) than the *gauche* form. This value was in agreement with earlier determined values of 107 ± 70 cm^{-1} (1.28 ± 0.84 kJ mol^{-1}) from electron diffraction study [162], 110 ± 50 cm^{-1} (1.32 ± 0.60 kJ mol^{-1}) from a microwave investigation [163], and 100 ± 10 cm^{-1} (1.20 ± 0.12 kJ mol^{-1}) from an infrared study of ethylamine in an argon matrix [164]. However, several of the earlier studies [165-168] reported the *gauche* conformer as the more stable form, and it is rather interesting that MP2(full)/6-311+G(2d,2p) calculations predict [161] the *gauche* conformer to be the more stable form by 66 cm^{-1} (0.79 kJ mol^{-1}). However, without the diffuse functions the *trans* form is predicted to be the more stable conformer by 32 cm^{-1} (0.38 kJ mol^{-1}).

These results clearly indicate that the enthalpy difference between the *gauche* and *trans* conformers of the NH_2 moiety will need to be determined experimentally rather than by theoretical predictions of organoprimary amines. Thus, it is of scientific interest to determine the effect of substituting one or more of the hydrogen atoms on β-carbon. One of the first molecules we investigated was 2-fluoroethylamine [170] where one of the hydrogen atoms on the β-carbon was replaced by a fluorine atom which is expected to have a significant effect on the C-C distance and it has potential to have five stable conformers, instead of two. With the utilization of variable temperature infrared spectra of xenon solutions we were able to determine the conformational stabilities of all five of the conformers of 2-fluoroethylamine [170].

The most stable conformer was the *Gg′* form with the *Gt* conformer the second most stable form with an enthalpy difference of 62 ± 8 cm^{-1} (0.74 ± 0.10 kJ mol^{-1}), where the first indicator is the NCCF dihedral angle (G=*gauche* or T= *trans*) and the second one

(g=*gauche* or t= *trans*) is the relative position of the lone pair of electrons on the nitrogen atom with respect to the β-carbon atom [*Gg′* is noted by the N-H eclipsing the fluoride]. The third, fourth, and fifth conformers in relative energy are the *Tg* (262 ± 26 cm^{-1}), *Tt* (289 ± 45 cm^{-1}), and *Gg* (520 ± 50 cm^{-1}), respectively, where it was not possible to determine whether the *Tg* or *Tt* was the more stable one. Thus the fluorine atom appears to have an effect on the conformer stability of the ethylene groups so we have continued our investigations of molecules with substitutions on the β-carbon atom of ethylamine with the determination of the conformational stabilities and structural parameters of n-propylamine which has a substitution of the methyl groups which is replacing one of the hydrogen atoms on the β-carbon. However this study is in progress and at the same time we have also replaced one of the hydrogen atoms on the α-carbon of ethylamine with a methyl group, i.e. isopropylamine to evaluate the effect of substitution on this carbon atom.

Therefore as a continuation of our study of the organoamines, we have again investigated vibrational spectra of isopropylamine with particular attention to the assignments for the fundamentals for both conformers, the enthalpy difference between the conformers and the structural parameters. In the first relatively complete vibrational investigation, the Raman spectra of gas, liquid and solid and the infrared spectra of the gas and solid of the normal species as well as the ND_2 isotopologue were investigated from 4000 to 50 cm^{-1} by Durig et al. [198]. From this study the enthalpy differences of 156 and 183 cm^{-1} (1.87 kJ mol^{-1} and 2.19 kJ mol^{-1}) for the d_0 and ND_2 species was found from the potential function obtained from the assignment of the far infrared spectra with the fundamentals of 236 and 221 cm^{-1} for NH_2 torsional modes of the *trans* and *gauche*

conformers, respectively. These values were significantly different from the value of 42 cm^{-1} (0.50 kJ mol^{-1}) reported by Kurgen and Jan [199] from a dilute CCl_4 solution with the *trans* conformer more stable.

The other studies up to this time of the first extensive spectroscopic investigations were detailed in this article [198] with energy differences ranging with the *gauche* conformer more stable to values near zero between the two forms. However, a more recent study [200] by using high-resolution infrared spectra of the gas and low temperature Argon matrix investigation resulted in some significantly different assignments for the fundamentals of both conformers and significantly larger enthalpy difference than the value from the previously reported [198] potential function. In addition to our interest in the enthalpy difference and the vibrational assignments we were interested in the structural parameters since only limited data have been reported**.** In the initial microwave study [201] the authors point out that the structure of the isopropyl group is relatively constant in a wide variety of substances, therefore, it was assumed that the structural parameters of the isopropyl group was nearly the same as those of the groups of seven other molecules so the ∠CCC was taken as 111.8° and the two C-C distances were equal for the *trans* conformer at 1.527 A° which reproduced the observed planar moment when the substitution value for the amine H---H distance. The nine moments of inertia from $(CH_3)_2CHNH_2$, $(CH_3)_2CHNHD$, and $(CH_3)_2CHND_2$ were fit with r(C-N) = 1.49 Å, ∠CCN = 108° and ∠HNC = 109° with estimated uncertainties of ± 0.02 Å and ± 2°. In a later microwave study [194] of $(CH_3)_2CHNH_2$ and $(CH_3)_2CHND_2$ by FT-microwave spectroscopy both centrifugal distortion constants and corrected quadrupole coupling constants as well as more accurate rotational constants were

reported but no information was given for the structural parameters. However a more recent electron diffraction investigation [202] was reported where the parameters were further refined by combining the moments of inertia from the microwave studies. In this study it was assumed that the molecule was 100% *trans* since the NH_2 change to the *gauche* form was not expected to affect significantly the heavy atom parameters. However, we believed that it is possible to obtain the structural parameters for the *trans* conformer more accurately than the values previously reported and estimate those for the *gauche* form which is in large abundance at ambient temperature. Therefore, the three major goals were to correct some of the earlier vibrational assignments, obtain a reliable enthalpy difference between the two conformers from which the concentrations of the two forms could be obtained at ambient temperature, and determine reliable structural parameters for both conformers.

In order to obtain a more reliable experimental value for the conformational enthalpy difference, we have investigated the variable temperature (-50 to -100 °C) Raman spectra (3500 to 100 cm^{-1}) of the sample dissolved in the liquified xenon. We have also reinvestigated the infrared spectra (4000 to 220 cm^{-1}) of the gas and solid. To support these experimental studies we have also obtained the harmonic force constants, infrared intensities, Raman activities, depolarization ratios, and vibrational frequencies from MP2(full)/6-31G(d) *ab intio* calculations. To obtain predictions on the conformational stabilities we have carried out MP2(full) *ab intio* and density functional theory (DFT) calculations by B3LYP method utilizing a variety of basis sets. The r_0 structural parameters have been obtained by combining the MP2(full)/6-311+G(d,p) *ab initio* predicted parameters with the previously reported rotational constants obtained

from the most recent microwave study [194]. The results of these spectroscopic, structural, and theoretical studies of isopropylamine are reported herein.

2. Experiment and theoretical methods

The sample of isopropylamine was purchased from Sigma-Aldrich Chemical Co., with stated purity of ≥99.5%. The sample was used with no further purifications.

The mid-infrared spectrum of the gas (Fig. 66A) and solid (Fig. 66E) were obtained from 4000 to 220 cm^{-1} on a Perkin-Elmer model 2000 Fourier transform spectrometer equipped with a Ge/CsI beamsplitter and a DTGS detector. Atmospheric water vapor was removed from the spectrometer housing by purging with dry nitrogen. The gas and solid spectra were obtained with a theoretical resolution of 0.5 cm^{-1} for the gas and 2 cm^{-1} for the solid with 128 interferograms added and truncated. Multiple annealings were required to obtain satisfactory spectra of the solid.

The Raman spectra (3500 to 100 cm^{-1}) of the sample dissolved in liquefied xenon (Fig. 67) at six different temperatures (-50 to -100^{o}C) were recorded on a Trivista 557 spectrometer consisting of a double f = 50 cm monochromator equipped with a 2000 lines mm^{-1} grating, a f = 70 cm spectrograph equipped with a 2400 lines mm^{-1} grating, and a back-illuminated LN2-cooled PI Acton Spec-10:2 kB/LN 2048 x 512 pixel CCD detector. For all experiments, the 514.5 nm line of a 2017-Ar S/N 1665 Spectra-Physics argon ion laser was used for Raman excitation, with the power set to 0.8 Watt. Signals related to the plasma lines were removed by using an interference filter. The frequencies were calibrated using Neon emission lines, and depending on the setup used, are expected to be accurate within 0.4 cm^{-1}. The experimental set-up used to investigate the solutions has been described before [23,24]. A home-built liquid cell equipped with four quartz

windows at right angles was used to record the spectra. The infrared and Raman bands assigned as fundamentals along with their proposed assignments and depolarization values are listed in Tables 104 and 105, respectively.

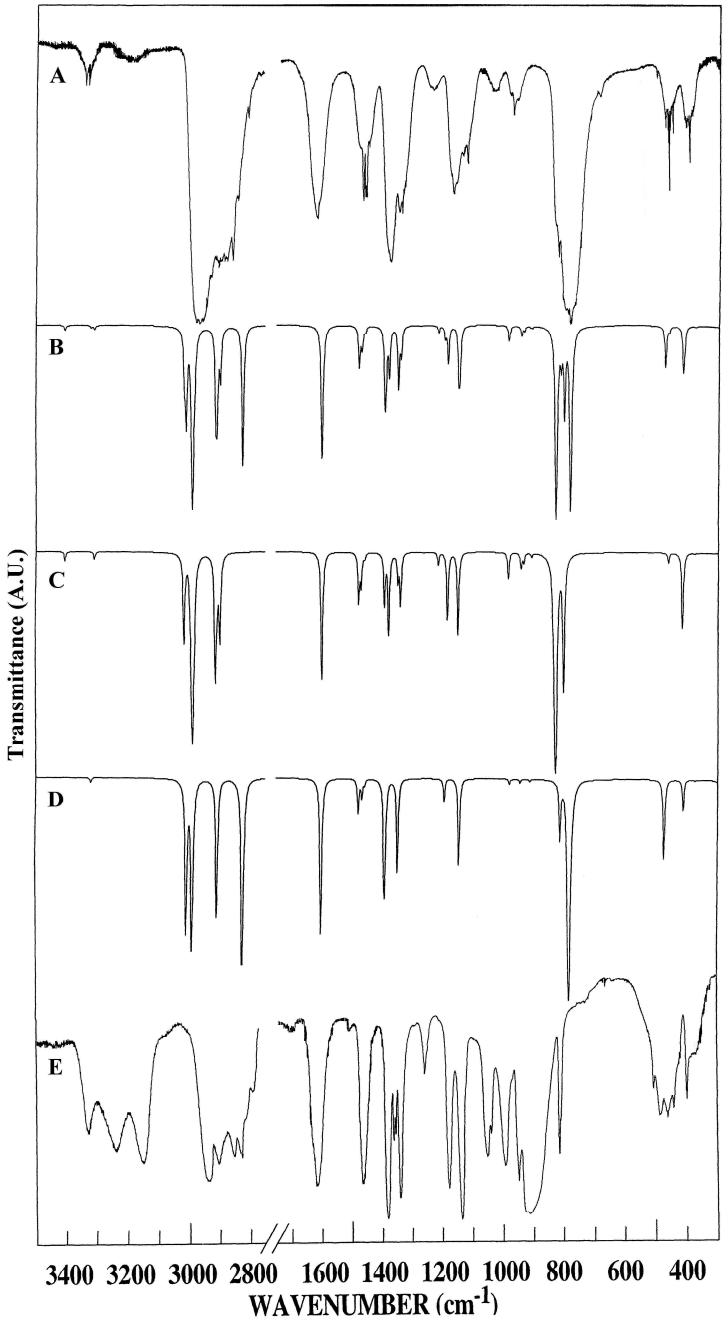

Figure 66. Experimental and predicted infrared spectra of isopropylamine: (A) gas; (B) simulated spectrum of *T* and *G*; enthalpy difference of 113 cm^{-1} at 25°C; (C) simulated spectrum of *G* conformer; (D) simulated spectrum of *T* conformer (D) solid.

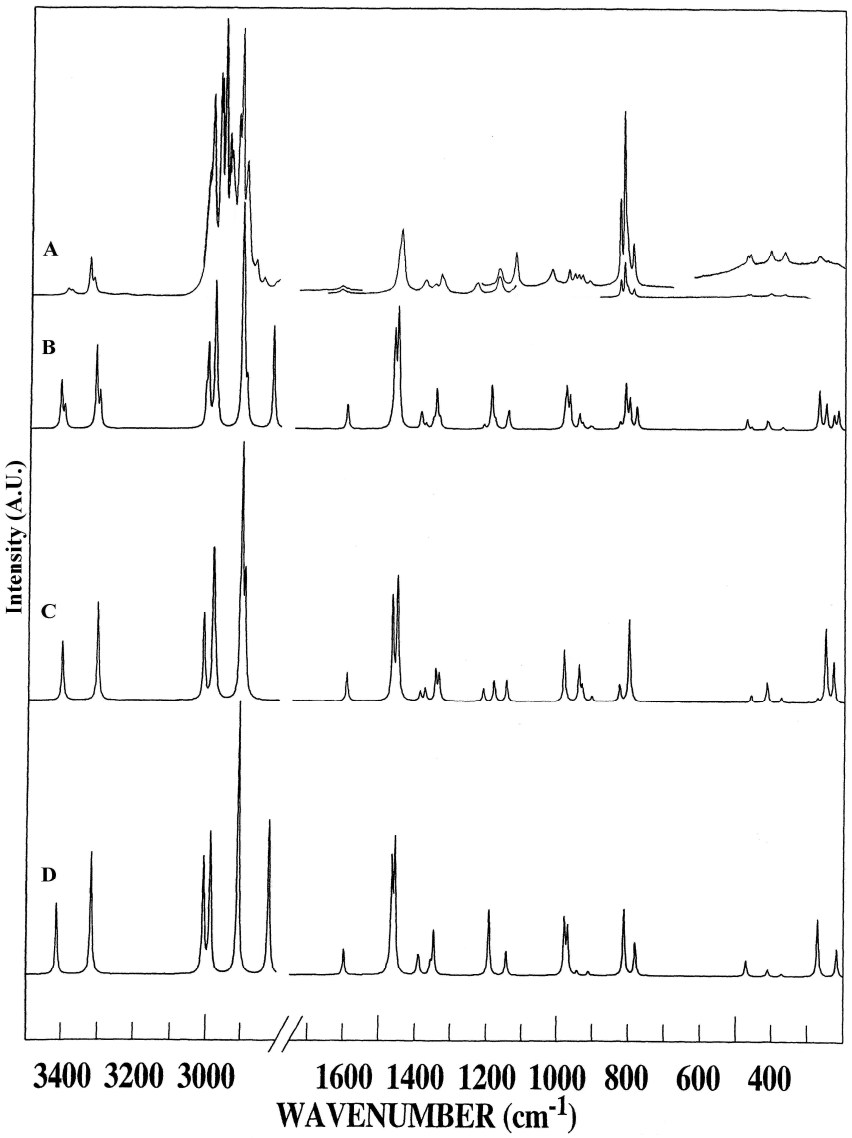

Figure 67. Experimental and predicted Raman spectra of isopropylamine: (A) xenon solution at -100°C; (B) simulated spectrum of *T* and *G;* enthalpy difference of 113 cm^{-1} at -100°C; (C) simulated spectrum of *G* conformer; (D) simulated spectrum of *T* conformer.

Table 104. Observed and calculated[a] frequencies (cm^{-1}) for *trans* isopropylamine.

	Vib. No.	Approximate Descriptions	*ab initio*	fixed scaled[b]	IR int.	Raman act.	dp ratio	IR Gas	xenon solution	Raman gas[c]	IR Solid	P.E.D.[d]	Band Contours B*	Band Contours C*
A′	ν_1	NH_2 symmetric stretch	3497	3318	0.7	106.4	0.12	3341	3325	3342	3347	$100S_1$	100	-
	ν_2	CH_3 antisymmetric stretch , in-plane, in phase	3207	3009	40.2	81.7	0.75	2960	2959		2960	$58S_2$, $42S_3$	20	80
	ν_3	CH_3 antisymmetric stretch , out-of- plane, in phase	3188	2990	37.6	76.3	0.74	2940	2937	2932	2947	$57S_3$,$42S_2$	87	13
	ν_4	CH_3 symmetric stretch, in phase	3102	2910	3.6	183.1	0.00	2920	2920	2918	2920	$99S_4$	96	4
	ν_5	CH stretch	3009	2823	72.2	100.6	0.37	2820	2821		2872	$99S_5$	3	97
	ν_6	NH_2 scissor	1722	1633	37.8	7.4	0.67	1621	1619		1614	$77S_6$,$21S_{14}$	70	30
	ν_7	CH_3 antisymmetric deformation, in-plane, in phase	1574	1478	6.5	1.0	0.71	1472	1470	1469	1467	$82S_7$,$10S_{12}$	37	63
	ν_8	CH_3 antisymmetric deformation , out-of-plane, in phase	1560	1465	3.1	26.1	0.75	1461	1458	1460	1459	$84S_8$,$10S_{11}$	2	98
	ν_9	CH_3 symmetric deformation, in phase	1475	1391	17.0	3.5	0.69	1382	1382	1388	1385	$87S_9$	82	18
	ν_{10}	CH bend	1430	1350	18.0	8.8	0.53	1352	1354		1350/1353	$68S_{10}$,$10S_{12}$,,$10S_9$	98	2
	ν_{11}	CH_3 rock , out-of-plane, in phase	1255	1196	4.3	4.2	0.63	1181	1180	1178	1180	$49S_{11}$,$14S_{17}$,$12S_{15}$	40	60
	ν_{12}	CH_3 rock, in plane, in phase	1205	1146	21.3	4.0	0.26	1128	1128	1130	1132	$33S_{12}$,$22S_{13}$,$17S_{16}$,$15S_{10}$	34	66
	ν_{13}	C-N stretch	1042	989	6.5	7.6	0.73	978	976	970	989	$33S_{13}$,$23S_{12}$,$14S_{14}$,$14S_{11}$,$10S_{15}$	4	96
	ν_{14}	NH_2 wag	918	871	130.1	4.2	0.75	786	793	792	810	$58S_{14}$,$15S_6$,$10S_{15}$,$10S_{12}$	34	66
	ν_{15}	C-C-C symmetric stretch	854	810	1.8	8.1	0.17	818	818	819	814/816	$57S_{15}$,$25S_{13}$,$10S_{11}$	69	31
	ν_{16}	C-C-N deformation, in-plane	489	474	13.0	0.8	0.50	472	472	472	471	$62S_{16}$,$15S_{17}$	68	32
	ν_{17}	C-C-C symmetric deformation	378	375	0.2	0.1	0.44	369[c]	369	368	370	$65S_{17}$,$20S_{16}$	53	47
	ν_{18}	CH_3 torsion, in-plane	288	270	0.3	0.0	0.40	270	272			$99S_{18}$	94	6
A″	ν_{19}	NH_2 antisymmetric stretch	3599	3414	0.0	65.3	0.75	3411[c]	3390	-		$100S_{19}$	-	-

ν_{20}	CH_3 antisymmetric stretch, in-plane, in phase	3203	3005	0.8	6.1	0.75	2960	2959	-	2960	$55S_{20},44S_{21}$	-	-
ν_{21}	CH_3 antisymmetric stretch, out-of- plane, out-of- phase	3185	2988	17.8	35.4	0.75	2930	2932	-	2927	$55S_{21},45S_{20}$	-	-
ν_{22}	CH_3 symmetric stretch, out-of- phase	3099	2908	31.0	5.3	0.75	2906	2906	-	2906	$99S_{22}$	-	-
ν_{23}	CH_3 antisymmetric deformation, in- plane, out-of- phase	1553	1459	0.2	1.3	0.75	1452	1449	-	1452	$40S_{23},41S_{24}$	-	-
ν_{24}	CH_3 antisymmetric deformation, out-of-phase	1551	1457	0.3	30.5	0.75	1452	1449	-	1452	$50S_{24},43S_{23}$	-	-
ν_{25}	CH bend	1477	1401	17.0	1.2	0.75	1382	1382	-	1385	$29S_{25},22S_{26},15S_{28},13S_{27}$	-	-
ν_{26}	CH_3 symmetric deformation, out-of-phase	1441	1362	0.9	2.2	0.75	1368	1364	-	1377	$74S_{26},16S_{25}$	-	-
ν_{27}	NH_2 twist	1307	1243	0.0	11.3	0.75	1243	1240	-	1246	$38S_{27},34S_{25},10S_{29}$	-	-
ν_{28}	C-C-C antisymmetric stretch	1081	1026	0.8	3.9	0.75	1030	1025	-	1039/1055	$48S_{28},37S_{27},10S_{29}$	-	-
ν_{29}	CH_3 rock, in plane, out-of- phase	1001	949	0.5	2.9	0.75	951	948	-	948	$69S_{29},23S_{28}$	-	-
ν_{30}	CH_3 rock, in plane, out-of- phase	963	912	0.5	0.3	0.75	918	918	-	907	$82S_{30},11S_{25}$	-	-
ν_{31}	C-C-N deformation, out-of- plane	417	413	5.2	0.3	0.75	404	405	-	397	$85S_{31}$	-	-
ν_{32}	NH_2 torsion	316	271	37.3	1.5	0.75	270	272	-		$71S_{32},27S_{33}$	-	-
ν_{33}	CH_3 torsion, out-of-phase	237	218	15.6	0.5	0.75	236[c]	238	-		$71S_{33},27S_{32}$	-	-

[a]MP2(full)/6-31G(d) *ab initio* calculations, scaled frequencies, infrared intensities (km/mol), Raman activities ($Å^4$/amu), depolarization ratios and potential energy distributions (P.E.D.s)

[b]MP2(full)/6-31G(d) fixed scaled frequencies with factors of 0.88 for CH stretches and deformations, 0.70 for the NH_2 torsion, 1.0 for heavy atom bends, and 0.90 for all other modes.

[c]Ref [198]

[d]Calculated with MP2(full)/6-31G(d) and contributions of less than 10% are omitted.

[*]A, B and C values in the last three columns are percentage infrared band contours.

Table 105. Observed and calculated[a] frequencies (cm^{-1}) for *gauche* isopropylamine.

Vib. No.[b]	Approximate Descriptions	*ab initio*	fixed scaled[c]	IR int.	Raman act.	dp ratio	IR gas	xenon solution	Raman gas[d]	P.E.D.[e]	Band Contours		
											A*	B*	C*
ν_{19}	NH_2 antisymmetric stretch	3588	3404	1.6	54.6	0.70	3393	3380	3393	$100S_{19}$	-	18	82
ν_1	NH_2 symmetric stretch	3486	3307	1.3	85.4	0.11	3327	3314	3328	$100S_1$	13	14	73
ν_3	CH_3 antisymmetric stretch , out-of- plane, in phase	3214	3015	17.9	63.3	0.70	2967	2968	2968	$26S_3,26S_2,24S_{21},22S_{20}$	53	41	6
ν_2	CH_3 antisymmetric stretch , in-plane, in phase	3186	2989	55.1	85.7	0.61	2940	2937	2945	$67S_2,18S_3,11S_{21}$	-	41	59
ν_{20}	CH_3 antisymmetric stretch, in-plane, in phase	3183	2986	22.4	42.6	0.70	2930	2932	2932	$51S_{20},39S_3$	12	41	46
ν_{21}	CH_3 antisymmetric stretch, out-of- plane, out-of- phase	3177	2981	13.9	19.1	0.71	2930	2932	2932	$57S_{21},27S_{20},13S_3$	35	4	61
ν_5	CH stretch	3104	2912	29.0	44.4	0.75	2920	2920	2918	$75S_{5,}17S_4$	-	6	94 94
ν_4	CH_3 symmetric stretch, in phase	3098	2906	7.3	160.4	0.07	2906	2906		$44S_4,28S_{22},21S_5$	35	65	-
ν_{22}	CH_3 symmetric stretch out-of-phase	3089	2897	17.1	74.5	0.01	2899	2899		$63S_{22},36S_4$	93	2	5
ν_6	NH_2 scissor	1720	1632	29.1	7.9	0.70	1621	1619		$77S_6,21S_{15}$	23	33	44
ν_7	CH_3 antisymmetric deformation, in-plane, in phase	1571	1476	9.5	0.7	0.66	1472	1470	1469	$77S_7,11S_8,10S_{12}$	2	14	84
ν_8	CH_3 antisymmetric deformation , out-of- plane, in phase	1565	1470	5.4	22.6	0.75	1466	1463		$72S_8,11S_7$	-	10	90
ν_{24}	CH_3 antisymmetric deformation, out-of- phase	1552	1457	0.7	4.2	0.75	1452	1449	1449	$75S_{24},10S_{23}$	78	2	20
ν_{23}	CH_3 antisymmetric deformation, in- plane, out-of- phase	1549	1454	0.3	28.9	0.75	1452	1449	1449	$85S_{23},10S_{24}$	28	39	33
ν_9	CH_3 symmetric deformation, in phase	1477	1395	11.4	4.7	0.74	1382	1382		$58S_9,10S_{10}$	19	77	4
ν_{26}	CH_3 symmetric deformation, out-of- phase	1461	1381	13.9	3.2	0.66	1377	1375	1370	$38S_{26},32S_9,11S_{25}$	83	-	17
ν_{10}	CH bend	1444	1363	3.9	6.8	0.73	1368	1364		$32S_{10},42S_{26},11S_{27}$	63	11	26
ν_{25}	CH bend	1413	1339	10.3	6.0	0.75	1339	1338	1338	$54S_{25},19S_{10},10S_{26}$	69	31	-
ν_{12}	CH_3 rock, in plane, in phase	1322	1259	4.3	2.6	0.71	1254	1256	1259	$18S_{12},30S_{27},15S_{16},10S_{11}$	-	94	6
ν_{11}	CH_3 rock , out-of- plane, in	1245	1185	7.2	3.8	0.71	1172	1173	1178		-	99	-

	phase									$28S_{11,}19S_{13},11S_{12},11S_{10}$			
ν_{28}	C-C-C antisymmetric stretch	1212	1156	26.3	3.3	0.72	1140	1141		$28S_{28,}19S_{29},11S_{11},10S_{25}$	82	15	3
ν_{13}	C-N stretch	1083	1026	2.8	3.7	0.72	1030	1025	1033	$30S_{13},43S_{12},14S_{14}$	18	2	80
ν_{27}	NH_2 twist	1012	960	0.7	6.5	0.75	951	948		$35S_{27},19S_{11},13S_{13},12S_{28}$	-	78	22
ν_{29}	CH_3 rock, in plane, out-of-phase	990	939	14.8	4.6	0.74	940	938		$45S_{29},34S_{28}$	44	54	2
ν_{30}	CH_3 rock, in plane, out-of-phase	957	907	2.9	0.7	0.75	918	918		$79S_{30},10S_{25}$	7	91	2
ν_{15}	NH_2 wag	946	897	143.9	1.9	0.71	826	830	826	$55S_{15},17S_{29},14S_{6}$	46	54	-
ν_{14}	C-C-C symmetric stretch	846	802	7.6	9.5	0.15	810	811		$62S_{14},24S_{13},10S_{11}$	26	74	-
ν_{16}	C-C-N deformation, in-plane	478	462	1.2	0.4	0.33	459	463	463	$58S_{16},18S_{17}$	80	17	3
ν_{31}	C-C-N deformation, out-of-plane	423	417	13.1	1.0	0.69	406	405	406	$80S_{31}$	-	97	3
ν_{17}	C-C-C symmetric deformation	379	376	0.1	0.2	0.39	369 [d]	369	368	$59S_{17},24S_{16}$	14	56	30
ν_{18}	CH_3 torsion, in-plane	295	275	1.0	0.1	0.55	270	272		$94S_{18}$	-	26	74
ν_{32}	NH_2 torsion	291	252	31.4	1.7	0.74	221[d]	223		$64S_{32},19S_{33}$	23	20	57
ν_{33}	CH_3 torsion, out-of- phase	249	230	15.2	0.8	0.74	236[d]	238		$64S_{33,}\ 33S_{32}$	23	21	56

[a] MP2(full)/6-31G(d) *ab initio* calculations, scaled frequencies, infrared intensities (km/mol), Raman activities ($Å^4$/amu), depolarization ratios and potential energy distributions (P.E.D.s)

[b] In order of decending frequency

[c] MP2(full)/6-31G(d) fixed scaled frequencies with factors of 0.88 for CH stretches and deformations, 0.70 for the NH_2 torsion,1.0 for heavy atom bends, and 0.90 for all other modes.

[d] Ref [198]

[e] Calculated with MP2(full)/6-31G(d) and contributions of less than 10% are omitted.

[*] A, B and C values in the last three columns are percentage infrared band contours.

Table 106. Calculated energies (hartree) and energy differences (cm^{-1}) for the two conformers and transition states of isopropylamine

Method/Basis Set	# *basis set*	Energy[a], E	Energy Differences, Δ		
		trans	*gauche*[b]	($t \rightarrow g$)[d] barrier	($g \rightarrow t$)[e] barrier
RHF/6-31G(d)	78	0.285678	116	910	1026
MP2(full)/6-31G(d)	78	0.863972	72	1014	1086
MP2(full)/6-31+G(d)	94	0.877327	228	807	1035
MP2(full)/6-31G(d,p)	105	0.941879	65	1000	1064
MP2(full)/6-31+G(d,p)	121	0.954027	237	774	1011
MP2(full)/6-311G(d,p)	126	1.062299	44	929	973
MP2(full)/6-311+G(d,p)	142	1.069475	204	768	972
MP2(full)/6-311G(2d,2p)	173	1.116801	85	883	968
MP2(full)/6-311+G(2d,2p)	189	1.122603	202	777	979
MP2(full)/6-311G(2df,2pd)	246	1.187136	84	877	962
MP2(full)/6-311+G(2df,2pd)	262	1.192526	197	772	969
Average MP2(full)		----------	71 / 201[c]	834 ± 70	970 ± 6
B3LYP/6-31G(d)	78	1.487268	-4	953	949
B3LYP/6-31+G(d)	94	1.497602	117	780	897
B3LYP/6-311G(d,p)	126	1.544412	15	854	870
B3LYP/6-311+G(d,p)	142	1.549361	125	723	848
B3LYP/6-311G(2d,2p)	173	1.552714	16	785	801
B3LYP/6-311+G(2d,2p)	189	1.557380	134	695	829
B3LYP/6-311G(2df,2pd)	246	1.556893	26	780	806
B3LYP/6-311+G(2df,2pd)	262	1.561466	138	689	827
B3LYP/aug-cc-pVTZ	391	1.566119	140	684	824
B3LYP Average		----------	85 ± 62	744 ± 64	829 ± 24

[a] Energy of conformer is given as –(E+173) H.
[b] Difference is relative to *trans* form and given in cm^{-1}.
[c] Average without diffuse functions / Average with diffuse functions.
[d] Difference is relative to *trans* form and given in cm^{-1}.
[e] Difference is relative to *guache* form and given in cm^{-1}.

A variety of basis sets as well as the corresponding ones with diffuse functions were employed with the Møller-Plesset perturbation method [21] to the second order

MP2 with full electron correlation as well as with the density functional theory by the B3LYP method. The predicted conformational energy differences are listed in Table 106.

In order to obtain descriptions of the molecular motions involved in the fundamental modes of isopropylamine, a normal coordinate analysis was carried out. The force field in Cartesian coordinates was obtained with the Gaussian 03 program at the MP2(full) level with the 6-31G(d) basis set. The internal coordinates used to calculate the G and B matrices are given for the *trans* and *gauche* conformers in Table 107 with the atomic numbering shown in Fig. S5. By using the B matrix [30], the force field in Cartesian coordinates was converted to force constants in internal coordinates. Subsequently, 0.88 was used as the scaling factor for the CH stretches and deformations, 0.70 for the NH_2 torsion, and 0.90 was used for all other modes excluding the heavy atom bends to obtain the fixed scaled force constants and resultant wavenumbers. A set of symmetry coordinates was used (Table S27) to determine the corresponding potential energy distributions (P.E.D.s). A comparison between the observed and calculated wavenumbers, along with the calculated infrared intensities, Raman activities, depolarization ratios and potential energy distributions for the *trans* and *gauche* conformers of isopropylamine are given in Tables 104 and 105, respectively.

Table 107. Structural parameters[a], rotational constants, and dipole moments for *trans* and *gauche* isopropylamine.

		trans					*gauche*		
Parameter	Int. Coor.	MP2(full)/ 6-311+G(d,p)	B3LYP/ 6-311+G(d,p)	ED[b]	MW[c]	adjusted r_0[d]	MP2(full)/ 6-311+G(d,p)	B3LYP/ 6-311+G(d,p)	Predicted r_0
r N_1-C_2	X_1	1.466	1.473	1.469(13)	1.49(2)	1.465(3)	1.466	1.472	1.465
r C_4-C_2	R_1	1.522	1.529	1.529(5)	1.527*	1.530(3)	1.522	1.530	1.530
r C_5-C_2	R_2	1.522	1.529	1.529(5)	1.527*	1.530(3)	1.530	1.537	1.538
r N_1-H_6	x_1	1.016	1.015	1.031*		1.019(3)	1.017	1.017	1.020
r N_1-H_7	x_2	1.016	1.015	1.031*		1.019(3)	1.016	1.015	1.019
r C_2-H_3	r_1	1.102	1.103	1.111*		1.102(2)	1.097	1.097	1.097
r C_4-H_9	r_2	1.094	1.094	1.104(15)		1.094(2)	1.096	1.096	1.096
r C_4-H_{11}	r_3	1.095	1.095	1.104(15)		1.095(2)	1.092	1.092	1.092
r C_4-H_{13}	r_4	1.094	1.093	1.104(15)		1.094(2)	1.093	1.093	1.093
r C_5-H_8	r_5	1.094	1.094	1.104(15)		1.094(2)	1.096	1.096	1.096
r C_5-H_{10}	r_6	1.095	1.095	1.104(15)		1.095(2)	1.095	1.094	1.095
r C_5-H_{12}	r_7	1.094	1.093	1.104(15)		1.094(2)	1.095	1.095	1.095
∠ $N_1C_2C_4$	ε_1	108.6	108.9	108.9(9)	108(2)	108.9(5)	108.4	108.8	108.7
∠ $N_1C_2C_5$	ε_2	108.6	108.9	108.9(9)	108(2)	108.9(5)	113.9	114.0	114.2
∠ $C_4C_2C_5$	η	111.4	111.7	114.4(16)	111.8*	111.0(5)	111.0	111.5	110.6
∠ $H_6N_1H_7$	γ	106.9	107.2	106.0		106.9(5)	106.5	107.0	106.5
∠ $C_2N_1H_6$	δ_1	110.3	110.9	111.5*	109(2)	110.3(5)	109.5	110.5	109.5
∠ $C_2N_1H_7$	δ_2	110.3	110.9	111.5*	109(2)	110.3(5)	110.3	110.9	110.3
∠ $N_1C_2H_3$	β_1	112.1	111.7	111.8*		112.1(5)	106.5	106.1	106.5
∠ $H_3C_2C_4$	β_2	108.1	107.8			108.0(5)	108.4	108.0	108.3
∠ $H_3C_2C_5$	β_3	108.1	107.8			108.0(5)	108.4	108.1	108.3
∠ $C_2C_4H_9$	ρ_1	109.7	110.3	111.1(32)		109.7(5)	110.1	110.6	110.0
∠ $C_2C_4H_{11}$	ρ_2	111.0	111.1	111.1(32)		111.0(5)	110.5	110.6	110.5

∠ $C_2C_4H_{13}$	ρ_3	110.8	110.9	111.1(32)	110.8(5)	111.0	111.2	111.0
∠ $C_2C_5H_8$	ρ_4	109.7	110.3	111.1(32)	109.7(5)	110.1	110.6	110.1
∠ $C_2C_5H_{10}$	ρ_5	111.0	111.1	111.1(32)	111.0(5)	111.0	111.0	111.0
∠ $C_2C_5H_{12}$	ρ_6	110.8	110.9	111.1(32)	110.8(5)	111.3	111.5	111.3
∠ $H_9C_4H_{11}$	α_1	108.3	108.0		108.3(5)	108.3	108.0	108.3
∠$H_{11}C_4H_{13}$	α_2	108.0	107.7		108.0(5)	109.0	108.7	109.0
∠ $H_9C_4H_{13}$	α_3	109.0	108.7		109.0(5)	107.9	107.6	107.9
∠ $H_8C_5H_{10}$	α_4	108.3	108.0		108.3(5)	108.1	107.9	108.1
∠$H_{10}C_5H_{12}$	α_5	108.0	107.7		108.0(5)	108.1	107.8	108.1
∠ $H_8C_5H_{12}$	α_6	109.0	108.7		109.0(5)	108.2	107.9	108.2
τ$H_6N_1C_2H_3$	τ_1	60.0	60.0		59.0(5)	-177.0	-178.8	-177.0
τ$H_7N_1C_2H_3$	τ_2	-60.0	-60.0		-59.0(5)	66.1	62.7	66.1
τ$H_8C_4C_2N_1$	τ_3	-59.4	-59.9		-59.8(5)	-62.3	-63.0	-62.3
τ$H_9C_5C_2N_1$	τ_4	59.4	59.9		59.8(5)	64.2	63.9	64.2
A		8391.30	8308.59	8331.92(2)	8332.77	8222.93	8135.66	8187.89
B		8016.30	7934.61	7977.32(2)	7977.08	7984.19	7896.97	7924.13
C		4689.37	4629.71	4657.17(8)	4656.62	4689.08	4625.39	4657.81
$\lvert\mu_a\rvert$		0.00	0.00	0.00		1.28	1.18	
$\lvert\mu_b\rvert$		0.07	0.07	0.10(4)		0.38	0.36	
$\lvert\mu_c\rvert$		1.42	1.34	1.19(3)		0.48	0.40	
$\lvert\mu_t\rvert$		1.42	1.34	1.19(3)		1.41	1.30	

[a]Bond distances in Å, bond angles in degrees, rotational constants in MHz, and dipole moments in Debye.
[b]Ref [202]; asterisk indicates fixed values.
[c] Structural parameters and dipole moments from ref [201], with rotational constants from ref [194]; asterisk indicates assumed values.
[d]Adjusted structural parameters with experimental rotational constants taken from Ref [194].

VIBRATIONAL ASSIGNMENT

The first comprehensive vibrational assignment for isoporpylamine [198] was made by utilizing the Raman spectra of the gas, liquid, and solid as well as the infrared spectra of the gas and solid for both the normal species along with the ND_2 molecule which made it possible to identify the modes involving mainly the amines. The vibrational assignments were made mostly based on existing assignments of corresponding vibrations of similar molecules. In the more recent report on the vibrational assignments [200] the authors utilized predictions from *ab intio* calculations with the 4-31G(N*) basis set and infrared spectral data from an argon matrix along with higher resolution for the FT-IR spectrum. Although one might expect the improved resolution would aid in making the vibrational assignment the breath of many of the bands resulted in little information for making the vibrational assignments but the *ab inito* predictions provided some guidance for assigning the fundamentals for the two conformers. Nevertheless there were only six fundamentals that were assigned as arising from the *trans* form with a similar number for the *gauche* conformer and the rest for both conformers. From the argon matrix, three additional fundamentals were assigned for each conformer in this region of the spectrum where they could not be separated from the spectrum of the gas. For the frequencies of the individual conformers there were only one for each form which differed from the earlier assignments. However, some of the assignments which were attributed to both conformers differed whether they were originally assigned as A' or A" modes while others have different vibrational descriptions or are not assigned. In fact there were only two that differed frequencies as fundamentals for the assigned bands for both conformers, one for the fundamentals assigned only to the

trans form and two for those assigned only to the *gauche* conformer as originally assigned. However, by the utilization of MP2(full)/6-31G(d) predicted vibrational wavenumbers along with *ab intio* predicted intensities, and depolarization ratios along with Raman data from xenon solutions it has been possible to assign a significantly larger number of the fundamentals for each of the conformers. This is important for obtaining the enthalpy difference since the fundamentals being used for the temperature study must be for a single confidently identified conformer. Therefore, we have attempted to assign all of the fundamentals for both conformers except for the carbon-hydrogen stretching modes. The most emphasis has been placed on the assignments for the fingerprint region from 1700 to 400 cm^{-1} where it was expected to find vibrational modes from the $(CH_3)_2CH$ moiety.

The assignments for the NH_2 stretching modes for both conformers were readily made from the Raman spectra of the xenon solution and from the Raman spectrum of the gas (Fig. 68) and they agree with the assignments previously reported. The assignments for the carbon-hydrogen stretches are similar to those previously reported with the frequencies for the fundamentals of the two conformers nearly the same except for the C-H mode where the *ab inito* calculations predicts a difference of 74 cm^{-1} with the fundamental of the *trans* form with the lower frequency. There appears to be a Fermi doublet at 2920 cm^{-1} and 2868 cm^{-1} so this lower frequency band is part of the Fermi doublet and cannot be the lower frequency CH stretching fundamental. Thus the weak band at 2821 cm^{-1} is assigned as the CH bend of the *trans* conformer but it could be the higher frequency band at 2851 cm^{-1}. However, it is doubtful that the *ab initio* prediction would be that far off.

The frequencies for the NH_2 scissors and the four CH_3 antisymmetric deformations also have essentially the same frequencies. However, most of the remaining fundamentals in the fingerprint spectral region have slightly different frequencies for the corresponding modes for the two conformers. For example, the two CH bends and the symmetric CH_3 deformations have slightly different frequencies for the two conformers. However, these eight fundamentals fall in relatively small frequency range of 1382 to 1339 cm^{-1} which results in a nondescript infrared band contour which makes it almost impossible to assign these fundamentals (Fig. 66A) from the infrared spectrum of the gas. However, the Raman spectrum of the xenon solution shows seven of the eight bands clearly (Fig. 69A). In the liquid these fundamentals appear as three rather broad lines.

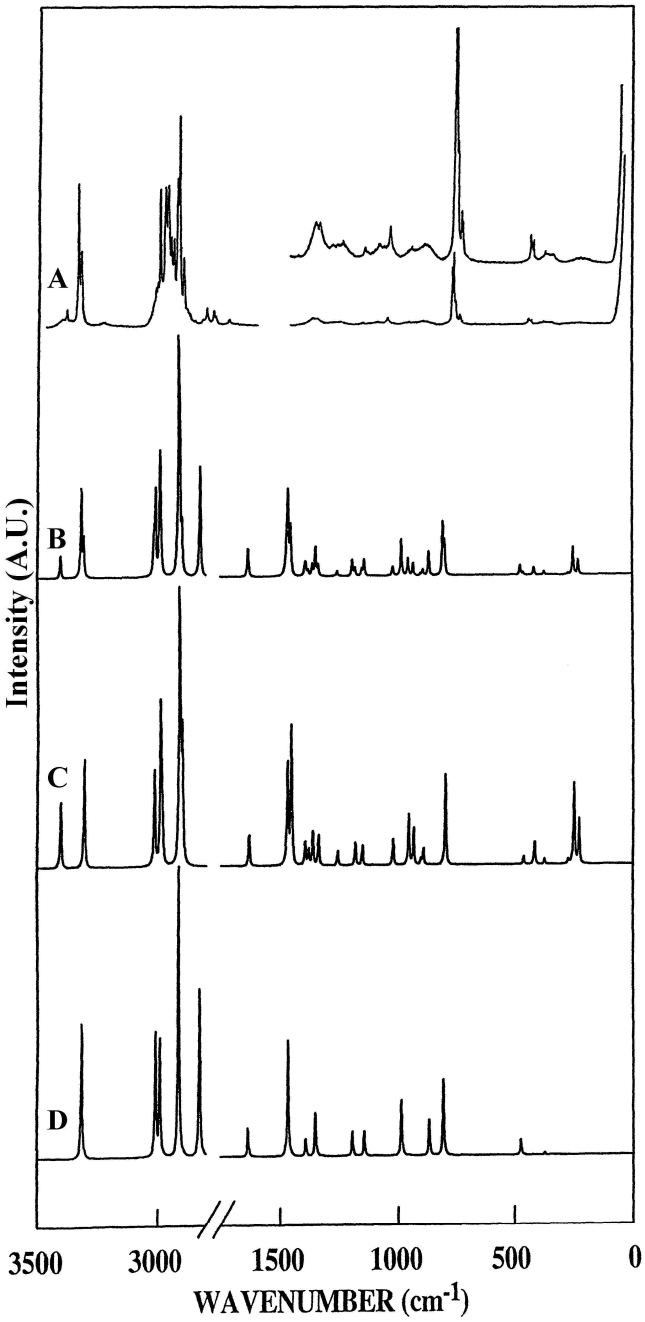

Figure 68. Experimental and predicted Raman spectra of gaseous isopropylamine: (A) Experimental; (B) simulated spectrum of *T* and *G;* enthalpy difference of 113 cm^{-1} at 25°C; (C) simulated spectrum of *G* conformer; (D) simulated spectrum of *T* conformer.

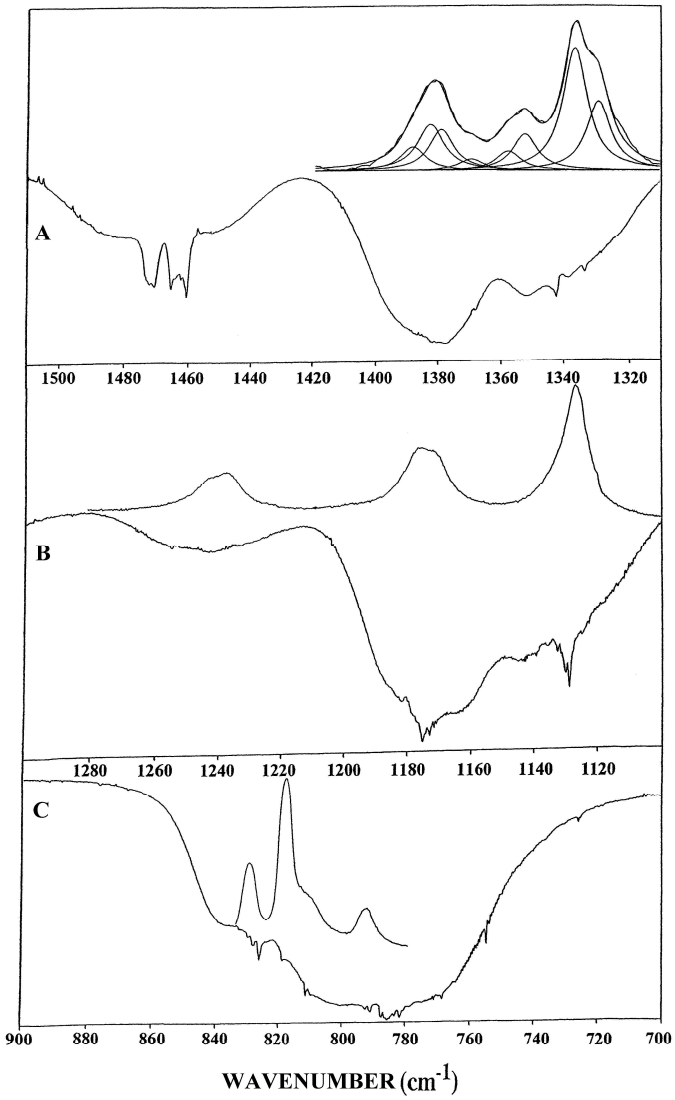

Figure 69. Raman spectra of the xenon solution (Top) and infrared spectra of the gaseous (Bottom) of isopropylamine (A) 1510 - 1310 cm^{-1}; (B) 1300 – 1100 cm^{-1}; (C) 900 – 700 cm^{-1}.

By using the Raman spectrum of the xenon solution the two predicted fundamentals in the 1200 cm^{-1} region are clearly observed whereas they simply appear as a very weak broad band in the infrared spectrum of the gas (Fig. 70). There are four fundamentals predicted in the 1100 cm^{-1} region at 1196, 1185, 1156, and 1146 cm^{-1} and again these fundamentals are clearly observed in the Raman spectrum of the xenon solution at 1180, 1173, 1141 and 1128 cm^{-1}. The two fundamentals of the *trans* conformer are clearly observed as Q-branches at 1181 and 1128 cm^{-1} (60%, 66% C-contour) in the infrared spectrum of the gas (Fig. 69B) (1178 and 1130 cm^{-1} Raman spectrum of the gas) but these fundamentals for the *gauche* conformer have predicted band contours of 99% B and 82% A type which makes it almost impossible to assign the B-type band but from the Raman spectrum they are observed at 1173 and 1141 $cm^{-1.}$

The third and most complex region for making vibrational assignments is from 900 to 700 cm^{-1} (Fig. 69C) where there are four fundamentals. On the high frequency side of the broad band in the infrared spectrum is a series of Q-branches at 826 cm^{-1} with two excited state bands falling to higher frequency and thus must be the NH_2 wag for the *gauche* conformer. The corresponding fundamental for the *trans* form is clearly observed at 786 cm^{-1} with a large number of hot band Q-branches falling to both high and low frequencies. There are also two weak bands at 818 and 810 cm^{-1} in the infrared spectrum which appear as a relatively strong Raman line at 818 cm^{-1} (xenon solution) for the *trans* conformer with a pronounced Q-branch at 811 cm^{-1} and a shoulder at the same frequency in the Raman spectrum. The assignments for the remaining fundamentals for both conformers are readily made and there is no need to discuss them.

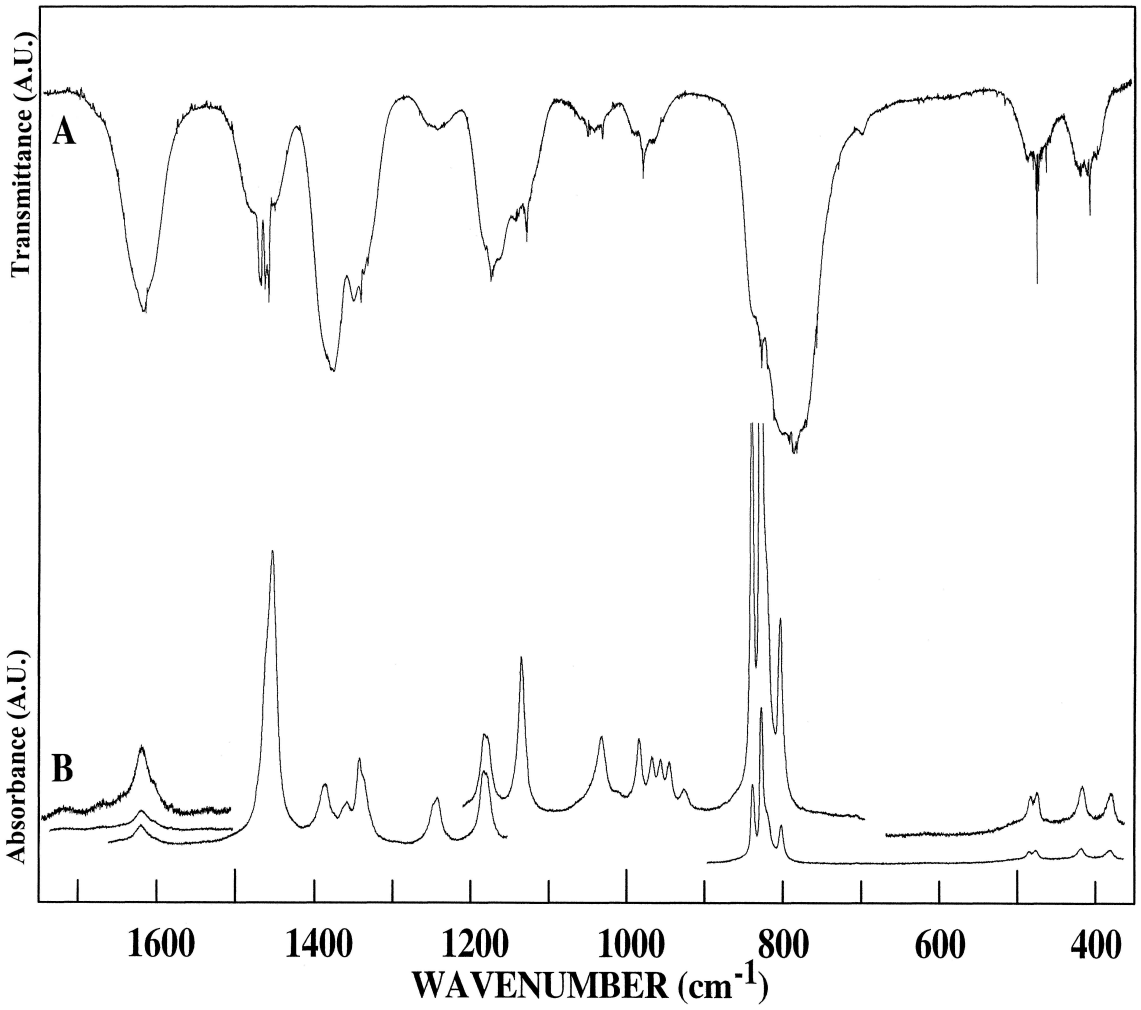

Figure 70. Spectra of isopropylamine (A) mid-infrared gas; (B) Raman Xe solution at -100°C.

These two examples clearly show that the better predictions from the *ab initio* calculations compared to the earlier study with predicted intensities and band contours with the Raman spectra of the xenon solutions it was possible to confidently assign the fundamentals for both conformers in this spectral region.

CONFORMATIONAL STABILITY

To determine the enthalpy differences among the two observed conformers of isopropylamine, the sample was dissolved in liquefied xenon and the Raman spectra were recorded as a function of temperature from -50 to -100°C. Relatively small interactions are expected to occur between xenon and the sample though the sample can associate with itself forming a dimmer, trimer or higher order complex. However, due to the very small concentration of sample self-association is greatly reduced. Therefore, only small wavenumber shifts are anticipated for the xenon interactions when passing from the gas phase to the liquefied xenon solutions except for the NH_2 modes. A significant advantage of this study is that the conformer bands are better resolved in comparison with those in the Raman spectrum of the liquid. From *ab initio* calculations, the dipole moments of the two conformers are predicted to have similar values and the molecular sizes of the two conformers are nearly the same, so the ΔH value obtained from the temperature dependent Raman study is expected to be near to that for the gas [16-20].

Once confident assignments have been made for the fundamentals of both conformers the task was then to find a pair or pairs of bands from which the enthalpy determination could be obtained. The bands should be sufficiently resolved as to determine their intensities. The selection of the bands to use in the enthalpy determination was complicated due to the presence of high intensity bands for both conformers and the near overlap of many modes. The fundamentals at 472 and 463 cm^{-1} were initially selected for the *trans* and *gauche* conformer as they are confidently assigned, satisfactory resolved, and a limited number of overtone and combination bands are possible. The band at 818 cm^{-1} C-C-C symmetric stretch/CN stretch was then selected for the *trans*

form as it was found that the intensity was not significantly affected by the underlying NH_2 bending mode which is weak in the Raman effect. The bands at 3390 and 3325 cm^{-1} were next selected for the *trans* conformer and the bands at 3380 and 3314 cm^{-1} were selected for the *gauche* form. From the frequency shift of the NH_2 stretching modes it is clear that this group interacts with the xenon atom. However, the shift for both the *trans* and *gauche* conformer bands are similar and, thus, the enthalpy difference is not expected to be significantly affected. Finally, the bands at 793 and 830 cm^{-1} (NH_2 wag modes) were also used for the *trans* and *gauche* conformers, respectively. Whether these bands would be used to determine the enthalpy difference depends on whether the results were consistent with the values obtained from the initially chosen pairs.

The intensities of the individual bands were measured as a function of temperature and their ratios were determined (Fig. 71). By application of the van't Hoff equation $-\ln K = \Delta H/(RT) - \Delta S/R$, the enthalpy difference was determined from a plot of $-\ln K$ versus $1/T$, where $\Delta H/R$ is the slope of the line and K is substituted with the appropriate intensity ratios, *i.e.* $I_{conf\text{-}1} / I_{conf\text{-}2}$, etc. It was assumed that ΔH, ΔS, and α are not functions of temperature in the range studied.

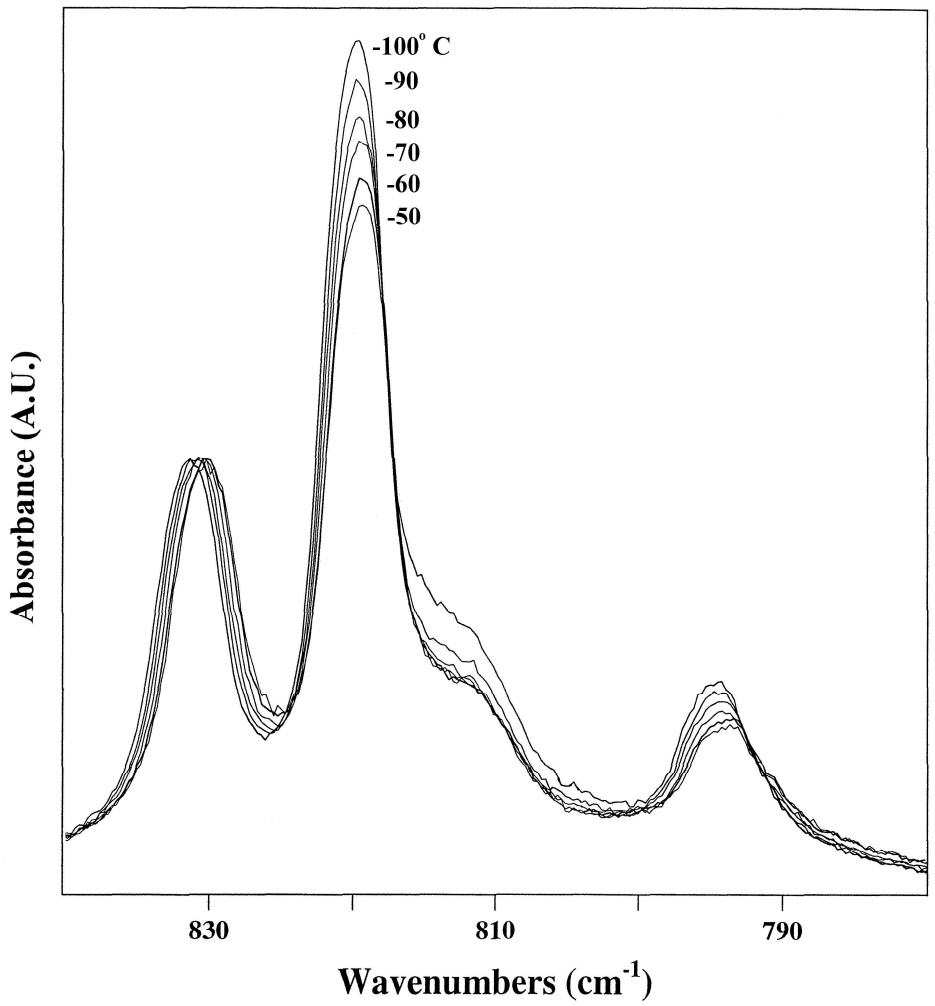

Figure 71. Raman spectra of isopropylamine in xenon solution at different temperatures.

Table 108. Temperature and intensity ratios of the *trans* and *gauche* bands of isopropylamine.

	T(°C)	1/T ($\times 10^{-3}$ K^{-1})	I_{3390} / I_{3380}	I_{3390} / I_{3314}	I_{3325} / I_{3380}	I_{3325} / I_{3314}	I_{3390} / I_{830} [b]	I_{3325} / I_{830} [b]	I_{818} / I_{830} [b]	I_{472} / I_{830} [b]
Liquid	–50.0	4.584	0.956	0.804	2.111	1.776	0.729	1.610	1.703	1.271
xenon	–60.0	4.692	1.011	0.850	2.222	1.869	0.771	1.695	1.771	1.288
	–70.0	4.923	1.056	0.888	2.278	1.916	0.805	1.737	1.873	1.305
	–80.0	5.177	1.111	0.935	2.367	1.991	0.847	1.805	1.941	1.373
	–90.0	4.460	1.167	0.981	2.433	2.047	0.890	1.856	2.034	1.424
	–100.0	5.775	1.233	1.037	2.544	2.140	0.941	1.941	2.119	1.475
ΔH[a]			134 ± 5	134 ± 5	95 ± 6	95 ± 6	135 ± 4	95 ± 6	118 ± 6	85 ± 7

	T(°C)	1/T ($\times 10^{-3}$ K^{-1})	I_{472} / I_{463}	I_{818} / I_{463}	I_{818} / I_{3380}	I_{818}/ I_{3314}	I_{3390} / I_{463}	I_{3325}/ I_{463}	I_{472}/ I_{3380}	I_{472}/ I_{3314}
Liquid	–50.0	4.584	0.781	1.047	2.233	1.879	0.448	0.990	1.667	1.402
xenon	–60.0	4.692	0.792	1.089	2.322	1.953	0.474	1.042	1.689	1.421
	–70.0	4.923	0.802	1.151	2.456	2.065	0.495	1.068	1.711	1.439
	–80.0	5.177	0.844	1.193	2.544	2.140	0.521	1.109	1.800	1.514
	–90.0	4.460	0.875	1.250	2.667	2.243	0.547	1.141	1.867	1.570
	–100.0	5.775	0.906	1.302	2.778	2.336	0.578	1.193	1.933	1.626
ΔH[a]			85 ± 7	118 ± 6	118 ± 6	118 ± 6	134 ± 5	95 ± 6	84 ± 7	84 ± 7

	T(°C)	1/T ($\times 10^{-3}$ K^{-1})	$I_{793}{}^{b}/ I_{3380}$	$I_{793}{}^{b}/ I_{3314}$	$I_{793}/ I_{830}{}^{b}$	$I_{793}{}^{b} / I_{463}$
Liquid	–50.0	4.584	0.440	0.336	0.305	0.188
xenon	–60.0	4.692	0.442	0.355	0.322	0.198
	–70.0	4.923	0.444	0.374	0.339	0.208
	–80.0	5.177	0.467	0.393	0.356	0.219
	–90.0	4.460	0.489	0.411	0.373	0.229
	–100.0	5.775	0.511	0.430	0.390	0.240
ΔH^{a}			131 ± 7	131 ± 8	131 ± 7	130 ± 6

[a] Average value $\Delta H = 113 \pm 2$ cm^{-1} (1.35 ± 0.03 kJ mol^{-1}) with the *trans* conformer the more stable form and the statistical uncertainty (1σ) obtained by utilizing all of the data as a single set.

[b] The 830 and 793 are NH_2 wag.

These nine bands, five *trans* and four *gauche*, were utilized for the determination of the enthalpy difference by combining them to form 20 band pairs. The enthalpy difference was determined from these 20 band pairs with a value of 113 ± 2 cm^{-1} (Table 108). This value is in reasonable agreement with the corresponding predicted values from *ab initio* calculations (Table 106). This error limit is derived from the statistical standard deviation of one sigma of the measured intensity data taken as a single data set, but it does not take into account small associations with the liquid xenon or the possible presence of overtones and combination bands in near coincidence of the measured fundamentals. The variations in the individual values are undoubtedly due to these types of interferences, but by taking several pairs, the effect of such interferences should cancel. However, this statistical uncertainty is probably better than can be expected from this technique and, therefore, an uncertainty of about 10% in the enthalpy difference is probably more realistic i.e. 113 ± 11 cm^{-1}. From the enthalpy difference the abundance of the *gauche* conformer present at ambient temperature is estimated to be 54 ± 1%.

STRUCTURAL PARAMETERS

Initial structural parameters for the isopropylamine were proposed from a microwave study [201] where a partial structure of *trans*-isopropylamine (Table 107) was determined by assuming the isopropyl group parameters by reproducing the planar moment for it. This was followed by another microwave study [194] two decades later where the rotational constants were determined for *trans*-isopropylamine as well as 2,2,2-trifluoroethylamine and aminoethanol but no structural parameters were reported for any of these molecules. From a later electron diffraction study [202] the structural parameters

were determined (Table 107) by fixing the structural parameters for the NH_2 moiety to the corresponding parameters previously reported [203] for the methylamine molecule.

We [51] have shown that *ab initio* MP2(full)/6-311+G(d,p) calculations predict the carbon-hydrogen r_0 structural parameters for more than fifty carbon-hydrogen distances to at least 0.002 Å compared to the experimentally determined [5] values from isolated CH stretching frequencies which agree to previously determined values from earlier microwave studies. Therefore, all of the carbon-hydrogen parameters can be taken from the MP2(full)/6-311+G(d,p) predicted values for the *trans* conformer of isopropylamine.

We have found that good structural parameters for hydrocarbons and many substituted ones can be determined by adjusting the structural parameters obtained from the *ab initio* MP2(full)/6-311+G(d,p) calculations to fit the rotational constants obtained from microwave experimental data by using a computer program "A&M" (*Ab initio* and Microwave) developed [5] in our laboratory. In order to reduce the number of independent variables, the structural parameters are separated into sets according to their types where bond distances in the same set keep their relative ratio, and bond angles and torsional angles in the same set keep their difference in degrees. This assumption is based on the fact that errors from *ab initio* calculations are systematic. Therefore, it should be possible to obtain "adjusted r_0" structural parameters for the six parameters with four heavy atoms and two NH_2 parameters by utilizing the previously reported six rotational constants from the earlier microwave study [194]. Therefore we have obtained the complete structural parameters for *trans* isopropylamine.

The resulting adjusted r_0 parameters are listed in Table 107, where it is believed that the N-C, C-C, and N-H distances should be accurate to ± 0.003 Å, the C-H distances are accurate to ± 0.002 Å, and the angles should be within ± 0.5°. The fit of the six determined rotational constants (Table 109) by the structural parameters for the *trans* conformer are good with the differences being less than 1 MHz. Therefore, it is believed that the suggested uncertainties are realistic values and the determined structural parameters are probably as accurate as can be obtained for the molecule in the gas phase by either electron diffraction or microwave substituted methods.

Table 109. Comparison of rotational constants obtained from *ab initio* MP2(full)/6-311+G(d,p) predictions, experimental values[a] from microwave spectra, and adjusted r_0 structural parameters for *trans* isopropylamine.

Conformer	Rotational constants	MP2(full)/ 6-311+G(d,p)	Experimental[a]	Adjusted r_0	$\|\Delta\|$
$(CH_3)_2CHNH_2$	A	8391.30	8331.92(2)	8332.77	0.85
	B	8016.30	7977.32(2)	7977.08	0.24
	C	4689.37	4657.17(8)	4656.62	0.55
$(CH_3)_2CHND_2$	A	7843.64	7806.17(1)	7806.42	0.25
	B	7537.32	7490.59(2)	7489.77	0.82
	C	4360.70	4331.79(8)	4332.33	0.54

[a] Ref. [194].

Additionally, we have also shown that the differences in predicted distances and angles from the *ab initio* calculations for different conformers of the same molecule can

usually be used as one parameter with the *ab initio* predicted differences except for some dihedral angles. Therefore we have predicted structural parameters for the *gauche* form of isopropylamine by applying the corresponding adjustments from the *trans* conformer to the MP2(full)/6-311+G(d,p) predicted parameters for the *gauche* form. These parameters should be close to the actual value except for the dihedral angles.

DISCUSSION

The vibrational assignments reported herein are based on a significant amount of information with the Raman spectrum of the xenon solution and predictions from the scaled *ab inito* MP2(full)/6-31G(d) calculations as well as the predicted infrared bands contours.

The *ab intio* Raman and infrared band intensities were also used but they seemed to be the least reliable of the data utilized. One of the possible reasons for significant difference in predicted and observed intensities could be the results of the association of the amine portion of the molecule with xenon. The evidence for the van der Waals molecules was the significant decreases in the NH stretching frequencies from the gas to the solutions i.e. 13 cm^{-1} lower for the *gauche* form and 21 and 16 cm^{-1} for the *trans* conformer. However, for the other fundamentals the difference between the frequencies in the gas and xenon solution is one or two wavenumbers except for the CCC antisymmetric stretch where the difference is five wavenumbers for both conformers. Finally, it should be noted that there is a very, very small amount of the dimer present in the xenon solution as evidence of the lack of the bands which are present at approximately 3225 cm^{-1} in xenon solutions.

For the *trans* conformer the *ab inito* predicted frequencies for A′ fundamentals with frequencies of 1600 cm^{-1} and below, except for the NH_2 wag was 8 cm^{-1} which represent 0.6% error. If all the fundamental frequencies are included the percent error increases to 0.8% since the CH stretches are poorly predicted. The predicted frequency for the NH_2 wag was too high with 0.9 scaling but it can be corrected with a scaling factor of 0.7. However, if this value is used it usually results in two or three unacceptable P.E.D. values. Since the NH_2 wag gives rise to a very intense infrared band, it is usually better to use 0.9 as the scaling factor so the other fundamentals are "normal". The percent error for the A″ modes for the *trans* form have similar errors to that of the A′ modes of the predicted frequencies and the percent error for the predictions for the *gauche* conformer are nearly the same. Thus the relatively small basis set of 6-31G(d) by the MP2(full) calculations with two or three scaling factors provides excellent predicted frequencies for aiding the vibrational assignments.

For the *trans* form the mixing is relatively small for the A′ modes except for the ν_{12} and ν_{13} which have only 33%S_{12} and $S_{13,}$ respectively, with 22% and 23% of each others symmetry coordinate. For the A″ modes only ν_{25} (CH bend) has a relatively small percentage of 29%S_{25} with 22%S_{26} the CH_3 symmetric deformation. Therefore, the approximate descriptions for the normal modes provide reasonable information on the molecular motions of vibrations. However, for the *gauche* conformer there is significantly more mixing with the vibration at 1254 cm^{-1} assigned as the CH_3 rock with only 18%S_{12} and 30%S_{27} (NH_2 twist) but the band at the 951 cm^{-1} has 35%S_{27} so this lower frequency band is described as the NH_2 twist. Therefore several of the approximate

descriptions for the fundamentals of the *gauche* form are more for bookkeeping than providing descriptions of the molecular motions.

The adjusted r_0 structural parameters have been determined for *trans* isopropylamine for six independent parameters (three distances and three angles) but the HNC angle did not change when the parameters were adjusted to fit the reported rotational constants. In the initial microwave study [201] only three parameters were determined which was the distance (Å) C-N = 1.49(2) and the angles (°) ∠NCC = 108(2) and ∠HNC = 109(2). The values obtained in the current study for the angles NCC and HNC are both within the error limits of the values from the previous study but again this is somewhat trivial due to the size of these error limits. The distance C-N obtained in the current study is somewhat lower than that obtained in the microwave study but this is relatively insignificant due to the large error limit of the previous study. The more recent electron diffraction work [202] agrees with the current study within the error limits for every parameter except the angle (°) ∠CCC = 114.4(16) which is 3.4 degrees higher than the value in the current study; however, when the error limits of nearly two degrees is taken into account this difference is also only minimally significant and so the value from this study is believed to be determined well. Thus, the structural parameters reported in the current study are believed to be accurate to within the stated error limits.

It is of interest to compare the structural parameters of isopropylamine with the corresponding parameters of other amine and isopropyl moieties. The methylamine structure has been well determined using electron diffraction to have the distances (Å) C-N = 1.471(3), N-H = 1.019(6) and angle (°) HNC = 111.5(7). The N-H distance and HNC angle change relatively little going from methylamine to isopropylamine; however, the C-

N bond distance is slightly shorter in the isopropylamine though it is within the experimental errors. It is also of interest to compare the isopropyl group with other isopropyl moieties. The structural parameters of isopropyl chloride have been determined from a microwave study [204] where the rotational constants of 11 isotopologues were used to determine the r_0 structural parameters. The parameters of interest are the distance (Å) C-C = 1.5202(14) and the angle (°) ∠CCC = 113.31(16). The isopropylamine C-C distance is longer by 0.010 Å than that for isopropyl chloride though this is lessened somewhat by the error limits of ± 0.0044 Å the difference is still significant though not unexpected. The ∠CCC angle is also significantly smaller for the isopropylamine by 2.31° but this is not unexpected as the chloride group is a larger substituent. Isopropyl alcohol is also of interest for comparing with isopropylamine and the structural parameters have been determined by a microwave study [205] where the parameters for the *trans* form are the distance (Å) C-C = 1.523(2) and the angle (°) ∠CCC = 112.3(1). These values have the same trend with the C-C distance longer in the isopropylamine and the ∠CCC angle shorter, though the differences in this case are less pronounced. It would be of interest to determine more amine and isopropyl moiety parameters so a more complete comparison could be made.

One of the major goals of this research was the determination of the enthalpy difference between the two conformers where there had been a large range of the values reported from nearly zero to a value slightly greater than 400 cm^{-1} (4.79 kJ mol^{-1}). If only the low frequency fundamentals at 463, 472, and 818 cm^{-1} and the four NH_2 stretches are used in conjunction with the three low frequency modes to determine the enthalpy difference a value of 104 ± 4 cm^{-1} (1.24 ± 0.05 kJ mol^{-1}) is determined. If the enthalpy

difference also includes the four determinations using the NH_2 stretches paired with each other the value increases slightly to 108 ± 3 cm^{-1} (1.29 ± 0.04 kJ mol^{-1}) and then finally including all twenty band pairs the value is 113 ± 2 cm^{-1} (1.35 ± 0.03 kJ mol^{-1}) where the statistical uncertainty is clearly unrealistic. Therefore we have simply indicated a more reasonable value of ± 11 cm^{-1} (0.13 kJ mol^{-1}). This value could be affected by the interaction of the amine with the xenon solution. However even if the value was increased by 50% it still would not reach near the most recently reported [200] value of ~400 cm^{-1}. This value was estimated based on the relative intensities of pairs of bands which were observed in the spectra of the argon matrix. These investigators utilized the CH_3 rock's relative intensities at 1183 and 1178 cm^{-1} assuming the α values would be equal. However, the α value of the *gauche* conformer is approximately half that of the *trans* form which would then indicate the bands should have nearly equal intensities rather than the 4:1 ratio observed by the authors for these bands in the argon matrix. From the Raman studies these two bands have nearly equal intensity which does not support the large enthalpy difference of ~400 cm^{-1}. Therefore, the use of the relative intensities in the argon matrix is questionable for determining the enthalpy difference.

To support the experimental values the *ab initio* energy differences have been determined by a variety of basis sets (Table 106). With diffuse functions the values are ~200 cm^{-1} with the *trans* form the more stable conformer, whereas, without diffuse functions the values are slightly less than 100 cm^{-1} which would be consistent with the values obtained in this study.

Also in the earlier study [198] the value of the *trans-gauche* barrier was determined to be ~1000 cm^{-1} whereas with the more recent assignments [200] in the far

infrared spectrum the splitting in the third energy level indicates the barrier should be much higher. However, the energy difference obtained from the various calculations give a value ~950 cm^{-1} (Table 106) which would be consistent with the barrier reported earlier in the initial extensive vibrational study.

The only way for a more confident determination of the enthalpy difference would require the use of a sample in a very low pressure gaseous phase. It is doubtful that this would be an easy experiment to determine the enthalpy and, therefore, the value obtained from the xenon solution must be considered the most confident enthalpy difference at this time. The use of enthalpy determinations from 20 band pairs indicates the accuracy of the determination by this technique.

In the most recent microwave study of isopropylamine the quadrupole coupling constants were determine from the spectral data as well as quartic centrifugal distortion constants. We have obtained the quadratic centrifugal distortion constants and the quadrupole coupling constants from the MP2(full)/6-311+G(d,p) calculations as well as the density functional theory by the B3LYP method utilizing the same basis set. These data are given in Table 110 and as can be seen from the values of the quadrupole coupling constants there is reasonable agreement with the predicted values for both calculations. However, the experiment distortion constants are significantly different than those predicted by both calculation methods. We have found in the past the *ab initio* calculations usually provide fairly good distortion and quadrupole coupling constants.

Table 110. Quadratic centrifugal distortion constants (kHz) and quadrupole coupling constants (MHz) for conformers of isopropylamine.

	Trans			*Gauche*	
	MP2(full)/ 6-311+G(d,p)	B3LYP/ 6-311+G(d,p)	Exp.[a]	MP2(full)/ 6-311+G(d,p)	B3LYP/ 6-311+G(d,p)
Δ_J	3.894	3.937	7.4(22)	3.793	3.874
Δ_{JK}	-2.293	-2.198	-12.94(53)	-1.434	-1.563
Δ_K	5.719	5.704	-9.6(52)	4.673	4.829
δ_J	1.451	1.469	0.1443(83)	1.376	1.414
δ_K	2.146	2.150	-6.43(72)	2.131	2.100
χ_{aa}	2.037	2.253	1.789(2)	-3.354	-3.667
χ_{bb}	2.664	2.840	2.566(4)	2.276	2.376
χ_{cc}	-4.701	-5.093	-4.355(4)	1.078	1.291

[a] Ref [194]

With the predicted structural parameters for the *gauche* conformer it is believed that the predicted rotational constants should be very close to those that would be obtained from a microwave study of this conformer. Therefore it would be interesting if such a study were carried out since the information obtained could be very useful in obtaining the *gauche* barrier using the splittings observed in the ground state. Nevertheless it is believed that the parameters that have been estimated should have rather small uncertainties with the uncertainties not larger than 0.005 Å for the heavy atom distances and 1° for the angles.

CHAPTER 18

INFRARED AND RAMAN SPECTRA, r_0 STRUCTURAL PARAMETERS, CONFORMATIONAL STABILITY, AND VIBRATIONAL ASSIGNMENT OF 2-CYANOETHYLAMINE

INTRODUCTION

The conformational stability determination of 1,2-disubstituted ethane molecules have provided some interesting challenges for structural scientists over the years. The 1,2-dihaloethane molecules provided good examples where it has been shown by infrared gas phase studies [206] that 1,2-difluoroethane has the *gauche* conformer more stable than the *trans* form by 280 ± 30 cm^{-1} (3.35 ± 0.36 kJ mol^{-1}) whereas 1,2-dichloroethane [207] has the *trans* conformer more stable than the *gauche* form by 323 ± 7 cm^{-1} (3.87 ± 0.09 kJ mol^{-1}) from variable temperature infrared studies of xenon solutions. This value was obtained from an average of four *gauche*/*trans* conformer pairs. Eight years later the enthalpy difference was again determined [20] for 1,2-dichloroethane for both the gas and two different noble gas solutions from variable temperature infrared studies. For the liquid xenon solution two conformer pairs which differed from those used in the earlier study [207] were utilized [20] from which a value of 272 ± 11 cm^{-1} (3.26 ± 0.13 kJ mol^{-1}) was obtained. However, from the determination in krypton solution only one conformer pair was used which differed from the two used from the xenon solution. The value from the krypton solution [20] was 318 ± 25 cm^{-1} (3.81 ± 0.30 kJ mol^{-1}) which is much lower than the value obtained for the gas [20] from one conformational pair with the enthalpy

difference of 410 ± 13 cm^{-1} (4.90 ± 0.15 kJ mol^{-1}). These results clearly show that more than one conformer pair needs to be used for enthalpy difference determinations but there may be slight differences from the two different rare gases.

Since many organoamines are important biomolecules such as aminoacids, proteins, etc, it is of scientific importance to determine the conformational stabilities of representative organoamine molecules. There have been recent studies of 3-$XCH_2CH_2NH_2$ molecules where X= F and NH_2 to identify the two or three conformers which are the most stable forms and determine their enthalpy differences. As a continuation of these scientific investigations, the molecule where X is the nitrile species was studied since it has been shown that this triple bonded moiety has significantly different effects on the conformational stabilities of X-methyl-cyclopropanes compared to molecules where the X is F or other halogens or hydrocarbons. The $H_2NCH_2CH_2CN$ molecule has been previously investigated by microwave spectroscopy [208] where two conformers were identified, the *Gg* and *Gt* forms (Fig. 72) where the Capital G is for *Gauche* for the orientation around the C-C bond and the lower cases g and t for *gauche* and *trans* orientation for the amine, but their enthalpy difference could not be determined. However in this study an estimated value of 0 ± 2 kJ/mol (0 ± 167 cm^{-1}) was reported and it also was reported that these two identified conformers were at least 4 kJ/mol (334 cm^{-1}) more stable than the other three possible conformers. Additionally, all the structural parameters except for the C-C-NH_2 angle and the C-C-C-N dihedral angle were estimated where the values for these estimated parameters were taken from the corresponding parameters of similar molecules. By using the assumed parameters and fitting the experimental rotational constants by changing the values for the angles determined

parameters were obtained for ∠CCN of 108.0(15)° for conformer I (*Gg*) and 114.0(15)° for form II (*Gt*) and for the heavy atom dihedral angles the values of 63(3)° and 59(3)° for conformers I and II, respectively, were reported.

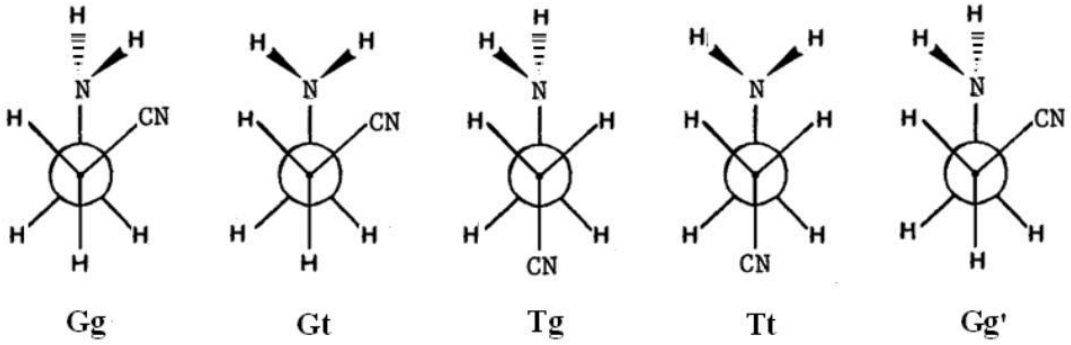

Figure 72. Five conformers of 2-cyanoethylamine.

To obtain the structural information and conformational stabilities of 2-cyanoethylamine, $H_2NCH_2CH_2CN$, we have investigated the infrared spectra of the gas and solid and the Raman spectrum of the liquid. To support these experimental studies we have also obtained the predicted harmonic force fields, infrared intensities, Raman activities, depolarization ratios, and vibrational frequencies from MP2/6-31G(d) *ab initio* calculations with full electron correlation. To obtain predictions for the conformational stabilities we have carried out MP2(full) *ab initio* and density functional theory (DFT) calculations by the B3LYP method by utilizing a variety of basis sets. The r_0 structural

parameters have been obtained by combining the MP2(full)/6-311+G(d,p) *ab initio* predicted parameters with the previously reported rotational constants obtained from the microwave study [208]. The results of these spectroscopic, structural and theoretical studies of 2-cyanoethylamine are reported herein.

EXPERIMENTAL AND THEORETICAL METHODS

The sample of 2-cyanoethylamine was purchased from Alfa Aesar with an estimated purity of 98%. The sample was used without further purification and its purity was verified from the infrared spectra of the gas.

The infrared spectrum of the gas (Fig. 73A) and solid (Fig. 73B) were obtained from 4000 to 220 cm^{-1} on a Perkin-Elmer model 2000 Fourier transform spectrometer equipped with a Ge/CsI beamsplitter and a DTGS detector. Atmospheric water vapor was removed from the spectrometer housing by purging with dry nitrogen. The spectra of the gas and solid were obtained with a theoretical resolution of 0.5 cm^{-1} for the gas and 2 cm^{-1} for the solid with 128 interferograms added and truncated. Multiple annealings were performed but a pure crystal could not be obtained, thereby the solid spectra is that of the amorphous solid at boiling liquid nitrogen temperatures.

The Raman spectra of the liquid (Fig. 74A) were recorded from 4000 to 40 cm^{-1} on a Spex model 1403 spectrophotometer equipped with a Spectra-Physics model 2017 argon ion laser operating on the 514.5 nm line. The laser power used was 1.5 W with a spectral bandpass of 3 cm^{-1}. The spectra of the liquid were recorded with the sample sealed in a Pyrex glass capillary. The measurements of the Raman frequencies are expected to be accurate to $\pm$ 2 cm^{-1}. All of the observed bands in the Raman spectra of the

liquid along with their proposed assignments and depolarization values are listed in Tables 111, 112, S28, and S29 for the *Gg*, *Gt*, *Tg*, and *Tt* conformers, respectively.

The LCAO-MO-SCF restricted Hartree-Fock calculations were performed with the Gaussian-03 program [22] using Gaussian-type basis functions. The energy minima with respect to nuclear coordinates were obtained by the simultaneous relaxation of all geometric parameters using the gradient method of Pulay [29]. Several basis sets as well as the corresponding ones with diffuse functions were employed with the Møller-Plesset perturbation method [21] to the second order (MP2(full)) as well as with the density functional theory by the B3LYP method. The predicted conformational energy differences are listed in Table 113.

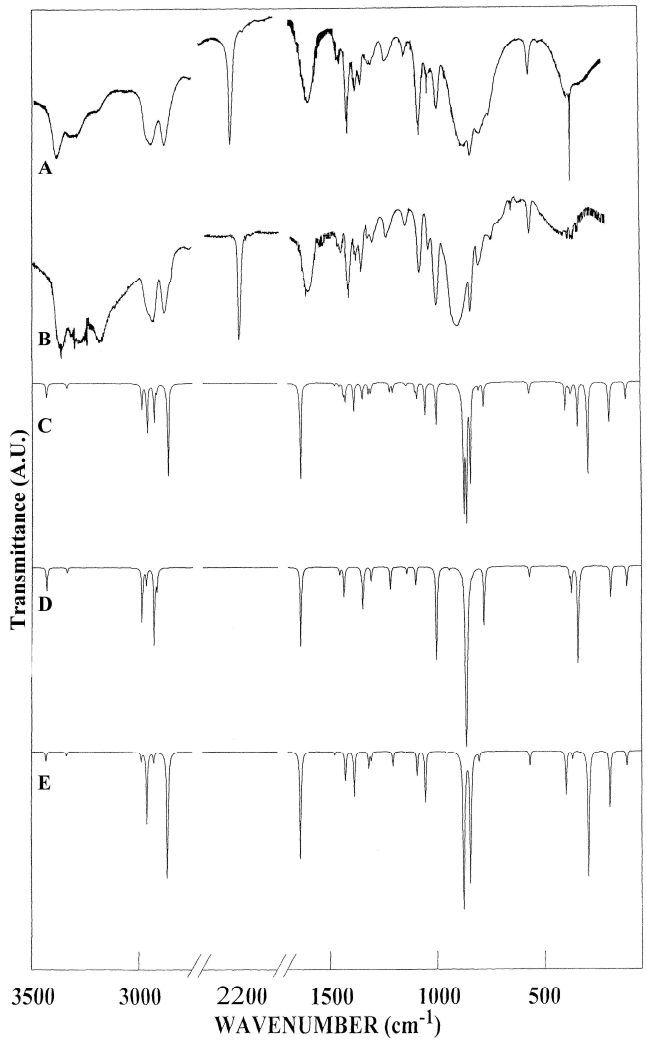

Figure 73. Experimental and predicted infrared spectra of 2-cyanoethylamine: (A) gas; (B) amorphous solid; (C) simulated spectrum of mixture of *Gg* and *Gt* (ΔH = 75 cm^{-1}) conformers at 25°C; (D) simulated *Gt* conformer; (E) simulated *Gg* conformer.

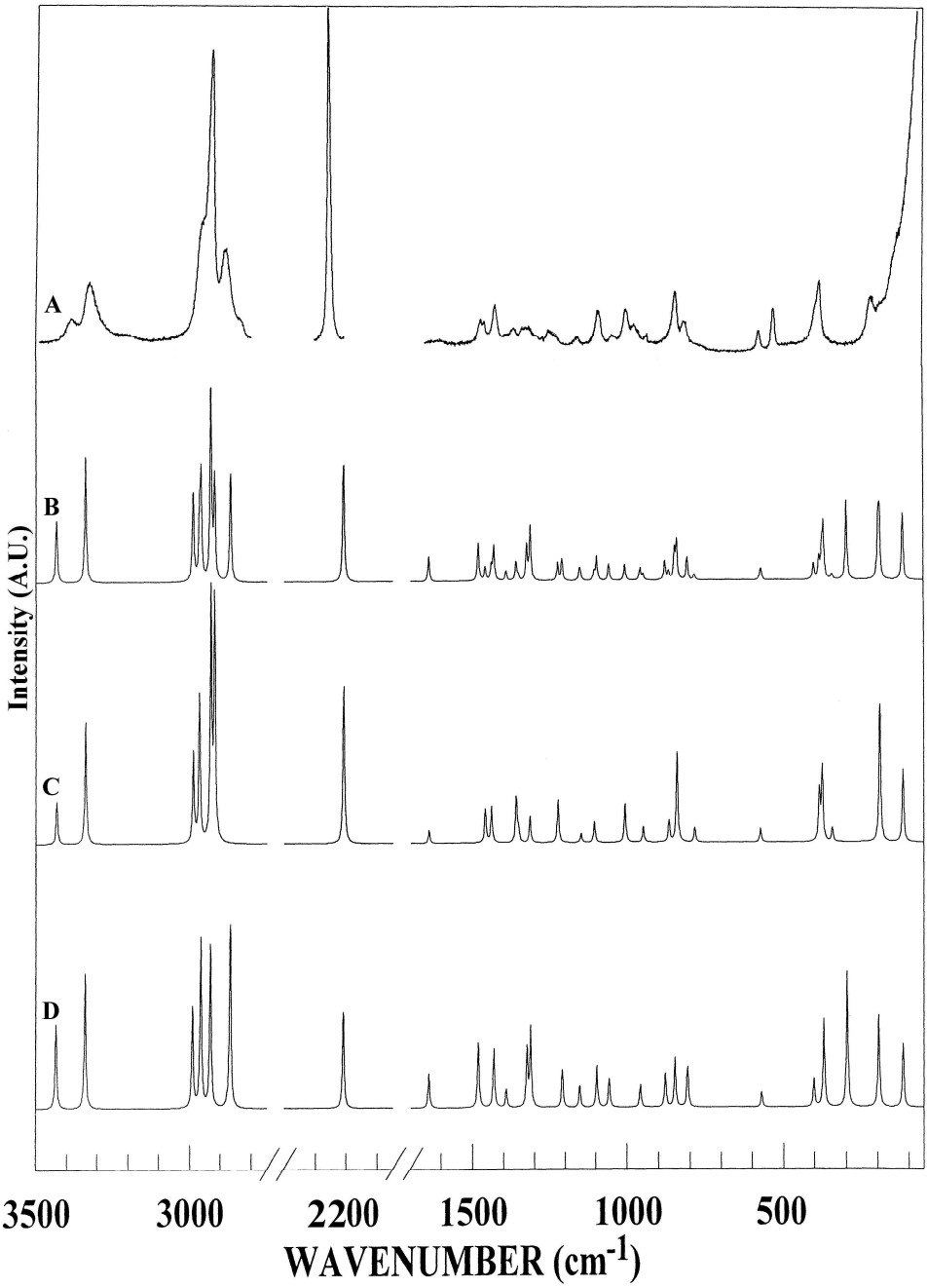

Figure 74. Experimental and predicted Raman spectra of 2-cyanoethylamine: (A) liquid; (B) simulated spectrum of mixture of *Gg* and *Gt* (ΔH = 75 cm^{-1}) conformers at 25°C; (C) simulated *Gt* conformer; (D) simulated *Gg* conformer.

Table 111. Observed and calculated[a] frequencies (cm^{-1}) and potential energy distributions (P.E.D.s) for the *Gg* conformer of 2-cyanoethylamine.

Vib. no.	Approximate description	ab initio	Fixed scaled[b]	IR int.	Raman act.	dp ratio	IR gas	IR solid	Raman Liquid	P.E.D.[c]	Contour[*] A	Contour[*] B	Contour[*] C
ν_1	NH_2 antisymmetric stretch	3619	3434	2.8	60.6	0.66	3380	3361	3383	$99S_1$	93	7	-
ν_2	NH_2 symmetric stretch	3519	3338	1.2	91.8	0.12	3317	3315	3324	$99S_2$	1	79	20
ν_3	β-CH_2 antisymmetric stretch	3187	2990	2.5	55.9	0.73	2994	2992	2988	$97S_3$	9	17	74
ν_4	α-CH_2 antisymmetric stretch	3159	2963	24.3	92.5	0.39	2967	2964	2960	$72S_4,26S_6$	49	38	13
ν_5	β-CH_2 symmetric stretch	3125	2931	2.9	87.4	0.11	2937	2930	2931	$97S_5$	10	90	-
ν_6	α-CH_2 symmetric stretch	3056	2867	56.3	95.3	0.21	2840	2846	2837	$74S_6,26S_4$	-	12	88
ν_7	C≡N stretch	2221	2208	0.2	32.9	0.27	2244	2245	2247	$89S_7,11S_{18}$	14	82	4
ν_8	NH_2 deformation	1728	1639	42.2	7.7	0.75	1603	1607	1599	$77S_8,22S_{19}$	3	79	18
ν_9	α-CH_2 deformation	1575	1481	1.0	12.7	0.72	1474	1472	1472	$98S_9$	74	22	4
ν_{10}	β-CH_2 deformation	1522	1431	8.6	11.0	0.71	1423	1420	1426	$95S_{10}$	12	53	35
ν_{11}	α-CH_2 rock	1465	1391	13.6	3.3	0.22	1386	1387	1389	$72S_{11},16S_{13}$	58	42	-
ν_{12}	β-CH_2 rock	1395	1324	4.7	9.9	0.63	1334	1336	1336	$60S_{12},23S_{15}$	3	79	19
ν_{13}	NH_2 twist	1381	1312	2.5	13.1	0.75	1313	1313	1315	$27S_{13},29S_{15},12S_{14,}$ $10S_{12}$, $10S_{11}$	2	93	4

ν_{14}	β-CH_2 twist	1273	1209	4.2	5.6	0.41	1216	1219	1219	$71S_{14},10S_{21},10S_{15}$	3	2	95
ν_{15}	α-CH_2 twist	1208	1151	0.5	3.0	0.60	1155	1158	1155	$31S_{15},27S_{13},13S_{12}$	86	-	14
ν_{16}	C-C(-N) stretch	1154	1096	7.1	5.4	0.72	1085	1090	1092	$21S_{16},29S_{17},11S_{11},10S_{21,}10S_{19,}10S_{13}$	10	20	71
ν_{17}	C-N stretch	1110	1057	15.9	3.6	0.15	1044	1050	1044	$31S_{17},28S_{20},24S_{21}$	4	32	64
ν_{18}	C-C(≡N) stretch	1003	956	0.6	2.5	0.70	973	978	976	$35S_{18},19S_{16},12S_{13,}10S_{21,}10S_{12}$	65	7	28
ν_{19}	NH_2 rock	922	878	92.9	3.3	0.53	856	925	953	$44S_{19},18S_{16,}\ 11S_{8,}10S_{21}$	3	13	84
ν_{20}	β-CH_2 wag	891	847	60.5	4.7	0.32	850	850	853	$35S_{20,}22S_{17,}18S_{19,}10S_{16,}10S_8$	6	23	70
ν_{21}	α-CH_2 wag	847	807	2.6	3.6	0.13	801	816	816	$24S_{21,}40S_{18,}14S_{16}$	29	28	43
ν_{22}	C-C-C bend	578	569	4.1	0.9	0.42	572	576	576	$35S_{22,}29S_{26,}12S_{23}$	38	22	40
ν_{23}	C-C-N bend	406	401	13.5	1.0	0.69	419	418	423	$50S_{23,}11S_{24,}11S_{26,}10S_{27,}\ 10S_{20}$	67	27	6
ν_{24}	C-C≡N out-of-plane bend	371	370	2.1	2.8	0.75	375	375	381	$66S_{24,}14S_{23,}10S_{26,}10S_{27}$	9	62	29
ν_{25}	NH_2 torsion	296	296	55.8	3.1	0.75	-	~430	212	$86S_{25}$	100	-	-
ν_{26}	C-C≡N in-plane bend	197	196	17.8	1.1	0.71	-	-	187	$32S_{26},28S_{22},25S_{27,}10S_{26}$	84	3	13
ν_{27}	C-C(N) torsion	118	118	4.4	1.4	0.73	-	-	118	$55S_{27},17S_{22},12S_{26,}10S_{24}$	7	89	4

[a] MP2(full)/6-31G(d) *ab initio* calculations, scaled frequencies, infrared intensities (km mol^{-1}), Raman activities ($Å^4$ u^{-1}), depolarization (dp) ratios and potential energy distributions (P.E.D.s).

[b] MP2(full)/6-31G(d) fixed scaled wavenumbers with factors of 0.88 for CH stretches, 1.0 for heavy atom bends, and 0.90 for all other modes.

[c] Calculated with MP2(full)/6-31G(d) and contributions of less than 10% are omitted.

[*] A, B and C values in the last three columns are percentage infrared band contours.

Table 112. Observed and calculated[a] frequencies (cm^{-1}) and potential energy distributions (P.E.D.s) for the *Gt* conformer of 2-cyanoethylamine.

Vib. no.	Approximate description	ab initio	Fixed scaled[b]	IR int.	Raman act.	dp ratio	IR gas	IR solid	Raman Liquid	P.E.D.[c]	Contour[*] A	Contour[*] B	Contour[*] C
ν_1	NH_2 antisymmetric stretch	3623	3432	6.9	31.3	0.73	3380	3361	3383	$100S_1$	44	22	34
ν_2	NH_2 symmetric stretch	3520	3337	1.5	83.9	0.05	3317	3315	3324	$100S_2$	-	98	2
ν_4	α-CH_2 antisymmetric stretch	3185	2988	17.3	50.9	0.74	2994	2992	2988	$90S_4$, $10S_3$	29	11	60
ν_3	β-CH_2 antisymmetric stretch	3163	2968	5.0	82.0	0.66	2967	2964	2960	$90S_3$, $10S_4$	-	83	17
ν_6	α-CH_2 symmetric stretch	3124	2930	27.0	134.0	0.09	2937	2930	2931	$98S_6$	24	48	28
ν_5	β-CH_2 symmetric stretch	3110	2918	5.7	129.4	0.07	2878	2880	2885	$99S_5$	-	76	24
ν_7	C≡N stretch	2220	2207	0.2	54.4	0.19	2244	2245	2247	$89S_7$,$11S_{18}$	61	39	-
ν_8	NH_2 deformation	1729	1639	27.9	2.9	0.73	1603	1607	1599	$77S_8$,$22S_{19}$	18	35	47
ν_9	α-CH_2 deformation	1552	1459	2.0	6.6	0.66	1458	1457	1460	$98S_9$	16	31	53
ν_{10}	β-CH_2 deformation	1530	1439	8.9	7.0	0.74	1423	1420	1426	$95S_{10}$	12	46	42
ν_{15}	α-CH_2 twist	1433	1359	1.8	8.0	0.73	1361	1371	1378	$49S_{15}$,$31S_{13}$,$10S_{11}$	42	58	-

ν_{11}	α-CH_2 rock	1425	1352	12.6	2.1	0.44	1361	1362	1366	$76S_{11},10S_{12}$	74	24	2
ν_{12}	β-CH_2 rock	1384	1314	4.1	4.4	0.38	1313	1313	1315	$59S_{12},12S_{13},11S_{21}$	10	59	31
ν_{14}	β-CH_2 twist	1286	1223	6.6	6.7	0.30	1242	1246	1249	$52S_{14},10S_{12},10S_{11}$	73	4	23
ν_{13}	NH_2 twist	1205	1147	1.9	1.3	0.59	1155	1158	1155	$19S_{13},26S_{15},16S_{14},10S_{12},10S_{11}$	19	5	76
ν_{17}	C-N stretch	1161	1104	5.4	2.8	0.47	1085	1090	1092	$54S_{17},12S_{14},12S_{20},10S_{19}$	-	68	32
ν_{16}	C-C(-N) stretch	1053	1005	35.1	4.7	0.51	1000	1008	999	$34S_{16},18S_{20},11S_{18},10S_{23},10S_{12}$	66	30	4
ν_{18}	C-C(≡N) stretch	992	947	0.7	1.7	0.36	966	963	966	$25S_{18},25S_{21},21S_{13},10S_{22}$	79	4	17
ν_{19}	NH_2 rock	912	866	182.9	2.1	0.08	844	912	937	$53S_{19},15S_{8},10S_{18},10S_{17}$	62	36	2
ν_{20}	β-CH_2 wag	881	840	0.9	8.6	0.20	850	850	845	$30S_{20},34S_{16},16S_{17}$	57	43	-
ν_{21}	α-CH_2 wag	826	784	18.8	1.3	0.06	760	757	750	$31S_{21},31S_{18},11S_{16},10S_{19},10S_{20}$	44	56	-
ν_{22}	C-C-C bend	581	572	3.2	0.8	0.31	572	576	576	$33S_{22},23S_{26},13S_{23},10S_{21}$	-	100	-
ν_{24}	C-C≡N out-of-plane bend	388	384	2.7	1.7	0.46	398	396	389	$43S_{24},27S_{23},11S_{27},10S_{20}$	40	9	51
ν_{23}	C-C-N bend	377	375	7.4	2.4	0.59	375	375	381	$28S_{23},29S_{26},17S_{24},13S_{25}$	22	41	37
ν_{25}	NH_2 torsion	344	343	37.1	0.4	0.57	245	~430	234	$77S_{25},15S_{24}$	33	17	50
ν_{26}	C-C≡N in-plane bend	192	192	9.3	1.6	0.75	-	-	187	$26S_{26},30S_{22},25S_{27},10S_{24}$	1	22	77
ν_{27}	C-C(N) torsion	118	118	6.0	1.6	0.72	-	-	118	$55S_{27},16S_{22},15S_{26}$	37	48	15

[a] MP2(full)/6-31G(d) *ab initio* calculations, scaled frequencies, infrared intensities (km mol^{-1}), Raman activities ($Å^4$ u^{-1}), depolarization (dp) ratios and potential energy distributions (P.E.D.s).

[b] MP2(full)/6-31G(d) fixed scaled wavenumbers with factors of 0.88 for CH stretches, 1.0 for heavy atom bends, and 0.90 for all other modes.

[c] Calculated with MP2(full)/6-31G(d) and contributions of less than 10% are omitted.

[*] A, B and C values in the last three columns are percentage infrared band contours.

Table 113. Calculated energies in (H) and energy differences (cm^{-1}) for the five conformers of 2-cyanoethylamine.

Method/Basis Set	# basis set	Energy[a], E	Energy Differences, Δ			
		Gg[b]	*Gt*[b]	*Tg*[b]	*Tt*[b]	*Gg'*[b]
RHF/6-31G(d)	87	-0.982440	61	100	323	517
MP2(full)/6-31G(d)	87	-1.707178	-10	326	400	563
MP2(full)/6-31+G(d)	107	-1.724295	117	358	524	624
MP2(full)/6-31G(d,p)	105	-1.759202	-28	307	329	521
MP2(full)/6-31+G(d,p)	125	-1.775510	112	332	470	582
MP2(full)/6-311G(d,p)	126	-1.912614	-57	292	301	518
MP2(full)/6-311+G(d,p)	146	-1.922720	75	326	441	549
MP2(full)/6-311G(2d,2p)	169	-1.974957	-29	289	347	551
MP2(full)/6-311+G(2d,2p)	189	-1.983791	83	286	408	582
MP2(full)/6-311G(2df,2pd)	234	-2.057871	-40	283	349	549
MP2(full)/6-311+G(2df,2pd)	254	-2.065785	67	286	401	581
MP2(full)/aug-cc-pVTZ	368	-2.072387	73	277	420	611
B3LYP/6-31G(d)	87	-2.409321	-145	159	110	556
B3LYP/6-31+G(d)	107	-2.422646	-24	124	184	565
B3LYP/6-311G(d,p)	126	-2.478557	-131	119	100	512
B3LYP/6-311+G(d,p)	146	-2.485712	-27	111	178	508
B3LYP/6-311G(2d,2p)	169	-2.486684	-132	131	114	504
B3LYP/6-311+G(2d,2p)	189	-2.493742	-20	120	173	517
B3LYP/6-311G(2df,2pd)	234	-2.493366	-130	117	110	484
B3LYP/6-311+G(2df,2pd)	254	-2.500132	-24	113	160	500
B3LYP/aug-cc-pVTZ	368	-2.506844	-20	120	163	503

[a]Energy of conformer is given as –(E+225) H.
[b]Difference is relative to Gg form and given in cm^{-1}.

In order to obtain a complete description of the molecular motions involved in the fundamental modes of $H_2NCH_2CH_2CN$, a normal coordinate analysis has been carried out. The force field in Cartesian coordinates was obtained with the Gaussian 03 program [22] at the MP2(full) level with the 6-31G(d) basis set. The internal coordinates used to calculate the **G** and **B** matrices are given in Table 114. By using the **B** matrix [30], the

force field in Cartesian coordinates was converted to a force field in internal coordinates. Subsequently, scaling factors of 0.88 for CH stretches and CH_2 deformation, and 0.90 for all other modes except the heavy atom bends were applied, along with the geometric average of the scaling factors for the interaction force constants, to obtain the fixed scaled force field and resultant wavenumbers. A set of symmetry coordinates was used (Table S30) to determine the corresponding potential energy distributions (P.E.D.s). A comparison between the observed and calculated wavenumbers, along with the calculated infrared intensities, Raman activities, depolarization ratios and potential energy distributions for the *Gg*, *Gt*, *Tg*, and *Tt* conformers are listed in Tables 111, 112, S28, and S29, respectively.

Table 114. Structural parameters (Å and °) and rotational constants (MHz) for the *Gg* and *Gt* conformers of 2-cyanoethylamine.

Structural parameters	*Internal coordinates*	*Gg*				*Gt*			
		MP2(full)/ 6-311+G(d,p)	B3LYP/ 6-311+G(d,p)	Microwave[a]	Adjusted r_0	MP2(full)/ 6-311+G(d,p)	B3LYP/ 6-311+G(d,p)	Microwave[a]	Adjusted r_0
r (N_1-C_2)	R_1	1.459	1.461	1.475	1.461(3)	1.452	1.452	1.475	1.453(3)
r (C_2-C_3)	R_2	1.531	1.540	1.548	1.535(3)	1.543	1.554	1.548	1.545(3)
r (C_3-C_4)	R_3	1.464	1.462	1.463	1.466(3)	1.462	1.460	1.463	1.463(3)
r (C_4≡N_5)	R_4	1.174	1.153	1.157	1.161(3)	1.174	1.154	1.157	1.161(3)
r (N_1-H_6)	r_1	1.014	1.014	1.017	1.014(3)	1.014	1.014	1.017	1.014(3)
r (N_1-H_7)	r_2	1.016	1.016	1.017	1.016(3)	1.015	1.014	1.017	1.015(3)
r (C_2-H_8)	r_3	1.093	1.093	1.091	1.093(2)	1.093	1.093	1.091	1.093(2)
r (C_2-H_9)	r_4	1.099	1.099	1.091	1.099(2)	1.094	1.093	1.091	1.094(2)
r (C_3-H_{10})	r_5	1.094	1.094	1.091	1.094(2)	1.095	1.095	1.091	1.095(2)
r (C_3-H_{11})	r_6	1.093	1.093	1.091	1.093(2)	1.095	1.095	1.091	1.095(2)
r (NH_6---C≡N)		3.862	3.948		3.884(5)	3.307	3.411		3.318(5)
r (NH_7---C≡N)		2.651	2.756		2.675(5)	2.715	2.821		2.727(5)
∠ $N_1C_2C_3$	A_1	109.5	110.5	108.0(15)	109.5(5)	115.8	116.7	114.0(15)	116.0(5)
∠ $C_2C_3C_4$	A_2	110.7	112.3	110.5	111.1(5)	110.9	112.3	110.5	111.1(5)
∠ $C_3C_4N_5$	A_3	177.7	178.6	180.0	177.4(5)	177.1	177.8	180.0	177.0(5)
∠ $H_6N_1H_7$	α_1	107.1	107.4		107.1(5)	107.6	108.3		107.6(5)
∠ $H_6N_1C_2$	α_2	110.6	111.2	111.0	110.6(5)	111.2	112.4	111.0	111.1(5)
∠ $H_7N_1C_2$	α_3	110.5	111.3	111.0	110.5(5)	111.2	112.2	111.0	111.2(5)
∠ $H_8C_2N_1$	π_1	108.4	108.2		107.7(5)	108.3	108.3		108.1(5)
∠ $H_9C_2C_3$	π_2	108.7	108.8	109.5	108.8(5)	107.8	107.3	109.5	107.8(5)
∠	π_3	110.7	110.1	109.5	110.7(5)	110.0	110.1	109.5	110.0(5)

$H_{10}C_3C_2$									
∠ $H_{11}C_3C_4$	π_4	108.6	108.5		109.0(5)	109.0	108.7		108.9(5)
∠ $H_9C_2N_1$	σ_1	114.3	114.3		114.9(5)	108.6	108.6		108.5(5)
∠ $H_8C_2C_3$	σ_2	107.9	107.4	109.5	107.9(5)	108.8	108.7	109.5	108.8(5)
∠ $H_{10}C_3C_4$	σ_3	108.6	108.3		107.8(5)	108.4	108.4		108.3(5)
∠ $H_{11}C_3C_2$	σ_4	109.4	109.4	109.5	109.4(5)	110.6	110.1	109.5	110.6(5)
∠ $H_8C_2H_9$	β_1	107.7	107.3		107.7(5)	107.3	106.8		107.3(5)
∠ $H_{10}C_3H_{11}$	β_2	108.7	108.1		108.7(5)	107.8	107.2		107.8(5)
τ $N_1C_2C_3C_4$	τ_1	-61.5	-64.7	-63(3)	-62.2(10)	58.2	60.2	59(3)	58.2(10)
A		10433.02	10825.10	10526.46(4)	10527.02	10220.02	10516.76	10281.38(2)	10282.23
B		3410.89	3263.00	3387.40(1)	3388.00	3367.34	3249.00	3367.75(4)	3367. 85
C		2789.35	2718.02	2781.57(1)	2780.99	2758.50	2699.03	2761.08(4)	2761.42
$\lvert\mu_a\rvert$		3.669				2.342			
$\lvert\mu_b\rvert$		2.169				2.813			
$\lvert\mu_c\rvert$		0.859				1.131			
$\lvert\mu_t\rvert$		4.348				3.381			

[a] Ref. [208]

The vibrational spectra were predicted from the MP2(full)/6-31G(d) calculations. The predicted scaled frequencies were used together with a Lorentzian function to obtain the simulated spectra. Infrared intensities were obtained based on the dipole moment derivatives with respect to Cartesian coordinates. The derivatives were transformed with respect to normal coordinates by $(\partial\mu_u/\partial Q_i) = \sum_j (\partial\mu_u/\partial X_j)L_{ij}$, where Q_i is the i^{th} normal coordinate, X_j is the j^{th} Cartesian displacement coordinate, and L_{ij} is the transformation matrix between the Cartesian displacement coordinates and the normal coordinates. The infrared intensities were then calculated by $(N\pi)/(3c^2)$ $[(\partial\mu_x/\partial Q_i)^2 + (\partial\mu_y/\partial Q_i)^2 + (\partial\mu_z/\partial Q_i)^2]$. A comparison of the experimental spectra of the gas and solid and simulated infrared spectra of the mixture of the two most stable conformers with relative concentrations calculated for the equilibrium mixture at 25ºC by using the experimentally determined enthalpy difference, pure *Gt* form, and pure *Gg* conformer are shown in Fig. 73 (A-E), respectively. The spectrum of the mixture should be compared to that of the infrared spectrum of the vapor at room temperature. The predicted spectrum is mostly in good agreement with the experimental spectrum which shows the utility of the scaled predicted frequencies and predicted intensities for supporting the vibrational assignment.

Additional support for the vibrational assignments was obtained from the simulated Raman spectra. The evaluation of Raman activity by using the analytical gradient methods has been developed [31-34] and the activity S_j can be expressed as: $S_j = g_j(45\alpha_j^2 + 7\beta_j^2)$, where g_j is the degeneracy of the vibrational mode j, α_j is the derivative of the isotropic polarizability, and β_j is the anisotropic polarizability. To obtain the Raman scattering cross sections, the polarizabilities are incorporated into S_j by multiplying S_j with $(1-\rho_j)/(1+\rho_j)$ where ρ_j is the depolarization ratio of the j^{th} normal

mode. The Raman scattering cross sections and calculated wavenumbers obtained from the Gaussian 03 program were used together with a Lorentzian function to obtain the simulated Raman spectra. Comparison of experimental Raman spectra of the liquid and the predicted Raman spectra of the mixture of the two most stable conformers with relative concentrations calculated for the equilibrium mixture at 25ºC by using the experimentally determined enthalpy difference, pure *Gt* form, and pure *Gg* conformer are shown in Fig. 74(A-D). The spectrum of the mixture should be compared to that of the Raman spectrum of the liquid at room temperature, though it must be noted that the predicted spectrum is that of a molecule in isolation therefore frequency and intensity changes are expected. The predicted spectrum is in reasonable agreement with the experimental spectrum which shows the utility of the predicted Raman spectra for the supporting vibrational assignments.

VIBRATIONAL ASSIGNMENT

From the microwave spectral study it was concluded that there are two conformers that are dominant and if there are other conformers present at ambient temperature their energy differences are sufficiently large so that large fractions of further conformers than the observed ones were ruled out [208]. However, from a subsequent theoretical study, it was concluded there were four conformations which could be identified as present in the gas phase at normal temperature since they all had almost equal total energies within 2 kJ/mol (167 cm^{-1}). These results were obtained by using the program TEXAS written by Pulay [209]. The essential feature of this program system is that energy gradients are calculated analytically, and complete geometry optimizations are carried out by the force relaxation method [29]. For carbon and nitrogen the

investigator [210] used a 4-21 Gaussian basis set of Pople et al. [211]. However these results are considerably different from those which we obtained from our calculations with much larger basis sets (aug-cc-pVTZ) with similar energies for the *Gg* and *Gt* forms but the third conformer had an energy difference of 277 cm^{-1} (3.31 kJ/mol) from Table 113.

Therefore we began the vibrational assignment expecting most of the observed bands would be for these two conformers. Also, since the difference between these two forms was the position of the NH_2 group, one figures most of the carbon-hydrogen fundamentals will have similar frequencies. Thus the spectrum of the gas was expected to be relatively simple.

The assignment of the carbon-hydrogen fundamentals were made based on "group frequencies", predicted frequencies from the *ab initio* calculations as well as the predicted intensities of the infrared bands and the Raman activities. However the depolarization values were of some utility for making assignments particularly for distinguishing bands for either the *Gg* or *Gt* conformer. The CH_2 modes were first assigned and then the NH_2 fundamentals and finally the heavy atom motions (Tables 111 and 112). It is interesting that many of the fundamentals for the *Gg* and *Gt* forms have nearly the same predicted frequencies for the CH_2 modes although some of the P.E.D.s are significantly different, i.e. ν_{13}, ν_{14}, ν_{15}, and ν_{16}.

The fundamentals of most interest are those of the heavy atom modes which should be most sensitive to the *gauche*(G)/*trans*(T) conformational changes i.e. rotation around the C-C bond which should aid in identifying vibrations arising from the forms with the lower abundance. The most interesting of these vibrations is the C-C-C bend

which is observed at 572 cm^{-1} for the *Gg* and *Gt* conformers but for the *Tg* this mode is observed at 526 cm^{-1} and for the *Tt* conformer at 517 cm^{-1}. However most of the other heavy atom vibrations have nearly the same frequencies.

CONFORMATIONAL STABILITY

There are five possible conformers of 2-cyanoethylamine (Fig. 72). The first conformational study for this molecule was a microwave study [208] where the enthalpy difference between *Gg* and *Gt* was estimated to be 0 ± 167 cm^{-1} (0 ± 2 kJ/mol) from intensity comparisons of the K_{-1} a-type R-branch transitions. This method was used since the dipole moments could not be determined. The remaining three conformers could not be assigned even though there were 20 or so unassigned lines so it was concluded that the remaining three conformers must be at least 334 cm^{-1} (4 kJ/mol) higher in energy. The next conformational study was a theoretical study [210] where the energy differences for the five possible conformers were predicted from *ab initio* calculations with the 4-21 gaussian basis set [211]. This basis set is fairly small by modern standards and there is significant disagreement with the predictions with the aug-cc-pVTZ basis set.

Due to the large uncertainty of the enthalpy difference for the two most stable conformers and the indefinite prediction of the remaining conformers' enthalpy differences the energy differences have been predicted (Table 113) with larger basis sets. Additionally the potential function for the rotation around the C-N bond was calculated (Fig. 75) by using the MP2(full) method with the 6-311+G(2d,2p) basis set, and an experimentally determined enthalpy difference has been obtained from band intensities of the infrared spectra of the vapor at room temperature. By utilizing the relative band intensities at room temperature from the infrared spectra of the gas an experimental

enthalpy difference can be determined. The bands at 1044 and 1000 cm^{-1} have been confidently assigned for the *Gg* and *Gt* conformers, respectively. The relative intensities were measured for these intense Q-branches and from this band pair the enthalpy difference was determined to be 75 cm^{-1} in the vapor phase. This value falls within the range given by the previous microwave study [208], but no uncertainty can be determined due to only one band pair being sufficiently resolved. The band at 526 cm^{-1} can be confidently assigned to the *Tg* conformer and its band intensity can be measured. With the band intensity of the 1044 cm^{-1} fundamental for the *Gg* form an enthalpy difference of 333 cm^{-1} (3.98 kJ/mol) was obtained. This value agrees with the previous microwave determination as well as the *ab initio* predictions but its certainty is questionable as the intensity of extremely weak bands is difficult to measure accurately. The remaining two conformers have significantly higher energy but only the *Tt* could be found in the infrared spectra of the gas as a low intensity Q-branch though the intensity could not be measured with enough accuracy to determine the enthalpy difference experimentally.

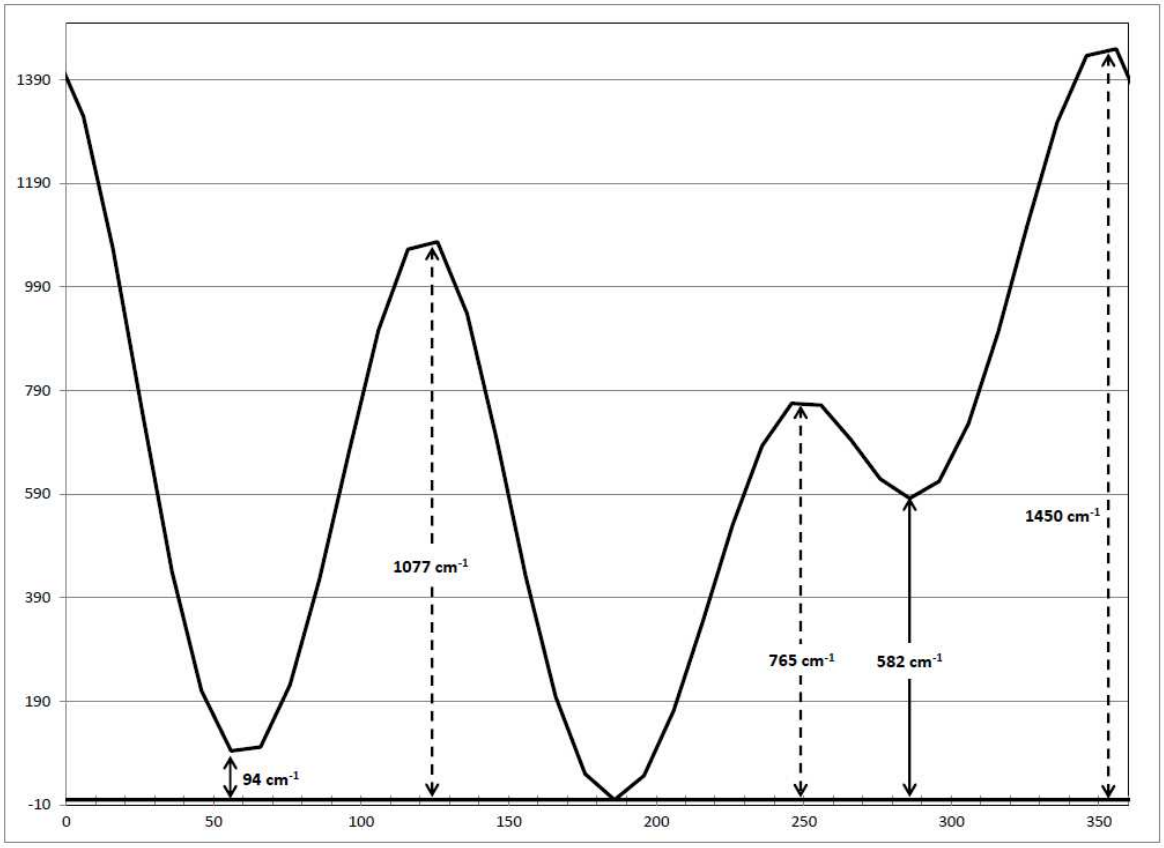

Figure 75. Potential function of rotation around the C-N bond (H_6-N_1-C_2-C_3 dihedral angle) for the gauche C-C-C-N heavy atom structure calculated using MP2(full) method with 6-311+G(2d,2p) basis set.

STRUCTURAL PARAMETERS

In the microwave study [208], all but two of the structural parameters were assumed for the two identified conformers and these parameters were assumed to be the same for both conformers. The two parameters that were fitted were the NCC angle and the NCCC dihedral angle. Due to these assumptions the structural parameters from the microwave study have large uncertainties. Therefore, we have determined the structural

parameters for the two conformers by utilizing the rotational constants previously reported from the microwave study [208]. Only one isotopic species was studied for the two conformers and, thus, only three rotational constants are available for each conformer.

We have found that good structural parameters for hydrocarbons and many substituted ones can be determined by adjusting the structural parameters obtained from the *ab initio* MP2(full)/6-311+G(d,p) calculations to fit the rotational constants obtained from microwave experimental data by using a computer program "A&M" (*Ab initio* and Microwave) developed [14] in our laboratory. In order to reduce the number of independent variables, the structural parameters are separated into sets according to their types where bond distances in the same set keep their relative ratio, and bond angles and torsional angles in the same set keep their difference in degrees. This assumption is based on the fact that errors from *ab initio* calculations are systematic. Additionally, we have also shown that the differences in predicted distances and angles from the *ab initio* calculations for different conformers of the same molecule can usually be used as one parameter with the *ab initio* predicted differences except for some dihedral angles. Therefore, it should be possible to obtain "adjusted r_0" structural parameters for the two conformers which have the determined rotational constants of 2-cyanoethylamine by utilizing the previously reported values from the earlier microwave study [208].

We [51] have shown that *ab initio* MP2(full)/6-311+G(d,p) calculations predict the r_0 structural parameters for more than fifty carbon-hydrogen distances to at least 0.002 Å compared to the experimentally determined values from isolated CH stretching frequencies which were compared [5] to previously determined values from earlier

microwave studies. Therefore, all of the carbon-hydrogen distances can be taken from the MP2(full)/6-311+G(d,p) predicted values for *Gg* and *Gt* conformers of 2-cyanoethylamine. The resulting adjusted r_0 parameters are listed in Table 114, where it is believed that the N-C, C-C and N-H distances should be accurate to ± 0.003 Å, the C-H distances should be accurate to ± 0.002 Å, and the angles should be within ± 0.5°.

The fit of the six determined rotational constants (Table 115) by the structural parameters for the *Gg* and *Gt* conformers is remarkably good with the largest differences being 0.80, 0.60 and the smaller ones of 0.30 and 0.10 MHz. Therefore, it is believed that the suggested uncertainties are realistic values and the determined structural parameters are probably as accurate as can be obtained for the molecule in the gas phase by the microwave substitution method.

Table 115. Comparison of experimental rotational constants obtained from microwave spectra and adjusted r_0 structural parameters of 2-cyanoethylamine.

Conformers	Rotational constants	Experimental[a]	Adjusted r_0	$\|\Delta\|$
Gg				
$H_2NCH_2CH_2CN$	A	10526.455(38)	10527.022	0.6
	B	3387.403(13)	3388.004	0.6
	C	2781.573(13)	2780.996	0.6
Gt				
$H_2NCH_2CH_2CN$	A	10281.375(19)	10282.233	0.8
	B	3367.7496(43)	3367.8466	0.1
	C	2761.0828(39)	2761.4188	0.3

[a]Ref [208].

DISCUSSION

The mixing was extensive for four modes; ν_{16} (21% C-C(-N) stretch, 29% C-N stretch) which has 6 contribution with 10% or more and ν_{13} (27% NH_2 twist), ν_{18} (35% C-C(≡N) stretch), ν_{20} (35% β-CH_2 wag), and ν_{23} (50% C-C-N bend) which have 5 contributions of 10% or more. Therefore several of the approximate descriptions for the fundamentals of the *Gg* form are more for bookkeeping than providing descriptions of the molecular motions.

The assignment was somewhat complicated by the nearly equal amounts of both conformers present. Therefore, significant reliance on the predicted wavenumbers was necessary to assign many of the modes with group frequencies also playing a significant role. Nevertheless the predicted wavenumbers for the *Gg* and *Gt* forms had average errors of 11 and 13 cm^{-1}, respectively. These errors correspond to percent errors of 0.7 and 0.8%. Where the C≡N stretch, NH_2 deformation, and NH_2 rock were excluded due to the well-known problems the MP2(full) method has predicting these modes. A significant amount of the error is due to the predictions for the C-C-N bending mode and the C-C(≡N) stretching mode but the assignments agree with previously reported group frequencies for these vibrations.

The predicted infrared intensities (Table 111 and 112) from the MP2 calculations for the C≡N stretch are poorly predicted as can be observed in Fig. 73 where the infrared spectra of the gas is 30 times more intense than that predicted. Similarly the Raman activities (Fig. 74) for this mode are almost three times more intense. These large differences are the result of the well-known problem from the MP2(full) calculations

which results in a predicted structural parameter for the triple bond being nearly 0.013 Å longer than the value determined for the adjusted r_0 value (Table 114).

To support the experimental enthalpy difference of 75 cm^{-1} for *Gg* to *Gt* in the vapor state the *ab initio* energy differences have been determined by a variety of basis sets (Table 113) for comparison. It is of particular interest that the energy difference from the MP2(full) method with the aug-cc-pVTZ basis set gives a value of 73 cm^{-1} and the 6-311+G(2d,2p) basis set which was used to generate the predicted potential function gives a value of 83 cm^{-1}. These values of the energy differences are in excellent agreement with the enthalpy difference for *Gg* to *Gt*. The order of stability by the *ab initio* MP2(full) calculation with the aug-cc-pVTZ basis set agrees with that predicted in the previous microwave study [208] and agrees with the spectral information obtained in the current study. However, it should be noted that the same method without diffuse functions gives the *Gt* conformer as being more stable. This is interesting as the diffuse functions seem to better account for the intramolecular hydrogen bonding of the amine with the cyanide as they account for the more distant portions of the molecular orbitals. The DFT calculations by the B3LYP method give the *Gt* conformer as being more stable for all basis sets though adding diffuse functions to the basis set lowers the predicted energy difference by approximately 100 cm^{-1}.

This order of stability seems to be largely the result of the amine group hydrogen-bonding to the π orbitals of the cyanide group. This can be demonstrated with the distances (Table 114) between the amine hydrogen and the cyanide carbon. The order of stability for the first two conformers closely mirrors this distance. The third (*Tg*) and fourth (*Tt*) conformers then are the heavy atom *trans* conformers where intramolecular

hydrogen bonding becomes impossible, though this is the heavy atom configuration that is the most stable in similar amine molecules without the possibility of intramolecular hydrogen bonding. The final possible conformer is the *Gg'* form where the NH_7---C≡N distance is 3.415 Å from the MP2(full)/6-311+G(d,p) calculation which is almost 1 Å larger than the same distance in the *Gg* conformer. This intramolecular hydrogen bonding is a significant influence on both the molecular conformation and structure of these amine molecules as is demonstrated in both this study and previous studies. [170,172]

In the current study the quadratic centrifugal distortion constants have been predicted by *ab initio* MP2(full) and DFT B3LYP calculations with the 6-311+G(d,p) basis set. These data are given in Table 116 and the values are all reasonably well predicted by the both the MP2(full) and B3LYP methods. However, the values predicted by the B3LYP method for Δ_K and δ_K are significantly different than those determined experimentally from the microwave study [208]. The quadrupole coupling constants for both the *Gg* and *Gt* conformers have been predicted by utilizing the MP2(full) and B3LYP methods with the 6-311+G(d,p) basis set to aid in any future microwave study.

Table 116. Quadratic centrifugal distortion constants (kHz) and quadrupole coupling constants (MHz) for *Gg* and *Gt* conformers of 2-cyanoethylamine.

	Gg			*Gt*		
	MP2(full)/ 6-311+G(d,p)	B3LYP/ 6-311+G(d,p)	Exp.[a]	MP2(full)/ 6-311+G(d,p)	B3LYP/ 6-311+G(d,p)	Exp.[a]
Δ_J	3.88	3.79	4.11(30)	3.797	3.687	4.066(38)
Δ_{JK}	-22.33	-23.50	-22.48(58)	-22.03	-23.69	-22.94(40)
Δ_K	62.6	78.58	52.8(60)	60.75	73.10	66.41(46)
δ_J	1.189	1.146	1.313(17)	1.1550	1.1108	1.2335(71)
δ_K	7.95	9.94	7.20(75)	7.23	8.02	8.33(27)
N_1						
χ_{aa}	1.9783	2.2298		-3.0510	-3.2699	
χ_{bb}	2.6797	2.7865		2.2215	2.5317	
χ_{cc}	-4.6580	-5.0162		0.8294	0.7382	
N_5						
χ_{aa}	-1.4340	-1.8227		-1.3839	-1.7231	
χ_{bb}	-0.2256	-0.1853		-0.3033	-0.3195	
χ_{cc}	1.6596	2.0080		1.6872	2.0425	

[a]Ref. [208]

The adjusted r_0 structural parameters have been determined for both the *Gg* and *Gt* conformers of 2-cyanoethylamine (Table 114). In the initial microwave study [208] only two parameters were determined for each conformer *Gg* [*Gt*] which were the angle (°) NCC = 108.0(15) [114.0(15)] and the dihedral angle (°) NCCC = -63(3) [59(3)]. These values have such large error limits that their agreement with the values obtained from the current study for the NCC angle and the NCCC dihedral angle has little meaning. These large differences are due to the assumed structural parameters used in the previous study where for the *Gg* conformer the heavy atom bond distances rN_1-C_2 and

rC_2-C_3 are 0.014 and 0.013 Å too long, respectively. For the *Gt* conformer the heavy atom bond distance rN_1-C_2 is 0.022 Å too long, but the rC_2-C_3 bond distance that was assumed is within 0.003 Å of that obtained in the present study.

The structure obtained in the current study should be accurate to within its error limits and is the most accurate structure that can be determined with the currently available information. This structure can be compared to other similar molecules such as the 2-fluoroethylamine [170] where the adjusted r_0 structural parameters were determined for the Gg [Gt] conformers with values for the distances (Å) of 1.466(3) [1.461(3)] for the C-N and 1.509(3) [1.516(3)] for the C-C. These distances have differences of +0.005 [+0.008] and -0.026 [-0.029] Å compared to the corresponding C-N and C-C bond distances for 2-cyanoethylamine. The difference in the C-N distance averages to approximately the sum of the error limits meaning it may be significant but may also be the errors of the methods. However, the difference in C-C distances is very large though to be expected for a fluoride substituent. This small difference in the C-N bond would seem to indicate the amine group is similarly affected by a fluorine in the 2-position as a cyanide in the 2-position though this similarity does not extend to identically affected.

These substituted ethyl amines are of interest with properties that often cannot be accurately predicted. An example of this is the study of the 2-fluoro substituted ethyl amine [170] the *Gg* to *Gt* energy difference is predicted by MP2(full)/aug-cc-pVQZ calculations to be 105 cm^{-1} which matches well with the experimentally determined enthalpy difference of 62 ± 8 cm^{-1}. It would seem from this result that the energy differences are well predicted by *ab initio* calculations. However, the next most stable conformer is predicted to have an energy difference of 464 cm^{-1} but compared to the

experimentally determined enthalpy difference of 262 ± 26 cm^{-1} it is very poorly predicted with nearly twice the energy. It would be of interest to obtain the enthalpy difference utilizing the variable temperature Raman spectra of the xenon solutions which would be much more accurate than the current value. Also of interest is the ethyl amine moiety with the alcohol substituent which has ten possible conformers and should exhibit both the behaviors of an amine and alcohol.

CHAPTER 19

THE r_0 STRUCTURAL PARAMETERS, CONFORMATIONAL STABILITY, BARRIERS TO INTERNAL ROTATION, AND VIBRATIONAL ASSIGNMENTS FOR TRANS AND GAUCHE ETHANOL

INTRODUCTION

The conformational stabilities and barriers to internal rotation of alcohols in the gas phase or in solution have provided significant challenges to structural scientist for years for a variety of reasons. The O-H barriers for those that have been determined are about one third or less than those obtained for methyl barriers so there is usually only the fundamental vibration and one excited state in the potential well which makes it difficult to obtain the barriers to internal rotation from the torsional frequencies. Also the determination of the conformational stability has been difficult to determine because of the association due to hydrogen bonding which is significant in the gas phase where vibrations due to the dimer as well as trimers can be observed.

The determination of the structural parameters for ethanol has not been without some serious problems. The first structural determination was an electron diffraction study [212] by Rouault and Gallagher that determined the CC and CO bond distances, the CH bond distances as one set, and the CCO angle. The first complete structural determination was a microwave study [213] where Kadzhar et al. used the principal moments of inertia obtained for ethanol and seven isotopomers to determine the structural parameters. This structural determination suffered from the assumption that the methyl hydrogens were all equivalent and the difference between the secondary moments of

inertia P'_{cc}-P_{cc} not being equal to zero. The next complete structural determination was another microwave study [214] by Culot where the rotational spectra of thirteen isotopomers of ethanol were used to determine the r_s structural parameters. In this study [214] it was concluded that the structural determination by the substitution method was unfavorable and the structural parameters obtained were not accurate, this conclusion was based on the finding that the effect of zero-point vibrations is rather large. This effect is even larger when the substitution is done on the in-plane hydrogen atom of the methyl group and the hydrogen atom of the OH group. Culot was aware that the zero-point vibrational effects due to the torsional oscillation of the methyl group resulted in less accurate structural parameters especially those involving the H_7 coordinates, Fig 76. This was followed by two microwave studies [215,216] by Quade et al. where the rotational constants for the *gauche* conformer were determined but no structural parameters were obtained in either study. There are remarkable discrepancies between previously obtained experimental structural parameters of ethanol and the theoretical predicted structural parameters for this molecule. There are also a number of complicating factors which undermine the validity of the structural parameters determined in the previous studies. Additionally, there are currently no structural parameters determined for the *gauche* conformer of ethanol. Therefore, to obtain a more complete determination of the structural parameters for ethanol we have combined the *ab initio* MP2(full)/6-311+G(d,p) predicted parameters with the eighteen experimentally determined rotational constants [214,215] for the two forms to obtain the complete structural parameters for both conformers of ethanol.

Figure 76. Ethanol showing atomic numbering.

EXPERIMENT AND THEORETICAL METHODS

The sample of ethanol was purchased from Sigma-Aldrich Chemical Co., with stated purity of $\geq$99%. The sample was further purified by low-temperature, low-pressure fractionation column and the purity of the sample was verified by comparing the infrared spectrum with that previously reported [217].

The mid-infrared spectrum of the gas (Fig. 77A) was obtained from 4000 to 300 cm^{-1} on a Perkin-Elmer model 2000 Fourier transform spectrometer equipped with a Ge/CsI beamsplitter and a DTGS detector. Atmospheric water vapor was removed from the spectrometer housing by purging with dry nitrogen. The theoretical resolution used to obtain the spectrum of the gas was 0.5 cm^{-1}. One hundred twenty eight interferograms were added and transformed with a boxcar truncation function. The frequencies for the

predicted and observed fundamentals for the *trans* and *gauche* conformers are listed in Tables 117 and 118, respectively.

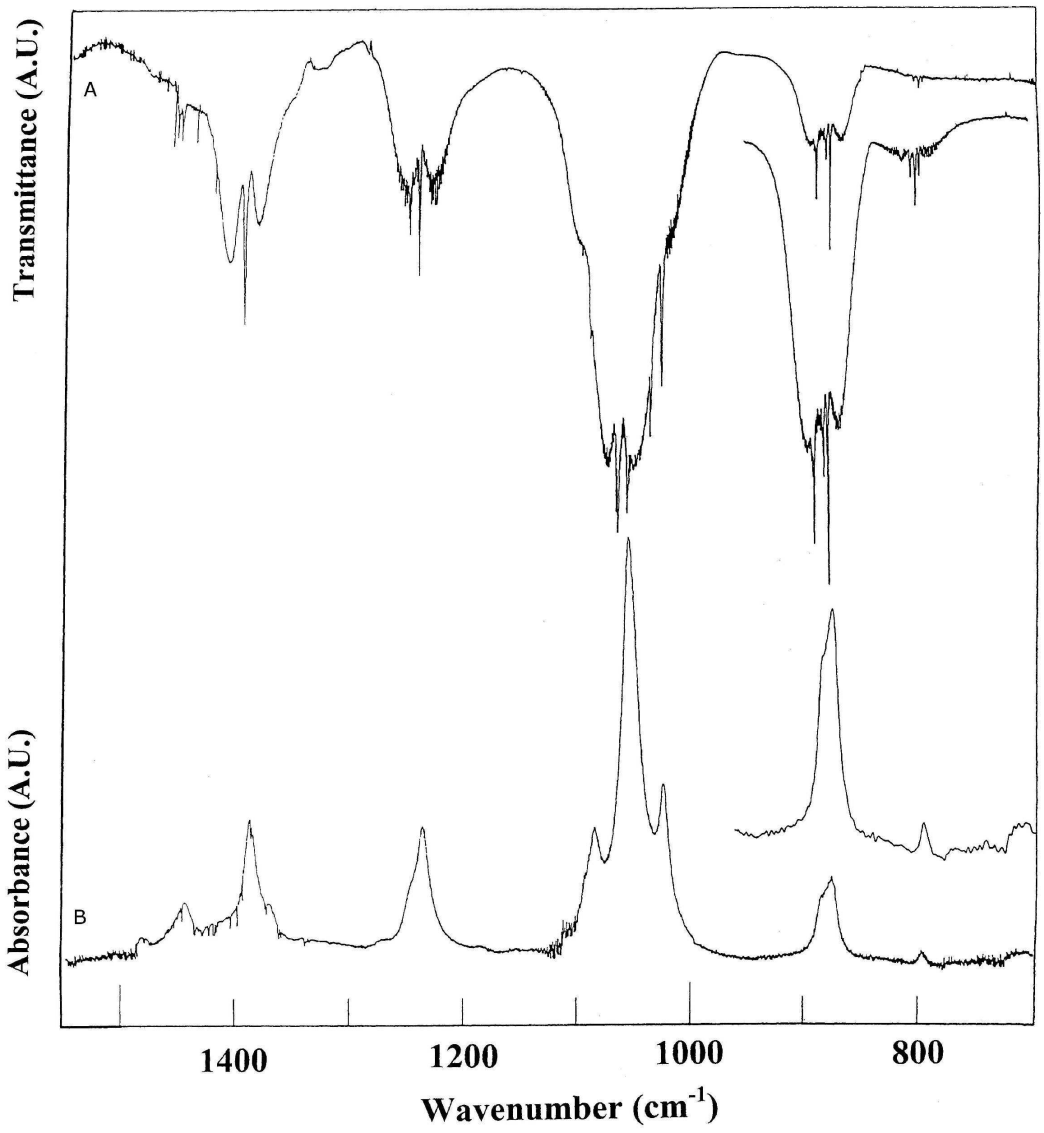

Figure 77. Mid-infrared spectra of ethanol (A) gas; (B) Xe solution at -60 °C.

TABLE 117. Observed and calculated frequencies (cm^{-1}) for *trans* ethanol.

Sym. block	Vib. No.	Fundamental	*ab initio*[a]	fixed scaled[b]	IR int.[c]	Raman act.[d]	IR gas	Xenon solution	Argon Matrix[f]	Raman gas[g]	P.E.D.[h]	Band Contours[i]	
												A	B
A′	ν_1	OH stretch	3779	3585	22.0	96.6	3676	3648	(3657.6)	3675	$100S_1$	94	6
	ν_2	CH_3 antisymmetric stretch	3211	3012	21.0	54.1	2992	2961	2995.6		$99S_2$	23	77
	ν_3	CH_3 symmetric stretch	3119	2926	11.3	98.6	2922	2920	2939.6		$99S_3$	89	11
	ν_4	CH_2 symmetric stretch	3062	2872	59.7	96.1	2888	2868	2900.5	2887	$100S_4$	-	100
	ν_5	CH_2 symmetric deformation	1598	1503	2.1	5.5	1500	1501	1490.2	1460	$92S_5$	77	23
	ν_6	CH_3 antisymmetric deformation	1567	1472	3.6	22.6	1480	1483	1462.8	1460	$84S_6$	21	79
	ν_7	CH_2 wag	1510	1431	16.8	6.1	1450	1446	1415.0	1430	$54S_7,18S_8,15S_9,10S_{11}$	83	17
	ν_8	CH_3 symmetric deformation	1456	1375	0.9	0.8	1367	1367	(1371.3)		$77S_8,19S_7$	80	20
	ν_9	COH bend	1312	1248	83.9	6.6	1241	1238	1240.3	1245	$55S_9,16S_7,15S_{12}$	52	48
	ν_{10}	CO stretch	1146	1090	18.1	6.1	1090	1086	1091.7	1093	$57S_{10},20S_{12}$	67	33
	ν_{11}	CC stretch	1079	1025	54.6	2.9	1027	1025	1025.0	1026	$51S_{11},21S_9,15S_{12}$	69	31
	ν_{12}	CH_3 rock	937	888	11.1	6.1	892	887	886.7	883	$32S_{12},36S_{10},29S_{11}$	70	30
	ν_{13}	CCO bend	427	420	13.1	0.2	418	419	416.5	422	$84S_{13},10S_{12}$	88	12
A″	ν_{14}	CH_3 antisymmetric stretch	3222	3022	21.9	44.1	2987	2965	2985.4		$99S_{14}$	-	-

ν_{15}	CH_2 antisymmetric stretch	3104	2912	62.4	77.9	2901	2884	2953.5	$99S_{15}$	-	-
ν_{16}	CH_3 antisymmetric deformation	1550	1455	5.1	16.7	1455	1453	(1445.1)	$93S_{16}$	-	-
ν_{17}	CH_2 twist	1337	1268	0.2	13.7	1275	1272	(1250.8)	$75S_{17},21S_{19}$	-	-
ν_{18}	CH_2 rock	1223	1160	4.7	3.6	1166	1156	(1083.2)	$57S_{18},25S_{19},15S_{17}$	-	-
ν_{19}	CH_3 rock	848	804	0.01	0.04	801	797	(812.1)	$46S_{19,}38S_{18}$	-	-
ν_{20}	OH torsion	316	300	109.0	4.0	202.6[e]		211	$82S_{20},15S_{21}$	-	-
ν_{21}	CH_3 torsion	265	251	33.8	0.7	244.4[e]		264	$82S_{21},16S_{20}$	-	-

[a]MP2(full)/6-31G(d) predicted values.
[b]MP2(full)/6-31G(d) fixed scaled frequencies with factors of 1.0 for the heavy atom bend, 0.88 for CH stretches and deformations, and 0.90 for all other modes.
[c]Scaled infrared intensities in km/mol from MP2(full)/6-31G(d) .
[d]Scaled Raman activities ($Å^4$/u) from MP2(full)/6-31G(d) .
[e] Ref [218]
[f] Ref [217], Bands marked in parenthesis belong to the *gauche* conformer.
[g] Ref [219]
[h]Calculated with MP2(full)/6-31G(d) and contributions of less than 10% are omitted.
[i]A, B and C values in the last three columns are percentage infrared band contours.

TABLE 118. Observed[a] and calculated frequencies (cm^{-1}) for *gauche* ethanol.

Vib. No.	Fundamental	*ab initio*[b]	fixed scaled[c]	IR int.[d]	Raman act.[e]	IR gas	Xenon solution	Raman gas[g]	P.E.D.[h]	Band Contours[i]		
										A	B	C
ν_1	OH stretch	3772	3579	18.5	61.1	3662	3636	3659	$100S_1$	17	43	40
ν_2	CH_3 antisymmetric stretch	3214	3015	24.7	42.3	2994	~2994		$63S_2,33S_3$	5	13	82
ν_3	CH_3 antisymmetric stretch	3193	2996	44.5	31.4	2987	2975	2985	$55S_3,20S_4,17S_2$	8	45	48
ν_4	CH_2 antisymmetric stretch	3175	2978	6.4	106.3	2972	2962		$52S_4,18S_2,18S_4,12S_6$	29	2	69
ν_5	CH_3 symmetric stretch	3105	2912	12.3	106.3	2936	2930	2939	$98S_5$	67	22	11
ν_6	CH_2 symmetric stretch	3077	2886	61.6	88.9	2912	2892	2914	$75S_6,25S_4$	-	70	30
ν_7	CH_2 symmetric deformation	1585	1490	0.3	3.0	1493	1492	1460	$84S_7,12S_8$	3	95	2
ν_8	CH_3 antisymmetric deformation	1561	1466	2.0	26.3	1465	1464	1460	$79S_8,15S_7$	25	75	-
ν_9	CH_3 antisymmetric deformation	1556	1461	7.0	15.1	1460	1460	1460	$91S_9$	9	6	85
ν_{10}	CH_3 symmetric deformation	1476	1396	30.8	5.8	1394	1388	1395	$58S_{10},31S_{11}$	100	-	-
ν_{11}	CH_2 wag	1450	1373	22.5	3.4	1373	1373	1370	$45S_{11},35S_{10},13S_{12}$	68	32	-
ν_{12}	COH bend	1417	1345	4.4	9.5	1342	1339	1340	$35S_{12},32S_{13},16S_{11}$	61	15	24
ν_{13}	CH_2 twist	1327	1259	10.2	5.2	1249	1248	1245	$42S_{13},26S_{18},13S_{12},12S_{14}$	80	14	6
ν_{14}	CH_2 rock/CH_3 rock	1174	1119	6.7	4.3	1117	1116	1117	$17S_{14},28S_{16},16S_{15},11S_{19},11S_{18}$	5	73	22
ν_{15}	CO stretch	1120	1063	59.5	5.9	1066	1055	1055	$51S_{15},44S_{17}$	89	11	-
ν_{16}	CH_3 rock/COH bend	1099	1044	57.3	1.4	1058	1055	1055	$19S_{16},32S_{12},15S_{14},11S_{18}$	62	38	-
ν_{17}	CC stretch	922	875	61.1	7.8	879	879	883	$36S_{17},31S_{15},30S_{16}$	66	33	1

ν_{18}	CH_3 rock	829	786	3.1	0.2	803	800		$43S_{18},43S_{14}$	14	43	43
ν_{19}	CCO bend	430	423	15.6	0.6	420	419	422	$81S_{19,}11S_{16}$	30	58	12
ν_{20}	OH torsion	330	313	128.1	3.3	243.1/ 195.8[f]			$89S_{20}$	39	32	29
ν_{21}	CH_3 torsion	285	270	9.4	0.3	274			$91S_{21}$	14	69	17

[a] Ref [217] assigned three gauche conformer bands; 3662.2, 1076.6, and 889.4 cm^{-1}.
[b] MP2(full)/6-31G(d) predicted values.
[c] MP2(full)/6-31G(d) fixed scaled frequencies with factors of 1.0 for the heavy atom bend, 0.88 for CH stretches and deformations, and 0.90 for all other modes.
[d] Scaled infrared intensities in km/mol from MP2(full)/6-31G(d) .
[e]Scaled Raman activities ($Å^4$/u) from MP2(full)/6-31G(d) .
[f] Ref [218]
[g] Ref [219]
[h] Calculated with MP2(full)/6-31G(d) and contributions of less than 10% are omitted.
[i]A, B and C values in the last three columns are percentage infrared band contours.

The mid-infrared spectra (4000 to 400 cm^{-1}) of the sample dissolved in liquefied xenon (Fig. 77B) were recorded on a Bruker model IFS-66 Fourier transform spectrometer equipped with a globar source, a Ge/KBr beamsplitter and a DTGS detector. In all cases, 100 interferograms were collected at 1.0 cm^{-1} resolution, averaged and transformed with a boxcar truncation function. For these studies, a specially designed cryostat cell was used. It consists of a copper cell with a path length of 4 cm with wedged silicon windows sealed to the cell with indium gaskets. The copper cell was enclosed in an evacuated chamber fitted with KBr windows. The temperature was maintained with boiling liquid nitrogen and monitored by two Pt thermo resistors.

The *ab initio* calculations were performed with the Gaussian-03 program [22] using Gaussian-type basis functions. The energy minima with respect to nuclear coordinates were obtained by the simultaneous relaxation of all geometric parameters using the gradient method of Pulay [29]. A variety of basis sets as well as the corresponding ones with diffuse functions were employed with the Møller-Plesset perturbation method [21] to the second order MP2 with full electron correlation as well as with the density functional theory by the B3LYP method and can be seen in Table 119.

TABLE 119. Calculated energies (hartree) and energy differences (cm^{-1}) for the two conformers and transition states of ethanol.

Method / Basis set	Basis functions	*trans*[a]	Δ^{b}_{tg}	CH_3 barrier[c]	CH_3 barrier[d]	($t \rightarrow g$) barrier[e]	($g \rightarrow g$) barrier[f]
MP2(full)/6-31G(d)	57	-0.528955	-30	1310	1402	477	639
MP2(full)/6-31+G(d)	69	-0.542510	66	1309	1422	442	554
MP2(full)/6-31G(d,p)	75	-0.582081	-29			398	495
MP2(full)/6-31+G(d,p)	87	-0.595132	59			448	620
MP2(full)/6-311G(d,p)	90	-0.693295	-108	1206	1321	467	683
MP2(full)/6-311+G(d,p)	102	-0.702059	-5	1252	1401	373	595
MP2(full)/6-311G(2d,2p)	123	-0.740875	14	1337	1492	395	449
MP2(full)/6-311+G(2d,2p)	135	-0.748375	73	1234	1415	392	422
MP2(full)/6-311G(2df,2pd)	174	-0.798083	26	1184	1274	423	444
MP2(full)/6-311+G(2df,2pd)	186	-0.805164	68	1238	1302	399	415
MP2(full)/cc-pVTZ	174	-0.142838	77	1203	1301		
MP2(full)/aug-cc-pVTZ	276	-0.811230	70	1268	1345		
MP2(full)/aug-cc-pVQZ	516	-0.892742	82	1240	1309		
B3LYP/6-31G(d)	57	-1.033805	-106	1215	1313	418	587
B3LYP/6-31+G(d)	69	-1.045630	26	1106	1206	421	483
B3LYP/6-311G(d,p)	90	-1.088124	-79	1192	1256	398	581
B3LYP/6-311+G(d,p)	102	-1.095063	22	1114	1196	367	484
B3LYP/6-311G(2d,2p)	123	-1.095358	-31	1210	1271	337	438
B3LYP/6-311+G(2d,2p)	135	-1.101692	32	1106	1207	342	406
B3LYP/6-311G(2df,2pd)	174	-1.099179	-19	1081	1131	360	444
B3LYP/6-311+G(2df,2pd)	186	-1.105504	38	1056	1134	350	404
B3LYP/cc-pVTZ	174	-1.105993	2	1083	1137		
B3LYP/aug-cc-pVTZ	276	-1.110261	49	1059	1137		
B3LYP/aug-cc-pVQZ	516	-1.121830	46	1310	1402		

[a]Energy of conformer is given as –(E+154) H.
[b]Difference is relative to *trans* form and given in cm^{-1} with a negative value indicating the *gauche* conformer is more stable.
[c]Methyl torsional barrier for the *trans* conformer.

[d]Methyl torsional barrier for the *gauche* conformer.
[e]Eclipsed form is a transition state that has the OH bond eclipsing the methylene CH bond.
[f]*Cis* form is a transition state that is rotated 180° from the *trans* conformer (OH bond eclipses the CC bond).

In order to obtain descriptions of the molecular motions involved in the fundamental modes of ethanol, a normal coordinate analysis was carried out. The force field in Cartesian coordinates was obtained with the Gaussian 03 program at the MP2(full) level with the 6-31G(d) basis set. The internal coordinates used to calculate the G and B matrices are given for the *trans* and *gauche* conformers in Table 120 with the atomic numbering shown in Fig. 78. By using the B matrix [30], the force field in Cartesian coordinates was converted to a force field in internal coordinates. Subsequently, 0.88 was used as the scaling factor for the CH stretches and deformations and 0.90 was used for all other modes excluding the heavy atom bend to obtain the fixed scaled force field and resultant wavenumbers. A set of symmetry coordinates was used (Table S31) to determine the corresponding potential energy distributions (P.E.D.s). A comparison between the observed and calculated wavenumbers, along with the calculated infrared intensities, Raman activities, depolarization ratios and potential energy distributions for the *trans* and *gauche* conformers of ethanol , are given in Tables 117 and 118, respectively.

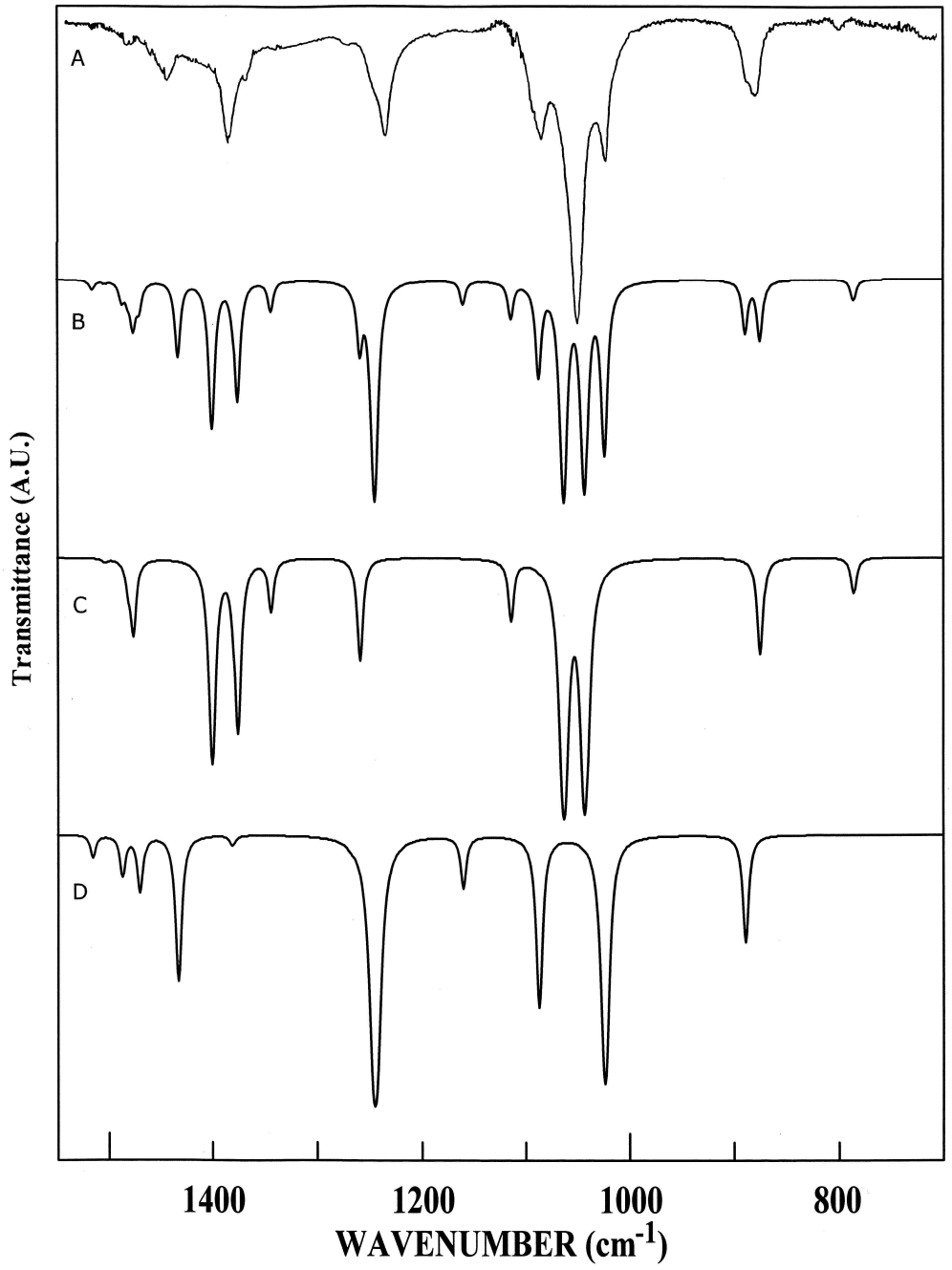

Figure 78. Comparison of experimental and predicted infrared spectra of ethanol: (A) Xe solution at -60 ºC; (B) simulated spectrum of mixture of *trans* and *gauche* conformers at -60^{o}C with ΔH = 62 cm^{-1}; (C) simulated spectrum of *gauche* conformer; (D) simulated spectrum of *trans* conformer.

TABLE 120. Structural parameters[a], rotational constants, and dipole moments for *trans* and *gauche* ethanol.

Parameter	*trans*								*gauche*		
	Int. Coor.	MP2(full)/ 6-311+G(d,p)	B3LYP/ 6-311+G(d,p)	ED[b]	MW[c]	MW[d] r_s	MW[e] r_s	adjusted r_0[f,g]	MP2(full)/ 6-311+G(d,p)	B3LYP/ 6-311+G(d,p)	adjusted r_0[f,g]
$r(O_3\text{-}H_4)$	R_1	0.960	0.962		0.936	0.956	0.9710 (6)	0.962 (3)	0.961	0.963	0.963 (3)
$r(C_2\text{-}O_3)$	R_2	1.426	1.431	1.40	1.426	1.428	1.431 (3)	1.432 (3)	1.424	1.429	1.430 (3)
$r(C_1\text{-}C_2)$	R3	1.513	1.517	1.50	1.533	1.524	1.512 (3)	1.519 (3)	1.519	1.524	1.523 (3)
$r(C_1\text{-}H_7)_{ip}$	r1	1.093	1.093	1.08	1.092	1.093	1.0878 (3)	1.095 (2)	1.094	1.095	1.096 (2)
$r(C_1\text{-}H_8)_{op}$	r2	1.092	1.093	1.08	1.092	1.093	1.0908 (2)	1.094 (2)	1.095	1.095	1.097 (2)
$r(C_1\text{-}H_9)_{op}$	r3	1.092	1.093	1.08	1.092	1.093	1.0908 (2)	1.094 (2)	1.092	1.093	1.094 (2)
$r(C_2\text{-}H_5)$	r4	1.097	1.099	1.08	1.092	1.100	1.0980 (4)	1.099 (2)	1.098	1.099	1.100 (2)
$r(C_2\text{-}H_6)$	r5	1.097	1.099	1.08	1.092	1.100	1.0980 (4)	1.099 (2)	1.091	1.092	1.093 (2)
$\angle C_2O_3H_4$	π_1	107.7	109.0		106.0	104.8	105.4 (1)	107.5 (5)	107.0	108.6	107.0 (5)
$\angle O_3C_2H_5$	π_2	110.6	110.4				109.8 (2)	110.8 (5)	110.6	110.4	110.4 (5)
$\angle O_3C_2H_6$	π_3	110.6	110.4				109.8 (2)	110.8 (5)	105.3	105.1	105.2 (5)
$\angle C_1C_2O_3$	α	107.6	107.9	109.5	107.4	107.6	107.77 (2)	107.6 (5)	112.3	113.0	112.5 (5)
$\angle C_1C_2H_5$	ρ_1	110.1	110.2		109.8	109.5	110.7 (2)	109.6 (5)	110.3	110.4	110.2 (5)

∠$C_1C_2H_6$	ρ_2	110.1	110.2		109.8	109.5	110.7 (2)	109.6 (5)	110.5	110.4	110.5 (5)
∠$H_5C_2H_6$	β	108.1	107.8				108.0 (2)	108.5 (5)	107.7	107.3	107.7 (5)
∠$H_7C_1C_2$	δ_1	110.4	110.4		109.8	110.7	110.5 (1)	110.0 (5)	110.7	110.6	110.7 (5)
∠$H_8C_1C_2$	δ_2	110.2	110.5		109.8	110.7	110.5 (1)	109.7 (5)	110.8	111.2	110.8 (5)
∠$H_9C_1C_2$	δ_3	110.2	110.5		109.8	110.7	110.5 (1)	109.7 (5)	110.3	110.7	110.2 (5)
∠$H_8C_1H_9$	μ_1	108.6	108.3				108.8 (2)	109.0 (5)	108.3	108.2	108.4 (5)
∠$H_7C_1H_8$	μ_2	108.6	108.3				108.8 (2)	109.0 (5)	107.8	107.6	107.9 (5)
∠$H_7C_1H_9$	μ_3	108.7	108.5				108.8 (2)	109.2 (5)	108.8	108.5	108.8 (5)
τ$H_4O_3C_2C_1$	τ_1	180.0	180.0	180.0	180.0	180.0	180.0	180.0	56.9	60.8	56.9 (5)
τ$H_7C_1C_2O_3$	τ_2	180.0	180.0	180.0	180.0	180.0	180.0	180.0	177.4	177.2	177.4 (5)
A		35060	35097		34890.8	34890.8	34891.73 (7)	34898.282	34252	34417	34173.8
B		9421	9320		9350.8	9350.8	9350.65 (2)	9352.933	9270	9122	9191.5
C		8189	8113		8135.0	8135.0	8135.22 (2)	8136.169	8161	8063	8100.4
$\|\mu_a\|$		0.014	0.043				0.058 (100)		1.597	1.419	
$\|\mu_b\|$		1.903	1.772				1.473 (100)		0.024	0.076	
$\|\mu_c\|$		0.000	0.000				0.000		1.338	1.233	

$\|\mu_t\|$	1.903	1.773	1.474 (100)	2.084	2.660

[a]Bond distances in Å, bond angles in degrees, rotational constants in MHz, and dipole moments in Debye.
[b]Ref [212].
[c]Assumed structural parameters, Ref [222]
[d]Ref [213]
[e]Ref [214]
[f]This study.
[g]Adjusted structural parameters with experimental rotational constants taken from Ref [215].

VIBRATIONAL ASSIGNMENT

To obtain information on the relative conformational enthalpy change between the two conformers a complete vibrational assignment is required for both conformers from 700 to 1300 cm^{-1} which is the usual region where conformer pairs can be identified. The lower spectral region will have the smallest number of combination and overtone bands possible so it is the best area to obtain the enthalpy difference. Since there is very little change in the force constants with conformational interchange of the OH rotor most of the fundamentals for the *trans* and *gauche* forms have nearly the same frequencies. Therefore as much information as can be obtained is needed to make the assignments of the fundamentals of the two forms.

First the vibrational spectrum were predicted from the MP2(full)/6-31G(d) calculations. The predicted scaled frequencies were used together with a Lorentzian function to obtain the calculated infrared spectra. Infrared intensities determined from MP2(full)/6-31G(d) calculations were obtained based on the dipole moment derivatives with respect to Cartesian coordinates. The derivatives were transformed with respect to normal coordinates by $(\partial\mu_u/\partial Q_i) = \sum_j (\partial\mu_u/\partial X_j)L_{ij}$, where Q_i is the i^{th} normal coordinate, X_j is the j^{th} Cartesian displacement coordinate, and L_{ij} is the transformation matrix between the Cartesian displacement coordinates and the normal coordinates. The infrared intensities were then calculated by $[(N\pi)/(3c^2)]\ [(\partial\mu_x/\partial Q_i)^2 + (\partial\mu_y/\partial Q_i)^2 + (\partial\mu_z/\partial Q_i)^2]$. In Fig. 78 a comparison of the experimental and simulated infrared spectra of ethanol is shown for the spectral region from 900 to 1500 cm^{-1}. The predicted spectrum is in relatively good agreement with the experimental spectrum which shows the utility of the scaled predicted frequencies and intensities for supporting the vibrational assignment.

To further support the vibrational assignments, we have simulated the Raman spectra from the *ab initio* MP2(full)/6-31G(d) results. The evaluation of Raman activity by using the analytical gradient methods has been developed [31-34]. The activity S_j can be expressed as: $S_j = g_j (45\alpha_j^2 + 7\beta_j^2)$, where g_j is the degeneracy of the vibrational mode j, α_j is the derivative of the isotropic polarizability, and β_j is that of the anisotropic polarizability. To obtain the polarized Raman scattering cross sections, the polarizabilities are incorporated into S_j by multiplying S_j with $(1-\rho_j)/(1+\rho_j)$, where ρ_j is the depolarization ratio of the j^{th} normal mode. The Raman scattering cross sections and calculated wavenumbers obtained from the Gaussian 03 program were used together with a Lorentzian function to obtain the simulated Raman spectra of the gas. The predicted spectrum of the mixture should be compared to that of the Raman spectrum of the gas (Fig. 79) and the relative intensities of the bands are of use in the vibrational assignment of the Raman data, particularly for the Raman spectra of the gas.

The earliest complete vibrational assignment was reported by Perchard and Josien [220] who prepared eleven isotopologues along with the normal species of ethanol for which the vibrations for the various segments were clearly identified. However the assignments were made based on the belief that the *gauche* conformer was the most stable form and in great abundance so most of the observed bands were assigned as *gauche* bands. However two years later Barnes and Hallam [217] carried out a vibrational study of ethanol by utilizing argon matrix isolation and concluded that the *trans* conformer was the more stable form and it was in the ratio of 2 to 1 so most of the observed fundamentals were assigned to the *trans* conformer. From a later Raman spectral study [219] the *trans* conformer was determined to be the more stable form from

their relative intensities to the bands assigned to the *gauche* form. This conclusion was supported by the potential function determined in that study which was further supported by an earlier microwave study [221]. Therefore we have re-investigated the vibrational spectra and made the assignments by utilizing *ab initio* predicted frequencies, infrared intensities and Raman activities along with infrared band contours. From the extensive predictions from the *ab initio* calculations it was possible to confidently assign practically all of the fundamentals for both conformers of ethanol (Tables 117 and 118).

CONFORMATIONAL STABILITY

To determine the enthalpy differences between the two conformers of CH_3CH_2OH, the sample was dissolved in liquefied xenon and the mid-infrared spectra were recorded as a function of temperature from -55 to -100°C. Relatively small interactions are expected to occur between xenon and the sample though the sample can associate with itself forming a dimer or trimer. Nevertheless, only small frequency shifts are anticipated for the xenon interactions when passing from the gas phase to the liquefied xenon solutions. A significant advantage of this study is that the conformer bands are better resolved in comparison with those in the infrared spectrum of the gas. From *ab initio* calculations, the dipole moments of the two conformers are predicted to have similar values and the molecular sizes of the two conformers are nearly the same, so the ΔH value obtained from the temperature dependent FT-IR study is expected to be close to that for the gas [16-20].

Once confident assignments have been made for the fundamentals of both conformers the task was then to find a pair or more of bands for which the enthalpy determination could be obtained. To minimize the effect of combination and overtone

bands in the enthalpy determination it is desirable to have the lowest frequency pair that is possible to use for the determination. Additionally, since there is clear evidence that the ethanol molecules associate in the gas phase it is certainly going to associate in the xenon solution, although it may be to a lesser amount. Nevertheless to ensure the association is minimized it is desirable to have vibrational fundamentals that are not significantly affected by dimerization or further association. Therefore the vibrations that have a large amount of methyl group (CH_3) vibrational motion were initially assessed. There is a band at 887 cm^{-1} for the *trans* conformer which has a large contribution from the CH_3 motion (41% S_{12}) as well as some CC stretch and CO stretch contributions. Therefore the methyl rock and CC stretch should be minimally affected by association. A similar band at 879 cm^{-1} for the *gauche* conformer is present and the difference in frequency is sufficient to be able to provide band contours with which to determine the relative intensities from -60 to -90°C. The antisymmetric rock which is in the lower frequency region could likewise be a good candidate but unfortunately the band is so weak that there is difficulty in separating the two vibrations even though they are predicted to be separated by 18 wavenumbers. An effort was also made to use the 1025 cm^{-1} band of the *trans* conformer but it appeared to be significantly affected by association since the determined enthalpy difference was relatively large. Therefore only one conformer pair was found that provided appropriate band intensities that could readily be determined as the temperature was lowered.

The intensities of the infrared bands were measured as a function of temperature and their ratios were determined. By application of the van't Hoff equation $-\ln K = \Delta H/(RT) - \Delta S/R$, the enthalpy difference was determined from a plot of $-\ln K$ versus $1/T$,

where ΔH/R is the slope of the line and K is substituted with the appropriate intensity ratios, *i.e.* I_{trans} / I_{gauche}. It was assumed that ΔH, ΔS, and α are not a function of temperature in the temperature range studied. This pair of bands was utilized for the determination of the enthalpy difference, and the resulting value of 62 ± 12 cm^{-1} (Table 121) and the van't Hoff plot is shown in Fig. 80. This value is consistent with the predicted value from *ab initio* calculations with large basis sets (Table 119). This error limit is derived from the statistical standard deviation of one sigma of the measured intensity data, but it does not take into account small associations with the liquid xenon or the interference of overtones and combination bands in near coincidence with the measured fundamentals. Thus, the abundance of the *trans* conformer present at ambient temperature is 40 ± 1%.

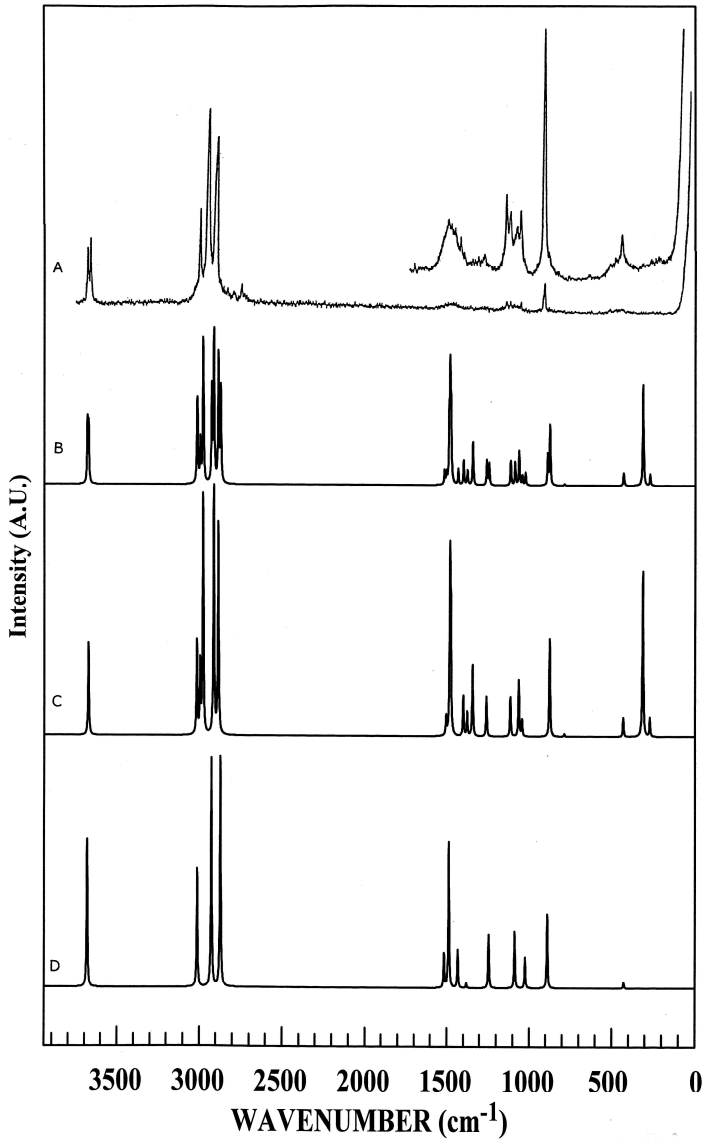

Figure 79. Comparison of experimental and predicted Raman spectra of ethanol: (A) gas [8]; (B) simulated spectrum of the mixture of *trans* and *gauche* conformers at 25ºC with ΔH = 62 cm^{-1}; (C) simulated spectrum of *gauche* conformer; (D) simulated spectrum of *trans* conformer A' block.

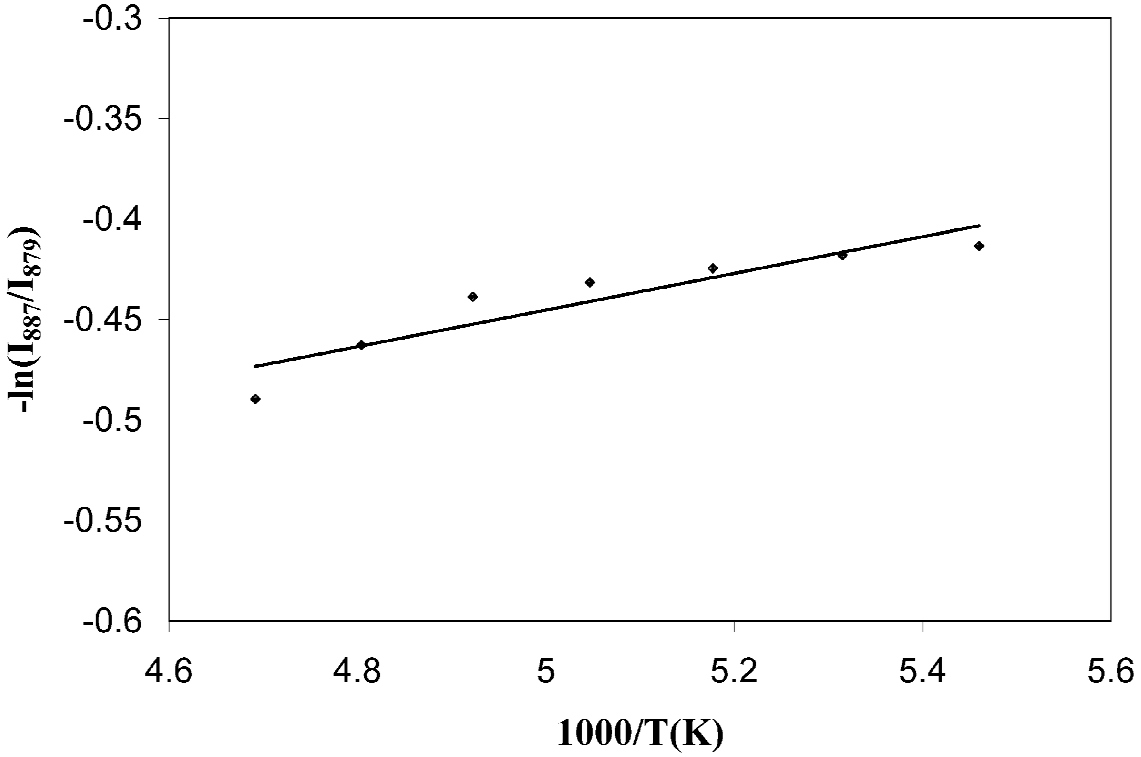

Figure 80. van't Hoff plot of $-\ln(I_{887}/I_{879})$ as a function of 1/T.

TABLE 121. Temperature and intensity ratios of the *trans* and *gauche* bands of ethanol.

	T(°C)	1/T ($\times 10^{-3}$ K^{-1})	I_{887} / I_{879}
Liquid xenon	–60.0	4.692	0.613
	–65.0	4.804	0.630
	–70.0	4.923	0.645
	–75.0	5.047	0.649
	–80.0	5.177	0.654
	–85.0	5.315	0.658
	–90.0	5.460	0.661
ΔH (cm^{-1})			62 ± 12

STRUCTURAL PARAMETERS

Initial structural parameters for the ethanol were proposed from an early electron diffraction study [212] where the structures of ethanol and ethyl mercaptan were determined by the visual method and the values are listed in Table 120. This study was followed by a large number of microwave investigations of this molecule but in only seven of these studies were structural parameters reported and in all of these investigations only the parameters for the *trans* form were given [213,214,222-226]. In the earliest of these studies [222-224] the structural parameters were transferred from the corresponding parameters for the haloethanes and methyl alcohol and the rotational constants resulting from these parameters agreed with the experimentally determined ones. In the two most extensive investigations [213,214] following the earlier ones the structural parameters were determined by the substitution method but ethanol is one of the most unfavorable cases as can be imagined as previously indicated for obtaining the parameters by Kraitchman's method and the values are listed in Table 120. Therefore, we believe the determination of the r_0 structural parameters will provide much more reliable ones than the r_s parameters previously reported [213,214].

We have found that good structural parameters for hydrocarbons and many substituted ones can be determined by adjusting the structural parameters obtained from the *ab initio* MP2(full)/6-311+G(d,p) calculations to fit the rotational constants obtained from microwave experimental data by using a computer program developed [14] in our laboratory. In order to reduce the number of independent variables, the structural parameters are separated into sets according to their types where bond distances in the

same set keep their relative ratio, and bond angles and torsional angles in the same set keep their difference in degrees. This assumption is based on the fact that errors from *ab initio* calculations are systematic. Additionally, we have also shown that the differences in predicted distances and angles from the *ab initio* calculations for different conformers of the same molecule can usually be used as one parameter with the *ab initio* predicted differences except for some dihedral angles. Therefore, it should be possible to obtain "adjusted r_0" structural parameters for both conformers of ethanol by utilizing the previously reported fifteen rotational constants from the microwave study [214] of the *trans* conformer along with the three rotational constants for the *gauche* conformer [215].

The carbon-hydrogen distances were taken as a single set and the three heavy atom parameters were then adjusted to provide the best fit of the 15 rotational constants for the *trans* conformer. The fit of the reported experimental rotational constants is shown in Table 122 and the agreement is considered satisfactory. The fit to four of the A rotational constants for the *trans* conformer have larger differences than those for the B and C rotational constants but the A rotational constants are four times larger than the B and C constants so only the A constants for the normal species and that for the molecule with the two ^{13}C atoms have differences larger than those for the other molecules which includes those for the *gauche* form. However by considering the *gauche* conformer as part of the set it is believed that the uncertainties in the determined structural parameters are the same for the *gauche* conformer as those for the *trans* form (Table 120).

TABLE 122. Comparison of rotational constants obtained from modified *ab initio*, MP2/6-311+G(d,p) structural parameters and those from microwave spectra for ethanol.

Isotopomer	Rotational constants	Observed	Calculated	$\|\Delta\|$
trans				
CH_3CH_2OH[a]	A	34891.7	34898.2	6.5
	B	9350.7	9352.0	1.3
	C	8135.2	8136.1	0.9
$^{13}CH_3CH_2OH$[a]	A	34748.9	34752.4	3.5
	B	9087.7	9087.7	0.0
	C	7927.9	7927.8	0.1
$CH_3{}^{13}CH_2OH$[a]	A	34125.1	34122.2	2.9
	B	9351.5	9351.9	0.4
	C	8093.0	8093.2	0.2
$CH_3CH_2{}^{18}OH$[a]	A	34446.1	34445.6	0.5
	B	8953.2	8952.8	0.4
	C	7809.8	7809.4	0.4
$^{13}CH_3{}^{13}CH_2OH$[a]	A	33975.0	33969.1	5.9
	B	9088.3	9087.4	0.9
	C	7887.0	7886.2	0.8
gauche				
CH_3CH_2OH[b]	A	34173.8	34172.1	1.7
	B	9191.5	9191.9	0.4
	C	8100.4	8099.6	0.8

[a]Values for the rotational constants taken from Ref [214].
[b]Values for the rotational constants taken from Ref [215].

DISCUSSION

All of the fundamentals chosen by Perchard and Josien [220] are fundamentals in our study and the bands which they assigned as combination bands are assigned as fundamentals for the *trans* conformer. All of the fundamentals selected in the matrix study [217] are also fundamentals in the current study but it was estimated that the amount of the *trans* conformer was twice the amount of the *gauche* form. However our

study shows that even though the *trans* is more stable the degeneracy of the *gauche* conformer results in it being 60 ± 1 % present at room temperature which resulted in many of the fundamentals assigned to *trans* bands when they are in fact *gauche* fundamentals (Table 117).

The *ab initio* predicted frequencies are in good agreement with the observed fundamentals with those for the *trans* form being predicted with an average difference of 8 cm^{-1} which is 0.5% error for the A′ block and slightly poorer with an average difference of 10 cm^{-1} (0.6 % error) for the A″ block these errors arises mainly from the carbon-hydrogen stretches and the CH_2 wag. For the *gauche* conformer the average difference is 8 cm^{-1} which is 0.5 % error. The advantage of the *ab initio* MP2(full)/6-31G(d) predictions is that the predicted frequencies are usually higher than the observed values or very close to the observed values.

A comparison of the predicted infrared spectrum with the experimental infrared spectrum of the xenon solution Fig. 78 indicates the intensities are very helpful in making the vibrational assignments. The Raman predicted activities are not as valuable but they help particularly when obtained from the gas for a molecule with some symmetry. Only the symmetric modes have the Q-branches which are quite sharp from which the band centers are easily determined (Fig. 79).

The predicted potential function from the *ab initio* MP2(full)/6-311+G(2d,2p) calculation is shown in Fig. 81 which is compared to the experimentally determined potential function [218] for the O-H internal rotation. The *trans* to *gauche* barrier is predicted to be essentially the same at 398 cm^{-1} as the experimentally determined value of 402.8 ± 0.1 cm^{-1}. However the *gauche* to *gauche* barrier is predicted to be 420 cm^{-1}

which is slightly higher than the experimental value of 399.1 ± 0.2 cm^{-1} but the difference shown in the figure is mainly due to the difference between the predicted energy difference of 73 cm^{-1} compared to the enthalpy difference of 45 cm^{-1} reported from the potential function. This enthalpy difference was fixed in the potential function to agree with the previously determined value of 41.2 cm^{-1} from microwave data [215]. In the current study the experimentally determined enthalpy difference of 62 ± 12 cm^{-1} was obtained which is in reasonable agreement with the earlier determined value from the microwave study.

We also predicted the barrier to methyl rotation for both conformers. For the *trans* conformer the predicted CH_3 barrier from the six largest basis sets is 1228 cm^{-1} compared to the experimentally determined value of 1185 ± 16 cm^{-1} (14.18 ± 0.19 kJ/mol) which was obtained from the torsional frequency [218]. It should be noted that the predicted value from MP2(full)/6-311+G(2d,2p) with 135 basis sets gives a value of 1234 cm^{-1} and the calculation from MP2(full)/aug-cc-pVQZ with 516 basis sets predicts a value of 1240 cm^{-1}(Table 119)! For the *gauche* conformer the CH_3 barrier was obtained from the double jumps in the Raman spectrum of the gas from which a value of 1251 ± 2 cm^{-1} (14.97 ± 0.02 kJ/mol) was obtained which should be compared to the predicted value of 1324 cm^{-1}. These predictions for both conformers indicate the *ab initio* values are reasonably good in providing values comparable to the experimentally determined ones and do not vary appreciably with basis set size. However the variation is significant from density functional theory calculations by the B3LYP method (Table 119).

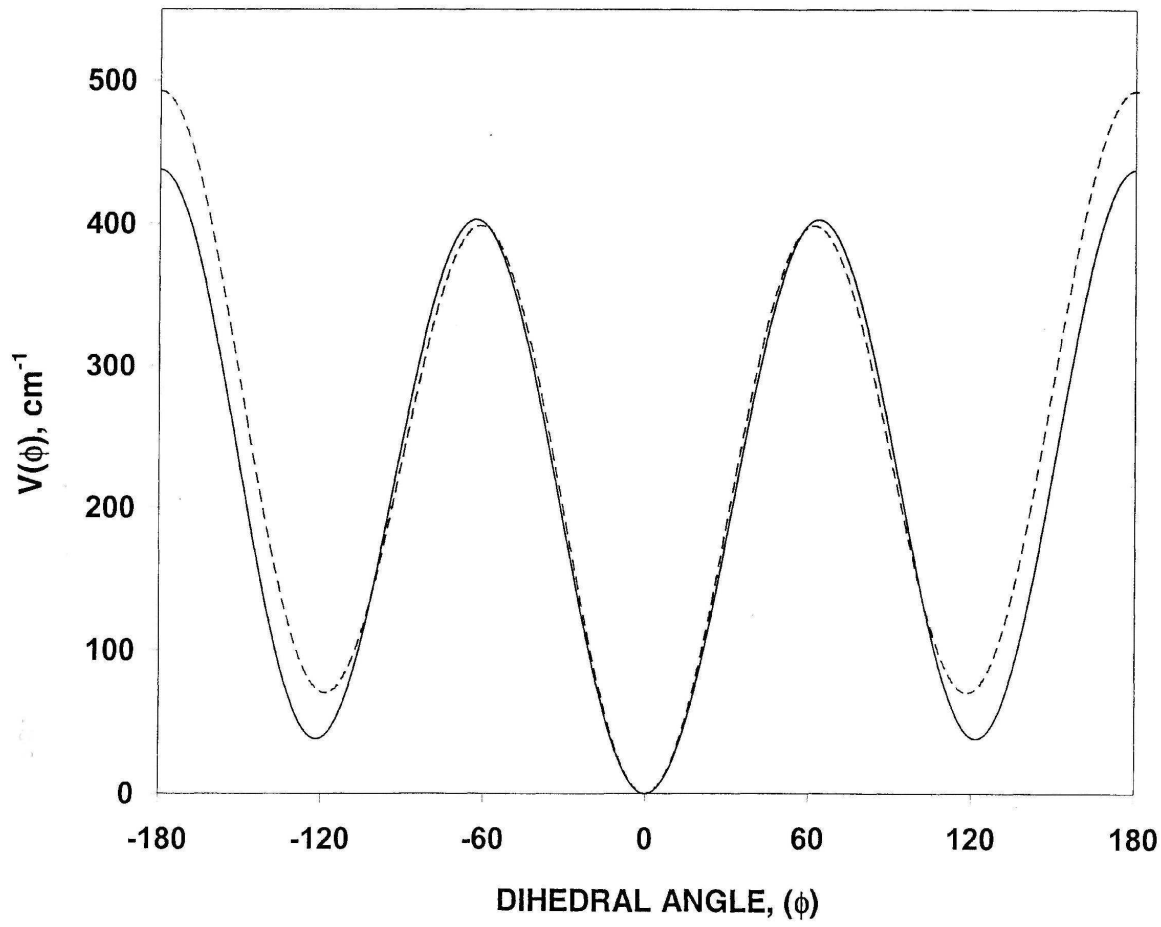

Figure 81. Predicted (dotted curve, from MP2(full)/6-311+G(2d,2p)) and experimental (solid curve[7]) potential function governing the hydroxyl torsion of ethanol.

The determination of the enthalpy was difficult because of the obvious association (probably a dimer) in the xenon solution as the temperature was lowered even with the four cm cell path and a concentration of about 10^{-4} molar. Attempts were made to obtain values from two other pairs but neither one gave a satisfactory van't Hoff plot. More reliable values for the enthalpy differences are obtained when several pairs can be used

but using the low frequency pair reduces the possible effects of combination bands affecting the change in intensity due to the temperature change.

To support the enthalpy determination the predicted intensities of the infrared bands were used along with the measured intensities at one temperature from which the enthalpy can be determined. The value determined from the 887/879 cm^{-1} pair was 97 cm^{-1}, for the 1025/1058 cm^{-1} pair 102 cm^{-1}, and the 1025/1066 cm^{-1} pair 114 cm^{-1} from which the average is 104 cm^{-1} with the *trans* conformer the more stable form. These values are slightly higher than the experimentally determined value but they support the relatively small enthalpy difference between the conformers.

The adjusted-r_0 parameters indicate the C_1-H_7 r_s distance is entirely too short after taking into account that the r_s parameters are smaller than the corresponding r_0 values. A similar problem should be noted for the $\angle C_1C_2H_5(H_6)°$ which has a reported value larger than the r_0 value. However the most dramatic difference is for the $\angle C_2C_3H_4$ where the r_s value is 105.4(1)° whereas the r_0 value is 107.5(5)°. The r(C_1-C_2) r_s distance is 0.006 Å shorter than the r_0 value but taking the reported uncertainties for each parameter they agree. Nevertheless the r_s values are remarkably good considering how unfavorable the ethanol molecule is for the determination of the r_s parameters. Finally it should be noted that the initially reported r_s value [213] reported for the C_1-C_2 distance of 1.524 Å is entirely too long compared to the other determination but most of the other parameters are in agreement with the r_0 values. Although no parameters have been reported for the *gauche* conformer it is believed that the values reported in the current study are quite reliable within the listed uncertainties.

The quadratic centrifugal distortion constants have been predicted from *ab initio* MP2(full) calculations with two basis sets and from density functional theory calculations by the B3LYP method with the same basis sets. Two different sets of experimental values have been reported [214,227] with those from the most recent study expected to be the most accurate. The B3LYP calculations usually give values in better agreement with the experimental values. This is true in the current case except for the Δ_{JK} constant where the experimental value is negative as predicted from the MP2(full) calculations but positive from the B3LYP calculations as shown in Table 123. Also it should be noted the difference between the values reported in the initial study [214] and those determined recently that have much smaller uncertainties. The values initially reported are relatively large compared to the more recently reported distortion constants. This result could affect the value of the A rotational constant where its fit is significantly poorer than the fits for the other two constants for most of the isotopic species.

TABLE 123. Quadratic centrifugal distortion constants (MHz) for *trans* and *gauche*-ethanol.

	trans- CH_3CH_2OH[a]					*gauche*- CH_3CH_2OH[a]			
	MP2(full)/ 6-31G(d)	MP2(full)/ 6-311+G(d,p)	B3LYP/ 6-31G(d)	B3LYP/ 6-311+G(d,p)	Exp.[b]	MP2(full)/ 6-31G(d)	MP2(full)/ 6-311+G(d,p)	B3LYP/ 6-31G(d)	B3LYP/ 6-311+G(d,p)
Δ_J	0.0099631	0.0101104	0.0101674	0.0103277	0.0085374 (8)	0.0113609	0.0116130	0.0120487	0.0123137
Δ_{JK}	-0.04685	-0.04692	0.01723	0.02065	-0.02878 (3)	-0.05510	-0.05756	-0.05844	-0.05570
Δ_K	0.4392	0.4535	0.2107	0.2145	0.2525 (1)	0.5019	0.5038	0.0531	0.5275
δ_J	0.0199325	0.0020267	0.0020146	0.0020494	0.0017377 (5)	0.0022464	0.0023068	0.0023786	0.0023832
δ_K	-0.06045	-0.08170	0.04460	0.04587	0.00668 (2)	-0.05519	-0.05932	-0.06428	-0.07317

[a] Quadratic centrifugal distortion constants are defined according to Watson's A-reduction for I^r representation.
[b] Values for the rotational constants taken from Ref [227].

CHAPTER 20

MICROWAVE, INFRARED, AND RAMAN SPECTRA, r_0 STRUCTURAL PARAMETERS, CONFORMATIONAL STABILITY, AND VIBRATIONAL ASSIGNMENT OF ALLYL THIOL

INTRODUCTION

Mono-substitution at the 3-position of propene, i.e. substituted allyl molecules, results in *cis* and *gauche* conformers where there has been considerable controversy concerning which conformer is the more stable rotamer. For example where the substitution is a methyl group (1-butene), the vibrational data clearly indicates that the more stable form is the *cis* conformer with an enthalpy difference of 64 ± 10 cm^{-1} (0.76 ± 0.12 kJ/mol), from variable temperature infrared spectra of rare gas solutions [228]. However, from the analysis of electron diffraction data, it was concluded [229], that the *gauche* conformer was the more stable form. Also, we have found that *ab initio* calculations may not give the correct conformer stability. For example *ab initio* calculations [230], at the MP2 level with a variety of basis sets with diffuse functions predict the *gauche* conformer to be the more stable form of 3-fluoropropene (allyl fluoride), CH_2=$CHCH_2F$, whereas the experimental results [231,14] clearly show the *cis* conformer to be the more stable rotamer.

When the substituent is an asymmetric rotor such as an OH, SH, NH_2 or PH_2 group there is the possibility of five different stable conformers with *cis* and *gauche* conformations around the C-C bond and *trans* and *gauche* conformations around the C-O (S,N,P) bond (Fig. 82). Only two of the five possible conformations of allyl alcohol (2-

propene-1-ol) have been identified from microwave studies [232-235]. The conformers are designated according to the relative position of the alcohol group (C = *cis* or G = *gauche*) to the double bond (rotation around the C-C bond) and the second one (t = *trans*, g = *gauche*, g′ = *gauche′*) to the relative position of the OH rotor i.e. rotation around the O-C bond. In two earlier microwave studies [232,234] only assignments were made for the *gauche-gauche* (*Gg*) conformer (or –ac,sc) but many lines were observed for a second form. In the most recent microwave study [235] lines which had been observed were assigned for the second conformer to be the *cis-gauche* (*Cg*) form. It was estimated that the two forms had nearly the same energy and these investigators planned to obtain more details on the conformational energies from rotational spectra. To the best of our knowledge such studies have not been reported. However from an earlier electron diffraction investigation [236] the authors reported the concentrations to be 57 ± 6% *Cg* and 43% *Gg* forms.

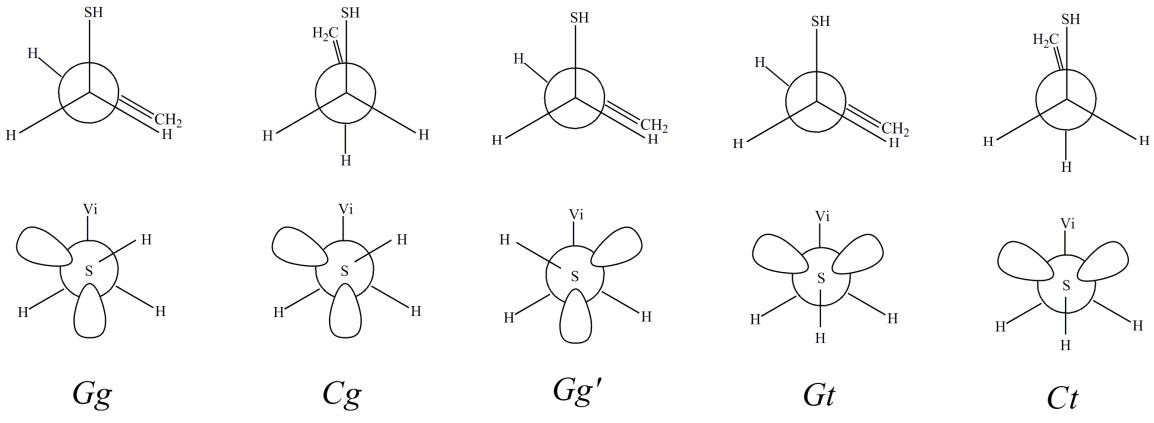

Figure 82. Possible stable conformers of allyl thiol.

Since there was considerable uncertainty which of the two identified conformers of allyl alcohol was the more stable species as well as little scientific information on the other three possible conformers, we [176] carried out variable temperature (-55 to -145°C) studies of the infrared spectra (4000 to 50 cm^{-1}) of the alcohol dissolved in liquid krypton and/or liquid xenon. From these data four of the five possible stable conformers were identified and their relative stabilities determined. The enthalpy differences have been determined between the most stable *Gg* conformer and the second most stable rotamer, *Cg*, to be 135 ± 14 cm^{-1} (1.62 ± 0.1 kJ/mol), and the third most stable conformer is *Ct* 260 ± 46 cm^{-1} (3.11 ± 0.6 kJ/mol), with the fourth most stable conformer *Gt* 337 ± 75 cm^{-1} (4.03 ± 0.9 kJ/mol). This experimentally determined order is consistent with the order of stability predicted by *ab initio* calculations *Gg* > *Cg* > *Ct* > *Gt* > *Gg′*. No evidence was obtained for the fifth conformer Gg′ which is predicted by most of the *ab initio* calculations to be less stable by an enthalpy difference of more than 500 cm^{-1} than the *Gg* form. The percentage of each conformer at ambient temperature was estimated to be *Gg* (54 ± 2%), *Cg* (28 ± 2%), *Ct* (8 ± 2%) and *Gt* (11 ± 3%).

As a continuation of these conformational stability studies of mono substituted allyl molecules we have turned our attention to allyl thiol (mercaptan), $H_2C{=}CHCH_2SH$, where again five possible conformations could be present. We have recorded variable temperature spectra in xenon solutions to identify the less stable conformers not identified by a microwave study [237] as well as the vibration investigation where all of the vibrations were assigned to one conformer [238].

From the microwave study [237] only the dihedral CCCS angle (124 ± 3°) and the gauche angle (50°) of the SH group were obtained from the six determined rotational constants with the remaining parameters estimated from the corresponding parameters of 3-fluoropropene [239] and methyl mercaptan [240]. Although there were a very large number of microwave lines measured the centrifugal distortion constants were not obtained which possibly could make a difference in the values of the rotational constants which are necessary for obtaining all of the structural parameters. Therefore we carried out FT-microwave studies to determine the distortion constants and obtain more accurate structural parameters.

Also to aid in identifying vibrations for additional conformers and to assign fundamentals for the less stable conformers for use in determining the enthalpy differences we have utilized *ab initio* calculations. We obtained the harmonic force fields, infrared intensities, Raman activities, depolarization ratios, and vibrational frequencies from MP2 6-31G(d) *ab initio* calculations with full electron correlation. Additionally MP2(full) *ab initio* and Density Functional Theory (DFT) calculations by the B3LYP method have been carried out with a variety of basis sets up to aug-cc-pVTZ as well as with diffuse functions to predict the conformational stabilities. The results of these spectroscopic, structural, and theoretical studies of allyl thiol are reported herein.

EXPERIMENTS

The sample of allyl thiol was purchased from Alfa Aesar, Shore Road, Heysham, Lancashire – United Kingdom with an estimated purity of 70%. The sample was further purified by a low-temperature, low-pressure fractionation column and the purity of the sample was verified from the infrared spectra of the gas.

Microwave spectra of the sample were recorded by using a “mini-cavity” Fourier-transform microwave spectrometer [25,26] at Kent State University. The Fabry-Perot resonant cavity is established by two 7.5-inch diameter diamond-tip finished aluminum mirrors with a 30.5-cm spherical radius. The Fabry-Perot cavity resides inside a vacuum chamber formed by a 6-way cross and a 15-inch long, 8-inch diameter extension tube. The two cavity mirrors are nominally separated by 30 cm.

The sample was entrained in a 70:30 Ne-He carrier gas mixture at 2 atm and expanded into the cavity to attain 4K using a reservoir nozzle [26] made from a modified Series-9 General Valve. The reservoir nozzle is mounted in a recessed region of the mirror flange, external to the vacuum chamber, and the expansion passes through a 0.182-inch diameter hole into the resonant cavity. The center of the expansion is offset from the center of the mirror by 1 inch.

The sample is irradiated by microwave radiation generated by an Agilent Technologies E8247C PSG CW synthesizer; details of the irradiation and heterodyne detection circuitry can be found in Ref. [27]. The vacuum system can accommodate pulse repetition rates of up to 15 s^{-1} while maintaining a pressure below 10^{-4} torr, and the instrument can scan 450 MHz in 6 hours while averaging 100 shots per scan segment. The frequencies for the measured transitions in the region of 10,500 to 22,000 MHz are listed in Table 124 along with their assignments. Also listed are the frequency differences between the measured values and the values obtained from the determined rotational and the centrifugal distortion constants (Table 125).

TABLE 124. Rotational transitional frequencies (MHz) for *Gg* form of allyl thiol in the ground state.

Transition	Ref [237]	ν (obs)	ν (obs) - ν (calc)
$2_{1,2} \leftarrow 1_{1,1}$	10898.92	10899.219	0.012
$2_{0,2} \leftarrow 1_{0,1}$	10993.34	10993.374	-0.003
$2_{1,1} \leftarrow 1_{1,0}$	11088.10	11088.764	-0.002
$7_{1,7} \leftarrow 7_{0,7}$	16007.21	16007.655	0.002
$6_{1,6} \leftarrow 6_{0,6}$	16321.54	16321.614	-0.002
$3_{1,3} \leftarrow 2_{1,2}$	16347.83	16348.462	-0.002
$3_{0,3} \leftarrow 2_{0,2}$	16488.72	16488.974	-0.002
$3_{2,2} \leftarrow 2_{2,1}$	16492.68	16491.840	-0.012
$3_{2,1} \leftarrow 2_{2,0}$	16492.68	16493.426	0.014
$5_{1,5} \leftarrow 5_{0,5}$	16594.46	16594.593	-0.004
$3_{1,2} \leftarrow 2_{1,1}$	16632.71	16632.771	-0.005
$4_{1,4} \leftarrow 4_{0,4}$	16824.56	16824.815	0.002
$3_{1,3} \leftarrow 3_{0,3}$	17010.96	17010.772	-0.001
$2_{1,2} \leftarrow 2_{0,2}$	17151.33	17151.286	0.000
$1_{1,1} \leftarrow 1_{0,1}$	17245.31	17245.458	0.002
$2_{1,1} \leftarrow 2_{0,2}$	17435.93	17435.630	0.001
$3_{1,2} \leftarrow 3_{0,3}$	17579.44	17579.430	0.000
$4_{1,4} \leftarrow 3_{1,3}$	21796.68	21797.310	0.001
$4_{0,4} \leftarrow 3_{0,3}$	21982.92	21983.270	0.001

The infrared spectrum of the gas (Fig. 83A) and solid (Fig. 84E) were obtained from 3500 to 220 cm^{-1} on a Perkin-Elmer model 2000 Fourier transform spectrometer equipped with a Ge/CsI beamsplitter and a DTGS detector. Atmospheric water vapor was removed from the spectrometer housing by purging with dry nitrogen. The spectra of the gas and solid were obtained with a theoretical resolution of 0.5 cm^{-1} for the gas and 2 cm^{-1} for the solid with 128 interferograms added and truncated. Multiple annealings were required to obtain a satisfactory spectrum of the solid.

TABLE 125. Rotational constants (MHz) and quadratic centrifugal distortion constants (kHz) for *Gg* conformer of allyl thiol.

	MP2(full)/ 6-31G(d)	MP2(full)/ 6-311+G(d,p)	B3LYP/ 6-31G(d)	B3LYP/ 6-311+G(d,p)	exp.[a]	exp.[b]
A	19734.253	19364.997	19872.537	20013.522	20041.7(1)	20041.439(4)
B	2810.886	2844.088	2745.188	2749.474	2795.7(1)	2795.830(1)
C	2714.357	2738.773	2652.192	2657.980	2701.1(1)	2701.084(1)
Δ_J	1.82	1.85	1.59	1.60		1.91(4)
Δ_{JK}	-51.3	-48.5	-44.9	-45.6		-54.8(2)
Δ_K	601	541	567	582		243(4)
δ_J	0.247	0.262	0.197	0.196		0.220(7)
δ_K	-12.9	-10.3	-12.1	-12.3		-10.2(1)

[a]Ref. [237]
[b]This study.

The mid-infrared spectra (3600 to 400 cm^{-1}) of the sample dissolved in liquefied xenon (Fig. 83B) at ten different temperatures (-55 to -100°C) were recorded on a Bruker model IFS-66 Fourier transform spectrometer equipped with a globar source, a Ge/KBr beamsplitter and a DTGS detector. In all spectral determinations, 100 interferograms were collected at 1.0 cm^{-1} resolution, averaged and transformed with a boxcar truncation function. For these studies, a specially designed cryostat cell was used. It consists of a copper cell with a path length of 4 cm with wedged silicon windows sealed to the cell with indium gaskets. The temperature was maintained with boiling liquid nitrogen and monitored by two Pt thermoresistors. After cooling to the designated temperature, a small amount of the sample was condensed into the cell and the system was then pressurized with the noble gas, which condensed in the cell, allowing the compound to dissolve.

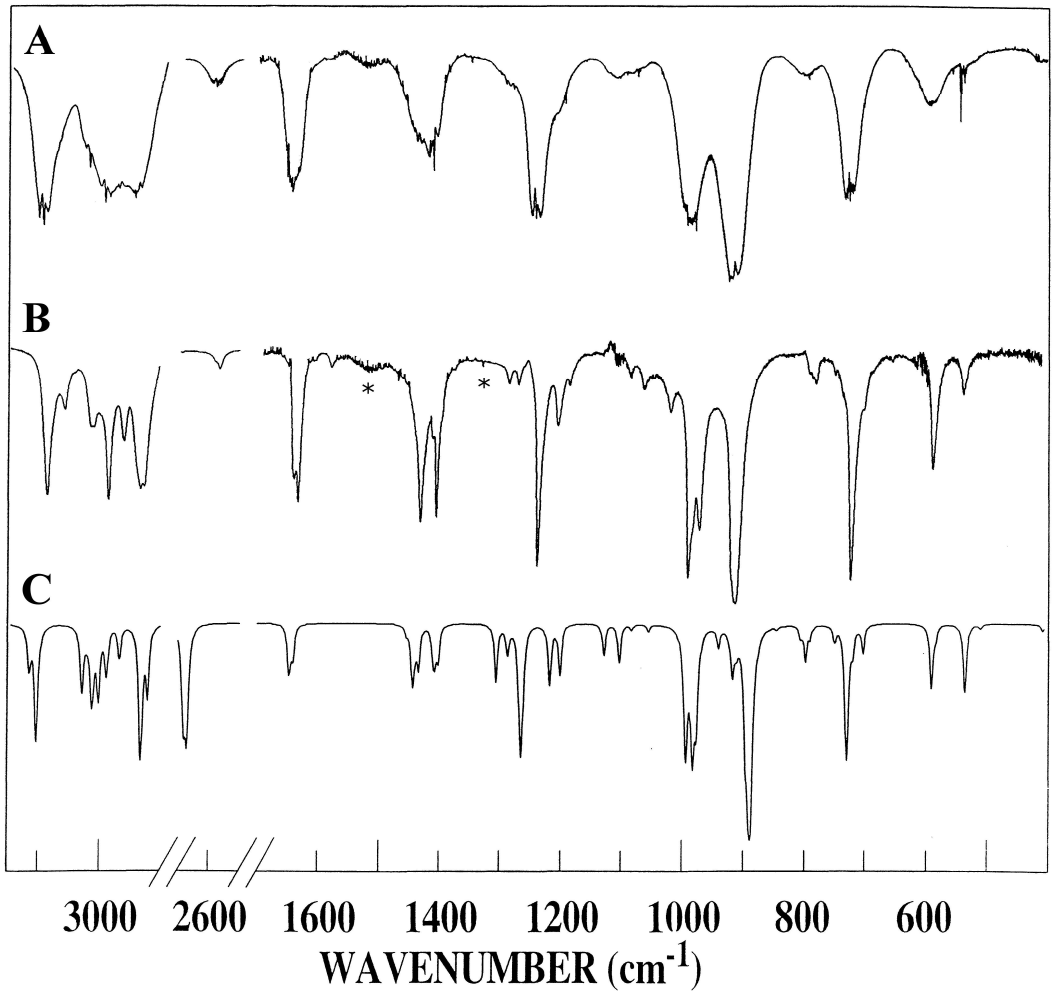

Figure 83. Comparison of experimental and calculated infrared spectra of allyl thiol: (A) observed spectrum of gas; (B) observed spectrum of xenon solution at -70°C, asterisk denotes location of impurity bands that develop soon after purification; (C) simulated spectrum of mixture of *Gg*, *Cg* ($\Delta H = 120$ cm^{-1}), *Gg′* ($\Delta H = 337$ cm^{-1}), and *Gt* ($\Delta H = 360$ cm^{-1}) conformers at 25°C.

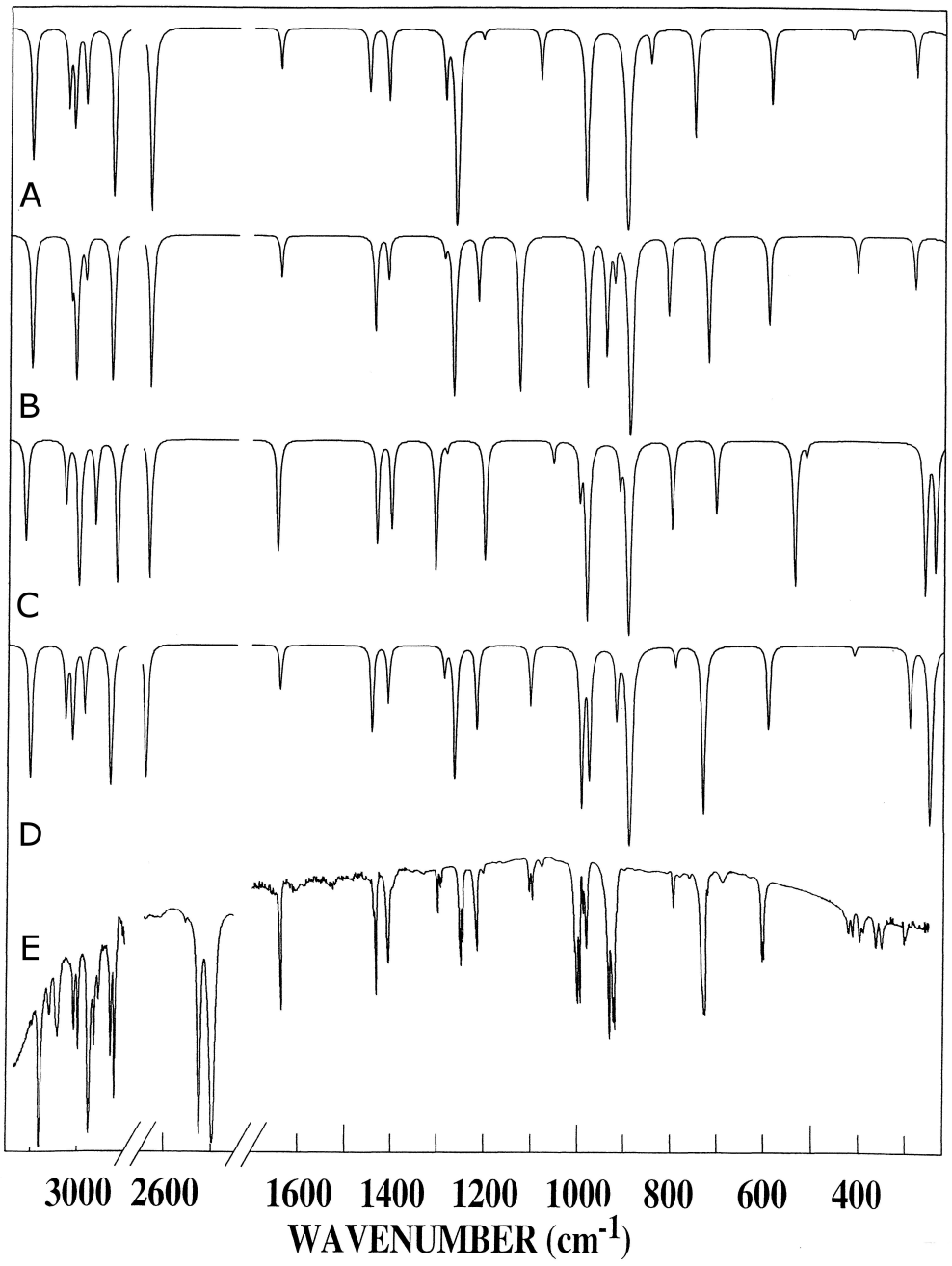

Figure 84. Comparison of experimental and calculated infrared spectra of solid allyl thiol: (A) simulated *Gt* conformer; (B) simulated *Gg′* conformer; (C) simulated *Cg* conformer; (D) simulated *Gg* conformer; (E) observed spectrum.

The Raman spectra of the liquid (Fig. 85A) were recorded from 3500 to 40 cm^{-1} on a Spex model 1403 spectrophotometer equipped with a Spectra-Physics model 2017 argon ion laser operating on the 514.5 nm line. The laser power used was 1.5 W with a spectral bandpass of 3 cm^{-1}. The spectra of the liquid were recorded with the sample sealed in a Pyrex glass capillary. The measurements of the Raman frequencies are expected to be accurate to ± 2 cm^{-1}. All of the observed bands in the Raman spectra of the liquid along with their proposed assignments and depolarization values are listed in Tables 126, 127, 128 and 129 for the *Gauche-gauche* (*Gg*), *Cis-gauche* (*Cg*), *Gauche-gauche'* (*Gg'*), and *Gauche-trans* (*Gt*) conformers, respectively.

TABLE 126. Observed and calculated[a] wavenumbers (cm^{-1}) for *Gg* form of allyl thiol.

Vib. No.	Approx. Description	*ab initio*	fixed scaled[b]	IR int.	Raman act.	dp ratio	IR gas	IR Xe soln.	Raman liquid	IR solid	P.E.D.[c]	Band Contours[d] A	B	C
ν_1	$=CH_2$ antisymmetric stretch	3307	3103	11.0	63.1	0.62	3094	3086	3085	3081	$97S_1$	23	14	63
ν_2	=C-H stretch	3228	3028	4.5	93.4	0.21	3018	3014	3011	3045/3042	$87S_2$	19	2	79
ν_3	$=CH_2$ symmetric stretch	3211	3013	6.4	52.1	0.14	2992	2984	2981	3007/2998	$89S_3$	17	-	83
ν_4	$-CH_2$ antisymmetric stretch	3185	2988	4.2	66.7	0.75	2983	2983	2981	2976	$97S_4$	28	1	71
ν_5	$-CH_2$ symmetric stretch	3125	2932	12.3	85.0	0.10	2935	2924	2927	2930/2921	$100S_5$	4	82	14
ν_6	-SH stretch	2784	2641	10.9	98.0	0.38	2599	2583	2573	2525/2497	$100S_6$	5	72	23
ν_7	-C=C- stretch	1730	1640	2.6	12.3	0.17	1645	1634	1636	1630	$67S_7,14S_9$	62	22	16
ν_8	$-CH_2$ scissoring	1535	1444	5.8	10.0	0.66	1440	1433	1433	1428	$85S_8,11S_9$	-	41	59
ν_9	$=CH_2$ scissoring	1493	1408	3.5	17.9	0.54	1412	1407	1409	1400	$66S_9,14S_8$	62	12	26
ν_{10}	=CH in plane bend	1356	1287	1.7	7.5	0.53	1287	1291	1294	1292	$43S_{10},24S_{11}$	67	32	1
ν_{11}	$-CH_2$ wag	1332	1264	11.2	17.1	0.53	1244	1240	1242	1245/1240	$68S_{11},20S_{10}$	61	32	7
ν_{12}	$-CH_2$ twist	1281	1218	5.6	19.4	0.65	1209	1210	1207	1211	$65S_{12},11S_{13},11S_{16}$	73	9	18
ν_{13}	-C-C- stretch	1160	1103	3.7	5.4	0.69	1093	1091	1094	1099/1092	$18S_{13},19S_{12},18S_{16},15S_{18},11S_{10}$	24	2	74
ν_{14}	=CH out of plane bend	1044	993	16.5	2.6	0.64	990	992	994	998/993	$47S_{14},20S_{15},10S_{18}$	58	41	1
ν_{15}	-SH bend	1028	976	11.0	2.3	0.70	974	974	972	984/978	$18S_{15},27S_{20},21S_{14},10S_{13}$	2	65	33

ν_{16}	$=CH_2$ rock	967	917	4.4	3.0	0.72	927	921	923	930	$44S_{16},33S_{13}$	92	8	-
ν_{17}	$=CH_2$ wag	937	889	39.0	0.1	0.60	918	914	919	922/919	$99S_{17}$	22	75	3
ν_{18}	$-CH_2$ rock	830	790	1.1	12.5	0.38	795	787	789	791/789	$39S_{18},22S_{19},21S_{15}$	33	34	33
ν_{19}	-C-S- stretch	765	729	18.1	14.5	0.44	730	724	726	727/725	$31S_{19},22S_{15},19S_{20},10S_{22}$	37	61	2
ν_{20}	$=CH_2$ twist	623	591	5.6	8.1	0.39	594	592	594	601/598	$45S_{20},31S_{19},10S_{14}$	1	77	22
ν_{21}	-C=C-C bend	420	409	0.5	3.3	0.26	413	-	413	418/409	$68S_{21},10S_{15}$	-	4	96
ν_{22}	-C-C-S- bend	298	292	5.3	3.8	0.73	286	-	288	300/297	$68S_{22},10S_{20}$	54	12	34
ν_{23}	-SH torsional	261	248	21.1	8.4	0.75	-	-	244	-	$91S_{23}$	18	12	70
ν_{24}	-C-C- torsional	109	103	0.6	5.9	0.74	-	-	110	-	$87S_{24}$	1	65	34

[a] MP2(full)/6-31G(d) *ab initio* calculations, scaled wavenumbers, infrared intensities (km/mol), Raman activities ($Å^4$/amu), depolarization ratios and potential energy distributions (P.E.D.s)

[b] MP2(full)/6-31G(d) fixed scaled wavenumbers with factors of 0.88 for CH stretches and CH_2 deformations, 1.0 for heavy atom bends, and 0.90 for all other modes.

[c] Calculated with MP2(full)/6-31G(d) and contributions of less than 10% are omitted.

[d] A, B and C values in the last three columns are percentage infrared band contours.

Figure 85. Comparison of experimental and calculated Raman spectra of liquid allyl thiol: (A) observed spectrum; (B) simulated spectrum of mixture of *Gg*, *Cg* (ΔH = 120 cm^{-1}), *Gg′* (ΔH = 337 cm^{-1}), and *Gt* (ΔH = 360 cm^{-1}) conformers at 25°C; (C) simulated *Gt* conformer; (D) simulated *Gg′* conformer; (E) simulated *Cg* conformer; (F) simulated *Gg* conformer.

TABLE 127. Observed and calculated[a] wavenumbers (cm^{-1}) for *Cg* form of allyl thiol.

Vib. No.[b]	Approx. Description	*ab initio*	fixed scaled[c]	IR int.	Raman act.	dp ratio	IR gas	IR Xe soln.	Raman liquid	P.E.D.[d]	Band Contours[e]		
											A	B	C
ν_1	$=CH_2$ antisymmetric stretch	3320	3115	7.1	42.1	0.67	3102	3086*	3085*	$100S_1$	99	1	-
ν_3	$=CH_2$ symmetric stretch	3229	3030	3.8	130.3	0.13	3025	3014*	3011*	$92S_3$	96	4	-
ν_2	=C-H stretch	3200	3002	13.2	80.3	0.39	2999	3009	3011*	$92S_2$	47	52	1
ν_4	$-CH_2$ antisymmetric stretch	3163	2967	5.5	76.3	0.75	2968	2958*	2962	$100S_4$	1	9	99
ν_5	$-CH_2$ symmetric stretch	3114	2921	12.6	107.3	0.11	2935*	2924*	2913	$100S_5$	99	1	-
ν_6	-SH stretch	2779	2636	11.8	105.3	0.36	2592	2583	2573*	$100S_6$	2	19	79
ν_7	-C=C- stretch	1737	1647	8.2	5.6	0.15	1653	1642	1636*	$69S_7,13S_9$	83	17	-
ν_8	$-CH_2$ scissoring	1526	1434	7.4	18.0	0.67	1433	1424	1433*	$99S_8$	44	56	-
ν_9	$=CH_2$ scissoring	1486	1402	5.9	7.5	0.64	1414	1401	1409*	$79S_9,10S_{10}$	1	98	1
ν_{11}	$-CH_2$ wag	1376	1306	10.6	5.4	0.53	1300	1291*	1294*	$74S_{11},11S_{10},10S_{13}$	86	13	1
ν_{10}	=CH in plane bend	1351	1283	0.5	12.5	0.61	1280	1275	1294*	$55S_{10},15S_{16},12S_7$	70	27	3
ν_{12}	$-CH_2$ twist	1266	1201	9.2	13.5	0.73	1196	1192	1195	$92S_{12}$	25	19	56
ν_{16}	$=CH_2$ rock	1107	1055	1.2	2.2	0.57	1075	1069	1094*	$4S_{16},14S_{10},11S_{13},10S_{11}$	3	73	24
ν_{18}	$-CH_2$ rock	1053	998	3.1	7.7	0.75			994*	$4S_{18},33S_{15},14S_{14},13S_{24}$	98	-	2

							90*	992*					
ν_{14}	=CH out of plane bend	1035	982	22.5	0.5	0.74	981	988	987	$46S_{14},38S_{20}$	2	-	98
ν_{13}	-C-C- stretch	960	911	2.2	4.6	0.63	927*	914*	923*	$56S_{13},24S_{16}$	89	11	-
ν_{17}	$=CH_2$ wag	940	892	32.6	0.0	0.48	922	914*	923*	$98S_{17}$	-	1	99
ν_{15}	-SH bend	839	798	6.0	5.4	0.53	803	792	789*	$35S_{15},32S_{18}$	5	35	60
ν_{19}	-C-S- stretch	735	702	4.6	9.0	0.19	703	707	705	$54S_{19},12S_{22},10S_{15}$	54	27	19
ν_{20}	$=CH_2$ twist	564	536	13.0	10.3	0.75	539	544	546	$54S_{20},22S_{18},17S_{14}$	1	1	98
ν_{21}	-C=C-C bend	526	511	0.7	3.3	0.51	-	-	511	$5S_{21},25S_{19},16S_{22},10S_{16}$	10	83	7
ν_{23}	-SH torsional	270	260	14.5	4.5	0.72	-	-	263	$53S_{23},26S_{22},19S_{21}$	55	20	25
ν_{22}	-C-C-S- bend	245	238	10.4	4.2	0.71	-	-	244*	$37S_{22},46S_{23},14S_{21}$	56	10	34
ν_{24}	-C-C- torsional	140	133	0.4	4.9	0.75	-	-	-	$87S_{24},18S_{14}$	2	30	68

[a] MP2(full)/6-31G(d) *ab initio* calculations, scaled wavenumbers, infrared intensities (km/mol), Raman activities ($Å^4$/amu), depolarization ratios and potential energy distributions (P.E.D.s)

[b] In order of descending frequency

[c] MP2(full)/6-31G(d) fixed scaled wavenumbers with factors of 0.88 for CH stretches and CH_2 deformations, 1.0 for heavy atom bends, and 0.90 for all other modes.

* under *Gg* fundamental

[d] Calculated with MP2(full)/6-31G(d) and contributions of less than 10% are omitted.

[e] A, B and C values in the last three columns are percentage infrared band contours.

TABLE 128. Observed and calculated[a] wavenumbers (cm^{-1}) for *Gg'* form of allyl thiol.

Vib. No.[b]	Approx. Description	*ab initio*	fixed scaled[c]	IR int.	Raman act.	dp ratio	IR gas	IR Xe soln.	Raman liquid	P.E.D.[d]	Band Contours[e]		
											A	B	C
ν_1	$=CH_2$ antisymmetric stretch	3309	3104	11.1	63.7	0.64				$98S_1$	24	29	47
ν_3	$=CH_2$ symmetric stretch	3219	3020	3.0	123.9	0.12				$61S_3,34S_2$	74	7	19
ν_2	=C-H stretch	3208	3010	12.8	12.5	0.66				$56S_2,37S_3$	1	5	94
ν_4	$-CH_2$ antisymmetric stretch	3187	2990	2.3	69.1	0.74				$91S_4$	1	41	58
ν_5	$-CH_2$ symmetric stretch	3127	2933	13.1	85.0	0.11				$99S_5$	3	96	1
ν_6	-SH stretch	2778	2635	14.5	110.8	0.39	2592	2583*	2573*	$100S_6$	1	8	91
ν_7	-C=C- stretch	1733	1642	2.4	11.1	0.16	1655	1645	1636*	$68S_7,14S_9$	62	6	32
ν_8	$-CH_2$ scissoring	1531	1440	6.7	9.2	0.65	1436	1429	1433*	$85S_8,11S_9$	-	53	47
ν_9	$=CH_2$ scissoring	1496	1411	2.5	17.4	0.52	1414	1415	1409*	$66S_9,14S_8$	62	15	23
ν_{10}	=CH in plane bend	1359	1289	0.9	10.5	0.52	1287*	1291*	1294*	$52S_{10},17S_7,13S_{11}$	28	12	60
ν_{11}	$-CH_2$ wag	1338	1269	16.2	10.4	0.50	1251	1245	1242*	$81S_{11},12S_{10}$	70	23	7
ν_{12}	$-CH_2$ twist	1281	1217	4.0	21.5	0.68	1209*	1210*	1207*	$72S_{12},10S_{16}$	56	16	28
ν_{13}	-C-C- stretch	1184	1128	15.1	7.0	0.75	1110	1113	1094*	$19S_{13},18S_{16},14S_{15},14S_{12},14S_{18}$	47	14	39

ν_{14}	=CH out of plane bend	1035	982	14.3	0.9	0.53	990*	992*	994*	$68S_{14},21S_{20}$	13	75	12
ν_{15}	-SH bend	991	940	9.3	6.6	0.75	918*	939	938	$33S_{15},24S_{13},22S_{18}$	2	1	97
ν_{16}	$=CH_2$ rock	972	923	2.2	1.3	0.75				$49S_{16},29S_{13}$	62	24	14
ν_{17}	$=CH_2$ wag	937	889	39.2	0.1	0.58	918*	914*	923*	$98S_{17}$	24	63	13
ν_{18}	$-CH_2$ rock	846	806	5.2	12.5	0.39	807	806	789*	$29S_{18},21S_{15},20S_{19},15S_{20},10S_{22}$	37	11	52
ν_{19}	-C-S- stretch	754	719	10.2	15.1	0.40	722	717	720	$35S_{19},20S_{15},19S_{18}$	63	37	-
ν_{20}	$=CH_2$ twist	622	590	6.0	8.3	0.39	594*	592*	594*	$45S_{20},31S_{19},10S_{14}$	-	76	24
ν_{21}	-C=C-C bend	413	402	2.0	3.5	0.24	413*		413*	$72S_{21},10S_{19}$	65	24	11
ν_{22}	-C-C-S- bend	288	283	3.1	5.2	0.71	286*		288*	$75S_{22},10S_{14}$	68	29	3
ν_{23}	-SH torsional	200	190	24.2	7.1	0.74				$93S_{23}$	43	49	8
ν_{24}	-C-C- torsional	100	95	0.6	5.0	0.75			110*	$88S_{24}$	1	95	4

[a] MP2(full)/6-31G(d) *ab initio* calculations, scaled wavenumbers, infrared intensities (km/mol), Raman activities ($Å^4$/amu), depolarization ratios and potential energy distributions (P.E.D.s)

[b] In order of descending frequency

[c] MP2(full)/6-31G(d) fixed scaled wavenumbers with factors of 0.88 for CH stretches and CH_2 deformations, 1.0 for heavy atom bends, and 0.90 for all other modes.

* under *Gg* fundamental

[d] Calculated with MP2(full)/6-31G(d) and contributions of less than 10% are omitted.

[e] A, B and C values in the last three columns are percentage infrared band contours.

TABLE 129. Observed and calculated[a] wavenumbers (cm^{-1}) for *Gt* form of allyl thiol.

Vib. No.[b]	Approx. Description	*ab initio*	fixed scaled[c]	IR int.	Raman act.	dp ratio	IR gas	IR Xe soln.	Raman liquid	P.E.D.[d]	Band Contours[e]		
											A	B	C
ν_1	$=CH_2$ antisymmetric stretch	3310	3105	10.7	62.5	0.63				$98S_1$	25	17	58
ν_2	=C-H stretch	3228	3028	4.9	101.9	0.19				$82S_2,13S_3$	23	5	72
ν_3	$=CH_2$ symmetric stretch	3213	3015	6.7	45.2	0.16				$84S_3,14S_2$	15	-	85
ν_4	$-CH_2$ antisymmetric stretch	3188	2991	4.7	68.2	0.75				$96S_4$	16	5	79
ν_5	$-CH_2$ symmetric stretch	3126	2932	17.6	88.0	0.08				$100S_5$	6	89	4
ν_6	-SH stretch	2778	2636	22.6	174.6	0.37	2592	2583*	2573*	$100S_6$	68	31	1
ν_7	-C=C- stretch	1734	1644	2.3	11.1	0.17	1650	1634*	1636*	$67S_7,14S_9$	59	22	19
ν_8	$-CH_2$ scissoring	1546	1454	3.9	9.4	0.70	1440*	1448	1433*	$91S_8$	17	22	61
ν_9	$=CH_2$ scissoring	1496	1411	4.5	16.2	0.53	1414	1415	1409*	$71S_9,11S_{10}$	67	-	33
ν_{10}	=CH in plane bend	1358	1288	4.0	10.1	0.46	1287*	1291*	1294*	$47S_{10},18S_{11},17S_7$	55	44	1
ν_{11}	$-CH_2$ wag	1332	1264	32.0	12.6	0.66	1244*	1240*	1242*	$75S_{11},17S_{10}$	62	34	4
ν_{12}	$-CH_2$ twist	1269	1207	0.5	16.6	0.67	1197	1210*	1207*	$54S_{12},15S_{16},14S_{13}$	37	5	58
ν_{13}	-C-C- stretch	1139	1083	3.0	5.1	0.62	1093		1094*	$18S_{13},14S_{16}$	53	1	46

								1091					
ν_{14}	=CH out of plane bend	1038	985	18.5	0.4	0.75	992*	992*	994*	$67S_{14},22S_{20}$	26	67	7
ν_{15}	-SH bend	1029	979	1.9	8.6	0.74	974*	974*	972*	$9S_{15},16S_{18},14S_{16},13S_{13}$	1	61	38
ν_{16}	$=CH_2$ rock	945	896	12.5	2.1	0.72	918*	914*	919*	$7S_{16},22S_{18},21S_{17},16S_{13}$	63	36	1
ν_{17}	$=CH_2$ wag	943	895	27.9	0.7	0.75	918*	914*	919*	$78S_{17}$	13	81	6
ν_{18}	$-CH_2$ rock	889	844	1.8	5.2	0.58			-	$36S_{18},30S_{15},16S_{13}$	2	4	94
ν_{19}	-C-S- stretch	786	749	7.9	26.2	0.43	747	741	743	$46S_{19},16S_{15},10S_{22}$	35	63	2
ν_{20}	$=CH_2$ twist	615	584	4.8	9.2	0.46	594*	592*	594*	$48S_{20},31S_{19},11S_{14}$	3	77	20
ν_{21}	-C=C-C bend	421	410	0.6	1.9	0.19	413*		413*	$75S_{21}$	95	4	1
ν_{22}	-C-C-S- bend	285	280	2.7	5.3	0.72	286*		288*	$74S_{22},10S_{20}$	90	5	5
ν_{23}	-SH torsional	200	191	25.0	7.6	0.72				$99S_{23}$	3	3	94
ν_{24}	-C-C- torsional	95	90	0.7	6.1	0.75			110*	$88S_{24}$	67	1	32

[a] MP2(full)/6-31G(d) *ab initio* calculations, scaled wavenumbers, infrared intensities (km/mol), Raman activities ($Å^4$/amu), depolarization ratios and potential energy distributions (P.E.D.s)

[b] In order of descending frequency

[c] MP2(full)/6-31G(d) fixed scaled wavenumbers with factors of 0.88 for CH stretches and CH_2 deformations, 1.0 for heavy atom bends, and 0.90 for all other modes.

* under *Gg* fundamental

[d] Calculated with MP2(full)/6-31G(d) and contributions of less than 10% are omitted.

[e] A, B and C values in the last three columns are percentage infrared band contours.

AB INITIO CALCULATIONS

The *ab initio* and DFT calculations were performed with the Gaussian-03 program [22]. The energy minima with respect to nuclear coordinates were obtained by the simultaneous relaxation of all geometric parameters using the gradient method of Pulay [29]. Several basis sets as well as the corresponding ones with diffuse functions were employed with the Møller-Plesset perturbation method [21] to the second order (MP2(full)) as well as with the DFT by the B3LYP method. The predicted conformational energy differences are listed in Table 130A.

In order to obtain descriptions of the molecular motions involved in the fundamental modes of allyl thiol, a normal coordinate analysis was carried out. The force field in Cartesian coordinates was obtained with the Gaussian 03 program at the MP2(full) level with the 6-31G(d) basis set. The internal coordinates used to calculate the G and B matrices are given in Table 131. By using the B matrix [30], the force field in Cartesian coordinates was converted to force constants in internal coordinates. Subsequently, 0.88 was used as the scaling factor for the force constants of the CH stretches and CH_2 deformations and 0.90 was used for all other force constants excluding those for the heavy atom bends to obtain the fixed scaled force constants and resultant wavenumbers. A set of symmetry coordinates was used (Table S32) to determine the corresponding potential energy distributions (P.E.D.s). A comparison between the observed and calculated wavenumbers, along with the calculated infrared intensities, Raman activities, depolarization ratios and potential energy distributions for the conformers of allyl thiol are given in Tables 126, 127, 128, and 129.

TABLE 130A. Calculated energies in (Hatrees) and energy differences (cm^{-1}) for the five possible conformers of allyl thiol.

Method/Basis Set	# basis sets	*Gg*	Energy Differences, Δ^b			
			Cg	*Gg'*	*Gt*	*Ct*
RHF/6-31G(d)	76	0.578849	648	455	386	1013
MP2(full)/6-31G(d)	76	1.106797	531	456	421	968
MP2(full)/6-31+G(d)	92	1.117720	672	466	475	1196
MP2(full)/6-31G(d,p)	94	1.159427	500	420	416	956
MP2(full)/6-31+G(d,p)	110	1.169967	635	430	467	1166
MP2(full)/6-311G(d,p)	116	1.383393	612	393	363	1050
MP2(full)/6-311+G(d,p)	132	1.388464	619	389	419	1167
MP2(full)/6-311G(2d,2p)	154	1.448385	465	464	421	878
MP2(full)/6-311+G(2d,2p)	170	1.452026	448	419	443	885
MP2(full)/6-311G(2df,2pd)	212	1.523721	434	455	426	803
MP2(full)/6-311+G(2df,2pd)	228	1.526879	420	419	451	816
MP2(full)/aug-cc-pVTZ	326	1.449537	266	401	419	607
Average MP2(full)	-	-	466 ± 121	420 ± 30	420 ± 28	887 ± 181
B3LYP/6-31G(d)	76	2.091124	613	451	465	1036
B3LYP/6-31+G(d)	92	2.098308	657	433	479	1099
B3LYP/6-311G(d,p)	116	2.156894	642	419	432	1027
B3LYP/6-311+G(d,p)	132	2.158826	626	392	456	1034
B3LYP/6-311G(2d,2p)	154	2.165347	612	416	395	969
B3LYP/6-311+G(2d,2p)	170	2.167219	586	383	421	958
B3LYP/6-311G(2df,2pd)	212	2.171261	588	402	400	926
B3LYP/6-311+G(2df,2pd)	228	2.173090	570	373	428	925
B3LYP/aug-cc-pVTZ	326	2.179899	571	364	405	891
Average B3LYP	-	-	607 ± 31	404 ± 29	431 ± 30	985 ± 68

[a]Energy of conformer is given as –(E+514) H.
[b]Difference is relative to *Gg* form and given in cm^{-1}.

TABLE 130B. Temperature and intensity ratios of the *Gg*, *Cg*, *Gg′*, and *Gt* bands of allyl thiol.

	T(°C)	1/T ($\times 10^{-3}$ K^{-1})	*Gg* → *Cg*				*Gg* → *Gg′*		*Gg* → *Gt*	
			I_{594} / I_{545}	I_{594} / I_{707}	I_{725} / I_{545}	I_{725} / I_{707}	I_{594} / I_{717}	I_{725} / I_{717}	I_{594} / I_{741}	I_{725} / I_{741}
Liquid xenon	-60	4.692	1.098	1.360	0.141	1.744	1.406	1.802	1.842	2.362
	-65	4.804	1.059	1.366	0.137	1.764	1.492	1.927	1.879	2.426
	-70	4.923	1.069	1.425	0.139	1.849	1.564	2.030	2.088	2.710
	-75	5.047	1.081	1.374	0.146	1.857	1.666	2.252	2.348	3.173
	-80	5.177	1.147	1.379	0.155	1.862	1.742	2.353	2.372	3.204
	-85	5.315	1.197	1.398	0.162	1.886	1.987	2.681	2.485	3.352
	-90	4.460	1.169	1.488	0.156	1.985	2.118	2.825	2.877	3.838
	-95	5.613	1.214	1.579	0.164	2.136	2.110	2.854	2.932	3.964
	-100	5.775	1.271	1.601	0.168	2.123	2.298	3.048	3.062	4.060
ΔH (cm^{-1})			110 ± 17	104 ± 21	135 ± 19	131 ± 14	324 ± 20	350 ± 24	346 ± 26	373 ± 33
ΔH (cm^{-1})[a]				120 ± 9				337 ± 16		360 ± 20

[a] Average value and statistical uncertainty (1σ) obtained by utilizing all of the data as a single set.

TABLE 131. Structural parameters (Å and degrees), rotational constants (MHz) and dipole moments (Debye) for *Gg* and *Cg* conformers of allyl thiol.

Structural Parameters	Int. coor.	Gg			Cg	
		MP2(full)/ 6-311+G(d,p)	MW[a]	Adjusted r_0[b]	MP2(full)/ 6-311+G(d,p)	Predicted r_0
rC=C	R_1	1.341	1.354*	1.343(3)	1.339	1.341
rC-C	R_2	1.494	1.486*	1.496(3)	1.503	1.505
rC-S	R_3	1.823	1.819*	1.827(3)	1.811	1.815
rS-H	r_1	1.336	1.335*	1.335(3)	1.336	1.335
rC_α-H_1	r_2	1.094	1.137*	1.094(2)	1.094	1.094
rC_α-H_2	r_3	1.092	1.127*	1.092(2)	1.095	1.095
rC_β-H	r_4	1.088	1.090*	1.088(2)	1.090	1.090
rC_γ-H_1	r_5	1.084	1.098*	1.084(2)	1.084	1.084
rC_γ-H_2	r_6	1.087	1.054*	1.087(2)	1.084	1.084
∠CCS	ϕ_1	111.9	110.9*	112.5(5)	117.0	117.6
∠CCC	ϕ_2	123.3	110.5*	123.4(5)	126.9	127.0
∠CSH	θ_1	95.1	96.5*	95.1(5)	95.7	95.7
$\angle SC_\alpha H_1$	θ_2	104.7		104.4(5)	109.5	109.2
$\angle SC_\alpha H_2$	θ_3	110.4		110.0(5)	105.0	104.6
$\angle C_\beta C_\alpha H_1$	σ_1	110.8	105.2*	110.8(5)	109.1	109.1
$\angle C_\beta C_\alpha H_2$	σ_2	110.7	107.4*	110.7(5)	109.3	109.3
$\angle C_\alpha C_\beta H$	σ_3	116.5	119.4*	116.5(5)	114.2	114.2
$\angle C_\gamma C_\beta H$	σ_4	120.2	119.0*	120.2(5)	118.9	118.9
$\angle C_\beta C_\gamma H_1$	σ_5	121.3	119.3*	121.3(5)	120.4	120.4
$\angle C_\beta C_\gamma H_2$	σ_6	121.2	121.5*	121.2(5)	121.7	121.7
$\angle H_1 C_\alpha H_2$	λ_1	108.1	111.4*	108.1(5)	106.3	106.3
$\angle H_1 C_\gamma H_2$	λ_2	117.5	119.3*	117.5(5)	117.8	117.8
$\tau C_\gamma C_\beta C_\alpha S$	τ_1	115.6	124(3)	118.7(5)	1.3	1.3
$\tau C_\beta C_\alpha SH$	τ_2	-54.6	50	-54.6(5)	60.3	60.3
A(MHz)		19365.0	20041.7(1)	20041.3	13156.2	13213.4
B(MHz)		2844.1	2795.7(1)	2795.6	3690.3	3644.6
C(MHz)		2738.8	2701.1(1)	2701.3	2979.1	2952.0
$\lvert\mu_a\rvert$		1.50	1.24		1.237	
$\lvert\mu_b\rvert$		0.14	0.21		0.765	
$\lvert\mu_c\rvert$		0.42	0.42		0.717	
$\lvert\mu_t\rvert$		1.56	1.33		1.622	

[a]proposed structural parameters, rotational constants, and dipole moments from reference [237], values with asterisk are assumed values.

[b]adjusted parameters using the microwave data from this study.

The vibrational spectra were predicted from the MP2(full)/6-31G(d) calculations. The predicted scaled frequencies were used together with a Lorentzian function to obtain the simulated spectra. Infrared intensities were obtained based on the dipole moment derivatives with respect to Cartesian coordinates. The derivatives were transformed with respect to normal coordinates by $(\partial\mu_u/\partial Q_i) = \sum_j (\partial\mu_u/\partial X_j)L_{ij}$, where Q_i is the i^{th} normal coordinate, X_j is the j^{th} Cartesian displacement coordinate, and L_{ij} is the transformation matrix between the Cartesian displacement coordinates and the normal coordinates. The infrared intensities were then calculated by $(N\pi)/(3c^2)$ $[(\partial\mu_x/\partial Q_i)^2 + (\partial\mu_y/\partial Q_i)^2 + (\partial\mu_z/\partial Q_i)^2]$. The infrared spectra of the vapor, xenon solutions, and the predicted infrared spectra for the mixture of the four conformers with relative concentrations calculated for the equilibrium mixture at 25ºC by using the experimentally determined enthalpy difference are shown in Fig. 83 (A-C), respectively. Also the predicted infrared spectra for the pure *Gt*, *Gg'*, *Cg*, and *Gg* conformers and the observed infrared spectra of the pure crystalline solid are shown in Fig. 84 (A-E), respectively. The predicted spectra are in good agreement with the experimental spectrum which shows the utility of the scaled predicted frequencies and predicted intensities for supporting the vibrational assignment.

Additional support for the vibrational assignments was obtained from the simulated Raman spectrum. The evaluation of Raman activity by using the analytical gradient methods has been developed [31-34] and the activity S_j can be expressed as: $S_j = g_j(45\alpha_j^2 + 7\beta_j^2)$, where g_j is the degeneracy of the vibrational mode j, α_j is the derivative of the isotropic polarizability, and β_j is the anisotropic polarizability. To obtain the Raman scattering cross sections, the polarizabilities are incorporated into S_j by multiplying S_j with $(1-\rho_j)/(1+\rho_j)$ where ρ_j is the depolarization ratio of the j^{th} normal

mode. The Raman scattering cross sections and calculated wavenumbers obtained from the Gaussian 03 program were used together with a Lorentzian function to obtain the simulated Raman spectra. Comparison of experimental Raman spectrum of the liquid and the mixture of the four conformers with relative concentrations calculated for the equilibrium mixture at 25ºC by using the experimentally determined enthalpy difference and the predicted Raman spectra for the pure *Gt*, *Gg'*, *Cg*, and *Gg* conformers are shown in Fig. 85(A-F). The spectrum of the mixture should be compared to that of the Raman spectrum of the liquid. The predicted spectrum is in reasonable agreement with the experimental spectrum which shows the utility of the predicted Raman spectra for supporting the vibrational assignments.

MICROWAVE SPECTRA

The relatively strong microwave lines were remeasured to obtain their frequencies to three significant figures in order to obtain more accurate rotational constants particularly for the "A" constant, as well as the centrifugal distortion constants. We were also interested in determining the r_0 structural parameters. The frequencies for these bands are listed in Table 124 along with the values which were initially reported [237]. As can be seen from the data the largest difference is 0.8 MHz and the average overall difference is 0.3 MHz. These differences did not significantly change the values of the rotational constants.

The experimentally determined rotational constants and the centrifugal distortion constants are listed in Table 125. It should be noted that the previously reported A rotational constant value differs only by 0.3 MHz than the value obtained in this study, where the previous study had an uncertainty of 0.1 MHz. The values of the determined

centrifugal distortion constants are in satisfactory agreement with the values predicted from the *ab intio* and DFT predicted values except for the value of Δ_K. The value obtained in the current study is suspect since it was determined from a limited number of transitions with relatively small values of K_a. Therefore we tried using some of the previously reported transitions where K_a values were a little larger than the ones listed in Table 124. However the result obtained with the additional transitions agreed with the initial value reported in this study within the listed uncertainty. This indicates the value obtained for Δ_K is a reasonable value within the listed uncertainty.

VIBRATIONAL ASSIGNMENT

In order to determine the enthalpy difference between the most stable *gauche* conformer and the other possible conformers it is essential to have a confident assignment for all of the fundamentals of the *gauche* form and identify vibrations which cannot be assigned to this conformer. These modes must be overtones, combination bands, or fundamentals of the other conformers. The initial vibrational assignment [238] of allyl thiol was made for only the *gauche* conformer. All of the previously reported bands were observed in the current study except for a band at 669 cm^{-1} which must be due to CO_2 or an impurity. No spectra were recorded of the solid in the initial study which would have indicated that some of these "extra bands" were due to another conformer since they disappear from the spectra of the solid with annealing.

The complete vibrational assignment for the most stable conformer was made by utilizing the frequencies predicted from the *ab initio* calculations along with the predicted band contours, the infrared intensities, Raman activities and the well known "group frequencies" for the allyl group. First the assignment was made for the most stable

conformer by utilizing the infrared spectrum of the crystalline solid which was annealed several times to verify the observed bands arose from a single conformer. This conformer was shown to be the *Gg* form as can be verified from the data in Fig. 84. The region below 1000 cm^{-1} is of particular interest as it is complex in the spectrum of the vapor and it is the region where the bands for the conformational determination will be taken. This region is greatly simplified in the spectrum of the solid allowing for confident assignment of the *Gg* conformer fundamentals. This can be demonstrated from the previous vibrational assignment [238] where the band at 982 cm^{-1} from the vapor phase was assigned as a combination band ($\nu_{17} + \nu_{23}$) whereas in the present study it is attributed to the ν_{15} fundamental based on the *ab initio* predictions and relative simplicity of the spectrum of the solid. This makes the assignment previously reported to be "shifted" down one fundamental. The region from 930 to 914 cm^{-1} is also a complex spectral region where two fundamentals were assigned at 929 and 918 cm^{-1} in the previous study and two other Q-branches were not assigned. With the aid of the spectrum of the solid the Gg fundamentals could be observed and it is clear that another conformer is present when the previously unassigned band at 921 cm^{-1} disappears with annealing. The region from 750 to 700 cm^{-1} was assigned to the RQP– branches of the single *Gg* fundamental in the previous study. However with higher resolution a distinct shoulder can be observed on the low frequency side of the band and with the spectra of the xenon solution three distinct shoulders can be observed at 707, 717, and 741 cm^{-1} where these bands disappear in the spectra of the solid. The shoulder at 703 cm^{-1} was observed in the spectrum of the gas from the previous study but it was not reported. Also of interest is the band at 539 cm^{-1} (Fig. 86) where it is observed as a sharp Q-branch but in the infrared spectra of the

xenon solutions the band is very distinct and can be confidently assigned as a fundamental of the Cg conformer. With all of the fundamentals assigned for the most stable conformer the *ab initio* predicted differences could be used to assign many of the fundamentals for the other conformers. These assigned fundamentals were verified by using the spectra of the variable temperature xenon solutions and the predicted band contours, intensities, and depolarization values. With a confident assignment of the most stable conformer the remaining bands were readily assigned to the three remaining conformers and they are listed in Tables 127, 128, and 129.

CONFORMATIONAL STABILITY

To determine the enthalpy differences among the four observed conformers of allyl thiol, the sample was dissolved in liquefied xenon and the mid-infrared spectra were recorded as a function of temperature from -55 to -100°C. Relatively small interactions are expected to occur between xenon and the sample though the sample can associate with itself forming a dimer, trimer or higher order complex. However, due to the very small concentration of sample ($\sim 10^{-4}$ molar) self-association is greatly reduced. Therefore, only small frequency shifts are anticipated from the xenon interactions when passing from the gas phase to the liquefied xenon solutions. A significant advantage of this study is that the conformer bands are better resolved in comparison with those in the infrared spectrum of the gas. From *ab initio* calculations, the dipole moments of the four conformers are predicted to have similar values and the molecular sizes of the four conformers are nearly the same, so the ΔH value obtained from the temperature dependent FT-IR study is expected to be close to that for the gas [16-20].

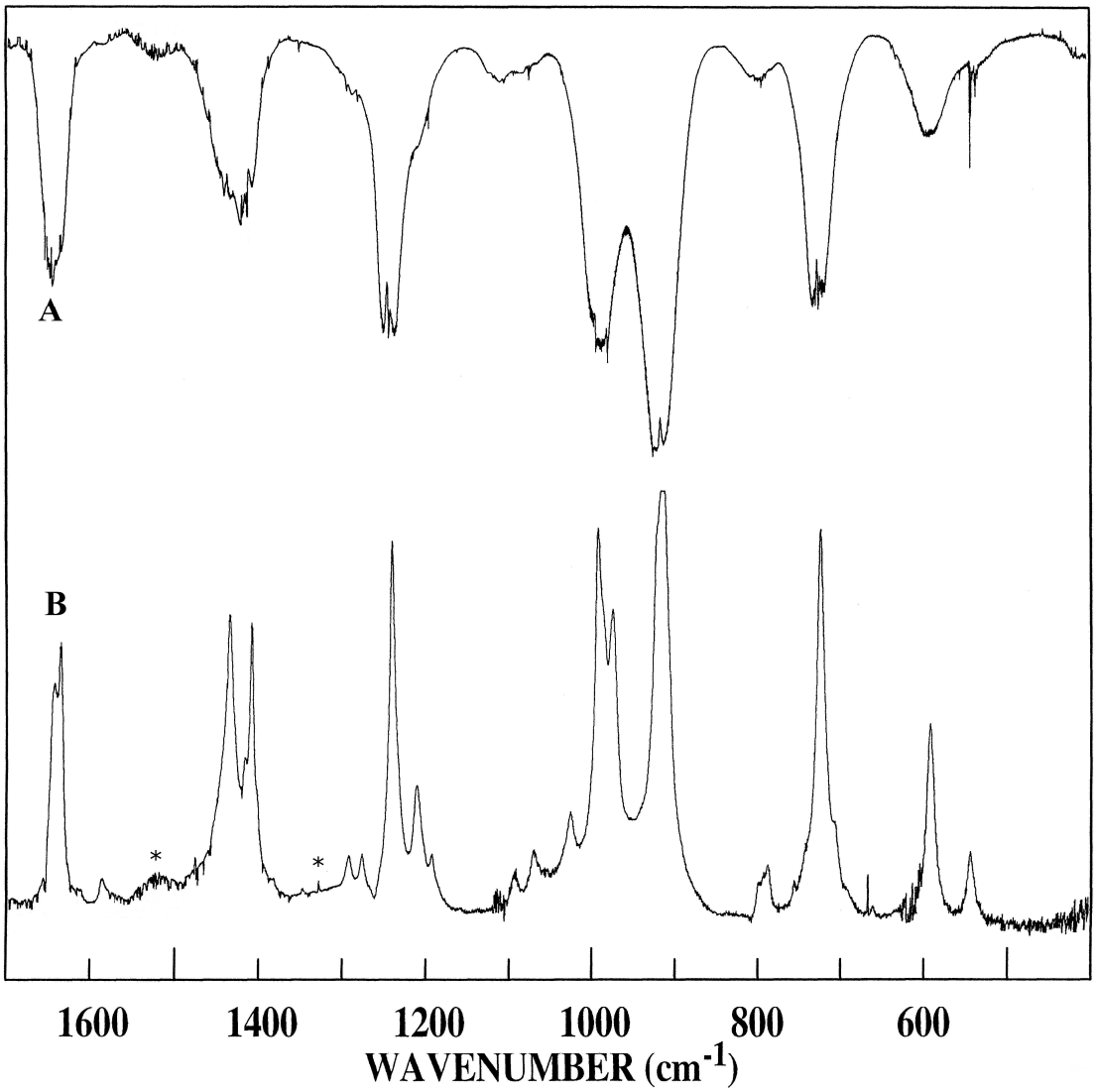

Figure 86. Mid-infrared spectra of allyl thiol (A) gas; (B) Xe solution at -70°C, asterisk denotes location of impurity bands that develop soon after purification.

Once confident assignments have been made for a significant number of the fundamentals of the four most abundant conformers the task was then to find a pair or pairs of bands from which the enthalpy determination could be obtained. To minimize the effect of combination and overtone bands in the enthalpy determination it is desirable to have the lowest frequency pair(s) that are possible to use for the determination. The bands should also be sufficiently resolved as to determine their intensities. The selection of the bands to use in the enthalpy determination was complicated due to the presence of all four conformers as well as from the lack of bands sufficiently resolved to determine their intensities. Initially the fundamentals at 725, 707, 717, and 741 cm^{-1} were selected for the *Gg*, *Cg*, *Gg'*, and *Gt* conformer bands, respectively, as they are sufficiently separated to obtain their intensities (Fig. 87) and they are in the lower frequency region of the spectrum. For the *Cg* conformer there was another band at 545 cm^{-1} that should be free of interfering bands. Finally the band at 594 cm^{-1} was selected for the *Gg* form as it does not appear to be significantly affected by underlying fundamentals from the other conformers.

The intensities of the individual bands were measured as a function of temperature (Fig. 88) and their ratios were determined. By application of the van't Hoff equation $-\ln K = \Delta H/(RT) - \Delta S/R$, the enthalpy difference was determined from a plot of $-\ln K$ versus $1/T$, where $\Delta H/R$ is the slope of the line and K is substituted with the appropriate intensity ratios, *i.e.* $I_{conf\text{-}1} / I_{conf\text{-}2}$, etc. It was assumed that ΔH, ΔS, and α are not functions of temperature in the range studied.

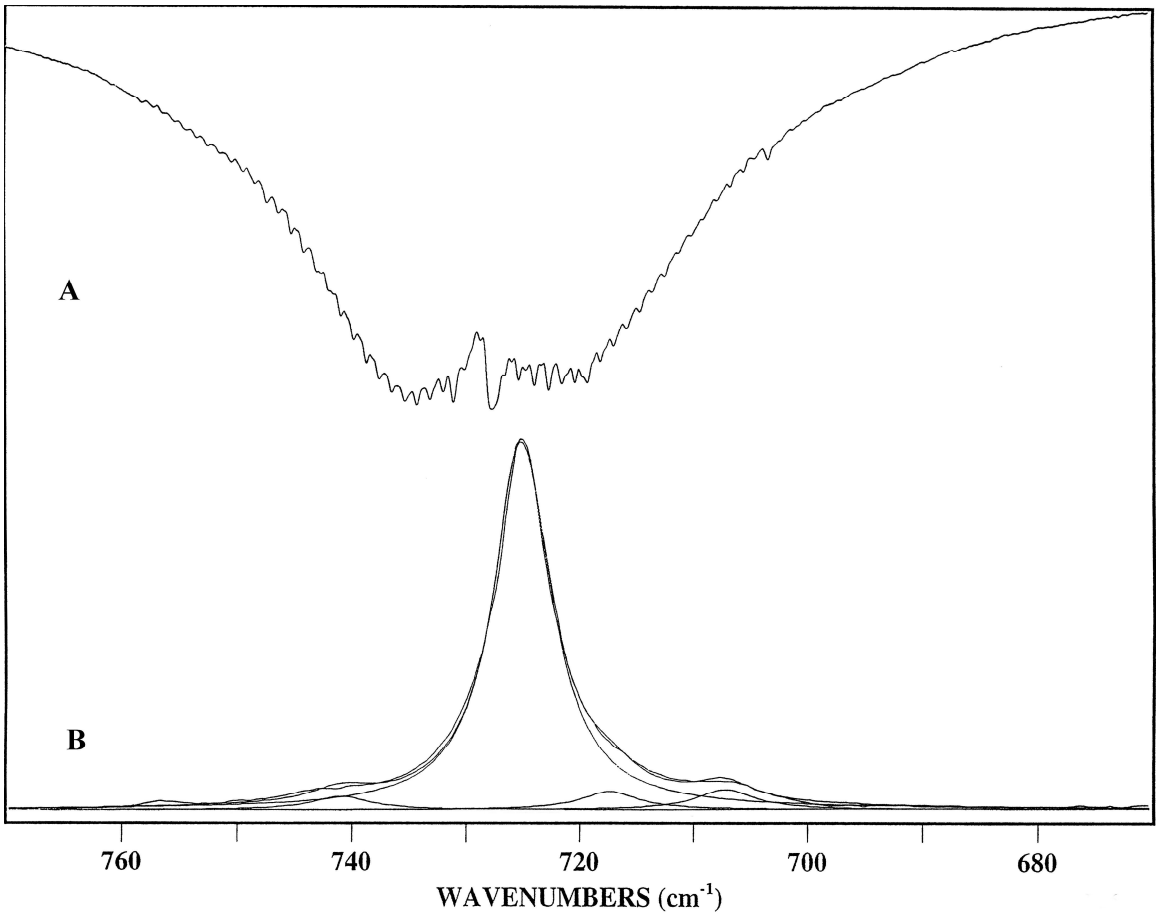

Figure 87. Fit of infrared spectra of xenon solution of allyl thiol.

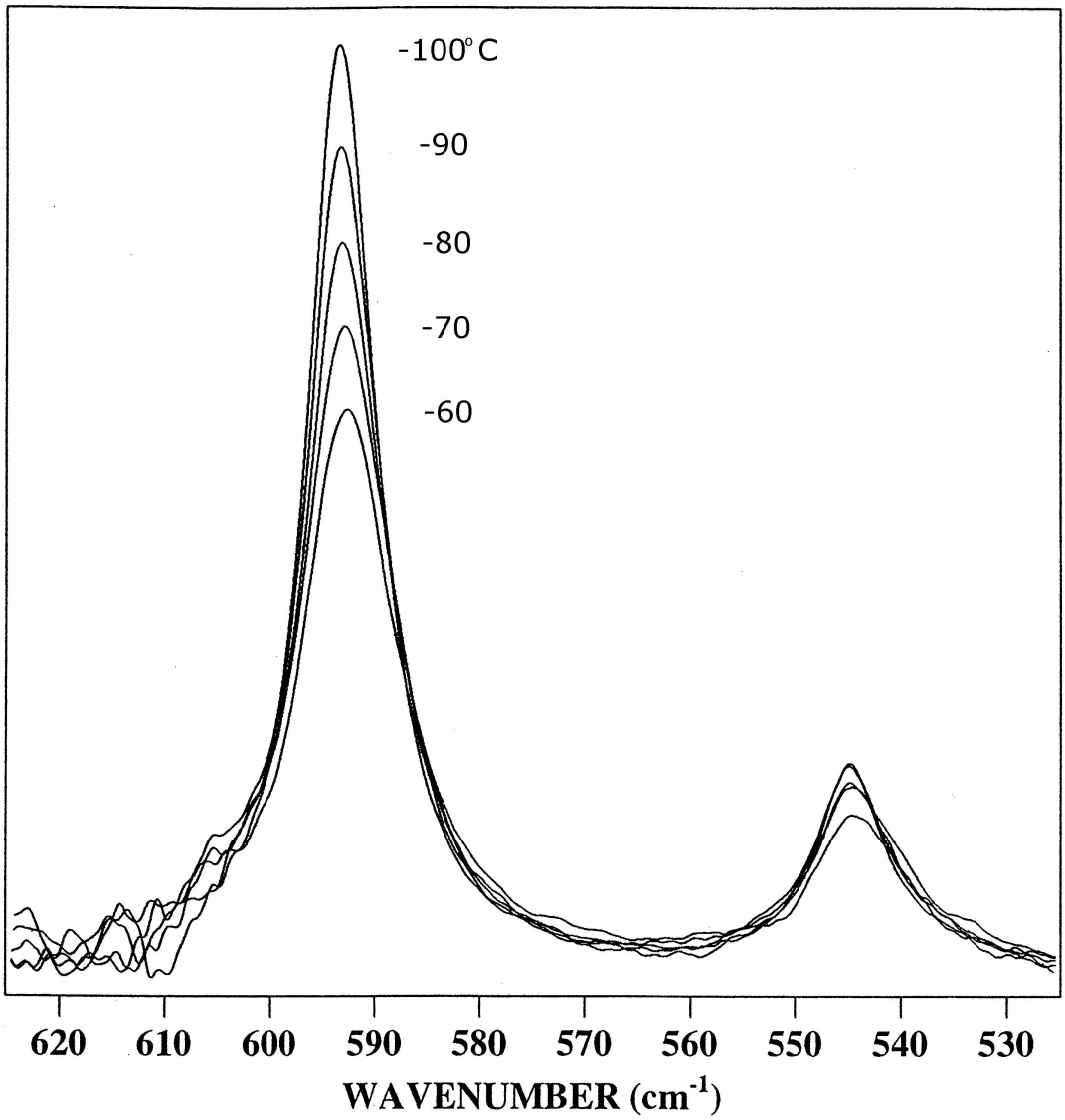

Figure 88. Temperature (-60 to -100°C) dependent infrared spectrum of allyl thiol dissolved in liquid xenon.

These six bands, were utilized for the determination of the enthalpy difference by combining them to form band pairs as shown in Table 130B. By using the four band pairs for the *Gg* and *Cg* conformers the enthalpy difference was determined with a value of 120 ± 9 cm^{-1}. Then the two band pairs for the *Gg* and *Gg′* forms were used to obtain the enthalpy difference of 337 ± 16 cm^{-1}. To determine the enthalpy difference for the *Gg* and *Gt* conformers the two corresponding band pairs were used for which a value of 360 ± 20 cm^{-1} was obtained. These values are consistent with the corresponding predicted values from *ab initio* calculations with the aug-cc-pVTZ basis set (Table 130A). For each enthalpy difference the listed error limit is derived from the statistical standard deviation of one sigma of the measured intensity data taken as a single data set, but it does not take into account small associations with the liquid xenon or the interference of overtones and combination bands in near coincidence with the measured fundamentals. However, this statistical uncertainty is probably better than can be expected from this technique for the Gg′ and Gt conformers with two band pairs. Therefore, an uncertainty of about 10% in the enthalpy difference is probably more realistic i.e. for Gg′ 337 ± 34 cm^{-1}, and for Gt 360 ± 36 cm^{-1} relative to the Gg form. From these enthalpy differences the relative abundance of the *Gg* conformer present at ambient temperature is estimated to be 52 ± 1%, with the remainder values of 29 ± 1% for the *Cg* conformer, 10 ± 1% *Gg′* form, and 9 ± 1% for the *Gt* form.

STRUCTURAL PARAMETERS

In the previous microwave study [237], only the dihedral angles τCCCS and τCCSH were determined for the Gg conformer with τCCCS fit to the ground state rotational constants which were determined without the distortion constants and τCCSH

determined using the Kraichman method. Therefore, we have again determined the rotational constants for the normal species of *Gg* allyl thiol with greater precision and from the newly determined rotational constants the adjusted r_0 structural parameters have been obtained.

We [51] have shown that *ab initio* MP2(full)/6-311+G(d,p) calculations predict the r_0 structural parameters for more than fifty carbon-hydrogen distances to at least 0.002 Å compared to the experimentally determined values from isolated CH stretching frequencies which were compared [5] to previously determined values from earlier microwave studies. Therefore, all of the carbon-hydrogen distances can be taken from the MP2(full)/6-311+G(d,p) predicted values. We have found that good structural parameters for hydrocarbons and many substituted ones can be determined by adjusting the structural parameters obtained from the *ab initio* MP2(full)/6-311+G(d,p) calculations to fit the rotational constants obtained from microwave experimental data by using a computer program "A&M" (*Ab initio* and Microwave) developed [14] in our laboratory. This assumption is based on the fact that errors from *ab initio* calculations are systematic. Therefore there are a total of 3 heavy atom distances, 2 heavy atom angles, and a heavy atom dihedral angle resulting in 6 heavy atom parameters to be determined using the three rotational constants obtained in this study. Therefore, it should be possible to obtain "adjusted r_0" structural parameters for the *Gg* conformer of allyl thiol by utilizing the rotational constants determined in this study and reasonable adjustments based on the ally alcohol where [176] the complete r_0 structure was adjusted to fit 13 previously reported rotational constants.

The fit of the three determined rotational constants by the structural parameters for the *Gg* conformer is remarkably good with the differences all less than 0.21 MHz. Therefore, it is believed that the suggested uncertainties are realistic values and the determined structural parameters are probably as accurate as can be obtained for the molecule in the gas phase by either electron diffraction or microwave substituted methods. The resulting adjusted r_0 parameters are listed in Table 131, where it is believed that the S-C, C-C, and S-H distances should be accurate to ± 0.003 Å, the C-H distances should be accurate to ± 0.002 Å, and the angles should be within ± 0.5°.

Additionally, we have also shown that the differences in predicted distances and angles from the *ab initio* calculations for different conformers of the same molecule can usually be used as one parameter with the *ab initio* predicted differences except for some dihedral angles. Therefore we have predicted structural parameters for the *Cg* form of allyl thiol by applying the corresponding adjustments from the *Gg* conformer to the MP2(full)/6-311+G(d,p) predicted parameters for the *Cg* form. These parameters should be close to the actual value except for the dihedral angles.

DISCUSSION

In general the mixing was only very extensive for ν_{13} which had extensive contributions from five symmetry coordinates, with the largest one having only 19%. Both ν_{15} and ν_{19} had contributions from four symmetry coordinates with the largest contributions of 27% and 31%, respectively. Therefore for most of the other vibrations the approximate descriptions provide a reasonable indication of the major vibrational motions involved.

The predicted frequencies from the MP2(full)/6-31G(d) calculations with the two scaling factors provided values with an average error of 9 cm^{-1} which is a percent error of 0.6%. The prediction of the S-H stretch was poor with a difference of 42 cm^{-1} though could be improved with a scaling factor of 0.88 applied to the corresponding force constant. Also the frequency for the $-CH_2$ wag was too high by 20 cm^{-1} whereas that for the $=CH_2$ wag was too low by 29 cm^{-1}. There are two other bands in the finger print spectral region that have 10 cm^{-1} differences between the predicted and observed frequencies whereas the remaining ones have single digit differences.

Since the far infrared spectrum of the gas was not recorded it was not possible to obtain meaningful information on the S-H torsional band. This mode is predicted to be relatively strong in the Raman spectrum but it is expected to be a very broad band in the spectrum of the liquid. The very broad Raman liquid line from 200 to 250 cm^{-1} under the 244 cm^{-1} line which is strongly polarized (Fig. 89) and assigned as the S-H torsion is quite questionable and requires additional investigation for obtaining more confident data on the S-H torsional mode with excited states.

One of the major goals of this research was the determination of the order of stability of the four stable conformers where only the *Gg* conformer had been observed in the previous studies [237,238] of allyl thiol. The order of stability and their enthalpy differences were obtained for the four stable conformers of allyl thiol as Gg > Cg (120 ± 9 cm^{-1}) > Gg′ (337 ± 34 cm^{-1}) ≥ Gt (360 ± 36 cm^{-1}), where the Gg′ and Gt order of stability cannot be determined. As can be seen in Table 130B the individual band pairs have small uncertainties and cover a relatively small range.

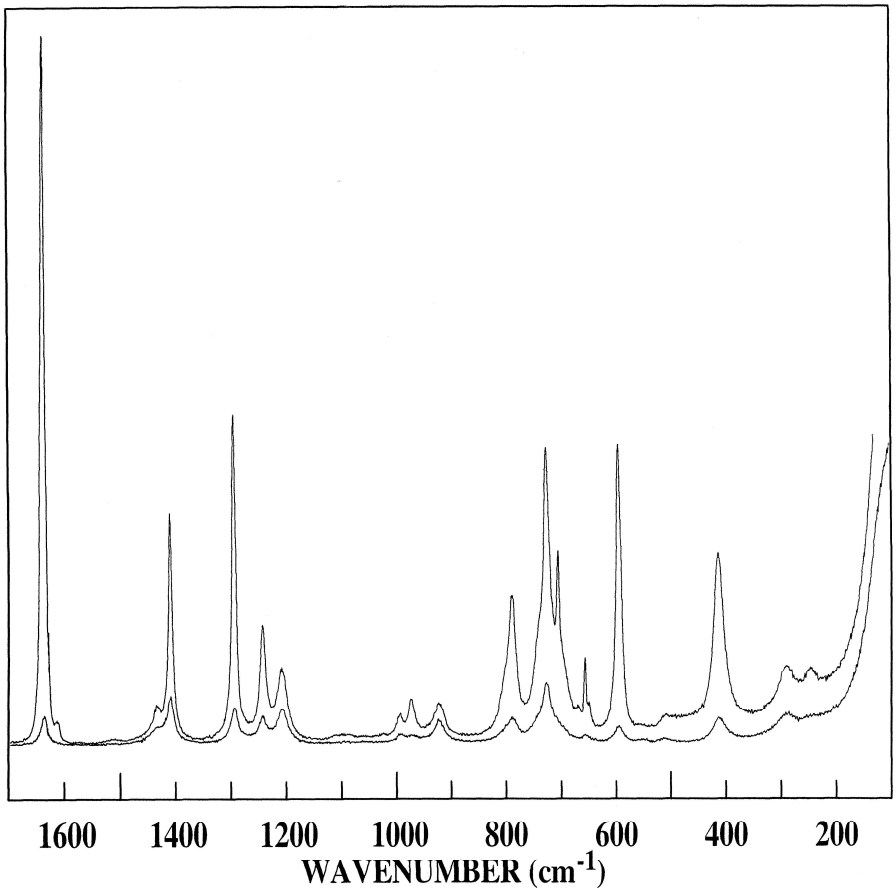

Figure 89. Raman spectra (100-1700 cm^{-1}) showing the polarized and the depolarized bands for allyl thiol.

There is evidence for the van der Waals complex with the sample where there is a significant decrease in the SH stretching frequency from the gas to the xenon solutions i.e. 16 cm^{-1} higher for the Gg form. However, for the other fundamentals the average difference between the frequencies in the gas and xenon solution is five wavenumbers except for the -C=C- stretch where the difference is 11 wavenumbers. This indicates some solvent effects on the infrared spectra of the xenon solutions but these shifts are

relatively minor for the fundamentals used in the determination of the enthalpy differences and the shifts are similar among the different conformers. The reported enthalpy differences are thereby believed to be accurate to within their stated uncertainties.

To support the experimental values the *ab initio* energy differences have been determined by a variety of basis sets (Table 130A) which can be compared to the experimentally determined enthalpy differences in Table 130B. The order of stability is reasonably well predicted by the *ab initio* MP2(full) calculation with the aug-cc-pVTZ basis set. However, the same method with less basis sets gives results that are significantly high for the *Cg* form but within a reasonable range for the *Gg′* and *Gt* conformers. The DFT calculations by the B3LYP method give similarly poor results for the *Cg* form but are even closer for the *Gg′* and *Gt* conformers. The order of stability changes for both methods depending on whether diffuse functions are included in the basis set and for the *ab initio* MP2(full) method even changes depending on the size of the basis set.

The adjusted r_0 structural parameters have been determined for Gg allyl thiol (Table 131). In the initial microwave study [237] only two parameters were determined which were the dihedral angles (°) τCCCS = 124(3) and τCCSH = 50. The values obtained in the current study for the dihedral angles CCCS and CCSH are both significantly different than those from the previous study even when the error limits from the previous study are considered. These discrepancies are due to the assumed structural parameters used in the previous study where the heavy atom bond distances for rC=C,

rC-C, and rC-S are 0.011, 0.010, and 0.008 Å different than the parameters from the current study.

The carbon skeletal structural parameters from this study should be comparable to other allyl-X moieties. The parameters from allyl alcohol, allyl amine, and allyl fluoride are listed in Table 132 where it can be observed that the rC=C distance varies only a small amount from the –SH, –OH, $–NH_2$, and –F substitutions with the values decreasing from –SH to –F. However the rC-C bond and ∠CCC angle change significantly depending on the substituent. It is clear from the data in Table 132 that the assumed allyl fluoride parameters used in the previous structural determination of allyl thiol were unfortunate poor assumptions as they are the parameters with the largest differences from the corresponding parameters in allyl thiol. The differences between the *ab initio* predictions and the adjusted r_0 structures obtained in each of the studies show small adjustments indicating the *ab initio* calculations give reasonably good predicted structural values for the allyl carbon skeleton group. Thus, the parameters reported in the current study are believed to be accurate to within the stated error limits.

In the current study the quadratic centrifugal distortion constants have been obtained (Table 125) from the rotational transitions listed in Table 124. These constants have also been predicted by *ab initio* MP2(full) and DFT B3LYP calculations with the 6-31G(d) and 6-311+G(d,p) basis sets. These data are given in Table 125 and the values of Δ_J, Δ_{JK}, δ_J, and δ_K are all reasonably well predicted by the MP2(full) method with the increase in basis set size showing no significant overall improvement. However, the value for Δ_K obtained experimentally is significantly different (less than half) those predicted by both calculation methods. We have found in the past the *ab initio* calculations usually

provide reasonably good distortion constants so this difference in the Δ_K constant is of interest and a future study of the rotational spectra of allyl thiol could obtain a more accurate Δ_K if more higher K_a value transitions could be obtained.

TABLE 132. Structural parameters (Å and degrees) for carbon skeleton gauche and cis forms of allyl alcohol, allyl amine, and allyl fluoride.

Structural Parameters	Gg allyl alcohol			Gg allyl amine		Gauche allyl fluoride		
	ED[a]	MW[b]	Adjusted r_0[c]	Adjusted r_0[d]	Adjusted r_0[e]	MW[f]	MW[g]	Adjusted r_0[h]
rC=C	1.335(5)	1.337	1.343(3)	1.339	1.339(3)	1.354(15)	1.335(3)	1.334
rC-C	1.496(8)	1.502	1.499(3)	1.499	1.501(3)	1.486(15)	1.490(4)	1.491
rC-X	1.431(5)	1.428	1.428(5)	1.466	1.468(3)	1.371(15)	1.394(4)	1.400
∠CCC	125.3(1.5)	123.9	122.8(5)	124.7	125.3(5)	121.6(10)	123.3(5)	123.8
$\tau C_\gamma C_\beta C_\alpha X$	112(1.5)	-122.9	122.7(10)	124.5	123.9(5)	127.1(30)	124.6(5)	125.7

Structural Parameters	Cg allyl alcohol		Ct allyl amine			Cis allyl fluoride		
	ED[a]	Adjusted r_0[c]	ED[i]	MW[j]	Adjusted r_0[d]	MW[f]	MW[g]	Adjusted r_0[h]
rC=C	1.334(5)	1.340(5)	1.334(7)	1.339(5)	1.338(4)	1.333(7)	1.333(3)	1.333
rC-C	1.500(8)	1.504(5)	1.501(3)	1.499(11)	1.510(4)	1.503(10)	1.495(4)	1.494
rC-X	1.425(5)	1.419(5)	1.463*	1.456(11)	1.459(4)	1.382(10)	1.388(4)	1.390
∠CCC	124.7(1.5)	124.7(5)	127.5(6)	125.7(2)	125.6(5)	124.6(8)	124.5(3)	123.6
$\tau C_\gamma C_\beta C_\alpha X$	22(9)	5.6(5)						

[a] r_z parameters; Ref [236]
[b] r_0 parameters; Ref [234]
[c] Ref [176]
[d] Ref [241]
[e] fit in current study using rotational constants from Ref [242]
[f] r_s parameters; Ref [239]
[g] r_0 parameters; Ref [84]
[h] Ref [14]
[i] Ref [243], asterisk denotes estimated value
[j] Pseudo r_s values; Ref [244]

With the predicted structural parameters for the *Cg* conformer it is believed that the predicted rotational constants should be very close to those that would be obtained from a microwave study of this conformer. Therefore it would be interesting if such a study were carried out since the information obtained could be very useful in obtaining the *gauche* barrier using the splittings observed in the ground state. Nevertheless it is believed that the parameters that have been estimated should have rather small uncertainties with the uncertainties not larger than 0.005 Å for the heavy atom distances and 1° for the angles. It would also be of interest to obtain the rotational constants and structural parameters for allyl phosphate, which could be useful for comparison with the previously obtained corresponding parameters of allyl amine.

REFERENCE LIST

[1] IUPAC. Compendium of Chemical Terminology, 2nd ed. (the "Gold Book"). Compiled by A. D. McNaught and A. Wilkinson. Blackwell Scientific Publications, Oxford (1997). XML on-line corrected version: http://goldbook.iupac.org (2006-) created by M. Nic, J. Jirat, B. Kosata; updates compiled by A. Jenkins. ISBN 0-9678550-9-8. doi:10.1351/goldbook.

[2] H. Herzberg, Molecular Spectra and Molecular Structure II. Infrared and Raman Spectra of Polyatomic Molecules. ISBN: 0894642693, 1991.

[3] P. Griffiths, J. M. Chalmers, Handbook of Vibrational Spectroscopy. ISBN: 9780470027325, 2012.

[4] D. A. Skoog, F. J. Holler, T. A. Nieman, Principles of Instrumental Analysis, 5th Edition. ISBN: 0030020786, 1998.

[5] D.C. McKean, J. Mol. Struct. 113 (1984) 251.

[6] J. L. Duncan, J. L. Harvie, D.C. McKean, J. Mol. Struct. 145 (1986) 225.

[7] S. Kumar, A. Barth, Biophys. J. 98 (2010) 1931.

[8] S. Kumar, A. Barth, J. Phys. Chem. B 115 (2011) 6784.

[9] S. Kumar, A. Barth, J. Phys. Chem. B 115 (2011) 11501.

[10] R. Nyquist, C. Putzig, M. Leugers, Handbook of Infrared and Raman Spectra of Inorganic Compounds and Organic Salts, 1st Edition. ISBN: 9780080878539, 1996.

[11] C. H. Townes, A. L. Schawlow, Microwave Spectroscopy. ISBN: 048661798X, 1955

[12] J. M. Brown, A. Carrington, Rotational Spectroscopy of Diatomic Molecules. ISBN: 0521530784, 2003.

[13] J. Kraitchman, Am. J. Phys. 21 (1953) 17.

[14] B. J. van der Veken, W. A. Herrebout, D. T. Durig, W. Zhao, J. R. Durig, J. Phys. Chem. A 103 (1999) 1976.

[15] C. Perez, S. Lobsiger, N. A. Seifert, D. P. Zaleski, B. Temelso, G. C. Shields, Z. Kisiel, B. H. Pate, Chem. Phys Let. 571 (2013) 1.

[16] M. O. Bulanin, J. Mol. Struct. 19 (1973) 59.

[17] B. J. van der Veken, F. R. DeMunck, J. Chem. Phys. 97 (1992) 3060.

[18] W. A. Herrebout, B. J. van der Veken, A. Wang, J. R. Durig, J. Phys. Chem. 97 (1995) 578.

[19] M. O. Bulanin, J. Mol. Struct. 73 (1995) 347.

[20] W. A. Herrebout, B. J. van der Veken, J. Phys. Chem. 100 (1996) 9671.

[21] C. Møller, M. S. Plesset, Phys. Rev. 46 (1934) 618.

[22] M. J. Frisch, G. W. Trucks, H. B. Schlegel, G. E. Scuseria, M. A. Robb, J. R. Cheeseman J. A. Montgomery Jr , T. Vreven, K. N. Kudin, J. C. Burant, J. M. Millam, S. S. Iyengar J. Tomasi, V. Barone, B. Mennucci, M. Cossi, G. Scalmani, N. Rega, G. A. Petersson, H. Nakatsuji, M. Hada, M. Ehara, K. Toyota, R. Fukuda, J. Hasegawa, M. Ishida, T. Nakajima, Y. Honda, O. Kitao, H. Nakai, M. Klene, X. Li, J. E. Knox, H. P. Hratchian, J. B. Cross, C. Adamo, J. Jaramillo, R. Gomperts, R. E. Stratmann, O. Yazyev, A. J. Austin, R. Cammi, C. Pomelli, J. W. Ochterski, P. Y. Ayala, K. Morokuma, G. A. Voth, P. Salvador, J. J. Dannenberg, V. G. Zakrzewski, S. Dapprich, A. D. Daniels, M. C. Strain, O.

Farkas, D. K. Malick, A. D. Rabuck, K. Raghavachari, J. B. Foresman, J. V. Ortiz, Q. Cui, A. G. Baboul, S. Clifford, J. Cioslowski, B. B. Stefanov, G. Liu, A. Liashenko, P. Piskorz, I. Komaromi, R. L. Martin, D. J. Fox, T. Keith, M. A. Al-Laham, C. Y. Peng, A. Nanayakkara, M. Challacombe, P. M. W. Gill, B. Johnson, W. Chen, M. W. Wong, C. Gonzalez, and J. A. Pople, Gaussian 03, Revision E.01, Gaussian, Inc., Pittsburgh, PA, 2003.

[23] W. A. Herrebout, N. Nagels, B. J. van der Veken, Chem. Phys. Chem. 10 (2009) 3054.

[24] B. Michielsen, J. J. J. Dom, B. J. van der Veken, S. Hessen, Z. Xue, M. A. Suhm, W. A. Herrebout, Phys. Chem. Chem. Phys. 12 (2010) 14034.

[25] R. D. Suenram, J. U. Grabow, A. Zuban, I. Leonov, Rev. Sci. Instrum. 70 (1999) 2127.

[26] R. D. Suenram, F. J. Lovas, D. F. Plusquellic, A. Lesarri, Y. Kawashima, J. O. Jensen, A. C. Samuels, J. Mol. Spectrosc. 211 (2002) 110.

[27] A. R. Conrad, N. H. Teumelsan, P. E. Wang, M. J. Tubergen, J. Phys. Chem. A 114 (2010) 336.

[28] G.G. Brown, B.C. Dian, K.O. Douglass, S.M. Geyer, S.T. Shipman, B.H. Pate, Rev. Sci. Instrum.79 (2008) 053103.

[29] P. Pulay, Mol. Phys. 17 (1969) 197.

[30] G.A. Guirgis, X. Zhu, Z. Yu, J.R. Durig, J. Phys. Chem. A 104 (2000) 4383.

[31] M.J. Frisch, Y. Yamaguchi, J.F. Gaw, H.F. Schaefer, III, J.S. Binkley, J. Chem. Phys. 84 (1986) 531.

[32] R.D. Amos, Chem. Phys. Lett. 124 (1986) 376.

[33] P.L. Polavarapu, J. Phys. Chem. 94 (1990) 8106.

[34] G.W. Chantry, in The Raman Effect, edited by A. Anderson (Marcel Dekker Inc., New York, 1971), Vol. 1, Chap. 2.

[35] H. Kim, W.D. Gwinn, J. Chem. Phys. 44 (1966) 865.

[36] W.G. Rothschild, B.P. Dailey, J. Chem. Phys. 36 (1962) 2931.

[37] M.Y. Fong, M.D. Harmony, J. Chem. Phys. 58 (1973) 4260.

[38] W.G. Rothschild, J. Chem. Phys. 45 (1966), 3599.

[39] C.S. Blackwell, L.A. Carreira, J.R. Durig, J.M. Karriker, R.C. Lord, J. Chem. Phys. 56 (1972) 1706.

[40] V.F. Kalasinsky, G.A. Guirgis, J.R. Durig, J. Mol. Struct. 39 (1977) 51.

[41] J.R. Durig, G.A. Guirgis, W.E. Bucy, D.A.C. Compton, V.F. Kalasinsky, J. Mol. Struct. 49 (1978) 323.

[42] V.F. Kalasinsky, W.C. Harris, P.W. Holtzclaw, T.S. Little, T.J. Geyer, J.R. Durig, J. Raman Spectrosc. 18 (1987) 581.

[43] J.R. Durig, T.J. Geyer, T.S. Little, M. Dakkouri, J. Phys. Chem. 89 (1985) 4307.

[44] B. Velino, L.B. Favero, W. Caminati, J. Mol. Spectrosc. 179 (1996) 168.

[45] W. Caminati, L.B. Favero, A. Maris, P.G. Favero, J. Mol. Struct. 376 (1996) 25.

[46] W. Caminati, B. Velino, M. Dakkouri, L. Schafer, K. Siam, J.D. Ewbank, J. Mol. Spectrosc. 123 (1987) 469.

[47] J.R. Durig, M.J. Lee, T.S. Little, Struct. Chem. 2 (1991) 195.

[48] J.R. Durig, J.J. Klaassen, A. Ganguly, T.K. Gounev, G.A. Guirgis, W. Lin, J. Struct Chem. 19 (2008) 935.

[49] J.R. Durig, L.A. Carreira, W.J. Lafferty, J. Mol. Spectrosc. 46 (1973) 187.

[50] D.L. Powell, A. Gatial, P. Klaeboe, C.J. Nielsen, A.J. Kondow, W.A. Boettner, A.M. Mulichak, Acta Chem. Scand. 43 (1989) 441.

[51] J.R. Durig, K.W. Ng, C. Zheng, S. Shen, Struct. Chem. 15 (2004) 149.

[52] L.N. Pauling, The Nature of the Chemical Bond , Cornell University, Ithaca, NY 3rd edition (1960).

[53] J.R. Durig, M.J. Lee, W. Zhao, T.S. Little, Struct. Chem. 3 (1992) 329.

[54] W. Caminati, B. Velino, R.G.D. Valle, J. Mol. Spectrosc. 129 (1988) 284.

[55] Y. Endo, M.C. Chang, E. Hirota, J. Mol. Spectrosc. 126 (1987) 63.

[56] B. Vogelsanger, W. Caminati, A. Bauder, Chem. Phys. Lett. 141 (1987) 245.

[57] J.R. Durig, A. Ganguly, A.M. El Defrawy, T.K. Gounev, G.A. Guirgis, Spectrochim. Acta 71A (2008) 1379.

[58] M.D. Harmony, R.N. Nandi, J.V. Tietz, J.I. Choe, S.J. Getty, S.W. Staley, J. Am. Chem. Soc. 105 (1983) 3947.

[59] M.L. Guennec, G. Wlodarczak, J. Burie, J. Demaison, J. Mol. Spectrosc. 154 (1992) 305.

[60] H. Maeder, H. M. Heise, H. Dreizler, Z. Naturforsch. A 29 (1974) 164.

[61] R.F. Curl Jr., J. Comput. Phys. 6 (1970) 367.

[62] J.R. Durig, A. Ganguly, A. M. El-Defrawy, G.A. Guirgis, T.K. Gounev, W.A. Herrebout, B.J. van der Veken J. Mol. Struct. 918 (2009) 64.

[63] J.R. Durig, A.Ganguly, J. J. Klaassen, G. A.Guirgis, J. Mol. Struct. 923 (2009) 28.

[64] W.G. Rothschild, J. Chem. Phys. 45 (1966) 1214.

[65] J.R. Durig, W.H. Green, J. Chem, Phys. 47 (1967) 673.

[66] A. Gatial, P. Klaeboe, C.J. Nielsen, D.L. Powell, D. Sülzle, A.J. Kondow, J. Raman Spectrosc. 20 (1989) 239.

[67] G. Bahnegyi, G. Fogarasi, P. Pulay, J. Mol. Struct. (THEOCHEM) 89 (1982) 1.

[68] J.R. Durig, T.S. Little, M.J. Lee, J. Raman Spectrosc. 20 (1989) 757.

[69] T. Inagusa, M. Hayashi, J. Mol. Spectrosc. 129 (1988) 160.

[70] M. Hayashi, C. Ikeda, T. Inagusa, J. Mol. Spectrosc. 139 (1990) 299.

[71] Y. Niide, J. Sci. Hiroshima Univ., 48A (1984) 23.

[72] F.M.K Lam, B.P. Dailey, J. Chem. Phys. 49 (1968) 1588.

[73] C. Ikeda, T. Inagusa, M. Hayashi, J. Mol. Spectrosc. 135 (1989) 334.

[74] J.R. Durig, X. Zhu, S. Shen, J. Mol. Struct. 570 (2001) 1.

[75] J.H. Carpenter, C.D. Gowland, D.C. Read, J.G. Smith, J. Mol. Spectrosc. 159 (1993) 192.

[76] H.M. Badawi, W.A. Herrebout, T.A. Mohamed, B.J. van der Veken, J.F. Sullivan, D.T. Durig, C. Zheng, K.S. Kalasinsky, J.R. Durig, J. Mol. Struct. 645 (2003) 89.

[77] J.R. Durig, A.M. El Defrawy, R.M. Ward, G.A. Guirgis, T.K. Gounev, J. Mol. Struct. 918 (2009) 26.

[78] W. Caminati, B. Vogelsanger, R. Meyer, G. Grassi, A. Bauder, J. Mol. Spectrosc. 131 (1988) 172.

[79] J.R. Durig, J.J. Klaassen, A. Ganguly, T.K. Gounev, P. Groner, J. Mol. Struct. 934 (2009) 66.

[80] J.R. Durig, J.N. Willis Jr., W.H. Green, J. Chem. Phys. 54 (1971) 1547.

[81] J. Demaison, J. Breidung, W. Thiel, D. Papousek, Struct. Chem. 10 (1999) 129.

[82] M. Hayashi, M. Fujitake, T. Inagusa, S. Miyazaki, J. Mol. Struct. 216 (1990) 9.

[83] M. Hayashi, T. Inagusa, J. Mol. Spectrosc. 138 (1989) 135.

[84] D.T. Durig, T.S. Little, T.G. Costner, J.R. Durig, J. Mol. Struct. 266 (1992) 277.

[85] G.A. Guirgis, H. Nanaie, J.R. Durig, J. Chem. Phys. 93 (1990) 3837.

[86] M. Hayashi, M. Fujitake, J. Mol. Struct. 146 (1986) 9.

[87] J.F. Sullivan, A. Wang, J.R. Durig, S.E. Godbey, Spectrochim. Acta 49A (1993) 1889.

[88] E. Bialkowska-Jaworska, M. Jaworski, Z. Kisiel, J. Mol. Struct. 350 (1995) 247.

[89] F. A. Miller, R. J. Capwell, R. C. Lord, D. G. Rea, Spectrochim. Acta 28A (1972) 603.

[90] J. R. Durig, A. C. Morrissey, J. Chem. Phys. 46 (1967) 4854.

[91] Ganguly, J. J. Klaassen, G. A. Guirgis, T. K. Gounev, J. R. Durig, Spectrochim. Acta 79A (2011) 831.

[92] Wurstner-Rock, H. D. Rudolph, J. Mol. Struct. 97 (1983) 327.

[93] J. R. Durig, T. J. Geyer, P. Groner, M. Dakkouri, Chem. Phys. 125 (1988) 299.

[94] J. R. Durig, T. S. Little, T. J. Geyer, M. Dakkouri, J. Phys. Chem. 93 (1989) 6296.

[95] M. Dakkouri, H. Oberhammer, J. Mol. Struct. 102 (1983) 315.

[96] A. Wurstner, H. D. Rudolph, paper E5, VIIth Colloquium on High Resolution Molecular Spectroscopy, Reading, 1981.

[97] J. J. Klaassen, I. D. Darkhalil, B. S. Deodhar, T. K. Gounev, R. M. Gurusinghe, M. J. Tubergen, P. Groner, and J. R. Durig, J. Phys. Chem. A 117 (2013) 6508.

[98] M. Dakkouri, J. Mol. Struct. 130 (1985) 289.

[99] J. R. Durig, A. D. Lopata, P. Groner, J. Chem. Phys. 66 (1977) 1888.

[100] K. -H. Chen, N. L. Allinger, J. Phys. Org. Chem. 12 (1999) 528.

[101] J. J. Klaassen, S. S. Panikar, G. A. Guirgis, H. W. Duke, J. K. Wyatt, J. R. Durig, J. Mol. Struct. 1032 (2013) 254.

[102] W. J. Adams, L.S. Bartell, J. Mol. Struct. 8 (1971) 199.

[103] E. C. R. Fabregue, Acad. Sci., Ser. B 280 (1975) 773.

[104] Hanai, K.; Katon, J. E. J. Mol. Struct. 70 (1981) 127.

[105] J. R. Durig, H. M.Badawi, H. D.Bist, T. S. Little, J. Mol. Struct. 190 (1988) 475.

[106] J.P. Guillory, L.S. Bartell, J. Chem. Phys. 43 (1965) 654.

[107] R.W. Kilb, C.-C. Lin, E.B. Wilson, J. Chem. Phys. 26 (1957) 1695.

[108] C.C. Lin, J.D. Swalen, Rev. Mod. Phys. 31 (1959) 841.

[109] P. Groner, H. Nanaie, J.R. Durig, J. Mol. Struct. 160 (1987) 37.

[110] P. Groner, J.R. Durig, D.D. DesMarteau, S.H. Hwang, J. Chem. Phys. 110 (1999) 9411.

[111] I. Mills, T. Cvitaš, K. Homann, N. Kallay, K. Kuchitsu, Quantities, Units, and Symbols in Physical Chemistry; Blackwell Science Ltd: Oxford, 1993.

[112] M. Hayashi, N. Inada, Y. Niide, J. Mol. Struct. 352/353 (1995) 325.

[113] K. Aarset, L.G. Faksnes, I. Nygaard, K. Hagen, J. Phys. Chem. 98 (1994) 2848.

[114] W. Lin, A. Ganguly, A.J. Minei, G.L. Lindeke, W.C. Pringle, S.E. Novick, J.R. Durig, J. Mol. Struct. 922 (2009) 83.

[115] L.S. Bartell, D.A. Kohl, B.L. Carroll, R. M. Gavin, J. Chem. Phys. 42 (1965) 3079.

[116] I.O.C. Ekejiuba, H.E. Hallam, Spectrochim. Acta A 26 (1970) 67.

[117] I.O.C. Ekejiuba, H.E. Hallam, Spectrochim. Acta A 26 (1970) 59.

[118] W.C. Harris, J.M. Karriker, J.R. Durig, J. Mol. Struct. 9 (1971) 139.

[119] J.I. Choe, M.D. Harmony, J. Mol. Spectrosc. 81 (1980) 480.

[120] R.N. Nandi, M.D. Harmony, J. Mol. Spectrosc. 98 (1983) 221.

[121] D.W. Wertz, W.E. Shasky, J. Chem. Phys. 55 (1971) 2422.

[122] L.A. Carreira, J. Chem. Phys. 55 (1971) 181.

[123] J.R. Durig, A.M. El Defrawy, A. Ganguly, T.K. Gounev, G.A. Guirgis, J. Phys. Chem A 113 (2009) 9675.

[124] R.C. Loyd, S.N. Mathur, M.D Harmony, J. Mol. Spectrosc. 72 (1978) 359.

[125] R.L. Hildebrandt, Q. Shen, J. Phys. Chem. 86 (1982) 587.

[126] P. Groner, M.J. Lee, J.R. Durig, J. Chem. Phys. 94 (1991) 3315.

[127] J.R. Durig, W. Zhao, X. Zhu, J. Mol. Struct. 521 (2000) 25.

[128] G.A. Guirgis, A.M. El Defrawy, T.K. Gounev, M.S. Soliman, J.R. Durig, J. Mol. Struct. 832 (2007) 73.

[129] M.D. Harmony, M.R. Strand, J. Mol. Spectrosc. 81 (1980) 308.

[130] J. Demaison, J. Cosléou, H. Bürger, E.B. Mkadmi, J. Mol. Spectrosc. 185 (1997) 384.

[131] J.R. Durig, C. Pan, G.A. Guirgis, Spectrochim. Acta A 59 (2003) 979.

[132] J.R. Durig, C. Pan, G.A. Guirgis, J. Mol. Struct. 688 (2004) 95.

[133] J. E. Kilpatrick, K. S. Pitzer, R. Spitzer, J. Am. Chem. Soc. 69 (1947) 2483.

[134] K. S. Pitzer, W. E. Donath, J. Am. Chem. Soc. 81 (1959) 3213.

[135] H. M. Badawi, W. A. Herrebout, C. Zheng, T. A. Mohamed, B. J. van der Veken, J. R. Durig, Struct. Chem. 14 (2003) 617.

[136] M. D. Harmony, V. W. Laurie, R. L. Kuczkowski, R. H. Schwendeman, D. A. Ramsay, F. J. Lovas, W. J. Lafferty, A. G. Maki, J. Phys. Chem. Ref. Data 8 (1979) 619.

[137] J. R. Durig, R. M. Ward, A. Ganguly, A. M. El Defrawy, K. G. Nelson, T. K. Gounev, M. S. Soliman, G. A. Guirgis, Vib. Spectrosc. 53 (2010) 45.

[138] T. Woldbaek, A. Berkessel, A. Horn, P. Klaeboe, Acta Chem. Scand. A 36 (1982) 719.

[139] C. J. Wurrey, S. Shen, X. Zhu, H. Zhen, J. R. Durig, J. Mol. Struct. 449 (1998) 203.

[140] G. A. Guirgis, C. J. Wurrey, Z. Yu, X. Zhu, J. R. Durig, J. Phys. Chem. A 103 (1999) 1509.

[141] F.A. Miller, R.G. Inskeep, J. Chem. Phys. 18 (1950) 1519.

[142] C.G. Le Fèvre, R.J.W. Le Fèvre, J. Chem. Soc. (1956) 3549.

[143] B. Curnutte, W.H. Shaffer, J. Mol. Spectrosc. 1 (1957) 239.

[144] J.R. Durig, D.W. Wertz, J. Chem. Phys. 49 (1968) 2118.

[145] I.O.C. Ekejiuba, H.E. Hallam, Spectrochim. Acta A 26 (1970) 57.

[146] W. Caminati, H. Oberhammer, G. Pfafferott, R.R. Filgueira, C.H. Gomez, J. Mol. Spectrosc. 106 (1984) 217.

[147] W. Caminati, A. Dell'Erba, G. Maccaferri, P.G. Favero, J. Mol. Spectrosc. 191 (1998) 45.

[148] J.R. Durig, A.M. El-Defrawy, A. Ganguly , S.S. Panikar, M.S. Soliman, J. Phys. Chem. A 115 (2011) 7473.

[149] J.R. Durig, S.S. Panikar, D.A. Obenchain, B.J. Bills, P.M. Lohan, R.A. Peebles, S.A. Peebles, P. Groner, G.A. Guirgis, M.D. Johnson, J. Chem. Phys. 136 (2012) 044306.

[150] J.R. Durig, S.S. Panikar, K.A. Glenn, Y. Zheng, G.A. Guirgis, Vib. Spectrosc. 55 (2011) 250.

[151] G.A. Guirgis, S.S. Panikar, J.J. Klaassen, S.S. Purohit, M.D. Johnston, J.R. Durig Spectrochim. Acta A 79 (2011) 858.

[152] G. Fritz, P. Schober, Z. Anorg. Allg. Chem. 372 (1970) 21.

[153] K. Turnbull, D.M. Ketcha, Comprehensive Heterocyclic Chemistry II 3 (1996) 795.

[154] G. Fritz, J. Mittag, Z. Anorg. Allg. Chem. 458 (1979) 37.

[155] L.F. Colegrove, J. Laane, J. Phys. Chem. 95 (1991) 6494.

[156] M. J. Frisch, G. W. Trucks, H. B. Schlegel, G. E. Scuseria, M. A. Robb, J. R. Cheeseman, G. Scalmani, V. Barone, B. Mennucci,G. A. Petersson, H. Nakatsuji, M. Caricato, X. Li, H. P. Hratchian, A. F. Izmaylov, J. Bloino, G. Zheng, J. L. Sonnenberg, M. Hada, M. Ehara, K. Toyota, R. Fukuda, J. Hasegawa, M. Ishida, T. Nakajima, Y. Honda, O. Kitao, H. Nakai, T. Vreven, J. A. Montgomery, Jr., J. E. Peralta, F. Ogliaro, M. Bearpark, J. J. Heyd, E. Brothers, K. N. Kudin, V. N. Staroverov, R. Kobayashi, J. Normand, K. Raghavachari, A. Rendell, J. C. Burant, S. S. Iyengar, J. Tomasi, M. Cossi, N. Rega, J. M. Millam, M. Klene, J. E. Knox, J. B. Cross, V. Bakken, C. Adamo, J. Jaramillo, R. Gomperts, R. E. Stratmann, O. Yazyev, A. J. Austin, R. Cammi, C. Pomelli, J. W. Ochterski, R. L. Martin, K. Morokuma, V. G. Zakrzewski, G. A. Voth, P. Salvador, J. J.

Dannenberg, S. Dapprich, A. D. Daniels, O. Farkas, J. B. Foresman, J. V. Ortiz, J. Cioslowski, D. J. Fox, Gaussian 09, Gaussian Inc., Wallingford CT, 2009.

[157] J.K.G. Watson, Mol. Phys. 15 (1968) 479.

[158] Z. Kisiel. PROSPE – Programs for Rotational Spectroscopy, available at <http://www.info.ifpan.edu.pl/~kisiel/prospe.htm>.

[159] D.O. Harris, G.G. Engerholm, C.A. Tolman, A.C. Luntz, R.A. Keller, H. Kim, W.D. Gwinn, J. Chem. Phys. 50 (1969) 2438.

[160] C. Zheng, M.R. Yazdi, V.F. Kalasinsky, J.R. Durig, J. Raman Spectrosc. 37 (2006) 52.

[161] J.R. Durig, C. Zheng, T.K. Gounev, W.A. Herrebout, B.J. van der Veken, J. Phys. Chem. A, 110 (2006) 5674.

[162] Y. Hamada, M. Tsuboi, K. Yamanouchi, K. Kuchitsu, J. Mol. Struct., 146 (1986) 253.

[163] E. Fischer, I. Botsker, J. Mol. Spectrosc., 104 (1984) 223.

[164] Y. Hamada, K. Hashiguchi, A.Y. Hirakawa, M. Tsuboi, M. Nakata, M. Tasumi, S. Kato, K. Morokuma, J. Mol. Spectrosc., 102 (1983) 123.

[165] J.R. Durig, Y.S. Li, J. Chem. Phys., 63 (1975) 4110.

[166] M. Tsuboi, K. Tamagake, A.Y. Hirakawa, J. Yamaguchi, H. Nakagawa, A.S. Manocha, E.C. Tuazon, W.G. Fateley, J. Chem. Phys., 63 (1975) 5177.

[167] A.S. Manocha, E.C. Tuazon, W.G. Fateley, J. Chem. Phys., 78 (1974) 803.

[168] L. Radom, W.J. Hehre, J.A. Pople, J. Am. Chem. Soc., 94 (1972) 2371.

[169] J.R. Durig, W.B. Beshir, S.E. Godbey, T.J. Hizer, J. Raman Spectrosc. 20 (1989) 311.

[170] J.R. Durig, A. Ganguly, C. Zheng, G.A. Gurigis, W.A. Herrebout, B.J. van der Veken, T.K. Gounev, J. Mol. Struct., 968 (2010) 36.

[171] K.M. Marstokk, H. Mollendal, Acta Chem. Scand. 36 (1982) 517.

[172] J. R. Durig, J. J. Klaassen, S. S. Panikar, I. D. Darkhalil, A. Ganguly, G. A. Guirgis, J. Mol. Struct. 993 (2011) 73.

[173] G. A. Guirgis, I. D. Darkhalil, J. J. Klaassen, A. Ganguly, J. K. Wyatt, J. R. Durig, J. Raman Spect. 43 (2012) 116.

[174] J. R. Durig, J. J. Klaassen, I. D. Darkhalil, W. A. Herrebout , J. J. J. Dom, B. J. van der Veken, J. Mol. Struct. 1009 (2012) 30.

[175] J. R. Durig, H. Deeb, I. D. Darkhalil, J. J. Klaassen, T. K. Gounev, A. Ganguly, J. Mol. Struct. 985 (2011) 202.

[176] J. R. Durig, A. Ganguly, A. M. El Defrawy, H. M. Badawi, W. A. Herrebout, B. J. van der Veken, G. A. Guirgis, T. K. Gounev, C. Zheng, J. Mol. Struct. 922 (2009) 114.

[177] E. Fischer, I. Botsker, J. Mol. Spectrosc. 104 (1984) 226.

[178] N. Sato, Y. Hamada, M. Tsuboi, Spectrochim. Acta. 43A (1987) 943.

[179] L. A. E. Batista De Carvalho, A. M. Amorim Da Costa, M. L. Duarte, J. J. C. Teixeira-Dias, Spectrochim. Acta. 44A (1988) 723

[180] V. H. Wolf, H. Ludwig, Bet Bunsenges. physik. chem. 68 (1964) 143.

[181] V. H. Wolf, H. Ludwig, Ber. Bunsenges. physik. chem. 71 (1967) 1107.

[182] V. H. Wolf, H. Ludwig, J. chem. Phys. 56 (1972) 5278.

[183] K. Yamanouchi, M. Sugie, H. Takeo, C. Matsumura, K. Kuchitsu, J. Phys. Chem. 88 (1984) 2315.

[184] L. A. E. Batista De Carvalho, A. M Amorim Da Costa, J. J. C. Teixeira-Dias, J. Mol. Struct. 218 (1990) 105.

[185] J. R. Durig, T. K. Gounev, M. S. Lee, T. S. Little, J. Mol. Struct. 327 (1994) 23.

[186] A. A. Abdurakhmanov, É. I. Veliyulin, R. A. Ragimova, L. M. Imanov, Zh. Struk. Khim. 22 (1981) 39.

[187] A. Maeda, F. C. De Lucia, E. Herbst, J. C. Pearson, J. Riccobono, E. Trosell, R. K. Bohn, Astrophys. J. Suppl. 162 (2006) 428.

[188] J. C. Dobrowolski, S. Ostrowski, R. Kolos, M. H. Jamroz, Vib. Spectrosc. 48 (2008) 82.

[189] T. Torgrimsen, P. Klaeboe, Acta Chem. Scand. 24 (1970) 1139.

[190] J.R. Durig, C. Zheng, R.D. Warren, P. Groner, C.J. Wurrey, T.K. Gounev, W.A. Herrebout, B.J. van der Veken, J. Phys. Chem., A 107 (2003) 7713.

[191] K.M. Marstokk, H. Møllendal, Acta. Chem. Scand., A 34 (1980) 15.

[192] V. F. Kalasinsky, H. V. Anjarla, J. Phys. Chem., 84 (1980) 1940.

[193] I. D. Warren, E. B. Wilson, J. Chem. Phys., 56 (1972) 2137.

[194] Ch. Keussen, H. Dreizler, Z. Naturforsch., 46a (1991) 527.

[195] H. Wolff, D. Horn, H.G. Rollar, Spectrochim. Acta., 29A (1973) 1835.

[196] J.R. Durig, P. Klaeboe, G.A. Guirgis, L.-F. Wang and J. Liu, Z. Physik. Chem. 191 (1995) 23.

[197] W.V. Cohen, U.S. Patent Number 3118945 19640121 1964.

[198] J.R. Durig, G.A. Guirgis and D.A.C. Compton, J. Phys. Chem., 83 (1979) 1313.

[199] P. J. Krueger and J. Jan, Can. J. Chem., 48 (1970) 3229.

[200] Y. Hamada, M. Tsuboi, M. Nakata and M. Tasumi, Chem. Phys., 125 (1988) 55.

[201] S. C. Mehrotra, L. L. Griffin, C. O. Britt and J. E. Boggs, J. Mol. Spectrosc., 64 (1977) 244.

[202] T. Iijima, T. Kondou and T. Takenaka, J. Mol. Struct., 445 (1998) 23.

[203] T. Iijima, Bull. Chem. Soc. Jpn., 59 (1986) 853.

[204] M. Meyer, J.U. Grabow, H. Dreizler and H.D. Rudolph, J. Mol Spectrosc., 151 (1992) 217.

[205] A.A. Abdurakhmanov, M.N. Elchiev and L.M. Imanov, Zh. Strukt. Khim., 15 (1972) 42.

[206] J.R. Durig, J. Liu, T.S. Little, V.F. Kalasinsky, J. Phys. Chem. 96 (1992) 8224.

[207] J.J. Turner, M. Poliakoff, S.M. Howdle, S.A. Jackson, J.G. McLaughlin, Faraday Discuss.Chem. Soc. 86 (1988) 271.

[208] O. A. Braathen, K. M. Marstokk, H. Møllendal, Acta. Chem. Scand. A 37 (1983) 493.

[209] P. Pulay, Theor. Chim. Acta 50 (1979) 299.

[210] P.N. Skancke, Acta. Chem. Scand. A 38 (1984) 95.

[211] P. Pulay, G. Fogarasi, F. Pang, J.E. Boggs, J. Am. Chem. Soc. 101 (1979) 2550.

[212] M. Rouault, G. Gallagher. Phys Rev. 75 (1949), 1319.

[213] C.O. Kadzhar, L.M. Imanov, I.D. Isaev. Academy of Sciences of the Azerbaijan SSR. 9 (1968), 375.

[214] J.P. Culot, 4th Austin Symp. on Molecular Structure. Paper T8 (1972), 47.

[215] R.K. Kakar, C.R. Quade. J. Chem. Phys. 76 (1980), 4300.

[216] S.F. Chun, C.R. Quade. J. Mol. Spectrosc. 199 (2000), 34.

[217] A.J. Barnes, H.E. Hallam. Trans. Faraday Soc. 66 (1970), 1932.

[218] J.R. Durig, R.A. Larsen, J. Mol. Struct. 238 (1989), 195.

[219] J.R. Durig, W.E. Bucy, C.J. Wurrey, J. Phys. Chem. 79 (1975), 988.

[220] J.P. Perchard, M.L. Josien, J. Chim. Phys. 65 (1968) 1834.

[221] R. Kakar, P.J. Seibt, J. Chem. Phys. 57 (1970), 988.

[222] L.M. Imanov, C.O. Kadzhar, I.D. Isaev. Opt. Spectrosc. 18 (1965) 344.

[223] W. Maier, Vth European Congress on Mol. Spectrosc. Buttersworth, London, 1962.

[224] J. Michielsen-Effinger, Bull. Classe Sci. Acad. Roy. Belg. 48 (1962) 438.

[225] J.P. Culot, Ann. Soc. Scient. Brux. 81 (1967) 272.

[226] J.P. Culot, Ann. Soc. Scient. Brux. 83 (1969) 65.

[227] J.C. Pearson, K.V.L.N. Sastry, M. Winnewisser, E. Herbst, F.C. De Lucia. J. Phys. Chem. Ref. Data. 24 (1995), 1.

[228] S. Bell, B. R. Drew, G. A. Guirgis, J. R. Durig, J. Mol. Struct. 553 (2000) 199.

[229] D. van Hemelrijk, L. Van den Enden, H. J. Giese, H. L. Sellers, L. Schaefer, J. Am. Chem. Soc. 102 (1980) 2189.

[230] B. Galabov, J. P. Kenny, H. F. Schaefer III, J. R. Durig, J. Phys. Chem. A 106 (2002) 3625.

[231] J. R. Durig, M. Zhen, H. L. Heusel, P. J. Joseph, P. Groner, T. S. Little, J. Phys. Chem. 89 (1985) 2877.

[232] A. N. Murty, R. F. Curl Jr, J. Chem. Phys. 46 (1967) 4176.

[233] A. I. Jaman, D. K. Ghosh, Pramana 17 (1981) 245.

[234] H. Badawi, P. Lorencak, K. W. Hillig II, M. Imachi, R. Kuczkowski, J. Mol. Struct. 162 (1987) 247.

[235] S. Melandri, P. G. Favero, W. Caminati, Chem. Phys. Lett. 223 (1994) 541.

[236] F. Vanhouteghem, W. Pyckhout, C. van Alsenoy, L. Van den Enden, H. J. Geise, J. Mol. Struct. 140 (1986), 33.

[237] K. V. L. N. Sastry, S. C. Dass, W. V. F. Brooks, A. Bhaumik, J. Mol. Spectrosc. 31 (1969) 54.

[238] C. S. Hsu, Spectrosc. Lett. 7 (1974) 139.

[239] E. Hirota, J. Chem. Phys. 42 (1965) 2071.

[240] T. Kojima, J. Phys. Soc. Jpn. 15 (1960) 1284.

[241] W. A. Herrebout, C. Zheng, B. J. Van der Veken, J. R. Durig, J. Mol. Struct. 645 (2003) 109.

[242] K. H. Wiedenmann, I. Botskor, H. D. Rudolph, O. L. Stiefvater, J. Mol. Struct. 190 (1988) 173.

[243] Y. Hamada, M. Tsuboi, K. Yamanouchi, T. Matsuzawa, K. Kuchitsu, J. Mol. Struct. 224 (1990) 345.

[244] I. Botskor, H. D. Rudolph, J. Mol. Spectrosc. 52 (1974) 457.

APPENDIX A

SUPPLEMENTAL INFORMATION

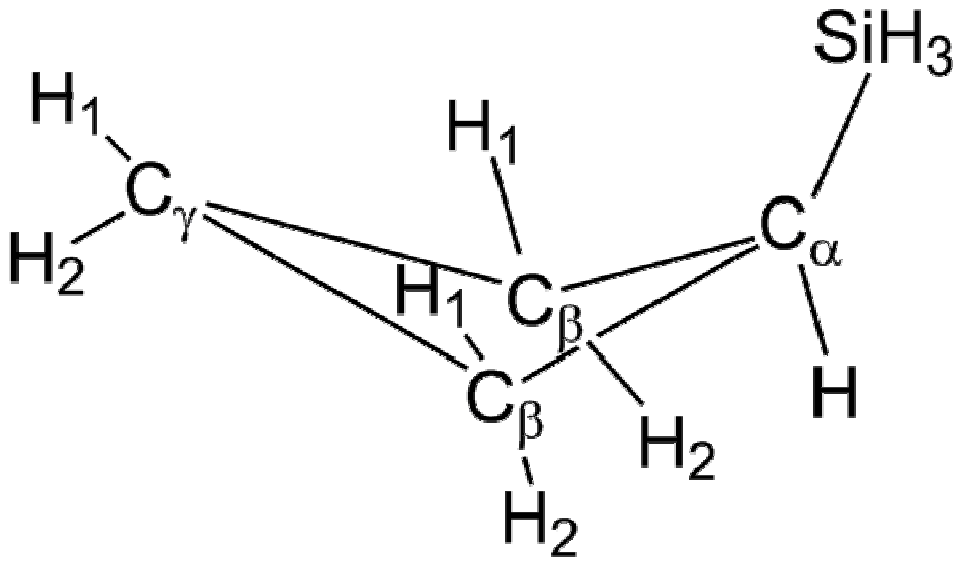

Figure S1. Labeled cyclobutylsilane molecule.

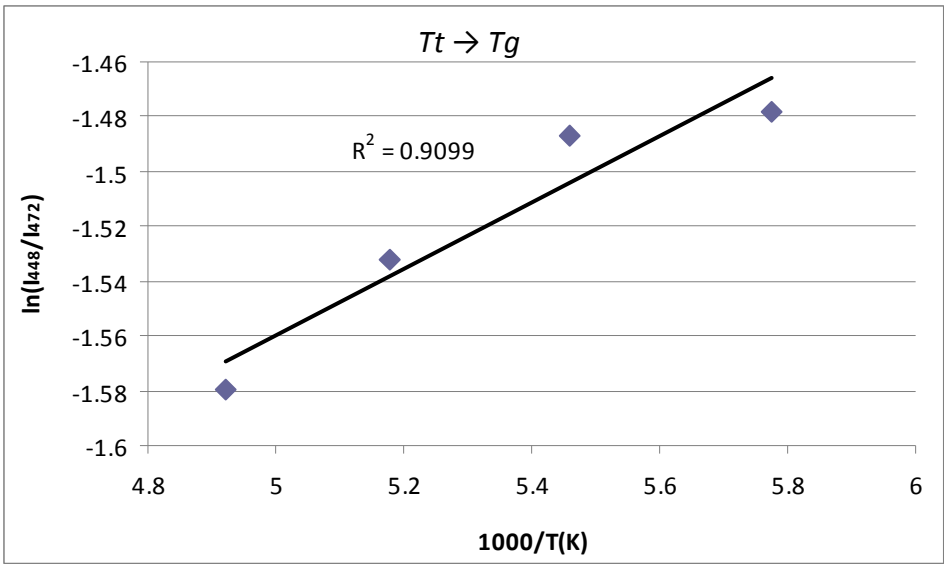
Tt → Tg
-1.46
-1.48
-1.5
-1.52
-1.54
-1.56
-1.58
-1.6
R2 = 0.9099
ln(I448/I472)
4.8
5
5.2
5.4
5.6
5.8
6
1000/T(K)

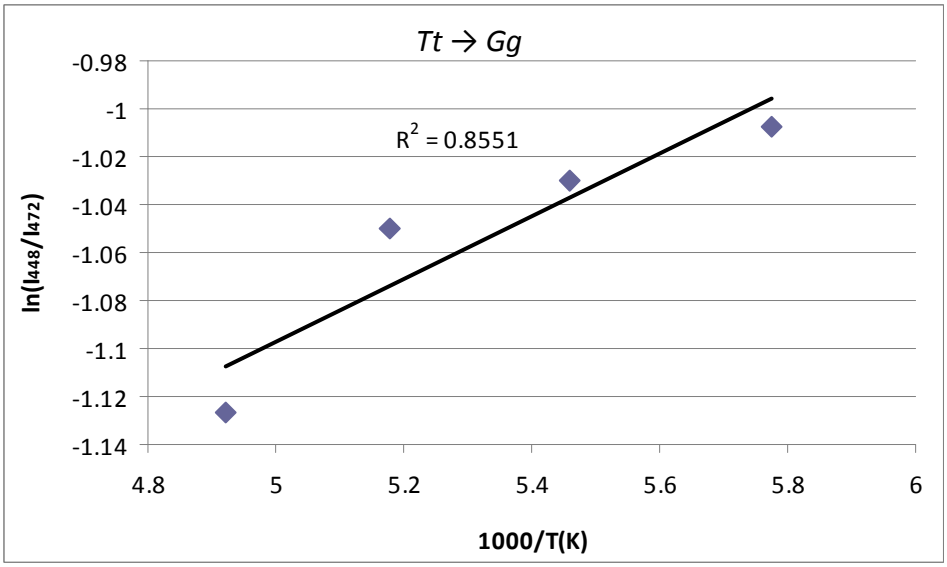
Tt → Gg
-0.98
-1
-1.02
-1.04
-1.06
-1.08
-1.1
-1.12
-1.14
R2 = 0.8551
ln(I448/I472)
4.8
5
5.2
5.4
5.6
5.8
6
1000/T(K)

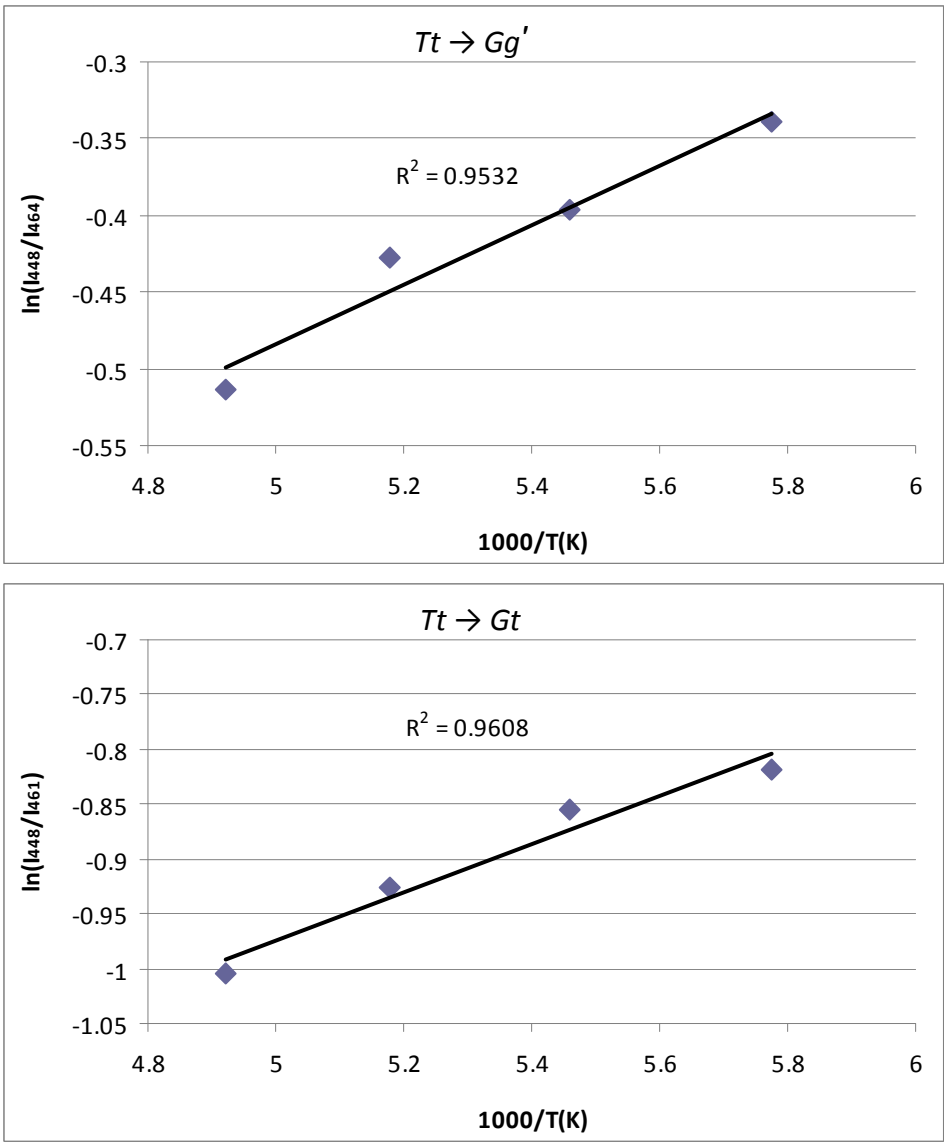

Figure S2. van't Hoff plot of $\ln(I_{conf1}/I_{conf2})$ as a function of 1/T.

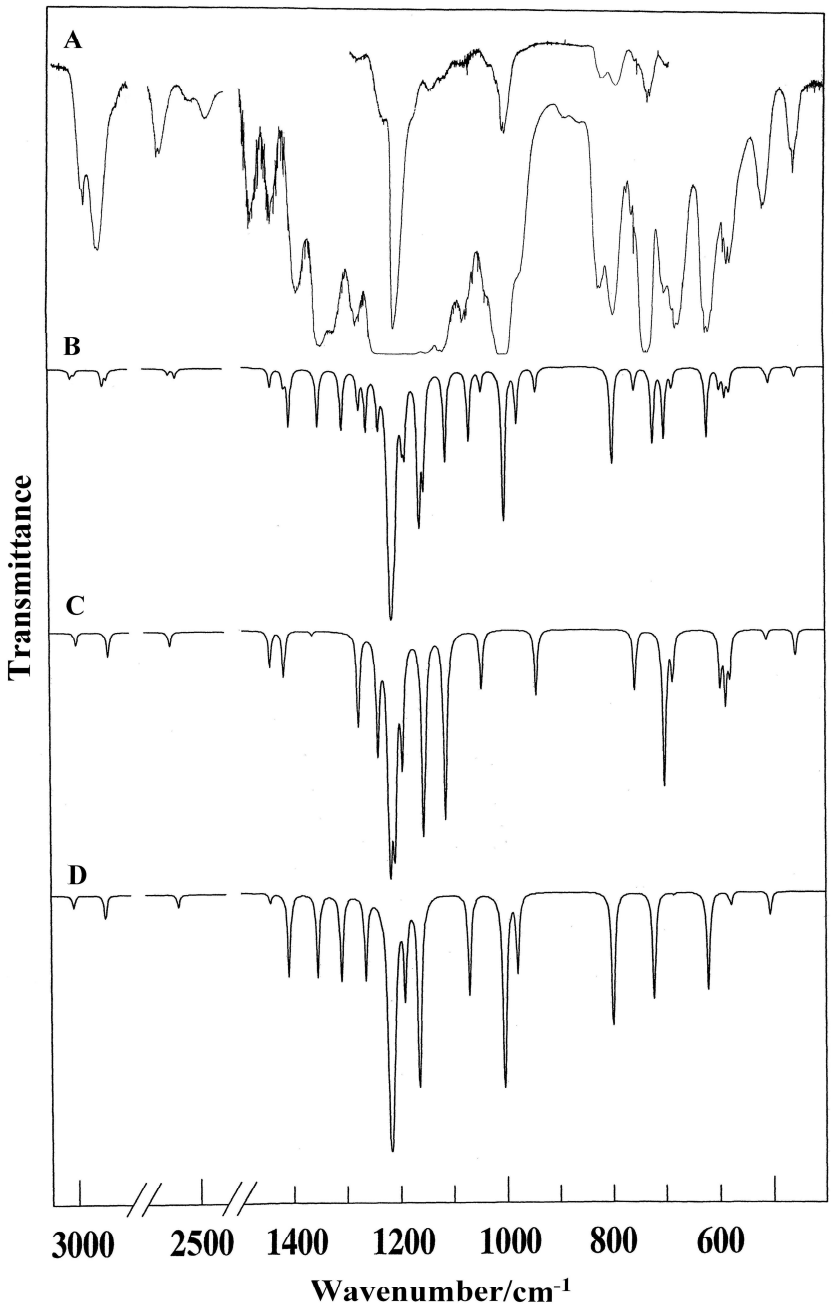

Figure S3. Comparison of experimental and predicted infrared spectra of 2,2,3,3,3-pentafluoropropylamine-ND_2: (A) gas; (B) simulated spectrum of *Tt* and *Tg*; enthalpy difference of 280 cm^{-1} at 25°C; (C) simulated spectrum of *Tg* conformer; (D) simulated spectrum of *Tt* conformer.

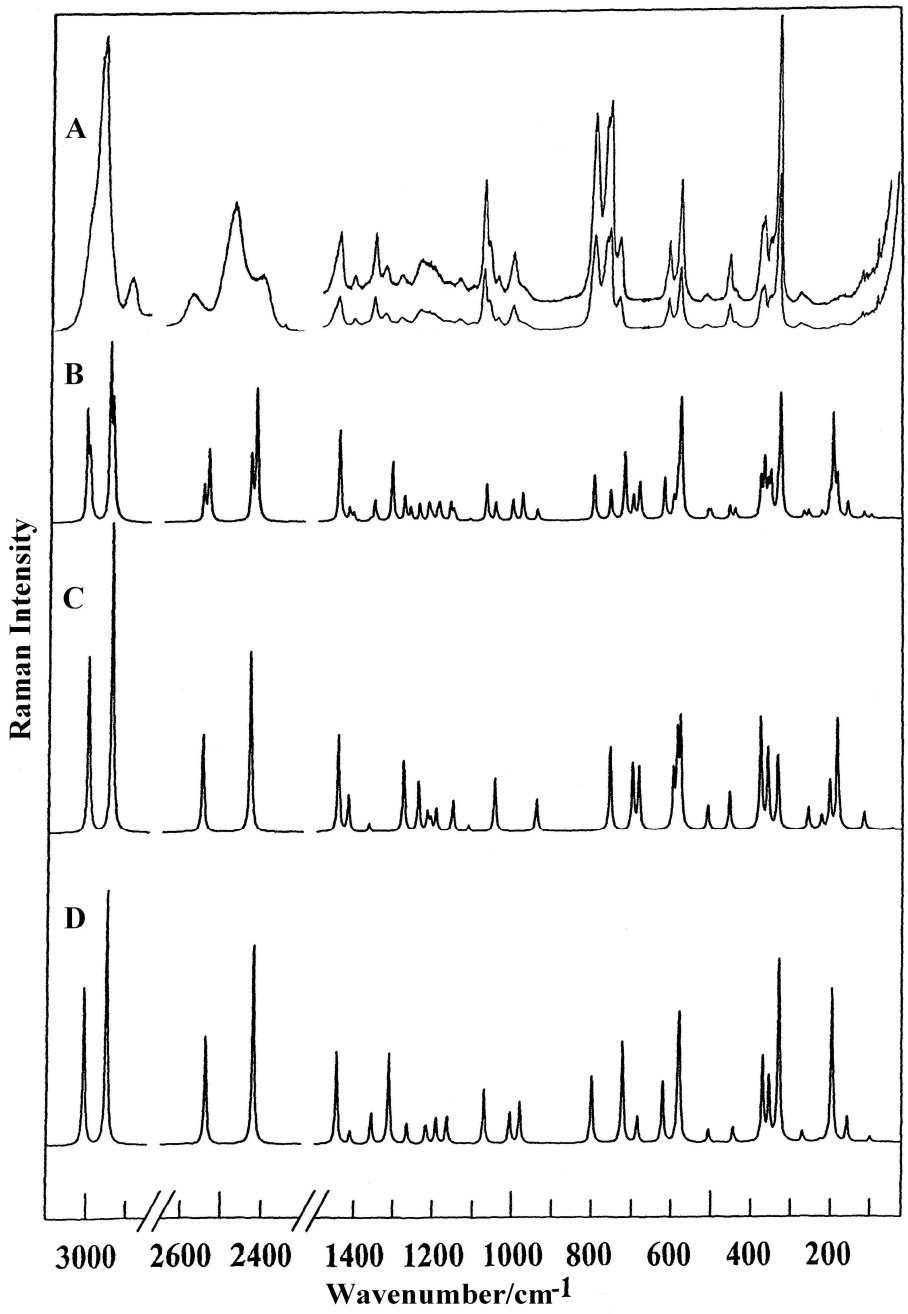

Figure S4. Comparison of experimental and predicted Raman spectra of 2,2,3,3,3-pentafluoropropylamine-ND_2: (A) liquid; (B) simulated spectrum of *Tt* and *Tg*; enthalpy difference of 280 cm^{-1} at 25°C; (C) simulated spectrum of *Tg* conformer; (D) simulated spectrum of *Tt* conformer.

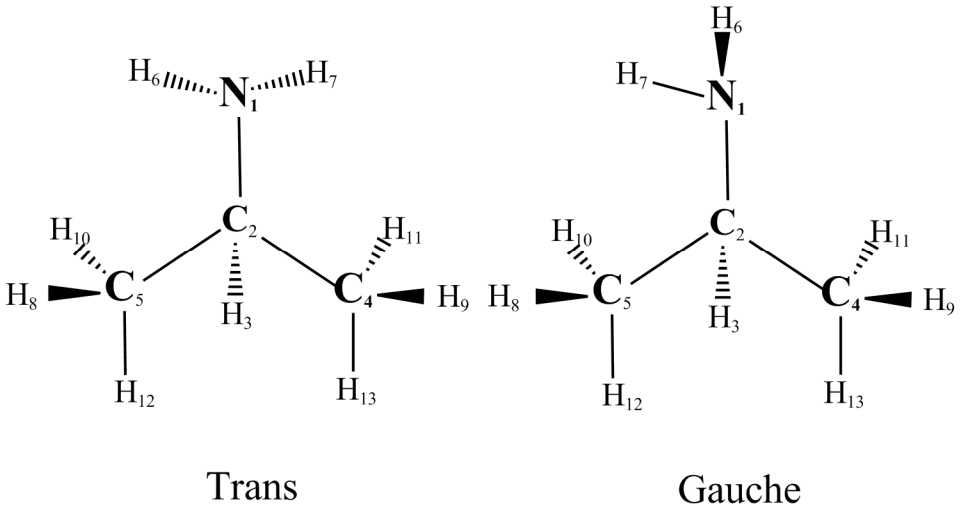

Figure S5. *Trans* and *gauche* conformers of isopropylamine showing atomic numbering.

VITA

Joshua John Klaassen was born on February 14, 1985, in San Antonio, Texas. He was educated in local public schools and graduated from Kelly Walsh High School in 1985. He received a Scholarship to the University of Nebraska Wesleyan in Lincoln, Nebraska, from which he graduated in 2007. His degree was a Bachelor of Science in Chemistry with a minor in Biology.

Joshua John Klaassen joined the University of Missouri-Kansas City in 2008 and promptly began publishing in international peer reviewed journals, publishing more than 24 publications as of this date with 21 of them in circulation.

Publications

J. J. Klaassen, I. D. Darkhalil, B. S. Deodhar, T. K. Gounev, R. M. Gurusinghe, M. J. Tubergen, P. Groner, J. R. Durig "Microwave and Infrared Spectra, Adjusted r_0 Structural Parameters, Conformational Stabilities, Vibrational Assignments and Theoretical Calculations of Cyclobutylcarboxylic Acid Chloride" J. Phys. Chem. A, 117, 6508 (2013).

G. A. Guirgis, **J. J. Klaassen**, B. H. Pate, N. A. Seifert, I. D. Darkhalil, B. S. Deodhar, J. K. Wyatt, H. W. Dukes, M. Kruger, J. R. Durig "Microwave, infrared, and Raman spectra, structural parameters, vibrational assignments and theoretical calculations of 1,3-disilacyclopentane" J. Mol. Struct., 1049, 400, (2013).

J. R. Durig, **J. J. Klaassen**, B. S. Deodhar, I. D. Darkhalil, W. A. Herrebout, J. J.J. Dom, B. J. van der Veken, S. S. Purohit, G. A. Guirgis, "Conformational and Structural Studies of Ethynylcyclopentane from Temperature Dependent Raman Spectra of Xenon Solutions and Ab Initio Calculations," J. Mol. Struct., 1044, 10 (2013).

B. H. Pate, N. A. Seifert, G. A. Guirgis, B. S. Deodhar, **J. J. Klaassen**, I. D. Darkhalil, J. A. Crow, J. K. Wyatt, H. W. Dukes, J. R. Durig, "Microwave, infrared, and Raman spectra, structural parameters, vibrational assignments and theoretical calculations of 1,1,3,3-tetrafluoro-1,3-disilacyclopentane" Chem. Phys., 416, 33 (2013).

S. S. Panikar, B. S. Deodhar, D. K. Sawant, **J. J. Klaassen**, J. Deng, J. R. Durig, "Raman and Infrared Spectra, r_o Structural Parameters, and

Vibrational Assignments of $(CH_3)_2PX$ where X=H, CN, and Cl," Spectrochim. Acta 103, 205 (2013).

J. R. Durig, I. D. Darkhalil, **J. J. Klaassen**, N. Nagels, W. A. Herrebout, B. J. van der Veken., "Conformational and structural studies of 2,2,2-trifluoroethylamine from temperature dependent Raman spectra of xenon solutions and ab initio calculations," J. Mol. Struct. 1032, 229 (2013).

G. A. Guirgis , **J. J. Klaassen**, B. S. Deodhar, D. K. Sawant, S. S. Panikar, H. W. Dukes, J. K. Wyatt, J. R. Durig, "Structure and conformation studies from temperature dependent infrared spectra of xenon solutions and ab initio calculations of cyclobutylgermane," Spectrochim. Acta, 99, 266 (2012).

J. J. Klaassen, S. S. Panikar, G. A. Guirgis, H. W. Duke, J. K. Wyatt, J. R. Durig, "Conformational and structural studies of cyclobutylsilane from temperature dependent infrared spectra of xenon solutions and ab initio calculations," J. Mol. Struct. 1032, 254 (2013).

J. R. Durig, I. D. Darkhalil, **J. J. Klaassen**, "Infrared and Raman Spectra, r_0 Structural Parameters, Conformational Stability, and Vibrational Assignment of 2-cyanoethylamine," J. Mol. Struct., 1023, 154 (2012).

J. R. Durig, I. D. Darkhalil, **J. J. Klaassen**, W. A. Herrebout, J. J. J. Dom, B. J. van der Veken, "Conformational and structural studies of n-propylamine from temperature dependent Raman and far infrared spectra of xenon solutions and ab initio calculations," J. Raman Spectrosc., 43, 1329 (2012).

J. R. Durig, **J. J. Klaassen**, I. D. Darkhalil, W. A. Herrebout, J. J. J. Dom, B. van der Veken, "Conformational and structural studies of isopropylamine from temperature dependent Raman spectra of xenon solutions and ab initio calculations," J. Mol. Struct. 1009, 30 (2012).

G. A. Guirgis, I. D. Darkhalil, **J. J. Klaassen**, A. Ganguly, J. K. Wyatt, J. R. Durig, "Conformational vibrational, and structural studies of 2,2,3,3,3-pentafluoropropylamine from Raman and infrared spectra of gas, liquid, xenon solutions, and solid supported by ab initio calculations," J. Raman Spectrosc. 43, 116 (2012).

J. R. Durig, **J. J. Klaassen**, B. S. Deodhar, T. K. Gounev, A. R. Conrad, M. J. Tubergen, "Microwave, Infrared, and Raman Spectra, r_0 Structural Parameters, Conformational Stability, and Vibrational Assignment of Allyl Thiol," Spectrochim. Acta, 87, 214 (2012).

G. A. Guirgis, S. S. Panikar, **J. J. Klaassen**, S. S. Purohit, M. D. Johnston, J. R. Durig, "Infrared and Raman Spectra, ab initio Calculations, Conformational Stability and Vibrational Assignment of 1-bromo-1-silacyclopentane," Spectrochim. Acta, 79, 858 (2011).

J. R. Durig, **J. J. Klaassen**, S. S. Panikar, I. D. Darkhalil, A. Ganguly, G. A. Guirgis, "Conformational and Structural Studies of 2,2-difluoroethylamine from Temperature Dependent Infrared Spectra of Xenon Solution and ab initio Calculations," J. Mol. Struct., 993, 73 (2011).

J. R. Durig, H. Deeb, I. D. Darkhalil, **J. J. Klaassen**, T. K. Gounev, A. Ganguly, "The r_0 Structural Parameters, Conformational Stability, Barriers to Internal Rotation, and Vibrational Assignments for trans and gauche Ethanol," J. Mol. Struct., 985, 202 (2011).

A. Ganguly, **J. J. Klaassen**, G. A. Guirgis, T. K. Gounev, J. R. Durig, "Conformational Stability, r_0 Structural Parameters, and Vibrational Assignments of Mono-substituted Cyclobutanes: Fluorocyclobutane," Spectrochim. Acta, 79, 831 (2011).

J. R. Durig, S. X. Zhou, **J. Klaassen**, A. Ganguly, "The Utilization of Low Frequency Raman Spectra of Gases for the Study of Molecules with Large Amplitude Vibration," Chin. J. Light Scatt., 21, 201 (2009).

J. R. Durig, **J. J. Klaassen**, A. Ganguly, P. Groner, "The r_0 Structural Parameters, Conformational Stability, and Vibrational Assignment of Equatorial and Axial Bromocyclobutane," J. Mol. Struct., 934, 66 (2009).

J. R. Durig, A. Ganguly, **J. J. Klaassen**, G. A. Guirgis, "The r_0 Structural Parameters, Conformational Stability, and Vibrational Assignment of Equatorial and Axial Cyanocyclobutane," J. Mol. Struct., 923, 28 (2009).

J. R. Durig, **J. J. Klaassen**, A. Ganguly, T. K. Gounev, G. A. Guirgis, W. Lin, "The r_0 Structural Parameters of Equatorial and Axial Chlorocyclobutane, Conformational Stability from Temperature Dependent Infrared Spectra of Xenon Solutions, and Vibrational Assignments" Struct. Chem., 19, 935 (2008).